

**Total Synthesis of (+)-Greek Tobacco Lactone,  
(+)-Plakortolide E, (-)-Plakortolide I  
and 3-*epi*-Hypatulin B**

**Inaugural-Dissertation**

to obtain the academic degree

Doctor rerum naturalium (Dr. rer. nat.)

submitted to the Department of Biology, Chemistry, Pharmacy

Freie Universität Berlin

by

**Stefan Leisering**

from Berlin

March 2022



Hiermit versichere ich, die vorliegende Dissertation selbstständig und ohne unerlaubte Hilfe angefertigt zu haben. Beim Verfassen der Dissertation wurden keine anderen als die im Text aufgeführten Hilfsmittel verwendet. Ein Promotionsverfahren zu einem früheren Zeitpunkt an einer anderen Hochschule oder einem anderen Fachbereich wurde nicht beantragt.

Hereby, I declare that the submitted thesis is my own work and was prepared autonomously without the help of other sources than the ones cited and acknowledged. The work was not submitted to any prior doctoral procedure and no doctoral examination has taken place to date.

Stefan Leisering, March 2022

The following work was carried out within the research group of Prof. Dr. MATHIAS CHRISTMANN from November 2015 until October 2021 at the Institute of Chemistry and Biochemistry of Freie Universität Berlin.

Date of Disputation: 08.06.2023

1<sup>st</sup> Reviewer: Prof. Dr. Mathias Christmann  
(Institute of Chemistry and Biochemistry, Freie Universität Berlin)

2<sup>nd</sup> Reviewer: Prof. Dr. Siegfried Eigler  
(Institute of Chemistry and Biochemistry, Freie Universität Berlin)





Parts of this dissertation have already been published in:

**Leisering, S.;** Riaño, I.; Depken, C.; Gross, L. J.; Weber, M.; Lentz, D.; Zimmer, R.; Stark, C. B. W.; Breder, A.; Christmann, M. Synthesis of (+)-Greek Tobacco Lactone via a Diastereoablative Epoxidation and a Selenium-Catalyzed Oxidative Cyclization. *Org. Lett.* **2017**, *19*, 1478–1481.

**Leisering, S.;** Mavroskoufis, A.; Voßnacker, P.; Zimmer, R.; Christmann, M. Synthesis of Plakortolides E and I Enabled by Base Metal Catalysis. *Org. Lett.* **2021**, *23*, 4731–4735.

Parts of this work were carried out in collaboration with SEBASTIAN PONATH. The described results give a complete representation of this collaboration and results obtained solely by SEBASTIAN PONATH are clearly identified as such.



# Table of Content

<b>Danksagung</b> .....	<b>I</b>
<b>Zusammenfassung</b> .....	<b>III</b>
<b>Abstract</b> .....	<b>VI</b>
<b>Abbreviations</b> .....	<b>IX</b>
<b>1 Introduction</b> .....	<b>1</b>
1.1 Natural Products.....	1
1.1.1 Primary and Secondary Metabolites .....	1
1.1.2 Terpenoids.....	1
1.2 Biosynthesis of Terpenoids .....	2
1.2.1 Biosynthesis of IPP and DMAPP.....	2
1.2.2 Prenyltransferases .....	3
1.2.3 Type I Terpenoid Cyclases .....	4
1.2.4 Type II Terpenoid Cyclases.....	6
1.3 Meroterpenoids .....	7
1.4 Natural Product Synthesis – Drug Development and Fundamental Research.....	9
<b>2 (+)-Greek Tobacco Lactone</b> .....	<b>11</b>
2.1 Introduction .....	11
2.1.1 Isolation of (+)-Greek Tobacco Lactone .....	11
2.1.2 Total Syntheses of (+)-Greek Tobacco Lactone .....	11
2.2 Objective .....	13
2.3 Publication .....	14
2.3.1 Synthesis of (+)-Greek Tobacco Lactone via a Diastereoablative Epoxidation and a Selenium-Catalyzed Oxidative Cyclization .....	14
<b>3 Cyclopropanation – Studies Towards the Intramolecular Methylenetransfer of 6,7-Alkenyl Epoxides</b> .....	<b>19</b>
3.1 Cyclopropanes in Natural Products .....	19
3.2 Synthesis of Cyclopropanes .....	19
3.3 Objective .....	22
3.4 Results.....	23
<b>4 (+)-Plakortolide E and (–)-Plakortolide I</b> .....	<b>31</b>
4.1 Introduction .....	31
4.1.1 Endoperoxide Natural Products and Malaria .....	31
4.1.2 Marine Natural Products.....	32
4.1.3 Characteristic Endoperoxide Metabolites of Marine Sponges.....	33
4.1.4 Isolation of Plakortolide E and Plakortolide I.....	33
4.1.5 Biosynthesis of Plakortolide E and Plakortolide I.....	34
4.1.6 Total Syntheses of Plakortolide E and Plakortolide I.....	35

4.2	Objective.....	36
4.3	Unpublished Results – Preliminary Studies .....	37
4.4	Publication.....	41
4.4.1	Synthesis of Plakortolides E and I Enabled by Base Metal Catalysis .....	41

## **5 Studies Towards the Total Synthesis of Hypatulin A and Hypatulin B..... 47**

5.1	Introduction .....	47
5.1.1	Characteristic Metabolites of Hypericum Plants.....	47
5.1.2	Biosynthesis of Hyperforin .....	48
5.1.3	Isolation of Hypatulin A and Hypatulin B.....	49
5.1.4	Biosynthesis of Hypatulin A and Hypatulin B .....	50
5.2	Objective.....	51
5.3	Unpublished Results – Preliminary Studies .....	52
5.3.1	Retrosynthetic Analysis of Hypatulin A and Hypatulin B.....	52
5.3.2	Preparation of Fragment A.....	52
5.3.3	Preparation of Fragment B .....	58
5.3.4	Coupling of Fragment A and Fragment B .....	60
5.3.5	Construction of the Second Quarternary Stereocenter .....	62
5.3.6	Installation of the Third Allyl Group .....	64
5.3.7	Preparation of Triketone rac-162.....	66
5.3.8	Installation of the Methoxycarbonyl Group .....	67
5.4	Publication.....	69
5.4.1	Synthesis of 3- <i>epi</i> -Hypatulin B Featuring a Late-Stage Photo-Oxidation in Flow .....	69

## **6 List of References and Illustration Credits ..... 75**

6.1	References.....	75
6.2	Illustration Credits.....	89

## **Appendix..... 91**

## Danksagung

An erster Stelle möchte ich mich bei meinem Doktorvater Prof. Dr. Mathias Christmann für die freundliche Aufnahme in seine Arbeitsgruppe und die große wissenschaftliche Freiheit bei der Bearbeitung der Forschungsprojekte bedanken.

Ich danke Herrn Prof. Dr. Siegfried Eigler für die freundliche Übernahme des Zweitgutachtens.

Mein ganz besonderer Dank gilt Prof. Dr. Christoph A. Schalley für die fortwährende Unterstützung und Förderung seit meinem Bachelorstudium sowie für die sehr angenehme und bereichernde Zusammenarbeit.

Auch danke ich Dr. Igor Linder für große Unterstützung während meines Bachelor- und Masterstudiums.

Patrick Voßnacker danke ich für die Hilfe bei all meinen Problemen und Fragen zu Einkristallstrukturanalysen und auch für die Durchführung einiger Messungen. Dr. Andreas Springer und Dr. Andreas Schäfer danke ich dafür, dass sie sich immer Zeit für meine Fragen zur Massenspektrometrie beziehungsweise NMR-Spektroskopie genommen haben.

Für das Korrekturlesen dieser Arbeit danke ich Dr. Merlin Kleoff, Dr. Sebastian Ponath, Marcel Gausmann, Bence Hartmayer, Tobias Olbrisch, Kamar Shakeri und Alexandros Mavroskoufis.

Außerdem möchte ich mich ganz herzlich bei Dr. Reinhold Zimmer für die Unterstützung und die Organisation innerhalb der Arbeitsgruppe bedanken. Weiterhin danke ich ihm dafür, dass er immer ein offenes Ohr für die Probleme der Mitarbeiter hatte.

Der Arbeitsgruppe Christmann danke ich für die freundliche und immer hilfsbereite Atmosphäre, die wunderbare Zeit und die vielen schönen Momente im Labor und auch darüber hinaus. Ganz besonders danke ich Dr. Sebastian Ponath für die lustigen, verrückten, aufregenden und schönen gemeinsamen Jahre im Labor und für die wunderbare Zusammenarbeit. Auch danke ich Tobias Olbrisch für die gemeinsame Zeit beim Sport sowie für die vielen kulinarischen Abende sowohl in diversen Restaurants als auch mit selbstgekochem Essen. Der Kochgruppe danke ich für viele erheiternde, entspannte und sättigende Abende. Weiterhin danke ich Dr. Merlin Kleoff für aufbauende Gespräche und die Hilfe beim Schreiben der Manuskripte.

Meinen Studenten Paul Richter, David Wisniewski, Sebastian Schötz, Kamar Shakeri und Alexandros Mavroskoufis sowie meinen Auszubildenden Sebastian Petrow, Anja Wulf und Laura Hagemann danke ich für gute Zusammenarbeit und die überaus große Unterstützung bei meinen Forschungsprojekten. Ein großes Dankeschön auch an Luise Schefzig für die große Unterstützung im Labor.

Ich möchte mich auch von Herzen bei Kamar Shakeri und Alexandros Mavroskoufis für die schönen gemeinsamen Abende und für die große Hilfe in schwierigen Zeiten bedanken. Ein riesiger Dank gilt hier auch Alexandra Zimmermann, die immer da war, um mich in all der Zeit aufzubauen und mir geholfen hat viele schwierige Momente zu überwinden.

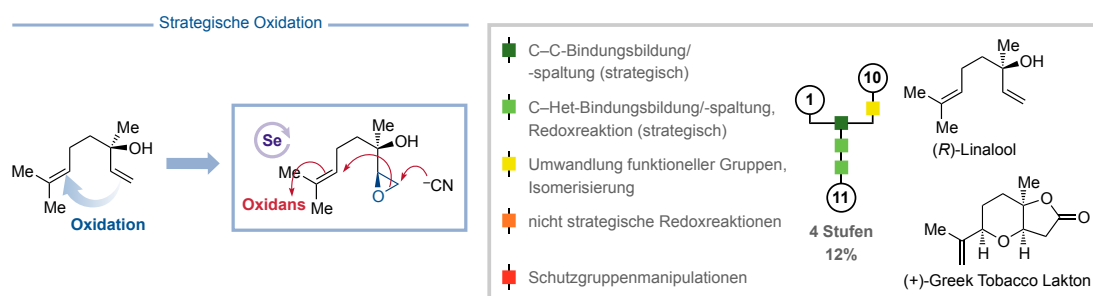
Abschließend gilt mein größter Dank meiner Familie, insbesondere meinen Eltern und Großeltern, für ihre immerwährende Unterstützung über all die Jahre, ohne die ich mein Studium und meine Promotion nicht in diesem Umfang und mit dieser Freiheit hätte durchführen können.



## Zusammenfassung

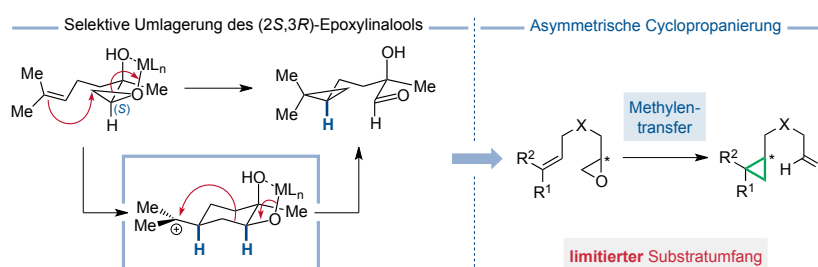
Im Rahmen dieser Arbeit wurden drei Projekte zur Synthese von insgesamt fünf Naturstoffen aus den Klassen der Terpene, Polyketide und Meroterpene bearbeitet.

Das erste Thema beschreibt eine vierstufige Totalsynthese des C<sub>11</sub>-Homoterpenoids (+)-Greek Tobacco Lacton, ein oxidatives Abbauprodukt, das aus den Blättern des griechischen Tabbaks isoliert wurde. Charakteristisch für diesen Naturstoff ist ein *cis*-fusioniertes Tetrahydropyran-Butyrolacton-Gerüst. Die Orientierung an verschiedenen Konzepten der Syntheseökonomie diente dabei der Entwicklung einer möglichst effizienten Synthese. Die Verwendung von (*R*)-Linalool, einem nachhaltigen und in großen Mengen verfügbaren C<sub>10</sub>-Startmaterial, ermöglichte dabei einen schnellen Aufbau des Kohlenstoffgerüsts einschließlich des ersten Stereozentrums. Schlüsselschritte der Synthese bilden die beiden strategischen Oxidationen der in (*R*)-Linalool vorhandenen Doppelbindungen. Die selektive Darstellung eines Isomers, von zwei möglichen epimeren Epoxiden, wurde durch eine Lewissäure-katalysierte Tandemsequenz, bestehend aus Epoxidierung und Epimerenspaltung, erreicht. Die anschließende Öffnung des Epoxids mit Cyanid lieferte zum einen ein Nitril als Carbonsäurevorläufer für das Lactonmotiv und zum anderen die sekundäre Hydroxylgruppe für die oxidative Cyclisierung zum Tetrahydropyranring. Letzteres wurde durch ein Selen-katalysiertes Redoxsystem mit NFSI oder molekularem Sauerstoff als terminales Oxidationsmittel realisiert. Interessanterweise stellte sich der Selen-basierte Katalysator gegenüber bewährten Palladiumkatalysatoren als überlegen heraus.



**Schema I.** Eine vierstufige Totalsynthese von (+)-Greek Tobacco Lacton ausgehend von (*R*)-Linalool wurde durch die strategische Oxidation der beiden Doppelbindungen erreicht. Das rechts abgebildete Flussdiagramm erlaubt eine qualitative Abschätzung der Effizienz der Synthese.

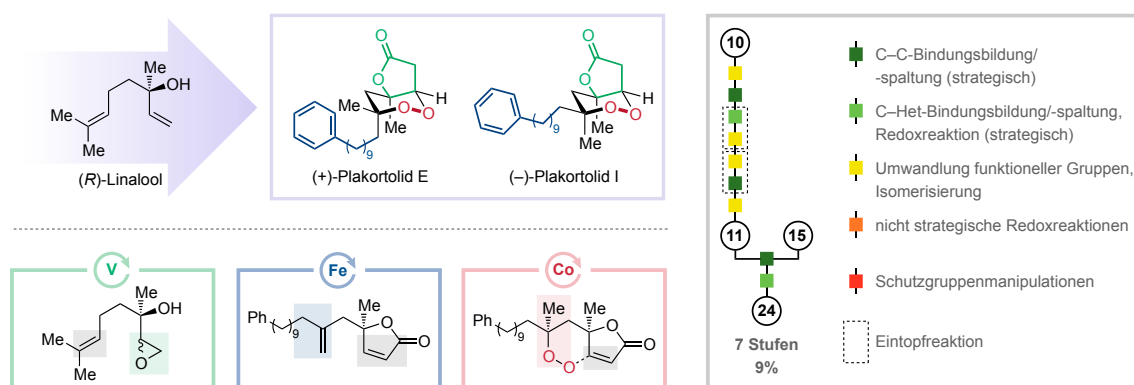
Im Zusammenhang der Synthese des (+)-Greek Tobacco Lactons wurde versucht eine Methode für die asymmetrische Cyclopropanierung von Alkenen über einen intramolekularen Methylentransfer zu entwickeln.



**Schema II.** Konzeptionelle Übertragung der angewandten Epimerenspaltung während der Synthese des (+)-Greek Tobacco Lactons auf eine generelle Methode zu asymmetrischen Cyclopropanierung von Alkenen.

Hierbei stellte sich allerdings heraus, dass der Substratumfang durch sehr spezifische Substitutionsmuster stark limitiert ist, weswegen das untersuchte System für eine allgemeine Anwendung ausgeschlossen wurde.

Das zweite Syntheseprojekt befasste sich mit der Synthese der beiden marinen Polyketide (+)-Plakortolid E und (-)-Plakortolid I. Beide Naturstoffe wurden aus Schwämmen der Familie *Plakinidae* isoliert und weisen ein Endoperoxidmotiv auf, welches bei vielen Sekundärmetaboliten häufig für wichtige biologische Aktivitäten verantwortlich ist. Die in dieser Arbeit beschriebene siebenstufige Synthese orientierte sich erneut an Konzepten zur Steigerung von Ökonomie und Effizienz. Dabei bildete der zuvor erschlossene Zugang zu substituierten  $\gamma$ -Butyrolactonen die Basis für die verfolgte Synthesestrategie. Im Anschluss an die Darstellung eines Butenolidintermediats ausgehend von (*R*)-Linalool lieferte die Modifikation des Prenylrests durch Redoxmanipulationen und die Einführung einer Methylengruppe ein allylisches Acetat. Dieses diente als Angriffspunkt für die beiden Schlüsselschritte, eine Eisen-katalysierte allylische Substitution zur Installation der Alkylkette sowie eine Cobalt-induzierte Endoperoxidbildung. Die Verwendung unedler und kostengünstiger Übergangsmetalle ermöglichte dabei chemoselektive Transformationen, wodurch die Verwendung von Schutzgruppen vermieden werden konnte. Weiterhin erlaubte die Entwicklung von Eintopfprotokollen, Reaktionsschritte zur Umwandlung von funktionellen Gruppen mit denen strategischer Bindungen zu verbinden und so die Kolbenökonomie der Synthese zu erhöhen.

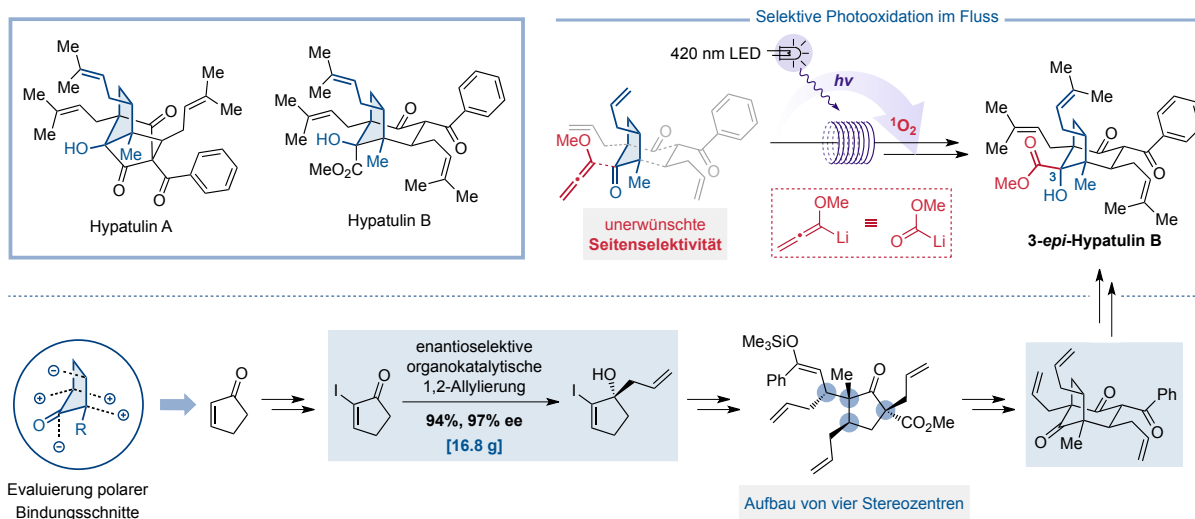


**Schema III.** Eine siebenstufige Totalsynthese von (+)-Plakortolid E und (-)-Plakortolid I unter Verwendung unedler Metalle. Das rechts abgebildete Flussdiagramm erlaubt eine qualitative Abschätzung der Effizienz der Synthese.

Der letzte Teil dieser Arbeit hatte die Synthese der beiden Meroterpenoide Hypatulins A und Hypatulins B zum Ziel. Vertreter dieser Substanzklasse, sogenannte polycyclische polyprenylierte Acylphloroglucinole (PPAP), weisen vielversprechende biologische Aktivitäten auf und wurden teilweise als Wirkstoffe in traditionellen Pflanzenheilmitteln identifiziert. Beide Naturstoffe wurden 2016 aus den Blättern des Großblumigen Johanniskrautes (*Hypericum patulum*) isoliert und durch die Verwendung von zweidimensionalen NMR-Experimenten und ECD-Spektroskopie charakterisiert. Sie besitzen dicht substituierte bi- beziehungsweise tricyclische Strukturen mit jeweils drei quarternären Stereozentren an einem Cyclopentanring. Der synthetische Ansatz, der in dieser Arbeit verfolgt wurde, orientierte sich an diesem zentralen fünfgliedrigen Ring, welcher durch retrosynthetische Analyse auf 2-Cyclopentenon als Startmaterial zurückgeführt wurde. Die Installation der Substituenten sowie der Aufbau von vier Stereozentren konnte mittels Carbonylchemie realisiert werden. Dabei wurde ein Enantiomerenüberschuss von 97% durch eine organokatalytische 1,2-Allylierung der Ketofunktionalität erzielt. Für den anschließenden Aufbau des bicyclischen Gerüsts war zunächst eine Dieckmann-Kondensation geplant. Aufgrund von Zersetzungsreaktionen musste jedoch auf eine Mukaiyama-Aldolreaktion ausgewichen werden. Der Aufbau des letzten Stereozentrums erwies sich ebenfalls als schwierig und lieferte ausschließlich das unerwünschte C-3-Epimer, so dass die Synthese der beiden



Naturstoffe nicht realisiert werden konnte. Die Darstellung des Naturstoffepimers 3-*epi*-Hypatulin B gelang stattdessen durch eine Methoxycarbonylierung unter Verwendung von lithiiertem Methoxyallen und der oxidativen Spaltung der Allengruppe mittels Singuletsauerstoff. Die Durchführung der Photooxidation in einem Flussprozess ermöglichte hierbei eine bessere Skalierbarkeit und höhere Reaktionsgeschwindigkeit als im Kolben. Nach anschließender Kreuzmetathese mit 2-Methylpropen wurde 3-*epi*-Hypatulin B in insgesamt 16 Stufen erhalten.

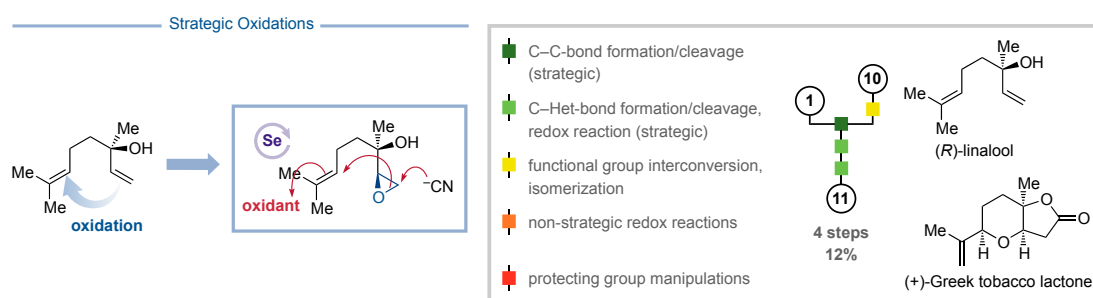


**Schema IV.** Synthese von 3-*epi*-Hypatulin B in 16 Stufen ausgehend von 2-Cyclopentenon. Schlüsselschritte sind eine hoehenantioselektive 1,2-Allylierung sowie eine im Fluss durchgeführte Photooxidation eines Methoxyallens.

## Abstract

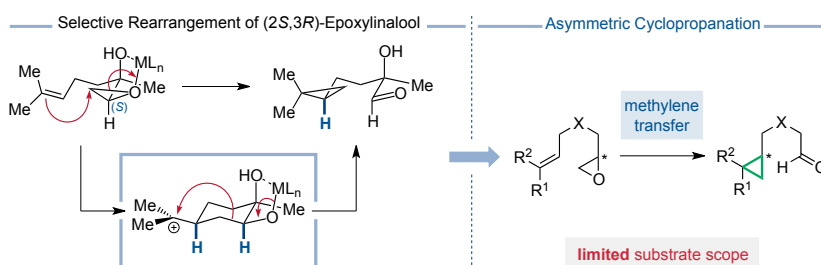
This thesis aimed at the total synthesis of five natural products belonging to the classes of terpenoids, polyketides and meroterpenoids.

The first project describes a short total synthesis of the  $C_{11}$ -homoterpenoid (+)-Greek tobacco lactone, an oxidative degradation product that was isolated from the sun-cured leaves of Greek tobacco. The natural product is characterised by a *cis*-fused tetrahydropyran-butyrolactone scaffold. In order to develop an efficient synthetic route, various concepts of synthesis economy were used as guidelines. The identification of (*R*)-linalool, an abundant and renewable chiral pool  $C_{10}$ -feedstock, as the starting material enabled the rapid construction of the carbon scaffold including the first stereocenter. Key steps of the synthesis are two strategic oxidations of the double bonds present in (*R*)-linalool thereby promoting formation of both cyclic motifs. The first oxidation process comprises the selective preparation of one of two possible epimeric epoxides via a tandem sequence of Lewis-acid catalysed epoxidation and resolution. Subsequent opening of the epoxide with cyanide afforded a nitrile functionality for the formation of the lactone as well as a secondary hydroxyl group for the construction of the tetrahydropyran core. The latter was achieved via a catalytic selenium-based redox system with either NFSI or molecular oxygen as the terminal oxidant. Interestingly, in this case, selenium proved to be a superior alternative to established palladium catalysts.



**Scheme I.** A total synthesis of (+)-Greek tobacco lactone in four steps was enabled by the strategic oxidation of both double bonds of (*R*)-linalool. The flow chart on the right gives a qualitative analysis of the efficiency of the synthesis.

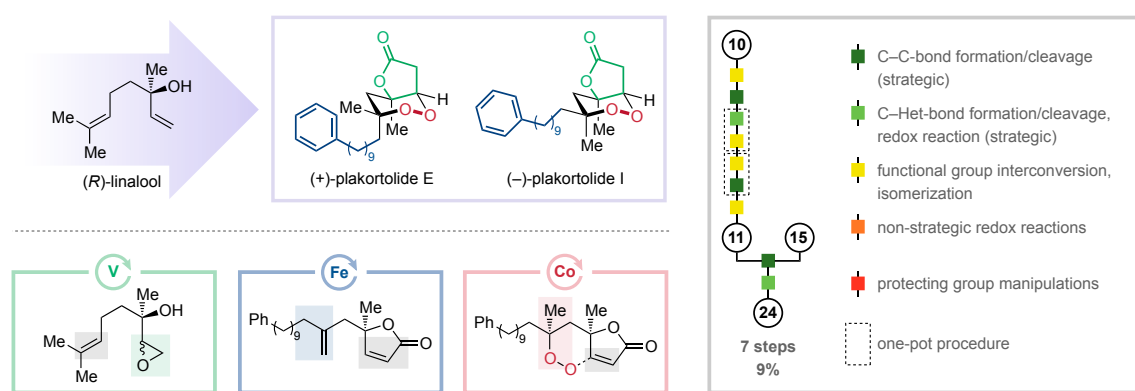
Regarding the Lewis-acid catalysed resolution of the epimeric epoxides via an intramolecular methylene transfer, the potential of this transformation for an asymmetric cyclopropanation of unactivated alkenes was investigated.



**Scheme II.** The attempted development of a method for the asymmetric cyclopropanation of alkenes, based on the employed resolution of the epimeric epoxides during the synthesis of (+)-Greek tobacco lactone.

Unfortunately, the reaction proved to require rather specific substitution patterns which severely limited the substrate scope. Thus, the investigated system was deemed unfeasible as a general method.

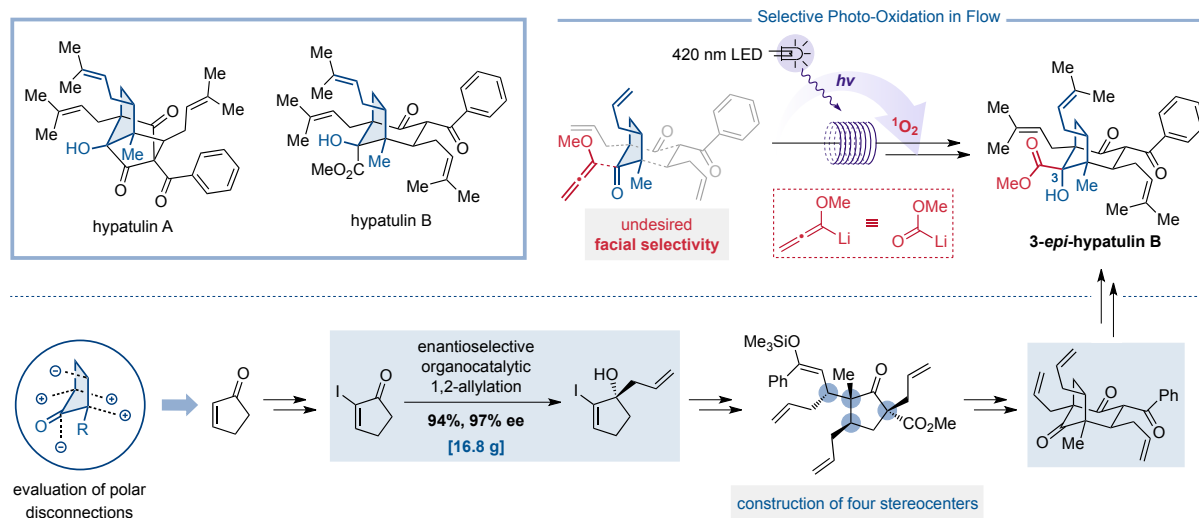
The second synthesis project focused on the total synthesis of the two marine polyketides (+)-plakortolide E and (-)-plakortolide I. Both natural products were isolated from sponges of the family *Plakinidae* and possess an endoperoxide, a motif that is often responsible for potent biological activities of secondary metabolites. With considerations for maximising aspects of synthesis economy in mind, a synthetic approach based on the previously developed route for the construction of substituted  $\gamma$ -butyrolactones from (*R*)-linalool was designed. Preparation of a butenolide intermediate via elimination of the secondary hydroxyl group was followed by modifications of the prenyl side chain to afford an allylic acetate that served as a platform for the two key steps of the synthesis. These steps constitute an iron-catalysed allylic substitution to install the alkyl chain and a cobalt-induced endoperoxide formation. By using earth-abundant transition metals to enable chemoselective transformations and developing one-pot operations to couple functional group interconversions with constructive bond formations the step and pot economy of the synthesis could be enhanced. Thus, a protecting group free synthesis of both natural products was achieved in seven steps.



**Scheme III.** A total synthesis of (+)-plakortolide E and (-)-plakortolide I in seven steps via chemoselective transformations enabled by base metals. The flow chart on the right gives a qualitative analysis of the efficiency of the synthesis.

The last part of this thesis deals with studies on the synthesis of the two novel meroterpenoids hypatulin A and hypatulin B. Members of this class of natural products, referred to as polycyclic polyprenylated acylphloroglucinols (PPAPs), have been identified as the active ingredients in some traditional plant-based remedies. Both natural products were isolated from the leaves of *Hypericum patulum* (goldencup St. John's wort) in 2016 and characterised by two-dimensional NMR experiments and ECD spectroscopy. The highly oxygenated bicyclic and tricyclic core of hypatulin A and hypatulin B, respectively, have a densely substituted cyclopentane core bearing three quarternary stereocenters. The synthetic approach described in this thesis focused on the five membered ring which was retrosynthetically traced back to 2-cyclopentenone as a suitable starting material. Installation of the substitutions and the generation of four stereocenters was realised by exploiting carbonyl chemistry. The first stereocenter was set via an enantioselective organocatalytic 1,2-allylation of the ketone achieving 97% enantiomeric excess. Formation of the bicyclic carbon scaffold was accomplished via a Mukaiyama aldol reaction as an initially envisaged Dieckmann condensation was unsuccessful due to degradation of the substrate. Since the construction of the last stereocenter proceeded exclusively with the undesired facial selectivity and delivered the epimeric product at C-3, the synthesis of both natural products could not be realised. Instead, the focus was redirected towards 3-*epi*-hypatulin B which was accessible via methoxycarbonylation through the addition of lithiated methoxyallene and an oxidative cleavage thereof with singlet oxygen. Translation of the photo-oxidation into a flow process resulted in an improved

scalability and a faster reaction compared to a batch process. Cross metathesis with 2-methylpropene eventually afforded 3-*epi*-hypatulin B over 16 steps in total.



**Scheme IV.** A synthesis of 3-*epi*-hypatulin B in 16 steps starting from 2-cyclopentenone. Key steps are a highly enantioselective 1,2-allylation and a photo-oxidation of an methoxyallene intermediate in flow.

## Abbreviations

---

Å	Angström
AAT	acetoacetyl-CoA thiolase
acac	acetylacetonate
ATP	adenosine triphosphate
ATR	attenuated total reflection
BAIB	bis(acetoxy)iodobenzene
BINOL	[1,1'-binaphthalene]-2,2'-diol
BPPS	(+)-bornyl pyrophosphate synthase
bpy	2,2'-bipyridine
br	broad
calcd	calculated
CMP	cytidine monophosphate
CMK	4-diphosphocytidyl-2-C-methyl-D-erythritol kinase
CMS	2-C-methyl-D-erythritol 4-phosphate cytidyltransferase
CoA	coenzyme A
COSY	correlation spectroscopy
Cy	cyclohexyl
$\delta$	chemical shift
d	day
DBU	1,8-diazabicyclo[5.4.0]undecane
1,2-DCE	1,2-dichloroethane
DDQ	2,3-dichloro-5,6-dicyano-1,4-benzoquinone
DFT	density-functional theory
(DHQD) <sub>2</sub> Pyr	hydroquinidine (2,5-diphenyl-4,6-pyrimidinediyl) diether
DIBAL-H	diisobutylaluminium hydride
DIPEA	<i>N,N</i> -diisopropylethylamine
DMAP	4-(dimethylamino)pyridine
DMDO	dimethyldioxirane
DMF	dimethylformamide
DMP	Dess-Martin periodinane
DMPU	<i>N,N'</i> -dimethylpropyleneurea
DMS	dimethyl sulfide
DMSO	dimethyl sulfoxide
dppe	1,3-bis(diphenylphosphino)ethane

dppp	1,3-bis(diphenylphosphino)propane
ECD	electronic circular dichroism
ee	enantiomeric excess
EGME	2-methoxyethanol
Enz	enzyme
equiv	equivalents
ESI	electrospray ionisation
EWG	electron withdrawing group
FID	flame ionisation detector
g	gram
GC	gas chromatography
GOESY	gradient-enhanced nuclear Overhauser effect spectroscopy
h	hour
1,5-HAT	1,5-hydrogen-atom transfer
HDS	HMB-PP synthase
HDR	HMB-PP reductase
HMB	( <i>E</i> )-4-hydrox-3-methyl-but-2-enyl
HMBC	heteronuclear multiple bond correlation
HMDS	hexamethyldisilazane
HMGCS	HMG-CoA synthase
HMGCR	HMG-CoA reductase
HMPA	hexamethylphosphoramide
HMQC	heteronuclear multiple quantum correlation
HPLC	high performance liquid chromatography
HRESIMS	high resolution electrospray ionisation mass spectrometry
HRMS	high resolution mass spectrometry
HSQC	heteronuclear single quantum correlation
Hz	Hertz
<i>i</i>	iso
IBX	2-iodoxybenzoic acid
IR	infrared spectroscopy
<i>J</i>	coupling constant
KHMDS	potassium hexamethyldisilazide
LED	light-emitting diode
LDA	lithium diisopropylamide
LiTMP	lithium 2,2,6,6-tetramethylpiperidine
m	multiplet

min	minute
MCS	2-C-methyl-D-erythritol 2,4-cyclodiphosphate synthase
MK	mevalonate kinase
MOM	methoxymethyl ether
m. p.	melting point
MPDC	mevalonate pyrophosphate decarboxylase
MS	mass spectrometry/ molecular sieves
Ms	methanesulfonyl
NADPH	nicotinamide adenine dinucleotide phosphate
NaHMDS	sodium hexamethyldisilazide
NCS	<i>N</i> -chlorosuccinimide
Nf	Nonafluorobutanesulfonyl
NFSI	<i>N</i> -fluorobenzenesulfonimide
NMR	nuclear magnetic resonance
NOE	nuclear Overhauser effect
NOESY	nuclear Overhauser effect spectroscopy
norAZADO	9-azanoradamantane <i>N</i> -oxyl
<i>o</i>	<i>ortho</i>
<i>p</i>	<i>para</i>
PKS	polyketide synthase
PMK	phosphomevalonate kinase
PP	pyrophosphate
PP <sub>i</sub>	pyrophosphate (inorganic)
ppm	parts per million
py	pyridine
q	quartet
rac	racemic
r.t.	room temperature
s	singlet
S <sub>N</sub> 2	nucleophilic substitution of 2 <sup>nd</sup> kinetic order
t	triplet
<i>t</i>	<i>tert</i>
TBAF	tetrabutylammonium fluoride
TBAT	tetrabutylammonium difluorotriphenylsilicate
TBD	1,5,7-triazabicyclo[4.4.0]dec-5-ene
TBHP	<i>tert</i> -butyl hydroperoxide
TBDPS	<i>tert</i> -butyldiphenylsilyl

---

TBS	<i>tert</i> -butyldimethylsilyl
TEMPO	(2,2,6,6-tetramethylpiperidin-1-yl)oxyl
<i>tet</i>	tetrahedral
Tf	trifluoromethanesulfonyl
TFE	2,2,2-trifluoroethanol
Th	thienyl
thd	2,2,6,6-tetramethyl-3,5-heptandione
THF	tetrahydrofuran
TLC	thin layer chromatography
TMEDA	<i>N,N,N',N'</i> -tetramethylethane-1,2-diamine
tol	tolyl
TPP	tetraphenylporphyrin
Ts	4-toluenesulfonyl

---



# 1 Introduction

## 1.1 Natural Products

### 1.1.1 Primary and Secondary Metabolites

Natural products are biogenic substances which are produced by organisms such as plants, animals, and microorganisms. Depending on their metabolic origin these organic compounds can be divided into two major classes. Primary metabolites constitute the basic building blocks of organisms essential for maintaining cellular homeostasis and life itself and include carbohydrates, lipids, amino acids, and nucleic acids.<sup>1</sup> These molecules exhibit intrinsic functions such as nutrient assimilation, energy storage and production, construction of cellular structures, enzymatic synthesis of all natural products, and encoding of genetic information (Figure 1).

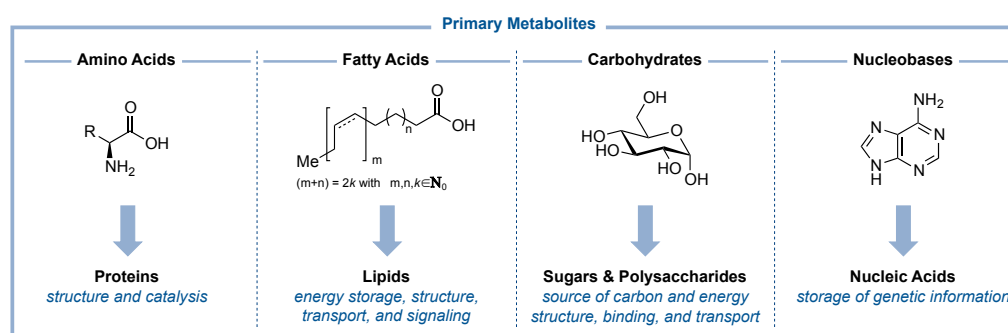


**Figure 1.** Primary metabolites and their biological functions.

Secondary metabolites, on the other hand, are not essential for the survival of an organism but are generally used to regulate ecological relationships providing specific evolutionary advantages that include defense against predators and competing organisms, attraction of sexual partners or pollinators, as well as interspecies communication for various other purposes.<sup>2,3,4</sup> In response to biotic and abiotic influences the evolution and expression of secondary metabolites is extremely adaptive and has led to a vast catalogue of compounds that can be divided into several structural classes such as terpenes and terpenoids, polyketides, and alkaloids.

### 1.1.2 Terpenoids

Terpenes and their oxidised derivatives, referred to as terpenoids<sup>†</sup>, constitute the largest and most structurally diverse class of natural products. The known terpenome with currently more than 80000 members, including steroids and carotenoids, accounts for nearly one third of all characterised natural compounds to date.<sup>5</sup> Due to their structural complexity, terpenoids possess a wide range of features, which give rise to a great number of applications. In particular, plants and their extracts, containing a plethora of these natural products, have provided the basis for traditional medicine systems and served as fragrances, flavors and pigments over the course of human history, culminating in a multi-billion dollar world market nowadays.<sup>6</sup> The importance of these natural products has propelled numerous studies and considerable research efforts in order to gain a deeper understanding of their biosynthesis, biological activities and roles in nature.<sup>7</sup>

<sup>†</sup> For the purpose of clarity, in this thesis the term 'terpenoid(s)' will be used to include terpenes.

Based on the pioneering works of WALLACH<sup>8</sup> and RUZICKA<sup>9</sup> terpenes and terpenoids are classified according to their carbon skeleton as multiples of the hydrocarbon unit isoprene (Figure 2). Further investigations, however, revealed that isoprene itself is not an intermediate in the biosynthetic pathways of terpenoids. Instead, its oxidised form isopentenyl pyrophosphate (**IPP**) and the isomeric dimethylallyl pyrophosphate (**DMAPP**) constitute the actual key building blocks.<sup>10,11</sup>

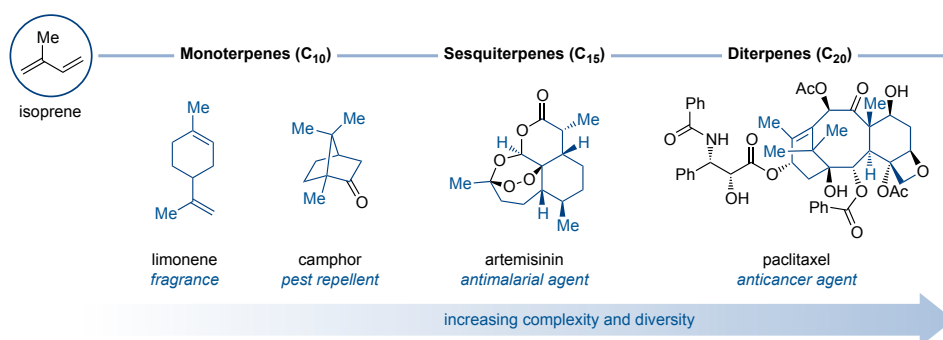
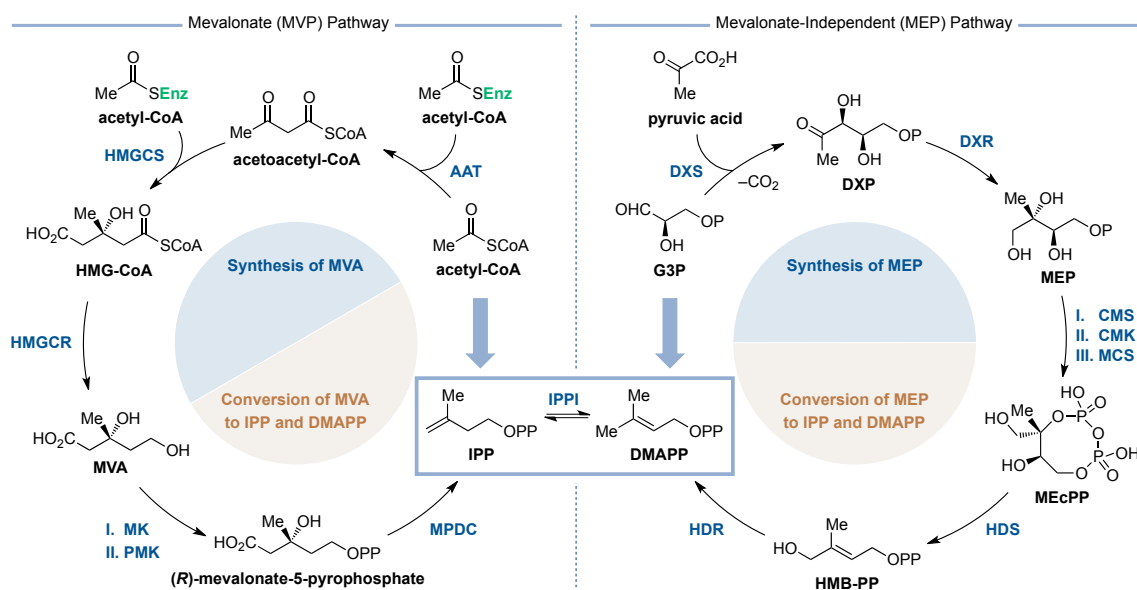


**Figure 2.** Examples of different types of terpenoids.

## 1.2 Biosynthesis of Terpenoids

### 1.2.1 Biosynthesis of IPP and DMAPP

Two distinct biogenetic pathways for the synthesis of these activated isoprene derivatives have been reported (Scheme 1).<sup>12</sup> Whereas all eukaryotes, archaea and some bacteria synthesise these universal terpenoid precursors via (*R*)-mevalonic acid (**MVA**),<sup>13,14</sup> an alternative pathway based on 2-*C*-methyl-D-erythritol 4-phosphate (**MEP**) is used by algae, eubacteria, cyanobacteria, and protozoa.<sup>15</sup> Interestingly, plants synthesise **IPP** via both metabolic pathways and their biosynthesis of terpenoids is usually compartmentalised. While sesqui- and triterpenoids are formed in the cytosol via the **MVA** pathway, mono- and diterpenoids as well as tetraterpenoids, which comprise essential pigments such as carotenoids, arise in the plastid organelles, where the **MEP** pathway is localised.<sup>15,16</sup> This compartmentalisation is in line with the hypothesised origin of chloroplasts resulting from the endosymbiosis between archaeal progenitors and blue-green algae.<sup>17</sup>



**Scheme 1.** Biosynthesis of **IPP** and **DMAPP** via the MVP and the MEP pathway.



process **DMAPP** is ionised to the corresponding allylic cation and coupled to the terminal double bond of the more nucleophilic **IPP** in a head-to-tail fashion accompanied by stereospecific deprotonation (Scheme 2). The product is geranyl pyrophosphate (**GPP**), a linear prenyl pyrophosphate, which, in turn, can be ionised and coupled to further **IPP** units. Consecutive head-to-tail condensations provide a range of acyclic intermediates with fixed lengths and stereochemistry, that serve as branch points in the next phase of the synthesis.<sup>5,18</sup>

Besides these regular prenyltransferases there are enzymes that catalyse irregular coupling reactions. Such head-to-head couplings generate further roots for considerably different carbon skeletons and include cyclopropanation, cyclobutanation and 1'-2 branching.<sup>19</sup> A prominent example is the biosynthesis of squalene, an important precursor for cholesterol, which in turn is an integral part of animal cell membranes and several biochemical pathways. The formation in two steps is catalysed by squalene synthase (**SQS**) and begins with the condensation of two molecules of **FPP** to form the cyclopropylcarbinyl intermediate presqualene pyrophosphate (**PSPP**).<sup>20</sup> Subsequent conversion to squalene involves a series of carbocation rearrangements that is initiated by the ionisation of the pyrophosphate and followed by a cyclopropylcarbinyl-cyclopropylcarbinyl rearrangement, presumably via a transient cyclobutyl cation.<sup>21</sup> Ring opening gives an allylic cation which is then trapped by an NADPH-dependent reduction process (Scheme 2).

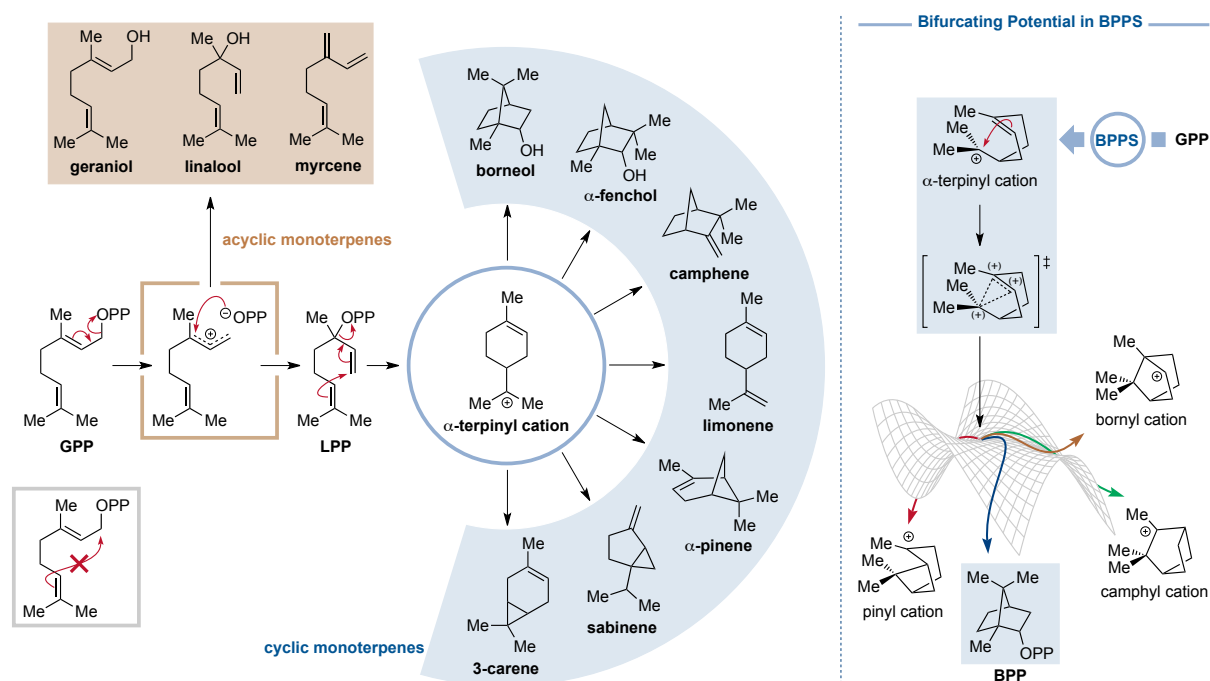
### 1.2.3 Type I Terpenoid Cyclases

These precursors, which determine the size of the final carbon skeleton, are converted through the action of terpenoid synthase enzymes, often called cyclases, to yield the parent scaffolds of various types of terpenoids.<sup>5,18</sup> This phase, which consists of rearrangement and/or cyclisation reactions, is mostly responsible for the vast structural diversity in terpenoid natural products. The underlying principle of these reactions is a cascade of multiple carbocation intermediates whereby the positive charge is transferred along the molecule by the intramolecular attack of double bonds to yield fused ring systems as well as ensuing WAGNER-MEERWEIN rearrangements such as hydride shifts, methyl migrations or ring expansions. The cascade is eventually terminated by deprotonation in the sense of a 1,2-elimination to yield an alkene, a 1,3-elimination to give the corresponding cyclopropane or trapping of the final carbocation by an exogenous nucleophile, often a molecule of water.<sup>5,18</sup> The intermediate positive charge can be stabilised in the active site of the cyclase by weak polar interactions with other charges, dipoles or quadrupoles. Especially cation- $\pi$  interactions with aromatic side chains of phenylalanine, tyrosine and tryptophane offer an efficient way for charge stabilisation without the risk of side reactions.<sup>5</sup> The precise spatial orientation and the controlled stabilisation of certain carbocation intermediates allow the enzyme to direct the reaction along a specific pathway. These types of cyclisation cascades are one of the most complex reactions found in nature, resulting in changes in bonding, hybridisation and stereochemistry of, on average, more than half of the substrate's carbon atoms.<sup>5</sup>

Terpenoid synthases, with some exceptions, generally fall into two main classes based on their initial substrate ionisation mechanism.<sup>5,18</sup> Class I terpenoid synthases trigger ionisation of prenyl pyrophosphates by metal ion-mediated coordination of the inorganic pyrophosphate anion to yield an allylic cation, whereas class II terpenoid synthases initiate the ionisation by protonation of the terminal double bond or the corresponding epoxide to yield a tertiary cation.<sup>5,18</sup> Depending on the size of the acyclic precursor these synthases produce different mono-, sesqui-, di- and sesterterpenoids.

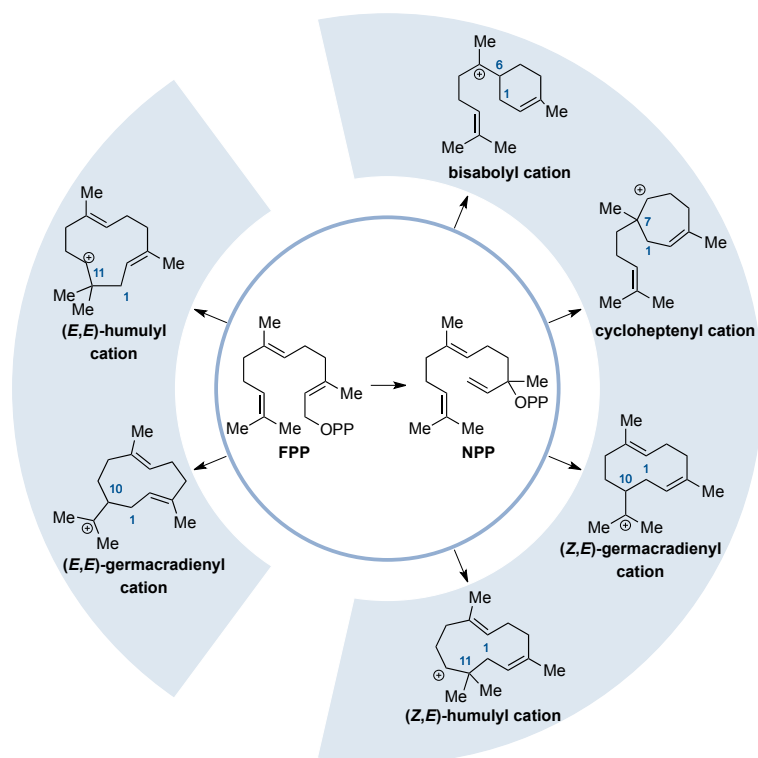
Monoterpenoid synthases generate acyclic, mono-, bi-, and in rare cases tricyclic products from the 10-carbon precursor **GPP**.<sup>22</sup> The corresponding cyclisation cascades proceed typically through the  $\alpha$ -terpinyl cation as the universal monocyclic intermediate (Scheme 3). However, formation of the 6-membered ring cannot occur from the *E*-configured double bond. The topological requirement for a 6-*endo-trig* cyclisation entails the necessity of an isomerisation step, which is achieved by ionisation of **GPP** to the *E*-allylic cation intermediate and subsequent readdition of the inorganic pyrophosphate anion at the tertiary position to yield linalyl

pyrophosphate (**LPP**). The resulting terminal double bond can adopt the required cisoid conformation that gives rise to the *Z*-allylic cation intermediate, thereby enabling C1–C6 bond formation.<sup>5</sup> These ionisation steps upstream to the  $\alpha$ -terpinyl cation allow the formation of acyclic monoterpenoids such as geraniol, linalool and myrcene by quenching of the allylic cation. Termination of the reaction cascade via deprotonation or addition of water can be preceded by numerous combinations of rearrangements and further cyclisations, resulting in a structurally and stereochemically diverse array of carbon skeletons.<sup>5</sup> However, while some terpenoid synthases are very specific and generate only one product, others produce several products from a single prenyl pyrophosphate precursor, thereby increasing the terpenoid structural diversity. Interestingly, (+)-bornyl pyrophosphate (**BPP**) synthase was shown to produce the product in only about 75% accompanied by minor quantities of other cyclic monoterpenoids.<sup>23</sup> Computational studies suggest that the 2-bornyl cation, arising from the initial formation of a pinyl cation, is a transition state, rather than an intermediate, and represents a bifurcation point leading to either **BPP** or camphene as a side product (Scheme 3).<sup>24</sup>



**Scheme 3.** Biosynthesis of various monoterpenes and monoterpenoids via type I cyclases.

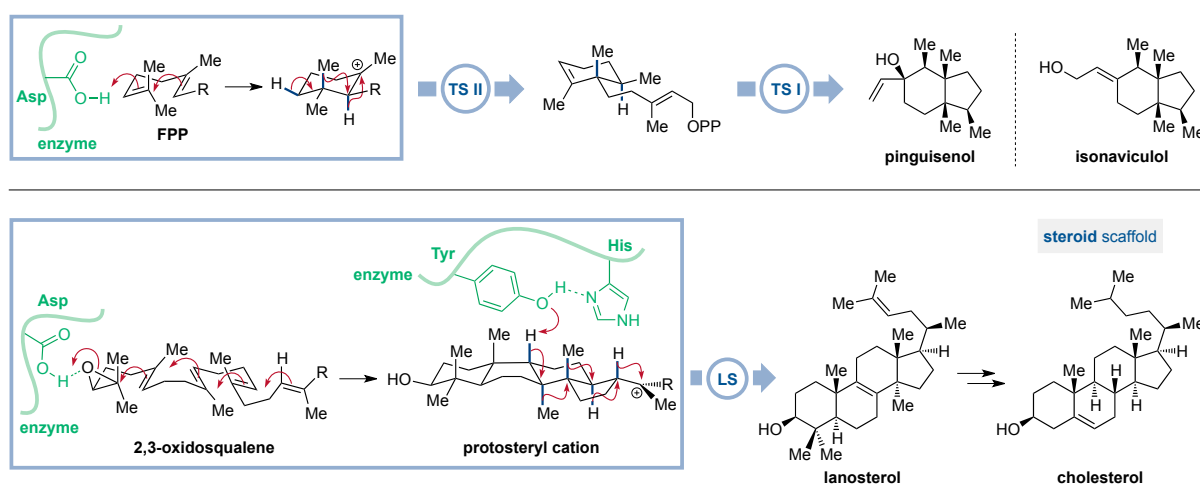
For higher order terpenoid synthases, the growing number of double bonds and gain in flexibility of the larger acyclic prenyl pyrophosphates result in additional carbon–carbon bond-forming trajectories and consequently in an increasingly diverse array of carbon skeletons.<sup>25,26</sup> In case of sesquiterpene synthases, the direct cyclisation of farnesyl pyrophosphate (**FPP**) may occur from the terminal double bond to give either the the (*E,E*)-humulyl cation or the (*E,E*)-germacradienyl cation (Scheme 4).<sup>5,26</sup> However, cyclisations from the central double bond require isomerisation to a *Z*-configured allylic cation analogous to the cyclisation of **LPP**. The corresponding cisoid nerolidyl pyrophosphate (**NPP**) eventually allows the formation of the bisabolyl cation and the cycloheptenyl cation as well as the (*Z,E*)-humulyl cation and the (*Z,E*)-germacradienyl cation (Scheme 4).<sup>5,26</sup> While monoterpenoid synthases are already able to generate a wide range of different carbon scaffolds from just one monocyclic carbocation intermediate, sesquiterpenoid synthases can draw from a larger pool of six diverse intermediates. Considering the numerous possible pathways of further cyclisation steps in combination with skeletal rearrangements, the tremendous impact of an additional unit of **IPP** in the acyclic precursor becomes apparent.



**Scheme 4.** Carbenium ions as precursors for sesquiterpenoid carbon scaffolds resulting from the cyclisation of **FPP** and **NPP** via sesquiterpenoid synthases.

### 1.2.4 Type II Terpenoid Cyclases

The additional double bond of **FPP** enables protonation induced cyclisations by type II cyclases starting from the opposing end of the linear precursor (Scheme 5). The protonation occurs most likely concerted with bond formation by general acid catalysis to yield a monocyclic tertiary carbocation. Depending on the size of the prenyl chain, meaning the number of available double bonds, these enzymes can produce up to five fused rings.<sup>5</sup>



**Scheme 5.** Examples of cyclisations via type II cyclases.

As with type I cyclases rearrangements, typically a sequence of concerted anti-periplanar hydride and methyl shifts, can accompany the cyclisation cascade to relocate the initial carbocation before termination. After completion of the type II catalysis, subsequent cyclisations can be triggered by ionisation of the remaining

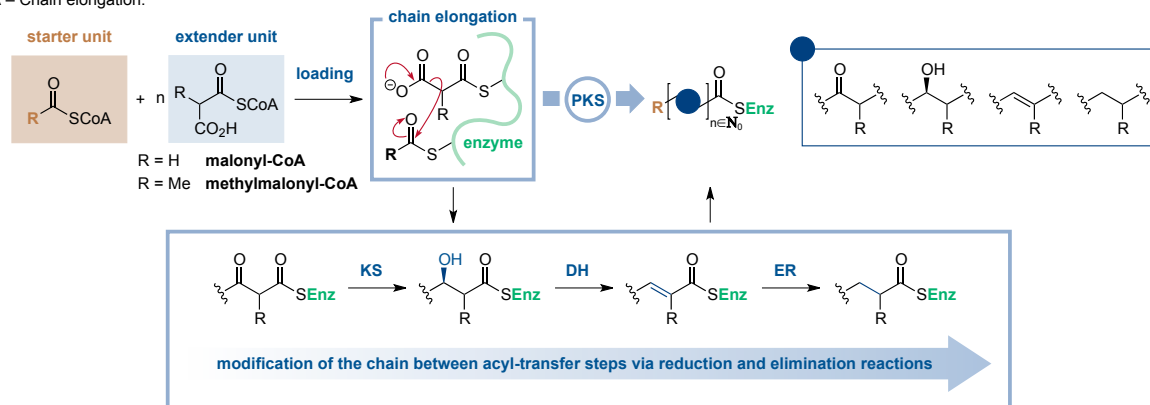
allylic pyrophosphate. These additional modes of cyclisation, class II and the combination of class I and II, further expand the scope of possible terpenoid products as is demonstrated by the biosynthesis of the pinguisane scaffold,<sup>12</sup> a *cis*-fused bicyclic framework that can be found in sesquiterpenoids such as pinguisenol and isonaviculol (Scheme 5, top).<sup>27,28</sup> While the same principles apply to diterpenoid and sesterterpenoid synthases, the cyclisation of squalene in prokaryotes or 2,3-oxidosqualene in eukaryotes by triterpene synthases proceeds exclusively via the protonation initiated mechanism due to the lack of an allylic pyrophosphate.<sup>5</sup> The resulting tetracyclic triterpenoids such as lanosterol serve as precursors for the class of steroids, an entire class of diverse carbon scaffolds on its own, via oxidative degradation pathways (Scheme 5, bottom).

### 1.3 Meroterpenoids

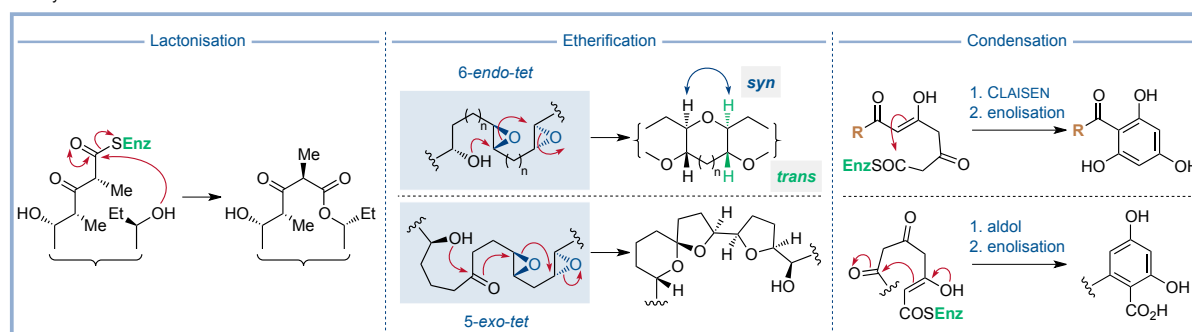
The beauty of the entire terpenoid biosynthesis apparatus lies in the fact that it gives rise to the vast and complex diversity of terpenoids from two simple building blocks.<sup>29</sup> However, nature goes even further and combines different biosynthetic machineries to create an almost infinite number of possible natural products. Meroterpenoids represent such a class of hybrid compounds that partially originate from the terpenoid pathway.<sup>30</sup> Although a plethora of biogenic substances produced by animals, plants, bacteria, and fungi match this definition, polyketide-terpenoid hybrids are by far the most numerous with 3,5-dimethylorsellinic acid (**DMOA**)<sup>31</sup> and acylphloroglucinol<sup>32</sup> derivatives representing the flagships of this subset of natural products.

The biosynthesis of these polyketide cores commences with the construction of a chain via iterative addition of extender units, usually malonyl-CoA or methylmalonyl-CoA, to an acyl-CoA starter unit (Scheme 6).<sup>33</sup>

A – Chain elongation.



B – Cyclisation modes.



**Scheme 6.** Proposed biosynthesis pathways of polyketides via chain elongation and different types of cyclisations.

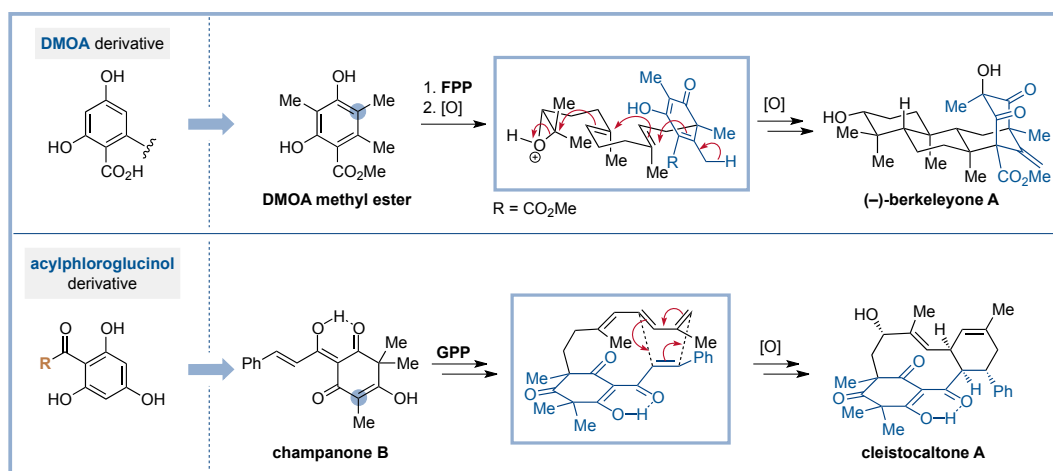
The chain extension step is catalysed by polyketide synthases (PKS) and proceeds via a CLAISEN-type condensation facilitated by the decarboxylation of the extender unit. After each addition, optional



transformations can alter the newly installed carbonyl fragment via the action of different catalytic domains. The sequential modification via reduction by ketoreductases (KR), dehydration by dehydratases (DH), and further reduction by enoyl reductases (ER) provides a variety of different degrees and combinations of functionalisation. Thus, each cycle may afford either a carbonyl group, a hydroxyl group, a double bond or a fully saturated ethylene group (Scheme 6).<sup>33</sup> The extension process is then repeated, adding two carbon units with each cycle to the acyl terminus, until the chain reaches a specific length. This biogenetic pathway is analogous to the construction of fatty acids. The crucial difference, however, is that polyketides may be left unprocessed, whereas fatty acid chains are defunctionalised. Unsaturated fatty acids are generated via isomerisation of the double bond at defined chain lengths. The *Z*-configured unsaturated carbonyl intermediate cannot be processed by the enoyl reductases and enters the next cycle of chain elongation.<sup>34</sup>

As with terpenoids, subsequent cyclisations create a pool of diverse polyketide natural products. The distinct functionalisation of the acyclic precursor serves as a template for different types of ring closing reactions that mould the final structure (Scheme 6). For instance, cyclic polyethers are proposed to be formed via the stereoselective epoxidation of polyene chains and a subsequent cascade of  $S_N2$  epoxide openings to form tetrahydrofurans and tetrahydropyrans. The resulting rings can be separated by at least one single bond or connected as either spiroketals or fused rings.<sup>33</sup> Interestingly, all marine polyether ladders, meaning molecules with extended fused-ring systems of cyclic ethers, exhibit a specific stereochemistry at their ring junctions resulting in a series of *trans*-fused rings typically arranged in a *syn*-fashion. Other cyclisation reactions include lactonisations, ketal formation, and aldol or CLAISEN condensations of polyketone chains to form aromatic rings (Scheme 6).<sup>33,35</sup> The latter two reactions account for the formation of **DMOA** and acylphloroglucinols.

Prenylation of the aromatic polyketide core, or derivatives thereof, via prenyltransferases initiates the second phase of the meroterpenoid biogenesis.<sup>5,30</sup> Subsequent modifications such as cyclisations and oxidations can give rise to various carbon scaffolds of polycyclic nature. For instance, (–)-berkeleyone A is synthesised via prenylation of **DMOA** methyl ester with **FPP**, followed by epoxidation to facilitate an acid catalysed cyclisation cascade akin to the cyclisation of 2,3-oxidosqualene.<sup>36</sup> The intermediate carbenium ion is ultimately trapped by the **DMOA** core and eliminated via deprotonation to give a tetracyclic product which is further oxidised (Scheme 7). Other cyclisation reactions may be initiated by allylic oxidation or involve nucleophilic attack of the electron-rich prenyl chains to protonated carbonyls or, as in the case of cleistocaltone A, intramolecular DIELS-ALDER reactions (Scheme 7).<sup>37</sup>



**Scheme 7.** Examples of meroterpenoid biosyntheses via prenylation of polyketide cores and subsequent transformations.



## 1.4 Natural Product Synthesis – Drug Development and Fundamental Research

The seemingly endless structural diversity of molecular architectures with their biological properties and functions provided by nature have fascinated and inspired mankind since ancient times, with the oldest records of herbal remedies dating as far back as Sumerian civilisation about 5000 years ago.<sup>38</sup> As many of these natural products have important biological and pharmaceutical applications, the development of chemical synthesis has had a tremendous impact on our modern civilisation elevating standards of living and increasing life expectancy.

With the realisation that specific molecular compounds are responsible for the pharmacological properties of plant extracts and the ensuing paradigm shift in the medicinal treatment of diseases, the isolation and synthetic production of these substances has garnered considerable scientific attention. Historical milestones are the discovery of the opiate morphine from *Papaver somniferum* poppies,<sup>39</sup> the first antibiotic penicillin from the fungus *Penicillium notatum*,<sup>40</sup> and the anticancer drug paclitaxel (Taxol®) from the Pacific yew tree *Taxus brevifolia*.<sup>41</sup> The supply of these and other compounds, listed as essential medicines by the World Health Organisation, is of great importance. Although some pharmaceutical substances such as morphine are still isolated from natural resources in large quantities,<sup>42</sup> the access to many other natural products is often limited by low yields and insufficient biomass. Therefore, the development of synthetic routes from readily available starting materials constitutes an indispensable alternative to natural sources. However, sometimes total syntheses of complex natural products prove to be rather tedious and inefficient resulting in low yields. In these cases the identification and isolation of other biochemically produced compounds, that may serve as advanced intermediates and can be converted to the target molecule via few transformations, may offer a solution. A prominent example is the semisynthesis of paclitaxel, starting from the more readily available 10-deacetylbaccatin III, as a total synthesis has not been feasible on an industrial scale and isolation from its natural source provides insufficient amounts to meet the global demand.<sup>41</sup>

With increasing insight into biochemical processes, modes of action, and molecular targets the focus shifted towards the design and synthesis of totally synthetic drugs.<sup>43</sup> However, despite recent advances in chemical techniques that allow for high-throughput screening to generate large compound libraries via combinatorial chemistry only about 33% of small-molecule drugs are exclusively of synthetic origin (Figure 3). The majority of approved drugs, on the other hand, consists of molecules that possess natural pharmacores or mimic natural product compounds.<sup>44</sup> To date, only three new chemical entities originating from combinatorial chemistry, the anti-cancer agents sorafenib (Nexavar®) and vemurafenib and the genetic disorder-inhibitor ataluren (Translarna®), have been approved (Figure 3).<sup>44</sup>

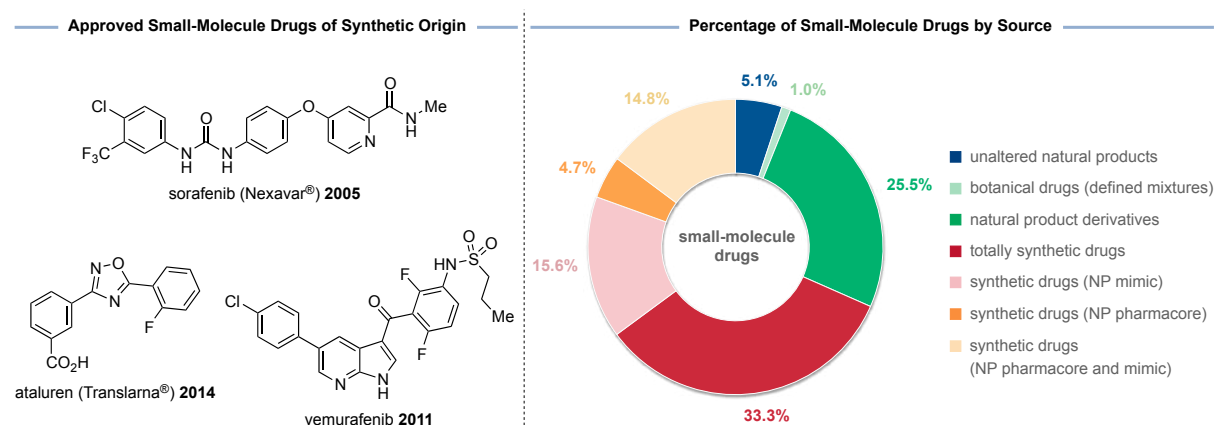


**Figure 3.** Small-molecule drugs that have been approved. Left: Approved drugs originating from combinatorial chemistry. Right: Percentage of drugs approved by the FDA from 1981–2019 categorised by origin (NP = natural product).<sup>44</sup>

In contrast to the diverse structural architectures of natural products, early combinatorial libraries predominantly focused on aromatic compounds neglecting intricate three-dimensional interactions with the molecular target.<sup>45</sup> In order to expand the bioactive chemical space covered by these libraries, the focus shifted to structural diversity, concerning functional groups, stereochemistry and molecular scaffolds.<sup>46</sup> In addition, the entirety of natural diversity has barely been explored and it is estimated that less than 10% has been investigated for biological activity and pharmacological potential.<sup>47</sup> Therefore, natural products still represent a major source for novel drug leads and the isolation and total synthesis thereof remains an indispensable discipline. Furthermore, total synthesis enables the analysis and evaluation of structure-activity relationships via selective derivatisation of lead structures.<sup>43</sup> This can lead to the identification of natural product analogues with enhanced pharmacological profiles or simplified structures as showcased by the development of the completely synthetic anti-cancer agent eribulin (Halaven®) which was derived from the marine natural product halichondrin B (Figure 4).<sup>48</sup>

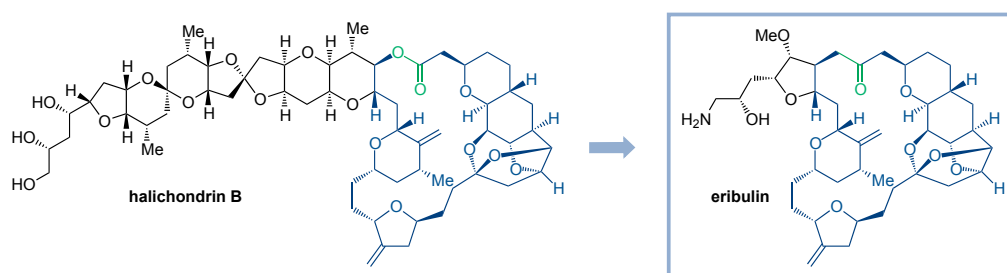


**Figure 4.** Structures of halichondrin B and eribulin.

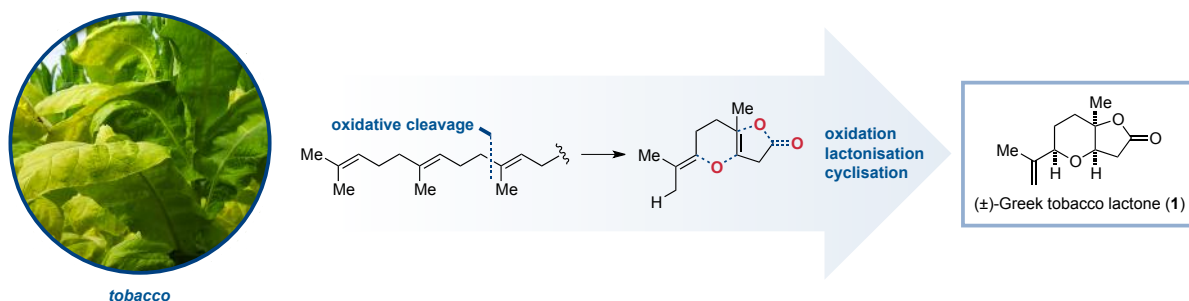
Besides the supply of pharmacologically active material, synthetic endeavours have inspired novel concepts and principles such as retrosynthetic<sup>49,50</sup> and conformational<sup>51</sup> analysis or considerations regarding atom,<sup>52</sup> redox,<sup>53</sup> step,<sup>54</sup> and pot<sup>55</sup> economy to provide guidelines for increasing the efficiency of a synthesis.<sup>56</sup> Many projects have led to the discovery of unknown reactivities, the development of new efficient methodologies to access complex structural motifs, as well as mechanistic studies providing a deeper understanding of chemical transformations and selectivities. Thus, the fields of organic and synthetic chemistry exceed purely industrial and pharmaceutical interests, providing fundamental research to expand knowledge and serve as a source for inspiration and innovation.

## 2 (+)-Greek Tobacco Lactone

### 2.1 Introduction

#### 2.1.1 Isolation of (+)-Greek Tobacco Lactone

In 1993, WAHLBERG and co-workers reported the isolation of the bicyclic Greek tobacco lactone (**1**) as one of thirteen butyrolactones found in sun-cured leaves of Greek tobacco.<sup>57</sup> Lactone **1** occurs in racemic form and possesses a *cis*-fused tetrahydropyran-butyrolactone scaffold. The authors proposed a biosynthetic pathway via degradative oxidation of acyclic isoprenoid precursors. The resulting C<sub>11</sub>-intermediate is oxygenated and undergoes lactonisation with subsequent cyclisation to form the *cis*-fused bicyclic system (Scheme 8). The isolation of Greek tobacco lactone (**1**) as a racemic mixture implies the lack of enantioselective oxidation processes.



**Scheme 8.** Proposed biosynthetic pathway and structure of (±)-Greek tobacco lactone (**1**).

The original structural assignment, which was derived from a combination of spectroscopic data, including IR, NOE and HMBC experiments, and mass spectrometric fragmentation studies, was later confirmed by three total syntheses.<sup>58,59,60</sup>

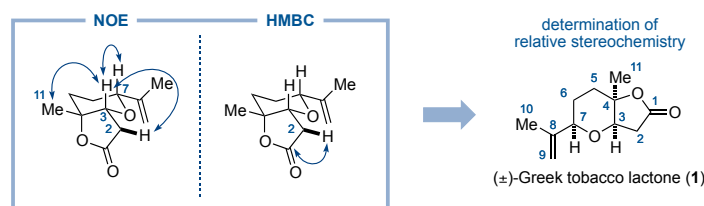
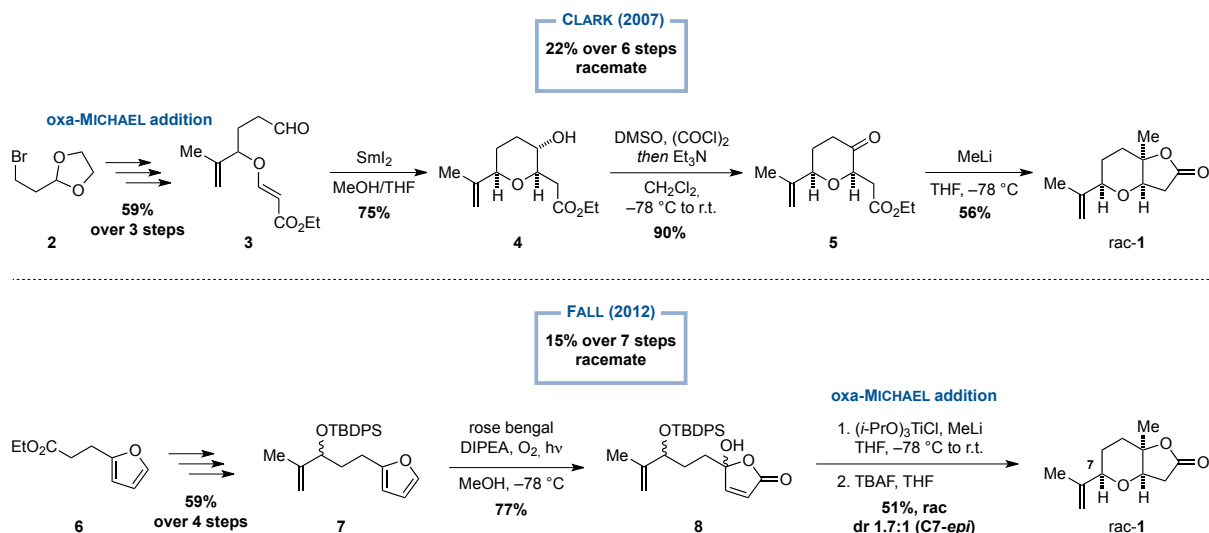


**Figure 5.** Determination of the relative stereochemistry highlighted by selected NOE and HMBC correlations.<sup>58</sup>

#### 2.1.2 Total Syntheses of (+)-Greek Tobacco Lactone

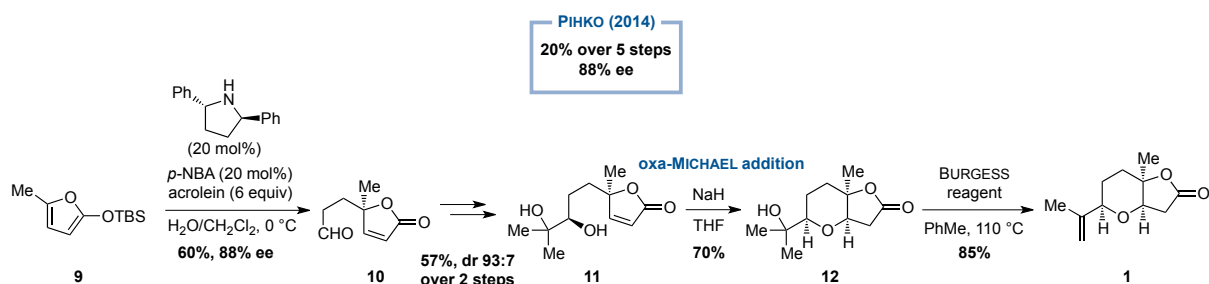
The first total synthesis of racemic Greek tobacco lactone (**1**) was published by CLARK and co-workers in 2007 (Scheme 2).<sup>58</sup> The authors pursued the strategy to construct natural products containing highly functionalised tetrahydropyran cores by employing reductive coupling reactions. The required cyclisation precursor **3** was obtained by the addition of the corresponding GRIGNARD reagent of bromide **2** to methacrolein, subsequent oxa-MICHAEL addition to ethyl propiolate, and deprotection. The reductive cyclisation of **3** was then accomplished using samarium(II) iodide. Oxidation of the secondary alcohol and subsequent treatment of the resulting ketone **5** with methyl lithium initiated lactone formation to give **1** as a racemate in a total yield of 22% over six steps (Scheme 9).

Five years later BESADA, FALL and co-workers published a second total synthesis by exploiting their methodology coined furan approach to oxacyclic systems, which is based on the oxidation of furans with singlet oxygen to generate functionalised butenolide scaffolds.<sup>59</sup> Their synthesis commenced with furan **6** by modifying the side chain to prepare an allylic alcohol for a late-stage oxa-MICHAEL addition. Oxidation of the furan moiety eventually afforded butenolide **8**, which, after methylation, was cyclised to racemic **1**. The product was obtained in a total yield of 15% over seven steps (Scheme 9).



**Scheme 9.** Total syntheses of racemic Greek tobacco lactone (**1**).

The first enantioselective total synthesis was reported by PIHKO and SIITONEN in 2014.<sup>60</sup> Starting from silyloxyfuran **9**, the butenolide core **10** was prepared by the reaction with acrolein in an asymmetric MUKAIYAMA-MICHAEL protocol, employing catalytic amounts of (2*R*,5*R*)-diphenylpyrrolidine and *para*-nitrobenzoic acid (*p*-NBA),<sup>61</sup> in 60% yield and in 88% enantiomeric excess. Subsequent WITTIG olefination and SHARPLESS asymmetric dihydroxylation afforded the cyclisation precursor **11** in 57% yield and in a diastereomeric ratio of 93:7. The synthesis was completed by base-induced oxa-MICHAEL addition to construct the tetrahydropyran core and dehydration of the tertiary alcohol. (+)-Greek tobacco lactone (**1**) was obtained in a total yield of 20% over five steps (Scheme 10).

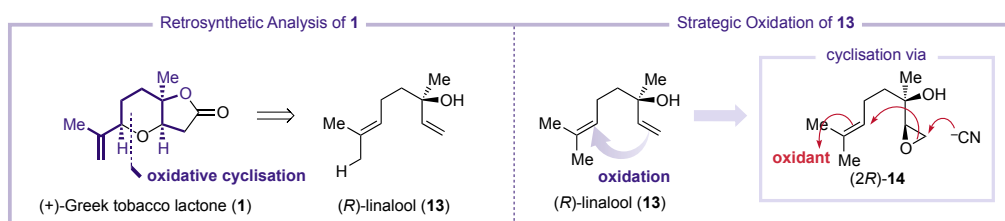


**Scheme 10.** The first enantioselective total synthesis of Greek tobacco lactone (**1**).

## 2.2 Objective

In contrast to the published syntheses, focusing on the construction the carbon framework from smaller carbon building blocks, it was envisaged to reduce the amount of carbon-carbon bond formations by strategic retrosynthetic cuts to identify suitable starting materials.

The retrosynthetic opening of the tetrahydropyran core by an oxidative cyclisation – as opposed to an oxa-MICHAEL addition – reveals two simple and readily available starting materials: the monoterpene (*R*)-linalool (**13**) and the one-carbon building block cyanide. Activation of both double bonds of (*R*)-linalool by oxidative transformations could give access to the fused bicyclic scaffold. Initial epoxidation of the terminal double bond would allow installation of the carboxyl carbanion equivalent and enable subsequent lactonisation. Oxidation of the prenyl double bond could then facilitate cyclisation with the epoxide-derived hydroxyl group to build the tetrahydropyran core (Scheme 11).



**Scheme 11.** Retrosynthetic analysis of (+)-Greek tobacco lactone (**1**) and strategic oxidations for key-bond formations.

The utilization of chiral and optically enriched or pure terpene natural products such as (*R*)-linalool enables several strategic approaches in synthesis planning. Due to their high abundance and general renewability, terpene building blocks represent an inexpensive and versatile pool of chiral starting materials for the chemical synthesis of complex natural products as well as pharmaceutical agents.<sup>62</sup> The identification of larger building blocks might minimise carbon-carbon bond forming reactions resulting in a more rapid construction of the carbon skeleton. Furthermore, the introduction of stereogenic centers by the starting materials omits the necessity for resolution or asymmetric catalysis to generate enantioenriched compounds and allows the installation of further stereogenic centers by substrate-induced diastereoselectivity.<sup>63</sup>

## 2.3 Publication

### 2.3.1 Synthesis of (+)-Greek Tobacco Lactone via a Diastereoablative Epoxidation and a Selenium-Catalyzed Oxidative Cyclization

---

<b>Authors</b>	Stefan Leisering, Iker Riaño, Christian Depken, Leona J. Gross, Manuela Weber, Dieter Lentz, Reinhold Zimmer, Christian B. W. Stark, Alexander Breder, and Mathias Christmann
<b>Journal</b>	<i>Org. Lett.</i> <b>2017</b> , <i>19</i> , 1478–1481
<b>DOI</b>	10.1021/acs.orglett.7b00484
<b>Abstract</b>	An asymmetric synthesis of the C11-homoterpenoid (+)-Greek tobacco lactone is developed starting from readily available ( <i>R</i> )-linalool. The synthesis is comprised of four operations and features a diastereoablative epoxidation and an oxidative tetrahydropyran formation using vanadium-, palladium-, and selenium-catalyzed cyclizations.
<b>Author Contribution</b>	<p>The concept of the manuscript was elaborated by S. Leisering, Dr. R. Zimmer and Prof. Dr. M. Christmann.</p> <p>The vanadium-catalysed oxidative cyclisation of compound <b>2</b> via intermediate <b>11</b> was carried out by L. J. Gross under the supervision of Prof. Dr. C. B. W. Stark and the selenium-catalysed oxidative cyclisation under photoredox conditions of <b>2</b> by C. Depken under the supervision of Prof. Dr. C. B. W. Stark. The palladium-mediated oxidative cyclisation experiments and synthesis of compounds <i>ent</i>-<b>12</b>, <b>13</b>, and <b>14</b> were performed by I. Riaño. The rest of the synthesis, including preparation of compound <b>8</b>, the collection of all associated analytical data, and the NMR experiments for the resolution of the diastereomeric epoxides <b>3a</b> and <b>3b</b>, were carried out by S. Leisering. The crystals of compounds <i>ent</i>-<b>12</b>, <b>13</b>, and <b>14</b> for X-ray diffraction analysis were provided by I. Riaño and the crystal of compound <b>8</b> for X-ray diffraction analysis was provided by S. Leisering. The X-ray diffraction measurements and analyses were performed by M. Weber and D. Lentz.</p> <p>The Manuscript was written by S. Leisering and Prof. Dr. M. Christmann.</p>

---

Permission for reproduction in print and electronic format for the purpose of this dissertation is granted by:

Copyright © 2017 American Chemical Society

# Synthesis of (+)-Greek Tobacco Lactone via a Diastereoablative Epoxidation and a Selenium-Catalyzed Oxidative Cyclization

Stefan Leisering,<sup>†</sup> Iker Riaño,<sup>†</sup> Christian Depken,<sup>‡</sup> Leona J. Gross,<sup>§</sup> Manuela Weber,<sup>†</sup> Dieter Lentz,<sup>†</sup> Reinhold Zimmer,<sup>†</sup> Christian B. W. Stark,<sup>\*,§</sup> Alexander Breder,<sup>\*,‡</sup> and Mathias Christmann<sup>\*,†,§</sup>

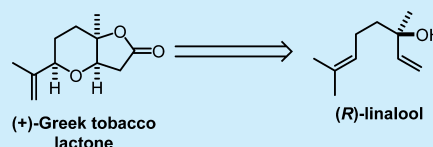
<sup>†</sup>Institut für Chemie und Biochemie, Freie Universität Berlin, Takustraße 3, 14195 Berlin, Germany

<sup>‡</sup>Institut für Organische und Biomolekulare Chemie, Universität Göttingen, Tammannstraße 2, 37077 Göttingen, Germany

<sup>§</sup>Institut für Organische Chemie, Universität Hamburg, Martin-Luther-King-Platz 6, 20146 Hamburg, Germany

## Supporting Information

**ABSTRACT:** An asymmetric synthesis of the C<sub>11</sub>-homoterpenoid (+)-Greek tobacco lactone is developed starting from readily available (*R*)-linalool. The synthesis is comprised of four operations and features a diastereoablative epoxidation and an oxidative tetrahydropyran formation using vanadium-, palladium-, and selenium-catalyzed cyclizations.



Many plants produce volatile C<sub>11</sub>-homoterpenes, such as (*E*)-4,8-dimethyl-1,3,7-nonatriene (DMNT, C<sub>11</sub>H<sub>18</sub>), to defend against herbivores by attracting their carnivorous predators (Figure 1).<sup>1</sup> It has been shown that DMNT is

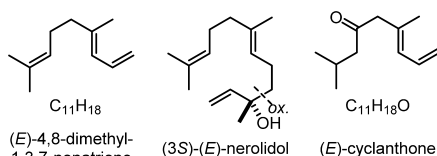


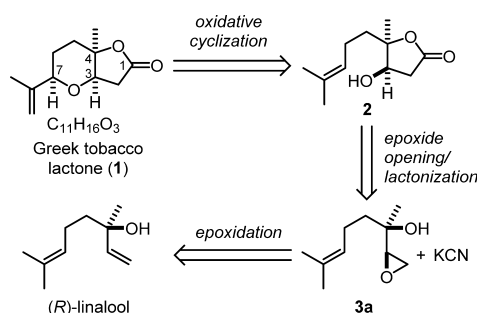
Figure 1. C<sub>11</sub>-homoterpenoids and their biosynthetic precursor.

biosynthetically derived from the sesquiterpenoid (3*S*)-(*E*)-nerolidol<sup>2</sup> via oxidative degradation by P450 monooxygenases.<sup>3</sup> For this reason, C<sub>11</sub>-homoterpenes are also referred to as tetranorsesquiterpenes. Mono-oxidized homoterpenes such as (*E*)-cyclanthonone<sup>4</sup> have been found as the major constituent of the floral scent of *Cyclanthus bipartitus* Poit., a neotropical plant in the family Cyclanthaceae. Higher oxidized C<sub>11</sub>-homoterpenes are rarely found in nature.<sup>5</sup> In 1993, Wahlberg et al. isolated the bicyclic homoterpenoid lactone **1** from the sun-cured leaves of Greek tobacco.<sup>6</sup> Although the exact biological role of this C<sub>11</sub>-homoterpenoid is not yet known, three syntheses of **1** have been reported by the groups of Clark,<sup>7</sup> Fall and Besada,<sup>8</sup> and Pihko.<sup>9</sup> Herein, we report a four-step synthesis of (+)-Greek tobacco lactone from the readily available monoterpene (*R*)-linalool.

A principal challenge in synthesis planning lies in the identification of larger building blocks within a given target molecule to minimize the number of carbon–carbon bond forming reactions.<sup>10</sup> In contrast to the previous approaches involving oxa-Michael additions to a butenolide and using smaller building blocks, we opted for an oxidative cyclization of hydroxyalkene **2** to form the tetrahydropyran. Accordingly, we identified (*R*)-linalool-derived epoxide **3a** as a ten-carbon chiral

building block and cyanide as nucleophilic equivalent of the carboxyl group (Scheme 1).

## Scheme 1. Retrosynthetic Analysis of (+)-Greek Tobacco Lactone



Our study commenced with the vanadium-catalyzed epoxidation of (*R*)-linalool.<sup>11</sup> Using a protocol published by Opatz et al.<sup>12</sup> as starting point, we obtained a 3:2 mixture of the diastereomeric epoxides in good yield slightly favoring the undesired diastereomer **3b**. As the chromatographic separation of the two diastereomers turned out to be difficult, we attempted to remove the undesired epoxide using Jacobsen's hydrolytic kinetic resolution.<sup>13</sup> To this end, the mixture of the diastereomeric epoxides was treated with catalyst **4**, and water was added in small portions. As expected, <sup>1</sup>H NMR analysis of the crude reaction mixture showed that only the desired epoxide had remained (Figure 2).

However, no signals for the expected diol could be found. Concomitant with the disappearance of the epoxide signals for diastereomer **3b**, an aldehyde and three cyclopropyl signals

Received: February 16, 2017

Published: March 3, 2017



## Organic Letters

## Letter

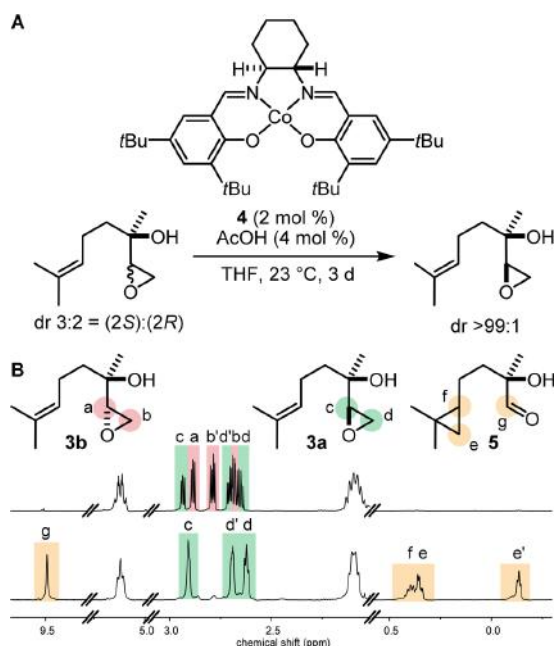
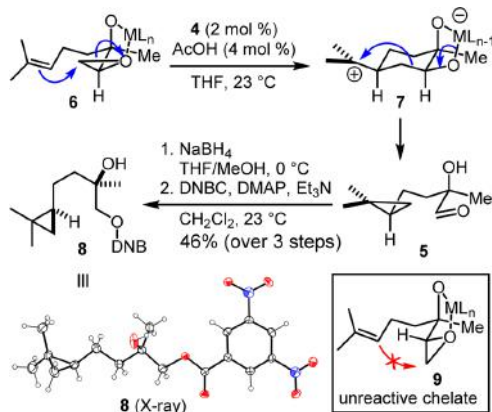


**Figure 2.** (A) Conditions for the resolution of the mixture of diastereomeric epoxides **3a** and **3b** and (B)  $^1\text{H}$  NMR analysis prior and after treatment with Jacobsen's catalyst **4**.

appeared. Sharpless et al.<sup>14</sup> identified an identical compound within a complex mixture of products<sup>15</sup> obtained by treatment of epoxide **3b** with 1.4 equiv of  $\text{Ti}(\text{O}i\text{Pr})_4$ . To shed light on the formation of cyclopropane **5**, we determined the configuration of the two stereogenic centers by X-ray analysis of dinitrobenzoate **8**.<sup>16</sup> In line with the Sharpless proposal, hydroxyl-directed Lewis acid activation of the epoxide via chelate **6** induces an intramolecular attack of the alkene. Subsequently, the resulting cationic cyclohexane intermediate **7** undergoes retro-homo-Prins fragmentation to form cyclopropyl aldehyde **5**. The stereogenic center at the cyclopropane is set by placing the isopropyl and methyl substituents in the equatorial positions of intermediate cyclohexane **7** (Scheme 2). For

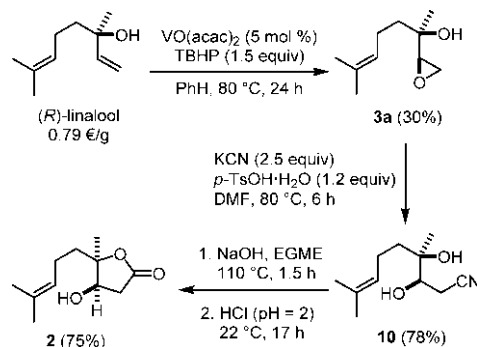
### Scheme 2. Mechanism of the Cyclopropane Formation and Determination of Its Absolute Configuration (Thermal Ellipsoid at 50% Probability)



diastereomeric chelate **9**, the alkene  $\pi$ - and epoxide  $\text{C}-\text{O}$   $\sigma^*$ -orbital overlap is insufficient for the initial epoxide opening step, leaving epoxide **3a** unreacted. As only 2 mol % of Jacobsen's catalyst decomposed the undesired epoxide diastereomer, we speculated that, upon increasing the reaction time,<sup>17</sup>  $\text{VO}(\text{acac})_2$  could not only epoxidize linalool but also effect the hydroxyl-mediated fragmentation in a catalytic diastereoblative manner.<sup>18</sup>

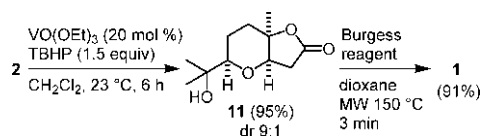
Gratifyingly, treatment of (*R*)-linalool with 5 mol % of  $\text{VO}(\text{acac})_2$  and 1.5 equiv of TBHP in refluxing benzene for 24 h afforded epoxide **3a** as a single diastereomer in 30% yield on a 10 g scale. Opening of the epoxide **3a** with cyanide could be realized using relatively costly  $\text{Et}_2\text{AlCN}$ <sup>19</sup> (72% yield). As a cost-efficient alternative, we used KCN and *p*-TsOH· $\text{H}_2\text{O}$  in DMF to afford nitrile **10** in 78% yield. Hydrolysis with NaOH and subsequent acidic lactonization provided lactone **2** in 75% yield (Scheme 3).

### Scheme 3. Synthesis of Lactone 2



Hartung et al.<sup>20</sup> have developed oxidative cyclizations of hydroxyalkenes<sup>21</sup> for the synthesis of tetrahydrofurans. The stereoselectivity is induced through coordination of the secondary alcohol to the vanadium catalyst. Encouraged by their results, we applied these conditions to lactone **2** (Scheme 4). Product **11** was formed in 95% yield with high

### Scheme 4. Vanadium-Catalyzed Oxidative Cyclization



diastereoselectivity (9:1). As shown previously by Pihko,<sup>9</sup> dehydration of **11** can be achieved using Burgess reagent.<sup>22</sup> In our case, under microwave irradiation in dioxane, (+)-**1** was produced in 91% yield. Although the two-step cyclization-elimination sequence described above was effective, we set our sights on a shortcut that would join an intramolecular hydroxymetalation and a  $\beta$ -hydride elimination using a single catalyst.

To this end, we took a closer look at  $\text{Pd}^{\text{II}}$ -mediated and -catalyzed Wacker-type cyclizations developed by Semmelhack<sup>23</sup> and Stoltz,<sup>24</sup> respectively. A single equivalent of palladium(II)-trifluoroacetate in DMSO under microwave conditions afforded tobacco lactone **1** in 41% as an 85:15 mixture of *C*7-diastereomers (Scheme 5). Along with the

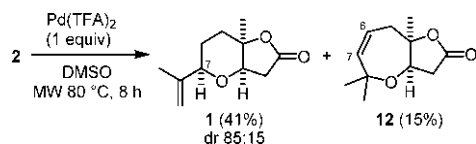


## Organic Letters

## Letter

desired product, we isolated  $\Delta^6$ -tetrahydrooxepine **12** from the endocyclic ring closure in 15% yield.

## Scheme 5. Palladium-Mediated Oxidative Cyclization



Changing the solvent to MeCN rendered **12** as the major product (32%) together with 8% of the regioisomeric  $\Delta^5$ -tetrahydrooxepine **13**.

Attempts at catalytic versions of the Wacker cyclization led to simple proton-mediated etherification to give hexahydrooxepine **14**, possibly through catalysis by hidden Brønsted acids.<sup>26</sup> Each of the three oxepines *ent*-**12**, **13**, and **14** was characterized unambiguously by X-ray crystallography as shown in Figure 3.

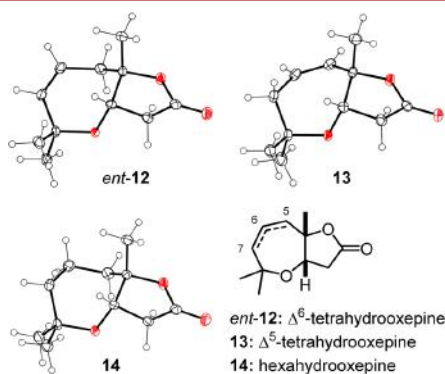
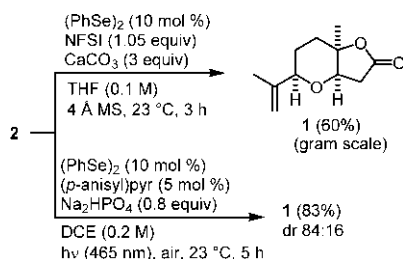


Figure 3. X-ray analyses of oxepines *ent*-**12**, **13**, and **14** (thermal ellipsoid at 50% probability).<sup>25</sup>

We recently showed diselenides to be cost-efficient and potent alternatives for conventional palladium catalysis in oxidative aminations<sup>27,28</sup> and acyloxylation<sup>29,30</sup> of unactivated alkenes. Our method relies on diphenyldiselenide as a catalytically active species and *N*-fluorobenzenesulfonimide (NFSI) as the terminal oxidant.<sup>31</sup> Slight modifications of these conditions eventually led to an efficient cyclization of **2** to **1** in 60% yield (Scheme 6).

Most recently, we developed a new selenium-catalyzed photoredox protocol for the oxidative allylic esterification of nonactivated alkenes utilizing air as the terminal oxidant.<sup>32</sup> Although the NFSI-based approach already achieved good

## Scheme 6. Selenium-Catalyzed Oxidative Cyclization



results, the use of ambient air as a complementary oxidant would appear more attractive and obviate stoichiometric amounts of byproducts other than water. Thus, we applied the selenium-based oxidation catalysis protocol for this synthesis. Consequently, the use of 10 mol % of (PhSe)<sub>2</sub> in the presence of 2,4,6-tri(4-methoxyphenyl)pyrylium tetrafluoroborate (5 mol %) under air-exposed conditions led to the clean cyclization of alcohol **2** to give target structure **1** in an improved yield of 83% (84:16 dr).

In summary, we have developed a short synthesis of (+)-Greek tobacco lactone (**1**) from readily available (*R*)-linalool. Key steps include a vanadium-catalyzed stereoablative epoxidation and an alkene hydroxylation using a selenium-based redox system with either NFSI or molecular oxygen as the terminal oxidant. Our example showcases how selenium can offer a powerful and superior alternative to the palladium-catalyzed alkoxylation of unactivated alkenes.

## ASSOCIATED CONTENT

## Supporting Information

The Supporting Information is available free of charge on the ACS Publications website at DOI: 10.1021/acs.orglett.7b00484.

X-ray crystallographic data for **8** (CIF)

X-ray crystallographic data for *ent*-**12** (CIF)

X-ray crystallographic data for **13** (CIF)

X-ray crystallographic data for **14** (CIF)

Experimental procedures and spectroscopic data (PDF)

## AUTHOR INFORMATION

## Corresponding Authors

\*E-mail: stark@chemie.uni-hamburg.de.

\*E-mail: abreder@gwdg.de.

\*E-mail: mathias.christmann@fu-berlin.de.

## ORCID

Christian B. W. Stark: 0000-0001-7180-8160

Mathias Christmann: 0000-0001-9313-2392

## Notes

The authors declare no competing financial interest.

## ACKNOWLEDGMENTS

We acknowledge the following grants for funding this project: Deutsche Forschungsgemeinschaft (DFG, Emmy Noether Fellowship to A.B. [BR 4907/1-1]) and the Fonds der Chemischen Industrie (FCI, Ph.D. Fellowship to C.D.). We thank the UPV/EHU predoctoral mobility program and Luise Schefzig and Kornel Ocytko (Freie Universität Berlin) for their experimental help.

## REFERENCES

- (1) Bouwmeester, H. J.; Verstappen, F. W. A.; Posthumus, M. A.; Dicke, M. *Plant Physiol.* **1999**, *121*, 173–180.
- (2) Boland, W.; Gäbler, A.; Gilbert, M.; Feng, Z. *Tetrahedron* **1998**, *54*, 14725–14736.
- (3) Lee, S.; Badiyan, S.; Bevan, D. R.; Herde, M.; Gatz, C.; Tholl, D. *Proc. Natl. Acad. Sci. U. S. A.* **2010**, *107*, 21205–21210.
- (4) Schultz, K.; Kaiser, R.; Knudsen, J. T. *Flavour Fragrance J.* **1999**, *14*, 185–190.
- (5) Shi, Y.-S.; Liu, Y.-B.; Ma, S.-G.; Li, Y.; Qu, J.; Li, L.; Yuan, S.-P.; Hou, Q.; Li, Y.-H.; Jiang, J.-D.; Yu, S.-S. *J. Nat. Prod.* **2015**, *78*, 1526–1535.

## Organic Letters

## Letter

- (6) Pettersson, T.; Eklund, A. M.; Wahlberg, I. *J. Agric. Food Chem.* **1993**, *41*, 2097–2103.
- (7) Clark, J. S.; Hayes, S. T.; Blake, A. J.; Gobbi, L. *Tetrahedron Lett.* **2007**, *48*, 2501–2503.
- (8) Zúñiga, A.; Pazos, G.; Besada, P.; Fall, Y. *Tetrahedron Lett.* **2012**, *53*, 4293–4295.
- (9) Siitonen, J.; Pihko, P. *Synlett* **2014**, *25*, 1888–1890.
- (10) (a) Winter, P.; Vaxelaire, C.; Heinz, C.; Christmann, M. *Chem. Commun.* **2011**, *47*, 394–396. (b) Winter, P.; Swatschek, J.; Willot, M.; Radtke, L.; Olbrisch, T.; Schäfer, A.; Christmann, M. *Chem. Commun.* **2011**, *47*, 12200–12202. (c) Swatschek, J.; Grothues, L.; Bauer, J. O.; Strohmann, C.; Christmann, M. *J. Org. Chem.* **2014**, *79*, 976–983.
- (11) Tertiary allylic alcohols constitute challenging substrates for asymmetric epoxidation: (a) Olivares-Romero, J. L.; Li, Z.; Yamamoto, H. *J. Am. Chem. Soc.* **2013**, *135*, 3411–3413. (b) Bryliakov, K. P.; Talsi, E. P.; Stas'ko, S. N.; Kholdeeva, O. A.; Popov, S. A.; Tkachev, A. V. *J. Mol. Catal. A: Chem.* **2003**, *194*, 79–88.
- (12) (a) Langhanki, J.; Rudolph, K.; Erkel, G.; Opatz, T. *Org. Biomol. Chem.* **2014**, *12*, 9707–9715. (b) Sharpless, K. B.; Michaelson, R. C. *J. Am. Chem. Soc.* **1973**, *95*, 6136–6137.
- (13) (a) Tokunaga, M. *Science* **1997**, *277*, 936–938. (b) Schaus, S. E.; Brandes, B. D.; Larrow, J. F.; Tokunaga, M.; Hansen, K. B.; Gould, A. E.; Furrow, M. E.; Jacobsen, E. N. *J. Am. Chem. Soc.* **2002**, *124*, 1307–1315.
- (14) Morgans, D. J.; Sharpless, K. B.; Traynor, S. G. *J. Am. Chem. Soc.* **1981**, *103*, 462–464.
- (15) Along with cyclopropane derivatives, cyclohexane-1,2-diols were identified.
- (16) CCDC 1534995 (8), 1534992 (*ent*-12), 1534994 (13), and 1534993 (14) contain the supplementary crystallographic data for this publication. These data can be obtained free of charge from The Cambridge Crystallographic Data Centre via [www.ccdc.cam.ac.uk/data\\_request/cif](http://www.ccdc.cam.ac.uk/data_request/cif).
- (17) In hindsight, this behavior could have been extrapolated from the comparison of literature-known epoxidations of linalool with VO(acac)<sub>2</sub>: (a) Ohloff, G.; Giersch, W.; Schulte-Elte, K. H.; Enggist, P.; Demole, E. *Helv. Chim. Acta* **1980**, *63*, 1582–1588. (b) Khomenko, T. M.; Tatarova, L. E.; Korchagina, D. V.; Barkhash, V. A. *Russ. J. Org. Chem.* **2002**, *38*, 498–506.
- (18) Mohr, J. T.; Ebner, D. C.; Stoltz, B. M. *Org. Biomol. Chem.* **2007**, *5*, 3571–3576.
- (19) Benedetti, F.; Berti, F.; Norbedo, S. *Tetrahedron Lett.* **1999**, *40*, 1041–1044.
- (20) (a) Hartung, J.; Schmidt, P. *Synlett* **2000**, 367–370. (b) Donges, M.; Amberg, M.; Niebergall, M.; Hartung, J. *J. Inorg. Biochem.* **2015**, *147*, 204–220.
- (21) For a review on direct oxidative diene cyclizations and related reactions in natural product synthesis, see: Adrian, J.; Gross, L. J.; Stark, C. B. W. *Beilstein J. Org. Chem.* **2016**, *12*, 2104–2123.
- (22) Atkins, G. M.; Burgess, E. M. *J. Am. Chem. Soc.* **1968**, *90*, 4744–4745.
- (23) Semmelhack, M. F.; Kim, C. R.; Dobler, W.; Meier, M. *Tetrahedron Lett.* **1989**, *30*, 4925–4928.
- (24) (a) Trend, R. M.; Ramtohl, Y. K.; Ferreira, E. M.; Stoltz, B. M. *Angew. Chem., Int. Ed.* **2003**, *42*, 2892–2895. (b) Trend, R. M.; Ramtohl, Y. K.; Stoltz, B. M. *J. Am. Chem. Soc.* **2005**, *127*, 17778–17788.
- (25) The oxepines were obtained from the cyclization of *ent*-2.
- (26) Dang, T. T.; Boeck, F.; Hintermann, L. *J. Org. Chem.* **2011**, *76*, 9353–9361.
- (27) (a) Trenner, J.; Depken, C.; Weber, T.; Breder, A. *Angew. Chem., Int. Ed.* **2013**, *52*, 8952–8956. (b) Ortgies, S.; Breder, A. *Org. Lett.* **2015**, *17*, 2748–2751.
- (28) For related selenium-catalyzed aminations, see: (a) Zhang, X.; Guo, R.; Zhao, X. *Org. Chem. Front.* **2015**, *2*, 1334–1337. (b) Guo, R.; Huang, J.; Huang, H.; Zhao, X. *Org. Lett.* **2016**, *18*, 504–507.
- (29) Krätzschar, F.; Käfel, M.; Delony, D.; Breder, A. *Chem. - Eur. J.* **2015**, *21*, 7030–7034.
- (30) For an asymmetric selenium-catalyzed lactonization, see: Kawamata, Y.; Hashimoto, T.; Maruoka, K. *J. Am. Chem. Soc.* **2016**, *138*, 5206–5209.
- (31) Li, Y.; Zhang, Q. *Synthesis* **2015**, *47*, 159–174.
- (32) Ortgies, S.; Depken, C.; Breder, A. *Org. Lett.* **2016**, *18*, 2856–2859.

### 3 Cyclopropanation – Studies Towards the Intramolecular Methylenetransfer of 6,7-Alkenyl Epoxides

#### 3.1 Cyclopropanes in Natural Products

Cyclopropanes are a widely distributed structural motif in natural products that display a broad range of important biological activities, including enzyme inhibition, plant growth and fruit ripening controls, as well as insecticidal, antifungal, and anticancer properties.<sup>64,65</sup> Prominent examples are the cholesteryl ester transfer protein (CETP) inhibitor (-)-U-106305 (**15**), the insecticide (+)-*trans*-chrysanthemic acid (**16**), and the promising anticancer agent (+)-ptaquiloside (**17**) (Figure 6). Furthermore, the presence of cyclopropane structures can enhance drugs leading to derivatives with increased potency or stability.<sup>66</sup> Therefore, cyclopropane-containing compounds represent valuable leads for the development of new pesticides and drugs and continue to be in the focus of organic synthesis, medicinal chemistry, and pharmacology.

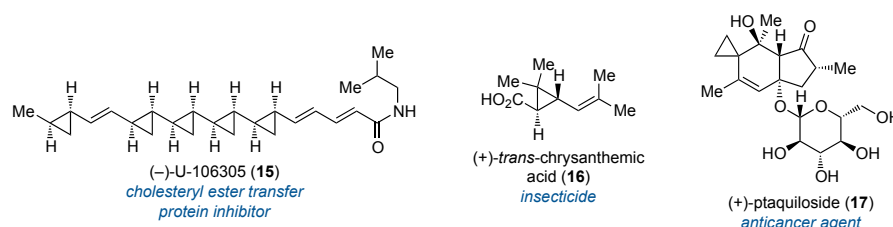
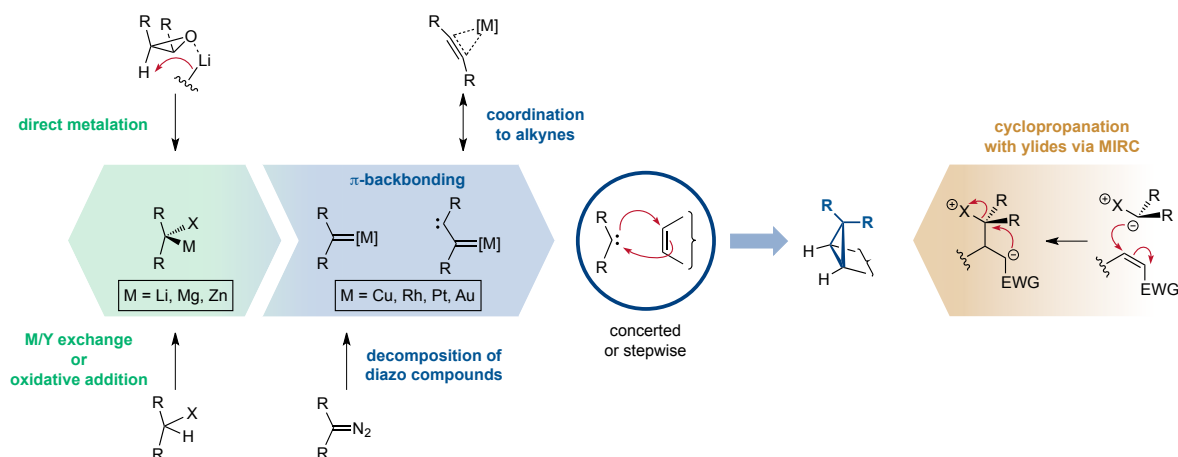


**Figure 6.** Cyclopropane-containing natural products and their biological properties.

#### 3.2 Synthesis of Cyclopropanes

Cyclopropanes are generally prepared either via the addition of carbene-like intermediates, meaning carbons with nucleophilic and electrophilic properties, to a double bond or intramolecular substitutions. The term ‘carbenoid’ was first introduced by CLOSS and MOSS in 1964 for these species and describes compounds, ‘which exhibit reactions qualitatively similar to those of carbenes without necessarily being free divalent carbon species.’<sup>67</sup> While carbenoids are structurally related to singlet carbenes, their ambiphilic character is generally realised in anionic carbon atoms that additionally bear a leaving group.<sup>68</sup> Depending on the nature of the double bond, different types of reagents with varying degrees of reactivity can be employed. Stabilisation of the negative charge can either be achieved by metals to generate metal carbenoids or by adjacent functionalities such as sulfonium or ammonium groups to give ylides, which can be considered a type of rather stable carbenoids (Scheme 12). While the former, in particular those with transition metals capable of forming vinylidene-based carbenoids with weak  $\pi$ -backbonding properties, have a stronger electrophilic character and react with electron-rich alkenes,<sup>68,69</sup> the latter exhibit more pronounced nucleophilic character and readily attack electron-deficient double bonds. Cyclopropane formation can occur concerted or in a stepwise manner (Scheme 12). In case of s-block metals and zinc carbenoids, the reaction usually proceeds concerted with retention of the stereochemistry of the alkene.

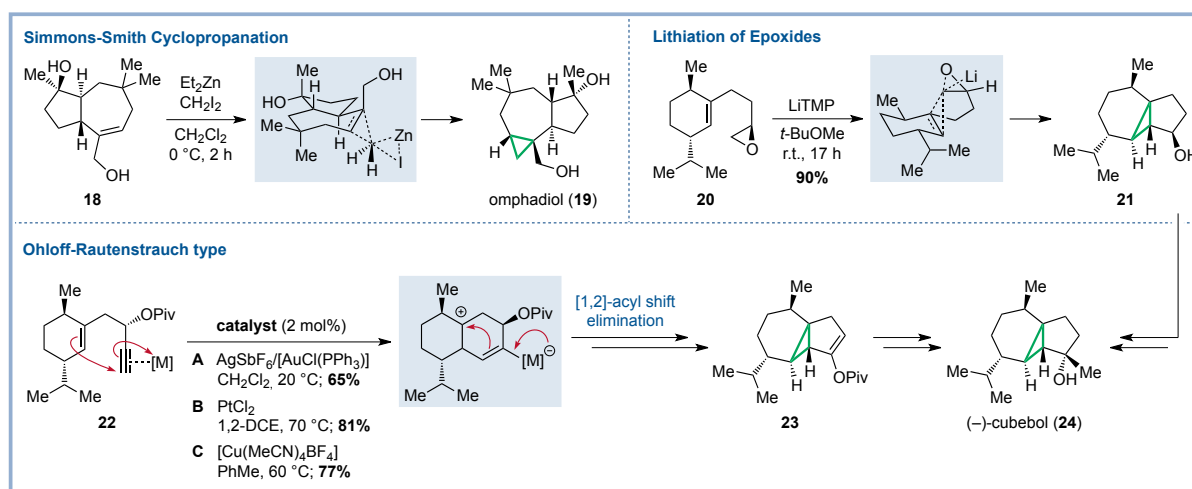


**Scheme 12.** Methods for cyclopropanation of alkenes. Left: Preparation of metal carbenoids and a simplified mechanism for the reaction with alkenes. Right: Cyclopropanation via ylides.

One of the most prominent methods involving reagents of this kind is the SIMMONS-SMITH cyclopropanation, which utilises zinc carbenoids.<sup>70</sup> Whereas the initial report from SIMMONS and SMITH in 1958 described the preparation of the active zinc species via oxidative addition of a zinc-copper couple to diiodomethane, various modifications to activate the zinc metal have been reported since then.<sup>71</sup> In 1966, FURUKAWA and co-workers reported an alternative preparation via zinc-halogen exchange between diethylzinc and diiodomethane,<sup>72</sup> which constitutes one of the most applied methods nowadays, counting numerous examples in total syntheses, such as the synthesis of omphadiol (**19**) reported by LIANG and co-workers (Scheme 13).<sup>73</sup> Besides oxidative addition and metal-halogen exchange, the direct metalation via deprotonation provides an alternative source for metal carbenoids. For instance, in 2004 HODGSON and co-workers disclosed a novel methodology for intramolecular cyclopropanations via the  $\alpha$ -lithiation of terminal epoxides, as already observed by CRANDALL and LIN in 1967,<sup>74</sup> and later applied their protocol to the total synthesis of (–)-cubebol (**24**) (Scheme 13).<sup>75</sup>

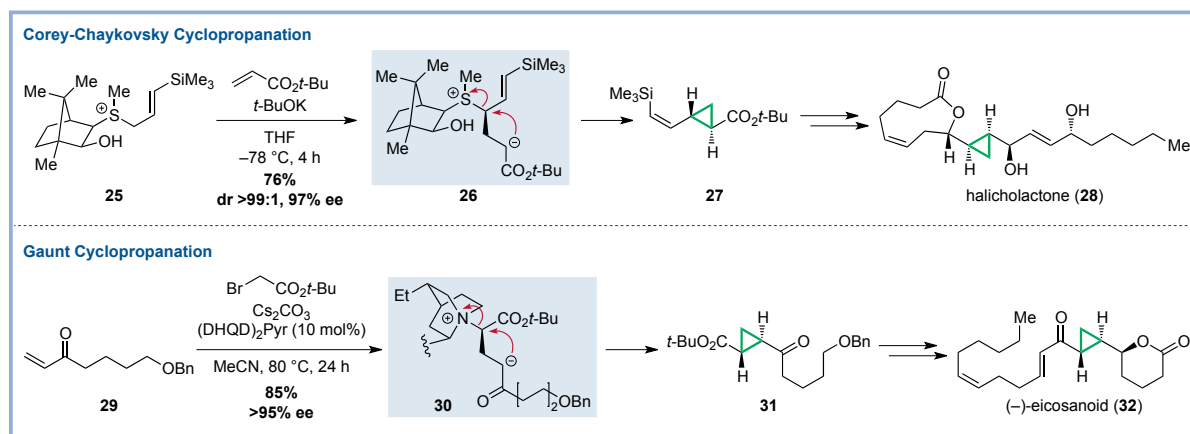
However, as these systems require stoichiometric amounts of organometallic reagent, transition metal catalysis remains one of the most efficient strategies for the construction of cyclopropanes.<sup>76</sup> Typical strategies for the *in situ* generation of transition-metal carbenoids include the decomposition of diazo compounds and the cyclisation of 1,*n*-enynes. The reaction of diazo compounds and more stable surrogates such as hydrazones have been widely used in combination with rhodium or copper catalysts,<sup>77</sup> whereas the activation of alkynes is dominated by gold and platinum catalysis.<sup>78</sup> To rationalise the reactivity of metal-vinylidene-based carbenoids derived from coordination of transition metals to alkynes, different mesomeric structures, corresponding to different coordination modes, can be analysed (Scheme 12). In the  $\eta^1$ -coordination mode both carbons of the alkyne exhibit weak carbene-like properties and therefore can act as an electrophile and as a nucleophile.<sup>78</sup> However, since the covalent character is rather weak, it can be considered as a polarised electrophilic  $\pi$ -system with an asymmetrical  $\eta^2$ -coordination to the metal center.<sup>79</sup> Thus, cyclopropanation is usually initiated by attack of the alkene, followed by trapping of the resulting carbenium ion. The resulting covalently bonded metal-carbenoid intermediate can then undergo further reactions typical for carbenes such as rearrangements or additional cyclopropanations.<sup>80</sup> In particular, OHLOFF-RAUTENSTRAUCH-type rearrangement constitutes a powerful reaction for the preparation of cyclopropanes embedded in a polycyclic environment. The reaction was first described by OHLOFF and co-workers in 1976 utilising zinc chloride and later rediscovered by RAUTENSTRAUCH during studies on palladium-catalysed NAZAROV-type cyclisations.<sup>81,82</sup> However, increasing awareness of its preparative potential emerged only with the work of FENSTERBAND, MALACRIA and MARCO-

CONTELLES in 2002,<sup>83</sup> propelling a series of research efforts.<sup>84</sup> While initial works focused on platinum(II) chloride as catalyst, FÜRSTNER and co-workers showed that gold(I) and gold(III) chlorides, usually in combination with silver salts, represent potent alternatives.<sup>85</sup> Naturally, many applications in total synthesis projects ensued. In their endeavour towards a total synthesis of (–)-cubebol (**24**), FEHR and GALINDO found that copper, gold and platinum salts are effective promoters for the envisaged cycloisomerisation reaction (Scheme 13).<sup>86</sup> Interestingly, the OHLOFF-RAUTENSTRAUCH rearrangement can be described via two different mechanistic scenarios, depending on whether [1,2]-acyl migration or cyclisation occurs first.<sup>85b</sup> In this particular case, DFT computational studies supported a mechanistic pathway with preceding cyclisation, as previously proposed by FÜRSTNER and co-workers, for platinum and gold catalysis, whereas calculations for copper were inconclusive.<sup>87</sup>



**Scheme 13.** Examples of cyclopropanations via metal-carbenoids in total synthesis.

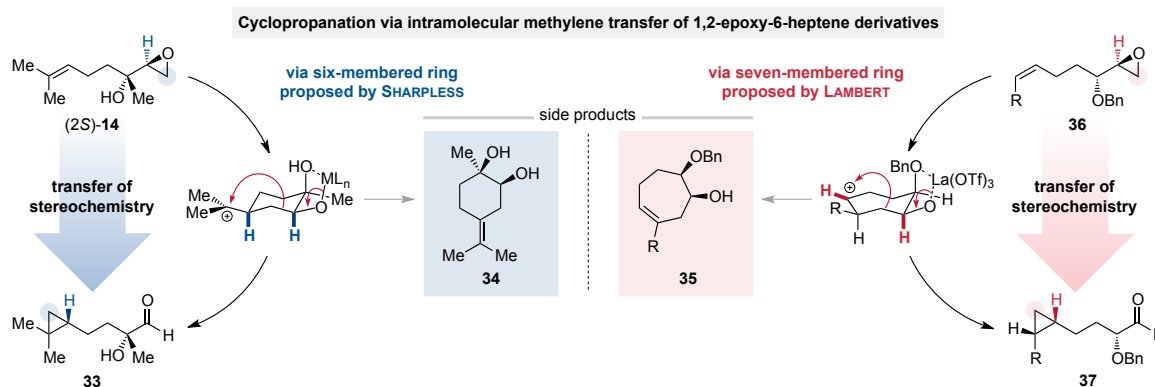
On the other hand, ylides can be regarded as nucleophiles and cyclopropane formation is initiated by irreversible conjugate addition to a MICHAEL system or electron-deficient double bonds in general. The resulting carbanion displaces the associated leaving group in an intramolecular nucleophilic substitution to give the cyclopropane. In systems with free rotation, the thermodynamically more stable *trans*-product is produced. Ylides, therefore, represent a powerful alternative to metal-carbenoids that generally give rather low conversions with electron-deficient alkenes. Moreover, the incorporation of chiral auxiliaries enables enantioselective variants of these reactions. For instance, TANG and co-workers developed the camphor-derived sulfonium salt **25** as a chiral ylide precursor for the enantioselective COREY-CHAYKOVSKY cyclopropanation of *t*-butyl acrylate in their total synthesis of halicholactone (**28**) (Scheme 14).<sup>88</sup> Concerning the advent of organocatalysis, the prospect of asymmetric catalytic systems have sparked great interest in further expanding the repertoire of synthetic tools available to organic chemists. Based on the seminal works of GAUNT and co-workers<sup>89</sup> on organocatalytic cyclopropanations using chiral tertiary amines, KUMARASWAMY and PADMAJA devised an enantioselective total synthesis of (–)-eicosanoid (**32**).<sup>90</sup> Mechanistically, the reaction proceeds via an ammonium ylide (**30**) generated *in situ* from the reaction between the catalyst and an  $\alpha$ -halo ester. Conjugate addition to enone **29** and ensuing intramolecular displacement of the ammonium leaving group furnished the cyclopropane **31** with concomitant regeneration of the catalyst (Scheme 14).



**Scheme 14.** Examples of cyclopropanations via ylides in the total synthesis of natural products.

### 3.3 Objective

Although these strategies offer powerful methods for chemo- and even stereoselective cyclopropanations some disadvantages remain, including the use of toxic and highly explosive diazocompounds, stoichiometric amounts of organometallic reagents or expensive transition metals, the necessity of chiral ligands or carefully prepared chiral reagents to induce stereoselectivity. With these considerations in mind, the vanadium-catalysed rearrangement of (2*S*,3*R*)-1,2-linalool epoxide ((2*S*)-**14**) (Scheme 15), which was exploited in the total synthesis of (+)-Greek tobacco lactone (**1**),<sup>91</sup> could represent a potential alternative to established methods for the enantioselective preparation of cyclopropanes.



**Scheme 15.** Mechanistic proposals for the methylene transfer of heptene-based alkenyl epoxides by SHARPLESS (left) and LAMBERT (right).

Following the works of SHARPLESS and MORGANS on the LEWIS-acid mediated intramolecular methylene transfer of  $\alpha$ -hydroxy epoxides to olefins,<sup>92</sup> two other groups have made similar observations. While MARSON and co-workers described the reaction in constrained ring systems with concomitant ring expansion via semi-pinacol rearrangement,<sup>93</sup> LAMBERT and HARDEE reported the first LEWIS-acid catalysed system and gave an elaborated investigation of the substrate scope and stereoselectivity for open-chain substrates.<sup>94</sup> Based on the isolation of cyclic side products such as **34** and **35**, presumably resulting from proton elimination of cationic species, similar mechanistic pathways, that account for the stereospecific formation of the observed cyclopropanes, have been proposed by all three groups. However, while SHARPLESS proposed a six-membered, HARDEE and LAMBERT postulated a seven-membered ring system as intermediate (Scheme 15). These



different observations can be rationalised by hyperconjugative stabilisation with respect to the degree of substitution on the alkenes and ensuing carbenium ions.

As all previous studies leveraged an adjacent hydroxyl group to promote cyclopropanation via chelation of the LEWIS acid, it was of interest to investigate a more general substrate scope in order to evaluate the feasibility of this method. Constraints such as requisite substitution patterns would severely limit the applicability in total synthesis. Therefore, different substrates that lack a directing group should be tested.

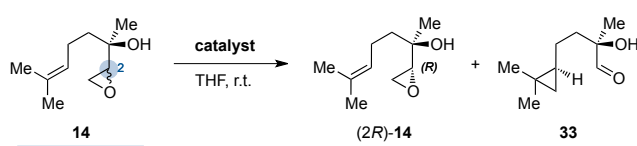
### 3.4 Results

It was first of interest to evaluate different LEWIS acids towards their ability to promote this intramolecular methylene transfer. Therefore, a mixture of both diastereomeric epoxides, obtained by vanadium-catalysed epoxidation of (*R*)-linalool (**13**),<sup>91</sup> was treated with different catalyst systems under the same conditions and the result was compared to the cobalt-mediated reaction with catalytic amounts of (salen)cobalt(II) complex **38** (Table 1, Entry 1). As a control experiment the reaction was performed solely with acetic acid as the catalytic system to test whether simple BRØNSTED-acid catalysis is sufficient to facilitate the reaction (Table 1, Entry 2). Since no conversion was observed at all, it was concluded that stronger coordinating LEWIS acids are required. Titanium tetraisopropoxide, which was already used by SHARPLESS in stoichiometric amounts to induce the rearrangement of (2*S*,3*R*)-1,2-linaloolepoxide, was tested (Table 1, Entry 3).<sup>92</sup> After three days, a diastereomeric ratio of 4.9:1 in favour of the *cis*- $\alpha$ -hydroxy epoxide was measured, which corresponds to a kinetic resolution by rearrangement of the *trans*- $\alpha$ -hydroxy epoxide to cyclopropane **33**. However, the result was inferior to the cobalt-salen-based catalyst system. In comparison, vanadyl acetylacetonate, which was the catalyst of choice for the one-pot protocol in the aforementioned total synthesis of (+)-Greek tobacco lactone, performed even worse under the same conditions and only marginally improved the diastereomeric ratio even after a reaction time of five days (Table 1, Entry 4). On the other hand, boron trifluoride diethyl etherate led only to degradation within minutes even at 0 °C (Table 1, Entry 5).

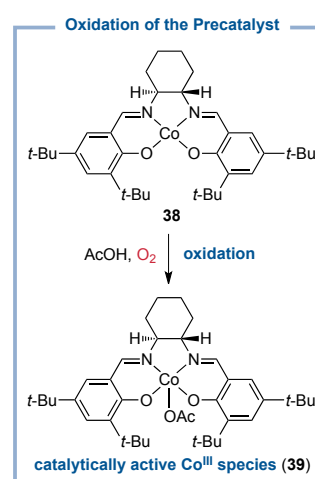
**Table 1.** Screening of different LEWIS acids as catalysts for the rearrangement (2*S*)-**14**.<sup>a</sup>

Entry	catalyst	<i>t</i>	Result <sup>b</sup>
1	<b>38</b> (2 mol%) AcOH (4 mol%)	3 d	dr >99:1
2	AcOH (10 mol%)	2 d	no conversion
3	Ti( <i>Oi</i> -Pr) <sub>4</sub> (10 mol%)	3 d	dr 4.9:1
4	VO(acac) <sub>2</sub> (10 mol%)	5 d	dr 1:1
5 <sup>c</sup>	BF <sub>3</sub> ·OEt <sub>2</sub> (12 mol%)	0.5 h	degradation

a) All reactions were performed on a 10 mg scale and in a concentration of 0.1 M. b) The reaction progress was monitored by GC-MS. c) The reaction was performed at 0 °C.



dr 1.4:1 (2*S*/2*R*)



Preliminary studies indicated that (salen)cobalt(II) complex **38** itself is not capable of facilitating the methylene transfer and only in combination with acetic acid yields the rearrangement product. This is in accordance with protocols for hydrolytic kinetic resolutions of racemic epoxides, where the corresponding (salen)cobalt(III) complex **39** is the catalytically active species.<sup>95</sup> Activation of the (salen)cobalt(II) precatalyst is achieved by oxidation with molecular oxygen in the presence of BRØNSTED acids.

With a promising catalytic system in hand, the influence of different substitution patterns on the alkyl chain between epoxide and alkene were investigated (Figure 7).

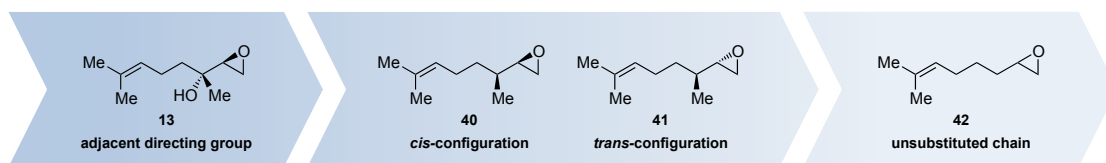
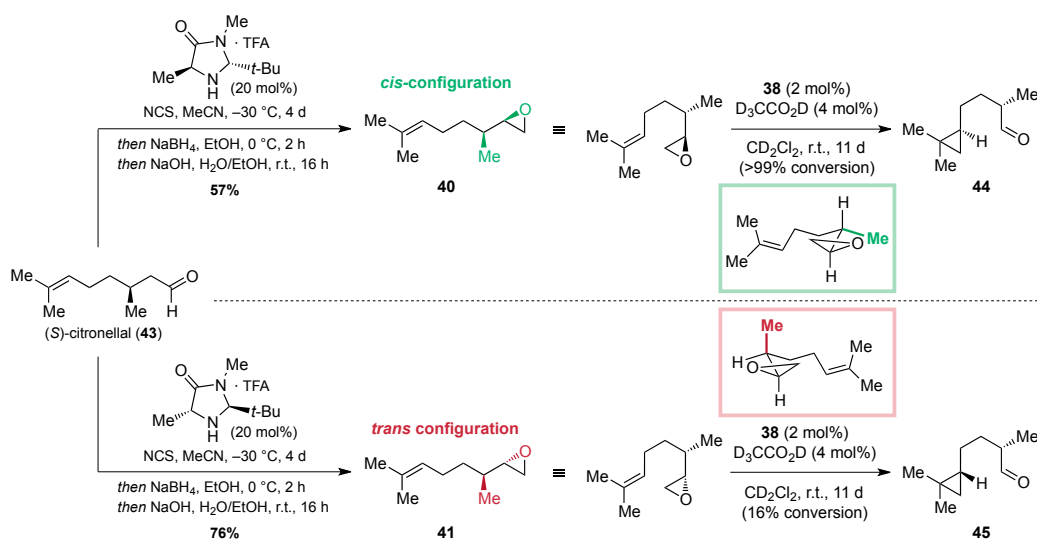


**Figure 7.** Substrates for the evaluation of the influence of different degrees of substitution on the alkyl chain.

Since all previous studies utilised the presence of an  $\alpha$ -hydroxyl directing group to promote rearrangement, it was of interest to evaluate the absence thereof. Both epimeric  $\alpha$ -methyl epoxides, the *cis*-configured epoxide **40** and the *trans*-configured epoxide **41**, were prepared from (*S*)-citronellal (**43**), which in turn was accessible by oxidation of commercially available enantioenriched (*S*)-citronellol. Subjection of (*S*)-citronellal to a one-pot procedure, consisting of  $\alpha$ -chlorination, reduction, and basic epoxide formation with either the L- or D-alanine-derived MACMILLAN catalyst, delivered the *cis*-epoxide **40** and the *trans*-epoxide **41** in 57% yield and 76% yield, respectively (Scheme 16).

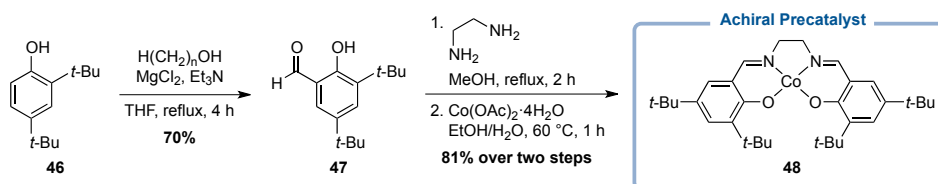


**Scheme 16.** Synthesis of epoxides **40** and **41** and subsequent investigation of the cobalt-catalysed methylene transfer.

Interestingly, when the two epimeric epoxides were subjected to (salen)cobalt(II) complex **38** and acetic acid a remarkable difference in reaction rates was observed. The reaction was much slower than with  $\alpha$ -hydroxy epoxide **13**, which can be attributed to the lack of a directing group. Furthermore, while the *cis*-epoxide **40**, bearing the same relative configuration with respect to the methyl group and epoxide moiety as the corresponding linalool-derived epoxide **13**, showed complete conversion after eleven days, <sup>1</sup>H-NMR analysis of the *trans*-epoxide **41** indicated only 16% conversion. The influence of the relative configuration on the reaction rates can be rationalised by steric interactions. The cyclic intermediate of *trans*-epoxide **41** bears the methyl group in axial position, which may render the reaction pathway less favourable compared to that of *cis*-

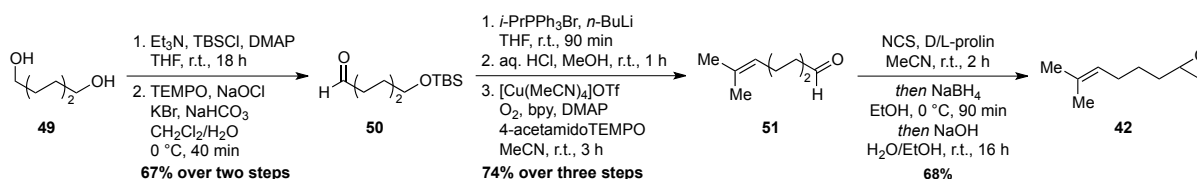


epoxide **40** with an equatorial positioned methyl group. Additionally, the reaction was performed with the (*R,R*)-enantiomer of complex **38** as a control experiment to determine whether stereoselectivity can be induced by chiral ligand and if matched or mismatched substrate-catalyst settings for stereocontrol are present. However, no influence was observed and the chiral backbone of the salen ligand was deemed inconsequential. Therefore, the preparation of an achiral (salen)cobalt(II) precatalyst in larger quantities was envisaged. Condensation of two equivalents of substituted salicylaldehyde **47**, available from phenol **46**,<sup>96</sup> with ethylenediamine and subsequent coordination of the resulting salen-based ligand to cobalt(II) afforded precatalyst **48** in 81% yield over two steps (Scheme 17).<sup>97,98</sup>



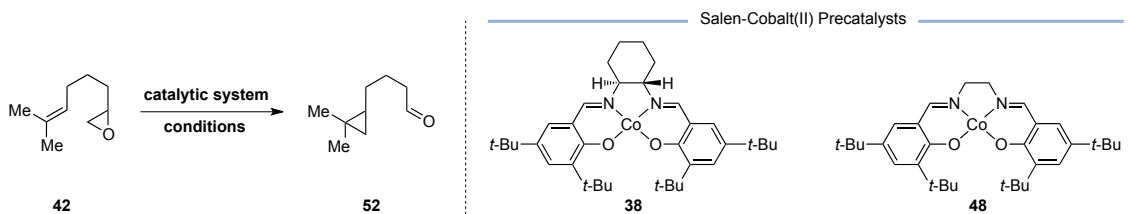
**Scheme 17.** Preparation of achiral precatalyst **48**.

Next, the influence of an unsubstituted alkyl chain was investigated. The required epoxide **42** was synthesised from aldehyde **51** analogous to both methylated substrates **40** and **41** via of  $\alpha$ -chlorination. Preparation of the aldehyde was accomplished by sequential oxidation of hexanediol (**49**) to introduce the prenyl moiety (Scheme 18).



**Scheme 18.** Preparation of epoxide **42**.

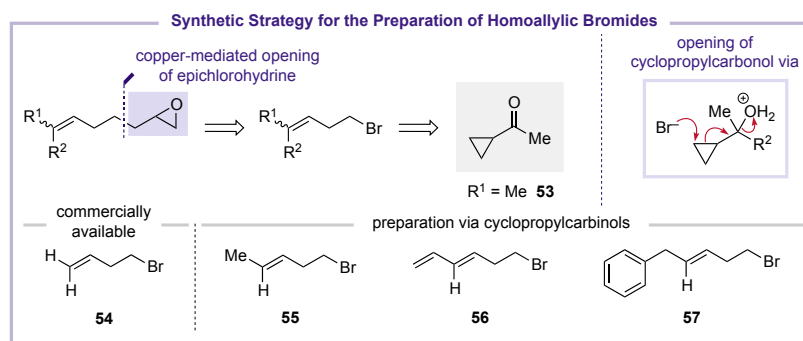
Employing achiral precatalyst **48** for the rearrangement of epoxide **42**, surprisingly, gave no conversion at ambient temperature after three days (Table 2, Entry 1). When the temperature was elevated to 50 °C, analysis by <sup>1</sup>H-NMR spectroscopy indicated a conversion of 76% after five days (Table 2, Entry 2). The same result was found, when the reaction was performed with cobalt(II) complex **38** as a control experiment (Table 2, Entry 3). Switching the solvent from dichloromethane to 1,2-dichloroethane allowed to perform the reaction at 80 °C resulting in complete conversion after one day (Table 2, Entry 4). On the other hand, utilising THF as the solvent gave only 50% conversion at 80 °C after 3 days (Table 2, Entry 5). Presumably, the etheral solvent acts as a competing LEWIS base and thus coordination of the solvent is preferred. For Comparison, in case of (2*S*,3*R*)-1,2-linaloolepoxide the hydroxyl group is the stronger LEWIS base and directs interaction between catalyst and epoxide via chelation. Scandium(III) triflate or LAMBERT's lanthanum(III) triflate system resulted exclusively in degradation (Table 2, Entries 6 and 7).

**Table 2.** Optimisation of the catalytic rearrangement of unsubstituted epoxide **42**.<sup>a</sup>


Entry	Catalyst	Additive	Solvent	<i>t</i>	<i>T</i>	Result <sup>b</sup>
1	<b>48</b> (2.5 mol%) AcOH (5 mol%)		CH <sub>2</sub> Cl <sub>2</sub>	3 d	r.t.	no conversion
2	<b>48</b> (2.5 mol%) AcOH (5 mol%)		CD <sub>2</sub> Cl <sub>2</sub>	5 d	50 °C	76% conversion <sup>c</sup>
3	<b>38</b> (2.5 mol%) AcOH (5 mol%)		CD <sub>2</sub> Cl <sub>2</sub>	5 d	50 °C	75% conversion <sup>c</sup>
4	<b>48</b> (2.5 mol%) AcOH (5 mol%)		1,2-DCE	1 d	80 °C	complete conversion
5	<b>48</b> (2.5 mol%) AcOH (5 mol%)		THF	3 d	80 °C	50% conversion
6	Sc(OTf) <sub>3</sub> (10 mol%)		1,2-DCE	1 d	40 °C	degradation
7	La(OTf) <sub>3</sub> (5 mol%)	2,6-lutidine (5 mol%) LiClO <sub>4</sub> (0.75 equiv)	1,2-DCE	1 d	r.t.	degradation

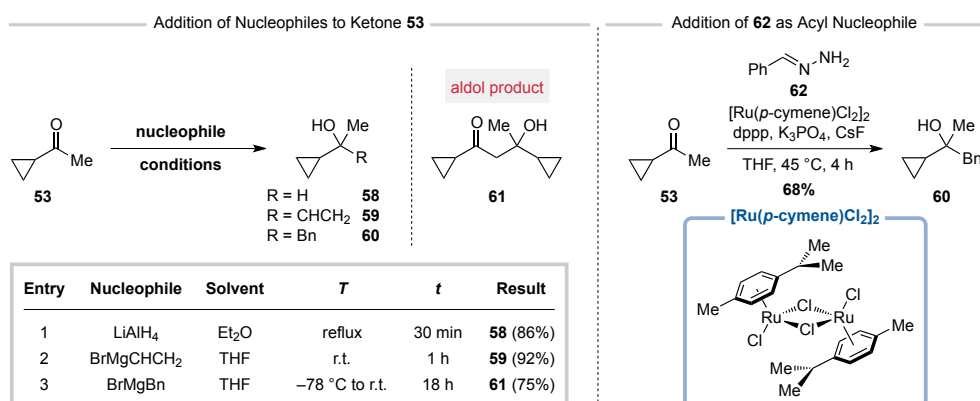
a) All reactions were performed on a 10 mg scale and in a concentration of 0.1 M. b) The reaction progress was monitored by GC-MS. c) The reaction progress was monitored by <sup>1</sup>H NMR.

Having evaluated the influence of substituents on the alkyl chain, concerning the degree of substitution, the relative configuration and the ability to direct the catalyst, it was further of interest to assess the nature of the alkene. Although the route towards epoxide **42** would allow for the introduction of other alkene moieties, a shorter avenue was desired. As a general approach, the copper-catalysed opening of epichlorohydrin with different homoallylic bromides was envisaged. The corresponding homoallylic bromides are either commercially available or can be prepared from cyclopropylcarbinols via treatment with hydrobromic acid (Scheme 19).

**Scheme 19.** Retrosynthetic analysis for the preparation of different homoallylic bromides.

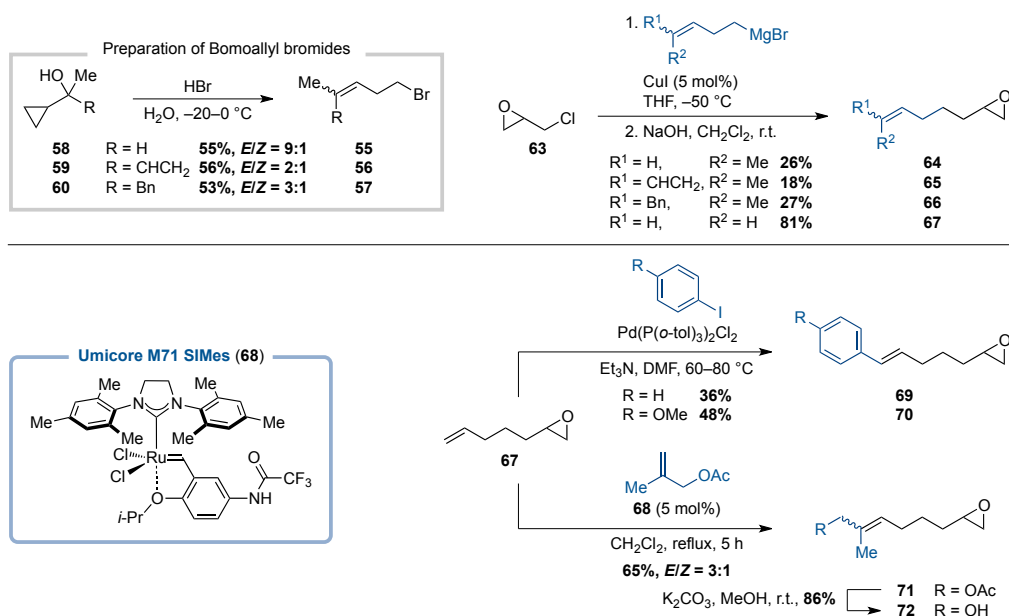
Cyclopropylcarbinols **58** and **59** were prepared by reaction of cyclopropyl methyl ketone (**53**) with lithium aluminium hydride and vinylmagnesium bromide, respectively (Scheme 19). Surprisingly, when the reaction was conducted with benzyl magnesium bromide as the nucleophile, addition of the GRIGNARD reagent to the

carbonyl was not observed. Instead, an aldol addition occurred and product **61** was isolated in 75% yield (Scheme 19). Cyclopropylcarbinol **60** was eventually available by ruthenium-catalysed addition of benzaldehyde hydrazone as a carbanion equivalent in 68% yield.<sup>99</sup>



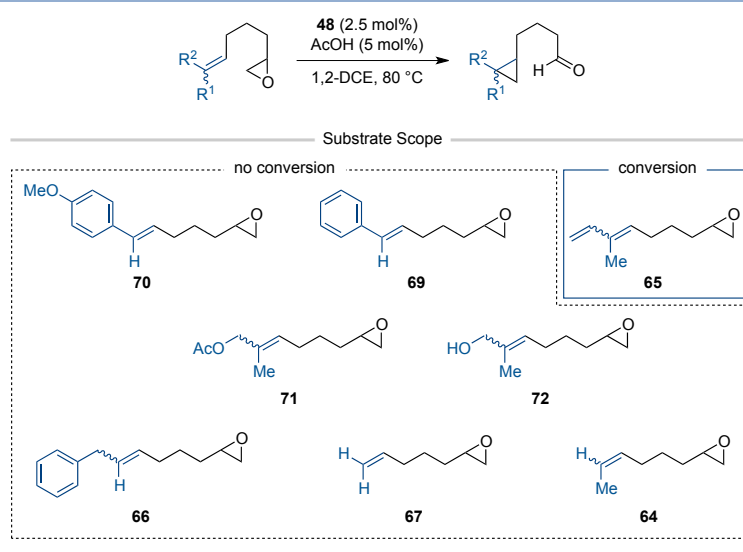
**Scheme 20.** Preparation of cyclopropylcarbinols via attack of various nucleophiles to cyclopropyl methyl ketone (**53**).

Subsequent treatment with hydrobromic acid in aqueous medium afforded homoallylic bromides **55**, **56** and **57** in moderate to good yields as mixtures of *E*- and *Z*-isomers. Preparation of the corresponding GRIGNARD reagents and copper-catalysed coupling to racemic epichlorohydrin (**63**) gave access to alkenyl epoxides **64**, **65** and **66** (Scheme 21). The terminal alkene **67** was accessible from commercially available 4-bromobut-1-ene and served further as a precursor for the aryl-substituted alkenes **69** and **70** via HECK coupling with iodobenzene and 1-iodo-4-methoxybenzene, as well as for epoxides **71** and **72** via metathesis with methallyl acetate and subsequent hydrolysis (Scheme 21).



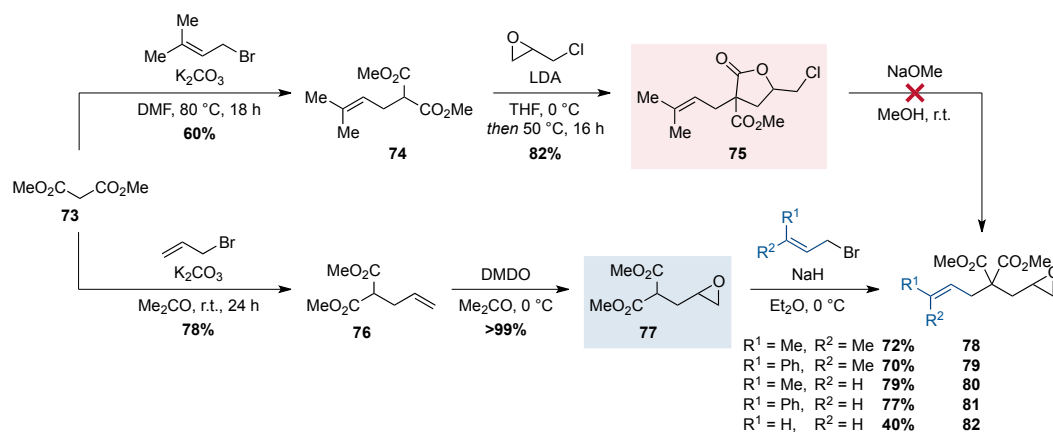
**Scheme 21.** Preparation of various alkenyl epoxides via copper-catalysed opening of epichlorohydrin and subsequent functionalisation of **67**.

Unfortunately, except for the vinyl-substituted substrate **65**, none of these alkenyl epoxides underwent methylene transfer (Table 3).

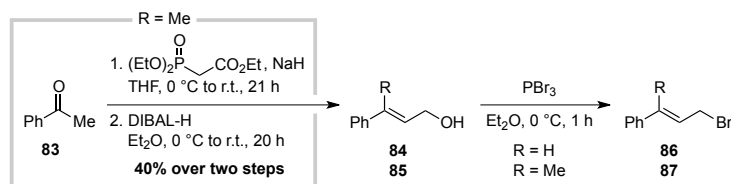
**Table 3.** Treatment of various alkenyl epoxides containing an unsubstituted alkyl chain with **48** and AcOH in 1,2-DCE.<sup>a</sup>

a) All reactions were performed on 60  $\mu\text{mol}$  scale and in a concentration of 0.1 M. The reaction progress was monitored by GC-MS.

Geminal disubstitution in acyclic chains tethering the two reaction centers accelerates intramolecular cyclisation reactions. This phenomenon is termed the *gem*-disubstituent effect, often also referred to as the THORPE-INGOLD effect.<sup>100</sup> Since the proposed mechanism for the methylene transfer involves a cyclisation step, it was of interest to apply this effect and evaluate its influence on the reaction. A suitable substrate design with two ester functionalities as the geminal substitutions would employ dimethyl malonate as the connecting building block, providing a potential access to the alkenyl-epoxide scaffold through double alkylation of the activated methylene with allylic bromides and epichlorohydrin (Scheme 22).



Preparation of bromides **86** and **87**

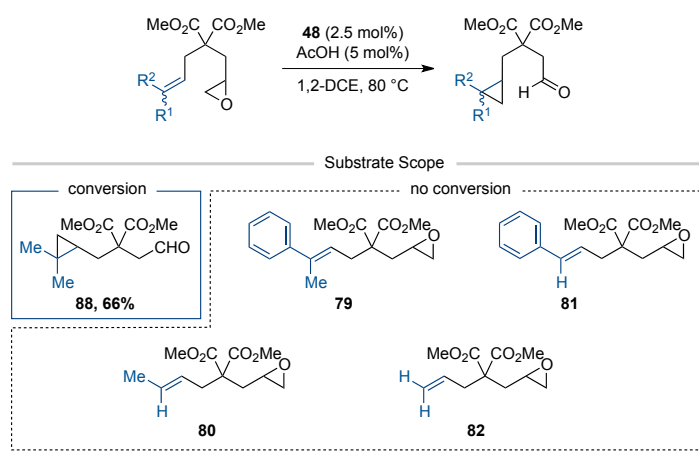
**Scheme 22.** Preparation of alkenyl epoxides bearing a geminal-disubstituted alkyl chain.

Initial efforts focussed on the installation of the epoxide on a later stage. However, when prenylated dimethyl malonate (**74**) was treated with epichlorohydrin under basic conditions, lactone **75** was isolated instead of the

desired epoxide (Scheme 22). Attempts to open the lactone with methoxide were unsuccessful. Therefore, the strategy was revised and it was envisioned to install the epoxide by epoxidation of an alkene. This was accomplished in a two-step sequence starting with the allylation of dimethyl malonate (**73**), followed by treatment with DMDO. Deprotonation of 1,3-diester **77** with sodium hydride and reaction with prenyl bromide afforded epoxide **78**. Varying the electrophile allowed the preparation of epoxides **79**, **80**, **81**, and **82**. Bromide **87** was available from acetophenone (**83**) in three steps.

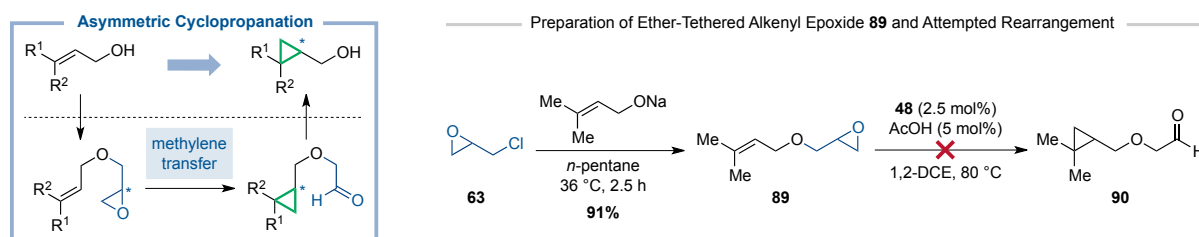
While epoxide **78** underwent complete conversion after 24 hours and the corresponding cyclopropane **88** could be isolated in 66% yield, none of the other epoxides reacted even after several days.

**Table 4.** Treatment of various alkenyl epoxides containing a geminal-disubstituted alkyl chain with **48** and AcOH in 1,2-DCE.<sup>a</sup>



a) All reactions were performed on 60  $\mu\text{mol}$  scale and in a concentration of 0.1 M. The reaction progress was monitored by GC-MS.

Finally, it was of interest to test whether this reaction could be translated into a general method for the stereoselective cyclopropanation of allylic alcohols. It was intended to functionalise the alcohol with epichlorohydrin and subsequently transfer the methylene group to the alkene. Reductive cleavage could then release the cyclopropanated alcohol. The advantage of this protocol is the direct transfer of stereochemistry from the epoxide, which can be introduced by employing the appropriate enantiomer of commercially available epichlorohydrin. Since alkenes with two methyl groups proved to be reliable substrates for the cobalt-catalysed cyclopropanation protocol, prenyl was chosen as a model substrate. Deprotonation with sodium in *n*-pentane as solvent, followed by treatment with limited equivalents of epichlorohydrin in order to suppress bisfunctionalisation of the epoxide gave product **89** in 91% yield with respect to epichlorohydrin. Unfortunately, no conversion to the corresponding cyclopropane **90** was observed under the investigated conditions (Scheme 23).



**Scheme 23.** Attempted method for the asymmetric cyclopropanation of allylic alcohols.

Based on these results, it was concluded that the intramolecular methylene transfer of alkenyl epoxides was deemed unsuitable as a general method for the cyclopropanation of alkenes. The investigated catalytic system proved problematic, requiring specific substitution patterns and thereby severely limiting the substrate scope.

## 4 (+)-Plakortolide E and (-)-Plakortolide I

### 4.1 Introduction

#### 4.1.1 Endoperoxide Natural Products and Malaria

Natural endoperoxides constitute a class of secondary metabolites with unique structural architectures and a variety of potent biological and pharmacological activities, including antibacterial, antitumor and antimalarial properties. Therefore, these compounds represent valuable sources in drug discovery and drug development as potential lead structures.<sup>101</sup>

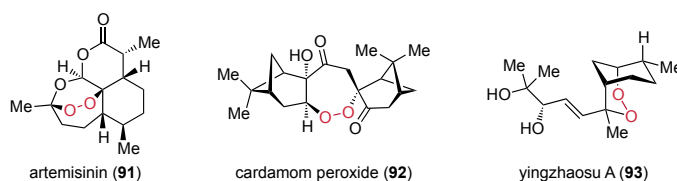


**Figure 8.** Natural products containing an endoperoxide motif.

The most prominent endoperoxide is the sesquiterpene lactone artemisinin (**91**) which was isolated in 1972 and identified as the active component in *Artemisia annua*, a common type of wormwood native to temperate regions of Asia.<sup>102</sup> This evergreen plant has been used for over 2000 years as a herbal remedy in traditional Chinese medicine to treat various diseases and symptoms such as jaundice, bacterial dysentery, fever and haemorrhoids.<sup>103</sup> Artemisinin and artemisinin-based drugs have proven especially valuable for combating malaria, an infectious disease caused by protozoan parasites of the genus *Plasmodium*, with *P. falciparum* being responsible for the most severe and fatal cases. The infection of the human host begins through the vector contribution of female mosquitos of the genus *Anopheles* (Figure 9).<sup>104</sup> Sporozoites transmitted during blood feeding rapidly migrate to the liver, where they invade hepatocytes. After a phase of differentiation and proliferation, merozoites are released which then infect mature human red blood cells, erythrocytes, and initiate cycles of asexual blood stage parasite growth, release and reinvasion. A small fraction of merozoites enter a phase of sexual development, producing gametocytes that can be taken up by *Anopheles* mosquitoes. The life cycle is then completed by sexual recombination of male and female gametes to form ookinetes, and eventually oocysts, which then produce sporozoites, ready for further infection.<sup>104</sup> Ensuing complications such as severe anemia, thrombocytopenia, and multiorgan dysfunction, including acute respiratory distress syndrome, acute renal failure, and cerebral herniation, constitute primary causes of death.<sup>105</sup> The highly potent anti-*Plasmodium* efficacy of artemisinin *in vitro* can be attributed to its endoperoxide pharmacophore embedded in a unique 1,2,4-trioxane structure. Although the exact mechanism of action has not been fully elucidated and is still controversial it has been proposed that iron(II)-induced degradation of the peroxide bond via one-electron reduction into free radicals – a pair of oxyl radical intermediats which then rearrange either via 1,5 hydrogen shift or  $\beta$ -scission into carbon-centred radicals as strong alkylating agents – causes oxidative stress and cellular damage (Figure 9).<sup>106</sup> Malaria parasites develop inside erythrocytes, hemoglobin-rich cells that contain iron(II)-centred porphyrin domains, of their human host. Within their digestive vacuole hemoglobin is then degraded by various proteases to release peptides and amino acids required for the parasite protein synthesis.<sup>107</sup> The iron(II)-containing heme moiety itself is not catabolised but rather oxidised into hemozoin, causing oxidative stress. Detoxification of hemozoin is achieved by the parasite through incorporation

into an insoluble non-toxic crystal lattice of heme dimers called hemozoin.<sup>108</sup> Hence, the abundance of iron(II)-heme, that becomes accessible upon degradation of hemoglobin, could serve as a potential source of activation.<sup>109</sup> This hypothesis is supported by the high activity of artemisinin-based drugs against trophozoites, in which hemoglobin catabolism peaks.<sup>110</sup> Furthermore, early ring stage parasites are effected as well, which can be explained by recent data suggesting that hemoglobin proteolysis and release of heme are already initiated at this stage.<sup>111</sup>

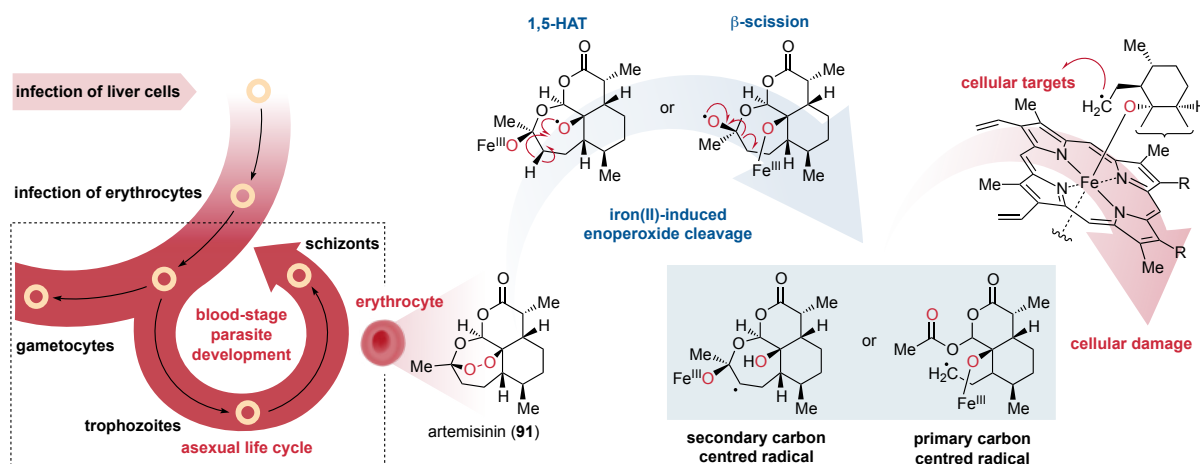


**Figure 9.** Human stages of the *Plasmodium*'s life cycle<sup>104</sup> and the proposed mechanism of artemisinin-based drugs.

The emerging resistance of parasites to traditional drugs such as quinine, chloroquine, and mefloquine and the discovery of artemisinin heralding a major breakthrough in the treatment of malaria fueled the exploration of endoperoxide-containing natural products as promising antimalarials.<sup>104,112</sup> While most of these naturally occurring cyclic peroxides possess a 1,2-dioxolane or 1,2-dioxane structure, such as yingzhaosu A (**93**) (Figure 8) which was isolated by LIANG and co-workers in 1979 from *Artabotrys uncinatus*,<sup>113</sup> some medium sized peroxide architectures have also been identified. For instance, the diterpenoid cardamom peroxide (**92**), which was isolated by CLARDY and co-workers in 1995 from *Amomum krervanh* Pierre, the fruit of Thai cardamom, features a distinct 1,2-dioxepane ring (Figure 8).<sup>114</sup>

#### 4.1.2 Marine Natural Products

Besides the large pool of terrestrial sources marine organisms have proven as prolific sources for endoperoxide natural products in recent years. However, compared to the rich history of plant-based extracts as remedies in traditional medicine and the identification of their phytoconstituents, the utilisation of marine-originated substances is still in its infancy.<sup>47</sup> With approximately 71% of the earth's surface covered by sea, the marine flora and fauna offer still uncharted resources for novel structures that cover unprecedented biologically relevant chemical space.<sup>115</sup> As a result of extreme conditions, such as high pressure, low oxygen concentrations and temperatures as well as the absence of light, that drastically differ from those in terrestrial habitats, a rich body of biodiversity, harbouring numerous unique secondary metabolites with intriguing biological activities, has emerged.<sup>47a</sup> A comparative analysis of molecular scaffolds showed that marine natural products are superior in terms of chemical novelty. Furthermore, marine organisms seem to have a higher incidence of significant bioactivity. This is reflected in a preclinical cytotoxicity screen, which revealed that approximately 1% of the tested marine samples exhibited antitumor properties compared to only 0.1% of the tested terrestrial samples.<sup>116</sup>



### 4.1.3 Characteristic Endoperoxide Metabolites of Marine Sponges

In this context marine sponges constitute an attractive source of structurally novel bioactive metabolites.<sup>117</sup> In particular, members of the genus *Plakortis* and *Plakinastrella*, both belonging to the family *Plakinidae*, have provided a large number of endoperoxide-containing polyketides with interesting pharmacological properties.<sup>118</sup>

Chondrillin (**94**), isolated from sponges of the genus *Chondrilla* by WELLS in 1976,<sup>119</sup> and plakortin (**95**), isolated from sponges of the genus *Plakortis* by FAULKNER and HIGGS in 1978,<sup>120</sup> were the first two of these cyclic peroxides isolated from marine sources (Figure 10). While chondrillin was shown to exhibit *in vitro* cytotoxicity against murine P388 leukaemia cells, plakortin possesses antimalarial activity against chloroquine-resistant strains of *Plasmodium falciparum*.<sup>121</sup> Ever since, a plethora of such plakortin type polyketides, many with either five- or six-membered endoperoxide subunits, have been isolated from marine sponges.<sup>101</sup>

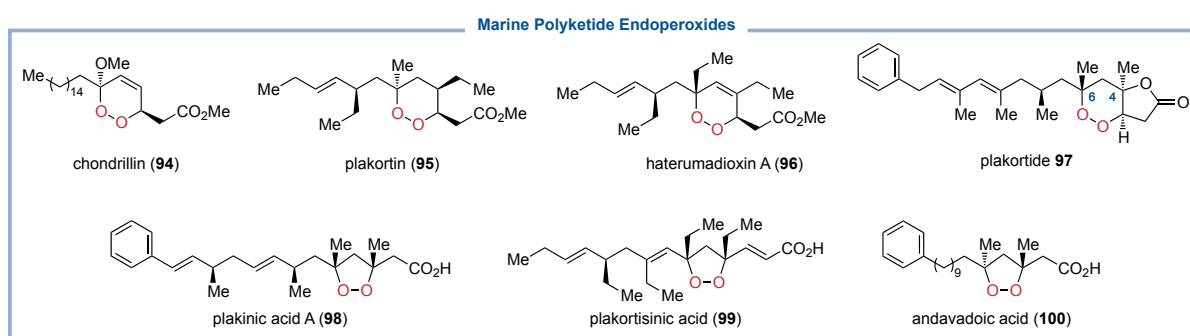


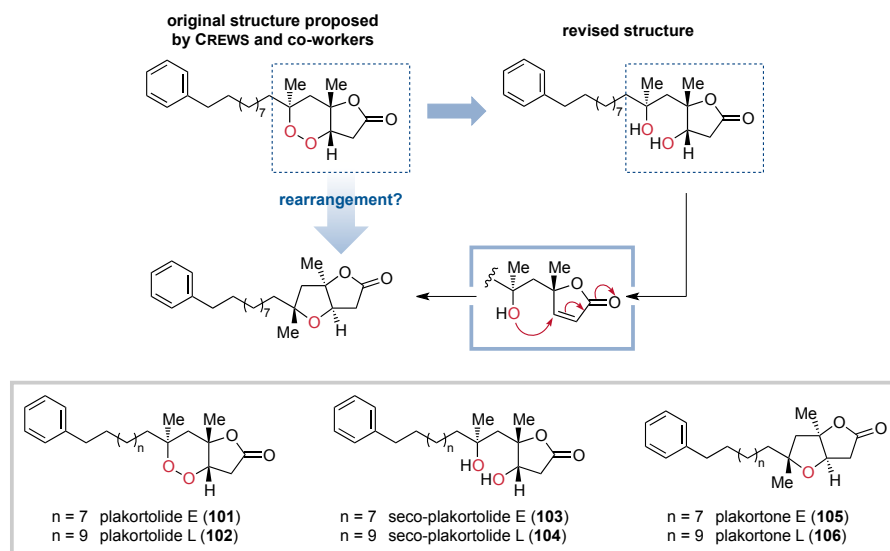
**Figure 10.** Various polyketide-endoperoxides from marine sources.<sup>101</sup>

### 4.1.4 Isolation of Plakortolide E and Plakortolide I

The first reported plakortolide **97** (Figure 10) was isolated by FAULKNER and STIERLE in 1980 from a Caribbean sponge of the genus *Plakortis*.<sup>122</sup> The structural assignment was elucidated by analysis of spectroscopic (IR, <sup>1</sup>H NMR and <sup>13</sup>C NMR) and mass spectrometric data in combination with oxidative degradation experiments. The relative and absolute stereochemistry was later determined by optical rotation computations.<sup>123</sup> Various plakortolides have been isolated since then, all characterised by the bicyclic 1,2-dioxane-fused butyrolactone with methyl substituents in C-4 and C-6 position as a common structural motif. Variations in the side chain comprise length, degree of saturation and methylation as well as the nature of terminal group, generally a phenyl or 4-hydroxyphenyl unit.

In 1995 CREWS and co-workers isolated a new plakortolide metabolite – initially coined plakortolide E – from a Fijian sponge of the genus *Plakortis* which exhibited *in vitro* activity against melanoma cancer cell lines.<sup>124</sup> The structure was assigned by NMR spectroscopy and mass spectrometry and the relative and absolute configuration of its stereogenic centers were determined by NOESY NMR experiments and the modified MOSHER's method respectively. Furthermore, the authors noted that rearrangement of some samples to plakortone **105** was observed after storage of approximately one year (Scheme 24). However, when GARSON and co-workers reported the isolation and characterisation of the homologous plakortolides L (**102**), its corresponding seco-derivative **104** and the stereochemically related plakortone **106**, the authors noticed that the previously published NMR data by CREWS and co-workers were in disagreement with the structural assignment.<sup>125</sup> Instead, the spectroscopic data matched those of seco-plakortolide L (**104**) except for alkyl chain length and absolute configuration, thereby explaining the rearrangement of CREW's samples to plakortone E

(**105**) via dehydration and oxa-MICHAEL addition (Scheme 24). This conclusion was confirmed by VATÈLE and BARNYCH in 2012 with the total synthesis of seco-plakortolide E (**103**) and plakortolide E (**101**), which corresponds to the initial structure proposed by CREWS and co-workers.<sup>126</sup>



**Scheme 24.** Structures of plakortolide E (**101**) and L (**102**) and rearrangement products.<sup>126</sup>

(-)-Plakortolide I (**107**) was isolated by FAULKNER and co-workers in 1998 from a Philippine sponge of the genus *Plakinastrella* (Figure 11).<sup>127</sup> Five years later the isolation of its supposed enantiomer, (+)-plakortolide I, from the extracts of the Madagascar marine sponge *Plakortis aff simplex* was reported by KASHMAN and co-workers.<sup>128</sup> However, with the works of VATÈLE and BARNYCH from 2012 it was shown that the metabolite isolated by KASHMAN and co-workers rather fits the structure **101** originally denoted plakortolide E (Figure 11).<sup>126</sup>

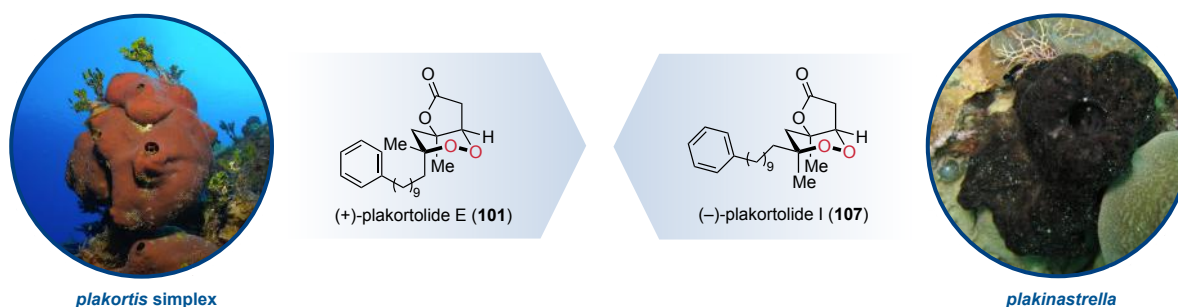
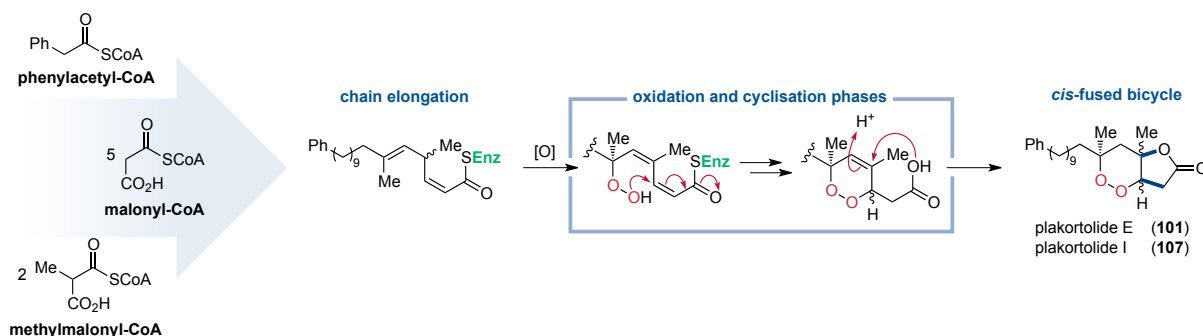


**Figure 11.** Structures of (+)-plakortolide E (**101**) and (-)-plakortolide I (**107**) which were isolated from sponges of the family *Plakinidae*.

#### 4.1.5 Biosynthesis of Plakortolide E and Plakortolide I

Although the biosynthesis of plakortin and plakortin-derived natural products is still a matter of debate, plausible biogenetic pathways have been proposed.<sup>129</sup> In general, all plakortin type polyketides could originate biosynthetically via some common linear precursors, which are accessible from acyl-CoA and malonyl-CoA building blocks through polyketide-synthase catalysed chain elongation (Scheme 25). Further functionalisation is then achieved by oxidation and cyclisation reactions. The endoperoxide scaffold could be generated either in a stepwise manner through a stereoselective hydroperoxide formation with molecular oxygen, similar to the biosynthesis of prostaglandins, and subsequent oxa-MICHAEL addition to the terminal  $\alpha,\beta$ -unsaturated carbonyl or in a concerted fashion via a DIELS-ALDER reaction of the acyclic diene with

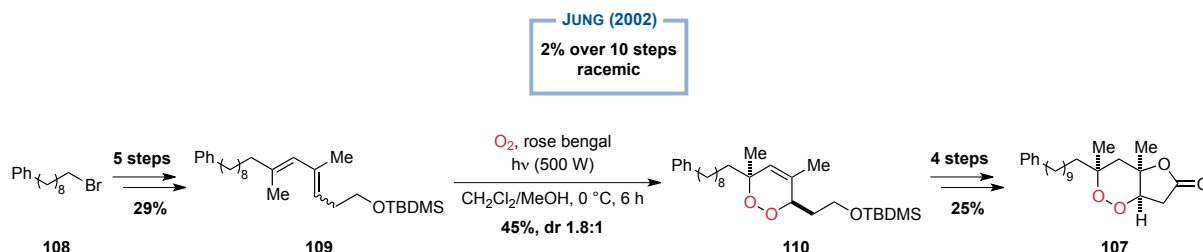
molecular oxygen (Scheme 25). The predicted stereochemical outcome of the latter, however, is in disagreement with the stereochemistry of some isolated compounds. Further transformations such as reduction of the endocyclic double bond, reductive cleavage of the peroxide, KORNBLUM-DELAMARE rearrangement, dehydrations or cyclisations give rise to a plethora structurally and stereochemically diverse plakortin-type polyketides. In the case of plakortolides, cyclisation by electrophilic addition of the carboxylic acid to the endocyclic double bond would furnish the butyrolactone core (Scheme 25).<sup>125</sup>



**Scheme 25.** Proposed biosynthesis of plakortolides via a common linear precursor for all plakortin-derived polyketides.

#### 4.1.6 Total Syntheses of Plakortolide E and Plakortolide I

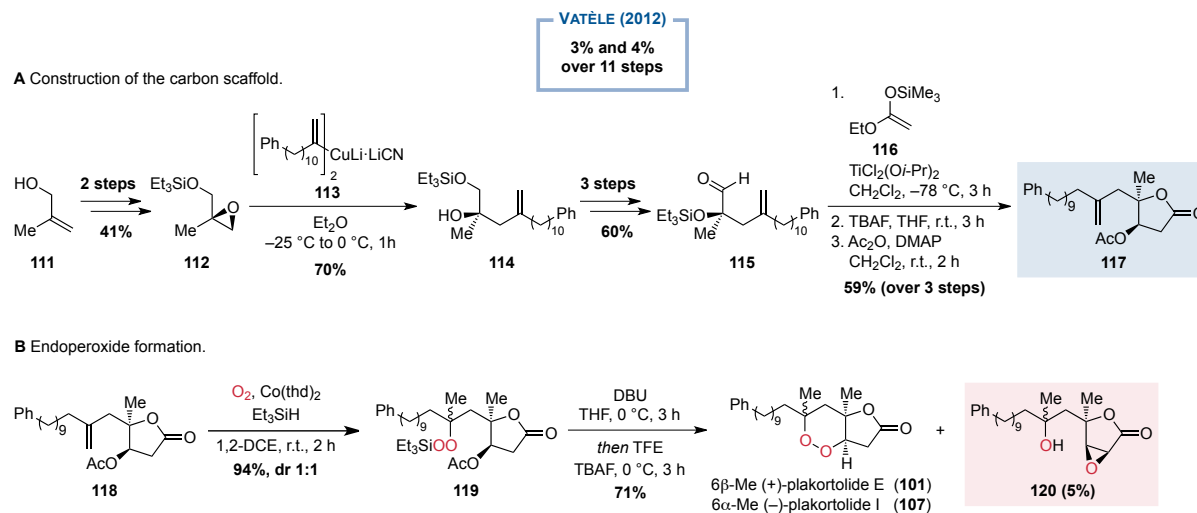
The first total synthesis of plakortolide I was described by JUNG and co-workers in 2002.<sup>130</sup> Starting from 1-bromo-10-phenyldecane (**108**) the carbon skeleton was built up by a sequence of GRIGNARD additions and a hydroboration to give diene **109**. Installation of the endoperoxide was achieved by addition of singlet oxygen in moderate yield of 45% and a diastereomeric ratio of 1.8:1 in favour of the desired product **110**. Oxidation of the primary alcohol and iodolactonisation followed by radical defunctionalisation eventually afforded racemic ( $\pm$ )-plakortolide I (**107**) (Scheme 26).



**Scheme 26.** First total synthesis of racemic plakortolide I by JUNG and co-workers.<sup>130</sup>

Ten years later VATÈLE and BARNYCH published the first enantioselective total synthesis of (–)-plakortolide I and its C6-epimer, which was shown to possess the structure of plakortolide E (Scheme 27).<sup>126a</sup> The carbon scaffold was constructed from protected 2-methylglycidol **112**, which in turn is available from  $\beta$ -methallyl alcohol (**111**) via enantioselective SHARPLESS epoxidation. Unfortunately, the authors did not report the enantiomeric excess. Epoxide opening with cuprate **113** and subsequent protection of the tertiary alcohol as well as oxidation of the primary alcohol delivered aldehyde **114**. MUKAIYAMA aldol addition with silyl ketene acetal **116** in the presence of TiCl<sub>2</sub>(*i*-OPr)<sub>2</sub> at –78 °C delivered selectively the *syn*-product. Deprotection of the tertiary alcohol promoted lactonisation while the secondary alcohol was subjected to acetylation with the purpose of generating a potential leaving group for late-stage butenolide formation. Installation of the endoperoxide was then planned in a two-step sequence, a MUKAIYAMA-ISAYAMA hydroperoxysilylation and an oxa-MICHAEL addition. Initial attempts lead to the formation of the butenolide via simple elimination of the acetate as well as epoxide **120**, presumably as the result of a WEITZ-SCHEFFER type epoxidation under the

basic conditions, as side products in considerable yield. In order to suppress undesired pathways the authors buffered the reaction mixture by the addition of 2,2,2-trifluoroethanol. The optimised conditions eventually afforded both natural products plakortolide E (**101**) and plakortolide I (**107**) in 37% yield and 34% yield, respectively (Scheme 27).



**Scheme 27.** Enantioselective total synthesis of (+)-plakortolide E (**101**) and (-)-plakortolide I (**107**) by VATÈLE and BARNYCH.<sup>126a</sup>

## 4.2 Objective

Despite the adoption of an artemisinin combination therapy (ACT) in the early 2000s to minimise the chance of developing resistances, several Southeast Asian countries have reported the emergence of parasites with decreased susceptibility to artemisinin derivatives and ACT partner drugs in recent years.<sup>104</sup> Regarding the life-threatening course of malaria the need for new antimalarial substances is therefore a constant focus in medicinal research. Inspired by the fascinating molecular structures and the pharmacological potential of marine endoperoxides, especially in the context of global interest in antimalarial drugs, the following part of this thesis pursued a rapid synthetic access towards plakortolide E and plakortolide I. Based on the total synthesis of (+)-Greek tobacco lactone (**1**), a common butyrolactone precursor was envisaged to constitute a general approach for the synthesis of various plakortolide natural products from linalool as a sustainable resource (Figure 12).

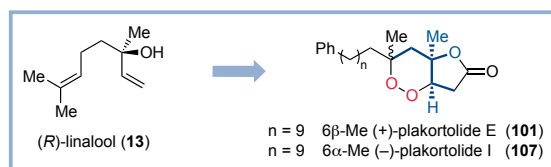
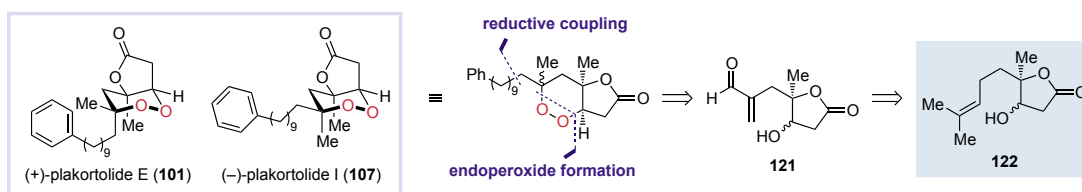


**Figure 12.** Development of an efficient synthesis of the endoperoxide-containing natural products (+)-plakortolide E (**101**) and (-)-plakortolide I (**107**) starting from (*R*)-linalool.

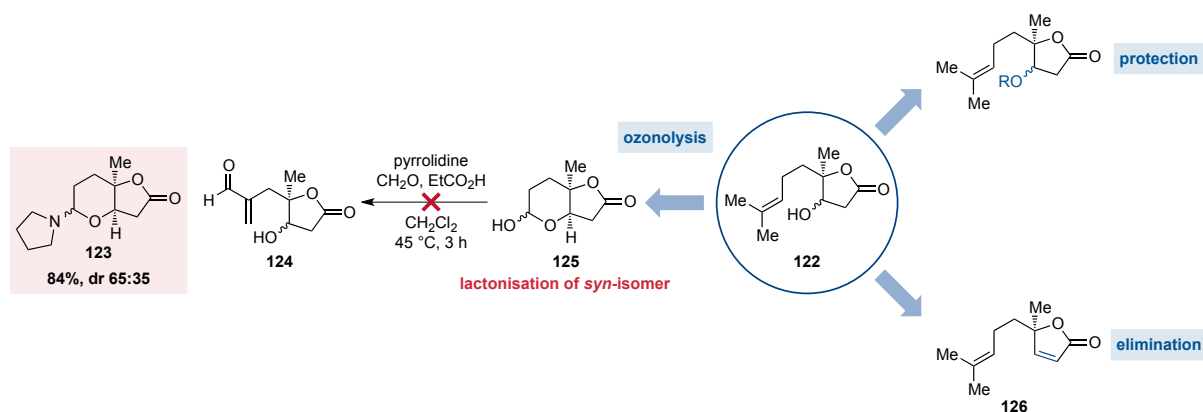
### 4.3 Unpublished Results – Preliminary Studies

Inspired by the total synthesis of (+)-Greek tobacco lactone (**1**)<sup>91</sup> both natural products **101** and **107** were retrosynthetically deconstructed to reveal butyrolactone **122** as a common precursor, available as previously described from (*R*)-linalool (**13**). Formation of the endoperoxide was based on the hydroperoxidation/oxa-MICHAEL addition sequence of VATÈLE and BARNYCH while installation of the side chain was envisioned by a reductive coupling to enal **121**. The  $\alpha,\beta$ -unsaturated aldehyde in turn could be accessible from the key intermediate **122** by modification of its prenyl chain (Scheme 28).



**Scheme 28.** Retrosynthetic analysis of (+)-plakortolide E (**101**) and (-)-plakortolide I (**107**).

Previous studies by F. BIENVENU revealed a challenge inherent to the substrate.<sup>131</sup> Whereas ozonolysis of the *trans*-butyrolactone of **122** furnished the corresponding aldehyde, that could be converted to the desired enal, the *cis*-butyrolactone of **122** resulted in formation of lactol **125** as a mixture of diastereomers, which were inert to the following  $\alpha$ -methylenation. Instead, only incorporation of pyrrolidine by formation of hemiaminal **123** under the organocatalytic conditions for the aldol condensation with formaldehyde was observed. Hence, in order to avoid forfeiting the *cis*-isomer, due to inhibition of  $\alpha$ -methylenation by lactol formation, either protection or elimination of the hydroxyl group was envisaged prior to ozonolysis (Scheme 29).

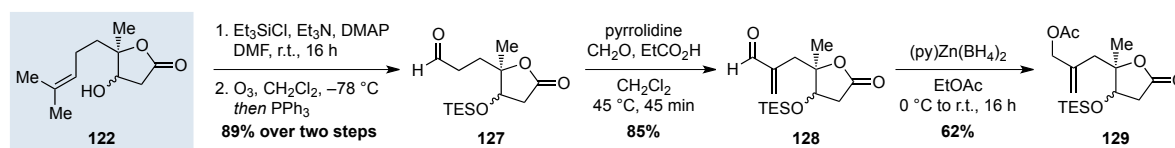


**Scheme 29.** Encountered challenges during preliminary studies and potential solutions.

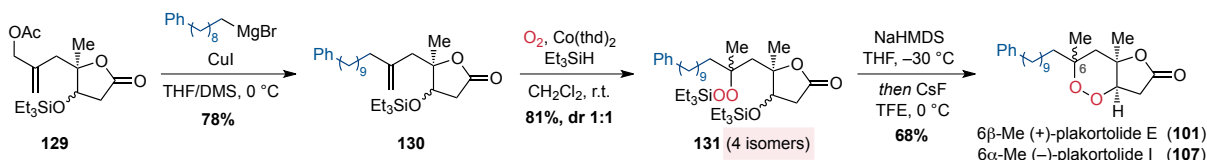
Both approaches were investigated by A. MAVROSKOUFIS.<sup>132</sup> Since a potential chemoselectivity challenge concerning the double bonds present in butenolide **126** could arise, protection of the alcohol with a silyl-based protecting group was pursued initially. Treatment of butyrolactone **122** with triethylsilylchloride under basic conditions and subsequent ozonolysis of the crude product afforded both diastereomeric aldehydes in very good yields. The following  $\alpha$ -methylenation and one-pot reductive acetylation eventually gave the allylic acetate **129** as precursor for the planned reductive coupling. Introduction of the side chain was then realised by copper-mediated substitution in 78% yield and the resulting alkene was subjected to MUKAIYAMA-ISAYAMA hydroperoxysilylation affording four diastereomers in 81% yield and a 1:1 diastereomeric ratio for each of the epimeric silyl alcohols. Sequential elimination of the silyl-protected alcohol with NaHMDS and

desilylation of the peroxide with CsF facilitated the desired oxa-MICHAEL addition to give both natural products in 68% yield in a one-pot process (Scheme 30).

**A** Synthesis of the coupling precursor (**129**).

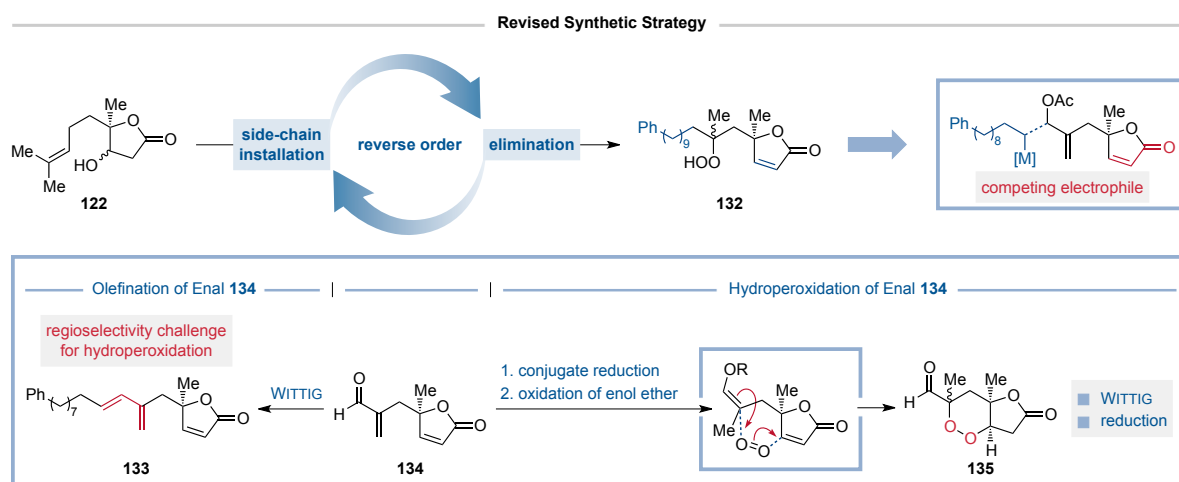


**B** Reductive coupling via allylic substitution and *endo*-peroxide formation.



**Scheme 30.** Synthesis of (+)-plakortolide E (**10**) and (-)-plakortolide I (**107**) enabled by protection of the alcohol.

However, this approach suffered from the use of protecting groups and the formation of complex mixtures with up to four diastereomeric products. Considering the alternative strategy of shifting the elimination to an earlier stage would solve both problems by removing the additional stereocenter and unprotected hydroxyl group. Unfortunately, preceding butenolide formation could render the side-chain installation via copper-catalysed allylic substitution inaccessible since the MICHAEL system represents a competing electrophile that is prone to react with cuprate reagents potentially yielding conjugate addition products (Scheme 31). To circumvent the challenge of organometal-based allylic substitutions the synthetic strategy was revised with enal **134** as the key intermediate and installation of the side chain was envisaged via WITTIG reaction followed by hydrogenation. However, hydroperoxidation would have to be performed prior to reduction of the double bond and further considerations of potential regioselectivity challenges reveal the necessity of an  $\alpha$ -oxidation of the aldehyde (Scheme 31). Typical protocols for this type of transformation proceed via deprotonation of the carbonyl and subsequent exposure to either triplet or singlet oxygen.<sup>133</sup>

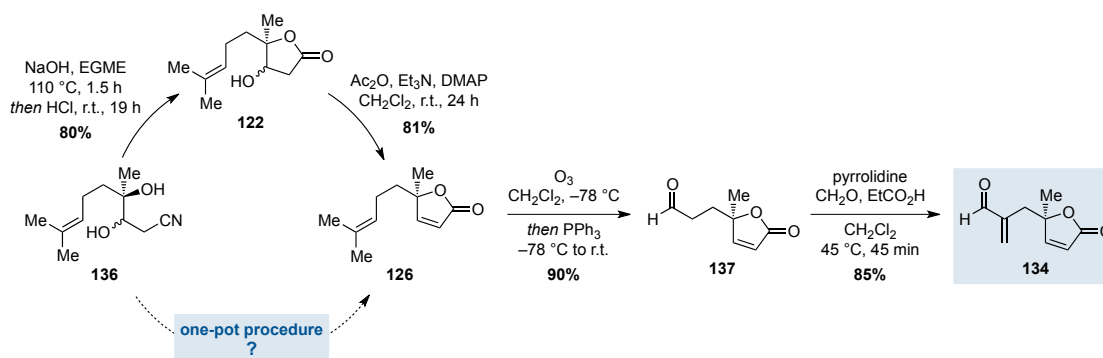


**Scheme 31.** Revised Synthetic Strategy with butenolide formation on an early stage and chemo- and regioselectivity considerations.

To this end, preparation of enal **134** was investigated. Elimination of the hydroxyl group was achieved by treatment of butyrolactone **122** with acetic anhydride in the presence of triethylamine and catalytic amounts



of DMAP. In order to further improve the synthesis a one-pot procedure of lactonisation and elimination could be envisioned to convert nitrile **135** directly into butenolide **126**. Functionalisation of the side chain via ozonolysis and  $\alpha$ -methylenation eventually afforded enal **134** in 77% yield over two steps (Scheme 32).



**Scheme 32.** Preparation of enal **134**.

Next, various conditions utilising triethylsilane for a conjugate reduction and *in situ* trapping of the resulting enolate were investigated. Surprisingly, a protocol by LIPSHUTZ and co-workers, employing STRYKER's reagent only provided the  $\alpha,\beta$ -saturated aldehyde (Table 5, Entry 1).<sup>134</sup> Although WILKINSON's catalyst already delivered the desired silyl enol ether **138** in 37% yield (Table 5, Entry 2),<sup>135</sup> the best results were obtained with palladium catalysts. While Pd/C afforded the product in 51% yield (Table 5, Entry 3),<sup>136</sup> a system of palladium-nanoparticles, generated from PdCl<sub>2</sub>/PCy<sub>3</sub>,<sup>137</sup> improved the yield significantly and silyl enol ether **138** was isolated in 85% yield (Table 5, Entry 4). Alternatively, a one-pot protocol reported by PIHKO and co-workers for the  $\alpha$ -hydroperoxidation of  $\alpha$ -substituted enals was tested.<sup>138</sup> The authors proposed the formation of metastable enols by conjugate reduction under aqueous and neutral conditions that upon exposure to air can undergo autoxidation to furnish the corresponding hydroperoxides. Unfortunately, neither the  $\alpha$ -hydroperoxide **141** nor any degradation product thereof could be identified and only the formation of the  $\alpha,\beta$ -saturated aldehyde **140** was observed. Presumably, tautomerisation is too rapid and the equilibrium is shifted almost exclusively towards the aldehyde, thereby suppressing/disabling the desired  $\alpha$ -oxidation.

**Table 5.** Conjugate reduction of enal **134** and *in situ* trapping of the enolate.

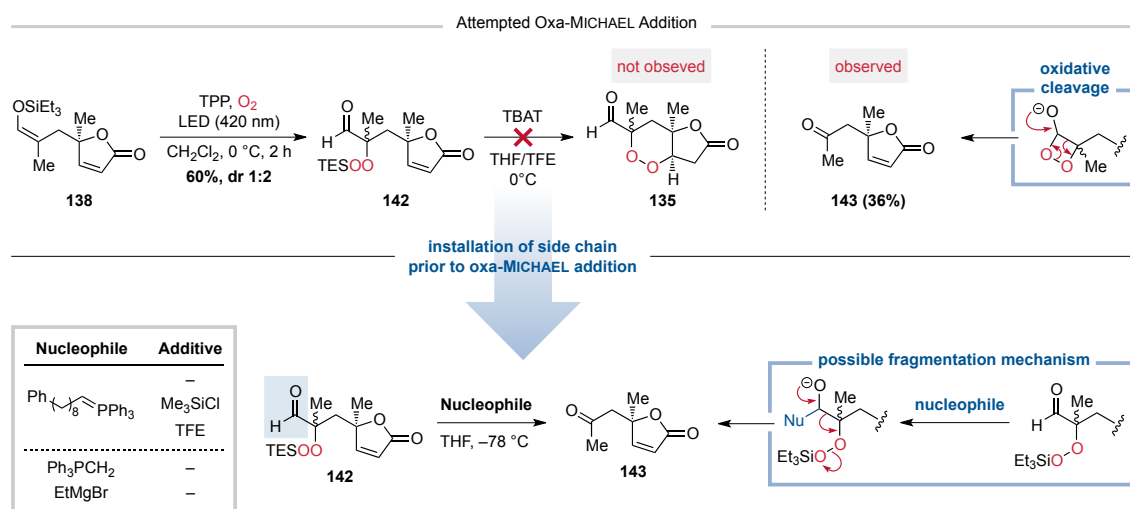
Entry	Catalyst	T	Yield
1	[(PPh <sub>3</sub> )CuH] <sub>6</sub> (5 mol%)	r.t.	0%
2 <sup>a</sup>	RhCl(PPh <sub>3</sub> ) <sub>3</sub> (5 mol%)	60 °C	37%
3	Pd/C (5 wt%)	r.t.	51%
4	PdCl <sub>2</sub> (1.5 mol%), PCy <sub>3</sub> (3 mol%)	r.t.	85%

a) The reaction was performed in anhydrous toluene.

With enol ether **138** in hand, installation of the peroxide was addressed. While the direct treatment with triplet oxygen resulted in no conversion, preceding desilylation to enhance nucleophilicity led only to degradation even at  $-78$  °C. It was speculated that undesired reactions can be attributed to the strong basic conditions, that

represent a challenge for aldehydes due to the tendency of aldol self-condensation as well as the instability of the anionic  $\alpha$ -peroxy products.<sup>133</sup> In order to maintain neutral conditions, singlet oxygen, which is well known to react with silyl enol ethers to give silylperoxy carbonyl compounds thereby avoiding anionic intermediates and corresponding degradation pathways, was tested. Gratifyingly, the reaction proceeded without noticeable formation of side products and the silylperoxide **142** could be isolated in 60% yield (Scheme 33). In contrast to the MUKAIYAMA-ISAYAMA hydroperoxysilylation the oxidation with singlet oxygen exhibits some degree of diastereoselectivity affording a mixture of two diastereomers in a ratio of 1:2. To initiate the envisioned oxa-MICHAEL addition deprotection was performed with TBAT in the presence of 2,2,2-trifluoroethanol as an acidic buffer. Surprisingly, ketone **143** was isolated as the only observable product in 36% yield. Presumably, 1,2-dioxetane formation is kinetically favoured followed by oxidative cleavage. Thus, it was necessary to install the side chain prior to deprotection of the hydroperoxide. Unfortunately, WITTIG reaction with triphenyl(9-phenylnonylidene)phosphorane afforded the same degradation product **143**. Oxidative cleavage in this case could be rationalised by a fragmentation mechanism which is initiated by the addition of nucleophiles to the aldehyde and subsequent collapse of the tetrahedral intermediate with triethylsiloxide as the leaving group. However, this would imply that degradation is faster than oxaphosphetane formation. Neither the addition of  $\text{Me}_3\text{SiCl}$  nor TFE to capture the alkoxide improved the reaction and only oxidative cleavage occurred (Scheme 33). When commercially available WITTIG salts or ethylmagnesium bromide as a control nucleophile were employed the same result was observed thereby supporting the mechanistic hypothesis.



**Scheme 33.** Attempted endoperoxide formation via oxa-MICHAEL addition.

Consequently, this approach was deemed unfeasible and a combination of both strategies, butenolide formation to avoid a complex mixture of diastereomers and protecting groups as well as the late-stage endoperoxide formation after installation of the side chain, was pursued. Further studies addressed the chemoselectivity challenge of an organometal-mediated allylic substitution in the presence of the  $\alpha,\beta$ -unsaturated lactone and thus enabled a seven-step synthesis of (+)-plakortolide E and (-)-plakortolide I.<sup>139</sup>



## 4.4 Publication

### 4.4.1 Synthesis of Plakortolides E and I Enabled by Base Metal Catalysis

---

<b>Authors</b>	Stefan Leisering, Alexandros Mavroskoufis, Patrick Voßnacker, Reinhold Zimmer, and Mathias Christmann
<b>Journal</b>	<i>Org. Lett.</i> <b>2021</b> , 23, 4731–4735
<b>DOI</b>	10.1021/acs.orglett.1c01457
<b>Abstract</b>	A protecting-group-free synthesis of two endoperoxide natural products, plakortolide E and plakortolide I, is reported. Key steps are a vanadium-mediated epoxidation, an iron-catalyzed allylic substitution, and a cobalt-induced endoperoxide formation. Our approach combines chemoselective bond-forming reactions and one-pot operations to forge an overall efficient synthesis.
<b>Author Contribution</b>	<p>The concept of the manuscript was elaborated by S. Leisering, Dr. R. Zimmer, and Prof. Dr. M. Christmann.</p> <p>A. Mavroskoufis optimised the conditions for both one-pot procedures. The rest of the synthesis, including the collection of all associated analytical data, was carried out by S. Leisering. The crystal of compound <b>1</b> for X-ray diffraction analysis was provided by S. Leisering and the measurement and analysis was performed by P. Voßnacker.</p> <p>The Manuscript was written by S. Leisering and Prof. Dr. M. Christmann.</p>

---

Permission for reproduction in print and electronic format for the purpose of this dissertation is granted by:

Copyright © 2021 American Chemical Society

## Synthesis of Plakortolides E and I Enabled by Base Metal Catalysis

Stefan Leisering, Alexandros Mavroskoufis, Patrick Voßnacker, Reinhold Zimmer, and Mathias Christmann\*



Cite This: *Org. Lett.* 2021, 23, 4731–4735



Read Online

ACCESS |



Metrics & More

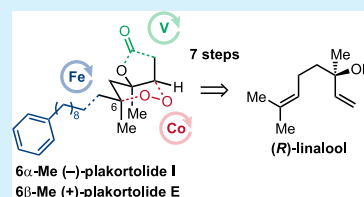


Article Recommendations



Supporting Information

**ABSTRACT:** A protecting-group-free synthesis of two endoperoxide natural products, plakortolide E and plakortolide I, is reported. Key steps are a vanadium-mediated epoxidation, an iron-catalyzed allylic substitution, and a cobalt-induced endoperoxide formation. Our approach combines chemoselective bond-forming reactions and one-pot operations to forge an overall efficient synthesis.



In synthesis planning, it is desirable to derive the target molecule from a carefully selected starting material through a sequence of successive construction steps with minimal functional group interconversions or protecting-group manipulations.<sup>1</sup> The concepts of atom,<sup>2</sup> redox,<sup>3</sup> step,<sup>4</sup> and pot<sup>5</sup> economy provide guidelines to evaluate different synthetic approaches and to design an efficient synthesis.<sup>6</sup> With these considerations in mind, we embarked on developing rapid syntheses of plakortolides E (1) and I (2) from (*R*)-linalool, a readily available monoterpene with a seven-carbon overlap with the bicyclic core structure of the target including one stereogenic center. Methodologically, we focused on the use of base metal catalysts for some anticipated challenging chemoselective transformations.<sup>7</sup>

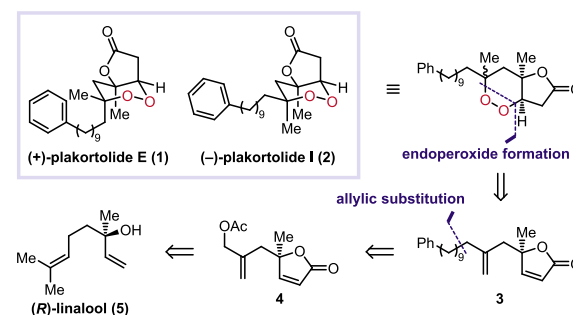
Endoperoxides from both terrestrial and marine sources constitute a class of natural products featuring a wide range of unique and often underexplored bioactivities.<sup>8</sup> For instance, several polyketide-derived endoperoxides such as plakinic acids, plakortides, and plakortolides show potential activity as antitumor, antibacterial, and antifungal agents.<sup>9</sup> Furthermore, terpene-based endoperoxides have proven as valuable compounds for combating malaria with artemisinin as the most important lead structure.<sup>10</sup>

The bicyclic 1,2-dioxane-fused butyrolactone plakortolide I (2) and its C6-epimer, plakortolide E (1), were isolated from marine sponges.<sup>11,12</sup> In 2002, Jung reported the first synthesis of racemic plakortolide I (2).<sup>13</sup> Ten years later, Vatele<sup>14</sup> described an asymmetric synthesis of (-)-plakortolide I (2) and (+)-plakortolide E (1).

In our retrosynthetic approach, we envisioned a late-stage endoperoxide formation by a tandem Mukaiyama hydroperoxidation/oxa-Michael addition sequence to access either of the two natural products. Installation of the side chain by allylic substitution would simplify both epimeric natural products 1 and 2 retrosynthetically to allyl acetate 4 which we traced back to our starting material 5. Herein, we report a seven-step synthesis of enantiopure (+)-plakortolide E (1) and

(-)-plakortolide I (2) from commercially available monoterpene (*R*)-linalool (5) (Scheme 1).

### Scheme 1. Retrosynthetic Analysis of (+)-Plakortolide E and (-)-Plakortolide I



The synthesis commenced with the chemoselective vanadium-catalyzed epoxidation of the terminal double bond providing the corresponding epoxide as an inconsequential mixture of two diastereomers (dr 3:2) in 74% yield (see the Supporting Information).<sup>16</sup> Opening of the epoxides with potassium cyanide under acidic conditions afforded nitrile 6 as a mixture of diastereomers (80% yield). Hydrolysis under basic conditions followed by acidic lactonization in an aqueous medium provided the corresponding butyrolactone in 80% yield after isolation (see the Supporting Information). In a subsequent step, elimination of the hydroxyl group was

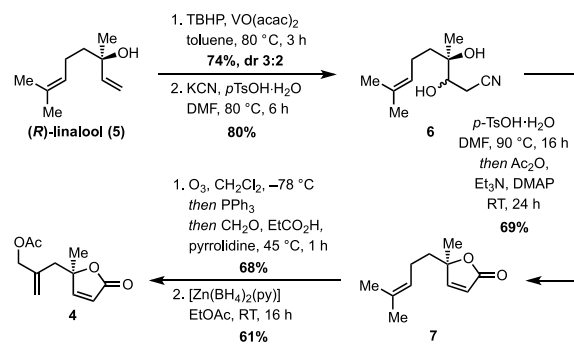
Received: April 28, 2021

Published: June 7, 2021



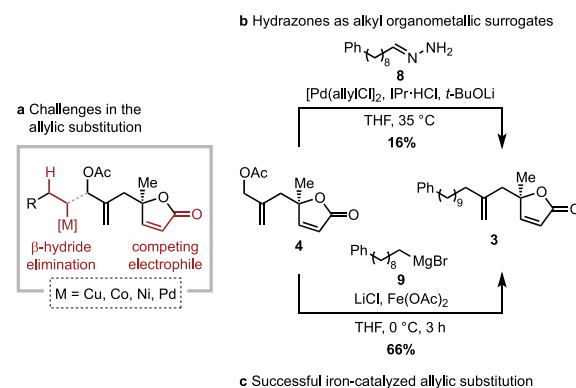
achieved by treatment with acetic anhydride in the presence of triethylamine to give the desired butenolide 7 in 81% yield. Gratifyingly, we found that the hydrolysis and the lactonization step could be combined in a tandem process mediated by *p*-TsOH·H<sub>2</sub>O in DMF. Upon treatment with acetic anhydride and triethylamine, elimination of the hydroxyl group was achieved, thus allowing the synthesis of butenolide 7 from nitrile 6 in a one-pot procedure with an overall yield of 69%. Butenolide 7 was subjected to a one-pot ozonolysis/ $\alpha$ -methylenation<sup>17</sup> (68% yield). The resulting enal was reduced by pyridine zinc borohydride in ethyl acetate to directly furnish allyl acetate 4 (Scheme 2).<sup>18</sup>

### Scheme 2. Synthesis of Allyl Acetate 4



With a precursor for the allylic substitution in hand, we investigated the installation of the side chain. Initial attempts to couple both fragments by cuprate-mediated allylic substitution failed. We recognized a chemoselectivity challenge imposed by the substrate, as it is known that many transition metals catalyze both allylic substitutions and conjugate additions.<sup>19</sup> To shut down the competing pathway, we investigated alternative processes.<sup>20</sup> Although palladium-catalyzed conjugate additions have been reported in recent years,<sup>21</sup> we anticipated that selectivity for the allylic substitution is achievable. However, typical nucleophiles for Tsuji–Trost-type reactions are either heteroatoms or stabilized carbanions, e.g., enolates, deprotonated sulfones and alkynes.<sup>20,22</sup> In contrast, the use of organomagnesium compounds is plagued by  $\beta$ -hydride elimination of the organometallic reagent or umpolung<sup>23</sup> of the  $\pi$ -allyl palladium complex into a nucleophile. When we examined the palladium-catalyzed allylic substitution with diethylzinc, we observed deoxygenation, presumably via  $\beta$ -hydride elimination and subsequent reductive elimination.<sup>24</sup> Although there have been reports by Maulide and co-workers to suppress those competing pathways and promote reductive elimination, their studies were limited to diethylzinc and required non-commercially available ligands.<sup>25</sup> Recently, Li and co-workers described a method for the palladium-catalyzed C-allylation of deprotonated hydrazones as surrogates for nonstabilized carbon nucleophiles.<sup>26</sup> When allyl acetate 4 was treated with hydrazone 8, the formation of coupling product 3 was observed, albeit in only 16% yield (Scheme 3). Next, we proceeded to investigate approaches involving cobalt, nickel, and iron catalysis as for these metals reactions with nonstabilized nucleophiles are described.<sup>27</sup> Unfortunately, attempts using cobalt and nickel suffered from either no conversion or decomposition. Recently, Jacobi von Wangelin

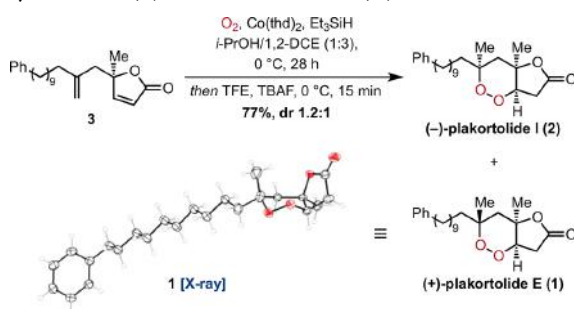
### Scheme 3. Chemoselective Allylic Substitution of 4



and co-workers showed that inexpensive Fe(OAc)<sub>2</sub> is an efficient catalyst for the allylic substitution with alkylmagnesium halides under mild conditions.<sup>27e</sup> Their protocol effectively inhibits competing  $\beta$ -hydride elimination without the need of stabilizing ligands or solvents. Initial treatment of allyl acetate 4 with alkylmagnesium bromide 9 in the presence of catalytic amounts of anhydrous Fe(OAc)<sub>2</sub> in Et<sub>2</sub>O gave no conversion, presumably due to limited solubility. Interestingly, we found that addition of anhydrous LiCl in THF afforded the desired product 3 in 66% yield (Scheme 3).<sup>27e</sup>

Having assembled the carbon skeleton, we addressed the remaining challenge of introducing the endoperoxide. Inspired by the application of cobalt-catalyzed hydrofunctionalizations with oxygen in total synthesis,<sup>28</sup> we anticipated a chemo- and regioselective hydroperoxidation of olefin 3 followed by an oxa-Michael addition in a tandem process to furnish both natural products 1 and 2. Based on the conditions employed by Vatele and Barnych, we treated 3 with Et<sub>3</sub>SiH and Co(thd)<sub>2</sub> in vigorously oxygen-saturated 1,2-dichloroethane.<sup>14</sup> Surprisingly, these conditions did not result in the conversion of the starting material even at prolonged reaction time or elevated temperature. We found that addition of protic solvents such as *i*-PrOH facilitated the conversion of olefin 3 which avoided undesired side reactions.<sup>14</sup> Under these conditions, the direct formation of endoperoxides 1 and 2 was observed, but was accompanied by decomposition of the products resulting in low isolated yields. Although decomposition reactions could be suppressed at 0 °C, the oxa-Michael addition was slowed and the intermediate was partially trapped as the corresponding silyl peroxide. This drawback was circumvented by *in situ* desilylation with TBAF in the presence of TFE (2,2,2-trifluoroethanol) to buffer the enolate resulting from the oxa-Michael reaction, thereby avoiding potential Weitz–Scheffer-type epoxidation.<sup>14,15</sup> This tandem endoperoxide formation afforded (–)-plakortolide I (2) in 42% yield, along with its C6-epimer (+)-plakortolide E (1) in 35% yield. Single crystals of 1 were grown and analyzed by X-ray analysis, thereby confirming the structure and absolute configuration of 1 and indirectly of 2 (Scheme 4).

To illustrate the efficiency of our synthesis, we applied a color-coded flowchart representation that was recently developed by our group (Figure 1).<sup>6c</sup> More than half of the transformations are strategic bond forming reactions that utilize all of the functional groups given by the chiral terpene starting material 5. Two functional group interconversions

Scheme 4. Tandem Endoperoxide Formation for the Synthesis of (+)-Plakortolide E and (-)-Plakortolide I<sup>a</sup>

<sup>a</sup>Thermal ellipsoids at 50% probability; disorder was omitted for clarity.

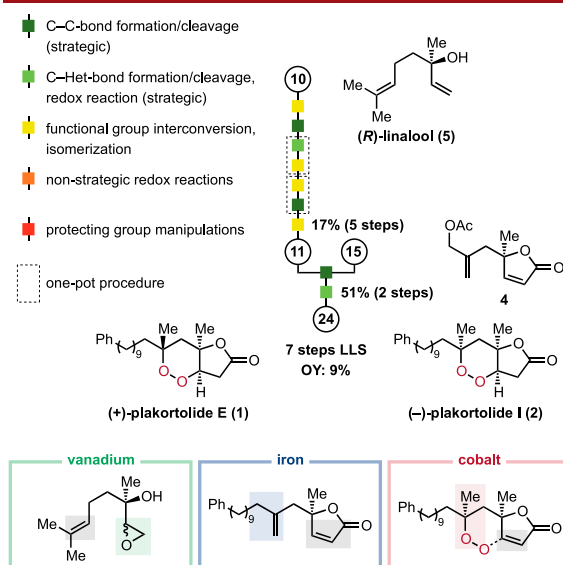


**Figure 1.** Flowchart representation of the synthesis of (+)-plakortolide E (1) and (-)-plakortolide I (2).

were combined with constructive bond formations in one-pot procedures to enhance the pot economy of the synthesis.

In conclusion, we have developed a concise synthesis of enantiopure (+)-plakortolide E (1) and (-)-plakortolide I (2) from commercially available (*R*)-linalool (5). By using  $\text{Fe}(\text{OAc})_2$  as catalyst, a chemoselective installation of the alkyl side chain was achieved in good yield.<sup>29</sup> This work demonstrates that a straightforward and protecting-group-free synthesis of endoperoxide natural products can be fueled by chemoselective transformations with earth-abundant transition-metal catalysts.

## ■ ASSOCIATED CONTENT

### Supporting Information

The Supporting Information is available free of charge at <https://pubs.acs.org/doi/10.1021/acs.orglett.1c01457>.

Experimental procedures and spectroscopic data (PDF)

## Accession Codes

CCDC 2074855 contains the supplementary crystallographic data for this paper. These data can be obtained free of charge via [www.ccdc.cam.ac.uk/data\\_request/cif](http://www.ccdc.cam.ac.uk/data_request/cif), or by emailing [data\\_request@ccdc.cam.ac.uk](mailto:data_request@ccdc.cam.ac.uk), or by contacting The Cambridge Crystallographic Data Centre, 12 Union Road, Cambridge CB2 1EZ, UK; fax: +44 1223 336033.

## ■ AUTHOR INFORMATION

### Corresponding Author

Mathias Christmann – Institute of Chemistry and Biochemistry, Freie Universität Berlin, 14195 Berlin, Germany; [orcid.org/0000-0001-9313-2392](https://orcid.org/0000-0001-9313-2392); Email: [mathias.christmann@fu-berlin.de](mailto:mathias.christmann@fu-berlin.de)

### Authors

Stefan Leisering – Institute of Chemistry and Biochemistry, Freie Universität Berlin, 14195 Berlin, Germany

Alexandros Mavroskoufis – Institute of Chemistry and Biochemistry, Freie Universität Berlin, 14195 Berlin, Germany

Patrick Voßnacker – Institute of Chemistry and Biochemistry, Freie Universität Berlin, 14195 Berlin, Germany

Reinhold Zimmer – Institute of Chemistry and Biochemistry, Freie Universität Berlin, 14195 Berlin, Germany

Complete contact information is available at:

<https://pubs.acs.org/10.1021/acs.orglett.1c01457>

### Notes

The authors declare no competing financial interest.

## ■ ACKNOWLEDGMENTS

We thank Luise Schefzig for preparative support and Merlin Kleoff (both at Freie Universität Berlin) for helpful discussions.

## ■ REFERENCES

- Hendrickson, J. B. Systematic Synthesis Design. IV. Numerical codification of construction reactions. *J. Am. Chem. Soc.* **1975**, *97*, 5784–5800.
- (a) Trost, B. M. The atom economy – a search for synthetic efficiency. *Science* **1991**, *254*, 1471–1477. (b) Trost, B. M. Atom Economy – A Challenge for Organic Synthesis: Homogeneous Catalysis Leads the Way. *Angew. Chem., Int. Ed. Engl.* **1995**, *34*, 259–281.
- Burns, N. Z.; Baran, P. S.; Hoffmann, R. W. Redox economy in organic synthesis. *Angew. Chem., Int. Ed.* **2009**, *48*, 2854–2867.
- (a) Wender, P. A.; Verma, V. A.; Paxton, T. J.; Pillow, T. H. Function-Oriented Synthesis, Step Economy, and Drug Design. *Acc. Chem. Res.* **2008**, *41*, 40–49. (b) Wender, P. A.; Miller, B. L. Synthesis at the molecular frontier. *Nature* **2009**, *460*, 197–201.
- (a) Hayashi, Y. Pot economy and one-pot synthesis. *Chem. Sci.* **2016**, *7*, 866–880. (b) Hayashi, Y. Time and Pot Economy in Total Synthesis. *Acc. Chem. Res.* **2021**, *54*, 1385–1398.
- (a) Newhouse, T.; Baran, P. S.; Hoffmann, R. W. The economies of synthesis. *Chem. Soc. Rev.* **2009**, *38*, 3010–3021. (b) Gaich, T.; Baran, P. S. Aiming for the Ideal Synthesis. *J. Org. Chem.* **2010**, *75*, 4657–4673. (c) Schwan, J.; Christmann, M. Enabling strategies for step efficient syntheses. *Chem. Soc. Rev.* **2018**, *47*, 7985–7995.
- (a) Zweig, J. E.; Kim, D. K.; Newhouse, T. R. Methods Utilizing First-Row Transition Metals in Natural Product Total Synthesis. *Chem. Rev.* **2017**, *117*, 11680–11752. (b) Beaumier, E. P.; Pearce, A. J.; See, X. Y.; Tonks, I. A. Modern applications of low-valent early transition metals in synthesis and catalysis. *Nat. Chem. Rev.* **2019**, *3*, 15–34. (c) Bullock, R. M.; Chen, J. G.; Gagliardi, L.; Chirik, P. J.;



- Farha, O. K.; Hendon, C. H.; Jones, C. W.; Keith, J. A.; Klosin, J.; Minter, S. D.; Morris, R. H.; Radosevich, A. T.; Raufuss, T. B.; Strotman, N. A.; Vojvodic, A.; Ward, T. R.; Yang, J. Y.; Surendranath, Y. Using nature's blueprint to expand catalysis with Earth-abundant metals. *Science* **2020**, *369*, No. eabc3183.
- (8) Bu, M.; Yang, B. B.; Hu, L. Natural Endoperoxides as Drug Lead Compounds. *Curr. Med. Chem.* **2016**, *23*, 383–405.
- (9) (a) Dembitsky, V. M.; Glorizova, T. M.; Poroikov, V. V. Natural Peroxy Anticancer Agents. *Mini-Rev. Med. Chem.* **2007**, *7*, 571–589. (b) Dembitsky, V. M. Bioactive peroxides as potential therapeutic agents. *Eur. J. Med. Chem.* **2008**, *43*, 223–251.
- (10) (a) Tu, Y. Artemisinin—A Gift from Traditional Chinese Medicine to the World (Nobel Lecture). *Angew. Chem., Int. Ed.* **2016**, *55*, 10210–10226. (b) Wang, J.; Xu, C.; Wong, Y. K.; Li, Y.; Liao, F.; Jiang, T.; Tu, Y. Artemisinin, the Magic Drug Discovered from Traditional Chinese Medicine. *Engineering* **2019**, *5*, 32–39.
- (11) Qureshi, A.; Salvà, J.; Harper, M.; Faulkner, D. J. New Cyclic Peroxides from the Philippine Sponge *Plakinastralla* sp. *J. Nat. Prod.* **1998**, *61*, 1539–1542.
- (12) (a) Rudi, A.; Afanii, R.; Gravalos, L. G.; Aknin, M.; Gaydou, E.; Vacelet, J.; Kashman, Y. Three New Cyclic Peroxides from the Marine Sponge *Plakortisaff simplex*. *J. Nat. Prod.* **2003**, *66*, 682–685. (b) Correction of the initially assigned structure to (+)-plakortolide E: Plakortolide Stereochemistry Revisited: Yong, K. W. L.; Barnych, B.; De Voss, J. J.; Vatele, J.-M.; Garson, M. J. The Checkered History of Plakortolides E and I. *J. Nat. Prod.* **2012**, *75*, 1792–1797.
- (13) Jung, M.; Ham, J.; Song, J. First Total Synthesis of Natural 6-Epiplakortolide. *Org. Lett.* **2002**, *4*, 2763–2765.
- (14) (a) Barnych, B.; Vatele, J.-M. Total Synthesis of *seco*-Plakortolide E and (–)-*ent*-Plakortolide I: Absolute Configurational Revision of Natural Plakortolide I. *Org. Lett.* **2012**, *14*, S64–S67. (b) Barnych, B. Synthetic studies towards plakortolides: asymmetric synthesis of *ent*-plakortolide I and *seco*-plakortolide E. Ph.D. Dissertation, Université Claude Bernard, Lyon I, 2011.
- (15) (a) Murakami, N.; Kawanishi, M.; Itagaki, S.; Horii, T.; Kobayashi, M. Facile construction of 6-carbomethoxymethyl-3-methoxy-1,2-dioxane, a core structure of spongean anti-malarial peroxides. *Tetrahedron Lett.* **2001**, *42*, 7281–7285. (b) Murakami, N.; Kawanishi, M.; Itagaki, S.; Horii, T.; Kobayashi, M. New Readily Accessible Peroxides with High Anti-Malarial Potency. *Bioorg. Med. Chem. Lett.* **2002**, *12*, 69–72.
- (16) Langhanki, J.; Rudolph, K.; Erkel, G.; Opatz, T. Total synthesis and biological evaluation of the natural product (–)-cyclonerodiol, a new inhibitor of IL-4 signaling. *Org. Biomol. Chem.* **2014**, *12*, 9707–9715.
- (17) Benohoud, M.; Erkkilä, A.; Pihko, P. M. ORGANO-CATALYTIC – METHYLENATION OF ALDEHYDES: PREPARATION OF 3,7-DIMETHYL-2-METHYLENE-6-OCTENAL. *Org. Synth.* **2010**, *87*, 201–208.
- (18) Zeynizadeh, B.; Setamdideh, D.; Faraji, F. Reductive Acetylation of Carbonyl Compounds to Acetates with Pyridine Zinc Borohydride. *Bull. Korean Chem. Soc.* **2008**, *29*, 76–80.
- (19) (a) Hayashi, T.; Yamasaki, K. Rhodium-Catalyzed Asymmetric 1,4-Addition and Its Related Asymmetric Reactions. *Chem. Rev.* **2003**, *103*, 2829–2844. (b) Alexakis, A.; Bäckvall, J. E.; Krause, N.; Pàmies, O.; Diéguez, M. Enantioselective Copper-Catalyzed Conjugate Addition and Allylic Substitution Reactions. *Chem. Rev.* **2008**, *108*, 2796–2823. (c) Bauer, I.; Knölker, H.-J. Iron Catalysis in Organic Synthesis. *Chem. Rev.* **2015**, *115*, 3170–3387. (d) Butt, N. A.; Zhang, W. Transition metal-catalyzed allylic substitution reactions with unactivated allylic substrates. *Chem. Soc. Rev.* **2015**, *44*, 7929–7967.
- (20) (a) Trost, B. M.; Crawley, M. L. Asymmetric Transition-Metal-Catalyzed Allylic Alkylations: Applications in Total Synthesis. *Chem. Rev.* **2003**, *103*, 2921–2944. (b) Lu, Z.; Ma, S. Metal-Catalyzed Enantioselective Allylation in Asymmetric Synthesis. *Angew. Chem., Int. Ed.* **2008**, *47*, 258–297.
- (21) (a) Cacchi, S.; Misioti, D.; Palmieri, G. The palladium-catalyzed conjugate addition type reaction of arylmercury compounds with  $\alpha,\beta$ -unsaturated ketones in a two-phase system. *Tetrahedron* **1981**, *37*, 2941–2946. (b) Nishikata, T.; Yamamoto, Y.; Miyaura, N. Conjugate Addition of Aryl Boronic Acids to Enones Catalyzed by Cationic Palladium(II)-Phosphane Complexes. *Angew. Chem., Int. Ed.* **2003**, *42*, 2768–2770. (c) Gutnov, A. Palladium-Catalyzed Asymmetric Conjugate Addition of Aryl-Metal Species. *Eur. J. Org. Chem.* **2008**, *2008*, 4547–4554. (d) Lin, S.; Lu, X. Cationic Pd(II)/Bipyridine-Catalyzed Conjugate Addition of Arylboronic Acids to  $\beta,\beta$ -Disubstituted Enones: Construction of Quaternary Carbon Centers. *Org. Lett.* **2010**, *12*, 2536–2539. (e) Gottumukkala, A. L.; Matcha, K.; Lutz, M.; de Vries, J. G.; Minnaard, A. J. Palladium-Catalyzed Asymmetric Quaternary Stereocenter Formation. *Chem. - Eur. J.* **2012**, *18*, 6907–6914. (f) Chen, W.; Chen, H.; Xiao, F.; Deng, G.-J. Palladium-catalyzed conjugate addition of arylsulfonyl hydrazides to  $\alpha,\beta$ -unsaturated ketones. *Org. Biomol. Chem.* **2013**, *11*, 4295–4298.
- (22) (a) Weaver, J. D.; Tunge, J. A. Decarboxylative Allylation using Sulfones as Surrogates of Alkanes. *Org. Lett.* **2008**, *10*, 4657–4660. (b) Trost, B. M.; Zhang, T.; Sieber, J. D. Catalytic asymmetric allylic alkylation employing heteroatom nucleophiles: a powerful method for C–X bond formation. *Chem. Sci.* **2010**, *1*, 427–440. (c) Li, Y.-X.; Xuan, Q.-Q.; Liu, L.; Wang, D.; Chen, Y.-J.; Li, C.-J. A Pd(0)-Catalyzed Direct Dehydrative Coupling of Terminal Alkynes with Allylic Alcohols To Access 1,4-Enynes. *J. Am. Chem. Soc.* **2013**, *135*, 12536–12539. (d) Akkarasamiyo, S.; Sawadjoon, S.; Orthaber, A.; Samec, J. S. M. Tsuji-Trost Reaction of Non-Derivatized Allylic Alcohols. *Chem. - Eur. J.* **2018**, *24*, 3488–3498.
- (23) (a) Tamaru, Y.; Tanaka, A.; Yasui, K.; Goto, S.; Tanaka, S. Highly Stereoselective Allylation of Benzaldehyde: Generation of a Stereochemically Defined Allylzinc Species from a  $\pi$ -Allylpalladium Intermediate and Diethylzinc. *Angew. Chem., Int. Ed. Engl.* **1995**, *34*, 787–789. (b) Howell, G. P.; Minnaard, A. J.; Feringa, B. L. Asymmetric allylation of aryl aldehydes: studies on the scope and mechanism of the palladium catalyzed diethylzinc mediated umpolung using phosphoramidite ligands. *Org. Biomol. Chem.* **2006**, *4*, 1278–1283. (c) Spielmann, K.; Niel, G.; de Figueiredo, R. M.; Campagne, J.-M. Catalytic nucleophilic ‘umpoled’  $\pi$ -allyl reagents. *Chem. Soc. Rev.* **2018**, *47*, 1159–1173.
- (24) (a) Yuan, K.; Scott, W. J. On the mechanism of the reduction of primary halides with Grignard reagents in the presence of (dppf)-PdCl<sub>2</sub> or (dppf)Pd(0). *J. Org. Chem.* **1990**, *55*, 6188–6194. (b) Fukuda, J.-i.; Nogi, K.; Yorimitsu, H. Cobalt-Catalyzed Reduction of Aryl Sulfones to Arenes by Means of Alkylmagnesium Reagents. *Asian J. Org. Chem.* **2018**, *7*, 2049–2052.
- (25) Misale, A.; Niyomchon, S.; Luparia, M.; Maulide, N. Asymmetric Palladium-Catalyzed Allylic Alkylation Using Dialkylzinc Reagents: A Remarkable Ligand Effect. *Angew. Chem., Int. Ed.* **2014**, *53*, 7068–7073.
- (26) Zhu, D.; Lv, L.; Li, C.-C.; Ung, S.; Gaom, J.; Li, C.-J. Umpolung of Carbonyl Groups as Alkyl Organometallic Reagent Surrogates for Palladium-Catalyzed Allylic Alkylation. *Angew. Chem., Int. Ed.* **2018**, *57*, 16520–16524.
- (27) (a) Qian, X.; Auffrant, A.; Felouat, A.; Gosmini, C. Cobalt-Catalyzed Reductive Allylation of Alkyl Halides with Allylic Acetates or Carbonates. *Angew. Chem., Int. Ed.* **2011**, *50*, 10402–10405. (b) Yonova, I. M.; Johnson, A. G.; Osborne, C. A.; Moore, C. E.; Morrisette, N. S.; Jarvo, E. R. Stereospecific Nickel-Catalyzed Cross-Coupling Reactions of Alkyl Grignard Reagents and Identification of Selective Anti-Breast-Cancer Agents. *Angew. Chem., Int. Ed.* **2014**, *53*, 2422–2427. (c) Yang, B.; Wang, Z.-X. Nickel-Catalyzed Alkylation or Reduction of Allylic Alcohols with Alkyl Grignard Reagents. *J. Org. Chem.* **2020**, *85*, 4772–4784. (d) Cahiez, G.; Avedissian, H. Highly Stereo- and Chemoselective Iron-Catalyzed Alkenylation of Organomagnesium Compounds. *Synthesis* **1998**, *1998*, 1199–1205. (e) Bernauer, J.; Wu, G.; Jacobi von Wangelin, A. Iron-catalyzed allylation-hydrogenation sequence as masked alkyl-alkyl cross-couplings. *RSC Adv.* **2019**, *9*, 31217–31223.
- (28) (a) Mukaiyama, T.; Isayama, S.; Inoki, S.; Kato, K.; Yamada, T.; Takai, T. Oxidation-Reduction Hydration of Olefins with Molecular Oxygen and 2-Propanol Catalyzed by Bis(acetylacetonato)cobalt(II). *Chem. Lett.* **1989**, *18*, 449–452. (b) Isayama, S.; Mukaiyama, T.

Novel Method for the Preparation of Triethylsilyl Peroxides from Olefins by the Reaction with Molecular Oxygen and Triethylsilane Catalyzed by Bis(1,3-diketonato)cobalt(II). *Chem. Lett.* **1989**, *18*, 573–576. (c) Isayama, S. An Efficient Method for the Direct Peroxygenation of Various Olefinic Compounds with Molecular Oxygen and Triethylsilane Catalyzed by a Cobalt(II) Complex. *Bull. Chem. Soc. Jpn.* **1990**, *63*, 1305–1310. (d) Crossley, S. W. M.; Obradors, C.; Martinez, R. M.; Shenvi, R. A. Mn-, Fe-, and Co-Catalyzed Radical Hydrofunctionalizations of Olefines. *Chem. Rev.* **2016**, *116*, 8912–9000.

(29) A version of this research was previously posted to ChemRxiv (2021-04-29): Leisering, S.; Mavroskoufis, A.; Voßnacker, P.; Zimmer, R.; Christmann, M. Synthesis of Plakortolides E and I Enabled by Base Metal Catalysis. *ChemRxiv* **2021**, DOI: [10.26434/chemrxiv.14501505.v1](https://doi.org/10.26434/chemrxiv.14501505.v1).

## 5 Studies Towards the Total Synthesis of Hypatulin A and Hypatulin B

### 5.1 Introduction

#### 5.1.1 Characteristic Metabolites of Hypericum Plants

The plant genus of *Hypericum* represents the largest of the nine genera within the family of *Hypericaceae* and comprises almost 500 species of perennial herbs, shrubs, and small trees.<sup>140</sup> *Hypericum* specimens, although generally absent from the poles, deserts, and low-altitude tropical areas, are nearly worldwide distributed and have been of great relevance due to their pharmaceutical and cosmeceutical properties.<sup>140</sup> These plants have been used in traditional medicine for the treatment of inflammations, bacterial and viral infections, burns, gastrointestinal disorders, and various other ailments and diseases for over 2000 years.<sup>140</sup> Moreover, as one of the oldest used and extensively studied medicinal herbs, *Hypericum perforatum*, commonly termed St. John's wort, has gained increasing attention due to its efficacy in the treatment of mild to moderate depressions in recent years. A variety of biologically active secondary metabolites that belong to different classes of natural products – with naphthodianthrones, phloroglucinols, flavonoids, and phenylpropanoids being the most prevalent – have been isolated from different *Hypericum* species. In particular, the phloroglucinol derivatives, which encompass polyprenylated acylphloroglucinols (PAPs) as well as polycyclic polyprenylated acylphloroglucinols (PPAPs), exhibit fascinating and complex chemical structures with intriguing biological activities that are responsible for many of the aforementioned pharmaceutical properties.<sup>30,141</sup> These types of meroterpenoids therefore represent lead structures for neuroscience, infectious disease, and oncology drug discovery programs. The most prominent phloroglucinol-derived meroterpenoid and one of the main bioactive compounds present in *Hypericum perforatum* is the neuroactive PPAP hyperforin (**144**) (Figure 13).<sup>142</sup> It is mainly accumulated in pistils and fruits where it presumably serves as a phytoconstituent to defend the reproductive parts of the plant.

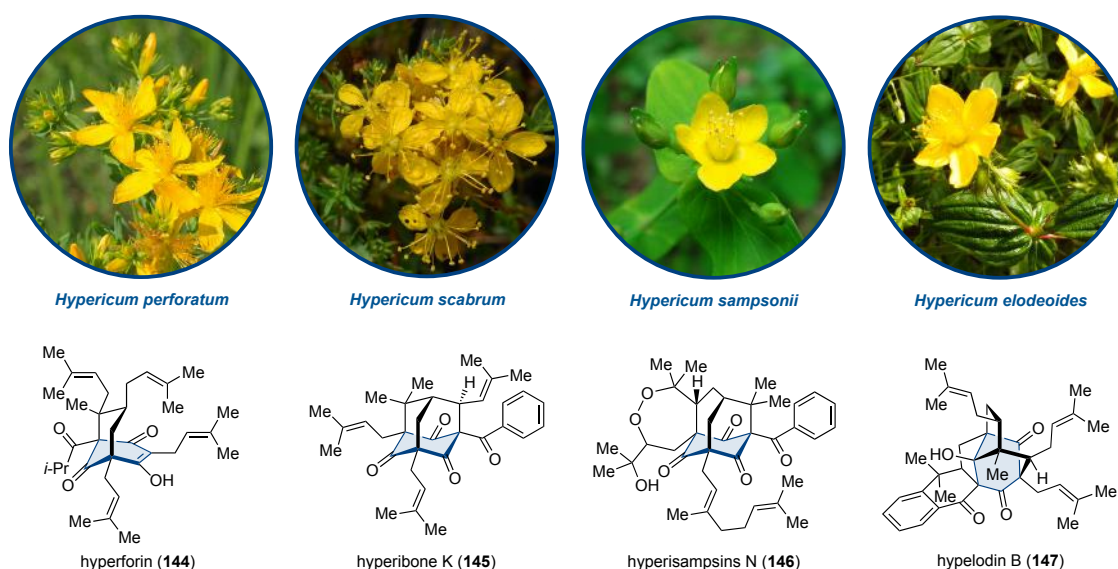


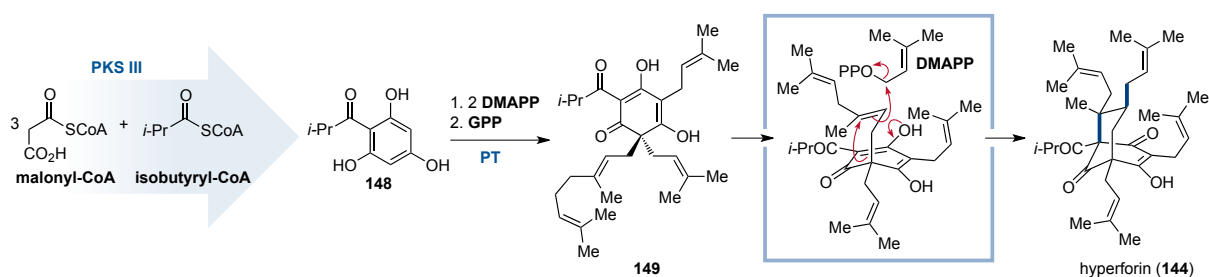
**Figure 13.** Examples of plants belonging to the genus *Hypericum* and PPAP natural products isolated therefrom.

Hyperforin exhibits activity against gram-positive bacteria including multiresistant *Staphylococcus aureus* strains as well as antiinflammatory action,<sup>143</sup> rationalising the traditional use of St. John's wort for the topical treatment of inflammatory skin diseases, burns, and superficial wounds. Furthermore, recent studies identified hyperforin as a potential anticancer agent by demonstrating its ability to inhibit proliferation and induce apoptosis both in *in vitro* and *in vivo* experiments.<sup>142</sup> In particular, hyperforin was shown to inhibit or modulate several neurotransmitter systems *in vitro* and therefore is likely responsible for the observed antidepressant and anxiolytic properties of the extracts of St. John's wort. While classical antidepressants act as competitive inhibitors for neurotransmitter transporters, instead, hyperforin indirectly affects the synaptosomal uptake due to a unique mechanism of action by elevating the intracellular sodium ion concentration. Studies indicate that this effect can be attributed either to the activation of nonselective cation channels (NSCCs)<sup>144</sup> or the induction of proton currents that cause cytosolic acidification which in turn fuels plasma-membrane sodium-proton exchangers.<sup>145</sup> Consequently, the gradient-driven synaptic reuptake, which requires sodium cation cotransport, of several neurotransmitters including serotonin, dopamine, noradrenaline, L-glutamate, and  $\gamma$ -aminobutyric acid (GABA) is inhibited.<sup>146</sup> This leads to changes in extracellular and intracellular concentrations of these neurotransmitters, explaining the observed pharmacological efficacy of hyperforin as an antidepressant.

Many other meroterpenoids related to PPAPs with unique and often densely-substituted caged-like structures and interesting biological activities such as hyperibone K (**145**),<sup>147</sup> hyperisampsins N (**146**),<sup>148</sup> and hypelodin B (**147**)<sup>149</sup> have been isolated from other *Hypericum* species (Figure 13).

### 5.1.2 Biosynthesis of Hyperforin

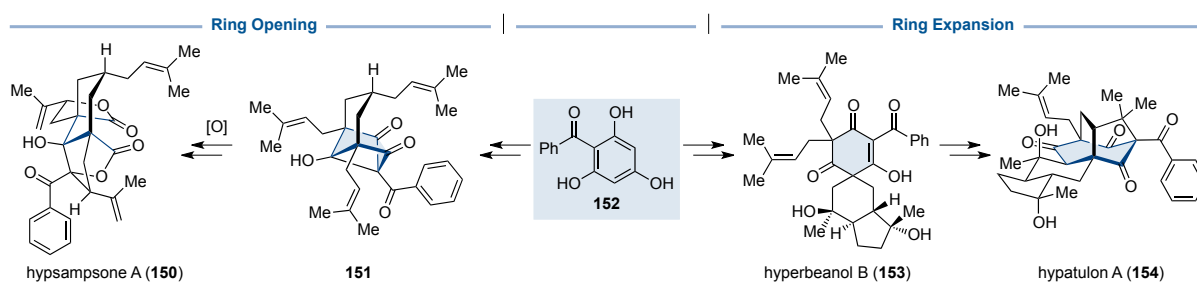
The biosynthesis of PAPs and PPAPs can be separated in two phases that represent a polyketide and a terpenoid biosynthetic pathway, respectively. The first phase is catalysed by a PKS type III and is initiated by formation of the acylphloroglucinol core, which is derived by condensation between one molecule of an acyl-CoA equivalent and three molecules of malonyl-CoA to yield a linear tetraketide intermediate that subsequently undergoes cyclisation.<sup>35</sup> In the case of hyperforin, isobutyryl-CoA serves as the acyl fragment and phloroisobutyrophenone (**148**) is obtained (Scheme 34). The second phase consists of stepwise prenylation by PTs with isoprenoid units such as **DMAPP** or higher homologues, which are derived predominantly through the MEP pathway, to give PAPs (Scheme 34). As is the case with terpenoid biosynthetic pathways, the initial prenylation phase can be succeeded by cyclisation reactions and rearrangements to add increased complexity and yield structurally diverse PPAPs. In regard to hyperforin, cyclisation is induced by prenylation of the geranyl side chain and the emerging carbenium ion is captured by the phloroglucinol to generate the bicyclic scaffold (Scheme 34).<sup>142c</sup>



**Scheme 34.** Two-phase biosynthesis of hyperforin (**1**).<sup>142c</sup>



Although the six-membered ring derived from its phloroglucinol precursor is often retained, rearrangements and oxidative cleavage reactions can result in ring expansions or contractions or even lead to seco-PPAPs via ring opening (Scheme 35).<sup>150,151</sup>



**Scheme 35.** Examples of modifications of the phloroglucinol-derived core via skeletal rearrangements.

### 5.1.3 Isolation of Hypatulins A and Hypatulins B

*Hypericum patulum*, commonly known as goldcup St. John's wort, is an evergreen shrub native to the provinces of Guizhou and Sichuan of China.<sup>152</sup> However, it has been naturalised in other countries such as Japan, India and South Africa and is widely cultivated in many temperate regions.<sup>153</sup> In 2016, TANAKA and KASHIWADA reported the isolation of two novel meroterpenoids, one possessing a contracted acylphloroglucinol- and the other a seco-acylphloroglucinol-derived motif, from the leaves of *hypericum patulum*.<sup>154</sup> The extraction of 1.48 kg of dried plant material yielded 36.9 mg and 3.6 mg of the two natural products, which were named hypatulins A (155) and hypatulins B (156), respectively (Figure 14).

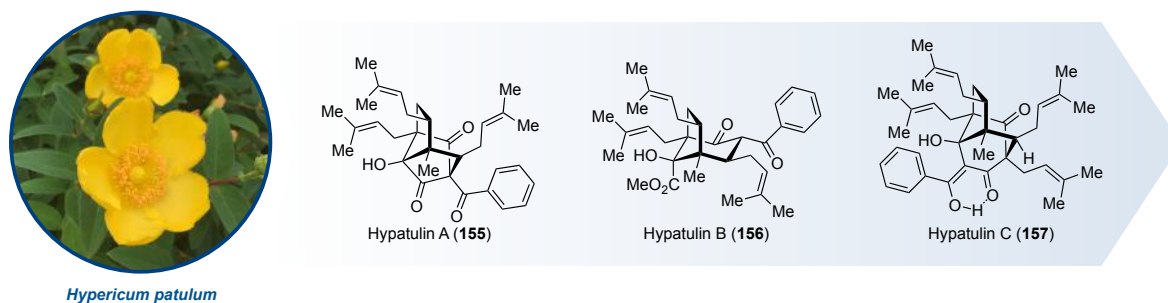


**Figure 14.** Structures of the natural products hypatulins A, B, and C isolated from *Hypericum patulum*.

After determination of the molecular formula by HRESIMS, the structures were derived by spectroscopic analysis, including COSY, HSQC, HMBC, and NOE experiments (Figure 15). The absolute configuration of the naturally occurring hypatulins A (155) was deduced by comparing the experimentally obtained ECD spectrum with the calculated spectra of both enantiomers. While hypatulins A has a unique highly oxygenated tricyclic octahydro-1,5-methanopentalene core, hypatulins B possesses a bicyclo[3.2.1]octane motif. Both natural products share a densely substituted cyclopentane core bearing four out of six stereocenters and were evaluated for their antimicrobial activity on strains of *Staphylococcus aureus*, *Bacillus subtilis*, and *Escherichia coli*. While hypatulins A exhibits activity against *Bacillus subtilis*, no activity could be observed for hypatulins B.

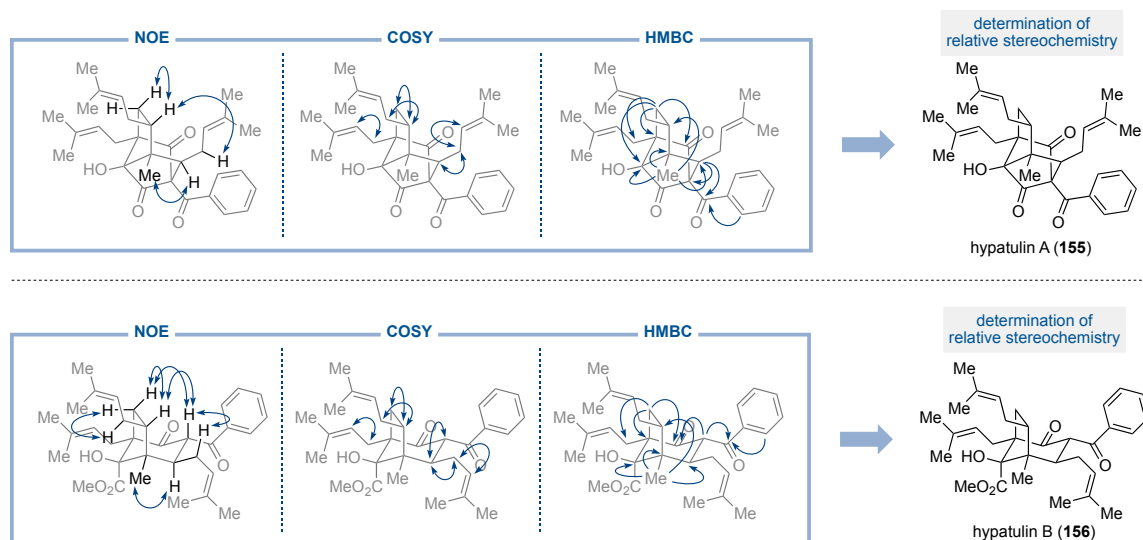
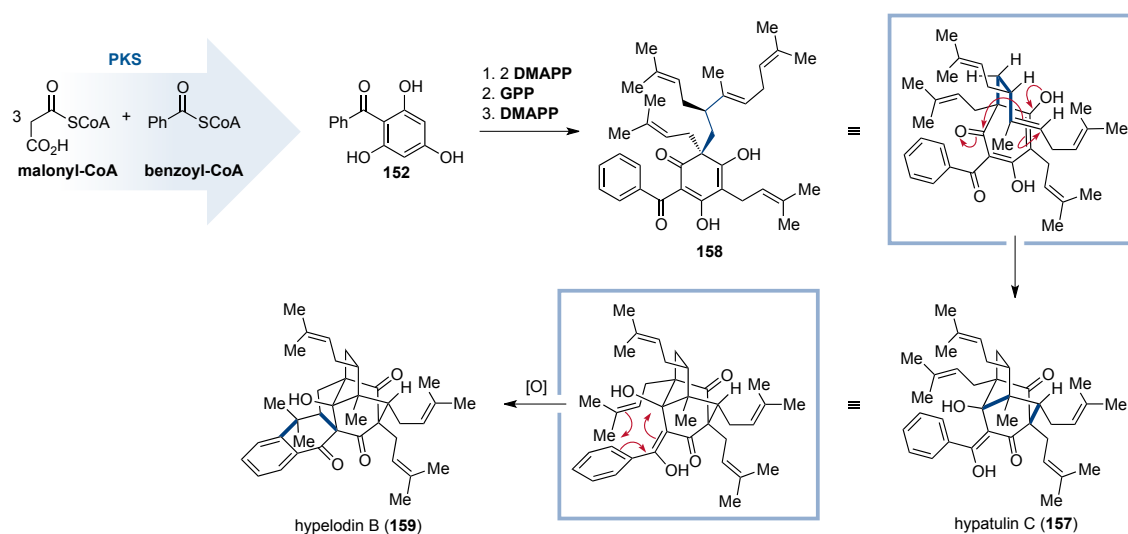


**Figure 15.** Elucidation of the relative stereochemistry of hypatulin A (**155**) and B (**156**) via key correlations obtained by 2D NMR spectroscopy experiments.<sup>154</sup>

### 5.1.4 Biosynthesis of Hypatulin A and Hypatulin B

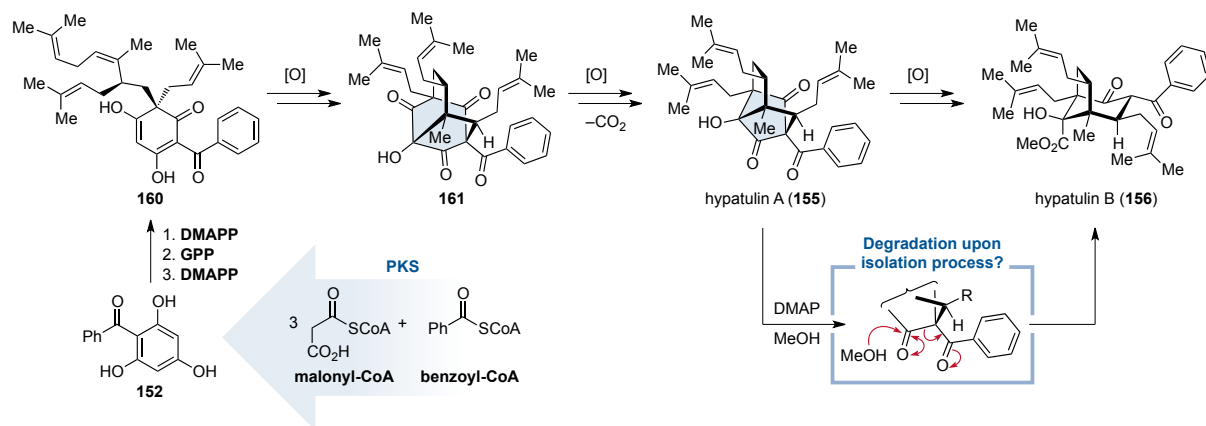
Additionally, after further investigation of the extracts from *Hypericum patulum* the same authors could isolate two other PPAPs in 2019 – the newly identified hypatulin C (**157**),<sup>155</sup> possessing a tricyclic [4.3.10<sup>3,7</sup>]-decane core with four prenyl groups, and the structurally related hypelodin B (**159**), which was already isolated from several other *Hypericum* species. The authors proposed a joint biosynthetic pathway for hypatulin C and hypelodin B (Scheme 36).<sup>155</sup> As is common for these PPAPs, the first steps build the polyketide chain from three molecules of malonyl-CoA and one molecule of an acyl-CoA, in this case benzoyl-CoA, followed by intramolecular condensation to yield acylphloroglucinol **152**. A sequence of prenylations and geranylation affords the precursor for the cyclisation cascade that eventually gives the polycyclic framework of hypatulin C (**157**). Further cyclisation of the phenone moiety and the adjacent prenyl group followed by oxidation would lead to hypelodin B (**159**).<sup>149,155</sup>



**Scheme 36.** Proposed biosyntheses of hypatulin C (**157**) and hypelodin B (**159**).<sup>149,155</sup>

A similar biosynthetic pathway, starting from the same acylphloroglucinol **152**, could be proposed for hypatulin A and hypatulin B (Scheme 37).<sup>154</sup> Polyprenylation, including installation of the geranyl group and

prenylation thereof, with only two instead of three equivalents of **DMAPP** would produce precursor **160**, thereby enabling a different cyclisation cascade. Oxidative decarboxylation would lead to ring contraction, generating the five-membered ring motif of hypatulin A. Hypatulin B could either be produced by oxidative cleavage and methylation through a biogenetic pathway or might be a side product during the extraction and isolation process. The authors were able to show the structural relationship between both natural products and support their structural assignment at position C-3 by chemical conversion of hypatulin A into hypatulin B (Scheme 37).<sup>154</sup>



**Scheme 37.** Proposed biosyntheses of hypatulins A (**155**) and B (**156**).<sup>154</sup>

## 5.2 Objective

Despite numerous synthetic approaches towards PPAPs with retained six-membered acylphloroglucinol motif, many rearranged congeners pose a synthetic challenge and require novel strategies for the construction of their densely substituted and highly oxygenated polycyclic scaffolds. Inspired by the complexity and the intriguing structural architectures of this class of natural products and their diverse biological profiles, the following part of this thesis was aimed at developing a convergent and concise enantioselective synthetic route towards the two novel meroterpenoids hypatulin A and hypatulin B. Although little biological activities have been reported for these two natural products, a synthetic avenue would enable further investigation of a potential pharmacological profile. In light of the highly oxygenated framework, it was envisaged to strategically exploit carbonyl chemistry for carbon-carbon forming reactions avoiding protecting groups or redox manipulations.

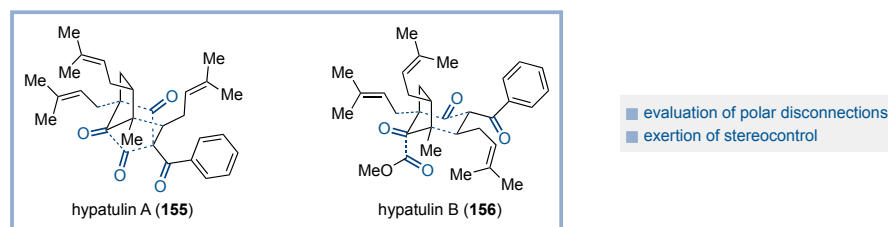
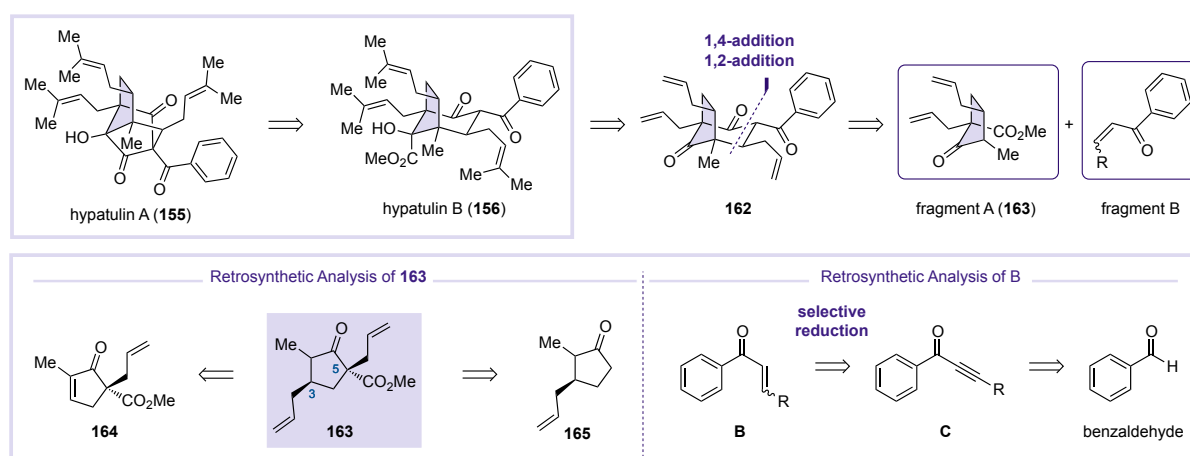


**Figure 16.** Assessment of synthetic strategies and examination of their feasibility towards the development of an efficient and enantioselective synthesis of the highly congested natural products hypatulin A and B as a major objective of this project.

### 5.3 Unpublished Results – Preliminary Studies

#### 5.3.1 Retrosynthetic Analysis of Hypatulin A and Hypatulin B

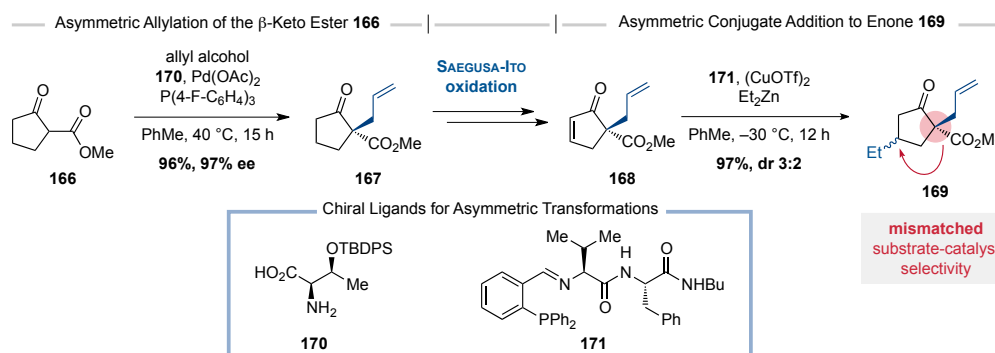
It was speculated that hypatulin A (**155**) could be derived from the easier accessible hypatulin B (**156**) via DIECKMANN or aldol cyclisation. Further retrosynthetic dissection by disconnecting the methoxycarbonyl group as well as simplifying the prenyl to allyl groups would trace both natural products back to triketone **162**. Construction of the bicyclic framework was envisaged by a sequence of 1,4-addition and 1,2-addition between fragments A (**163**) and B (Scheme 38). For the preparation of cyclopentanone **163** there two possible retrosynthetic cuts, differentiated by the order in which the substituents are installed, leading to either cyclopentenone **163** or cyclopentanone **164**. Fragment B on the other hand, could be accessible via selective reduction of an alkyne resulting from nucleophilic addition to benzaldehyde and subsequent oxidation.



**Scheme 38.** Retrosynthetic analysis of hypatulin A (**155**) and hypatulin B (**156**).

#### 5.3.2 Preparation of Fragment A

In light of the retrosynthetic analysis outlined above, an approach based on the retrosynthetic cut towards cyclopentenone **164** was devised with 2-methoxycarbonyl cyclopentanone (**166**) as the starting material. It was first necessary to identify suitable conditions for the stereoselective preparation of both stereocenters. Therefore, installation of the methyl group was omitted and enone **168** was envisaged as precursor for the conjugate addition (Scheme 39).



**Scheme 39.** Attempted asymmetric allylation and conjugate addition to construct both stereocenters of ketone **169**.

Construction of the first stereocenter was achieved by S. PONATH via an asymmetric allylation protocol by YOSHIDA using chiral ligand **170** to yield  $\beta$ -keto ester **167** in 96% yield and 97% enantiomeric excess.<sup>156</sup>

Subsequent SAEGUSA-ITO oxidation<sup>157</sup> via a two-step sequence prepared enone **168** for the intended allylation. Although there are examples for enantioselective conjugate additions to cyclic enons with many catalyst systems showing promising results, these systems are often sensitive to ring size and substitution patterns.<sup>158</sup> HOVEYDA and co-workers developed an efficient protocol for the conjugate addition of dialkylzinc species to cyclic enons of various ring sizes promoted by asymmetric copper-catalysis with peptide-based phosphine ligands such as ligand **171**.<sup>159</sup> However, since the protocol requires the utilisation of stoichiometric amounts of organozinc reagents, which have to be prepared in advance, the feasibility of this system was tested with commercially available diethylzinc. Unfortunately, the catalyst system exhibited a poor diastereoselectivity of 3:2 indicating a mismatched substrate-catalyst setting.

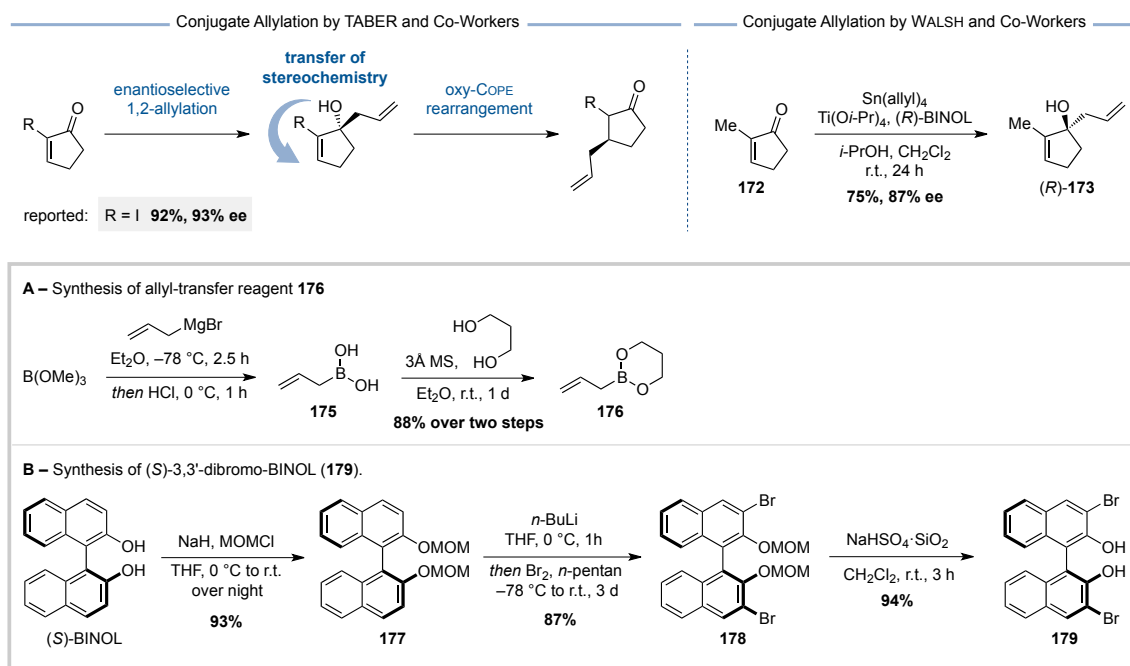
Thus, the retrosynthetic analysis was revisited and another approach based on cyclopentanone **165** with 2-methylcyclopent-2-enone (**172**) as the starting material was devised. First attempts to construct the stereocenter in  $\beta$ -position were made with a system developed by HOVEYDA and co-workers.<sup>159</sup> The required diallylzinc was prepared via boron-zinc exchange from triallylborane.<sup>160,161</sup> These conditions, however, resulted only in the formation of the 1,2-addition product **173** (Table 6, Entry 1) with higher catalyst loading and lower temperatures exhibiting no influence on the chemoselectivity (Table 6, Entry 2). Next, a catalytic system for the enantioselective conjugate addition of cuprates using NHC ligand **175**, as reported by ALEXAKIS and co-workers, was tested.<sup>162</sup> This system benefits from the use of GRIGNARD reagents, which are in most cases easier to prepare or even commercially available, instead of organozinc compounds. Various alkyl GRIGNARD reagents, including unbranched, branched, and even cyclic alkyl chains, could be added to **173** with moderate to good enantiomeric excesses.<sup>162</sup> However, all attempts using allylmagnesium bromide were unsuccessful and only gave the 1,2-addition product **173** as well (Table 6, Entries 3–6). Since the a slight excess of organomagnesium reagent is used to reduce the copper(II) precatalyst, it was speculated that allyl GRIGNARD might not be able to promote the formation of the required oxidation state. However, when a copper(I) catalyst was employed the same result was obtained (Table 6, Entry 5). The use of THF as solvent to improve solubility and facilitate formation of the active catalyst had no improving effect on the chemoselectivity as well (Table 6, Entry 6).

**Table 6.** Attempted copper-catalysed conjugate addition of allyl nucleophiles to 2-methylcyclopent-2-enone (**172**).<sup>a</sup>

Entry	M	Catalyst	Ligand	Solvent	T
1	Zn(allyl)	Cu(OTf) <sub>2</sub> (1 mol%)	<b>171</b> (2 mol%)	PhMe	-30 °C
2	Zn(allyl)	Cu(OTf) <sub>2</sub> (2 mol%)	<b>171</b> (5 mol%)	PhMe	-45 °C
3	MgBr	Cu(OTf) <sub>2</sub> (1.5 mol%)	<b>171</b> (2 mol%)	Et <sub>2</sub> O	-30 °C
4	MgBr	Cu(OTf) <sub>2</sub> (11 mol%)	<b>174</b> (14 mol%)	Et <sub>2</sub> O	-30 °C
5	MgBr	Cu(OTf)·PhH (1 mol%)	<b>174</b> (1.4 mol%)	Et <sub>2</sub> O	-30 °C
6	MgBr	Cu(OTf)·PhH (1 mol%)	<b>174</b> (1.4 mol%)	THF	-45 °C

a) The results were analysed by TLC and <sup>1</sup>H NMR spectroscopy of the crude products.

Since both catalytic systems disfavoured the conjugate addition, in it was concluded that the direct enantioselective allylation in  $\beta$ -position of enone **172** is unfeasible with the employed systems. In general, enantioselective conjugate allylation to  $\alpha,\beta$ -unsaturated carbonyl compounds, in particular cyclic enones, still poses a challenge underlined by the relatively scarce literature compared to that of conjugate alkylation reactions.<sup>163,164</sup> The main difficulty described arises from the inability of many catalytic systems to chemoselectively override the inherent preference for the 1,2-addition.<sup>163b</sup> To provide a formal solution to this challenging transformation, TABER and co-workers took advantage of the 1,2-addition by a subsequent oxy-Cope rearrangement resulting in the formation of the 1,4-addition product and transfer of stereochemistry (Scheme 40).<sup>165</sup> Enantioselective allylation of the ketone was achieved by applying SCHAUS organocatalytic protocol with allylboronate **176** as the allyl donor and 3,3'-dibromo-BINOL **179** as the enantioselective catalyst.<sup>166</sup> Both, reagent and catalyst, are easily accessible in 2 to 3 steps. TABER and co-workers showed that several  $\alpha$ -iodo and  $\alpha$ -alkyl functionalised five-, six- and seven-membered cyclic ketones could be prepared in moderate to excellent yields and high enantiomeric excesses. Furthermore, the iodinated addition products can be used in cross-coupling reactions prior to oxy-COPE rearrangement thereby enabling the introduction of a variety of substituents in  $\alpha$ -position.<sup>165</sup> Although methylated allylic alcohol (*R*)-**173** can be prepared by the direct asymmetric allylation of **172** according to a procedure by WALSH and co-workers,<sup>167</sup> the strategy by TABER and co-workers via 2-iodocyclopent-2-enone was reported to give higher enantiomeric excess (Scheme 40).



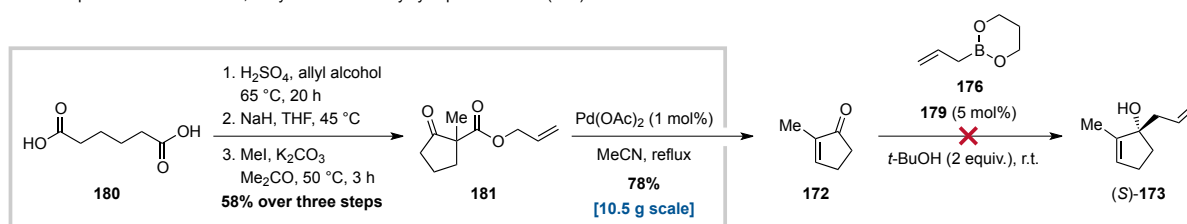
**Scheme 40.** Strategies for enantioselective conjugate allylations by TABER and co-workers and by WALSH and co-workers.

The system was first tested with 2-methylcyclopentenone (**172**), which is either commercially available or can be prepared on a multi-gram scale from inexpensive adipinic acid (**181**) (Scheme 41). Although the enantioselective allylation reaction was published for 2-methylcyclohexanone by TAUBER and co-workers, albeit with noticeably lower yields than all other examples,<sup>165</sup> allylation with the five-membered homologue resulted in no conversion. On the other hand, when  $\alpha$ -iodocyclopentenone (**183**), which can be prepared in one step from cyclopentenone **182**,<sup>168</sup> was subjected to the enantioselective allylation conditions, the reaction proceeded smoothly and the desired product was isolated in 94% yield and 97% enantiomeric excess (Scheme

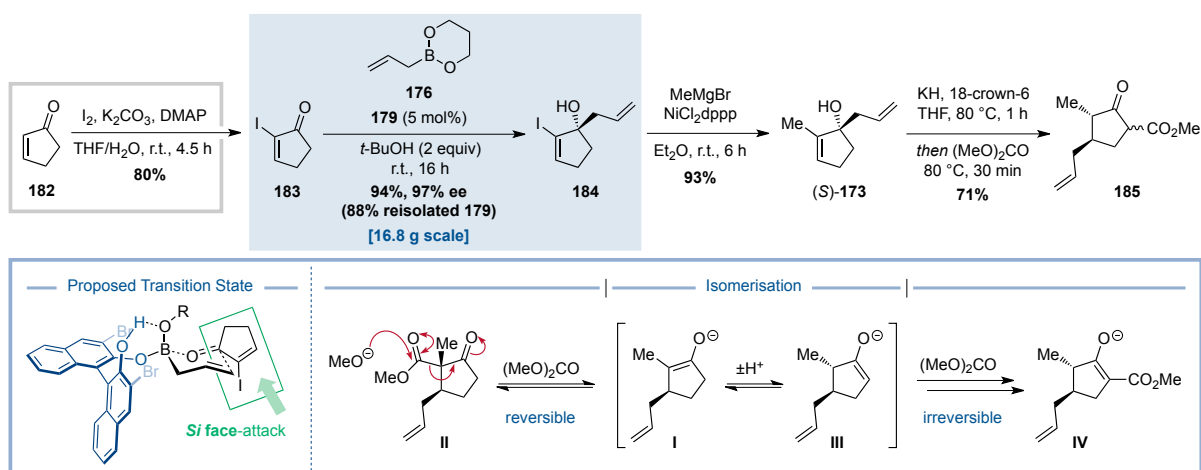


41). Installation of the methyl group was achieved by a KUMADA cross-coupling reaction and the subsequent conversion to  $\beta$ -keto ester **185** could be realised in a one-pot procedure by trapping the *in situ* formed enolate with dimethyl carbonate. The exclusive formation of the thermodynamic product **185** can be rationalised by the susceptibility of  $\alpha,\alpha$ -disubstituted  $\beta$ -keto esters to undergo retro-CLAISEN reaction in the presence of alkoxide bases.<sup>169</sup> The initially formed product **II** is prone to attack by the released methoxide, due to the lack of an  $\alpha$ -proton between both carbonyls, and thus can revert to enolate **I**. However, methoxide can also deprotonate **II** in the unfunctionalised  $\alpha$ -position, thereby providing catalytic amounts of a proton source which enables equilibration between **I** and **III**. Methoxycarbonylation of **III**, on the other hand, is irreversible since the subsequent deprotonation leads to enolate **IV** as a thermodynamic sink that eventually shifts the entire preceding equilibrium towards the desired product **185** (Scheme 41).

A – Attempted enantioselective 1,2-allylation of 2-methylcyclopent-2-enone (**172**).



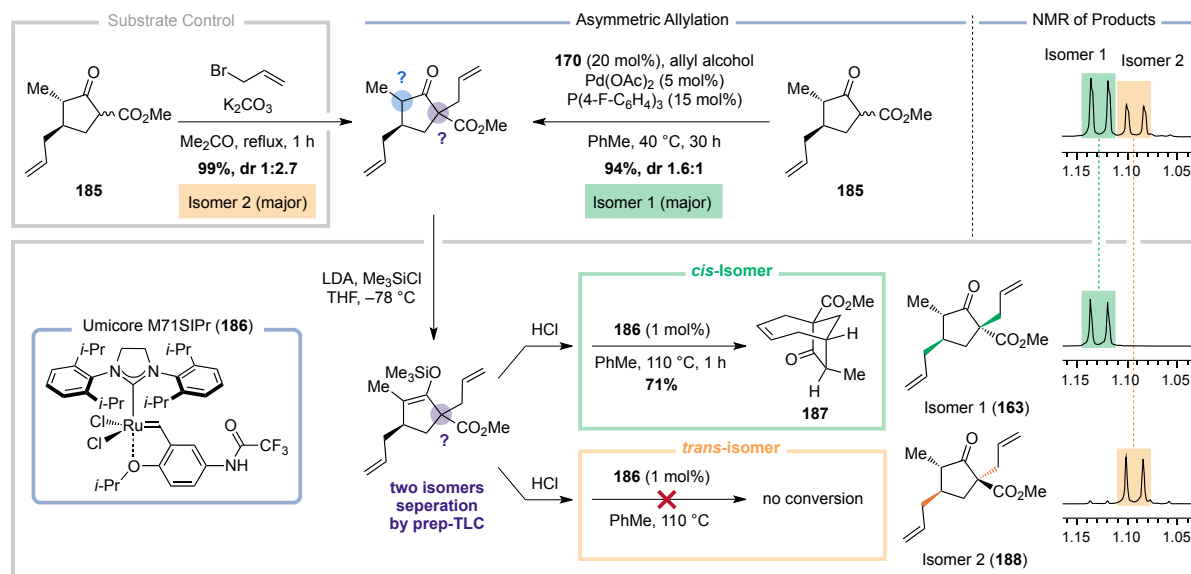
B – Enantioselective 1,2-allylation of 2-iodocyclopent-2-enone (**183**) and subsequent transformations for the preparation of cyclopentanone **185**.



**Scheme 41.** Preparation of  $\beta$ -keto ester **185** via the enantioselective allylation strategy of cyclic enones reported by TABER and co-workers.

With  $\beta$ -keto ester **185** in hand, construction of the quaternary stereocenter was pursued. To test whether allylation could be achieved in a diastereoselective fashion via substrate control, **185** was treated with allyl bromide in the presence of potassium carbonate in acetone. The reaction proceeded with 99% yield and a moderate diastereoselectivity of 2.7:1 (Scheme 42). On the other hand, when the enantioselective allylation protocol by YOSHIDA was applied the diastereoselectivity was reversed favouring the other isomer in a ratio of 1.6:1. These results could suggest a mismatched case between stereochemical control of the substrate and the asymmetric catalytic system, with the latter not being able to completely override the inherent bias. However, epimerisation of the methylated  $\alpha$ -position could also account for the observation of two isomers. To elucidate the stereochemistry of both obtained products, the mixture was subjected to enolisation to form the corresponding silyl enol ethers. As no convergence was observed, the two isomers were deduced to be epimers at the quaternary stereocenters. Separation by preparative thin layer chromatography and desilylation with

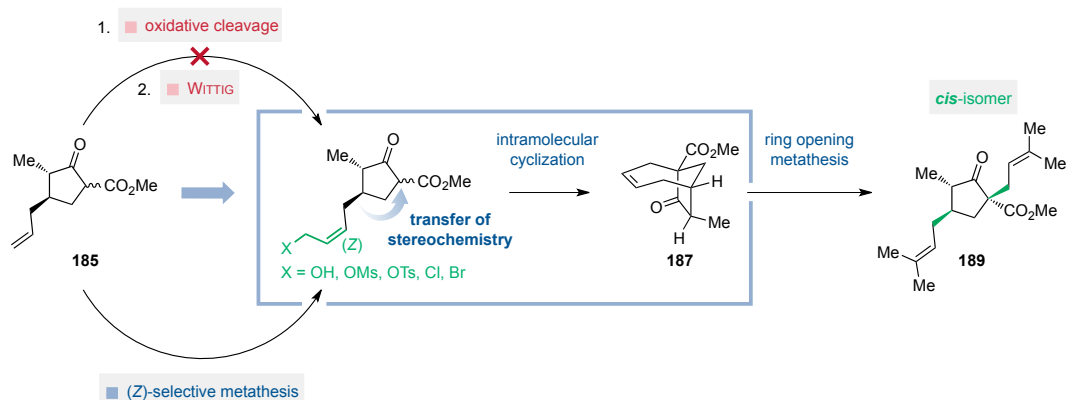
aqueous hydrogen chloride afforded the initial epimeric ketones. Surprisingly, in both cases protonation occurred in a stereoselective manner to yield a single configuration at the methylated  $\alpha$ -position. The configuration is presumably set by the adjacent stereocenter to yield a *trans*-relationship.<sup>158a,162</sup> Both epimers were then subjected to olefin metathesis with the premise that only a *cis*-relationship between both allyl groups would enable cyclisation. While isomer 1 (**163**) afforded the bicyclic product **187**, isomer 2 (**188**) gave no conversion, revealing the former to possess the desired configuration (Scheme 42).



**Scheme 42.** Alkylation of  $\beta$ -keto ester **185** and elucidation of the resulting stereochemistry.

Since the construction of the quaternary stereocenter via direct allylation of the  $\beta$ -keto ester proceeded with low diastereoselectivity, an alternative approach was pursued. Inspired by the concept of TABER and co-workers to transfer stereochemistry within the substrate, the intention was to further exploit the allyl group in  $\beta$ -position. Functionalisation to form a *Z*-configured olefin that contains a new allylic position with a leaving group at its terminus could pose a suitable precursor for an intramolecular cyclisation to form bicyclic product **187** (Scheme 43). This revised strategy would allow the direct transfer of stereochemical information from the first stereocenter and thereby bypassing the substrate imposed bias for the facial selectivity in intermolecular allylation reactions. Subsequent ring opening metathesis could introduce both prenyl groups leading to cyclopentanone **190**. Unfortunately, initial attempts to introduce the *Z*-configured olefin via an oxidative cleavage/WITTIG sequence were unsuccessful, since a variety of different methods, such as ozonolysis and periodate cleavage in combination with preceding dihydroxylation or epoxidation, failed to give the required aldehyde intermediate. To avoid the challenging oxidation step a direct functionalisation by olefin cross metathesis was envisioned. Owing to its broad applications in synthetic organic and material chemistry, olefin metathesis has found its way into repertoire of organic chemists as a powerful transformation for the construction of carbon-carbon bonds. In pursuit of a mechanistic understanding and expanding limitations of imparting stereochemical control on the product formation in order to access kinetic *Z*-olefins, considerable research efforts have pushed the development of catalysts capable of promoting *Z*-selective cross metathesis reactions.<sup>170</sup>





**Scheme 43.** Strategy for an intramolecular transfer of stereochemistry to generate the second stereocenter.

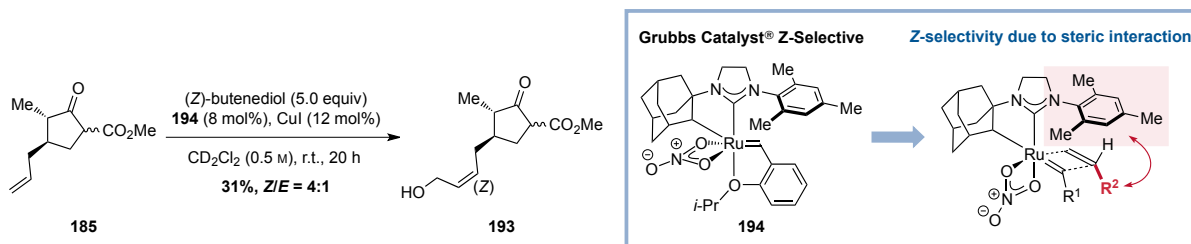
However, in order to evaluate different olefins and to find suitable conditions, initial reactions were conducted with common ruthenium-based metathesis catalysts (Table 7).<sup>171</sup> Reactions with allyl halides in excess (Table 7, Entry 1–2) gave no conversion.<sup>172</sup> The same results were observed with allyl acetate (Table 7, Entry 3). Neither the addition of titanium tetraisopropoxide to disarm chelating functional groups such as 1,3-dicarbonyls (Table 7, Entry 4),<sup>173</sup> nor microwave irradiation (Table 7, Entry 5)<sup>174</sup> had a facilitating influence on the reaction. Gratifyingly, the use of (*Z*)-butenediol<sup>175</sup> in the presence of catalytic amounts of copper iodide<sup>176</sup> resulted in the formation of allylic alcohol **192** in 53% yield (Table 7, Entry 6).

**Table 7.** Optimisation of the cross metathesis of  $\beta$ -keto ester **185** with various olefins.<sup>a</sup>

Entry	Catalyst	Alkene	Additive	Solvent	T	Result <sup>b</sup>
1	<b>190</b> (10 mol%)	allyl chloride (8.0 equiv)		CH <sub>2</sub> Cl <sub>2</sub> (0.3 M)	50 °C	no conversion
2	<b>186</b> (2 mol%)	allyl bromide (2.5 equiv)		CH <sub>2</sub> Cl <sub>2</sub> (0.5 M)	35 °C	no conversion
3	<b>190</b> (3 mol%)	allyl acetate (3.0 equiv)		CH <sub>2</sub> Cl <sub>2</sub> (0.1 M)	60 °C	no conversion
4	<b>190</b> (3 mol%)	allyl acetate (3.0 equiv)	Ti(O <i>i</i> -Pr) <sub>4</sub> (15 mol%)	CH <sub>2</sub> Cl <sub>2</sub> (0.1 M)	60 °C	no conversion
5	<b>192</b> (4 mol%)	allyl acetate (3.0 equiv)		1,2-DCE (0.1 M)	100 °C	no conversion
6	<b>186</b> (8 mol%)	( <i>Z</i> )-butenediol (5.0 equiv)	CuI (12 mol%)	CD <sub>2</sub> Cl <sub>2</sub> (0.5 M)	r.t.	20 h, 53% of <b>192</b> (X = OH)

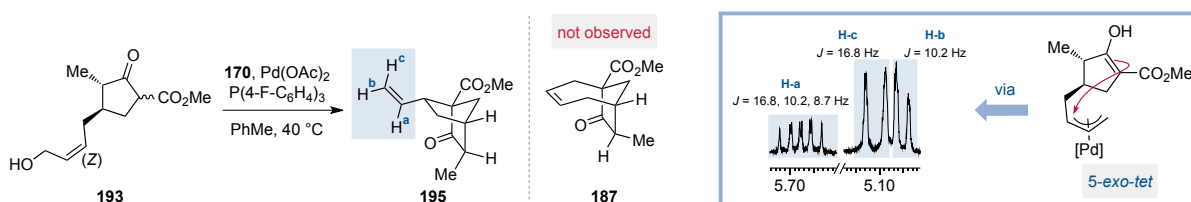
a) The reactions were performed on a 25 mg scale. b) The reaction was monitored by <sup>1</sup>H NMR spectroscopy.

When these conditions were applied to the *Z*-selective cross-metathesis reaction with the Grubbs Catalyst® *Z*-Selective (**194**) olefin **193** was isolated in 31% yield as a *Z/E* mixture with a ratio of 4:1 (Scheme 44).



**Scheme 44.** *Z*-Selective cross metathesis between  $\beta$ -keto ester **185** and (*Z*)-butenediol.

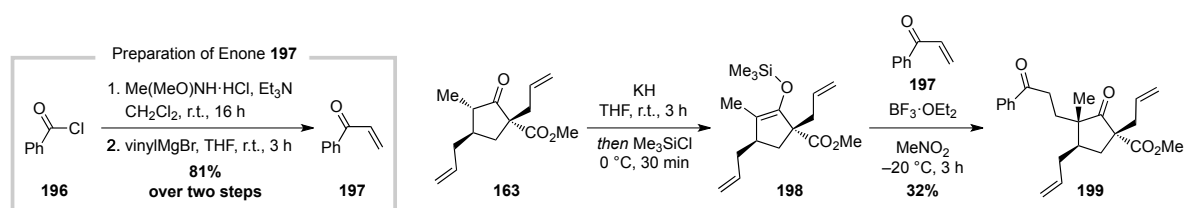
Attempts to activate the alcohol with thionyl chloride or mesyl chloride for the subsequent cyclisation failed. Instead of a two step sequence with initial formation of a leaving group, was envisioned to use the previously applied conditions by YOSHIDA for the direct allylation of  $\beta$ -keto esters with allylic alcohols to facilitate ring closure in one pot. Unfortunately,  $^1\text{H}$  NMR spectroscopic analysis of the crude product indicated formation of the undesired product **195** containing a five-membered ring and an exocyclic double bond (Scheme 45). Although allylic substitutions usually proceeds through an  $\text{S}_{\text{N}}2$  pathway, palladium-catalysis generates an  $\eta^3$ -allyl-palladium complex, thereby activating both positions and as a result favouring the *5-exo-tet* cyclisation as clearly underlined by these observations.



**Scheme 45.** Attempted cyclisation of olefin **193** via palladium-catalysed allylic substitution.

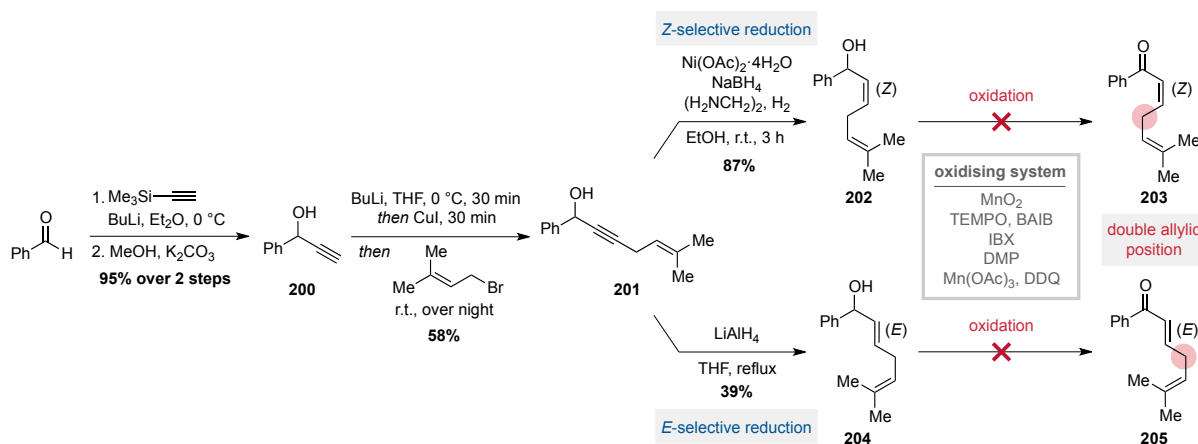
### 5.3.3 Preparation of Fragment B

Since this approach remained unsuccessful as well, further efforts were focused on coupling fragment A (**163**) to suitable enones in order to evaluate the synthetic strategy outlined in the retrosynthetic analysis (Scheme 38). Phenylvinyl ketone (**197**), readily accessible from benzoyl chlorid (**196**) in two steps,<sup>177</sup> was selected as a model substrate to identify suitable conditions for the intended conjugate addition. S. PONATH could show that the presence of LEWIS acids such as boron trifluoride diethyl etherate successfully promoted the coupling of silyl enol ether **198** and enone **197**, albeit with moderate yields (Scheme 46). Attempts to prepare the corresponding enone by SAEGUSA-ITO oxidation<sup>157</sup> for subsequent installation of the third allyl group, however, failed.



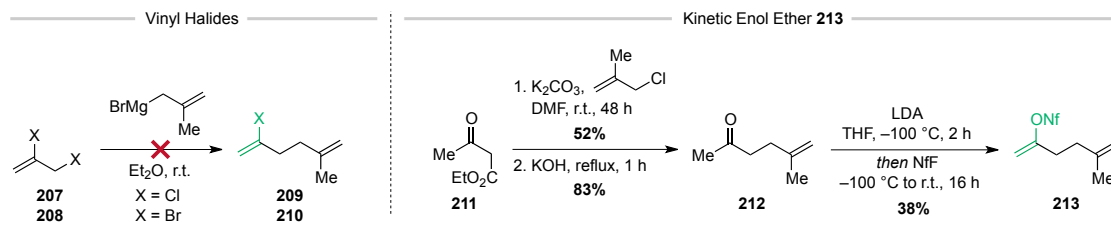
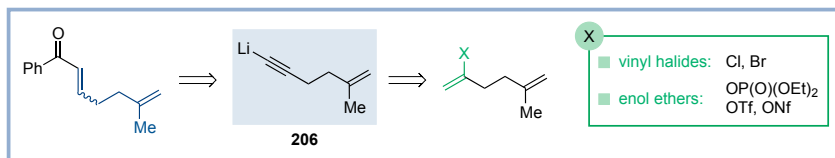
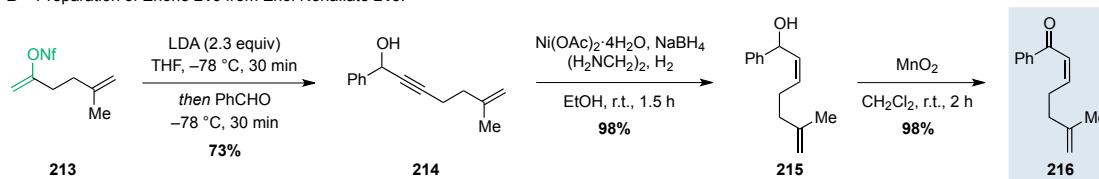
**Scheme 46.** Construction of the second quaternary stereocenter via conjugate addition to enone **197** as a model substrate.

Encouraged by this result, substituted enons were investigated. This strategy would allow the incorporation of a prenyl group into fragment B, thereby avoiding late-stage allylation. Since the configuration of the double bond of the enone might influence the facial selectivity of the conjugate addition an alkyne was envisaged as a common precursor for preparation of *E*- and *Z*-enons. Access to such an intermediate **201** was realised in three steps, starting from commercially available benzaldehyde (Scheme 47). The addition of trimethylsilyl acetylene under basic conditions, followed by deprotection in methanol gave propargyl alcohol **200** in 95% yield over 2 steps.<sup>178</sup> Propargylic alcohol **201** was then obtained by a subsequent copper-catalysed allylic substitution with prenyl bromide as the electrophile in 58% yield.<sup>179</sup> Reduction with hydrogen in the presence of P2-nickel<sup>180</sup> allowed for the selective conversion to the *Z*-configured olefin **202**, while lithium aluminiumhydride<sup>179</sup> delivered selectively the *E*-olefin **204** (Scheme 47). Unfortunately, in both cases the final oxidation of the benzylic/allylic hydroxyl group failed with a variety of oxidising systems under mild conditions.<sup>181</sup> Rapid degradation was observed which might be attributed the double allylic position between the unsaturated carbonyl and the prenyl group resulting in undesired side reactions.



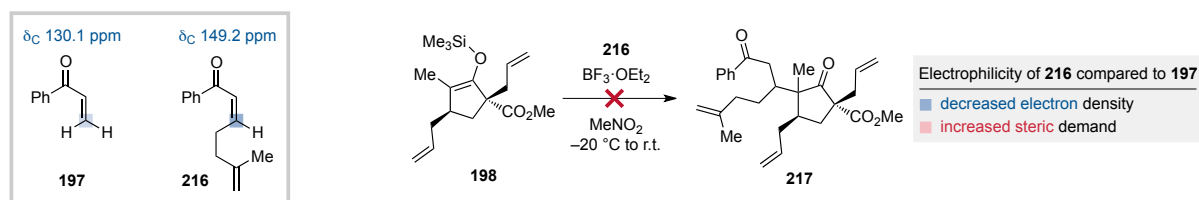
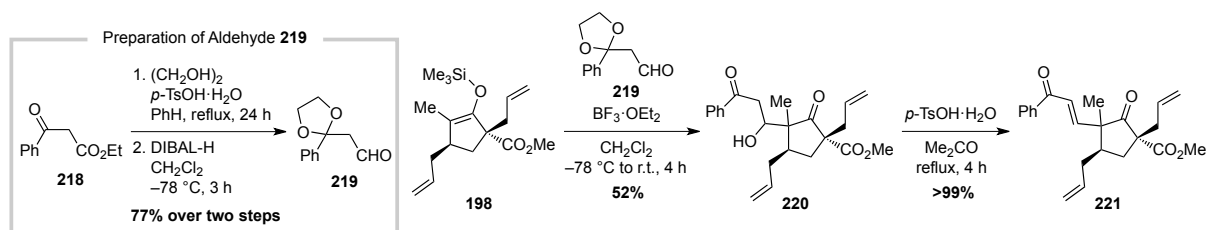
**Scheme 47.** Attempted preparation of enones **203** and **205**.

To avoid such side reactions, it was intended to shift the double bond to the terminal position. However, since in this approach the corresponding electrophile would lack an allylic position for the copper-catalysed coupling with propargylic alcohol **200**, it was necessary to install the terminal alkene moiety on the alkynyllithium nucleophile prior to addition to benzaldehyde. Such an intermediate **206** could be obtained via elimination from a suitable vinylic precursor (Scheme 48).<sup>182</sup> Attempts to prepare the corresponding vinylic bromide **209** or chloride **210** failed.<sup>183</sup> Although complete conversion of the starting material was observed, the products could not be isolated. Alternatively, the use of enol ethers appeared promising.<sup>184</sup> The corresponding ketone **212** was prepared from ethyl acetoacetate (**211**) in a two-step sequence.<sup>185</sup> Initial attempts to synthesise enol nonaflate **213** at  $-78$  °C suffered from the formation of an inseparable mixture of the kinetic and thermodynamic enol ethers.<sup>186</sup> In order to suppress deprotonation at the undesired thermodynamic  $\alpha$ -position, lower temperatures were tested. Eventually, when ketone **212** was deprotonated with lithium diisopropylamide at  $-100$  °C and then treated with nonafllyl fluoride enol nonaflate **213** could be isolated in 38% yield. Elimination of enol nonaflate **213** and *in situ* deprotonation of the resulting alkyne with lithium diisopropylamide, followed by the addition of benzaldehyde afforded propargylic alcohol **214** in 73% yield. Subsequent *Z*-selective hydrogenation with P2-nickel and oxidation with manganese dioxide delivered enone **216** (Scheme 48).

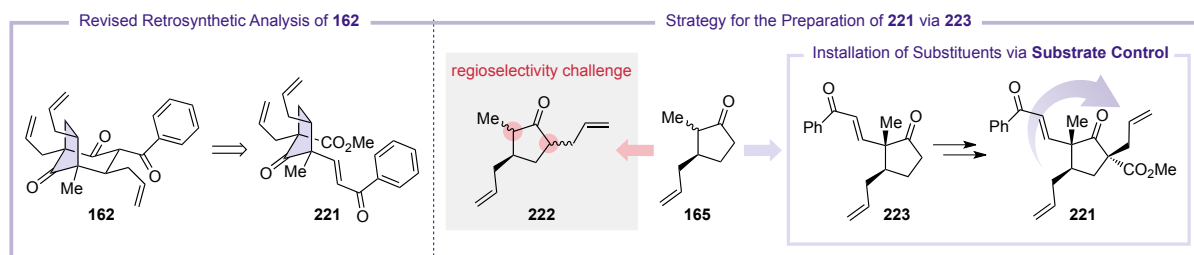
A – Preparation of a Suitable Precursor for Alkynyllithium **206**.B – Preparation of Enone **216** from Enol Nonafate **213**.Scheme 48. Preparation of enone **216** via enol nonafate **213**.

## 5.3.4 Coupling of Fragment A and Fragment B

With fragment A and fragment B in hand, the coupling of both was attempted. Unfortunately, when the previously tested conditions were applied, no formation of the 1,4-addition product was observed (Scheme 49). Presumably, the higher degree of substitution of the electrophile hinders approach of the densely substituted silyl enol ether **198**. Based on these results, the use of enones as coupling partners was deemed unfeasible and the strategy was changed to employ the less sterically demanding aldehyde **219**, which was prepared in two steps from  $\gamma$ -keto ester **218**.<sup>187</sup> Gratifyingly, MUKAIYAMA aldol addition promoted by boron trifluoride diethyl etherate proceeded concomitant with deacetalisation and  $\beta$ -hydroxy ketone **220** could be isolated in 52% yield as a single diastereoisomer by S. PONATH.<sup>188,189</sup> Furthermore, the use of **219** provides a suitable precursor for enone formation via dehydration, thereby avoiding the challenging oxidation of ketone **199**. Refluxing the aldol product **220** under acidic conditions in acetone delivered enone **221**.

A – Attempted conjugate addition of silyl enol ether **198** to enone **216**.B – Preparation of enone **221** via MUKAIYAMA-aldol addition and subsequent dehydration.Scheme 49. Evaluation of enone **216** and aldehyde **219** as suitable coupling partners for silyl enol ether **198**.

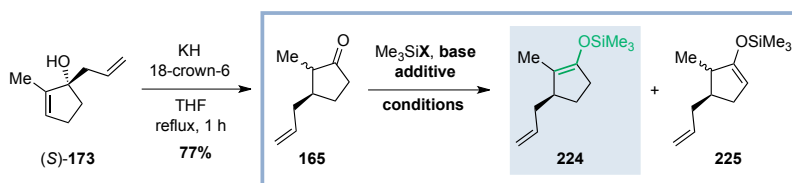
With all substituents installed on the cyclopentanone core, optimisation of the stereoselectivity was addressed. Instead of relying on ligand-induced diastereoselectivity, a strategy, that utilises the inherent substrate-control for facial selectivity, was pursued. While it can be speculated that changing the order of methoxycarbonylation and allylation would give the desired isomer as the major product, this sequence would generate an intermediate **222** with two monofunctionalised  $\alpha$ -positions posing a regioselectivity challenge for the introduction of the methyl ester. Thus, it was necessary to construct the other quaternary stereocenter via hydroxyalkylation of ketone **165** in advance (Scheme 50).



**Scheme 50.** New retrosynthetic analysis of triketone **162** and synthetic strategy via cyclopentanone **223**.

Ketone **165** was accessible via oxy-COPE rearrangement of allylic alcohol (*S*)-**173**. For the preparation of the desired silyl enol ether **224**, required for a MUKAIYAMA aldol reaction, conditions with weak amine bases were investigated (Table 8). The resulting ammonium salts should act as a proton source allowing equilibration under thermodynamic conditions with the more substituted silyl enol ether predominating. The use of trimethylsilyl iodide and hexamethyldisilazane in a non-polar solvent, as reported by MILLER and MCKEAN for the preparation of thermodynamic silyl enol ethers at ambient temperature, only gave a 50:50-mixture of both regioisomers **224** and **225** (Table 8, Entry 1).<sup>190</sup> Surprisingly, treatment of ketone **165** with trimethylsilyl chloride and triethylamine in the presence of sodium iodide in acetonitrile at 100 °C gave the same result (Table 8, Entry 2).<sup>191</sup> When DMF was used as solvent an improvement of the regioisomeric ratio in favour of the desired thermodynamic product was observed (Table 8, Entries 3). Moreover, the use of catalytic amounts of sodium iodide were sufficient at higher temperatures leading to similar yields. When the temperature was increased to 145 °C the product was isolated in 94% yield and a regioisomeric ratio of 93:7 (Table 8, Entry 4).

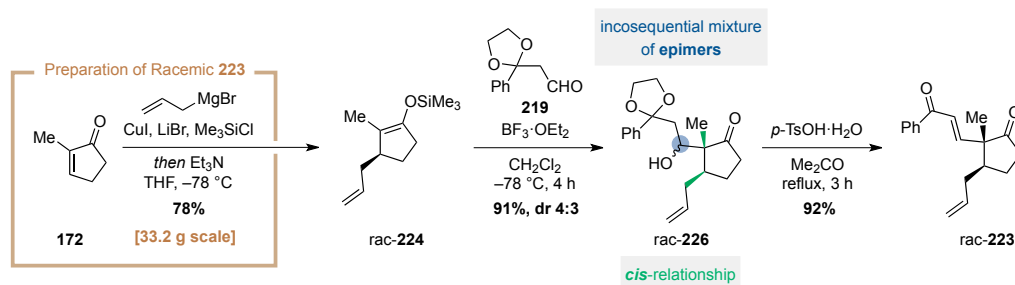
**Table 8.** Evaluation of different conditions for the preparation of the thermodynamic silyl enol ether **224**.



Entry	Me <sub>3</sub> SiX	Base	Additive	Solvent	T	t	Result <sup>a</sup>
1	Me <sub>3</sub> SiI (2.2 equiv)	HMDS (2.4 equiv)		pentane	-20 °C to r.t.	16 h	n.d. (50:50)
2	Me <sub>3</sub> SiCl (5.0 equiv)	Et <sub>3</sub> N (5.0 equiv)	NaI (1.5 equiv)	MeCN	100 °C	16 h	79% (49:51)
3	Me <sub>3</sub> SiCl (3.0 equiv)	Et <sub>3</sub> N (3.3 equiv)	NaI (10 mol%)	DMF	120 °C	20 h	72% (75:25)
4	Me <sub>3</sub> SiCl (3.0 equiv)	Et <sub>3</sub> N (3.3 equiv)	NaI (5 mol%)	DMF	145 °C	21 h	94% (93:7)

a) The ratio was determined by <sup>1</sup>H NMR spectroscopy. The yields were determined by isolation.

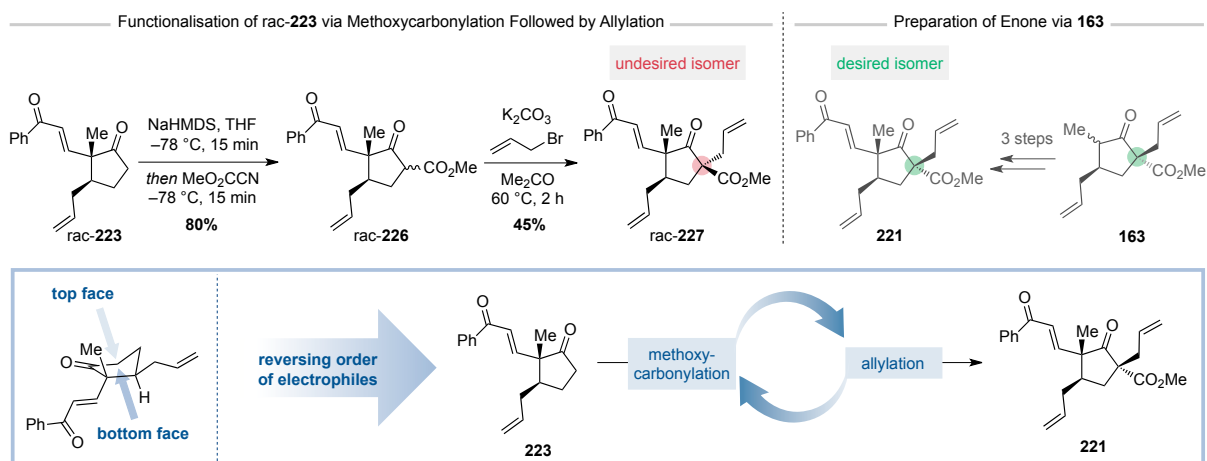
Having identified a suitable pathway towards enantioenriched silyl enol ether **224**, further studies were conducted with the easier accessible racemate, which can be prepared in one step from 2-methylcyclopent-2-enone (**172**) on a multi-gram scale (Scheme 51).<sup>192</sup> Hence, all following reactions were conducted with racemic mixtures. The aforementioned sequence of MUKAIYAMA aldol reaction with aldehyde **219**, delivering an incosequential mixture of epimers that converge in the next step, and tandem deacetalisation/dehydration afforded enone **rac-223** in very good yields. Since the sequential functionalisation of cyclopentenones via conjugate addition and subsequent  $\alpha$ -alkylation usually gives *trans*-relationships between both substituents,<sup>162</sup> because the electrophile approaches from the less hindered face of the enolate, enone **rac-223** was deduced to possess the desired *cis*-relationship between methyl and allyl group. This was supported by NOE correlations and proven by X-ray crystal structure analysis on later stages.



**Scheme 51.** Preparation of racemic enone **223** starting from 2-methylcyclopent-2-enone (**172**).

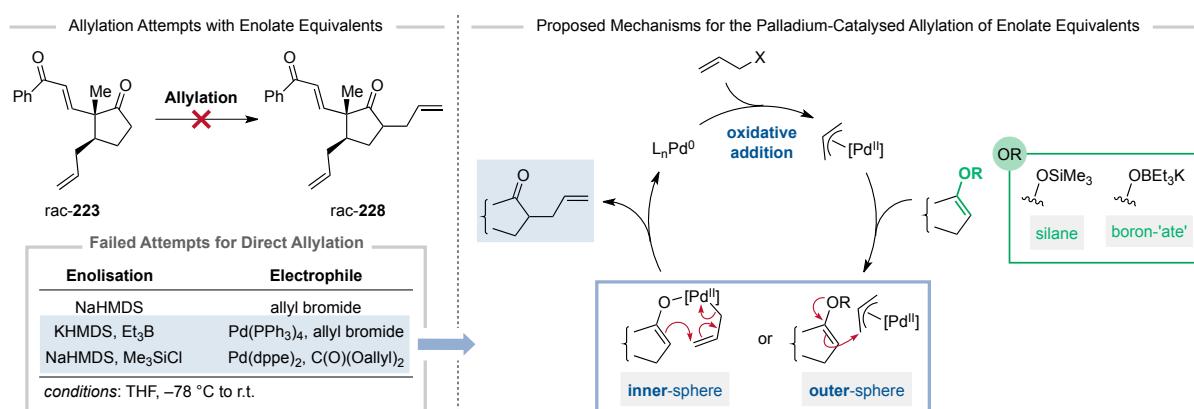
### 5.3.5 Construction of the Second Quarternary Stereocenter

For the construction of the second quarternary stereocenter, different methoxycarbonylation reagents were tested. While the use of dimethoxy carbonate resulted in no conversion, methyl chloroformate only gave the *O*-carbonylated product. Eventually, when methyl cyanofornate was used the desired  $\beta$ -keto ester **rac-226** was isolated in 80% (Scheme 52).<sup>193</sup> Treatment with allyl bromide and potassium carbonate in acetone delivered the undesired isomer as revealed by comparison of the NMR data of the previously synthesised  $\beta$ -keto ester **221** (Scheme 52). In accordance with the previous findings these results indicate that approach of the second electrophile is entirely under substrate control and exclusively proceeds with the undesired facial selectivity. Thus, the desired isomer should be accessible by reversing the order of allylation and methoxycarbonylation leveraging the substrate-inherent bias.



**Scheme 52.** Evaluation of substrate bias on the construction of the second quarternary stereocenter.

Therefore, various allylation protocols employing different electrophiles were tested. Unfortunately, ketone **rac-223** was rather inert towards reaction with allyl bromide and either no conversion was observed or degradation upon warming to ambient temperature (Scheme 53). Similar challenges have been reported for other cyclic ketones. Previous reports by COVEY and co-workers noted the resistance of a Hajos-Parrish ketone derived cyclohexanone to several alkylation attempts.<sup>194</sup> During their investigations, the authors found that allylation was feasible by applying NEGISHI's protocol for the reaction of preformed potassium enoxyborates with allylic electrophiles in the presence of a palladium(0) catalyst.<sup>195</sup> The reaction is proposed to proceed via formation of a  $\pi$ -allyl palladium(II) complexes resulting from the oxidative addition of the allyl reagent to the catalyst. The cationic palladium species exhibits pronounced electrophilic character and readily reacts with enolate complex. Allylation can either occur via an outer-sphere mechanism in a  $S_N2$ -like manner or an inner-sphere mechanism involving transmetalation to generate a palladium-enolate species followed by [3,3']-reductive elimination (Scheme 53).<sup>196,197</sup> However, when ketone **rac-223** was deprotonated with KHMDS, followed by sequential addition of triethylborane and a mixture of allyl bromide and catalytic  $Pd(PPh_3)_4$ , even after several hours at ambient temperature, no conversion was observed (Scheme 53). A similar protocol, utilising silyl enol ethers as enolate equivalents for the reaction with  $\pi$ -allyl palladium(II) electrophiles, was described by TSUJI and co-workers, circumventing challenges associated with simple ketones.<sup>198</sup> Unfortunately, *in situ* formation of the corresponding silyl enol ether and subsequent treatment with diallyl carbonate in the presence of catalytic  $Pd(dppe)_2$  resulted in no conversion as well.

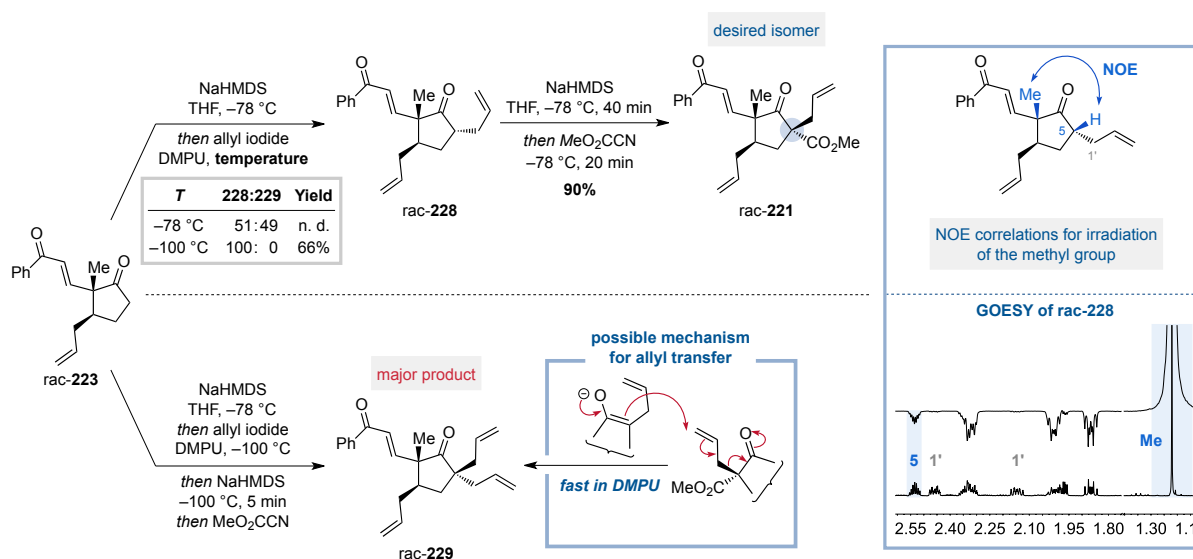


**Scheme 53.** Attempted direct allylation of ketone **rac-223** and the proposed mechanisms for palladium-catalysed systems.

As several examples in the literature for five- and six-membered cyclic ketones noted the use of HMPA and allyl iodide, initial attempts were conducted by applying these conditions.<sup>199</sup> Gratifyingly, deprotonation of ketone **rac-223** with LDA and treatment of the resulting enolate with allyl iodide in the presence of HMPA delivered the desired product. Moreover, telescoping the allylation and subsequent methoxycarbonylation under these conditions into a one-pot process was achieved by S. PONATH affording ketone **rac-221** in 54% yield on a 100 mg scale. As exchange of HMPA with DMPU gave the same result, further experiments were performed with the latter. Attempts to upscale the reaction, however, failed resulting in poor yields and dialkylated ketone **rac-229** as the major product. As it was unclear, which conditions facilitated the formation of **rac-220**, the monoalkylated ketone **rac-228** was isolated and then subjected to methoxycarbonylation in the presence of DMPU to simulate the conditions during the one-pot process. Analysis of the reaction by TLC revealed that formation of  $\beta$ -keto ester **rac-221** was fast within the first minutes. Unfortunately, with progressing consumption of ketone **rac-228** the appearance of **rac-229** was noted and, after several minutes,



formation of the dialkylated product predominated, even at  $-100\text{ }^{\circ}\text{C}$ . In light of these observations, it was speculated that the  $\alpha$ -alkylated  $\beta$ -keto ester **rac-228** acts as a powerful allylating agent in the presence of DMPU, thereby rendering a one-pot process unfeasible on larger scales.



**Scheme 54.** Left: Preparation of  $\beta$ -keto ester **rac-221** via direct allylation of ketone **rac-223** and attempted one-pot procedure. Right: GOESY experiment and NOE analysis to elucidate the stereochemistry for **rac-228**.

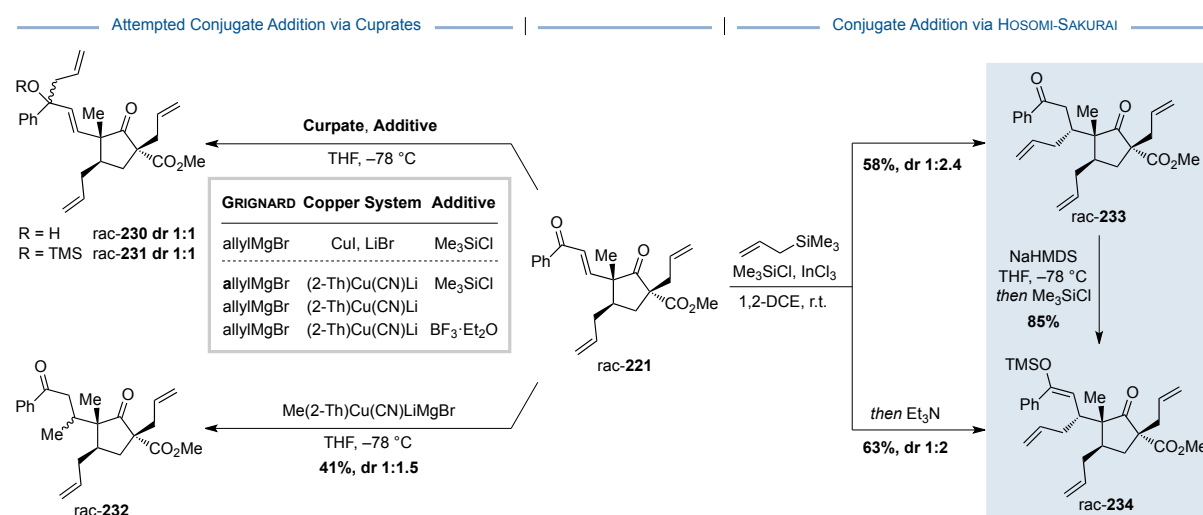
The relative configuration of the monoalkylated product **rac-228** was elucidated by GOESY experiments and analysis of the observed NOE correlations.

### 5.3.6 Installation of the Third Allyl Group

With enone **rac-221** prepared, the attention was turned towards the installation of the third and final allyl group. Initial efforts were focused on the use of allyl organocopper(I) reagents to facilitate conjugate addition. However, exposure of enone **rac-221** to allyl cuprate, generated from allylmagnesium bromide and CuI in the presence of LiBr, furnished exclusively the 1,2-addition product (Scheme 55). This result might be attributed to the steric encumbrance of the enone owing to its neopentyl-like position. Hence, the use of LIPSHUTZ-type cuprates<sup>200</sup> derived from copper(I) cyanide was explored, as these types of cuprates are reported in some instances to be more reactive and therefore capable of promoting conjugate addition to even highly congested enones.<sup>200a,201</sup> Unfortunately, reaction with cuprates prepared from 2-thienyl(cyano)copper(I) lithium<sup>200</sup> and allylmagnesium bromide exhibited the same selectivity and neither the addition of trimethylsilyl chloride<sup>202</sup> nor boron trifluoride diethyl etherate<sup>200a,203</sup> encouraged conjugate addition (Scheme 55). A control experiment was performed with a methyl cuprate, prepared from the same LIPSHUTZ precursor<sup>200</sup> and methylmagnesium bromide, in order to assess whether addition to the carbonyl group is favoured in general. The methylated product **rac-232** was isolated in 41% yield as a 1:1.5 mixture of diastereomers and no formation of 1,2-addition was observed (Scheme 55). These findings could suggest that, in case of allyl cuprates, other mechanistical pathways, which might predominate under certain conditions, are available. As the reaction of enone **rac-221** with allyl cuprates turned out to result solely in addition to the carbonyl, other systems were investigated. In light of various literature precedents for conjugate allylation, the HOSOMI-SAKURAI reaction,<sup>204</sup> employing allyltrimethylsilane as allyl donor, was considered a promising alternative. Therefore, several conditions were tested by S. PONATH. The screening of several LEWIS acids revealed that typical systems employing stoichiometric amounts of either titanium tetrachloride<sup>204</sup> or boron trifluoride diethyl etherate failed resulting in rapid degradation. Other systems using catalytic iron(III) chloride,<sup>205</sup> iodine<sup>206</sup> or indium in combination with trimethylsilyl chloride,<sup>207</sup> however, gave either very low or no

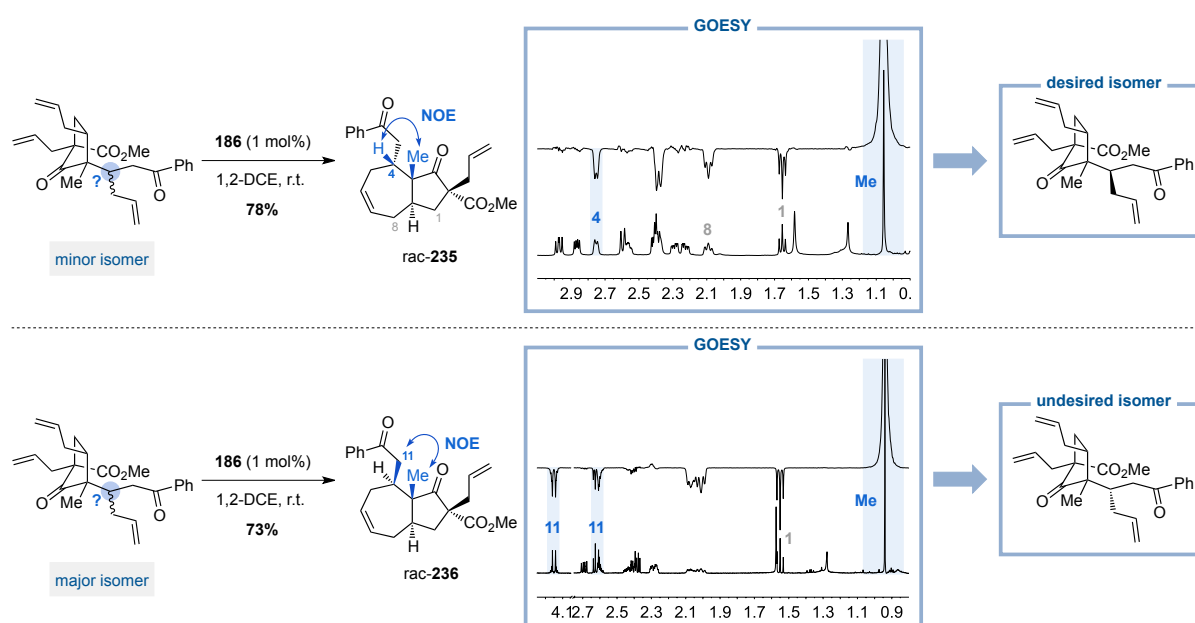


conversion at all. Eventually, the use of indium(III) chloride in the presence of trimethylsilyl chloride, as reported by LEE and co-workers, proved to deliver the best results.<sup>208</sup> Under these conditions the desired product **rac-233** could be isolated in 58% yield as a mixture of two diastereomers (dr 1:2.4) (Scheme 55). Interestingly, partial trapping of the enolate with trimethylsilyl chloride was observed during the reaction and addition of triethylamine following complete conversion of enone **rac-221** led to the isolation of silyl enol ether **rac-234** in 63% yield as a mixture of diastereomers (dr 1:2). Alternatively, the preparation of the silyl enol ether can be achieved in a two-step sequence starting from enone **rac-221** via enolisation of the SAKURAI product **rac-233**.



**Scheme 55.** Attempted and successful conjugate allylation of enone **rac-221**.

In order to elucidate the relative configurations, both diastereomeric ketons were separated by HPLC and subsequently cyclised via ring-closing metathesis to yield the corresponding seven-membered rings **rac-234** and **rac-236**. Subjection to GOESY experiments and analysis of the resulting NOE correlations, unfortunately, indicated that the observed minor isomer possess the desired configuration, which was confirmed by X-ray crystal structure analysis on a later stage (Scheme 56).

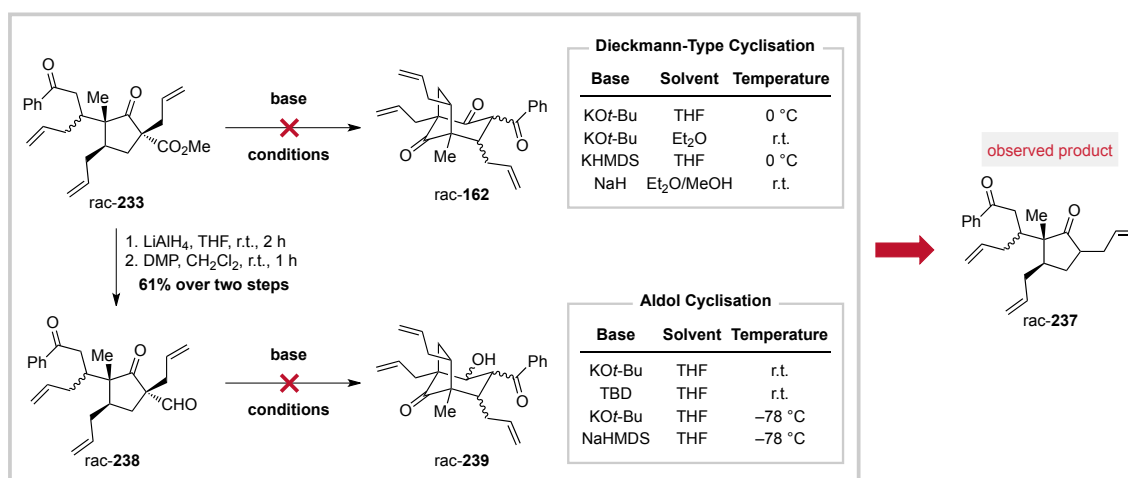


**Scheme 56.** Ring-closing metathesis of both diastereomeric allylation products and elucidation of the respective relative configuration via GOSEY experiments.

Further attempts, including variation of temperature and solvent, as well as attempted conformational locking via ring closing metathesis or introduction of other nucleophiles, to reverse the selectivity remained unsuccessful.

### 5.3.7 Preparation of Triketone rac-162

Having assembled the carbon skeleton of the cyclisation precursor rac-233, the construction of the bicyclic intermediate rac-162 was addressed. All attempts by S. PONATH to close the six-membered ring under basic conditions via a DIECKMANN-type reaction resulted in degradation and only the decarboxylation product rac-237 was isolated (Scheme 57). It is noteworthy that all experiments were conducted under careful exclusion of water regarding solvent and base since it was speculated at first that decarboxylation could be triggered by ester hydrolysis. Moreover, at temperatures below  $-20\text{ }^{\circ}\text{C}$  no conversion was observed.



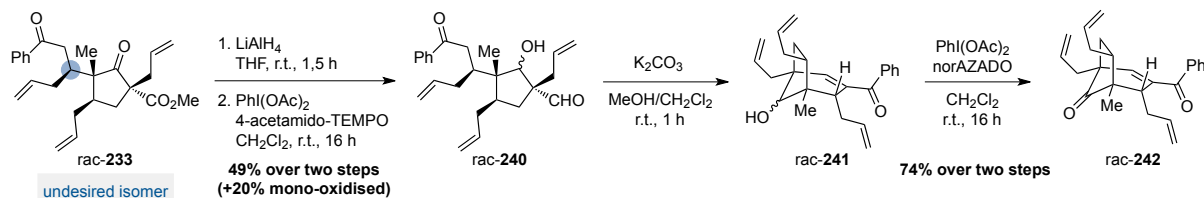
**Scheme 57.** Attempted DIECKMANN and aldol cyclisation of cyclopentanones rac-233 and rac-238, respectively.

Thus, it was envisaged to perform the cyclisation at lower temperatures via an aldol reaction in order to shut down undesired degradation. Preparation of the requisite aldehyde rac-238 was achieved by sequential reduction and oxidation in 61% yield over two steps. Unfortunately, when aldehyde rac-238 was exposed to basic conditions to promote enolate formation and subsequent aldol cyclisation, the same degradation product was observed irrespective of temperature and the employed base (Scheme 57). It was speculated that the cyclopentanone initiates fragmentation via a retro-CLAISEN-type reaction to release ring strain.

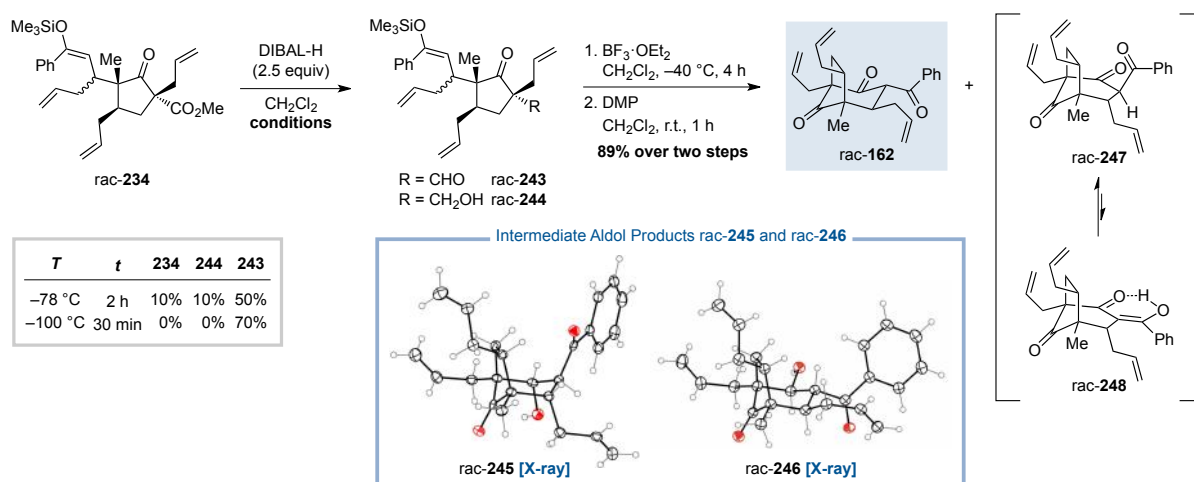
To avoid such undesired pathways, it was envisaged to reduce the ketone prior to cyclisation. It should be noted that the following reactions were conducted with the undesired isomer to test the feasibility of this approach. Global reduction of rac-233 with lithium aluminium hydride and subsequent selective oxidation employing ANELLI-like conditions with bis(acetoxy)iodobenzene as terminal oxidant<sup>209</sup> allowed for the preparation of the corresponding aldehyde rac-240 in 49% yield as a mixture of epimers (Scheme 58). Eventually, mild basic conditions in a protic medium afforded two diastereomeric cyclisation products,<sup>210</sup> which after oxidation yielded a single isomer. Analysis of the NMR spectroscopic data, however, revealed the  $\alpha,\beta$ -unsaturated ketone as the product rac-242 and in hindsight rac-241 as a mixture of epimeric aldol condensation products (Scheme 58). Based on these results, it was concluded that mild and non-basic conditions prevent fragmentation and the aldol reaction in general provides a suitable pathway to access the bicyclic scaffold. In order to suppress the undesired elimination, lower temperatures and the exclusion of protic solvents were investigated. These conditions are typically employed in MUKAIYAMA aldol reactions using silyl enol ethers as neutral enolate equivalents.<sup>188</sup> However, preparation of a suitable aldol precursor required selective reduction of the ester while preserving the benzylic ketone. For this purpose, protection of the ketone was envisioned by exploiting silyl enol ether rac-234 which is accessible from enone rac-221 in one

pot via the aforementioned HOSOMI-SAKURAI conditions with triethylamine. When a diastereomeric mixture of ester **rac-234** was treated with DIBAL at  $-78\text{ }^{\circ}\text{C}$ , the desired product **rac-243** could be isolated in 50% yield, however, overreduction to the primary alcohol **rac-244** occurred as a side reaction. Lowering the temperature to  $-100\text{ }^{\circ}\text{C}$  suppressed formation of side product and the aldehyde was isolated in an increased yield of 70% (Scheme 58).

**A** – Attempted Aldol cyclisation via Aldehyde **rac-240**.



**B** – Aldol cyclisation via Aldehyde **rac-234**.



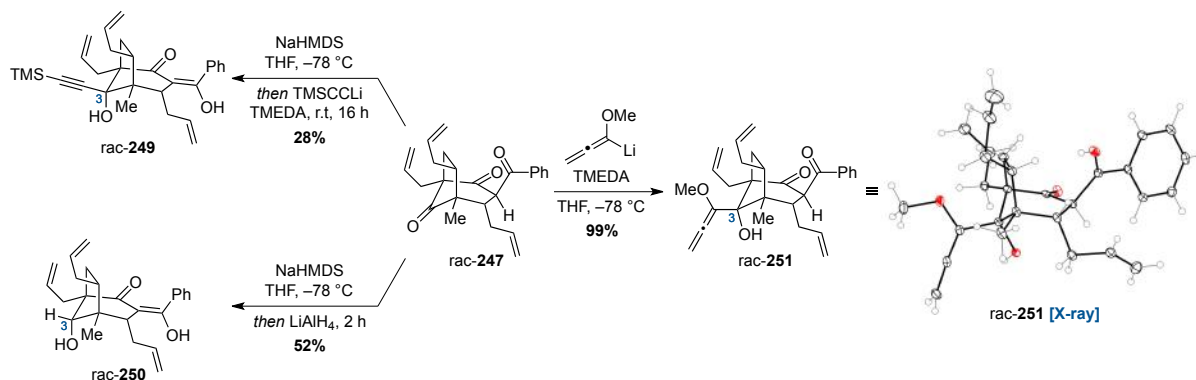
**Scheme 58.** Attempted and successful aldol cyclisation to prepare triketones **rac-162** and **rac-247**.

The subsequent intramolecular MUKAIYAMA aldol reaction with boron trifluoride diethyl etherate proceeded with high conversion and afforded a mixture of four diastereomers. Samples of the two major aldol products **rac-245** and **rac-246** were separated and subjected to X-ray crystal structure analysis confirming the previous assignment of minor and major product resulting from the HOSOMI-SAKURAI allylation. Eventually, oxidation of the crude product gave both bicyclic products **rac-162** and **rac-247** which could be separated by column chromatography at this stage. The undesired epimer **rac-247** was found to be in equilibrium with its enol form, whereas **rac-162** adopts the thermodynamically stable form with allyl and acyl substituents equatorial positioned.

### 5.3.8 Installation of the Methoxycarbonyl Group

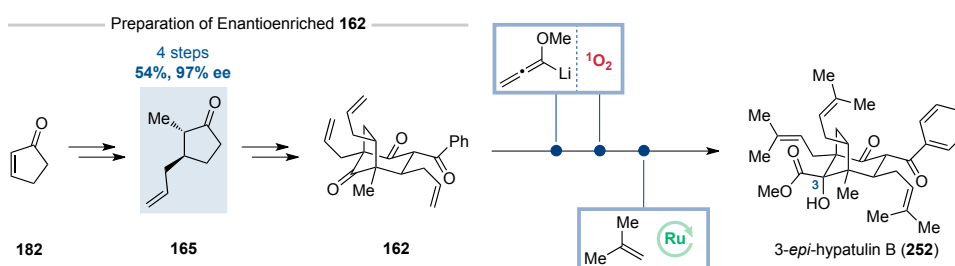
With the bicyclic triketone **rac-162** in hand, the remaining challenge of introducing the final carbonyl functionality was addressed. To identify suitable acyl or carboxylate carbanion equivalents preliminary test reactions were conducted with the undesired triketone **rac-247**. Initial attempts, including transhydrocyanation,<sup>211</sup> by S. PONATH to introduce a cyano group were unsuccessful as no conversion of the starting material was observed. It was assumed that stronger nucleophiles, that add irreversible to the ketone, are required. However, when switching to lithiated 1,3-dithiane<sup>212</sup> no conversion was observed at lower temperatures while warming to ambient temperature resulted in degradation. On the other hand, smaller nucleophiles, such as hydride, lithiated alkynes, and lithiated methoxyallene,<sup>213</sup> added successfully to triketone **rac-247** (Scheme 59). Unfortunately, X-ray crystal structure analysis of **rac-251** and NMR analysis of **rac-249**

and **rac-250** revealed that addition occurred with the undesired facial selectivity leading to the epimeric configuration of the natural product at C-3 in all cases.



**Scheme 59.** Addition on small nucleophiles to triketone **rac-247**.

Since all attempts to reverse the facial selectivity, including for instance ring-closing metathesis of the cyclopentane-associated allyl groups to shield the observed trajectory for nucleophilic attack, remained unsuccessful, synthetic efforts were focused on the synthesis of 3-*epi*-hypatulin B (**252**). During the course of further studies the developed route was applied to enantioenriched ketone **165** and the methyl ester could successfully be installed via a sequence of methoxyallene addition and subsequent oxidative cleavage with singlet oxygen. Unfortunately, the methoxycarbonylation proceeded again with the undesired facial selectivity. However, investigation of an olefin cross metathesis ultimately enabled the synthesis of enantioenriched 3-*epi*-hypatulin B (**252**) in 16 steps starting from cyclopentenone **182**.



**Scheme 60.** Synthesis of 3-*epi*-hypatulin B.

## 5.4 Publication

### 5.4.1 Synthesis of 3-*epi*-Hypatulin B Featuring a Late-Stage Photo-Oxidation in Flow

---

<b>Authors</b>	Stefan Leisering, Sebastian Ponath, Kamar Shakeri, Alexandros Mavroskoufis, Merlin Kleoff, Patrick Voßnacker, Simon Steinhauer, Manuela Weber, Mathias Christmann
<b>Journal</b>	<i>Org. Lett.</i>
<b>DOI</b>	submitted
<b>Abstract</b>	<p>A total synthesis of 3-<i>epi</i>-hypatulin B, a highly oxygenated and densely functionalized bicyclic scaffold, is reported. The carbon skeleton was prepared by functionalization of a cyclopentanone core and an intramolecular Mukaiyama aldol reaction. The synthesis features a late-stage photo-oxidation of a methoxyallene intermediate for the installation of an ester functionality. Problems encountered during the batch process were solved by translation of the transformation into a flow protocol. Our synthesis highlights the value of flow chemistry to enable challenging steps in natural product synthesis.</p>
<b>Author Contribution</b>	<p>The concept of the manuscript and the retrosynthetic analysis was elaborated by S. Leisering, Dr. S. Ponath and Prof. Dr. M. Christmann.</p> <p>K. Shakeri and A. Mavroskoufis helped with the preparation of compound <b>5</b> and the investigation of some nucleophiles for addition to compound <b>4</b>. The preliminary studies and the route towards compound <b>11</b> was developed in collaboration with Dr. S. Ponath. The attempted Dieckmann cyclisations were carried out by Dr. S. Ponath. The rest of the synthesis was carried out by S. Leisering. The associated analytical data were collected by S. Leisering and Dr. S. Ponath. The crystals of compounds <b>4</b>, (10<i>R</i>)-<b>8</b>, <b>14</b> and <b>15</b> for X-ray diffraction analysis was provided by S. Leisering and the measurements and analyses were performed by M. Weber and S. Steinhauer. P. Voßnacker helped with the analysis of the data.</p> <p>The Manuscript was written by S. Leisering, Dr. M. Kleoff and Prof. Dr. M. Christmann.</p>

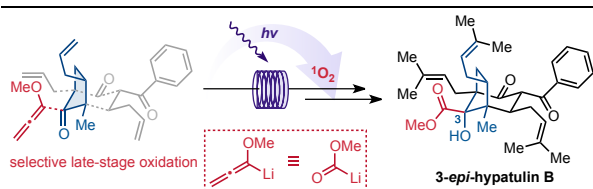
---

## Synthesis of 3-*epi*-Hypatulin B Featuring a Late-Stage Photo-Oxidation in Flow

Stefan Leisering, Sebastian Ponath, Kamar Shakeri, Alexandros Mavroskoufis, Merlin Kleoff, Patrick Voßnacker, Simon Steinhauer, Manuela Weber, Mathias Christmann\*

Institute of Chemistry and Biochemistry, Freie Universität Berlin, Takustraße 3, 14195 Berlin, Germany

Supporting Information Placeholder



**ABSTRACT:** A total synthesis of 3-*epi*-hypatulin B, a highly oxygenated and densely functionalized bicyclic scaffold, is reported. The carbon skeleton was prepared by functionalization of a cyclopentanone core and an intramolecular Mukaiyama aldol reaction. The synthesis features a late-stage photo-oxidation of a methoxyallene intermediate for the installation of an ester functionality. Problems encountered during the batch process were solved by translation of the transformation into a flow protocol. Our synthesis highlights the value of flow chemistry to enable challenging steps in natural product synthesis.

Polycyclic polyprenylated acylphloroglucinols (PPAPs) are a family of meroterpenoids with fascinating and complex chemical structures.<sup>1</sup> Due to a wide range of intriguing biological activities, PPAPs represent potential lead structures for neuroscience, infectious disease, and oncology drug discovery programs.<sup>2</sup> Thus, several synthetic approaches, some of which culminated in elegant total syntheses, have been devised.<sup>3</sup> The most prominent congener, the neuroactive hyperforin (**1**), is one of the main bioactive compounds in *Hypericum perforatum* (St. John's wort) (Scheme 1).<sup>4</sup> While many of the isolated PPAPs retain the six-membered ring of their acylphloroglucinol progenitors, subsequent rearrangements and oxidative cleavages can result in ring expansions, contractions, or ring openings.<sup>5</sup>

In 2016, Tanaka, Kashiwada, and co-workers reported the isolation of two novel meroterpenoids with a contracted acylphloroglucinol- and a seco-acylphloroglucinol-derived motif, respectively, from the leaves of *hypericum patalum*.<sup>6</sup> Whereas hypatulin A (**2**) has a highly oxygenated tricyclic octahydro-1,5-methanopentalene core, hypatulin B (**3**) possesses a bicyclo[3.2.1]octane motif. Both natural products have a densely substituted cyclopentane core bearing four stereocenters, three of them being quaternary (Scheme 1).

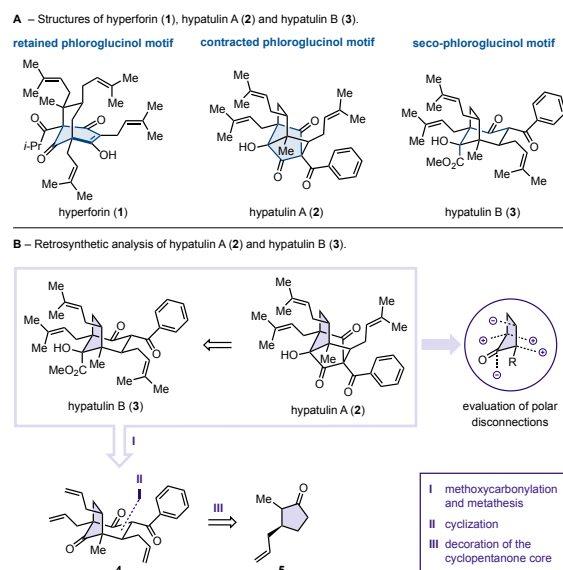
Hypatulin A (**2**) and B (**3**) were evaluated for their antimicrobial activity on strains of *Staphylococcus aureus*, *Bacillus subtilis*, and *Escherichia coli*. Hypatulin A exhibited activity against *Bacillus subtilis*.

According to Tanaka, Kashiwada, and co-workers hypatulin B (**3**) could be produced by oxidative cleavage and methylation through a biogenetic pathway from hypatulin A (**2**). The structural assignment of C-3 was supported by chemical conversion of hypatulin A (**2**) into hypatulin B (**3**) by a retro-Dieckmann-type cleavage using *N,N*-dimethylaminopyridine (DMAP) in MeOH.

We speculated that the easier accessible hypatulin B (**3**) could be transformed into hypatulin A (**2**) via cyclization. Simplification of hypatulin B (**3**) by methoxycarbonylation and subsequent metathesis would lead to triketone **4**. Construction of the bicyclic scaffold was envisaged by a Dieckmann-type cyclization and installation of the substituents was intended by stereoselective functionalizations of ketone **5** (Scheme 1).



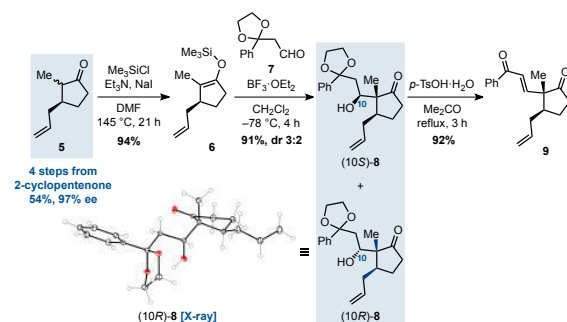
### Scheme 1. Different PPAPs and Retrosynthetic Analysis of Hypatulin A (2) and Hypatulin B (3)



The synthesis commenced with cyclopentanone **5**, which was prepared in 97% enantiomeric excess in analogy to a procedure by Taber and co-workers in four steps starting from 2-cyclopentenone.<sup>7</sup> Enolization under thermodynamic control afforded silyl enol ether **6** in 94% yield and in a 93:7 ratio of constitutional isomers (Scheme 2).<sup>8</sup> Subsequent Mukaiyama aldol addition with aldehyde **7** proceeded in 91% yield and generated the first of three quaternary stereocenters of the cyclopentane core. A 3:2-mixture of two diastereomers was obtained, providing, after separation, one diastereomer as a crystalline solid. X-ray crystal structure analysis revealed (10*R*)-**8** to possess the desired *cis*-relationship between methyl and allyl substituent. Both diastereomers were subjected to a tandem deacetalization/elimination affording enone **9**. As both diastereomers **8** converge into enone **9**, it can be deduced that they are diastereomers at C-10, thus rendering the low diastereoselectivity inconsequential for the further synthesis (Scheme 2). With enone **9** in hand, construction of the second quaternary center bearing a methyl ester and an allyl group was pursued. Initial attempts to install the ester first, followed by an allylation resulted in the exclusive formation of the undesired diastereomer. Thus, the order of the electrophile additions was reversed. Interestingly, allylation of the corresponding enolate with allyl iodide in the presence of *N,N'*-dimethylpropyleneurea (DMPU) at  $-78\text{ }^{\circ}\text{C}$  gave a mixture of unreacted starting material, mono-, and bisallylated products. However, by decreasing the reaction temperature to  $-100\text{ }^{\circ}\text{C}$  monoallylation was achieved exclusively. Subsequent methoxycarbonylation was performed by deprotonation with NaHMDS and treatment with methyl cyanofor-

mate providing the desired isomer **10** in 59% over two steps (Scheme 3).

### Scheme 2. Synthesis of Enone 9 (Thermal Ellipsoids at 50% Probability)

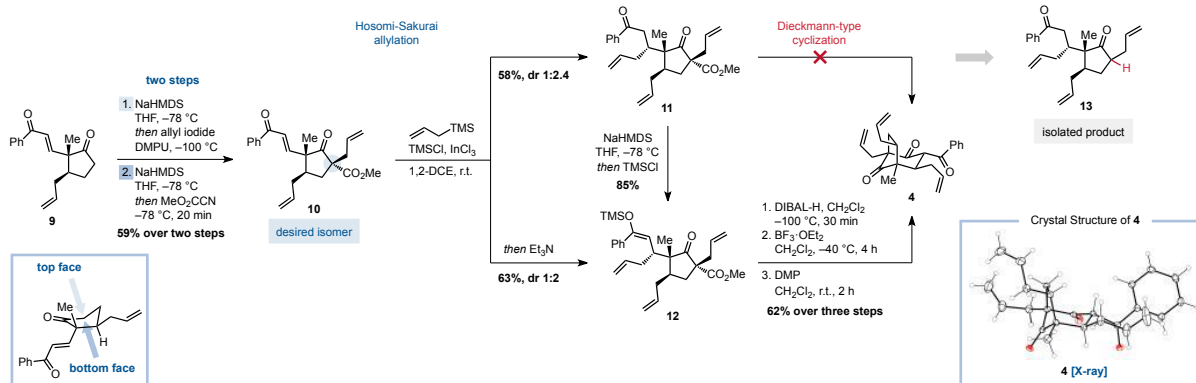


Attempts to telescope both reactions into a one-pot protocol<sup>9</sup> revealed that the allylation step requires DMPU as solvent, while methoxycarbonylation in the presence of DMPU resulted in degradation (Scheme 3).

An attempted conjugate addition of an allyl cuprate to the enone **10** failed and provided exclusively the corresponding 1,2-addition product. Therefore, a Hosomi-Sakurai reaction with allyltrimethylsilane was investigated.<sup>10</sup> A screening of various Lewis acids, including titanium tetrachloride,<sup>10</sup> boron trifluoride diethyl etherate, iron(III) chloride,<sup>11</sup> iodine,<sup>12</sup> and indium in combination with trimethylsilyl chloride,<sup>13</sup> revealed indium(III) chloride<sup>14</sup> in the presence of trimethylsilyl chloride to be the best system. Under these conditions, the 1,4-addition product **11** was isolated in 58% yield as a mixture of two diastereomers (dr 1:2.4) (Scheme 3). During the reaction, partial trapping of the enolate with trimethylsilyl chloride was observed. When triethylamine was added after completion of the conjugate addition, silyl enol ether **12** was obtained exclusively in 63% yield as a mixture of two diastereomers (dr 1:2) (Scheme 3). The configuration was determined three steps later by X-ray crystallographic analysis of intermediate **4**. Unfortunately, the desired product turned out to be the minor diastereomer. Attempts to reverse the stereoselectivity were unsuccessful.

Next, we aimed to construct bicyclic triketone **4** in a Dieckmann-type cyclization of the highly substituted cyclopentanone **11**.<sup>15</sup> Unfortunately, a variety of different conditions resulted in the formation of **13** (Scheme 3). To suppress decarboxylation, reduction of the ester to the corresponding aldehyde and subsequent aldol cyclization was attempted. When ester **12** was treated with DIBAL-H at  $-78\text{ }^{\circ}\text{C}$ , overreduction to the primary alcohol was a major side reaction. By lowering the temperature to  $-100\text{ }^{\circ}\text{C}$ , the corresponding aldehyde could be isolated in 70% yield. The subsequent intramolecular Mukaiyama aldol reaction with boron trifluoride etherate afforded a mixture of epimeric  $\beta$ -hydroxy ketones.<sup>17</sup> Oxidation of the crude mixture of both

**Scheme 3. Synthesis of Key Intermediate Triketone 4 (Thermal Ellipsoids at 50% Probability; Disorder Was Omitted for Clarity)<sup>16</sup>**



epimers with Dess-Martin periodinane (DMP)<sup>18</sup> eventually gave triketone **4** in 62% yield over three steps (Scheme 3). With the bicyclic carbon framework assembled, the introduction of the remaining carbonyl functionality was addressed. Different d1-reagents either as acyl anion equivalents or masked carbonyl equivalents were considered.<sup>19</sup> While bulky reagents such as lithiated dithianes<sup>20</sup> gave no conversion, smaller nucleophiles such as methoxyallenyl-lithium<sup>21</sup> or cyanide were added successfully to the ketone (Scheme 4). In all cases, the 1,3-diketone was 'disarmed' by *in situ* deprotonation with NaHMDS. Unfortunately, X-ray and NMR analysis revealed that addition of all nucleophiles proceeded with the undesired facial selectivity. As all our attempts to obtain the epimeric tertiary alcohol were unsuccessful, we redirected our synthetic efforts towards 3-*epi*-hypatulin B (**17**).

Attempted conversion of cyanohydrin **14** to the corresponding ester **16** resulted in the desilylation and cyanide elimination leading to ketone **4**. In contrast, the addition of methoxyallenyl-lithium is irreversible and methoxyallene **15** was isolated in 72% yield (Scheme 4). Next, we attempted the oxidative cleavage of the allenyl moiety to the corresponding ester **16**.<sup>22</sup> Although examples for ozonolysis of enol ethers in the presence of less electron-rich olefins have been reported, controlled addition of a solution of ozone, even at  $-115^{\circ}\text{C}$ , resulted in complete degradation of the starting material.<sup>23</sup> Alternatively, enol ethers can be reacted with singlet oxygen leading to dioxetanes, which decompose to the corresponding esters.<sup>24</sup> Singlet oxygen exhibits high chemo- and regioselectivity depending on substitution patterns, conformations and stereoelectronic effects of the substrates.<sup>25</sup> Gratifyingly, when methoxyallene **15** was treated with singlet oxygen generated with tetraphenylporphyrin (TPP) as photocatalyst in a test reaction the product could be isolated. As we experienced scale-up problems on a scale larger than 10 mg, we contemplated the application of flow-chemistry.<sup>26</sup> Recently, we developed a modu-

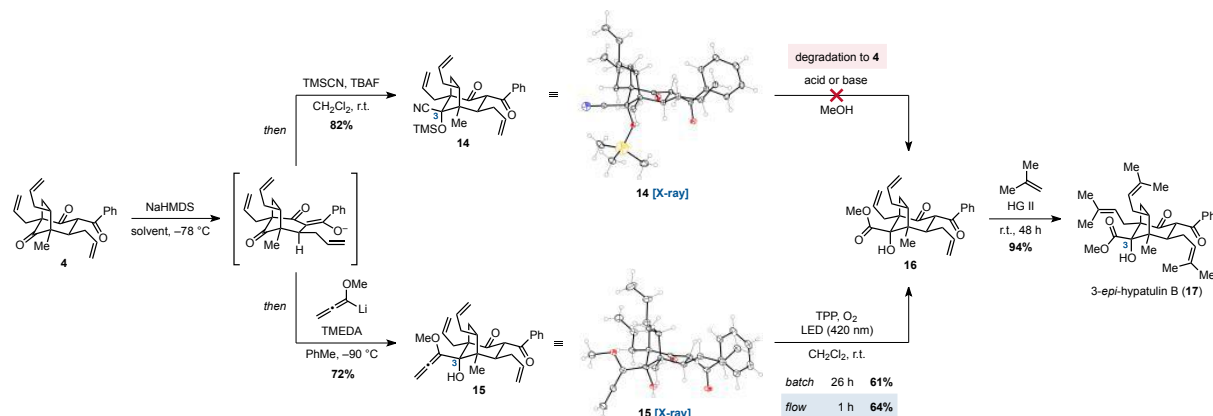
lar, and argon-driven flow platform especially designed for the robustification of late-stage transformations in natural product synthesis.<sup>27</sup> In particular, gas reactions and photo-reactions can be significantly accelerated and upscaled in flow.<sup>28</sup> Therefore, we translated the oxidative cleavage of methoxyallene **15** to ester **16** into a flow process. After optimizing reaction parameters, the desired ester **16** was obtained in a slightly higher yield of 64% and a remarkably shorter reaction time of 60 minutes compared with 26 hours in batch (Scheme 4). Most importantly, in flow, this transformation could be conducted on a 56 mg scale providing sufficient material for the final step of the synthesis.

Ester **16** was then subjected to cross metathesis conditions.<sup>29</sup> Initial reactions using 2-methyl-2-butene as a dimethylvinylcarbene source resulted in a mixture of products with dimethylated and monomethylated allyl groups. Therefore, the metathesis reaction was performed with gaseous 2-methylpropene in a pressure tube providing 3-*epi*-hypatulin B (**17**) in 94% yield (Scheme 4).<sup>30</sup>

In conclusion, we completed a synthesis of 3-*epi*-hypatulin B (**17**) in 16 steps starting from 2-cyclopentenone. The synthetic key challenge was to construct the unique bicyclic core motif in an efficient way, which was achieved by introducing all required substituents to a cyclopentane core, followed by a Mukaiyama aldol cyclization. The introduction of the last carbonyl fragment led to the undesired epimer of the tertiary alcohol. However, synthesis of 3-*epi*-hypatulin B could be achieved utilizing an oxidative cleavage of an enol ether species in presence of competing alkene functionalities. This reaction could be performed in flow allowing larger scale, shorter reaction time and a slightly higher yield. Our synthesis demonstrates the value of combining an efficient approach to a highly functionalized ring system with the virtue of flow chemistry for the robustification of late-stage transformations in natural product synthesis.



**Scheme 4. Methoxycarbonylation via Late-Stage Oxidation in Flow and Alkene Metathesis for the Formation of 3-*epi*-Hypatulin (17) (Thermal Ellipsoids at 50% Probability)<sup>16</sup>**



## ASSOCIATED CONTENT

### Supporting Information.

The Supporting Information is available free of charge on the ACS Publications website.

X-ray crystallographic data for **4** (CIF)

X-ray crystallographic data for (**10R**)-**8** (CIF)

X-ray crystallographic data for **14** (CIF)

X-ray crystallographic data for **15** (CIF)

Experimental procedures and spectroscopic data (PDF)

## AUTHOR INFORMATION

### Corresponding Author

\*E-mail: mathias.christmann@fu-berlin.de

### ORCID

Mathias Christmann: 0000-0001-9313-2392

### Notes

The authors declare no competing financial interest.

## ACKNOWLEDGMENT

We thank Luise Schefzig and Bence Hartmayer (both Freie Universität Berlin) for preparative support. We thank Dr. Daniel Franz (Freie Universität Berlin) for the recording of SCXRD data for compound **15**. We would like to acknowledge the assistance of the Core Facility BioSupraMol supported by the DFG.

## REFERENCES

- (1) Shen, X.; Ting, C. P.; Xu, G.; Maimone, T. J. Programmable mero-terpene synthesis. *Nat. Commun.* **2020**, *11*, 508.
- (2) Yang, X.-W.; Grossman, R. B.; Xu, G. Research Progress of Polycyclic Polyprenylated Acylphloroglucinols. *Chem. Rev.* **2018**, *118*, 3508–3558.

- (3) a) Tsukano, C.; Siegel, D. R.; Danishefsky, D. J. Differentiation of Nonconventional “Carbanions”—The Total Synthesis of Nemorosone and Clusianone. *Angew. Chem. Int. Ed.* **2007**, *46*, 8840–8844; b) Qi, J.; Porco, J. A. Rapid Access to Polyprenylated Phloroglucinols via Alkylative Dearomatization–Annulation: Total Synthesis of (±)-Clusianone. *J. Am. Chem. Soc.* **2007**, *129*, 12682–12683; c) Biber, N.; Möws, K.; Plietker, B. The total synthesis of hyperpauanone, hyperibone L, epiclusianone and oblongifolin A. *Nat. Chem.* **2011**, *3*, 938–942; d) Bellavance, G.; Barriault, L. Total Syntheses of Hyperforin and Papuaforins A–C, and Formal Synthesis of Nemorosone through a Gold(I)-Catalyzed Carbocyclization. *Angew. Chem. Int. Ed.* **2014**, *53*, 6701–6704; e) Sparling, B. A.; Tucker, J. K.; Moebius, D. C.; Shair, M. D. Total Synthesis of (–)-Nemorosone and (+)-Secohyperforin. *Org. Lett.* **2015**, *17*, 3398–3401; f) Ting, C. P.; Maimone, T. J. The Total Synthesis of Hyperforin. *Synlett* **2016**, *27*, 1443–1449.

- (4) a) Gurevich, A. I.; Dobrynin, V. N.; Kolosov, M. N.; Popravko, S. A.; Ryabova, I. D.; Chernov, B. K.; Derbentseva, N. A.; Aizenman, B. E.; Garagulya, A. D. Hyperforin, an Antibiotic from *Hypericum perforatum*. *Antibiotiki* **1971**, *16*, 510–513; b) Bystrov, N. S.; Chernov, B. K.; Dobrynin, V. N.; Kolosov, M. N. The Structure of Hyperforin. *Tetrahedron Lett.* **1975**, *16*, 2791–2794; c) Beerhues, L. Hyperforin. *Phytochemistry* **2006**, *67*, 2201–2207; d) Richard, J.-A. Chemistry and Biology of the Polycyclic Polyprenylated Acylphloroglucinol Hyperforin. *Eur. J. Org. Chem.* **2014**, 273–299.

- (5) a) Liu, Y.-Y.; Ao, Z.; Xue, G.-M.; Wang, X.-B.; Luo, J.-G.; Kong, L.-Y. Hypatulone A, a Homoadamantane-Type Acylphloroglucinol with an Intricately Caged Core from *Hypericum patulum*. *Org. Lett.* **2018**, *20*, 7953–7956; b) Zhang, Z.-Z.; Zeng, Y.-R.; Li, Y.-N.; Hu, Z.-X.; Huang, L.-J.; Gu, W.; Hao, X.-J.; Yuan, C.-M. Two new seco-polycyclic polyprenylated acylphloroglucinol from *Hypericum sampsonii*. *Org. Biomol. Chem.* **2021**, *19*, 216–219.

- (6) Tanaka, N.; Yano, Y.; Tatano, Y.; Kashiwada, Y. Hypatulins A and B, Meroterpenes from *Hypericum patulum*. *Org. Lett.* **2016**, *18*, 5360–5363.

- (7) Taber, D. F.; Gerstenhaber, D. A.; Berry, J. F. Enantioselective Conjugate Allylation of Cyclic Enones. *J. Org. Chem.* **2011**, *76*, 7614–7617.

- (8) a) Rochin, C.; Babot, O.; Moulines, F.; Duboudin, F. Synthèse Régiosélective de Trisenoxysilanes. *J. Organomet. Chem.* **1984**, *273*, C7–C10; b) Cazeau, P.; Duboudin, F.; Babot, O.; Dunogues, J. A New Practical Synthesis of Silyl Enol Ethers: Part I. From Simple Aldehydes and Ketones. *Tetrahedron* **1987**, *43*, 2075–2088.

- (9) Vaxelaire, C.; Winter, P.; Christmann, M. One-Pot Reactions Accelerate the Synthesis of Active Pharmaceutical Ingredients. *Angew. Chem. Int. Ed.* **2011**, *50*, 3605–3607.

- (10) Hosomi, A.; Sakurai, H. Chemistry of organosilicon compounds. 99. Conjugate addition of allylsilanes to  $\alpha,\beta$ -enones. A New method of stereoselective introduction of the angular allyl group in fused cyclic  $\alpha,\beta$ -enones. *J. Am. Chem. Soc.* **1977**, *99*, 1673–1675.
- (11) Xu, L.; Yang, M.; Qiu, H.; Lai, G.; Jiang, J. Efficient Iron-Catalyzed Sakurai–Michael Addition of Allyltrimethylsilane to Chalcones. *Synth. Commun.* **2008**, *38*, 1011–1019.
- (12) Yadav, J. S.; Reddy, B. V. S.; Sadasiv, K.; Satheesh, G. 1,4-Conjugate addition of allyltrimethylsilane to  $\alpha,\beta$ -unsaturated ketones. *Tetrahedron Lett.* **2002**, *43*, 9695–9697.
- (13) Lee, P. H.; Seomoon, D.; Kim, S.; Nagaiah, K.; Damle, S. V.; Lee, K. Efficient Addition of Allylsilanes to  $\alpha,\beta$ -Enones Using Catalytic Iridium and Trimethylsilyl Chloride. *Synthesis* **2003**, 2189–2193.
- (14) Lee, P. H.; Lee, K.; Sung, S.-y.; Chang, S. The Catalytic Sakurai Reaction. *J. Org. Chem.* **2001**, *66*, 8646–8649.
- (15) a) Dieckmann, W. Zur Kenntniss der Ringbildung aus Kohlenstoffketten. *Ber.* **1894**, *27*, 102–103; x) Wang, L.; Sun, L.; Wang, X.; Wu, R.; Zhou, H.; Zheng, C.; Xu, H. Me<sub>2</sub>AlSEt-Promoted Domino Dieckmann Cyclization Enables the Total Synthesis of Polycyclic Poly-prenylated Acylphloroglucinols. *Org. Lett.* **2019**, *21*, 8075–8079.
- (16) Crystal structures of compounds **4**, **14** and **15** were only obtained from racemic mixtures, since preliminary studies were conducted from the racemate of silyl enol ether **6** (see Supporting Information). Compound **13** was only obtained as a racemate as well.
- (17) a) Mukaiyama, T.; Koichi, N.; Kazuo, B. NEW ALDOL TYPE REACTION. *Chem. Lett.* **1973**, *2*, 1011–1014; b) Li, C.; Tu, S.; Wen, S.; Li, S.; Chang, J.; Shao, F.; Lei, X. Total Synthesis of the G2/M DNA Damage Checkpoint Inhibitor Psilostachyin C. *J. Org. Chem.* **2011**, *76*, 3566–3570.
- (18) Dess, D. B.; Martin, J. C. Readily accessible 12-I-5 oxidant for the conversion of primary and secondary alcohols to aldehydes and ketones. *J. Org. Chem.* **1983**, *48*, 4155–4156.
- (19) Hase, T. A.; Koskimies, J. K. A Compilation of References on Formyl and Acyl Anion Synthesis. *Aldrichimica Acta*, **1981**, *14*, 73–77.
- (20) a) Seebach, D.; Corey, E. J. Generation and synthetic applications of 2-lithio-1,3-dithianes. *J. Org. Chem.* **1975**, *40*, 231–237; b) Gröbel, B.-T.; Seebach, D. Umpolung of the Reactivity of Carbonyl Compounds Through Sulfur-Containing Reagents. *Synthesis* **1977**, 357–402; c) Yus, M.; Nájera, C.; Foubelo, F. The role of 1,3-dithianes in natural product synthesis. *Tetrahedron* **2003**, *59*, 6147–6212; d) Smith, A. B.; Adams, C. M. Evolution of Dithiane-Based Strategies for the Construction of Architecturally Complex Natural Products. *Acc. Chem. Res.* **2004**, *37*, 365–377.
- (21) For reviews of lithiated methoxyallenes as building blocks and carbonyl carbanion equivalents, see: a) Zimmer, R. Alkoxyallenes – Building Blocks in Organic Synthesis. *Synthesis* **1993**, 165–178; b) Zimmer, R.; Reissig, H.-U. Alkoxyallenes as Building Blocks for Organic Synthesis. *Chem. Soc. Rev.* **2014**, *43*, 2888–2903.
- (22) For examples of oxidative cleavage of methoxyallenes, see: a) Zimmer, R.; Taszarek, M.; Scheffig, L.; Reissig, H.-U. Reaction of a Polycyclic Diketone with Lithiated Methoxyallene: Synthesis of New Functionalized Cage Compounds. *Synlett* **2008**, 2046–2050; b) Bressel, B.; Reissig, H.-U. A New Approach to Neuraminic Acid Analogues via 1,2-Oxazines. *Org. Lett.* **2009**, *11*, 527–530.
- (23) a) Coulthard, G.; Erb, W.; Aggarwal, V. K. Stereocontrolled organocatalytic synthesis of prostaglandin PGF<sub>2a</sub> in seven steps. *Nature* **2012**, *489*, 278–281; b) Fisher, T. J.; Dussault, P. H. Alkene ozonolysis. *Tetrahedron* **2017**, *73*, 4233–4258.
- (24) Jefford, C. W.; Kohmoto, S.; Boukouvalas, J.; Burger, U. Reaction of Singlet Oxygen with Enol Ethers in the Presence of Acetaldehyde. Formation of 1,2,4-Trioxanes. *J. Am. Chem. Soc.* **1983**, *105*, 6498–6499.
- (25) a) Sivaguru, J.; Saito, H.; Poon, T.; Omonuwa, T.; Franz, R.; Jockusch, S.; Hooper, C.; Inoue, Y.; Adam, W.; Turro, N. J. Stereoselective Photooxidation of Encarbamates: Reactivity of Ozone vs Singlet Oxygen. *Org. Lett.* **2005**, *7*, 2089–2092; b) Bayer, P.; Pérez-Ruiz, R.; Jacobi von Wangelin, A. Stereoselective Photooxidations by the Schenck Ene Reaction. *ChemPhotoChem* **2018**, *2*, 559–570; c) Bayer, P.; Schachtner, J.; Májek, M.; Jacobi von Wangelin, A. Visible light-mediated photo-oxygenation of arylcyclohexenes. *Org. Chem. Front.* **2019**, *6*, 2877–2883.
- (26) a) Pastre, J. C.; Browne, D. L.; Ley, S. V. Flow chemistry syntheses of natural products. *Chem. Soc. Rev.* **2013**, *42*, 8849–8869; b) Plutschack, M. B.; Pieber, B.; Gilmore, K.; Seeberger, P. H. The Hitchhiker's Guide to Flow Chemistry. *Chem. Rev.* **2017**, *117*, 11796–11893.
- (27) Kleoff, M.; Schwan, J.; Christmann, M.; Heretsch, P. A Modular, Argon-Driven Flow Platform for Natural Product Synthesis and Late-Stage Transformations. *Org. Lett.* **2021**, *23*, 2370–2374.
- (28) a) Su, Y.; Straathof, N. J. W.; Hessel, V.; Noël, T. Photochemical Transformations Accelerated in Continuous-Flow Reactors: Basic Concepts and Applications. *Chem. Eur. J.* **2014**, *20*, 10562–10589; b) Ghogare, A. A.; Greer, A. Using Singlet Oxygen to Synthesize Natural Products and Drugs. *Chem. Rev.* **2016**, *116*, 9994–10034; c) Cambié, D.; Bottecchia, C.; Straathof, N. J. W.; Hessel, V.; Noël, T. Applications of Continuous-Flow Photochemistry in Organic Synthesis, Material Science, and Water Treatment. *Chem. Rev.* **2016**, *116*, 10276–10341; d) Mallia, C. J.; Baxendale, I. R. The Use of Gases in Flow Synthesis. *Org. Process Res. Dev.* **2016**, *20*, 327–360.
- (29) a) Schuster, M.; Blechert, S. Olefin Metathesis in Organic Chemistry. *Angew. Chem. Int. Ed. Engl.* **1997**, *36*, 2036–2056; b) Fürstner, A. Olefin Metathesis and Beyond. *Angew. Chem. Int. Ed.* **2000**, *39*, 3012–3043; c) Chatterjee, A. K.; Choi, T.-L.; Sanders, D. P.; Grubbs, R. H. A General Model for Selectivity in Olefin Cross Metathesis. *J. Am. Chem. Soc.* **2003**, *125*, d) Grubbs, R. H. Olefin metathesis. *Tetrahedron* **2004**, *60*, 7117–7140;
- (30) Uwamori, M.; Nakada, M. Stereoselective total synthesis of ( $\pm$ )-hyperforin via intramolecular cyclopropanation. *Tetrahedron Lett.* **2013**, *54*, 2022–2025.

## 6 List of References and Illustration Credits

### 6.1 References

- (1) Maeda, H. A. Evolutionary Diversification of Primary Metabolism and Its Contribution to Plant Chemical Diversity. *Front. Plant Sci.* **2019**, *10*, 881.
- (2) Maplestone, R. A.; Stone, M. J. The evolutionary role of secondary metabolites — a review. *Gene* **1992**, *115*, 151–157.
- (3) Kliebenstein, D. J. Secondary metabolites and plant/environment interactions: a view through *Arabidopsis thaliana* tinged glasses. *Plant Cell Environ.* **2004**, *27*, 675–684.
- (4) Nishida, R. Chemical ecology of insect–plant interactions: ecological significance of plant secondary metabolites. *Biosci. Biotechnol. Biochem.* **2014**, *78*, 1–13.
- (5) Christianson, D. W. Structural and Chemical Biology of Terpenoid Cyclases. *Chem. Rev.* **2017**, *117*, 11570–11648.
- (6) a) Maimone, T. J.; Baran, P. S. Modern synthetic efforts towards biologically active terpenes. *Nat. Chem. Bio* **2007**, *3*, 396–407; b) Bohlmann, J.; Keeling, C. I. Terpenoid biomaterials. *Plant. J.* **2008**, *54*, 656–669.
- (7) Gershenzon, J.; Dudareva, N. The function of terpene natural products in the natural world. *Nat. Chem. Bio.* **2007**, *3*, 408–414.
- (8) Wallach, O. Zur Kenntniss der Terpene und der ätherischen Oele; Fünfte Abhandlung. *Liebigs Ann. Chem.* **1887**, *239*, 1–54.
- (9) Ruzicka, L. The isoprene rule and the biogenesis of terpenic compounds. *Experientia* **1953**, *9*, 357–367.
- (10) a) Chaykin, S.; Law, J.; Phillips, A. H.; Bloch, K. PHOSPHORYLATED INTERMEDIATES IN THE SYNTHESIS OF SQUALENE. *PNAS* **1958**, *44*, 998–1004; b) Rilling, H. C.; Bloch, K. On the Mechanism of Squalene Biogenesis from Mevalonic Acid. *J. Biol. Chem.* **1959**, *234*, 1424–1432.
- (11) a) Lynen, F.; Eggerer, H.; Henning, U.; Kessel, I. Farnesyl-pyrophosphat und 3-Methyl- $\Delta^3$ -butenyl-1-pyrophosphat, die biologischen Vorstufen des Squalens. Zur Biosynthese der Terpene, III. *Angew. Chem.* **1958**, *70*, 738–742; b) Lynen, F. Biosynthetic pathways from acetate to natural products. *Pure Appl. Chem.* **1967**, *14*, 137–168.
- (12) a) Dewick, P. M. The biosynthesis of C<sub>5</sub>–C<sub>25</sub> terpenoid compounds. *Nat. Prod. Rep.* **2002**, *19*, 18–1222; b) Kuzuyama, T. Mevalonate and Nonmevalonate Pathways for the Biosynthesis of Isoprene Units. *Biosci. Biotechnol. Biochem.* **2002**, *66*, 1619–1627.
- (13) a) Bloch, K. The biological synthesis of cholesterol. *Science*, **1965**, *150*, 19–28; b) Katsuki, H.; Bloch, K. Studies on the biosynthesis of ergosterol in yeast: Formation of methylated intermediates. *J. Biol. Chem.* **1967**, *242*, 222–227; c) Lynen, F. Biosynthetic pathways from acetate to natural products. *Pure Appl. Chem.* **1967**, *14*, 137–167.
- (14) Goldstein, J. L.; Brown, M. S. Regulation of the mevalonate pathway. *Nature* **1990**, *343*, 425–430.
- (15) a) Rohmer, M. The discovery of a mevalonate-independent pathway for isoprenoid biosynthesis in bacteria, algae and higher plants. *Nat. Prod. Rep.* **1999**, *16*, 565–574; ; b) Dubey, V. S.; Bhalla, R.; Luthra, R. An overview of the non-mevalonate pathway for terpenoids biosynthesis in plants. *J. Biosci.* **2003**, *28*, 637–646; c) Eisenreich, W.; Bacher, A.; Arigoni, D.; Rohdich, F. Biosynthesis of isoprenoids via the non-mevalonate pathway. *Cell. Mol. Life Sci.* **2004**, *61*, 1401–1426.
- (16) Okada, K. The biosynthesis of isoprenoids and the mechanisms regulating it in plants. *Biosci. Biotechnol. Biochem.* **2011**, *75*, 1219–1225.
- (17) Archibald, J. M. Endosymbiosis and Eukaryotic Cell Evolution. *Curr. Biol.* **2015**, *25*, R911–R921.

- (18) a) Christianson, D. W. Structural Biology and Chemistry of the Terpenoid Cyclases. *Chem. Rev.* **2006**, *106*, 3412–3442; b) Gao, Y.; Honzatko, R. B.; Peters, R. J. Terpenoid synthase structures: a so far incomplete view of complex catalysis. *Nat. Prod. Rep.* **2012**, *29*, 1153–1175.
- (19) Thulasiram, H. V.; Erickson, H. K.; Poulter, C. D. Chimeras of Two Isoprenoid Synthases Catalyze All Four Coupling Reactions in Isoprenoid Biosynthesis. *Science* **2007**, *316*, 73–76.
- (20) a) Lin, F.-Y.; Liu, C.-I.; Liu, Y.-L.; Zhang, Y.; Wand, K.; Jeng, W.-Y.; Ko, T.-P.; Cao, R.; Wang, A. H.-J.; Oldfield, E. Mechanism of action and inhibition of dehydrosqualene synthase. *PNAS* **2010**, *107*, 21337–21342; b) Liu, C.-I.; Jeng, W.-Y.; Chang, W.-J.; Shih, M.-F.; Ko, T.-P.; Wang, A. H.-J. Structural insights into the catalytic mechanism of human squalene synthase. *Acta. Cryst.* **2014**, *D70*, 231–241.
- (21) Blagg, B. S. J.; Jarstfer, M. B.; Rogers, D. H.; Poulter, C. D. Recombinant Squalene Synthase. A Mechanism for the Rearrangement of Presqualene Diphosphate to Squalene. *J. Am. Chem. Soc.* **2002**, *124*, 8846–8853.
- (22) a) Banthorpe, D. V.; Charlwood, B. V.; Francis, M. J. O. Biosynthesis of monoterpenes. *Chem. Rev.* **1972**, *72*, 115–155; b) Croteau, R. Biosynthesis and Catabolism of Monoterpenoids. *Chem. Rev.* **1987**, *87*, 929–954.
- (23) Wise, M. L.; Savage, T. J.; Katahira, E.; Croteau, R. Monoterpene Synthases from Common Sage (*Salvia officinalis*): cDNA ISOLATION, CHARACTERIZATION, AND FUNCTIONAL EXPRESSION OF (+)-SABINENE SYNTHASE, 1,8-CINEOLE SYNTHASE, AND (+)-BORNYL DIPHOSPHATE SYNTHASE. *J. Biol. Chem.* **1998**, *273*, 14891–14899.
- (24) Major, D. T.; Weitman, M. Electrostatically Guided Dynamics—The Root of Fidelity in a Promiscuous Terpene Synthase? *J. Am. Chem. Soc.* **2012**, *134*, 47, 19454–19462.
- (25) Cordell, G. A. Biosynthesis of sesquiterpenes. *Chem. Rev.* **1976**, *76*, 425–460.
- (26) Vattekkatte, A.; Garms, S.; Brandt, W.; Boland, W. Enhanced structural diversity in terpenoid biosynthesis: enzymes, substrates and cofactors. *Org. Biomol. Chem.* **2018**, *16*, 348–362.
- (27) Asakawa, Y.; Toyota, M.; Aratani, T. Un nouvel alcool sesquiterpénique de *Porella vernicosa* et *Porella densifolia* (hépatiques). *Tetrahedron Lett.* **1976**, *17*, 3619–3622.
- (28) Tori, M.; Arbiyanti, H.; Taira, Z.; Asakawa, Y. Terpenoids of the liverwort *Frullanoides densifolia* and *Trocholejeunea sandvicensis*. *Phytochemistry* **1993**, *32*, 335–348.
- (29) Christianson, D. W. Roots of Biosynthetic Diversity. *Science* **2007**, *316*, 60–61.
- (30) a) Matsuda, Y.; Abe, I. Biosynthesis of fungal meroterpenoids. *Nat. Prod. Rep.* **2016**, *33*, 26–53; b) Shen, X.; Ting, C. P.; Xu, G.; Maimone, T. J. Programmable meroterpene synthesis. *Nat. Commun.* **2020**, *11*, 508.
- (31) Matsuda, Y.; Abe, I. Biosynthesis of over of novel synthetic methodologies and reagents during natural product synthesis in the post-palytoxin erungal meroterpenoids. *Nat. Prod. Rep.* **2016**, *33*, 26–53.
- (32) a) Ciochina, R.; Grossman, R. B. Polycyclic polyprenylated acylphloroglucinols. *Chem. Rev.* **2006**, *106*, 3963–3986; b) Yang, X.-W., Grossman, R. B.; Xu, G. Research progress of polycyclic polyprenylated acylphloroglucinols. *Chem. Rev.* **2018**, *118*, 3508–3558.
- (33) a) Gallimore, A. R. The biosynthesis of polyketide-derived polycyclic ethers. *Nat. Prod. Rep.* **2009**, *26*, 266–280; b) Xie, X.; Garg, A.; Khosla, C.; Cane, D. E. Mechanism and Stereochemistry of Polyketide Chain Elongation and Methyl Group Epimerization in Polyether Biosynthesis. *J. Am. Chem. Soc.* **2017**, *139*, 3283–3292.
- (34) Gurr, M. I. 5 - The Biosynthesis of Unsaturated Fatty Acids. In *Biochemistry of Lipids*; Goodwin, T. W., Ed.; Butterworth-Heinemann, 1974; pp 181–235.
- (35) Katsuyama, Y.; Ohnishi, Y. Chapter Sixteen - Type III Polyketide Synthases in Microorganisms. In *Methods in Enzymology*; Hopwood, D. A., Ed.; Academic Press, 2012; Vol. 515, pp 359–377.
- (36) Geris, R.; Simpson, T. J. Meroterpenoids produced by fungi. *Nat. Prod. Rep.* **2009**, *26*, 1063–1094.



- (37) Song, J.-G.; Su, J.-C.; Song, Q.-Y.; Huang, R.-L.; Tang, W.; Hu, L.-J.; Huang, X.-J.; Jiang, R.-W.; Li, Y.-L.; Ye, W.-C.; Wang, Y. Cleistocaltones A and B, Antiviral Phloroglucinol–Terpenoid Adducts from *Cleistocalyx operculatus*. *Org. Lett.* **2019**, *21*, 9579–9583
- (38) a) Hassan, H. M. A. A Short History of the Use of Plants as Medicines from Ancient Times. *Chimia* **2015**, *69*, 622–623; b) Dias, D. A.; Urban, S.; Roessner, U. A Historical Overview of Natural Products in Drug Discovery. *Metabolites* **2012**, *2*, 303–336.
- (39) a) Sertürner, F. III. Säure im Opium. *Journal der Pharmacie für Aerzte, Apotheker und Chemisten* **1805**, *13*, 234–235; b) Sertürner, F. I. Nachtrag zur Charakteristik der Säure im Opium. *Journal der Pharmacie für Aerzte, Apotheker und Chemisten* **1805**, *13*, 236–241.
- (40) Fleming, A. On the Antibacterial Action of Cultures of a Penicillium, with Special Reference to their Use in the Isolation of *B. influenzae*. *Br. J. Exp. Pathol.* **1929**, *10*, 226–236.
- (41) Rao, K. V. Taxol and Related Taxanes. I. Taxanes of *Taxus brevifolia* Bark. *Pharm. Res.* **1993**, *10*, 521–524.
- (42) Frackenpohl, J. Morphin und Opioid-Analgetika. *Chem. Unserer Zeit* **2000**, *34*, 99–112.
- (43) a) Heilmann, J. Wirkstoffe auf Basis biologisch aktiver Naturstoffe. *Chem. Unserer Zeit* **2007**, *41*, 376–389; b) Atanasov, A. G.; Waltenberger, B.; Pferschy-Wenzig, E. M.; Linder, T.; Wawrosch, C.; Uhrin, P.; Temml, V.; Wang, L.; Schwaiger, S.; Heiss, E. H.; Rollinger, J. M.; Schuster, D.; Breuss, J. M.; Bochkov, V.; Mihovilovic, M. D.; Kopp, B.; Bauer, R.; Dirsch, V. M.; Stuppner, H. Discovery and resupply of pharmacologically active plant-derived natural products: A review. *Biotechnol. Adv.* **2015**, *33*, 1582–1614.
- (44) Newman, D. J.; Cragg, G. M. Natural Products as Sources of New Drugs over the Nearly Four Decades from 01/1981 to 09/2019. *J. Nat. Prod.* **2020**, *83*, 770–803.
- (45) Feher, M.; Schmidt, H. M. Property Distributions: Differences between Drugs, Natural Products, and Molecules from Combinatorial Chemistry. *J. Chem. Inf. Comput. Sci.* **2003**, *43*, 218–227.
- (46) Galloway, W. R. J. D.; Isidro-Llobet, A.; Spring, D. R. Diversity-oriented synthesis as a tool for the discovery of novel biologically active small molecules. *Nature Comm.* **2010**, *1*, 80.
- (47) a) Cragg, G. M.; Newman, D. J. Biodiversity: A continuing source of novel drug leads. *Pure Appl. Chem.* **2005**, *77*, 7–24; b) Cragg, G. M.; Newman, D. J. Natural products: A continuing source of novel drug leads. *Biochim. Biophys. Acta, Gen. Subj.* **2013**, *1830*, 3670–3695.
- (48) Yu, M. J.; Zheng, W.; Seletsky, B. M.; Littlefield, B. A.; Kishi, Y. Chapter 14 - Case History: Discovery of Eribulin (HALAVEN™), a Halichondrin B Analogue That Prolongs Overall Survival in Patients with Metastatic Breast Cancer. *Annu. Rep. Med. Chem.* **2011**, *46*, 227–241.
- (49) Corey, E. J.; Ohno, M.; Mitra, R. B.; Vatakencherry, P. A. Total Synthesis of Longifolene. *J. Am. Chem. Soc.* **1964**, *86*, 478–485.
- (50) a) Corey, E. J. Retrosynthetic thinking—essentials and examples. *Chem. Soc. Rev.* **1988**, *17*, 111–133; b) Corey, E. J. The Logic of Chemical Synthesis: Multistep Synthesis of Complex Carbogenic Molecules (Nobel Lecture). *Angew. Chem. Int. Ed. Engl.* **1991**, *30*, 455–465.
- (51) Barton, D. H. R. The conformation of the steroid nucleus. *Experientia* **1950**, *6*, 316–320.
- (52) a) Trost, B. M. The atom economy – a search for synthetic efficiency. *Science* **1991**, *254*, 1471–1477; b) Trost, B. M. Atom Economy – A Challenge for Organic Synthesis: Homogeneous Catalysis Leads the Way. *Angew. Chem., Int. Ed. Engl.* **1995**, *34*, 259–281.
- (53) Burns, N. Z.; Baran, P. S.; Hoffmann, R. W. Redox economy in organic synthesis. *Angew. Chem., Int. Ed.* **2009**, *48*, 2854–2867.
- (54) a) Wender, P. A.; Verma, V. A.; Paxton, T. J.; Pillow, T. H. Function-Oriented Synthesis, Step Economy, and Drug Design. *Acc. Chem. Res.* **2008**, *41*, 40–49; b) Wender, P. A.; Miller, B. L. Synthesis at the molecular frontier. *Nature* **2009**, *460*, 197–201.
- (55) a) Hayashi, Y. Pot economy and one-pot synthesis. *Chem. Sci.* **2016**, *7*, 866–880; b) Hayashi, Y. Time and Pot Economy in Total Synthesis. *Acc. Chem. Res.* **2021**, *54*, 1385–1398.

- (56) a) Newhouse, T.; Baran, P. S.; Hoffmann, R. W. The economies of synthesis. *Chem. Soc. Rev.* **2009**, *38*, 3010–3021; b) Gaich, T.; Baran, P. S. Aiming for the Ideal Synthesis. *J. Org. Chem.* **2010**, *75*, 4657–4673; c) Schwan, J.; Christmann, M. Enabling strategies for step efficient syntheses. *Chem. Soc. Rev.* **2018**, *47*, 7985–7995.
- (57) Pettersson, T.; Eklund, A. M.; Wahlberg, I. New Lactones from Tobacco. *J. Agric. Food Chem.* **1993**, *41*, 2097–2103.
- (58) Clark, J. S.; Hayes, S. T.; Blake, A. J.; Gobbi, L. Synthesis of a lactone natural product found in Greek tobacco. *Tetrahedron Lett.* **2007**, *48*, 2501–2503.
- (59) Zúñiga, A.; Pazos, G.; Besada, P.; Fall, Y. Synthesis of Greek tobacco lactonic natural product and its analogues. *Tetrahedron Lett.* **2012**, *53*, 4293–4295.
- (60) Siitonen, J.; Pihko, P. Total Synthesis of (+)-Greek Tobacco Lactone. *Synlett* **2014**, *25*, 1888–1890.
- (61) Kempainen, E. K.; Sahoo, G.; Valkonen, A.; Pihko, P. M. Mukaiyama–Michael Reactions with Acrolein and Methacrolein: A Catalytic Enantioselective Synthesis of the C17–C28 Fragment of Pectenotoxins. *Org. Lett.* **2012**, *14*, 1086–1089.
- (62) a) Ho, T.-L. *Enantioselective Synthesis. Natural Products from Chiral Terpenes*; John Wiley & Sons, 1992; b) Gaich, T.; Mulzer, J. Chiral Pool Synthesis: Starting from Terpenes. In *Comprehensive Chirality*; Elsevier, 2012; Vol. 2, pp 163–206; c) Brill, Z. G.; Condakes, L.; Ting, C. P.; Maimone, T. J. *Chem. Rev.* **2017**, *117*, 11753–11795.
- (63) Mulzer, J. Introductory Remarks: Chiral Pool Syntheses and Diastereoselective Reactions. In *Comprehensive Chirality*; Elsevier, 2012; Vol. 2, pp 1–8.
- (64) a) Staudinger, H. and Ruzicka, L. Insektentötende Stoffe I. Über Isolierung und Konstitution des wirksamen Teils des dalmatinischen Insektenpulvers. *Helv. Chim. Acta* **1924**, *7*, 177–235; b) Arlt, D.; Jautelat, M.; Lantsch, R. Synthesis of Pyrethroid Acids. *Angew. Chem., Int. Ed. Engl.* **1981**, *20*, 703–722; c) Barrett, A. G. M.; Doubleday, W. W.; Hamprecht, D.; Kasdorf, K.; Tustin, G. J.; White, A. J. P.; Williams, D. J. Assembly of the antifungal agent FR-900848 and CETP inhibitor U-106305: studies on remarkable multicyclopropane natural products. *Chem. Commun.* **1997**, 1693–1700; d) Yamada, K.; Ojika, M.; Kigoshi, H. Ptaquiloside, the major toxin of bracken, and related terpene glucosides: chemistry, biology and ecology. *Nat. Prod. Rep.* **2007**, *24*, 798–813; e) Okada, M.; Ito, S.; Matsubara, A.; Iwakura, I.; Egoshi, S.; Ueda, M. Total syntheses of coronatines by exo-selective Diels–Alder reaction and their biological activities on stomatal opening. *Org. Biomol. Chem.* **2009**, *7*, 3065–3073; f) Hiratsuka, T.; Suzuki, H.; Minami, A.; Oikawa, H. Stepwise cyclopropanation on the polycyclopropanated polyketide formation in jawsamycin biosynthesis. *Org. Biomol. Chem.* **2017**, *15*, 1076–1079.
- (65) a) Suckling, J. The Cyclopropyl Group in Studies of Enzyme Mechanism and Inhibition. *Angew. Chem. Int. Ed.* **1988**, *27*, 537–552; b) Faust, R. Fascinating Natural and Artificial Cyclopropane Architectures. *Angew. Chem. Int. Ed.* **2001**, *40*, 2251–2253; c) Pietruszka, J. Synthesis and Properties of Oligocyclopropyl-Containing Natural Products and Model Compounds. *Chem. Rev.* **2003**, *103*, 1051–1070; d) Wessjohann, L. A.; Brandt, W.; Thiemann, T. Biosynthesis and Metabolism of Cyclopropane Rings in Natural Compounds. *Chem. Rev.* **2003**, *103*, 1625–1648; e) Chen, D. Y.-K.; Pouwer, R. H.; Richard, J.-A. Recent advances in the total synthesis of cyclopropane-containing natural products. *Chem. Soc. Rev.* **2012**, *41*, 4631–4642.
- (66) a) Marson, C. M. New and unusual scaffolds in medicinal chemistry. *Chem. Soc. Rev.* **2011**, *40*, 5514–5533; b) Fukuda, H.; Muromoto, R.; Takakura, Y.; Ishimura, K.; Kanada, R.; Fushihara, D.; Tanabe, M.; Matsubara, K.; Hirao, T.; Hirashima, K.; Abe, H.; Arisawa, M.; Matsuda, T.; Shuto, S. Design and Synthesis of Cyclopropane Congeners of Resolvin E2, an Endogenous Proresolving Lipid Mediator, as Its Stable Equivalents. *Org. Lett.* **2016**, *18*, 6224–6227; c) Mizuno, A.; Kameda, T.; Kuwahara, T.; Endoh, H.; Ito, Y.; Yamada, S.; Hasegawa, K.; Yamano, A.; Watanabe, M.; Arisawa, M.; Shuto, S. Cyclopropane-Based Peptidomimetics Mimicking Wide-Ranging Secondary Structures of Peptides: Conformational Analysis and Their Use in Rational Ligand Optimization. *Chem. Eur. J.* **2017**, *23*, 3159–3168; d) Nirogi, R.; Mohammed, A. R.; Shinde, A. K.; Ravella, S. R.; Bogaraju, N.; Subramanian, R.; Mekala, V. R.; Palacharla, R. C.; Muddana, N.; Thenttu, J. B.; Bhyrapuneni, G.; Abraham, R.; Jasti, V. Discovery

- and Development of 3-(6-Chloropyridine-3-yloxymethyl)-2-azabicyclo[3.1.0]hexane Hydrochloride (SUVN-911): A Novel, Potent, Selective, and Orally Active Neuronal Nicotinic Acetylcholine  $\alpha 4\beta 2$  Receptor Antagonist for the Treatment of Depression. *J. Med. Chem.* **2020**, *63*, 2833–2853.
- (67) Closs, G. L.; Moss, R. A. Carbenoid Formation of Arylcyclopropanes from Olefins, Benzal Bromides, and Organolithium Compounds and from Photolysis of Aryldiazomethanes. *J. Am. Chem. Soc.* **1962**, *86*, 4042–4053.
- (68) Gessner, V. H. Stability and reactivity control of carbenoids: recent advances and perspectives. *Chem. Commun.* **2016**, *52*, 12011–12023.
- (69) a) Wang, Y.; Muratore, M. E.; Echavarren, A. M. Gold Carbene or Carbenoid: Is There a Difference? *Chem. Eur. J.* **2015**, *21*, 7332–7339.
- (70) a) Simmons, H. E.; Smith, R. D. A New Synthesis of Cyclopropanes from Olefins. *J. Am. Chem. Soc.* **1958**, *80*, 5323–5324; b) Simmons, H. E.; Smith, R. D. A New Synthesis of Cyclopropanes. *J. Am. Chem. Soc.* **1959**, *81*, 4256–4264.
- (71) a) Denis, J. M.; Girard, C.; Conia, J. M. Improved Simmons-Smith Reactions. *Synthesis* **1972**, 549–551; b) Rieke, R. D.; Li, P. T.-J.; Burns, T. P.; Uhm, S. T. Preparation of highly reactive metal powders. New procedure for the preparation of highly reactive zinc and magnesium metal powders. *J. Org. Chem.* **1981**, *46*, 4323–4324; c) Repič, O.; Vogt, S. Ultrasound in organic synthesis: cyclopropanation of olefins with zinc-diiodomethane. *Tetrahedron Lett.* **1982**, *23*, 2729–2732; d) Friedrich, E. C.; Lunetta, S. E.; Lewis, E. J. Titanium(IV) chloride catalyzed cyclopropanations of alkenes using zinc dust, copper(I) chloride, and dihalomethanes. *J. Org. Chem.* **1989**, *54*, 2388–2390; e) Friedrich, E. C.; Lewis, E. J. Acetyl chloride promoted cyclopropanations of alkenes with dibromomethane using zinc dust and copper(I) chloride in ether. *J. Org. Chem.* **1990**, *55*, 2491–2494; f) Takai, K.; Kakiuchi, T.; Utimoto, K. A Dramatic Effect of a Catalytic Amount of Lead on the Simmons-Smith Reaction and Formation of Alkylzinc Compounds from Iodoalkanes. Reactivity of Zinc Metal: Activation and Deactivation. *J. Org. Chem.* **1994**, *59*, 2671–2673.
- (72) Furukawa, J.; Kawabata, N.; Nishimura, J. A novel route to cyclopropanes from olefins. *Tetrahedron Lett.* **1966**, *7*, 3353–3354.
- (73) Zhou, L.; Yao, Y.; Xu, W.; Liang, G. Total Syntheses of ( $\pm$ )-Omphadiol and ( $\pm$ )-Pyxidatol C through a Cis-Fused 5,7-Carbocyclic Common Intermediate. *J. Org. Chem.* **2014**, *79*, 5345–5350.
- (74) Crandall, J. K.; Lin, L.-H. C. Base-promoted reactions of epoxides. III. Carbenoid decomposition in acyclic derivatives. *J. Am. Chem. Soc.* **1967**, *89*, 4526–4527.
- (75) a) Hodgson, D. M.; Chung, Y. K.; Paris, J.-M. Intramolecular Cyclopropanation of Unsaturated Terminal Epoxides. *J. Am. Chem. Soc.* **2004**, *126*, 8664–8665; b) Hodgson, D. M.; Salik, S. Thieme Chemistry Journal Awardees – Where Are They Now? Synthesis of (–)-Cubebol by Intramolecular Cyclopropanation of a Terminal Epoxide. *Synlett* **2009**, 1730–1732.
- (76) Wu, W.; Lin, Z.; Jiang, H. Recent advances in the synthesis of cyclopropanes. *Org. Biomol. Chem.* **2018**, *16*, 7315–7329.
- (77) a) Merlic, C. A.; Zechman, A. L. Selectivity in Rhodium(II) Catalyzed Reactions of Diazo Compounds: Effects of Catalyst Electrophilicity, Diazo Substitution, and Substrate Substitution. From Chemoselectivity to Enantioselectivity. *Synthesis* **2003**, 1137–1156; Honma, M.; b) Takeda, H.; Takano, M.; Nakada, M. Development of Catalytic Asymmetric Intramolecular Cyclopropanation of  $\alpha$ -Diazo- $\beta$ -Keto Sulfones and Applications to Natural Product Synthesis. *Synlett* **2009**, 1695–1712; c) Padawa, A. Domino reactions of rhodium(II) carbenoids for alkaloid synthesis. *Chem. Soc. Rev.* **2009**, *38*, 3072–3081.
- (78) Zhang, L.; Sun, J.; Kozmin, S. A. Gold and Platinum Catalysis of Enyne Cycloisomerization. *Adv. Synth. Catal.* **2006**, *348*, 2271–2296.
- (79) a) Nevado, C.; Cárdenas, D. J.; Echavarren, A. M. Reaction of Enol Ethers with Alkynes Catalyzed by Transition Metals: 5-*exo-dig* versus 6-*endo-dig* Cyclizations via Cyclopropyl Platinum and Gold Carbene-Complexes. *Chem. Eur. J.* **2003**, *9*, 2627–2635; b) Nieto-Oberhuber, C.; Muñoz, M. P.; Buñuel, E.; Nevado, C.; Cárdenas, D. J.; Echavarren, A. M. *Angew. Chem. Int. Ed.* **2004**, *43*, 2402–2406; c) Soriano, E.; Marco-Contelles, J. Mechanistic Insights on the Cycloisomerization of



- Polyunsaturated Precursors Catalyzed by Platinum and Gold Complexes. *Acc. Chem. Res.* **2009**, *42*, 1026–1036.
- (80) a) Jiménez-Núñez, E.; Echavarren, A. M. Gold-Catalyzed Cycloisomerizations of Enynes: A Mechanistic Perspective. *Chem. Rev.* **2008**, *108*, 3326–3350; b) Pérez-Galán, P.; Herrero-Gómez, E.; Hog, D. T.; Martin, N. J. A.; Maseras, F.; Echavarren, A. M. Mechanism of the gold-catalyzed cyclopropanation of alkenes with 1,6-enynes. *Chem. Sci.* **2011**, *2*, 141–149.
- (81) Strickler, H., Davis, J. B., Ohloff, G. Zur Cyclisierung von Dehydrolinalylacetat in Gegenwart von Zinkchlorid. *Helv. Chim. Acta* **1976**, *59*, 1328–1332.
- (82) Rautenstrauch, V. 2-Cyclopentenones from 1-Ethynyl-2-propenyl Acetates. *J. Org. Chem.* **1984**, *49*, 950–952.
- (83) Mainetti, E.; Mouriès, V.; Fensterbank, L.; Malacria, M.; Marco-Contelles, J. The Effect of a Hydroxy Protecting Group on the PtCl<sub>2</sub>-Catalyzed Cyclization of Dienynes—A Novel, Efficient, and Selective Synthesis of Carbocycles. *Angew. Chem. Int. Ed.* **2002**, *41*, 2132–2135.
- (84) a) Harrak, Y.; Blaszykowski, C.; Bernard, M.; Cariou, K.; Mainetti, E.; Mouriès, V.; Dhimane, A.-L.; Fensterbank, L.; Malacria, M. PtCl<sub>2</sub>-Catalyzed Cycloisomerizations of 5-En-1-yn-3-ol Systems. *J. Am. Chem. Soc.* **2004**, *126*, 8656–8657; b) Blaszykowski, C.; Harrak, Y.; Gonçalves, M.-H.; Cloarec, J.-M.; A.-L.; Fensterbank, L.; Malacria, M. PtCl<sub>2</sub>-Catalyzed Transannular Cycloisomerization of 1,5-Enynes: A New Efficient Regio- and Stereocontrolled Access to Tricyclic Derivatives. *Org. Lett.* **2004**, *6*, 3771–3774; c) Prasad, B. A. B.; Yoshimoto, F. K.; Sarpong, R. Pt-Catalyzed Pentannulations from In Situ Generated Metallo-Carbenoids Utilizing Propargylic Esters. *J. Am. Chem. Soc.* **2005**, *127*, 12468–12469; d) Anjum, S.; Marco-Contelles, J. PtCl<sub>2</sub>-mediated cycloisomerization of unsaturated propargylic carboxylates. *Tetrahedron* **2005**, *61*, 4793–4803.
- (85) a) Mamane, V.; Gress, T.; Krause, H.; Fürstner, A. Platinum- and Gold-Catalyzed Cycloisomerization Reactions of Hydroxylated Enynes. *J. Am. Chem. Soc.* **2004**, *126*, 8654–8655; b) Fürstner, A.; Hannen, P. Platinum- and Gold-Catalyzed Rearrangement Reactions of Propargyl Acetates: Total Syntheses of (–)- $\alpha$ -Cubebene, (–)-Cubebol, Sesquicarene and Related Terpenes. *Chem. Eur. J.* **2006**, *12*, 3006–3019.
- (86) Fehr, C.; Galindo, J. Synthesis of (–)-Cubebol by Face-Selective Platinum-, Gold-, or Copper-Catalyzed Cycloisomerization: Evidence for Chirality Transfer. *Angew. Chem. Int. Ed.* **2006**, *45*, 2901–2904.
- (87) Fehr, C.; Winter, B.; Magpantay, I. Synthesis of (–)-Cubebol by Face-Selective Platinum-, Gold-, or Copper-Catalyzed Cycloisomerization: Evidence of Chirality Transfer and Mechanistic Insights. *Chem. Eur. J.* **2009**, *15*, 9773–9784.
- (88) a) Ye, S.; Huang, Z.-Z.; Xia, C.-A.; Tang, Y.; Dai, L.-X. A Novel Chiral Sulfonium Ylide: Highly Enantioselective Synthesis of Vinylcyclopropanes. *J. Am. Chem. Soc.* **2002**, *124*, 2432–2433; b) Zhu, C.-Y.; Cao, X.-Y.; Zhu, B.-H.; Deng, C.; Sun, X.-L.; Wang, B.-Q.; Shen, Q.; Tang, Y. Application of Asymmetric Ylide Cyclopropanation in the Total Synthesis of Halicholactone. *Chem. Eur. J.* **2009**, *15*, 11465–11468.
- (89) Bremeyer, N.; Smith, S. C.; Ley, S. V.; Gaunt, M. J. An Intramolecular Organocatalytic Cyclopropanation Reaction. *Angew. Chem. Int. Ed.* **2004**, *43*, 2681–2684.
- (90) Kumaraswamy, G.; Pdumaja, M. Enantioselective Total Synthesis of Eicosanoid and Its Congener, Using Organocatalytic Cyclopropanation, and Catalytic Asymmetric Transfer Hydrogenation Reactions as Key Steps. *J. Org. Chem.* **2008**, *73*, 5198–5201.
- (91) Leisering, S.; Riaño, I.; Depken, C.; Gross, L. J.; Weber, M.; Lentz, D.; Zimmer, R.; Stark, C. B. W.; Breder, A.; Christmann, M. Synthesis of (+)-Greek Tobacco Lactone via a Diastereoblabative Epoxidation and a Selenium-Catalyzed Oxidative Cyclization. *Org. Lett.* **2017**, *19*, 1478–1481.
- (92) Morgans Jr., D. J.; Sharpless, K. B.; Traynor, S. G. Epoxy alcohol rearrangements: hydroxyl-mediated delivery of Lewis acid promoters. *J. Am. Chem. Soc.* **1981**, *103*, 462–464.

- (93) Marson, C. M.; Oare, C. A.; McGregor, J.; Walsgrove, T.; Grinterb, T. J.; Adams, H. A sequential stereocontrolled cyclopropane ring formation and semi-pinacol rearrangement. *Tetrahedron Lett.* **2003**, *44*, 141–143.
- (94) Lanthanum(III) Triflate-Catalyzed Cyclopropanation via Intramolecular Methylene Transfer. Hardee, D. J.; Lambert, T. H. *J. Am. Chem. Soc.* **2009**, *131*, 7536–7537.
- (95) Tokunaga, M.; Larrow, J. F.; Kakiuchi, F.; Jacobsen, E. N. Asymmetric Catalysis with Water: Efficient Kinetic Resolution of Terminal Epoxides by Means of Catalytic Hydrolysis. *Science* **1997**, *277*, 936–938.
- (96) Zeng, C.; Yuan, D.; Zhao, B.; Yao, Y. Highly Enantioselective Epoxidation of  $\alpha,\beta$ -Unsaturated Ketones Catalyzed by Rare-Earth Amides  $[(\text{Me}_3\text{Si})_2\text{N}]_3\text{RE}(\mu\text{-Cl})\text{Li}(\text{THF})_3$  with Phenoxy-Functionalized Chiral Prolinols. *Org. Lett.* **2015**, *17*, 2242–2245.
- (97) For preparation of the salen ligand, see: Kshirsagara, V. S.; Garadea, A. C.; Manea, R. B.; Patilb, K. R.; Yamaguchi, A.; Shiraic, M.; Rode, C. V. Characterization of clay intercalated cobalt-salen catalysts for the oxidation of *p*-cresol. *Appl. Catal. A* **2009**, *370*, 16–23.
- (98) For preparation of the (salen)cobalt(II) complex **xxx**, see: Kowalski, G.; Pielichowski, J. A New Polyaniline-Based Catalyst for the Oxidation of Alkenes. *Synlett* **2002**, 2107–2109.
- (99) Wang, H.; Dai, X.-J.; Li, C.-J. Aldehydes as alkyl carbanion equivalents for additions to carbonyl compounds. *Nat. Chem.* **2017**, *9*, 374–478.
- (100) Beesley, R. M.; Ingold, C. K.; Thorpe, J. F. CXIX.—The formation and stability of *spiro*-compounds. Part I. *spiro*-Compounds from cyclohexane. *J. Chem. Soc., Trans.* **1915**, *107*, 1080–1106.
- (101) a) Jung, M.; Kim, H.; Lee, K.; Park, M. Naturally occurring peroxides with biological activities. *Mini Rev. Med. Chem.* **2003**, *3*, 159–165; b) Dembitsky, V. M.; Glorizova, T. A.; Poroikov, V. V. Natural Peroxy Anticancer Agents. *Mini Rev. Med. Chem.* **2007**, *7*, 571–589; c) Dembitsky, V. M. Bioactive peroxides as potential therapeutic agents. *Eur. J. Med. Chem.* **2008**, *43*, 223–251.
- (102) Tu, Y. The discovery of artemisinin (qinghaosu) and gifts from Chinese medicine. *Nat. Med.* **2011**, *17*, 1217–1220.
- (103) Ekiert, H.; Świątkowska, J.; Klin, P.; Rzepiela, A.; Szopa, A. *Artemisia annua* – Importance in Traditional Medicine and Current State of Knowledge on the Chemistry, Biological Activity and Possible Applications. *Planta Med.* **2021**, *87*, 584–599.
- (104) Blasco, B.; Leroy, D.; Fidock, D. A. Antimalarial drug resistance: linking *Plasmodium falciparum* parasite biology to the clinic. *Nat. Med.* **2017**, *23*, 917–928.
- (105) Sarkar, P. K.; Ahluwalia, G.; Vijayan, V. K.; Talwar, A. Critical Care Aspects of Malaria. *J. Intensive Care Med.* **2009**, *25*, 93–103.
- (106) O'Neill, P. M.; Posner, G. H. A Medicinal Chemistry Perspective on Artemisinin and Related Endoperoxides. *J. Med. Chem.* **2004**, *47*, 2945–2964; Bousejra-El Garah, F.; Wong, M. H.-L.; Amewu, R. K.; Muangnoicharoen, S.; Maggs, J. L.; Stigliani, J.-L.; Park, B. K.; Chadwick, J.; Ward, S. A.; O'Neill, P. M. Comparison of the Reactivity of Antimalarial 1,2,4,5-Tetraoxanes with 1,2,4-Trioxolanes in the Presence of Ferrous Iron Salts, Heme, and Ferrous Iron Salts/Phosphatidylcholine. *J. Med. Chem.* **2011**, *54*, 6443–6455; Posner, G. H.; O'Neill, P. M. Knowledge of the Proposed Chemical Mechanism of Action and Cytochrome P450 Metabolism of Antimalarial Trioxanes Like Artemisinin Allows Rational Design of New Antimalarial Peroxides. *Acc. Chem. Res.* **2004**, *37*, 397–404.
- (107) Sigala, P. A. and Goldberg, D. E. The peculiarities and paradoxes of *Plasmodium* heme metabolism. *Annu. Rev. Microbiol.* **2014**, *68*, 259–278.
- (108) Combrinck, J. M.; Mabothe, T. E.; Ncokazi, K. K.; Ambele, M. A.; Taylor, D.; Smith, P. J.; Hoppe, H. C.; Egan, T. J. Insights into the role of heme in the mechanism of action of antimalarials. *ACS Chem. Biol.* **2013**, *8*, 133–137.
- (109) Wang, J.; Zhang, C.-J.; Chia, W. N.; Loh, C. C. Y.; Li, Z.; Lee, Y. M.; He, Y.; Yuan, L.-X.; Lim, T. K.; Liu, M.; Liew, C. X.; Lee, Y. Q.; Zhang, J.; Lu, N.; Lim, C. T.; Hua, Z.-C.; Liu, B.; Shen, H.-M.; Tan, K. S. W.; Lin, Q. Haem-activated promiscuous targeting of artemisinin in *Plasmodium falciparum*. *Nat. Commun.* **2015**, *6*, 10111.

- (110) Klonis, N.; Xie, S. C.; McCaw, J. M.; Crespo-Ortiz, M. P.; Zaloumis, S. G.; Simpson, J. A.; Tilley, L. Altered temporal response of malaria parasites determines differential sensitivity to artemisinin. *Proc. Natl. Acad. Sci. USA* **2013**, *110*, 5157–5162.
- (111) Xie, S. C.; Dogovski, C.; Hanssen, E.; Chiu, F.; Yang, T.; Crespo, M. P.; Stafford, C.; Batinovic, S.; Teghu, S.; Charman, S.; Klonis, N.; Tilley, L. Haemoglobin degradation underpins the sensitivity of early ring stage *Plasmodium falciparum* to artemisinins. *J. Cell Sci.* **2016**, *129*, 406–416.
- (112) Terent'ev, A. O.; Borisov, D. A.; Vil', V. A.; Dembitsky V. M. Synthesis of five- and six-membered cyclic organic peroxides: Key transformations into peroxide ring-retaining products. *Beilstein J. Org. Chem.* **2014**, *10*, 34–114.
- (113) Liang, X.-T.; Yu, D.-Q.; Wu, W.-L.; Deng, H.-C. THE STRUCTURE OF YINGZHAOSU A. *Acta Chim. Sin.* **1979**, *37*, 215–230.
- (114) Kamchonwongpaisan, S.; Nilanonta, C.; Tarnchompoo, B.; Thebtaranonth, C.; Thebtaranonth, Y.; Yuthavong, Y.; Kongsaree, P.; Clardy, J. An antimalarial peroxide from *Amomum krervanh* Pierre. *Tetrahedron Lett.* **1995**, *36*, 1821–1824.
- (115) a) Pomponi, S. A.; The bioprocess–technological potential of the sea. *J. Biotechnol.* **1999**, *70*, 5–13; b) Munro, M. H. G.; Blunt, J. W.; Dumdei, E. J.; Hickford, S. J. H.; Lill, R. E.; Li, S.; Battershill, C. N.; Duckworth, A. R. The discovery and development of marine compounds with pharmaceutical potential. *J. Biotechnol.* **1999**, *70*, 15–25; c) Sponga, F.; Cavaletti, L.; Lazzarini, A.; Borghi, A.; Ciciliato, I.; Marinelli, D. L. F. Biodiversity and potentials of marine-derived microorganisms. *J. Biotechnol.* **1999**, *70*, 65–69; d) Martins, A.; Vieira, H.; Gaspar, H.; Santos, D. Marketed Marine Natural Products in the Pharmaceutical and Cosmeceutical Industries: Tips for Success. *Mar. Drugs* **2014**, *12*, 1066–1101.
- (116) Montaser, R.; Luesch, H. Marine natural products: a new wave of drugs? *Future Med. Chem.* **2011**, *3*, 1475–1489.
- (117) Faulkner, D. J. Marine natural products. *Nat. Prod. Rep.* **1999**, *16*, 155–198.
- (118) Casteel, D. A. Peroxy natural products. *Nat. Prod. Rep.* **1999**, *16*, 55–73.
- (119) Wells, R. J. A novel peroxyketal from a sponge. *Tetrahedron Lett.* **1976**, *17*, 2637–2638.
- (120) Higgs, M. D.; Faulkner, D. J. Plakortin, an antibiotic from *Plakortis halichondrioides*. *J. Org. Chem.* **1978**, *43*, 3453–3457.
- (121) Fattorusso, E.; Parapini, S.; Campagnuolo, C.; Basilico, N.; Tagliatela-Scafati, O.; Taramelli, D. Activity against *Plasmodium falciparum* of cycloperoxide compounds obtained from the sponge *Plakortis simplex*. *Antimicrob. Chemother.* **2002**, *50*, 883–888.
- (122) Stierle, D. B.; Faulkner, D. J. Metabolites of three marine sponges of the genus *Plakortis*. *J. Org. Chem.* **1980**, *45*, 3396–3401.
- (123) Perry, T. L.; Dickerson, A.; Khan, A. A.; Kondru, R. K.; Beratan, D. N.; Wipf, P.; Kelly, M.; Harmann, M. T. New peroxy lactones from the Jamaican sponge *Plakinastrella onkodes*, with inhibitory activity against the AIDS opportunistic parasitic infection *Toxoplasma gondii*. *Tetrahedron* **2001**, *57*, 1483–1487.
- (124) Varoglu, M.; Peters, B. M.; Crews, P. The Structure and Cytotoxic Properties of Polyketide Peroxides from a *Plakortis* Sponge. *J. Nat. Prod.* **1995**, *58*, 27–36.
- (125) Yong, K. W. L.; De Voss, J. J.; Hooper, J. N. A.; Garson, M. J. Configurational Assignment of Cyclic Peroxy Metabolites Provides an Insight into Their Biosynthesis: Isolation of Plakortolides, *seco*-Plakortolides, and Plakortones from the Australian Marine Sponge *Plakinastrella clathrata*. *J. Nat. Prod.* **2011**, *74*, 194–207.
- (126) a) Barnych, B.; Vatèle, J.-M. Total Synthesis of *seco*-Plakortolide E and (–)-*ent*-Plakortolide I: Absolute Configurational Revision of Natural Plakortolide I. *Org. Lett.* **2012**, *14*, 564–567; b) Yong, K. W. L.; Barnych, B.; DeVoss, J. J.; Vatèle, J.-M.; Garson, M. J. Plakortolide Stereochemistry Revisited: The Checkered History of Plakortolides E and I. *J. Nat. Prod.* **2012**, *75*, 1792–1797.
- (127) Qureshi, A.; Salvà, J.; Harper, M.; Faulkner, D. J. New Cyclic Peroxides from the Philippine Sponge *Plakinastrella* sp. *J. Nat. Prod.* **1998**, *61*, 1539–1542.

- (128) Rudi, A.; Afanii, R.; Gravalos, L. G.; Akinin, M.; Gaydou, E.; Vacelet, J.; Kashman, Y. Three New Cyclic Peroxides from the Marine Sponge *Plakortisaff simplex*. *J. Nat. Prod.* **2003**, *66*, 682–685.
- (129) Li, Q.; Yang, H.; Tang, Y. Recent advances in the synthesis of plakortin-type polyketides. *Org. Biomol. Chem.* **2020**, *18*, 9371–9384.
- (130) Jung, M.; Ham, J.; Song, J. First Total Synthesis of Natural 6-Epiplakortolide. *Org. Lett.* **2002**, *4*, 2763–2765.
- (131) Bienvenu, F.; Studien zur Synthese von Plakortolid I. Bachelor thesis, Freie Universität Berlin, Berlin, 2016.
- (132) Mavroskoufis, A. Unpublished results. Freie Universität Berlin, Berlin, 2020.
- (133) Chen, B.-C.; Zhou, P.; Davis, F. A.; Ciganek, E.  $\alpha$ -Hydroxylation of Enolates and Silyl Enol Ethers. In *Organic Reactions*; Overman, L. E., Ed.; John Wiley & Sons, 2003; Vol. 62, pp 1–356.
- (134) Lipshutz, B. H.; Chrisman, W.; Noson, K.; Papa, P.; Sclafani, J. A.; Vivian, R. W.; Keith, J. M. Copper Hydride-Catalyzed Tandem 1,4-Reduction/Alkylation Reactions. *Tetrahedron* **2000**, *56*, 2779–2788.
- (135) Ichibakase, T.; Kaneko, T.; Orito, Y.; Kotani, S.; Nakajima, M. Construction of quaternary carbon centers by a base-catalyzed enantioselective aldol reaction and related reactions of trimethoxysilyl enol ethers. *Tetrahedron* **2012**, *68*, 4210–4224.
- (136) Tuokko, S.; Pihko, P. M. Palladium on Charcoal as a Catalyst for Stoichiometric Chemo- and Stereoselective Hydrosilylations and Hydrogenations with Triethylsilane. *Org. Process Res. Dev.* **2014**, *18*, 1740–1751.
- (137) Benohoud, M.; Tuokko, S.; Pihko, P. M. Stereoselective Hydrosilylation of Enals and Enones Catalysed by Palladium Nanoparticles. *Chem. Eur. J.* **2011**, *17*, 8404–8413.
- (138) Tuokko, S.; Pihko, P. M. Palladium on Charcoal Catalyzed 3,4-Hydroperoxidation of  $\alpha$ -Substituted Enals with Triethylsilane and Water. *Synlett* **2016**, *27*, 1649–1652.
- (139) Leisering, S.; Mavroskoufis, A.; Voßnacker, P.; Zimmer, R.; Christmann, M. Synthesis of Plakortolides E and I Enabled by Base Metal Catalysis. *Org. Lett.* **2021**, *23*, 4731–4735.
- (140) a) Silva, A. R.; Taofiq, O.; Ferreira, I. C. F. R.; Barros, L. *Hypericum* genus cosmeceutical application – A decade comprehensive review on its multifunctional biological properties. *Ind. Crops Prod.* **2021**, *159*, 113053; b) Nürk, N. M.; Crockett, S. L. Morphological and phytochemical diversity among *Hypericum* species of the Mediterranean Basin. *Med. Aromat. Plant Sci. Biotechnol.* **2011**, *5*, 14–28; c) Tanaka, N.; Kashiwada, Y. Characteristic metabolites of *Hypericum* plants: their chemical structures and biological activities. **2021**, *75*, 423–433; d) Marrelli, M.; Statti, G.; Conforti, F.; Menichini, F. New Potential Pharmaceutical Applications of *Hypericum* Species. **2016**, *16*, 710–720; e) Mir, M. Y.; Hamid, S.; Kamili, A. N.; Hassan, Q. P. Sneak peek of *Hypericum perforatum* L.: phytochemistry, phytochemical efficacy and biotechnological interventions. *J. Plant Biochem. Biotechnol.* **2019**, *28*, 357–373; f) Patočka, J. The chemistry, pharmacology, and toxicology of the biologically active constituents of the herb *Hypericum perforatum* L. *J. Appl. Biomed.* **2003**, *1*, 61–70; g) Bridi, H.; Gabriela de Carvalho Meirelles; Gilsane Lino von Poser. Structural diversity and biological activities of phloroglucinol derivatives from *Hypericum* species. *Phytochemistry* **2018**, *155*, 203–232.
- (141) Yang, X.-W.; Grossman, R. B.; Xu, G. Research Progress of Polycyclic Polyprenylated Acylphloroglucinols. *Chem. Rev.* **2018**, *118*, 3508–3558.
- (142) a) Gurevich, A. I.; Dobrynin, V. N.; Kolosov, M. N.; Popravko, S. A.; Ryabova, I. D.; Chernov, B. K.; Derbentseva, N. A.; Aizenman, B. E.; Garagulya, A. D. Hyperforin, an Antibiotic from *Hypericum perforatum*. *Antibiotiki* **1971**, *16*, 510–513; b) Bystrov, N. S.; Chernov, B. K.; Dobrynin, V. N.; Kolosov, M. N. The Structure of Hyperforin. *Tetrahedron Lett.* **1975**, *16*, 2791–2794; c) Beerhues, L. Hyperforin. *Phytochemistry* **2006**, *67*, 2201–2207; d) Richard, J.-A. Chemistry and Biology of the Polycyclic Polyprenylated Acylphloroglucinol Hyperforin. *Eur. J. Org. Chem.* **2014**, 273–299.
- (143) Albert, D.; Zündorf, I.; Dingermann, T.; Müller, W. E.; Steinhilber, D.; Werz, O. Hyperforin is a dual inhibitor of cyclooxygenase-1 and 5-lipoxygenase. *Biochem. Pharmacol.* **2002**, *64*, 1767–1775.
- (144) a) Treiber, K.; Singer, A.; Henke, B.; Müller, W. E. Hyperforin activates nonselective cation channels (NSCCs). *Br. J. Pharmacol.* **2005**, *145*, 75–83; b) Leuner, K.; Kazanski, V.; Müller, M.; Essin, K.



- Henke, B.; Gollasch, M.; Harteneck, C.; Müller, W. E. Hyperforin—a key constituent of St. John's wort specifically activates TRPC6 channels. *FASEB J.* **2007**, *21*, 4101–4111.
- (145) Sell, T. S.; Belkacemi, T.; Flockerzi, V.; Beck, A. Protonophore properties of hyperforin are essential for its pharmacological activity. *Sci. Rep.* **2014**, *4*, 7500.
- (146) Chatterjee, S. S.; Bhattacharya, S. K.; Wonnemann, M.; Singer, A.; Müller, W. E. Hyperforin as a possible antidepressant component of hypericum extracts. *Life Sci.* **1998**, *63*, 499–510.
- (147) Tanaka, N.; Takaishi, Y.; Shikishima, Y.; Nakanishi, Y.; Bastow, K.; Lee, K. H.; Honda, G.; Ito, M.; Takeda, Y.; Kodzhimatov, O. K.; Ashurmetov, O. Prenylated benzophenones and xanthenes from *Hypericum scabrum*. *J. Nat. Prod.* **2004**, *67*, 1870–1875.
- (148) Zhu, H.-C.; Chen, C.-M.; Zhang, J.-W.; Guo, Y.; Tan, D.-D.; Wie, G.-Z.; Yang, J.; Wand, J.-P.; Luo, Z.-W.; Xue, Y.-B.; Zhang, Y.-H. Hyperisampsins N and O, two new benzoylated phloroglucinol derivatives from *Hypericum sampsonii*. *Chin. Chem. Lett.* **2017**, *28*, 986–990.
- (149) Hashida, C.; Tanaka, N.; Kawazoe, K.; Murakami, K.; Sun, H.-D.; Takaishi, Y.; Kashiwada, Y. Hypelodins A and B, polyprenylated benzophenones from *Hypericum elodeoides*. *J. Nat. Med.* **2014**, *68*, 737–742.
- (150) Liu, Y.-Y.; Ao, Z.; Xue, G.-M.; Wang, X.-B.; Luo, J.-G.; Kong, L.-Y. Hypatulone A, a Homoadamantane-Type Acylphloroglucinol with an Intricately Caged Core from *Hypericum patulum*. *Org. Lett.* **2018**, *20*, 7953–7956.
- (151) Zhang, Z.-Z.; Zeng, Y.-R.; Li, Y.-N.; Hu, Z.-X.; Huang, L.-J.; Gu, W.; Hao, X.-J.; Yuan, C.-M. Two new seco-polycyclic polyprenylated acylphloroglucinol from *Hypericum sampsonii*. *Org. Biomol. Chem.* **2021**, *19*, 216–219.
- (152) Royal Botanic Gardens, Kew. Plants of the World Online.  
<http://www.plantsoftheworldonline.org/taxon/urn:lsid:ipni.org:names:927423-1>  
(Accessed 13.09.2021).
- (153) United States Department of Agriculture. Agricultural Research Service.  
<https://npgsweb.ars-grin.gov/gringlobal/taxon/taxonomydetail?id=19598>  
(Accessed 14.09.2021).
- (154) Tanaka, N.; Yano, Y.; Tatano, Y.; Kashiwada, Y. Hypatulins A and B, Meroterpenes from *Hypericum patulum*. *Org. Lett.* **2016**, *18*, 5360–5363.
- (155) Tanaka, N.; Niwa, K.; Yano, Y.; Kashiwada, Y. Prenylated benzophenone derivatives from *Hypericum patulum*. *J. Nat. Med.* **2019**, *74*, 264–268.
- (156) Yoshida, M. Asymmetric  $\alpha$ -Allylation of  $\alpha$ -Substituted  $\beta$ -Ketoesters with Allyl Alcohols. *J. Org. Chem.* **2017**, *82*, 12821–12826.
- (157) Ito, Y.; Hirao, Saegusa, T. Synthesis of  $\alpha,\beta$ -Unsaturated Carbonyl Compounds by Palladium(II)-Catalyzed Dehydrosilylation of Silyl Enol Ethers. *J. Org. Chem.* **1978**, *43*, 1011–1013.
- (158) a) Li, K.; Alexakis, A. Asymmetric Conjugate Addition to  $\alpha$ -Halo Enones: Dramatic Effect of Styrene on the Enantioselectivity. *Angew. Chem. Int. Ed.* **2006**, *45*, 7600–7603; b) Vuagnoux-d'Augustin, M.; Alexakis, A. Copper-Catalyzed Asymmetric Conjugate Addition of Trialkylaluminum Reagents to Trisubstituted Enones: Construction of Chiral Quaternary Centers. *Chem. Eur. J.* **2007**, *13*, 9647–9662; c) Wencel, J.; Rix, D.; Jennequin, T.; Labat, S.; Crévisy, C.; Mauduit, M. Chiral phosphinoazomethinylate salts as new 'one-step available' ligands for copper-catalyzed asymmetric conjugate addition. *Tetrahedron: Asymmetry* **2008**, *19*, 1804–1809; d) Harutyunyan, S. R.; den Hartog, T.; Geurts, K.; Minnaard, A. J.; Feringa, B. L. Catalytic Asymmetric Conjugate Addition and Allylic Alkylation with Grignard Reagents. *Chem. Rev.* **2008**, *108*, 2824–2852; e) Palais, L.; Alexakis, A. Copper-catalyzed asymmetric conjugate addition with Grignard reagents and SimplePhos ligands. *Tetrahedron: Asymmetry* **2009**, *20*, 2866–2870.
- (159) Degrado, S. J.; Mizutani, H.; Hoveyda, A. H. Modular Peptide-Based Phosphine Ligands in Asymmetric Catalysis: Efficient and Enantioselective Cu-Catalyzed Conjugate Additions to Five-, Six-, and Seven-Membered Cyclic Enones. *J. Am. Chem. Soc.* **2001**, *123*, 755–756.

- (160) For the preparation of Diallylzinc, see: Thiele, K.-H.; Zdunneck, P. Darstellung und Eigenschaften des Diallylzinks. *J. Organomet. Chem.* **1965**, *4*, 10–17.
- (161) For the preparation of triallylborane, see: a) Brown, H. C.; Racherla, U. S. Organoboranes. 44. A convenient, highly efficient synthesis of triorganylboranes via a modified organometallic route. *J. Org. Chem.* **1986**, *51*, 427–432; b) Thiedemann, B.; Gliese, P. J.; Hoffmann, J.; Lawrence, P. G.; Sönnichsen, F. D.; Staubitz, A. High molecular weight poly(*N*-methyl-*B*-vinylazaborine) – a semi-inorganic B–N polystyrene analogue. *Chem. Commun.* **2017**, *53*, 7258–7261.
- (162) Germain, N.; Guénee, L.; Mauduit, M.; Alexakis, A. Asymmetric Conjugate Addition to  $\alpha$ -Substituted Enones/Enolate Trapping. *Org. Lett.* **2013**, *16*, 118–121.
- (163) For an examples of enantioselective allylation to  $\alpha,\beta$ -unsaturated aldehydes, see: a) Ooi, T.; Kondo, Y.; Maruoka, K. Conjugate Allylation to  $\alpha,\beta$ -Unsaturated Aldehydes with the New Chemzyme p-F-ATPH. *Angew. Chem. Int. Ed.* **1997**, *36*, 1183–1185; b) Berger, M.; Carboni, D.; Melchiorre, P. Photochemical Organocatalytic Regio- and Enantioselective Conjugate Addition of Allyl Groups to Enals. *Angew. Chem. Int. Ed.* **2021**, *60*, 26373–26377.
- (164) For an example of enantioselective allylation to cyclic enones, see: Shizuka, M.; Snapper, M. L. Catalytic Enantioselective Hosomi–Sakurai Conjugate Allylation of Cyclic Unsaturated Ketoesters. *Angew. Chem. Int. Ed.* **2008**, *47*, 5049–5051.
- (165) Taber, D. F.; Gerstenhaber, D. A.; Berry, J. F. Enantioselective Conjugate Allylation of Cyclic Enones. *J. Org. Chem.* **2011**, *76*, 7614–7617.
- (166) Barnett, D. S.; Moquist, P. N.; Schaus, S. E. The Mechanism and an Improved Asymmetric Allylboration of Ketones Catalyzed by Chiral Biphenols. *Angew. Chem. Int. Ed.* **2009**, *48*, 8679–8682.
- (167) Kim, J. G.; Waltz, K. M.; Garcia, I. F.; Kwiatkowski, D.; Walsh, P. J. Catalytic Asymmetric Allylation of Ketones and a Tandem Asymmetric Allylation/Diastereoselective Epoxidation of Cyclic Enones. *J. Am. Chem. Soc.* **2004**, *126*, 12580–12585.
- (168) Lin, H.; Xiao, L.-J.; Zhou, M.-J.; Yu, H.-M.; Xie, J.-H.; Zhou, Q.-L. Enantioselective Approach to (–)-Hamigeran B and (–)-4-Bromohamigeran B via Catalytic Asymmetric Hydrogenation of Racemic Ketone To Assemble the Chiral Core Framework. *Org. Lett.* **2016**, *18*, 1434–1437.
- (169) a) Kutz, W. M.; Adkins, H. THE ALCOHOLYSIS OF CERTAIN 1,3-DIKETONES AND BETA-KETONIC ESTERS. *J. Am. Chem. Soc.* **1930**, *52*, 4391–4399; b) Gupta, S. K. An Exceptionally Facile Reaction of  $\alpha,\alpha$ -Dichloro- $\beta$ -keto Esters with Base. *J. Org. Chem.* **1973**, *38*, 4081–4082.
- (170) a) Quigley, B. L.; Grubbs, R. H. Ruthenium-catalysed Z-selective cross metathesis of allylic-substituted olefins. *Chem. Sci.* **2014**, *5*, 501–506; b) Herbert, M. B.; Grubbs, R. H. Z-Selective Cross Metathesis with Ruthenium Catalysts: Synthetic Applications and Mechanistic Implications. *Angew. Chem. Int. Ed.* **2015**, *54*, 2–9; c) Montgomery, T. P.; Johns, A. M.; Grubbs, R. H. Recent Advancements in Stereoselective Olefin Metathesis Using Ruthenium Catalysts. *Catalysts* **2017**, *7*, 87; d) Ogba, O. M.; Warner, N. C.; O’Leary, D. J.; Grubbs, R. H. Recent advances in ruthenium-based olefin metathesis. *Chem. Soc. Rev.* **2018**, *47*, 4510–4544; e) Dawood, K. M.; Nomura, K. Recent Developments in Z-Selective Olefin Metathesis Reactions by Molybdenum, Tungsten, Ruthenium, and Vanadium Catalysts. *Adv. Synth. Catal.* **2021**, *363*, 1970–1997.
- (171) Chatterjee, A. K.; Choi, T.-L.; Sanders, D. P.; Grubbs, R. H. A General Model for Selectivity in Olefin Cross Metathesis. *J. Am. Chem. Soc.* **2003**, *125*, 11360–11370.
- (172) a) Bandini, M.; Cozzi, P. G.; Licciulli, S.; Umani-Ronchi, A. A Cross Metathesis Based Protocol for the Effective Synthesis of Functionalised Allyl Bromides and Chlorides. *Synthesis* **2004**, 409–414; b) Chung, W.-j.; Carlson, J. S.; Bedke, D. K.; Vanderwal, C. D. A Synthesis of the Chlorosulfolipid Mytilipin A via a Longest Linear Sequence of Seven Steps. *Angew. Chem. Int. Ed.* **2013**, *52*, 1–5.
- (173) Bai, C.-X.; Lu, C.-B.; Zhang, W.-Z.; Feng, X.-J. Lewis-acid assisted cross metathesis of acrylonitrile with functionalized olefins catalyzed by phosphine-free ruthenium carbene complex. *Org. Biomol. Chem.* **2005**, *3*, 4139–4142.
- (174) Michaut, A.; Boddaert, T.; Coquerel, Y.; Rodriguez, J. Reluctant Cross-Metathesis Reactions: The Highly Beneficial Effect of Microwave Irradiation. *Synthesis* **2007**, 2867–2871.

- (175) Dumas, A.; Müller, D. S.; Curbet, I.; Toupet, L.; Rouen, M.; Baslé, O.; Mauduit, M. Synthesis and Application of Stereoretentive Ruthenium Catalysts on the Basis of the M7 and the Ru–Benzylidene–Oxazinone Design. *Organometallics* **2018**, *37*, 829–834.
- (176) Voigtritter, K.; Ghorai, S.; Lipshutz, B. H. Rate Enhanced Olefin Cross-Metathesis Reactions: The Copper Iodide Effect. *J. Org. Chem.* **2011**, *76*, 4697–4702.
- (177) Lan, Y.; Chang, X.-H.; Fan, P.; Shan, C.-C.; Liu, Z.-B.; Loh, T.-P.; Xu, Y.-H. Copper-Catalyzed Silylperoxidation Reaction of  $\alpha,\beta$ -Unsaturated Ketones, Esters, Amides, and Conjugated Enynes. *ACS Catal.* **2017**, *7*, 7120–7125.
- (178) Zheng, M.; Wu, F.; Chen, K.; Zhu, S. Styrene as  $4\pi$ -Component in Zn(II)-Catalyzed Intermolecular Diels–Alder/Ene Tandem Reaction. *Org. Lett.* **2016**, *18*, 3554–3557.
- (179) Hodgson, D. M.; Arif, T. Convergent Synthesis of Trisubstituted Z-Allylic Esters by Wittig–Schlosser Reaction. *Org. Lett.* **2012**, *12*, 4204–4207.
- (180) a) Brown, C. A.; Ahju, V. K. Catalytic hydrogenation. VI. Reaction of sodium borohydride with nickel salts in ethanol solution. P-2 Nickel, a highly convenient, new, selective hydrogenation catalyst with great sensitivity to substrate structure. *J. Org. Chem.* **1973**, *38*, 2226–2230; For conditions for the preparation of Z-alkene **202**, see: b) Durand, S. A Large Scale and Concise Synthesis of  $\gamma$ -Linolenic Acid from 4-Chlorobut-2-yn-1-ol. *Synthesis* **1998**, 1015–1018.
- (181) For the oxidation with manganese dioxide, see: a) Kinoshita, M.; Takami, H.; Taniguchi, M.; Tamai, T. An Enantiospecific Synthesis of the C-21–C-37 Segment of the Aglycon of Amphotericin B. *Bull. Chem. Soc. Jpn.* **1987**, *60*, 2151–2161; for the oxidation with DDQ and Mn(OAc)<sub>3</sub>, see: b) Cosner, C. C.; Cabrera, P. J.; Byrd, K. M.; Thomas, A. M. A.; Helquist, P. Selective Oxidation of Benzylic and Allylic Alcohols Using Mn(OAc)<sub>3</sub>/Catalytic 2,3-Dichloro-5,6-dicyano-1,4-benzoquinone. *Org. Lett.* **2011**, *13*, 2071–2073; for oxidation with TEMPO and PhI(OAc)<sub>2</sub>, see: c) Regioselective Catalytic Asymmetric C-Alkylation of Isoxazolinones by a Base-Free Palladacycle-Catalyzed Direct 1,4-Addition. *Angew. Chem. Int. Ed.* **2015**, *54*, 2788–2791.
- (182) Negishi, E.-i.; Zhang, Y.; Bagheri, V. Highly stereoselective synthesis of exocyclic alkenes via cyclialkylation. *Tetrahedron Lett.* **1987**, *28*, 5793–5796.
- (183) Snider, B. B.; Kiselgof, J. Y.; Foxman, B. M. Total Synthesis of ( $\pm$ )-Isosteviol and ( $\pm$ )-Beyer-15-ene-3 $\beta$ ,19-diol by Manganese(III)-Based Oxidation Quadruple Free-Radical Cyclization. *J. Org. Chem.* **1998**, *63*, 7945–7952.
- (184) Negishi, E.; King, A. O.; Klima, W. L.; Patterson, W.; Silveira Jr., A. Conversion of methyl ketones into terminal acetylenes and (E)-trisubstituted olefins of terpenoid origin. *J. Org. Chem.* **1980**, *45*, 2526–2528.
- (185) Breton, N. L.; Martinho, M.; Kabytaev, K.; Topin, J.; Mileo, E.; Blocquel, D.; Habchi, J.; Longhi, S.; Rockenbauer, A.; Golebiowski, J.; Guigliarelli, B.; Marque, S. R. A.; Belle, V. Diversification of EPR signatures in site directed spin labeling using a  $\beta$ -phosphorylated nitroxide. *Physical Chemistry Chemical Physics* **2014**, *16*, 4202–4209.
- (186) McCammant, M. S.; Shigeta, T.; Sigman, M. S. Palladium-Catalyzed 1,3-Difunctionalization Using Terminal Alkenes with Alkenyl Nonaflates and Aryl Boronic Acids. *Org. Lett.* **2016**, *18*, 1792–1795.
- (187) For acetalisation, see: a) Le-Hocine, M. B.; Khac, D. D.; Fetizon, M.; Prance, T. A Photochemical Approach to a Potential Precursor of the Bicyclo [6.4.0] Dodecane Ring System of Taxane Diterpenes. *Synthetic Commun.* **1992**, *22*, 1871; for reduction with DIBAL-H, see: b) Davis, F. A.; Zhang, H.; Lee, S. H. Masked Oxo Sulfinimines (N-Sulfinyl Imines) in the Asymmetric Synthesis of Proline and Pipcolic Acid Derivatives. *Org. Lett.* **2001**, *3*, 759–762.
- (188) Mukaiyama, T.; Koichi, N.; Kazuo, B. NEW ALDOL TYPE REACTION. *Chem. Lett.* **1973**, *2*, 1011–1014.
- (189) Shanghui, C. L.; Wen, S.; Li, S.; Chang, J.; Shao, F.; Lei, X. Total Synthesis of the G2/M DNA Damage Checkpoint Inhibitor Psilostachyin C. *J. Org. Chem.* **2011**, *76*, 3566–3570.



- (190) Miller, R. D.; Mckean, D. R. The Facile Silylation of Aldehydes and Ketones using Trimethylsilyl Iodide: An Exceptionally Simple Procedure for the Generation of Thermodynamically Equilibrated Trimethylsilylenol Ethers. *Synthesis* **1979**, 730–732.
- (191) Rochin, C.; Babot, O.; Moulines, F.; Duboudin, F. Synthèse Régioselective de Trisenoxysilanes. *J. Organomet. Chem.* **1984**, 273, C7–C10.
- (192) Michalak, K.; Michalak, M.; Wicha, J. Construction of the Tricyclic 5–7–6 Scaffold of Fungi-Derived Diterpenoids. Total Synthesis of ( $\pm$ )-Heptemerone G and an Approach to Danishefsky's Intermediate for Guanacastepene A Synthesis. *J. Org. Chem.* **2010**, 75, 8337–8350.
- (193) Crabtree, S. R.; Chu, W. L. A.; Mander, L. N. C-Acylation of Enolates by Methyl Cyanofornate: An Examination of Site- and Stereoselectivity. *Synlett* **1990**, 169–170.
- (194) a) Scaglione, J. B.; Rath, N. P.; Covey, D. F. First Synthesis of Enantiopure 1,6-Difunctionalized Dodecahydrobenz[f]indenes. *J. Org. Chem.* **2005**, 70, 1089–1092; b) Jastrzebska, I.; Scaglione, J. B.; DeKoster, G. T.; Rath, N. P.; Covey, D. F. Palladium-Catalyzed Potassium Enoxyborate Alkylation of Enantiopure Hajos–Parrish Indenone To Construct Rearranged Steroid Ring Systems. *J. Org. Chem.* **2007**, 72, 4837–4843.
- (195) For the allylation via enoxyborates, see: a) Negishi, E.; Matsushita, H.; Chatterjee, S.; John, R. A. Selective carbon-carbon bond formation via transition metal catalysis. 29. A highly regio- and stereospecific palladium-catalyzed allylation of enolates derived from ketones. *J. Org. Chem.* **1982**, 47, 3188–3190; b) Negishi, E.; Luo, F. T.; Pecora, A. J.; Silveira Jr.; A. 1,4- and 1,5-Diketones via palladium-catalyzed allylation of potassium enoxyborates. *J. Org. Chem.* **1983**, 48, 2427–2430.
- (196) For examples proceeding via an outer-sphere mechanism, see: a) Wei, T. D.; Helmchen, G.; Kazmaier, U. Synthesis of amino acid derivatives via enantio- and diastereoselective Pd-catalyzed allylic substitutions with a non-stabilized enolate as nucleophile. *Chem. Commun.* **2002**, 12, 1270–1271; b) Mukherjee, S.; List, B. Chiral Counteranions in Asymmetric Transition-Metal Catalysis: Highly Enantioselective Pd/Brønsted Acid-Catalyzed Direct  $\alpha$ -Allylation of Aldehydes. *J. Am. Chem. Soc.* **2007**, 129, 11336–11337; c) Jiang, G.; List, B. Direct Asymmetric  $\alpha$ -Allylation of Aldehydes with Simple Allylic Alcohols Enabled by the Concerted Action of Three Different Catalysts. *Angew. Chem. Int. Ed.* **2011**, 50, 9471–9474.
- (197) For an example proceeding via an inner-sphere mechanism, see: Bai, D.-C.; Yu, F.-L.; Wang, W.-Y.; Chen, D.; Li, H.; Liu, Q.-R.; Ding, C.-H.; Chen, B.; Hou, C.-L. Palladium/N-heterocyclic carbene catalysed regio and diastereoselective reaction of ketones with allyl reagents via inner-sphere mechanism. *Nat. Commun.* **2016**, 7, 11806.
- (198) For the allylation via silyl enol ether, see: Tsuji, J.; Minami, I.; Shimizu, I. Palladium-Catalyzed Allylation of Ketones and Aldehydes with Allylic Carbonates via Silyl Enol Ethers under Neutral Conditions. *Chem. Lett.* **1983**, 12, 1325–1326.
- (199) a) Shimada, Y.; Nakamura, M.; Suzuka, T.; Matsui, J.; Tatsumi, R.; Tsutsumi, K.; Morimoto, T.; Kurosawa, H.; Kakiuchi, K. A new route for the construction of the AB-ring core of Taxol. *Tetrahedron Lett.* **2003**, 44, 1401–1403; b) Toyota, M.; Sasaki, M.; Ihara, M. Diastereoselective Formal Total Synthesis of the DNA Polymerase  $\alpha$  Inhibitor, Aphidicolin, Using Palladium-Catalyzed Cycloalkenylation and Intramolecular Diels-Alder Reactions. *Org. Lett.* **2003**, 5, 1193–1194; c) Magauer, T.; Mulzer, J.; Tiefenbacher, K. Total Syntheses of ( $\pm$ )-Echinopine A and B: Determination of Absolute Stereochemistry. *Org. Lett.* **2009**, 11, 5306–5309; d) Uwamori, M.; Saito, A.; Nakada, M. Stereoselective Total Synthesis of Nemorosone. *J. Org. Chem.* **2012**, 77, 5098–5107; e) Wang, Y.; Jäger, A.; Gruner, M.; Lübken, T.; Metz, P. Enantioselective Total Synthesis of 3 $\beta$ -Hydroxy-7 $\beta$ -kemp-8(9)-en-6-one, a Diterpene Isolated from Higher Termites. *Angew. Chem. Int. Ed.* **2017**, 56, 15861–15865.
- (200) a) Lipshutz, B. H.; Parker, D. A.; Nguyen, S. L.; McCarthy, K. E.; Barton, J. C.; Whitney, S. E.; Kotsuki, H. *Tetrahedron* **1986**, 42, 2873–2879; b) Lipshutz, B. H.; Koerner, M.; Parker, D. A. 2-thienyl(cyano)copper lithium. A lower order, stable “cuprate in a bottle” precursor to higher order reagents. *Tetrahedron Lett.* **1987**, 28, 945–948.

- (201) Schneider, L. M.; Schmiedel, V. M.; Pecchioli, T.; Lentz, D.; Merten, C.; Christmann, M. Asymmetric Synthesis of Carbocyclic Propellanes. *Org. Lett.* **2017**, *19*, 2310–2313.
- (202) Linderman, R. J.; Godfrey, A.; Horne, K. A. A reactivity umpolung route to cyclic homoenolate aldol products via  $\alpha$ -alkoxyorganocuprate conjugate additions. *Tetrahedron Lett.* **1987**, *28*, 3911–3914.
- (203) Lipshutz, B. H.; Parker, D. A.; Kozlowski, J. A.; Nguyen, S. L. Effects of Lewis acids on higher order, mixed cuprate couplings. *Tetrahedron Lett.* **1984**, *25*, 5959–5962.
- (204) Hosomi, A.; Sakurai, H. Chemistry of organosilicon compounds. 99. Conjugate addition of allylsilanes to  $\alpha,\beta$ -enones. A New method of stereoselective introduction of the angular allyl group in fused cyclic  $\alpha,\beta$ -enones. *J. Am. Chem. Soc.* **1977**, *99*, 1673–1675.
- (205) Xu, L.; Yang, M.; Qiu, H.; Lai, G.; Jiang, J. Efficient Iron-Catalyzed Sakurai–Michael Addition of Allyltrimethylsilane to Chalcones. *Synth. Commun.* **2008**, *38*, 1011–1019.
- (206) Yadav, J. S.; Reddy, B. V. S.; Sadasiv, K.; Satheesh, G. 1,4-Conjugate addition of allyltrimethylsilane to  $\alpha,\beta$ -unsaturated ketones. *Tetrahedron Lett.* **2002**, *43*, 9695–9697.
- (207) Lee, P. H.; Seomoon, D.; Kim, S.; Nagaiah, K.; Damle, S. V.; Lee, K. Efficient Addition of Allylsilanes to  $\alpha,\beta$ -Enones Using Catalytic Indium and Trimethylsilyl Chloride. *Synthesis* **2003**, 2189–2193.
- (208) Lee, P. H.; Lee, K.; Sung, S.-y.; Chang, S. The Catalytic Sakurai Reaction. *J. Org. Chem.* **2001**, *66*, 8646–8649.
- (209) Mico, A. D.; Margarita, R.; Parlanti, L.; Vescovi, A.; Piancatelli, G. A Versatile and Highly Selective Hypervalent Iodine(III)/2,2,6,6-Tetramethyl-1-piperidinyloxy-Mediated Oxidation of Alcohols to Carbonyl Compounds. *J. Org. Chem.* **1997**, *62*, 6974–6977.
- (210) Williams, B. M.; Trauner, D. Expedient Synthesis of (+)-Lycopalhine A. *Angew. Chem. Int. Ed.* **2016**, *55*, 2191–2194.
- (211) Lukashev, N. V.; Kazantsev, A. V.; Beletskaya, I. P. Hydro- and Silylcyanation of Cholic Acid Derivatives. Synthesis of Novel Pincer Ligands Based on Litocholic Acid. *Russ. J. Org. Chem.* **2014**, *50*, 1389–1396.
- (212) a) Seebach, D.; Corey, E. J. Generation and synthetic applications of 2-lithio-1,3-dithianes. *J. Org. Chem.* **1975**, *40*, 231–237; b) Yus, M.; Nájera, C.; Foubelo, F. The role of 1,3-dithianes in natural product synthesis. *Tetrahedron* **2003**, *59*, 6147–6212; c) Smith, A. B.; Adams, C. M. Evolution of Dithiane-Based Strategies for the Construction of Architecturally Complex Natural Products. *Acc. Chem. Res.* **2004**, *37*, 365–377.
- (213) a) Zimmer, R.; Taszarek, M.; Schefzig, L.; Reissig, H.-U. Reaction of a Polycyclic Diketone with Lithiated Methoxyallene: Synthesis of New Functionalized Cage Compounds. *Synlett* **2008**, 2046–2050; b) Bressel, B.; Reissig, H.-U. A New Approach to Neuraminic Acid Analogues via 1,2-Oxazines. *Org. Lett.* **2008**, *10*, 527–530; Reviews: c) Zimmer, R.; Reissig, H.-U. Alkoxyallenes as Building Blocks for Organic Synthesis. *Chem. Soc. Rev.* **2014**, *43*, 2888–2903. d) Zimmer, R. Alkoxyallenes – Building Blocks in Organic Synthesis. *Synthesis* **1993**, 165–178.

## 6.2 Illustration Credits

Scheme 8, p. 11

*Tobacco*: The photograph was downloaded from pixabay and edited for the scheme.

Source: [https://cdn.pixabay.com/photo/2018/09/20/22/32/tobacco-3691983\\_960\\_720.jpg](https://cdn.pixabay.com/photo/2018/09/20/22/32/tobacco-3691983_960_720.jpg)  
(Accessed 18.11.2021).

Licence free. Photograph credited to Markus Distelrath.

Figure 11, p. 34

*Plakortis simplex*: The photograph was downloaded from porifera.myspecies.info and edited for the figure.

Source: [http://bioweb.uwlax.edu/bio203/2011/pluym\\_conn/P.%20simplex%202.jpg](http://bioweb.uwlax.edu/bio203/2011/pluym_conn/P.%20simplex%202.jpg)  
(Accessed 04.10.2021).

Permission granted by: Copyright © Scott Nichols.

*Plakinastrella*: The photograph was downloaded from bioweb.uwlax.edu and edited for the figure.

Source: [https://porifera.myspecies.info/sites/porifera.myspecies.info/files/styles/large/public/p26\\_bocas\\_2009\\_182\\_0.jpg?itok=y8ZWvjHN](https://porifera.myspecies.info/sites/porifera.myspecies.info/files/styles/large/public/p26_bocas_2009_182_0.jpg?itok=y8ZWvjHN)  
(Accessed 04.10.2021).

Free for use as per Creative Common Licence. Photograph credited to Robert W. Thacker, Christina Diaz, Chris Freeman.

Figure 12, p. 47

*Hypericum perforatum*: The photograph was downloaded from pixabay and edited for the scheme.

Source: [https://cdn.pixabay.com/photo/2013/03/01/18/11/flowers-87580\\_960\\_720.jpg](https://cdn.pixabay.com/photo/2013/03/01/18/11/flowers-87580_960_720.jpg)  
(Accessed 13.09.2021).

Licence free. Photograph credited to Emilian Robert Vicol.

*Hypericum scabrum*: The photograph was downloaded from freenatureimages and edited for the scheme.

Source: <http://www.freenatureimages.eu/plants/Flora%20D-I/Hypericum%20scabrum/Hypericum%20scabrum%204%2C%20Saxifraga-Ed%20Stikvoort.jpg>  
(Accessed 13.09.2021).

Permission granted by: Copyright © Saxifraga and Ed Stikvoort.

*Hypericum sampsonii*: Reuse with permission from (Silva, A. R.; Taofiq, O.; Ferreira, I. C. F. R.; Barros, L. *Ind. Crops Prod.* **2021**, 159, 113053) © 2011 Elsevier Ltd. (License No.: 5266590981269).

*Hypericum elodeoides*: The photograph was downloaded from efloraofindia and edited for the scheme.

Source: [https://08511630493324166816.googlegroups.com/attach/160b76564827d191/Hypericum%204%20\(2\).JPG?part=0.2&view=1&vt=ANaJVrErjP5XSZqJx3WTEEn6LYnsKpVisal uABn9gZMKl5Tc9Ahr0N5zeeWXyx5Fix2b3ha1e1\\_7jM7FbdmCLOs8-QWrnKib5FlvuDiooqZ3Xaygu1Hg\\_Kc](https://08511630493324166816.googlegroups.com/attach/160b76564827d191/Hypericum%204%20(2).JPG?part=0.2&view=1&vt=ANaJVrErjP5XSZqJx3WTEEn6LYnsKpVisal uABn9gZMKl5Tc9Ahr0N5zeeWXyx5Fix2b3ha1e1_7jM7FbdmCLOs8-QWrnKib5FlvuDiooqZ3Xaygu1Hg_Kc)  
(Accessed 04.03.2022).

Permission granted by: Copyright © Nidhan Singh.

Figure 14, p. 49

*Hypericum patulum*: The photograph was downloaded from pixabay and edited for the scheme.

Source: [https://cdn.pixabay.com/photo/2018/10/21/18/05/image-3763331\\_960\\_720.jpg](https://cdn.pixabay.com/photo/2018/10/21/18/05/image-3763331_960_720.jpg)  
(Accessed 13.09.2021).

Licence free. Photograph credited to 日本語.

## Appendix

### Supporting Information – Synthesis of (+)-Greek Tobacco Lactone

#### Supporting Information

## Synthesis of (+)-Greek Tobacco Lactone via a Diastereoablative Epoxidation and a Selenium-Catalyzed Oxidative Cyclization

Stefan Leisering,<sup>†</sup> Iker Riaño,<sup>†</sup> Christian Depken,<sup>‡</sup> Leona J. Gross,<sup>§</sup> Manuela Weber,<sup>†</sup> Dieter Lentz,<sup>†</sup> Reinhold Zimmer,<sup>†</sup> Christian B. W. Stark,<sup>\*,§</sup> Alexander Breder,<sup>\*,‡</sup> and Mathias Christmann<sup>\*,†</sup>

<sup>†</sup>Institut für Chemie und Biochemie, Freie Universität Berlin, Takustr. 3, 14195 Berlin, Germany

<sup>‡</sup>Institut für Organische und Biomolekulare Chemie, Georg-August-Universität, Tammannstr. 2, 37077 Göttingen, Germany

<sup>§</sup>Institut für Organische Chemie, Universität Hamburg, Martin-Luther-King-Platz 6, 20146 Hamburg, Germany

#### Table of Content

General Information .....	S2
Experimental Procedures and Analytical Data .....	S2
<sup>1</sup> H- and <sup>13</sup> C-NMR Spectra .....	S8
GC Chromatogram .....	S19

## General Information

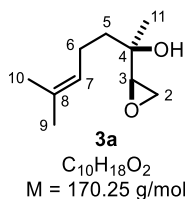
Dry dichloromethane, tetrahydrofuran and toluene were provided by purification with a MBraun SPS-800 solvent system using solvents of HPLC grade purchased from Fischer Scientific. Dry *N,N*-dimethylformamide and methanol were purchased from Acros Chemicals. Triethylamine was distilled from calcium hydride and stored under argon over KOH. Solvents for extraction, crystallization and flash column chromatography were purchased in technical grade and distilled under reduced pressure prior to use. Unless otherwise indicated, all starting materials and reagents were purchased from commercial distributors and used without further purification. Microwave-assisted reactions were done in a microwave oven "micro Chemist" from MLS GmbH.

Products were purified by flash column chromatography on silica gel 60 M (0.040-0.063 mm, 230-400 mesh, Macherey-Nagel). TLC-analyses was performed on silica gel coated aluminum plates ALUGRAM® Xtra SIL G/UV<sub>254</sub> purchased from Macherey-Nagel. Products were detected by UV light at 254 nm and by using staining reagents (based on KMnO<sub>4</sub> and anisaldehyd).

<sup>1</sup>H NMR and <sup>13</sup>C NMR spectral data were recorded on Bruker (AC 500, AVIII 700) and JEOL (ECX 400, Eclipse 500) spectrometer. The chemical shifts (δ) are listed in parts per million (ppm) and are reported relative to the corresponding residual solvent signal (CDCl<sub>3</sub>: δ<sub>H</sub> = 7.26 ppm, δ<sub>C</sub> = 77.16 ppm). Integrals are in accordance with assignments; coupling constants (*J*) are given in Hz. Multiplicity is indicated as follows: s (singlet), d (doublet), t (triplet), q (quartet), m (multiplet), dd (doublet of doublet), s<sub>br</sub> (broad singlet), etc. <sup>13</sup>C-NMR spectra are <sup>1</sup>H-broadband decoupled. For detailed peak assignments 2D spectra were measured (COSY, HMQC, HMBC). The numbering of the carbon atoms was based on Wahlberg's initial assignment of the isolated Tobacco lactone. IR spectra were measured with a Jasco spectrometer (FT/IR-4100) equipped with an ATR unit. High resolution mass spectra were measured with an Agilent 6210 ESI-TOF (10 μL/min, 1.0 bar, 4 kV) instrument. Melting points were determined by digital melting point apparatus (Stuart SMP30) and are uncorrected. Optical rotations values were determined with a Jasco P-2000 polarimeter at the temperatures given. Diastereomeric ratios were determined by <sup>1</sup>H NMR or gas chromatography with an Agilent 7890B instrument on a chiral column. The specific conditions are given in each case.

## Experimental Procedures and Analytical Data

### (*R*)-6-Methyl-2-((*S*)-oxiran-2-yl)hept-5-en-2-ol (**3a**)



(*R*)-Linalool (10.0 g, 64.8 mmol, 1.00 equiv) and VO(acac)<sub>2</sub> (0.86 g, 3.24 mmol, 5 mol%) were dissolved in toluene (250 mL) under argon atmosphere and the solution was refluxed for 10 min. Then a solution of TBHP in decane (5.5 M, 17.7 mL, 97.2 mmol, 1.50 equiv) was added over 1 h and the resulting reaction mixture was stirred at 80 °C for 20 h. The mixture was cooled to ambient temperature, washed with saturated aqueous NaHCO<sub>3</sub> solution (100 mL) and brine (100 mL) and dried over anhydrous MgSO<sub>4</sub>. The solvent was removed under reduced pressure and the crude product was purified by column chromatography (SiO<sub>2</sub>, pentane/Et<sub>2</sub>O, 10:1 to 4:1) to give epoxide **3a** (3.29 g, 19.3 mmol, 30%, d.r. >99:1) as a slightly yellow oil. The diastereomeric ratio was determined by chiral GC analysis (Lipodex-E, 100 °C, isothermal, 1.1 mL/min, He, *t<sub>R</sub>* (**3a**) = 19.79 min, *t<sub>R</sub>* (**3b**, not observed) = 20.77 min).

[α]<sub>D</sub><sup>22</sup> = -5.2 (*c* = 1.00, CHCl<sub>3</sub>).

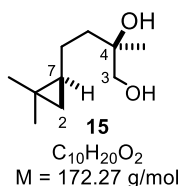
<sup>1</sup>H NMR (400 MHz, CDCl<sub>3</sub>): δ = 1.19 (s, 3 H, H-11), 1.59–1.66 (m, 5 H, H-5, H-9/H-10), 1.68 (s, 3 H, H-9/H-10), 1.77 (s, 1 H, OH), 2.08–2.18 (m, 2 H, H-6), 2.69 (dd, <sup>2</sup>*J* = 5.1 Hz, <sup>3</sup>*J* = 4.1 Hz, 1 H, H-2), 2.77 (dd, <sup>2</sup>*J* = 5.1 Hz, <sup>3</sup>*J* = 2.8 Hz, 1 H, H-2), 2.97 (dd, <sup>3</sup>*J* = 4.1, 2.8 Hz, 1 H, H-3), 5.09–5.16 ppm (m, 1 H, H-7).

<sup>13</sup>C NMR (126 MHz, CDCl<sub>3</sub>): δ = 17.7 (C-9/C-10), 22.3 (C-6), 22.8 (C-11), 25.8 (C-9/C-10), 41.3 (C-5), 43.4 (C-2), 57.8 (C-3), 69.4 (C-4), 124.2 (C-7), 132.0 ppm (C-8).

IR (ATR):  $\tilde{\nu}$  = 3447, 2972, 2919, 2857, 1451, 1377, 1261, 1115, 915, 874, 837, 810, 755 cm<sup>-1</sup>.

HRMS (ESI, pos.): *m/z* calcd for C<sub>10</sub>H<sub>18</sub>O<sub>2</sub>Na<sup>+</sup> [M+Na]<sup>+</sup>: 193.1199, found 193.1202.

### (*R*)-4-((*S*)-2,2-Dimethylcyclopropyl)-2-methylbutane-1,2-diol (**15**)



A solution of both diastereomeric epoxides **3b** and **3a** in a ratio of 1.4:1 (1.18 g, 6.91 mmol, 1.00 equiv), (*S,S*)-Jacobsen's catalyst **4** (83.4 mg, 0.14 mmol, 2 mol%) and AcOH (16 μL, 0.28 mmol, 4 mol%) in THF (1.4 mL) was stirred at 23 °C. The reaction progress was monitored by chiral GC. After 3 d the conversion of **3b** was complete and MeOH (1.4 mL) and NaBH<sub>4</sub> (26.0 mg, 6.91 mmol, 1.00 equiv) were added at 0 °C and the reaction mixture was stirred for 40 min at this temperature. Then saturated

aqueous  $\text{NH}_4\text{Cl}$  solution (1 mL) was added and the mixture was stirred until no further gas evolution was observed. The solution was extracted with EtOAc ( $3 \times 1$  mL) and the combined organic layers were dried over anhydrous  $\text{Na}_2\text{SO}_4$ . The solvent was removed under reduced pressure and the crude product was purified by column chromatography ( $\text{SiO}_2$ , pentane/ $\text{Et}_2\text{O}$ , 4:1 to 1:2) to give alcohol **15** (377 mg, 2.19 mmol, 54% based on **3b**) as a brown oil.

$[\alpha]_{\text{D}}^{25} = 9.4$  ( $c = 1.00$ ,  $\text{CHCl}_3$ ).

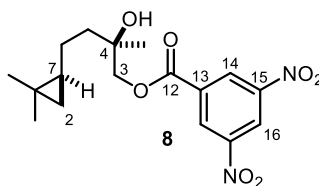
$^1\text{H NMR}$  (700 MHz,  $\text{CDCl}_3$ ):  $\delta = -0.13$  (dd,  $^3J = 5.3$  Hz,  $^2J = 4.2$  Hz, 1 H, H-2), 0.35 (dd,  $^3J = 8.4$  Hz,  $^2J = 4.2$  Hz, 1 H, H-2), 0.40–0.45 (m, 1 H, H-7), 1.00 (s, 3 H, H-9/H-10), 1.02 (s, 3 H, H-9/H-10), 1.13 (s, 3 H, H-11), 1.26–1.39 (m, 2 H, H-6), 1.52 (td,  $J = 12.8$  Hz,  $J = 4.8$  Hz, 1 H, H-5), 1.59 (td,  $J = 12.8$  Hz,  $J = 4.8$  Hz, 1 H, H-5), 3.39 (d,  $^2J = 11.0$  Hz, 1 H, H-3), 3.44 ppm (d,  $^2J = 11.0$  Hz, 1 H, H-3).

$^{13}\text{C NMR}$  (176 MHz,  $\text{CDCl}_3$ ):  $\delta = 15.6$  (C-8), 19.8 (C-2), 19.9 (C-9/C-10), 23.2 (C-11), 24.2 (C-6), 25.0 (C-7), 27.7 (C-9/C-10), 39.2 (C-5), 70.0 (C-3), 73.1 (C-4) ppm.

IR (ATR):  $\tilde{\nu} = 3384, 2972, 2938, 2866, 1455, 1376, 1053$   $\text{cm}^{-1}$ .

HRMS (ESI, pos.):  $m/z$  calcd for  $\text{C}_{10}\text{H}_{20}\text{O}_2\text{Na}^+$  [ $\text{M}+\text{Na}$ ] $^+$ : 195.1356, found 195.1355.

#### (*R*)-4-((*S*)-2,2-Dimethylcyclopropyl)-2-hydroxy-2-methylbutyl 3,5-dinitrobenzoate (**8**)



$\text{C}_{17}\text{H}_{22}\text{N}_2\text{O}_7$   
M = 366.37 g/mol

To a solution of alcohol **15** (100 mg, 0.58 mmol, 1.00 equiv) in dichloromethane (3.6 mL) was added 3,5-dinitrobenzoyl chloride (200 mg, 0.87 mmol, 1.50 equiv), followed by the addition of  $\text{Et}_3\text{N}$  (120  $\mu\text{L}$ , 0.87 mmol, 1.50 equiv). The reaction mixture was stirred at 23  $^\circ\text{C}$  for 1.5 h. Then saturated aqueous  $\text{NaHCO}_3$  solution (3 mL) was added and the mixture was extracted with EtOAc ( $3 \times 3$  mL). The combined organic extracts were washed with brine (3 mL) and dried over anhydrous  $\text{Na}_2\text{SO}_4$ . The solvent was removed under reduced pressure and the residue was purified by column chromatography ( $\text{SiO}_2$ , pentane/ $\text{EtOAc}$ , 8:1 to 7:1) to afford ester **8** (182 mg, 0.50 mmol, 86%) as a colorless solid. Crystallization from benzene/pentane gave crystals suitable for X-ray diffraction.

$[\alpha]_{\text{D}}^{25} = -0.9$  ( $c = 1.00$ ,  $\text{CHCl}_3$ ).

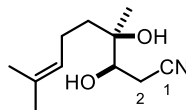
$^1\text{H NMR}$  (700 MHz,  $\text{CDCl}_3$ ):  $\delta = -0.10$  (dd,  $^3J = 5.3$  Hz,  $^2J = 4.2$  Hz, 1 H, H-2), 0.39 (dd,  $^3J = 8.5$  Hz,  $^2J = 4.2$  Hz, 1 H, H-2), 0.47 (dtd,  $^3J = 8.5, 7.1, 5.3$  Hz, 1 H, H-7), 1.02 (s, 3 H, H-9/H-10), 1.04 (s, 3 H, H-9/H-10), 1.32 (s, 3 H, H-11), 1.37–1.47 (m, 2 H, H-6), 1.68–1.75 (m, 2 H, H-5), 4.33 (d,  $^2J = 11.2$  Hz, 1 H, H-3), 4.36 (d,  $^2J = 11.2$  Hz, 1 H, H-3), 9.15 (d,  $^4J = 2.2$  Hz, 2 H, H-14), 9.22 ppm (t,  $^4J = 2.2$  Hz, 1 H, H-16).

$^{13}\text{C NMR}$  (176 MHz,  $\text{CDCl}_3$ ):  $\delta = 15.7$  (C-8), 19.8 (C-2), 19.9 (C-9/C-10), 24.1 (C-11), 24.1 (C-6), 24.8 (C-7), 27.6 (C-9/C-10), 39.7 (C-5), 72.0 (C-4), 73.0 (C-3), 122.7 (C-16), 129.6 (C-14), 133.9 (C-13), 148.8 (C-15), 162.7 ppm (C-12).

IR (ATR):  $\tilde{\nu} = 3101, 2980, 2941, 2865, 1732, 1543, 1342, 1273, 1164, 921$   $\text{cm}^{-1}$ .

HRMS (ESI, pos.):  $m/z$  calcd for  $\text{C}_{17}\text{H}_{22}\text{N}_2\text{O}_7\text{Na}^+$  [ $\text{M}+\text{Na}$ ] $^+$ : 389.1319, found 389.1329.

#### (3*R*,4*R*)-3,4-Dihydroxy-4,8-dimethylnon-7-enitrile (**10**)



**10**  
 $\text{C}_{11}\text{H}_{19}\text{NO}_2$   
M = 197.28 g/mol

A solution of epoxide **3a** (5.49 g, 32.3 mmol, 1.00 equiv) in DMF (10 mL) was added to a suspension of KCN (5.25 g, 80.6 mmol, 2.50 equiv) and  $p\text{-TsOH}\cdot\text{H}_2\text{O}$  (7.36 g, 38.7 mmol, 1.20 equiv) in DMF (54 mL) at 40  $^\circ\text{C}$  and the resulting reaction mixture was stirred at 80  $^\circ\text{C}$  for 6 h. The solution was cooled to 0  $^\circ\text{C}$ , quenched with saturated aqueous  $\text{NaHCO}_3$  solution (50 mL) and water (50 mL) and extracted with EtOAc ( $3 \times 100$  mL). The combined organic extracts were washed with brine ( $3 \times 100$  mL) and dried over anhydrous  $\text{Na}_2\text{SO}_4$ . The solvent was removed under reduced pressure and the crude product was purified by column chromatography ( $\text{SiO}_2$ , pentane/ $\text{EtOAc}$ , 4:1 to 2:1) to give nitrile **10** (4.96 g, 25.1 mmol, 78%) as a colorless oil that crystallized in the fridge.

$[\alpha]_{\text{D}}^{20} = +26.2$  ( $c = 1.00$ ,  $\text{CHCl}_3$ ).

m.p. 55–57  $^\circ\text{C}$ .



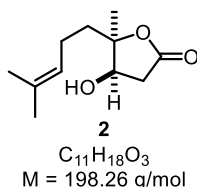
**<sup>1</sup>H NMR** (500 MHz, CDCl<sub>3</sub>): δ = 1.13 (s, 3 H, H-11), 1.50–1.57 (m, 2 H, H-5), 1.61 (s, 3 H, H-9/H-10), 1.68 (s, 3 H, H-9/H-10), 2.02–2.09 (m, 2 H, H-6), 2.29–2.39 (m, 1 H, OH), 2.57 (d, <sup>3</sup>J = 7.9 Hz, 1 H, H-2), 2.57 (d, <sup>3</sup>J = 5.0 Hz, 1 H, H-2), 3.26–3.43 (m, 1 H, OH), 3.75–3.81 (m, 1 H, H-3), 5.06–5.12 ppm (m, 1 H, H-7).

**<sup>13</sup>C NMR** (126 MHz, CDCl<sub>3</sub>): δ = 17.8 (C-9/C-10), 21.2 (C-2), 21.7 (C-11), 22.3 (C-6), 25.8 (C-9/C-10), 38.5 (C-5), 72.7 (C-3), 74.2 (C-4), 119.0 (C-1), 123.8 (C-7), 132.7 ppm (C-8).

**IR** (ATR):  $\tilde{\nu}$  = 3422, 2972, 2919, 2858, 2254, 1377, 1068 cm<sup>-1</sup>.

**HRMS** (ESI, pos.): *m/z* calcd for C<sub>11</sub>H<sub>19</sub>NO<sub>2</sub>Na<sup>+</sup> [M+Na]<sup>+</sup>: 220.1308, found 220.1328; *m/z* calcd for C<sub>22</sub>H<sub>38</sub>N<sub>2</sub>O<sub>4</sub>Na<sup>+</sup> [2M+Na]<sup>+</sup>: 417.2724, found 417.2749.

**(4*R*,5*R*)-4-Hydroxy-5-methyl-5-(4-methylpent-3-en-1-yl)dihydrofuran-2(3*H*)-one (2)**



A solution of nitrile **10** (3.00 g, 15.2 mmol, 1.00 equiv) in ethylene glycol monomethyl ether (15 mL) and NaOH (2 M, 40 mL) was stirred at 110 °C for 1.5 h. The reaction mixture was cooled to 0 °C, acidified with HCl (2 M) until pH = 2 and stirred for further 17 h while slowly warming up to room temperature. The solution was extracted with Et<sub>2</sub>O (4 × 100 mL). The combined organic extracts were washed with brine (150 mL) and dried over anhydrous Na<sub>2</sub>SO<sub>4</sub>. The solvent was removed under reduced pressure and the crude product was purified by column chromatography (SiO<sub>2</sub>, pentane/EtOAc, 3:1 to 1:1) to give lactone **2** (2.25 g, 11.4 mmol, 75%) as a slightly yellow oil.

$[\alpha]_D^{21}$  = +21.3 (*c* = 1.00, CHCl<sub>3</sub>).

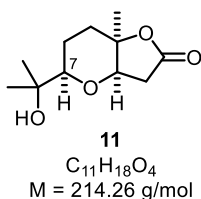
**<sup>1</sup>H NMR** (700 MHz, CDCl<sub>3</sub>): δ = 1.33 (s, 3 H, H-11), 1.61 (s, 3 H, H-9/H-10), 1.68 (s, 3 H, H-9/H-10), 1.77 (ddd, <sup>2</sup>J = 14.0 Hz, <sup>3</sup>J = 10.2, 6.7 Hz, 1 H, H-5), 1.83 (ddd, <sup>2</sup>J = 14.0 Hz, <sup>3</sup>J = 9.8, 6.1 Hz, 1 H, H-5), 2.05–2.16 (m, 2 H, H-6), 2.50 (dd, <sup>2</sup>J = 18.1 Hz, <sup>3</sup>J = 2.4 Hz, 1 H, H-2), 2.78 (d, <sup>3</sup>J = 4.7 Hz, 1 H, OH), 2.88 (s<sub>br</sub>, 1 H, OH), 2.93 (dd, <sup>2</sup>J = 18.1 Hz, <sup>3</sup>J = 6.2 Hz, 1 H, H-2), 4.15–4.20 (m, 1 H, H-3), 5.10–5.17 ppm (m, 1 H, H-7).

**<sup>13</sup>C NMR** (176 MHz, CDCl<sub>3</sub>): δ = 17.8 (C-9/C-10), 22.5 (C-6), 23.2 (C-11), 25.8 (C-9/C-10), 34.1 (C-5), 38.6 (C-2), 73.6 (C-3), 90.0 (C-4), 123.5 (C-7), 133.0 (C-8), 175.5 ppm (C-1).

**IR** (ATR):  $\tilde{\nu}$  = 3438, 2971, 2921, 2858, 1748, 1173, 1080, 1067, 952, 929 cm<sup>-1</sup>.

**HRMS** (ESI, pos.): *m/z* calcd for C<sub>11</sub>H<sub>18</sub>O<sub>3</sub>K<sup>+</sup> [M+K]<sup>+</sup>: 237.0888, found 237.0919; *m/z* calcd for C<sub>22</sub>H<sub>36</sub>O<sub>6</sub>Na<sup>+</sup> [2M+Na]<sup>+</sup>: 419.2404, found 419.2441.

**(3*aR*,5*R*,7*aR*)-5-(2-Hydroxypropan-2-yl)-7*a*-methylhexahydro-2*H*-furo[3,2-*b*]pyran-2-one (11)**



To a solution of vanadium(V)oxytriethoxide (3.00 μL, 15.8 μmol, 10 mol%) in dichloromethane (2.0 mL) under N<sub>2</sub>-atmosphere was added TBHP (43.0 μL, 237 μmol, 1.50 equiv) and the reaction mixture was stirred at 23 °C. Lactone **2** (31.0 mg, 158 μmol, 1.00 equiv) dissolved in dichloromethane (1.0 mL) was added via cannula. The reaction mixture was stirred for 4 h and then more vanadium(V)oxytriethoxide (3.00 μL, 15.8 μmol, 10 mol%) was added. After 2 h the reaction was complete and the solvent was removed under reduced pressure. The crude product was purified via flash chromatography (SiO<sub>2</sub>, CH<sub>2</sub>Cl<sub>2</sub>/MeOH, 95:5). The diastereomeric products were obtained as colorless oils (**11**: 28.8 mg, 134 μmol, 85% and 7-*epi*-**11**: 3.50 mg, 16.0 μmol, 10%) with a diastereometric ratio of 9:1 favoring the (7*R*)-diastereoisomer as the major product.

**(7*R*)-diastereoisomer (11):**

**<sup>1</sup>H NMR** (600 MHz, CDCl<sub>3</sub>): δ = 1.13 (s, 3 H, H-10), 1.16 (s, 3 H, H-9), 1.30 (s, 3 H, H-11), 1.51–1.60 (m, 2 H, H-6), 1.64–1.73 (m, 1 H, H-5), 2.25–2.36 (m, 2 H, H-5, OH), 2.51 (d, <sup>2</sup>J = 17.5 Hz, 1 H, H-2), 2.89 (dd, <sup>2</sup>J = 17.5 Hz, <sup>3</sup>J = 4.3 Hz, 1 H, H-2), 3.14 (dd, <sup>3</sup>J = 10.2 Hz, <sup>3</sup>J = 2.6 Hz, 1 H, H-7), 4.07 ppm (d, <sup>3</sup>J = 4.2 Hz, 1 H, H-3).

**<sup>13</sup>C NMR** (150 MHz, CDCl<sub>3</sub>): δ = 20.8 (C-6), 24.1 (C-10), 25.2 (C-11), 25.7 (C-9), 32.3 (C-5), 38.2 (C-2), 71.8 (C-8), 78.0 (C-3), 82.0 (C-4), 82.3 (C-7), 175.7 ppm (C-1).

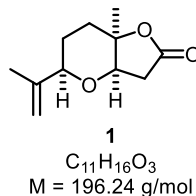
**(7*S*)-diastereoisomer (7-*epi*-11):**

**<sup>1</sup>H NMR** (600 MHz, CDCl<sub>3</sub>): δ = 1.34 (s, 3 H, H-11), 1.56 (s, 3 H, H-10), 1.61 (s, 3 H, H-9), 1.59–1.68 (m, 1 H, H-6), 1.67–1.87 (m, 1 H, H-6), 1.91–2.00 (m, 1 H, H-5), 2.09–2.19 (m, 1 H, H-5), 2.54 (dd, <sup>2</sup>J = 18.1 Hz, <sup>3</sup>J = 1.3 Hz, 1 H, H-2), 2.96 (dd, <sup>2</sup>J = 18.0 Hz, <sup>3</sup>J = 6.1 Hz, 1 H, H-2), 3.53 (dd, <sup>3</sup>J = 10.8 Hz, <sup>3</sup>J = 1.8 Hz, 1 H, H-7), 4.22 ppm (dd, <sup>3</sup>J = 6.1 Hz, <sup>3</sup>J = 1.5 Hz, 1 H, H-3).

$^{13}\text{C}$  NMR (150 MHz,  $\text{CDCl}_3$ ):  $\delta$  = 23.6 (C-11), 25.8 (C-6), 27.4 (C-10), 29.3 (C-9), 30.5 (C-5), 38.6 (C-2), 74.0 (C-3), 75.6 (C-8), 78.8 (C-7), 89.6 (C-4), 175.2 ppm (C-1).

All other data were in accordance with published data.<sup>1</sup>

**(3a*R*,5*R*,7a*R*)-7a-Methyl-5-(prop-1-en-2-yl)hexahydro-2H-furo[3,2-*b*]pyran-2-one (1)**



**Elimination of alcohol 11**

A mixture of alcohol **11** (43.0 mg, 0.20 mmol, 1.00 equiv) and Burgess' reagent (96.0 mg, 0.40 mmol, 2.00 equiv) in 1,4-dioxane (1 mL) was sealed in a reaction vial and submitted to a microwave reactor. The reaction mixture was irradiated for 1 min with a capacity of 150 W to reach a temperature of 150 °C and stirred for 3 min at this temperature. After cooling down to ambient temperature the crude mixture was directly subjected to silica gel chromatography ( $\text{SiO}_2$ , pentane/EtOAc, 4:1). The dehydration product **1** (35.8 mg, 0.18 mmol, 91%) was obtained as a colorless oil.

**Palladium-catalyzed cyclization**

A mixture of lactone **2** (34.8 mg, 176  $\mu\text{mol}$ , 1.00 equiv.) and palladium trifluoroacetate (60.2 mg, 176  $\mu\text{mol}$ , 1.00 equiv.) in dry DMSO (1.8 mL) under argon atmosphere, was stirred at 80 °C using microwave irradiation for 8 h. The reaction mixture was allowed to cool to ambient temperature and then filtered through silica gel. The filtrate was concentrated under reduced pressure and purified by column chromatography (hexane/EtOAc, 4:1 to 1:1) to give a mixture of **1** and 7-*epi*-**1** (14.3 mg, 73.0  $\mu\text{mol}$ , 41%) as a colourless oil with a diastereomeric ratio of 85:15 and **12** (5.20 mg, 26.0  $\mu\text{mol}$ , 15%) as a white solid.

**Selenium-catalyzed cyclization with NFSI**

To a suspension of lactone **2** (2.00 g, 10.1 mmol, 1.00 equiv) and 4Å molecular sieves (200 mg) in THF (100 mL)  $\text{CaCO}_3$  (3.03 g, 30.3 mmol, 3.00 equiv) and  $(\text{PhSe})_2$  (0.31 g, 1.01 mmol, 10 mol%) were added. Then NFSI (3.34 g, 10.6 mmol, 1.05 equiv) was added in small portions over 1 h. The reaction mixture was stirred for further 2 h and then diluted with  $\text{Et}_2\text{O}$  (50 mL) and filtered through celite. The solvent was removed under reduced pressure and the crude product was purified by column chromatography ( $\text{SiO}_2$ , pentane/EtOAc, 10:1 to 5:1) to give **1** (1.20 g, 6.10 mmol, 60%) as a colorless oil.

**Selenium-catalyzed cyclization with oxygen**

A solution of lactone **2** (150 mg, 813  $\mu\text{mol}$ , 1.00 equiv),  $(\text{PhSe})_2$  (25.0 mg, 81.0  $\mu\text{mol}$ , 10 mol%), 2,4,6-tris(4-methoxyphenyl)pyrylium tetrafluoroborate (19.0 mg, 4.00  $\mu\text{mol}$ , 5 mol%) and  $\text{Na}_2\text{HPO}_4$  (90 mg, 651  $\mu\text{mol}$ , 0.80 equiv) in dichloroethane (4.2 mL) was subjected to blue light irradiation (465 nm, 7200 lux) and stirred at 700 rpm with a cross-shaped magnetic stirrer for 5 h under an atmosphere of air (balloon). Once the reaction was complete all volatile materials were removed under reduced pressure and the crude mixture was purified by column chromatography ( $\text{SiO}_2$ , pentane/EtOAc, 8:1) to yield **1** (102 mg, 553  $\mu\text{mol}$ , 68%) as colorless oil and 7-*epi*-**1** (20.0 mg, 107  $\mu\text{mol}$ , 13%) as a colorless oil with small amounts of **1** (3.00 mg, 15.0  $\mu\text{mol}$ , 2%).

**(7*R*)-diastereoisomer 1:**

$[\alpha]_D^{25} = +40.8$  ( $c = 1.00$ ,  $\text{CHCl}_3$ ).

$^1\text{H}$  NMR (700 MHz,  $\text{CDCl}_3$ ):  $\delta$  = 1.29 (s, 3 H, H-11), 1.56–1.60 (m, 1 H, H-6), 1.63–1.74 (m, containing s at 1.70, 5 H, H-5, H-6, H-10), 2.26–2.30 (m, 1 H, H-5), 2.51 (dd,  $^2J = 17.5 \text{ Hz}$ ,  $J = 0.9 \text{ Hz}$ , 1 H, H-2), 2.87 (dd,  $^2J = 17.5 \text{ Hz}$ ,  $^3J = 4.3 \text{ Hz}$ , 1 H, H-2), 3.71 (d,  $^3J = 10.4 \text{ Hz}$ , H-7), 4.06 (d,  $^3J = 4.3 \text{ Hz}$ , 1 H, H-3), 4.82–4.84 (m, 1 H, H-9), 4.94–4.95 ppm (m, 1 H, H-9).

$^{13}\text{C}$  NMR (176 MHz,  $\text{CDCl}_3$ ):  $\delta$  = 18.5 (C-10), 25.2 (C-6), 25.3 (C-11), 32.4 (C-5), 38.3 (C-2), 77.6 (C-3), 78.7 (C-7), 81.7 (C-4), 111.5 (C-9), 144.9 (C-8), 175.9 ppm (C-1).

IR (ATR):  $\tilde{\nu} = 2976, 2927, 2851, 1777, 1288, 1077, 935 \text{ cm}^{-1}$ .

HRMS (ESI, pos.):  $m/z$  calcd for  $\text{C}_{11}\text{H}_{16}\text{O}_3\text{Na}^+$  [ $\text{M}+\text{Na}$ ] $^+$ : 219.0992, found 219.0993;  $m/z$  calcd for  $\text{C}_{22}\text{H}_{32}\text{O}_6\text{Na}^+$  [ $2\text{M}+\text{Na}$ ] $^+$ : 415.2091, found 415.2094.

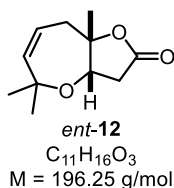
**Compounds *ent*-12 and 13**

To a round-bottom flask lactone *ent*-**2** (24.2 mg, 122  $\mu\text{mol}$ , 1.00 equiv) and palladium trifluoroacetate (41.9 mg, 122  $\mu\text{mol}$ , 1.00 equiv) were added and dissolved in acetonitrile (0.5 mL). The flask was evacuated and flooded with  $\text{O}_2$  (3 $\times$ ) and then stirred at 80

<sup>1</sup> Siitonen, J.; Pihko, P. *Synlett* 2014, 25, 1888–1890.

°C under O<sub>2</sub> atmosphere (1 atm) for 90 min. The mixture was allowed to cool and then filtered over silica gel. The filtrate was concentrated under reduced pressure and the residue was purified by column chromatography (hexane/EtOAc, 4:1 to 3:1) to yield tetraoxepine *ent*-**12** (12.5 mg, 64.0 μmol, 52%) and tetraoxepine **13** (4.40 mg, 22.0 μmol, 18%).

**(3a*S*,8a*S*)-5,5,8a-Trimethyl-3,3a,8,8a-tetrahydrofuro[3,2-*b*]oxepin-2(3*H*)-one (*ent*-**12**):**



[α]<sub>D</sub><sup>20</sup> = -52.2 (*c* = 0.50, CH<sub>2</sub>Cl<sub>2</sub>).

m.p. 87–89 °C.

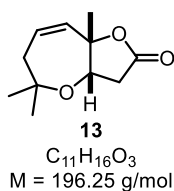
<sup>1</sup>H NMR (700 MHz, CDCl<sub>3</sub>): δ = 1.24 (s, 3 H, H-9/H-10), 1.32 (s, 3 H, H-9/H-10), 1.33 (d, <sup>4</sup>*J* = 1.0 Hz, 3 H, H-11), 2.16 (dd, <sup>2</sup>*J* = 12.8 Hz, <sup>3</sup>*J* = 8.8 Hz, <sup>5</sup>*J* = 0.7 Hz, 1 H, H-5), 2.47 (dt, <sup>2</sup>*J* = 13.8 Hz, <sup>5</sup>*J* = 0.7 Hz, 1 H, H-2), 2.91 (dd, <sup>2</sup>*J* = 13.8 Hz, <sup>3</sup>*J* = 7.0 Hz, 1 H, H-2), 3.06 (dddq, <sup>2</sup>*J* = 12.8 Hz, <sup>3</sup>*J* = 5.4 Hz, <sup>4</sup>*J* = 2.5, 1.0 Hz, 1 H, H-5), 4.07 (d, <sup>3</sup>*J* = 7.0 Hz, 1 H, H-3), 5.38 (ddd, <sup>3</sup>*J* = 11.0 Hz, <sup>4</sup>*J* = 2.5, 0.6 Hz, 1 H, H-7), 5.51 ppm (ddd, <sup>3</sup>*J* = 11.0, 8.8, 5.4 Hz, 1 H, H-6).

<sup>13</sup>C NMR (176 MHz, CDCl<sub>3</sub>): δ = 23.4 (C-9/C-10), 25.2 (C-9/C-10), 29.3 (C-11), 32.8 (C-5), 36.8 (C-2), 73.8 (C-3), 79.2 (C-8), 90.4 (C-4), 121.3 (C-6), 138.1 (C-7), 175.2 (C-1).

IR (ATR):  $\tilde{\nu}$  = 2974, 2935, 2871, 1773, 1085, 1071, 954 cm<sup>-1</sup>.

HRMS (ESI, pos.): *m/z* calcd for C<sub>11</sub>H<sub>16</sub>O<sub>3</sub>Na<sup>+</sup> [M+Na]<sup>+</sup>: 219.0992, found 219.0097.

**(3a*S*,8a*S*)-5,5,8a-Trimethyl-3,3a,5,6-tetrahydrofuro[3,2-*b*]oxepin-2(8a*H*)-one (**13**):**



[α]<sub>D</sub><sup>20</sup> = -28.5 (*c* = 0.20, CH<sub>2</sub>Cl<sub>2</sub>).

m.p. 125–127 °C.

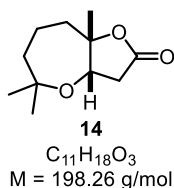
<sup>1</sup>H NMR (400 MHz, CDCl<sub>3</sub>): δ = 1.17 (s, 3 H, H-9/H-10), 1.20 (s, 3 H, H-9/H-10), 1.39 (s, 3 H, H-11), 1.93 (ddd, <sup>2</sup>*J* = 14.8 Hz, <sup>3</sup>*J* = 8.6, <sup>4</sup>*J* = 1.0 Hz, 1 H, H-7), 2.33–2.38 (m, 1 H, H-7), 2.48 (dt, <sup>2</sup>*J* = 18.1 Hz, *J* = 0.7 Hz, 1 H, H-2), 2.96 (dd, <sup>2</sup>*J* = 18.1 Hz, <sup>3</sup>*J* = 6.5 Hz, 1 H, H-2), 4.17 (d, <sup>3</sup>*J* = 6.5 Hz, 1 H, H-3), 5.68 (ddd, <sup>3</sup>*J* = 11.0, 8.6, 5.8 Hz, 1 H, H-6), 5.77–5.79 ppm (m, 1 H, H-5).

<sup>13</sup>C NMR (176 MHz, CDCl<sub>3</sub>): δ = 24.9 (C-11), 26.1 (C-9/C-10), 27.7 (C-9/C-10), 36.7 (C-7), 37.4 (C-2), 72.9 (C-3), 76.4 (C-8), 91.9 (C-4), 123.8 (C-6), 132.6 (C-5), 174.6 ppm (C-1).

IR (ATR):  $\tilde{\nu}$  = 2975, 2930, 2874, 1765, 1074 cm<sup>-1</sup>.

HRMS (ESI, pos.): *m/z* calcd for C<sub>11</sub>H<sub>16</sub>O<sub>3</sub>Na<sup>+</sup> [M+Na]<sup>+</sup>: 219.0992, found 219.1002.

**(3a*S*,8a*S*)-5,5,8a-Trimethylhexahydrofuro[3,2-*b*]oxepin-2(3*H*)-one (**14**)**



**Method A**

To a flame-dried round-bottom flask lactone *ent*-**2** (39.6 mg, 200 μmol, 1.00 equiv), palladium(II) chloride (7.10 mg, 40.0 μmol, 20 mol%) and copper(II) chloride (80.6 mg, 600 μmol, 3.00 equiv) were added under argon atmosphere. Then dried methanol (0.8 mL) was added and the reaction was stirred at 50 °C for 1 d. The volatile materials were removed under reduced pressure and the crude mixture was purified by column chromatography (hexane/EtOAc, 3:1 to 1:1) to afford hexahydrooxepine **14** (11.0 mg, 55.5 μmol, 28%) as a white solid.

**Method B**

To a flame-dried round-bottom flask lactone *ent-2* (20.4 mg, 103  $\mu$ mol, 1.00 equiv), benzoquinone (22.3 mg, 206  $\mu$ mol, 2.00 equiv), 1,2-bis(phenylsulfinyl)ethane]palladium acetate (5.20 mg, 10.0  $\mu$ mol, 10 mol%) and silver trifluoromethanesulfonate (2.60 mg, 10  $\mu$ mol, 10 mol%) were added under argon atmosphere. Then dried dioxane (0.3 mL) was added and the reaction was stirred at 80 °C for 18 h. The mixture was allowed to cool and then brine (5 mL) was added, followed by the extraction with EtOAc (3  $\times$  5 mL). The combined organic layers were dried over anhydrous Na<sub>2</sub>SO<sub>4</sub>. The solvent was removed under reduced pressure and the residue purified by column chromatography (hexane/EtOAc, 3:1 to 2:1) to afford hexahydrooxepine **14** (12.5 mg, 63.0  $\mu$ mol, 61%) as a white solid.

$[\alpha]_D^{20} = -26.2$  ( $c = 0.50$ , CH<sub>2</sub>Cl<sub>2</sub>).

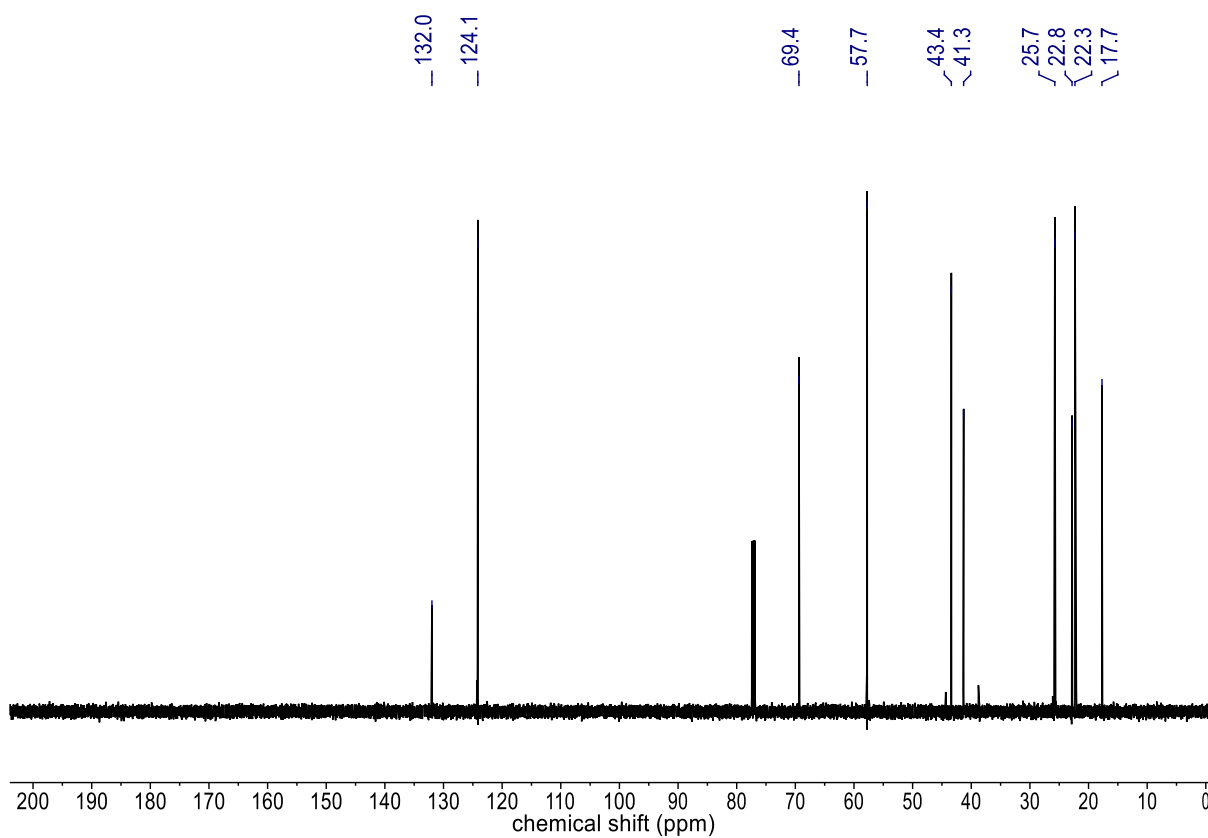
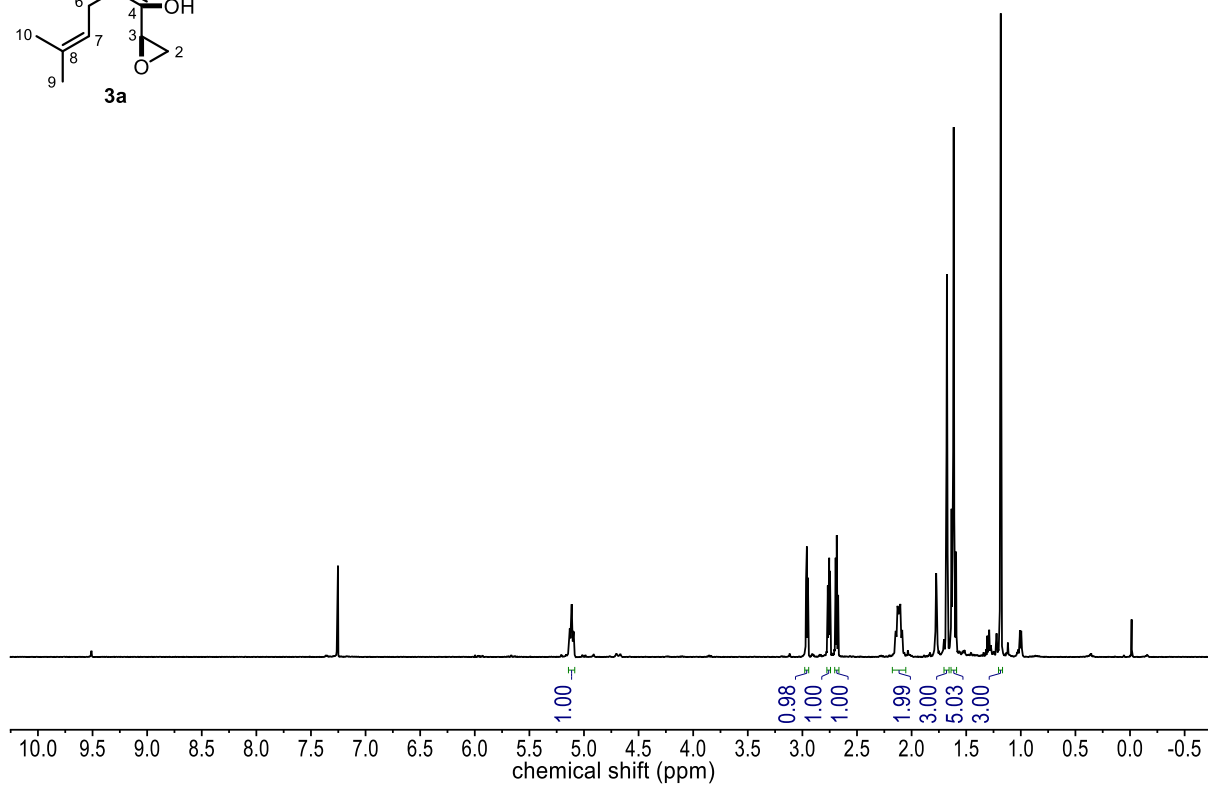
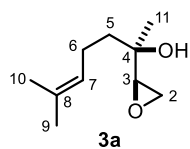
**m.p.** 79–81 °C.

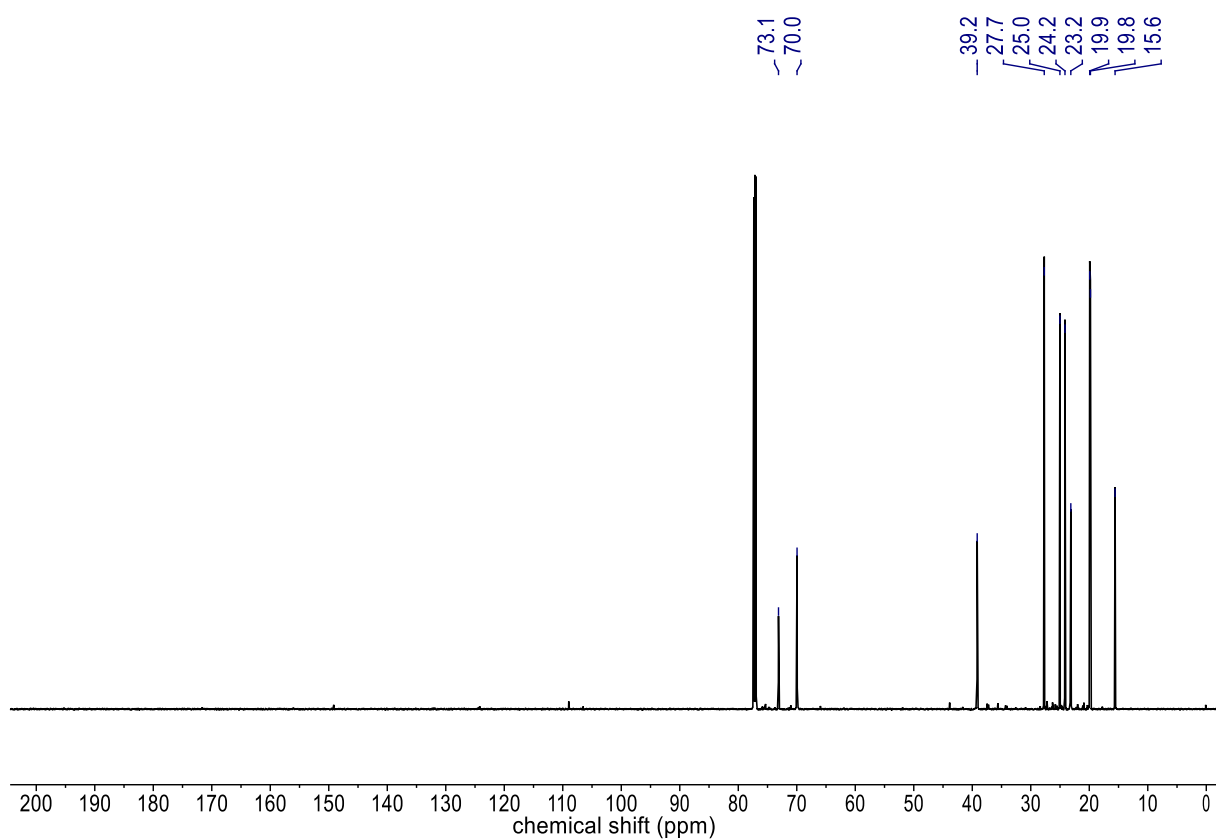
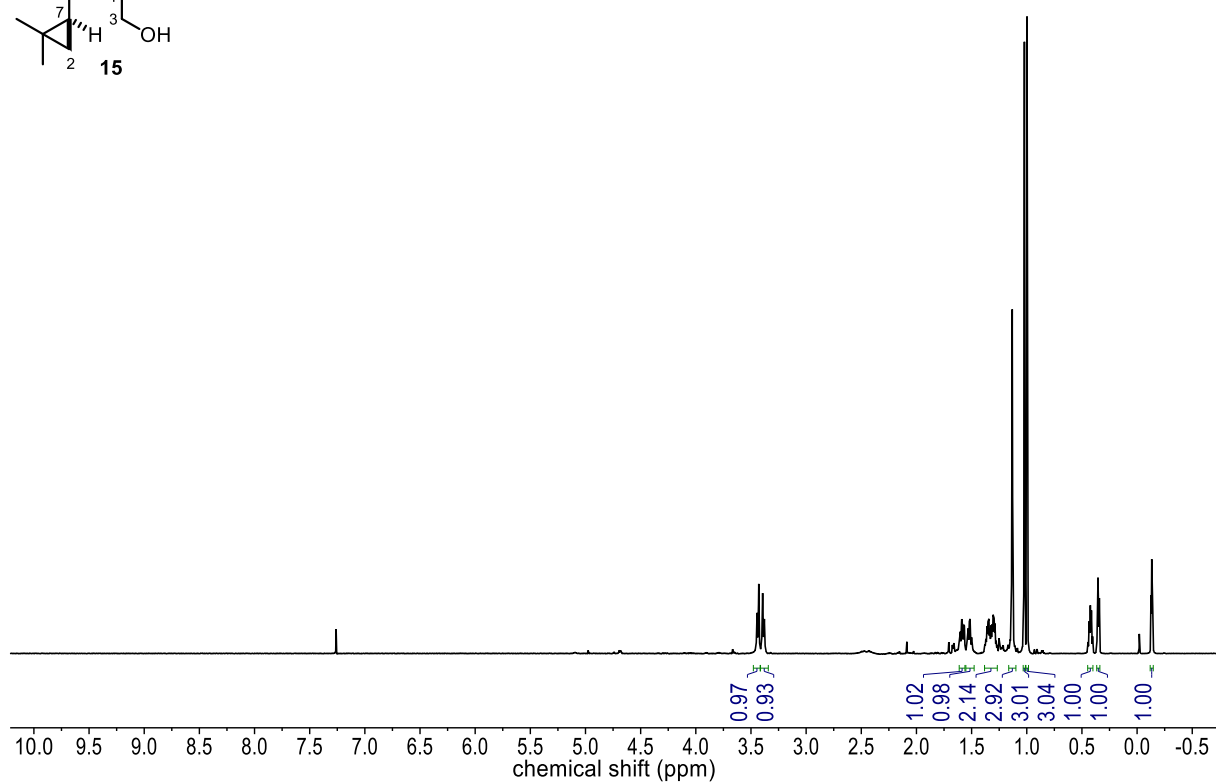
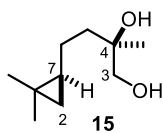
**<sup>1</sup>H NMR** (400 MHz, CDCl<sub>3</sub>):  $\delta = 1.13$  (s, 3 H, H-9/H-10), 1.22 (s, 3 H, H-9/H-10), 1.33 (d,  $J = 0.8$  Hz, 3 H, H-11), 1.42–1.51 (m, 2 H, H-6, H-7), 1.59–1.67 (m, 1 H, H-7), 1.74–1.84 (m, 2 H, H-5, H-6), 2.14–2.25 (m, 1 H, H-5), 2.45 (d,  $^2J = 18.7$  Hz, 1 H, H-2), 2.96 (dd,  $^2J = 18.7$  Hz,  $^3J = 7.7$  Hz, 1 H, H-2), 4.01 ppm (d,  $^3J = 7.7$  Hz, 1 H, H-3).

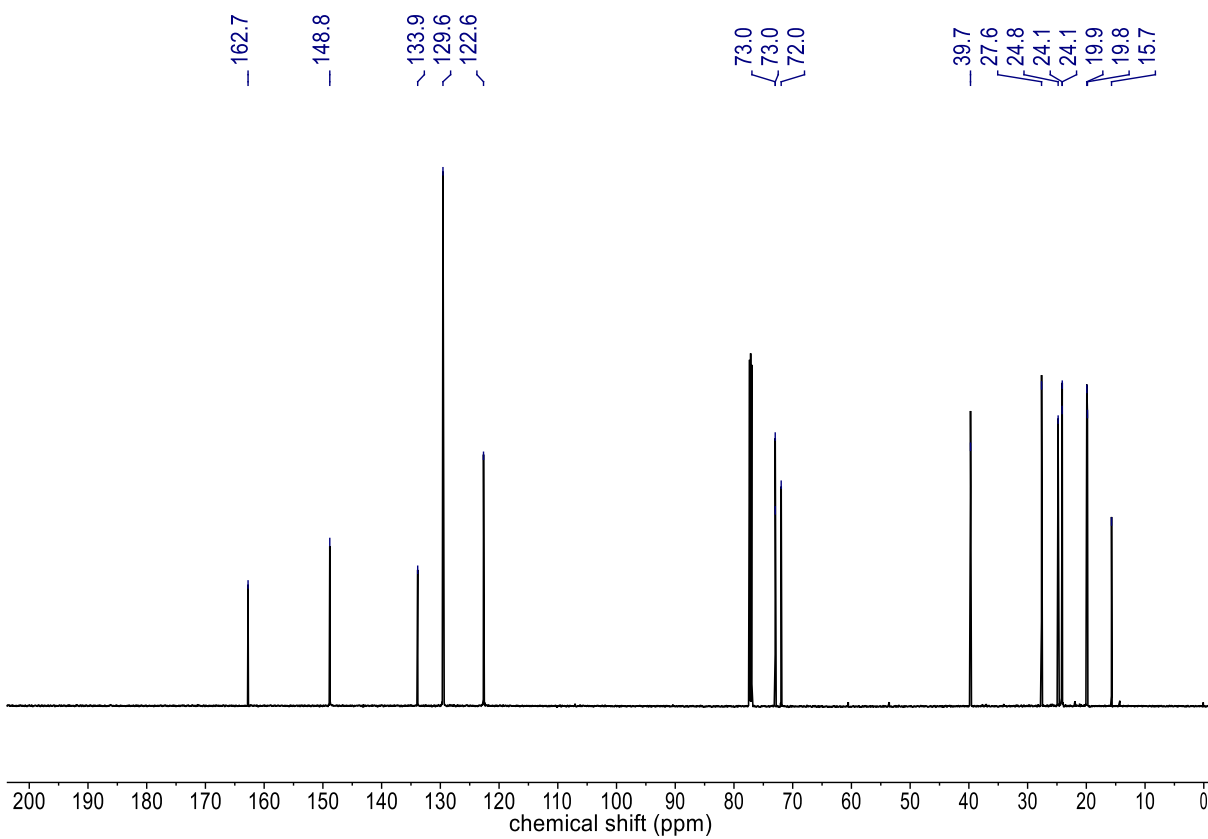
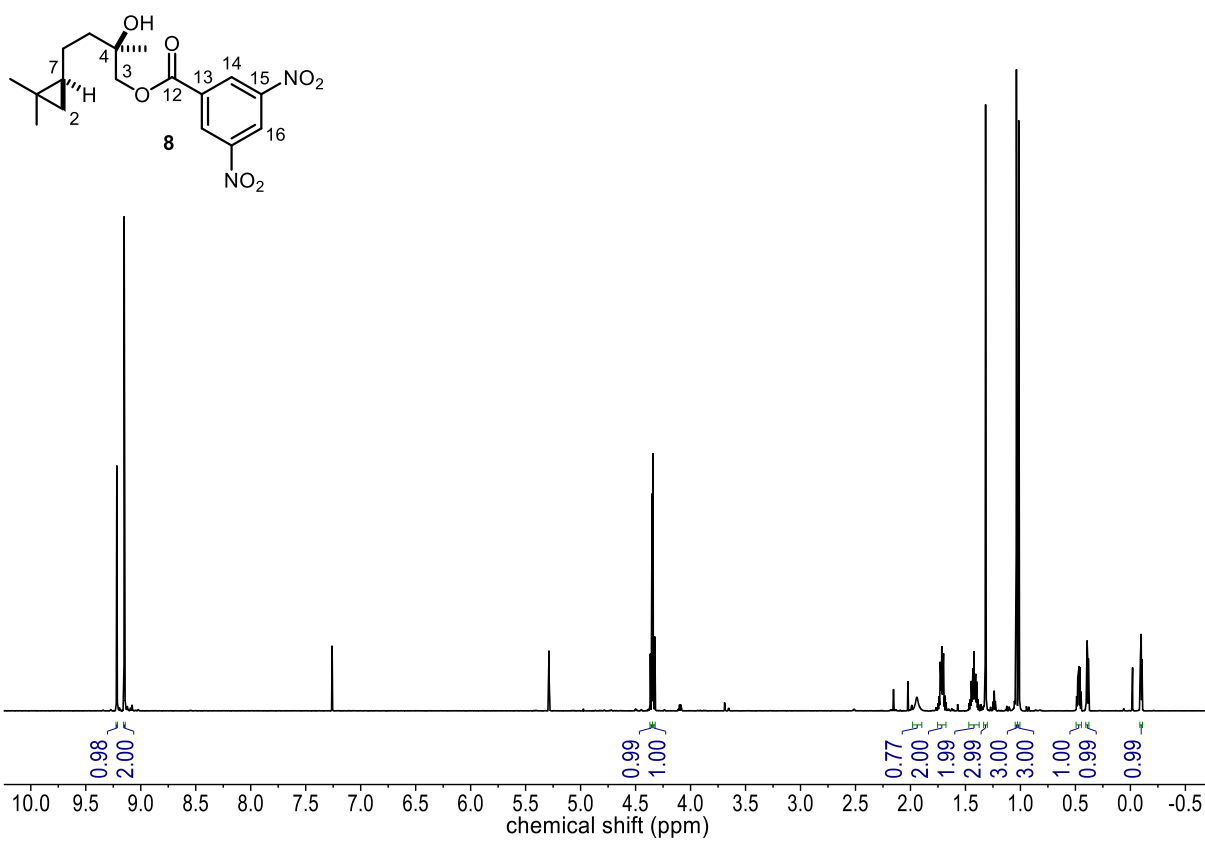
**<sup>13</sup>C NMR** (176 MHz, CDCl<sub>3</sub>):  $\delta = 18.6$  (C-6), 23.2 (C-11), 26.9 (C-9/C-10), 27.6 (C-9/C-10), 32.9 (C-5), 36.1 (C-7), 37.3 (C-2), 73.4 (C-3), 77.2 (C-8), 90.9 (C-4), 175.2 ppm (C-1).

**IR** (ATR):  $\tilde{\nu} = 2972, 2934, 2871, 1766, 1199, 1079, 946$  cm<sup>-1</sup>.

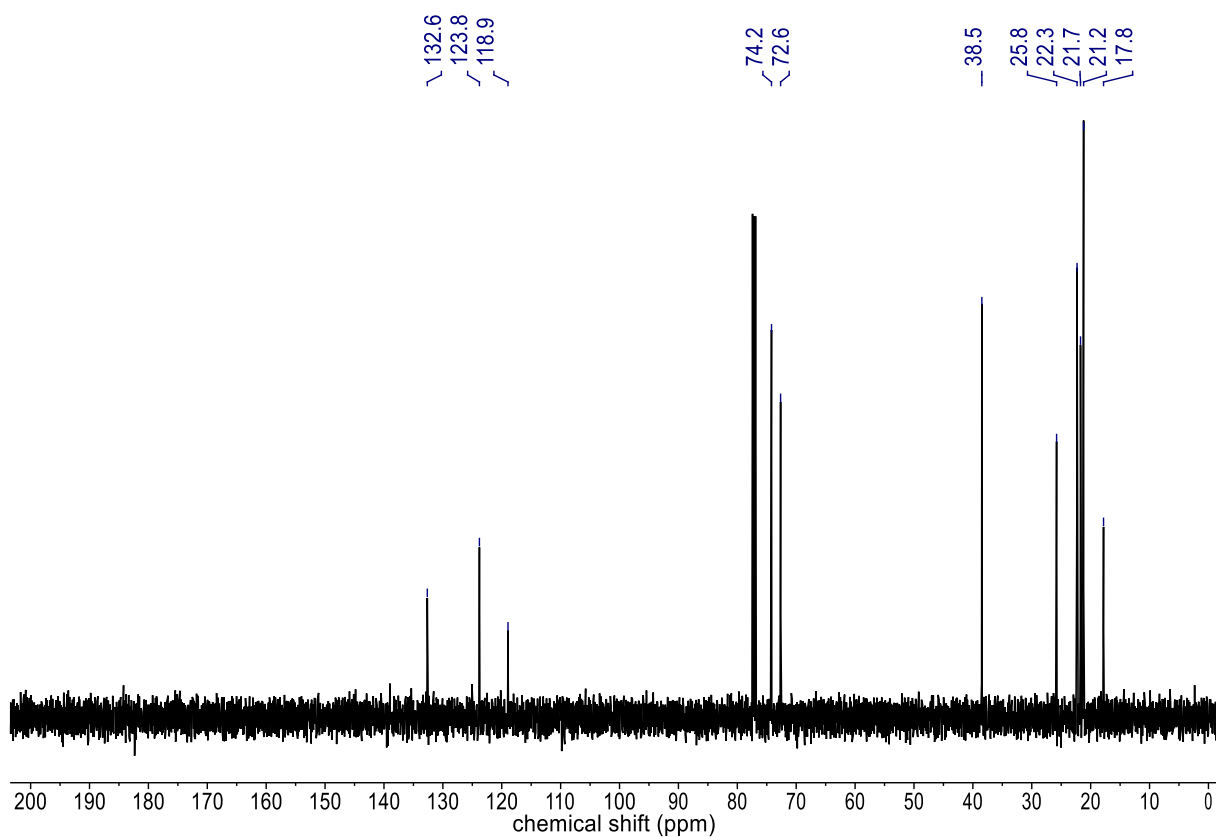
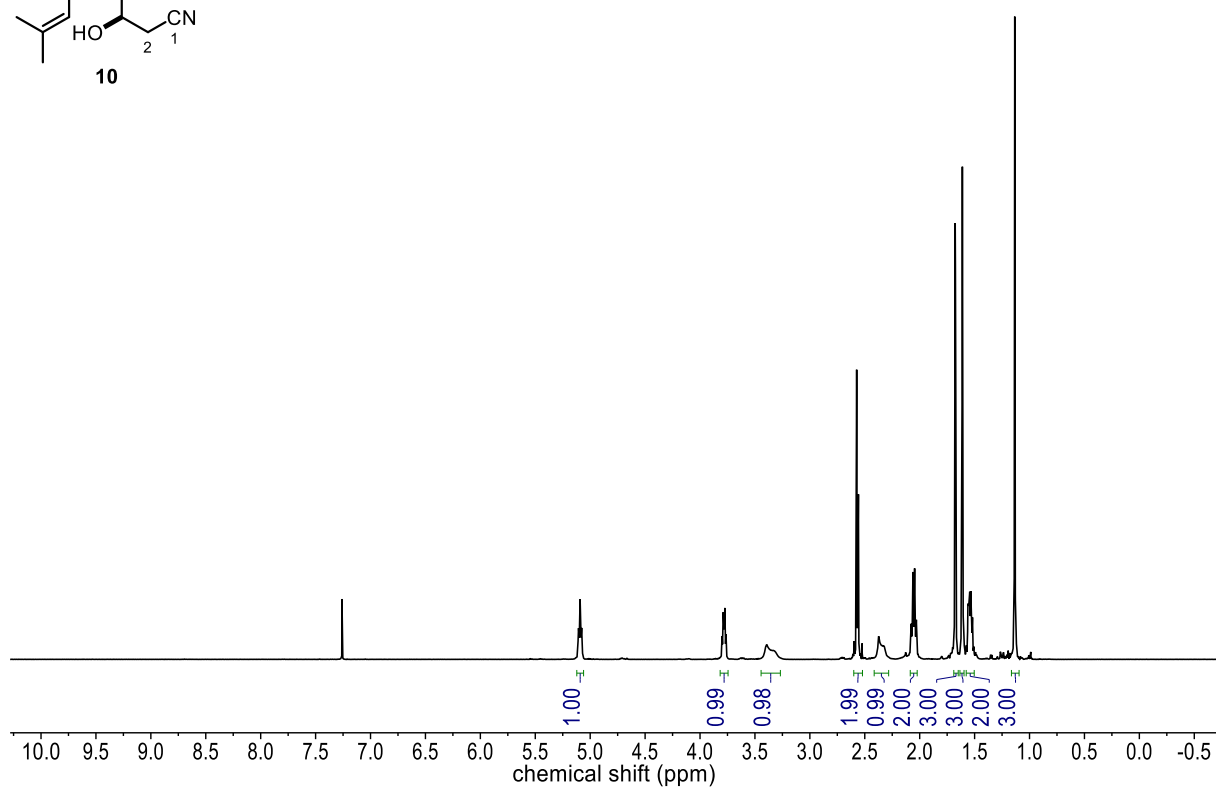
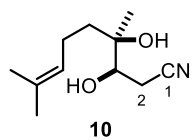
**HRMS** (ESI, pos.):  $m/z$  calcd for C<sub>11</sub>H<sub>18</sub>O<sub>3</sub>K<sup>+</sup> [M+K]<sup>+</sup>: 237.0888, found 237.0893.

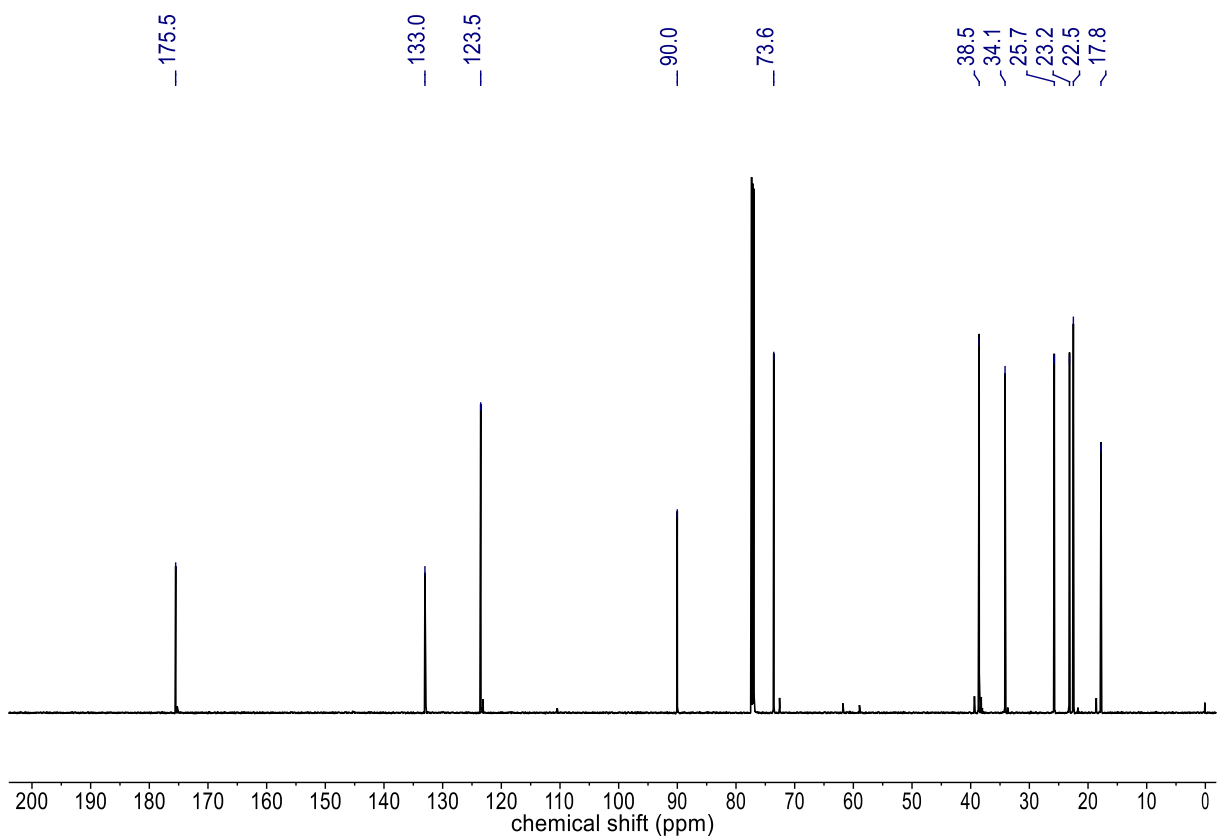
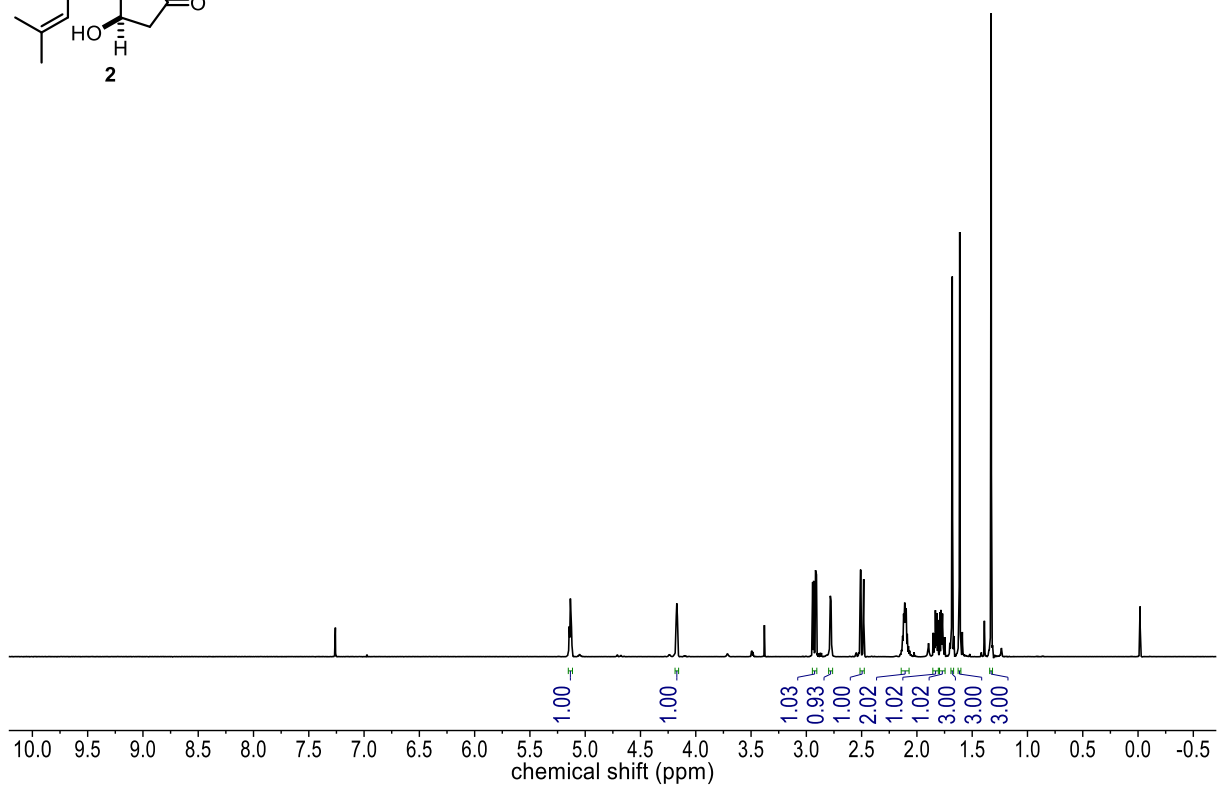
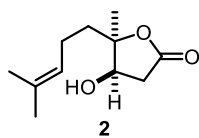
**<sup>1</sup>H- and <sup>13</sup>C- NMR Spectra**

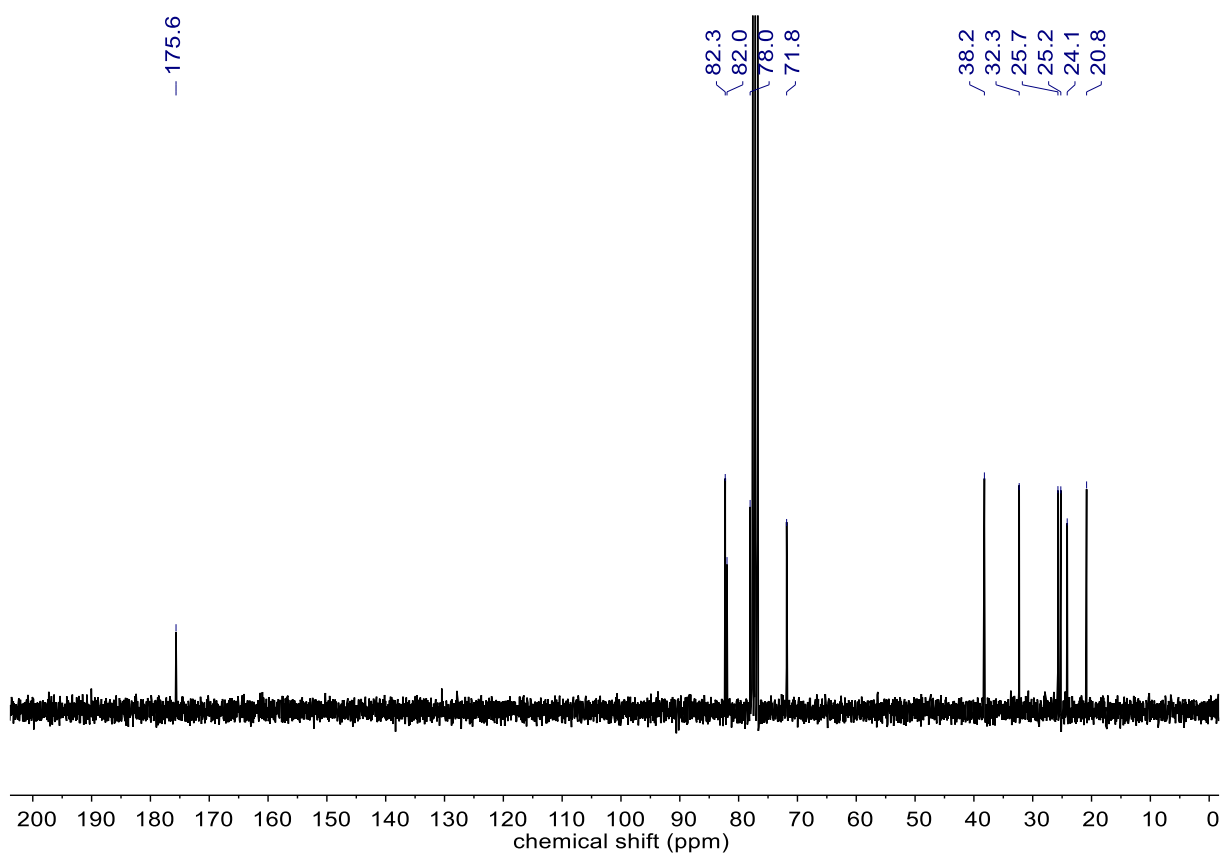
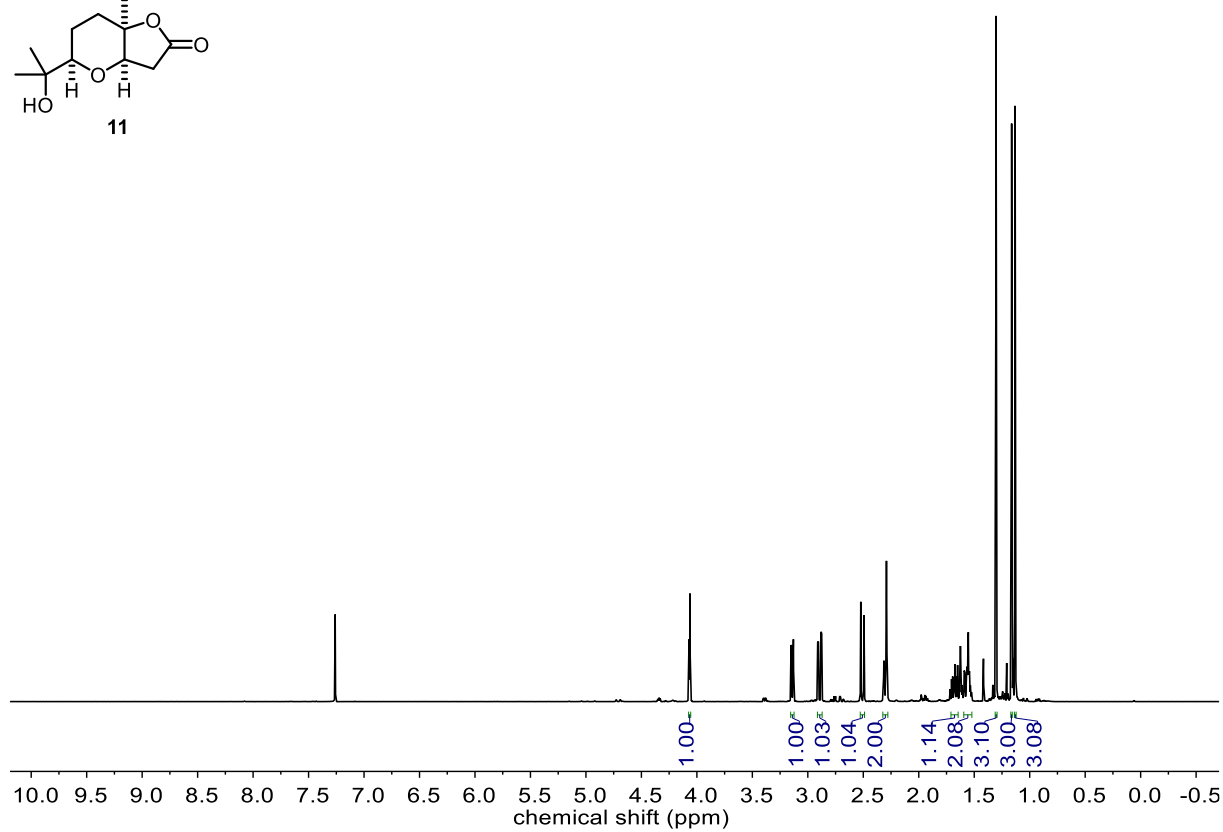
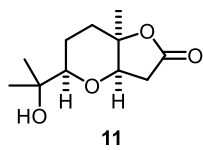


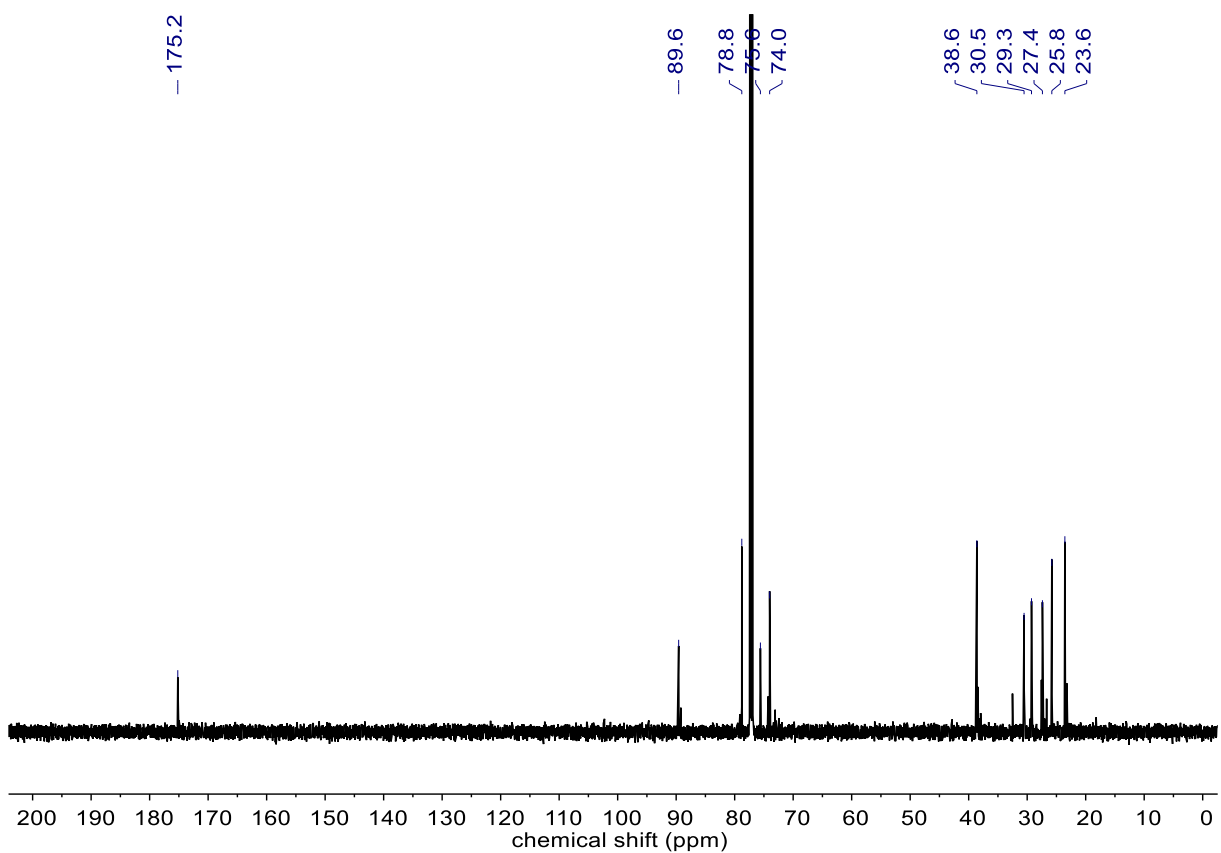
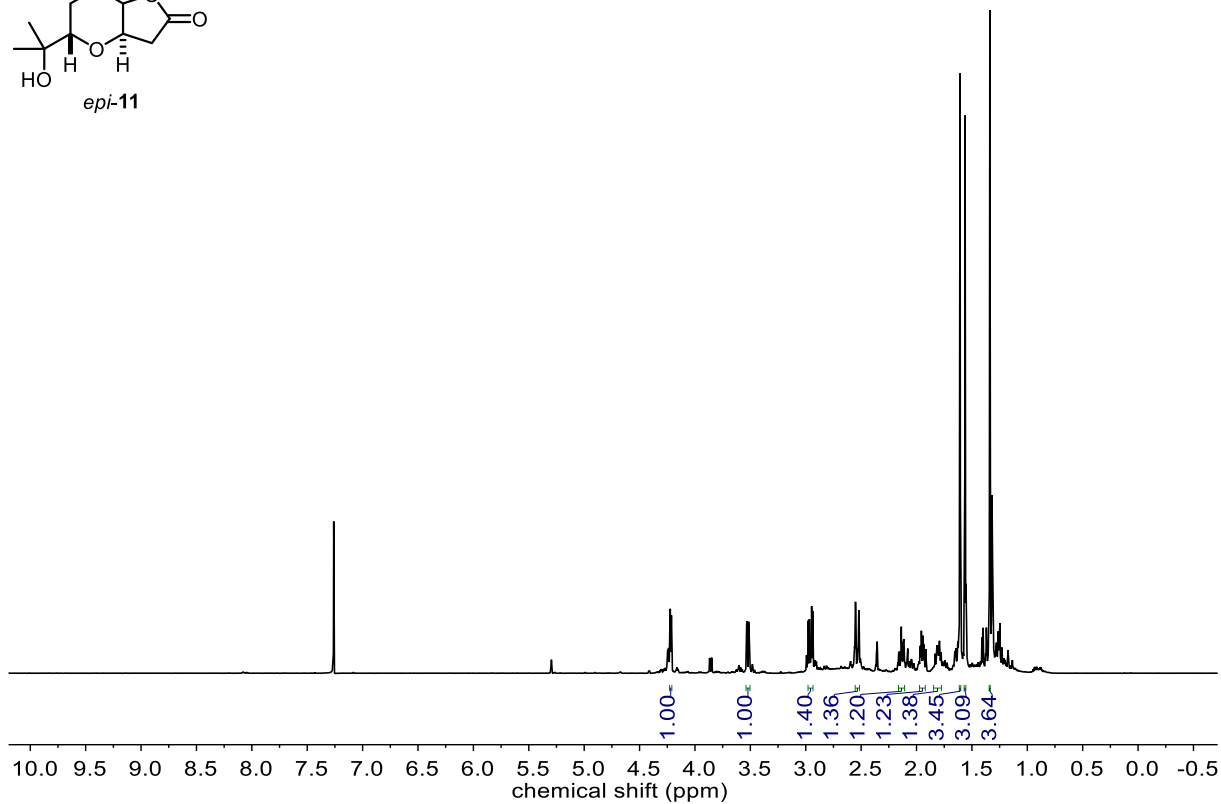
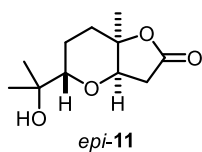


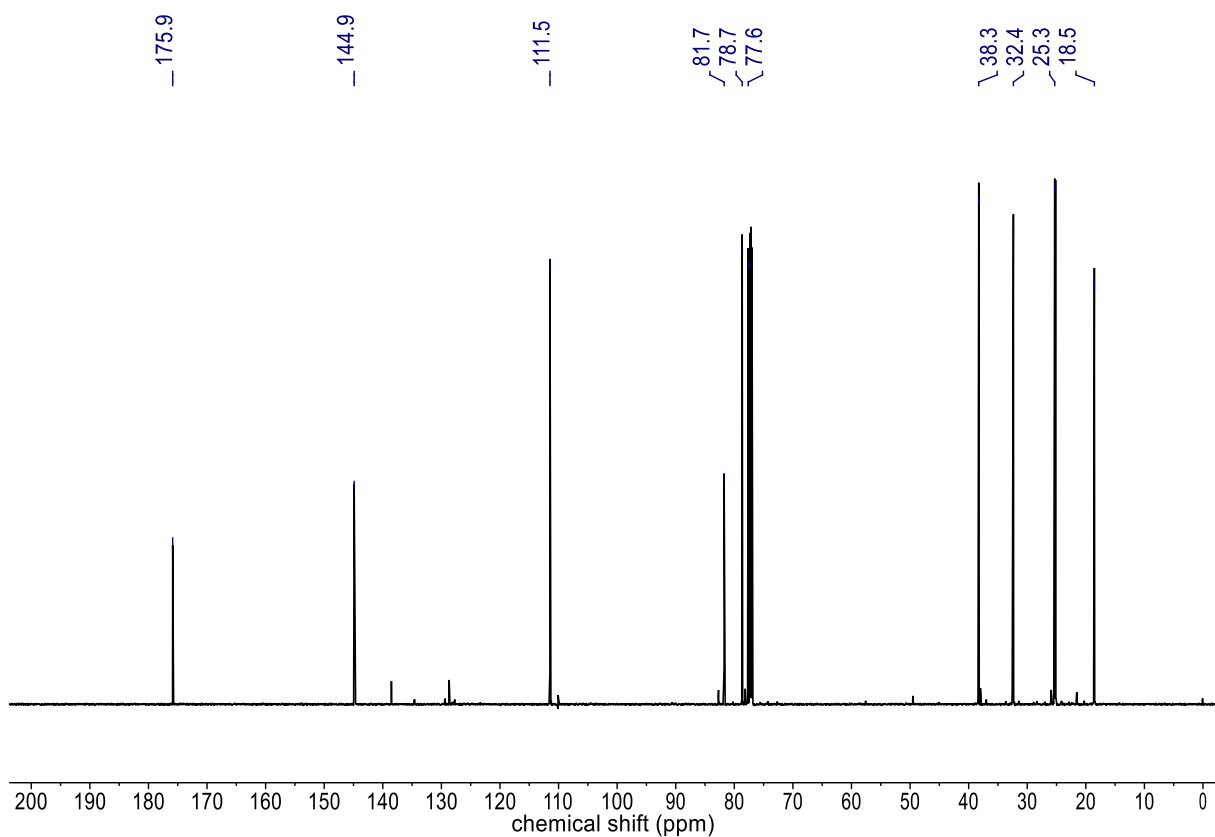
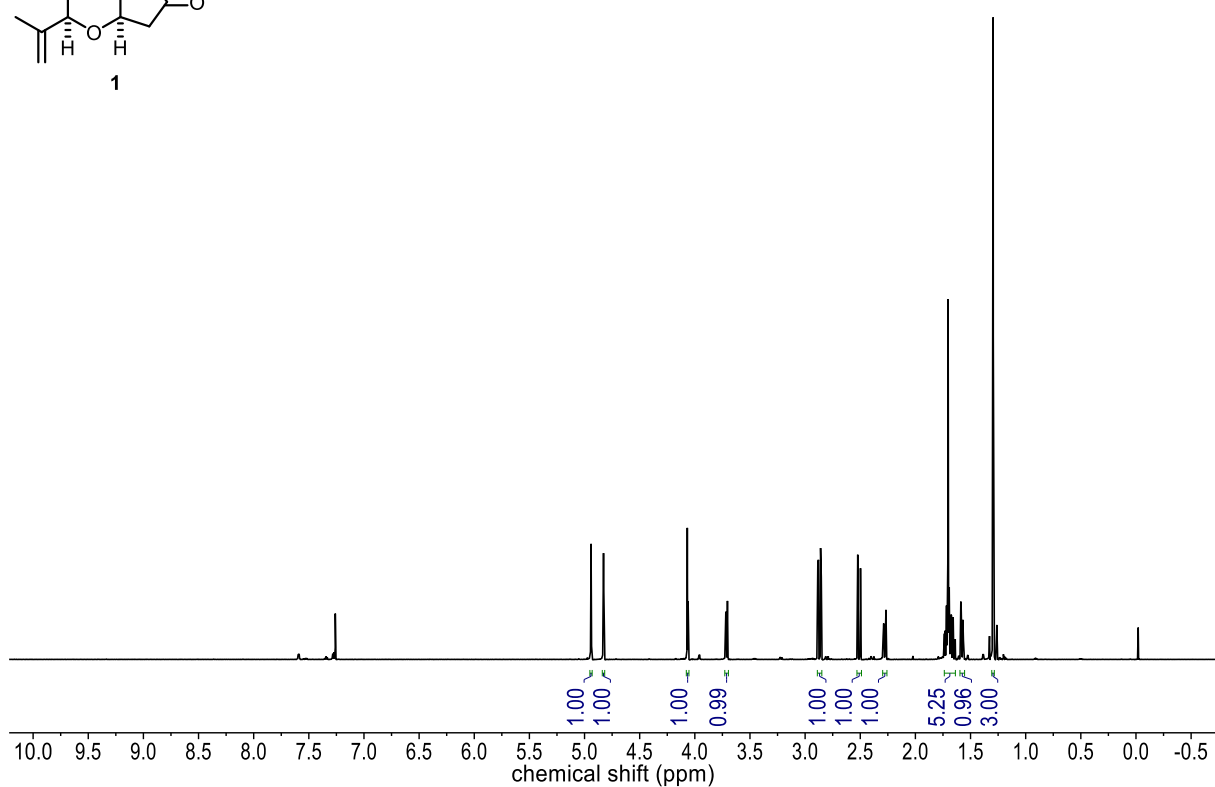
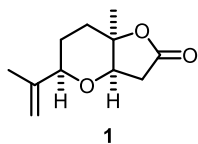


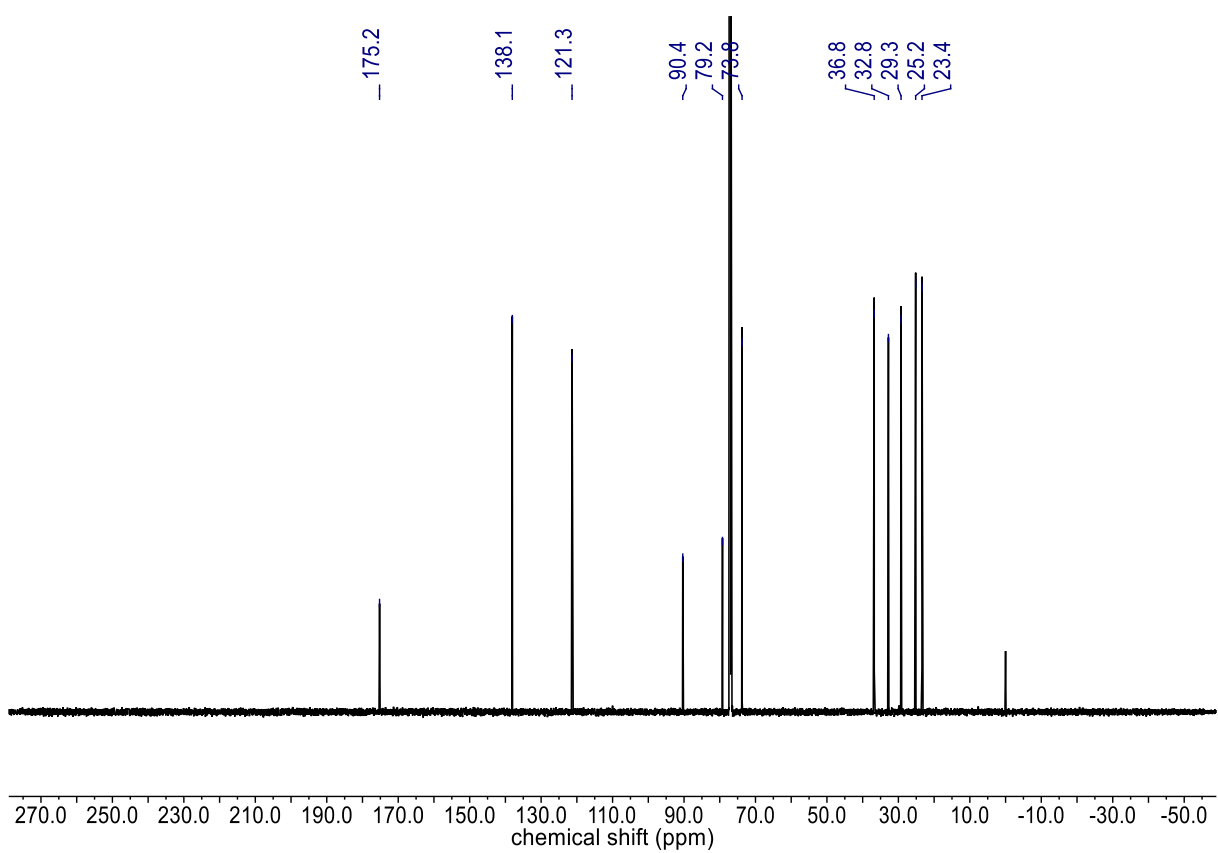
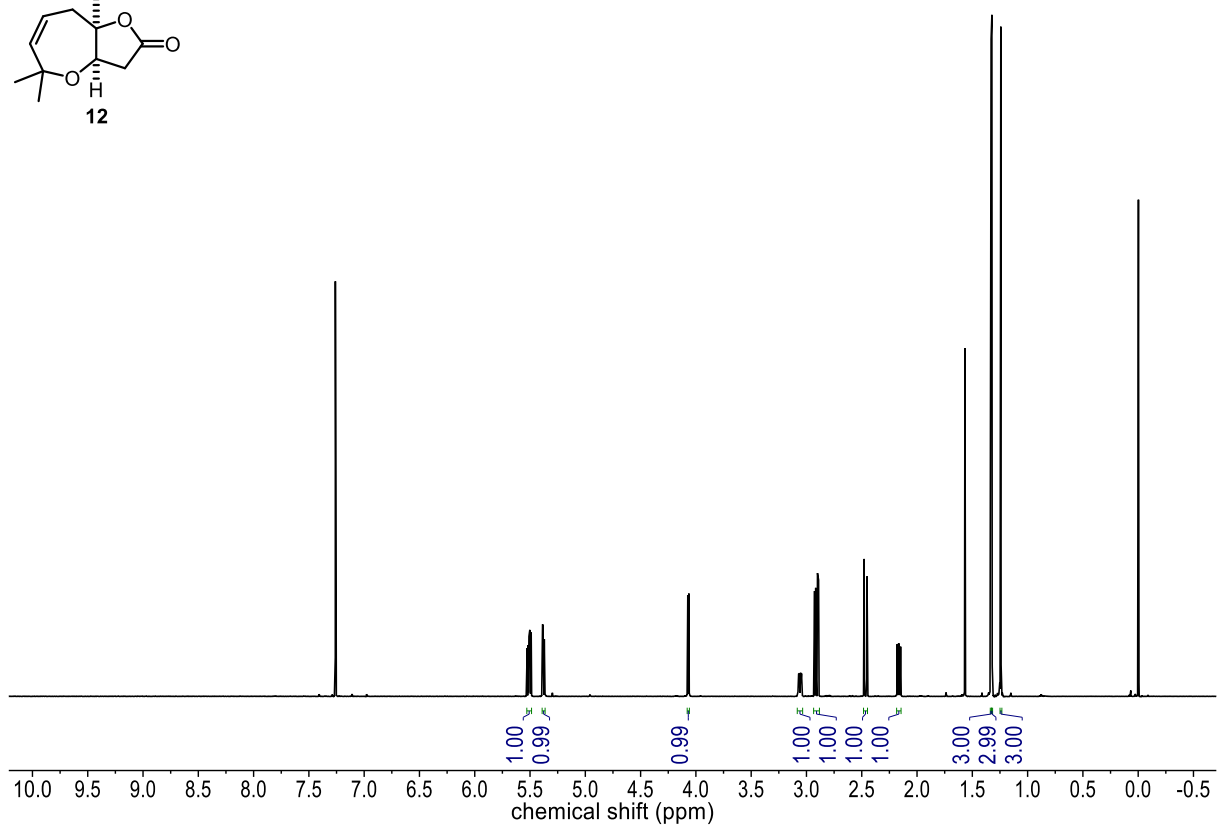
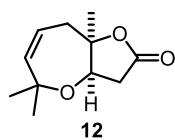


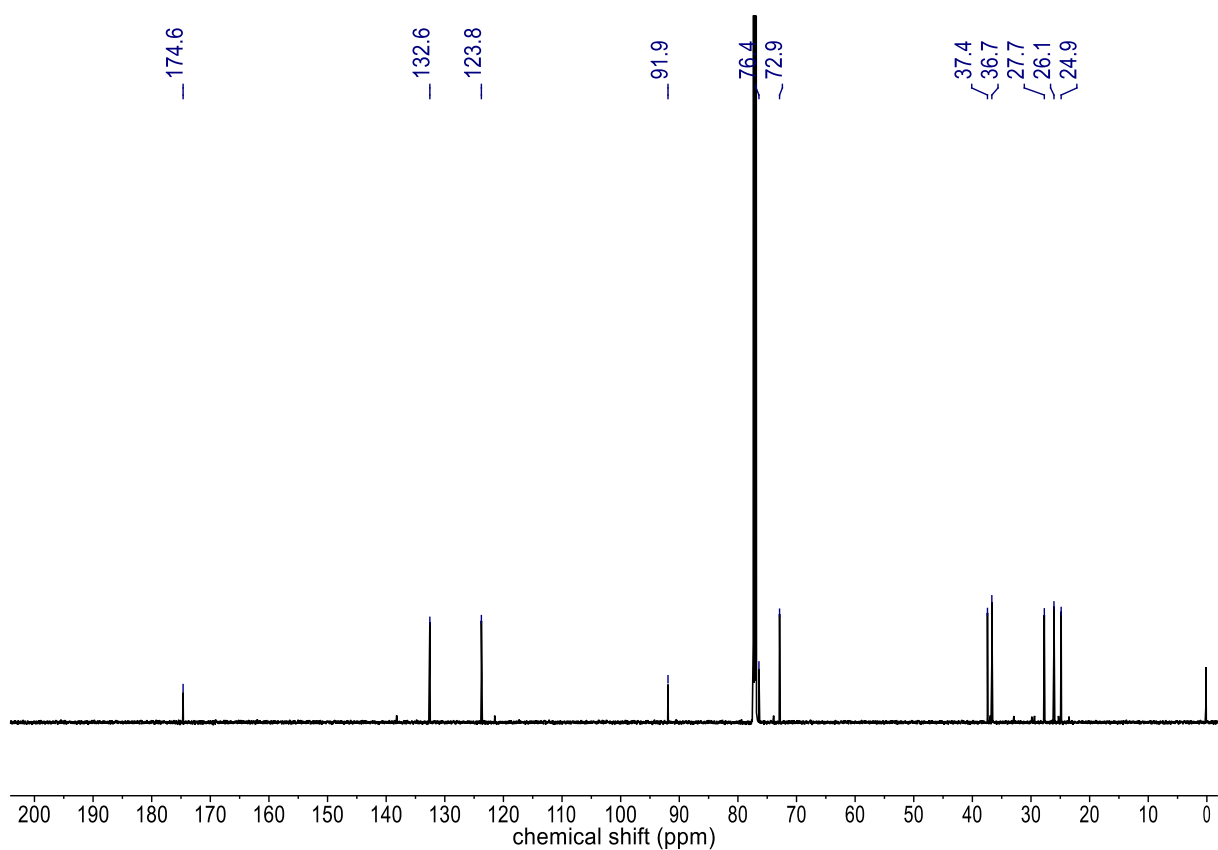
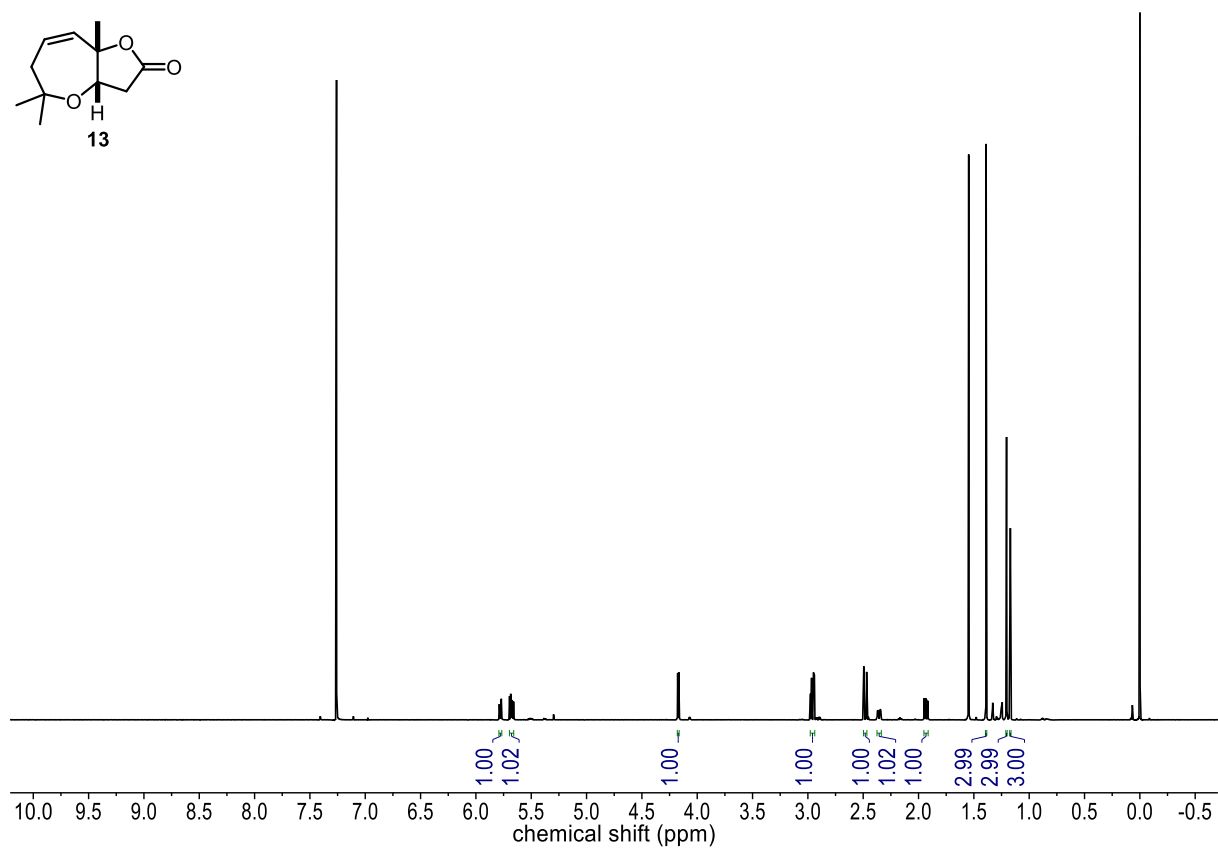
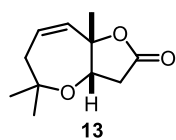




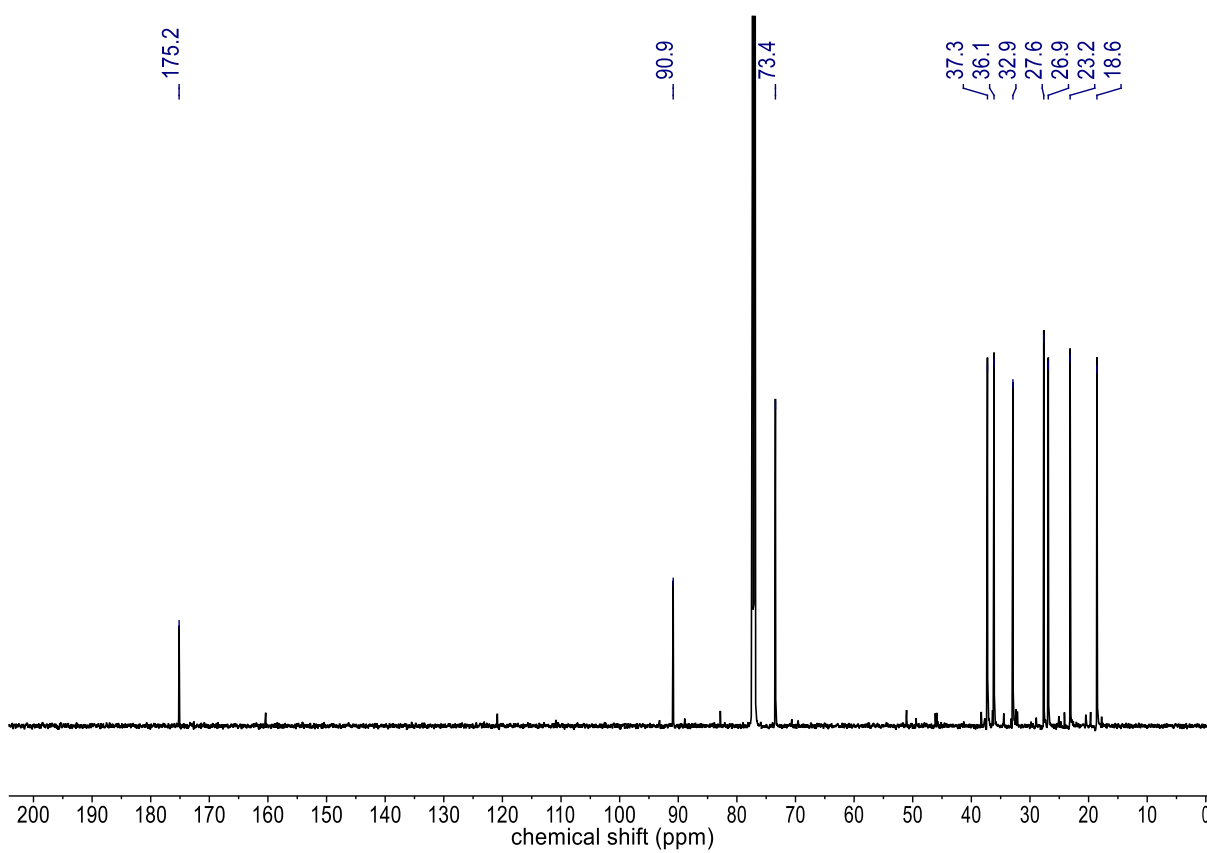
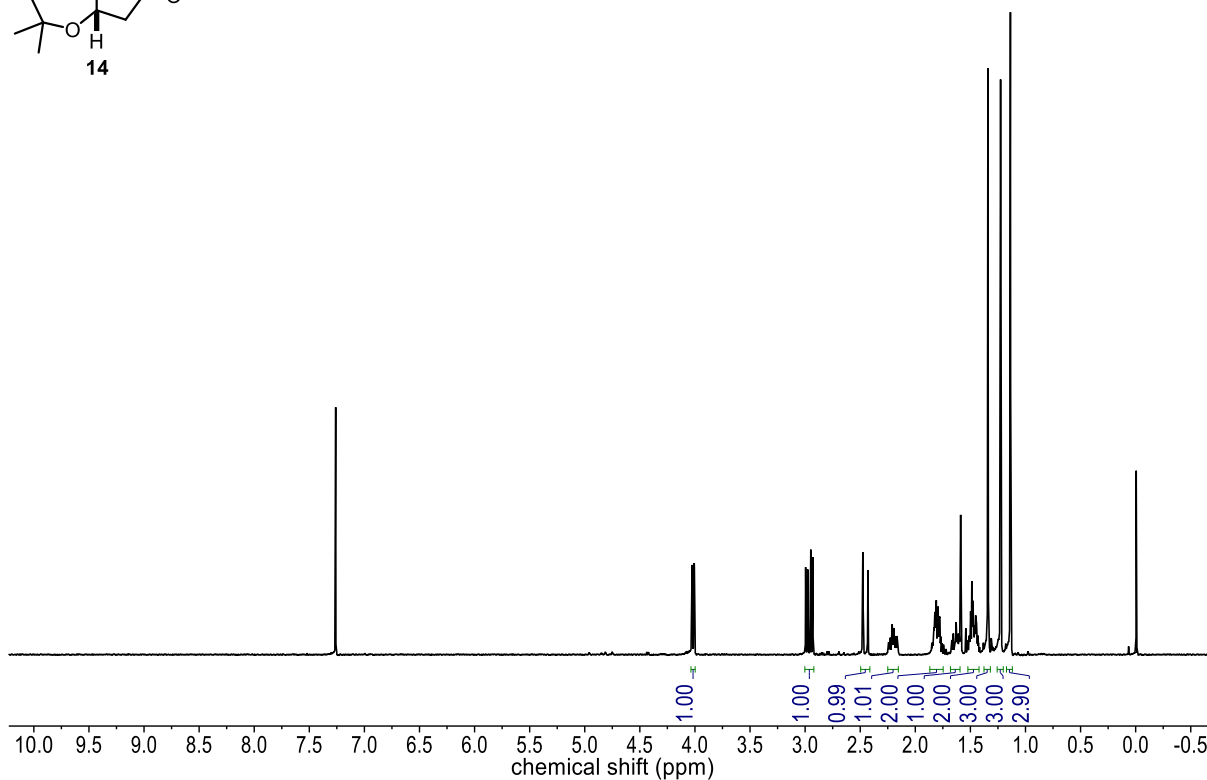
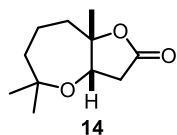




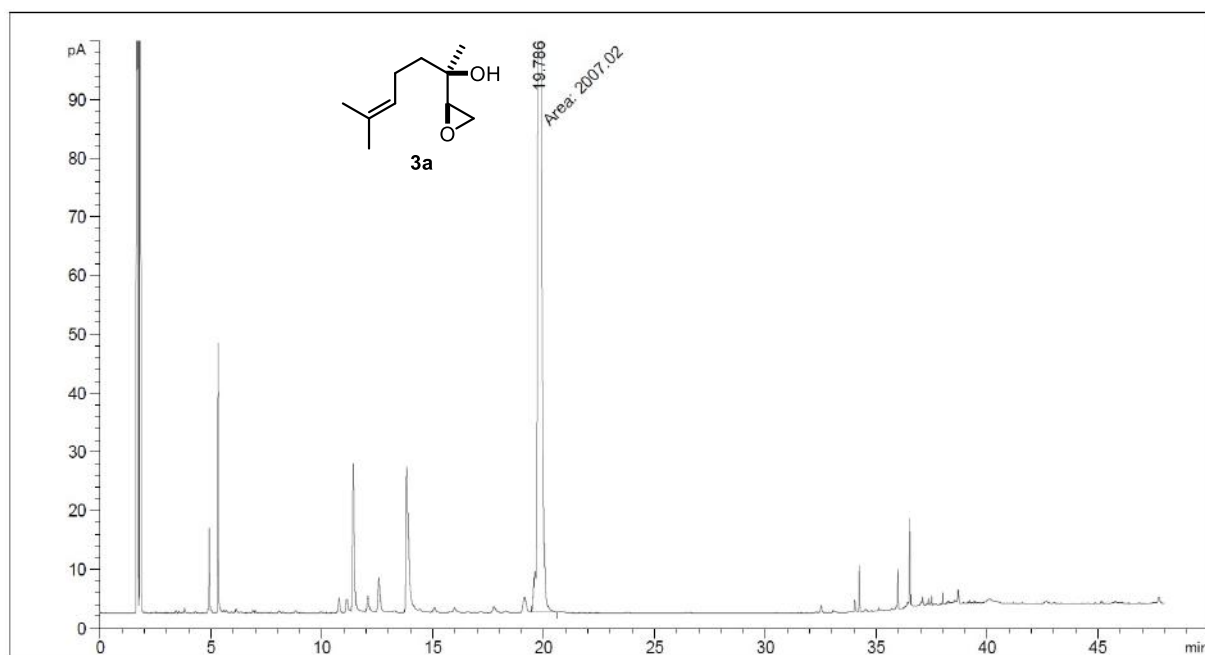








## GC Chromatogram of reaction mixture after 20 h.

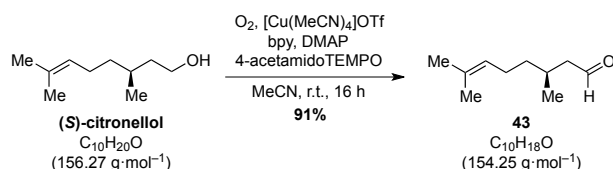


## Unpublished Results – Cyclopropanation

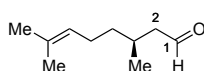
The same general working methods have been used.

### Experimental Procedures and Analytical Data

#### (*S*)-Citronellal (**43**)

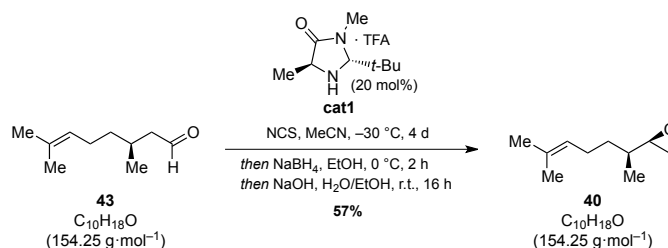


To a solution of (*S*)-citronellol (6.00 g, 38.4 mmol, 1.0 equiv) in MeCN (77 mL) were added sequentially  $[\text{Cu}(\text{MeCN})_4]\text{OTf}$  (723 mg, 1.92 mmol, 5 mol%), 2,2'-biyridine (300 mg, 1.92 mmol, 5 mol%), 4-acetamido TEMPO (409 mg, 1.92 mmol, 5 mol%), and DMAP (469 mg, 3.84 mmol, 10 mol%). The resulting brown reaction mixture was stirred under an oxygen atmosphere at ambient temperature for 16 h. The reaction was accompanied by a change of colour from brown to green. Then  $\text{H}_2\text{O}$  (65 mL) was added and the solution was extracted with a 8:1-mixture of *n*-pentane/ $\text{Et}_2\text{O}$  ( $4 \times 100$  mL). The combined organic extracts were dried over anhydrous  $\text{Na}_2\text{SO}_4$  and filtered through a plug of silica eluting with a 4:1-mixture of *n*-pentane/ $\text{Et}_2\text{O}$ . The filtrate was concentrated under reduced pressure to furnish (*S*)-citronellal (**43**) (5.38 g, 34.9 mmol, 91%) as a colourless oil.



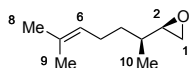
$^1\text{H NMR}$  (400 MHz,  $\text{CDCl}_3$ ):  $\delta$  = 9.75 (d,  $J$  = 2.6 Hz, 1H, H-1), 5.11 – 5.05 (m, 1H, H-6), 2.41 (ddd,  $J$  = 16.0, 5.6, 2.0 Hz, 1H, H-2), 2.23 (ddd,  $J$  = 16.0, 8.0, 2.7 Hz, 1H, H-2), 2.13 – 1.92 (m, 3H,  $\text{CH}_2$ , CH), 1.69 (s, 3H, Me), 1.60 (s, 3H, Me), 1.42 – 1.33 (m, 1H,  $\text{CH}_2$ ), 0.97 (d,  $J$  = 6.7 Hz, 3H) ppm.

#### (*R*)-2-((*S*)-6-Methylhept-5-en-2-yl)oxirane (**40**)



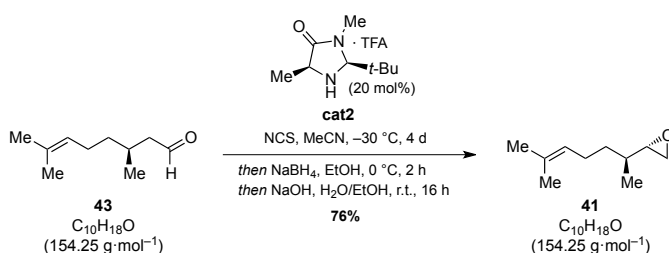
A solution of (*S*)-citronellal (**43**) (3.24 g, 21.0 mmol, 1.0 equiv) in MeCN (100 mL) was cooled to  $-30^\circ\text{C}$ , MACMILLAN catalyst **cat1** (1.19 g, 4.20 mmol, 20 mol%) and NCS (3.65 g, 27.3 mmol, 1.3 equiv) were added and the reaction mixture was for 4 d at the same temperature. Then EtOH (27 mL) and  $\text{NaBH}_4$  (1.99 mg, 52.5 mmol, 2.5 equiv) were added and stirring was continued for 2 h at  $0^\circ\text{C}$ . After 90 min, a solution of NaOH (18.7 g, 468 mmol, 22.3 equiv) in a 2:1-mixture of  $\text{H}_2\text{O}/\text{EtOH}$  (135 mL) was added, the cooling bath was removed and the reaction mixture was stirred at ambient temperature for 16 h. The solution was extracted with a 8:1-mixture of *n*-pentane/ $\text{Et}_2\text{O}$  ( $4 \times 100$  mL), dried over  $\text{Na}_2\text{SO}_4$ , and concentrated under reduced

pressure. The crude product was purified by preparative column chromatography ( $\text{SiO}_2$ , *n*-pentane/ $\text{Et}_2\text{O}$ , 40:1) to yield epoxide **40** (1.67 g, 11.9 mmol, 57%) as a colourless oil.

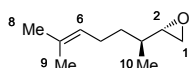


$^1\text{H NMR}$  (400 MHz,  $\text{CDCl}_3$ ):  $\delta$  = 5.07 (dddt,  $J$  = 6.9, 5.5, 2.6, 1.3 Hz, 1H, H-6), 2.76 (dd,  $J$  = 5.0, 4.0 Hz, 1H, H-1), 2.69 (ddd,  $J$  = 6.8, 4.0, 2.8 Hz, 1H, H-2), 2.53 (dd,  $J$  = 5.0, 2.8 Hz, 1H, H-1), 2.09 – 1.96 (m, 2H,  $\text{CH}_2$ ), 1.68 (q,  $J$  = 1.3 Hz, 2H, H-8), 1.60 (s, 3H, H-9), 1.47 – 1.39 (m, 1H, H-3), 1.35 – 1.27 (m, 2H,  $\text{CH}_2$ ), 1.03 (d,  $J$  = 6.3 Hz, 3H, H-10) ppm.

### (*S*)-2-((*S*)-6-Methylhept-5-en-2-yl)oxirane (**41**)

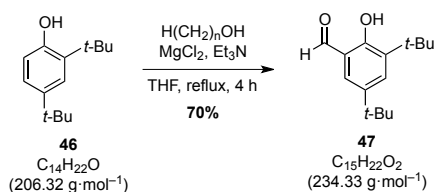


A solution of (*S*)-citronellal (**43**) (2.25 g, 14.6 mmol, 1.0 equiv) in MeCN (71 mL) was cooled to  $-30^\circ\text{C}$ , MACMILLAN catalyst **cat2** (828 mg, 2.91 mmol, 20 mol%) and NCS (2.53 g, 18.9 mmol, 1.3 equiv) were added and the reaction mixture was for 4 d at the same temperature. Then EtOH (19 mL) and  $\text{NaBH}_4$  (1.38 mg, 36.4 mmol, 2.5 equiv) were added and stirring was continued for 2 h at  $0^\circ\text{C}$ . After 90 min, a solution of NaOH (13.0 g, 324 mmol, 22.3 equiv) in a 2:1-mixture of  $\text{H}_2\text{O}/\text{EtOH}$  (95 mL) was added, the cooling bath was removed and the reaction mixture was stirred at ambient temperature for 16 h. The solution was extracted with a 8:1-mixture of *n*-pentane/ $\text{Et}_2\text{O}$  ( $4 \times 100$  mL), dried over  $\text{Na}_2\text{SO}_4$ , and concentrated under reduced pressure. The crude product was purified by column chromatography ( $\text{SiO}_2$ , *n*-pentane/ $\text{Et}_2\text{O}$ , 40:1) to yield epoxide **41** (1.55 g, 11.1 mmol, 76%) as a colourless oil.



$^1\text{H NMR}$  (400 MHz,  $\text{CDCl}_3$ ):  $\delta$  = 5.11 (ddp,  $J$  = 8.5, 5.6, 1.4 Hz, 1H, H-6), 2.76 – 2.69 (m, 2H, H-1, H-2), 2.48 (dd,  $J$  = 4.7, 3.1 Hz, 1H, H-1), 2.15 – 1.98 (m, 2H,  $\text{CH}_2$ ), 1.68 (q,  $J$  = 1.3 Hz, 3H, H-8), 1.61 (s, 3H, H-9), 1.59 – 1.54 (m, 1H, H-3), 1.38 – 1.32 (m, 2H,  $\text{CH}_2$ ), 0.93 (d,  $J$  = 6.6 Hz, 3H, H-10) ppm.

### 3,5-Di-*tert*-butyl-2-hydroxybenzaldehyde (**47**)

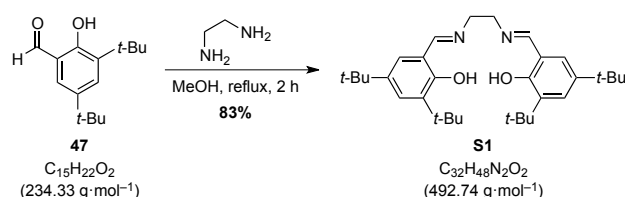


A flame-dried two-necked round bottom flask equipped with a reflux condenser was charged with phenol **46** (10.3 g, 50.0 mmol, 1.0 equiv),  $\text{MgCl}_2$  (7.14 g, 75.0 mmol, 1.5 equiv),  $\text{Et}_3\text{N}$  (14 mL), and anhydrous THF

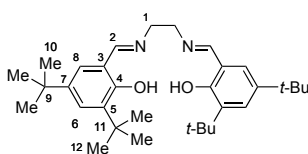
(150 mL) under an argon atmosphere. The Suspension was stirred at ambient temperature for 30 min followed by the addition of *p*-formaldehyde (3.00 g, 100 mmol, 2.0 equiv). The reaction mixture was heated to reflux for 4 h. After cooling to ambient temperature, the reaction was quenched by the addition of aqueous 1.4 M HCl (50 mL). The layers were separated and the aqueous phase was extracted with EtOAc (4 × 30 mL). The combined organic phases were dried over anhydrous Na<sub>2</sub>SO<sub>4</sub> and the solvent was removed under reduced pressure. The crude product was purified by column chromatography (SiO<sub>2</sub>, *n*-pentane/EtOAc, 20:1 to 10:1) to yield aldehyde **47** (8.20 g, 35.0 mmol, 70%) as a faint yellow solid.

<sup>1</sup>H NMR (400 MHz, CDCl<sub>3</sub>): δ = 11.64 (s, 1H, OH), 9.87 (s, 1H, CHO), 7.59 (d, *J* = 2.5 Hz, 1H, CH), 7.34 (d, *J* = 2.5 Hz, 1H, CH), 1.43 (s, 9H, *t*-Bu), 1.33 (s, 9H, *t*-Bu) ppm.

### Preparation of 48

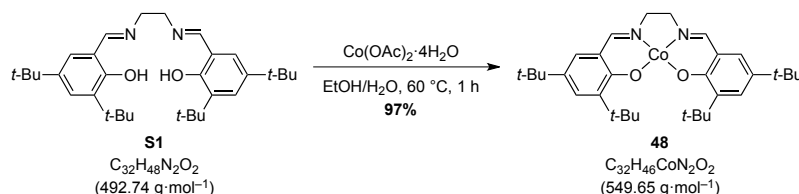


A round bottom flask charged with 1,2-ethylenediamine (1.18 g, 1.5 mL, 19.6 mmol, 1.0 equiv) and anhydrous MeOH (50 mL) and as solution of aldehyde **47** (9.20 g, 39.3 mmol, 2.0 equiv) in anhydrous MeOH (70 mL) was added dropwise. The reaction mixture was heated to reflux and stirred for 2 h. After cooling to 0 °C, the resulting yellow precipitate was separated by filtration, washed with MeOH, and dried under reduced pressure to afford salen ligand **S1** (7.98 g, 16.2 mmol, 83%) as a yellow solid.



<sup>1</sup>H NMR (700 MHz, CDCl<sub>3</sub>): δ = 1.30 (s, 18 H, H-10), 1.45 (s, 18 H, H-12), 3.93 (s, 4 H, H-1), 7.08 (d, *J* = 2.5 Hz, 2 H, H-8), 7.38 (d, *J* = 2.5 Hz, 2 H, H-6), 8.40 (s, 2 H, H-2), 13.64 (s, 2 H, OH) ppm.

<sup>13</sup>C NMR (176 MHz, CDCl<sub>3</sub>): δ = 29.6 (C-12), 31.6 (C-10), 34.3 (C-9), 35.2 (C-11), 59.7 (C-1), 118.0 (C-3), 126.2 (C-8), 127.2 (C-6), 136.8 (C-5), 140.2 (C-7), 158.2 (C-4), 167.7 (C-2) ppm.

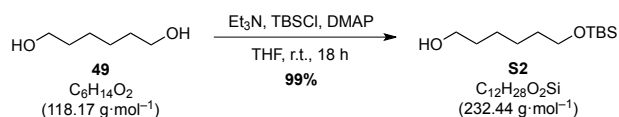


A flame-dried two-necked round bottom flask was charged with salen ligand **S1** (7.98 g, 16.2 mmol, 1.0 equiv) and anhydrous EtOH (260 mL) under an argon atmosphere and heated to 60 °C. A solution of Co(OAc)<sub>2</sub>·4H<sub>2</sub>O (4.50 g, 18.2 mmol, 1.1 equiv) in H<sub>2</sub>O (33 mL) was added dropwise and stirring was continued for 1 h. After cooling to ambient temperature, the resulting orange precipitate was separated by filtration, washed with EtOH (100 mL) and dried under reduced pressure. The crude product was

recrystallised from EtOH under an argon atmosphere to yield cobalt(II) complex **48** (8.62 g, 15.7 mmol, 97%) as an orange solid.

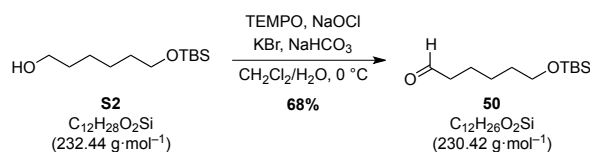
HRMS (ESI, pos. mode):  $m/z$  calcd for  $C_{32}H_{47}CoN_2O_2^+$   $[M+H]^+$ : 550.2964, found 550.2955.

### Preparation of 6-((*tert*-butyldimethylsilyl)oxy)hexanal (**50**)



To a solution of 1,6-hexandiol (**49**) (20.0 g, 169 mmol, 2.0 equiv), in anhydrous THF (560 mL) were added DMAP (1.03 g, 8.46 mmol, 10 mol%), TBSCl (12.8 g, 84.6 mmol, 1.0 equiv), and  $Et_3N$  (11.7 mL, 8.56 g, 84.6 mmol, 1.0 equiv). The reaction mixture was stirred at ambient temperature for 18 h. Then  $H_2O$  (400 mL) was added, the layers were separated and the aqueous phase was extracted with EtOAc (3 × 300 mL). The combined organic extracts were dried over anhydrous  $MgSO_4$  and the solvent was removed under reduced pressure. The crude product was purified by column chromatography ( $SiO_2$ , *n*-pentane/EtOAc, 8:1 to 3:1) to yield alcohol **S2** (19.5 g, 83.9 mmol, 99%) as a colourless oil.

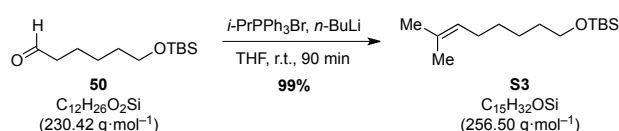
<sup>1</sup>H NMR (400 MHz,  $CDCl_3$ ):  $\delta$  = 3.64 (t,  $J$  = 6.5 Hz, 2H,  $CH_2O$ ), 3.60 (t,  $J$  = 6.5 Hz, 2H,  $CH_2O$ ), 1.63 – 1.48 (m, 4H,  $CH_2$ ), 1.41 – 1.32 (m, 5H,  $CH_2$ , OH), 0.89 (s, 9H, *t*-Bu), 0.04 (s, 6H, Me) ppm.



To a solution of alcohol **S2** (7.00 g, 30.1 mmol 1.0 equiv) in dichloromethane (75 mL) were added TEMPO (235 mg, 1.51 mmol, 5 mol%), KBr (3.94 g, 33.1 mmol, 1.1 equiv), and 5 wt% aqueous  $NaHCO_3$  (120 mL). The suspension was cooled to 0 °C and an aqueous NaOCl (23 mL, 27.6 g, 48.2 mmol, 1.6 equiv) was added dropwise over a period of 40 min. The reaction was quenched by the addition of saturated aqueous  $Na_2S_2O_3$  (40 mL) and the aqueous layer was extracted with dichloromethane (2 × 100 mL). The combined organic phases were dried over anhydrous  $MgSO_4$  and the solvent was removed under reduced pressure. Purification of the crude product by column chromatography ( $SiO_2$ , *n*-pentane/EtOAc, 14:1 to 1:1) afforded aldehyde **50** (4.73 g, 20.5 mmol, 68%) as a colourless oil.

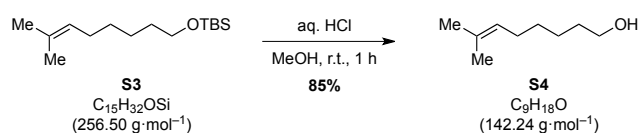
<sup>1</sup>H NMR (400 MHz,  $CDCl_3$ ):  $\delta$  = 9.77 (t,  $J$  = 1.8 Hz, 1H, H-1), 3.60 (t,  $J$  = 6.4 Hz, 2H, H-6), 2.43 (td,  $J$  = 7.4, 1.8 Hz, 2H, H-2), 1.65 (dt,  $J$  = 15.1, 7.4 Hz, 2H, H-3), 1.59 – 1.49 (m, 2H,  $CH_2$ ), 1.43 – 1.34 (m, 2H,  $CH_2$ ), 0.89 (s, 9H, *t*-Bu), 0.04 (s, 6H, Me) ppm.

### Preparation of 7-methyloct-6-enal (**51**)



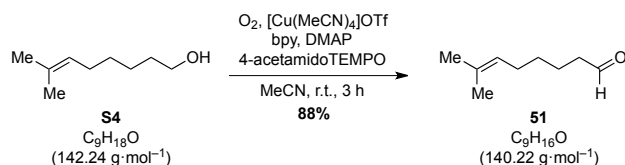
A flame-dried round bottom flask was charged with isopropyltriphenylphosphonium bromide (8.30 g, 21.6 mmol, 1.05 equiv) and anhydrous THF (70 mL). The suspension was cooled to 0 °C and *n*-BuLi (2.5 M in hexanes, 8.54 mL, 21.3 mmol, 1.04 equiv) was slowly added. The resulting dark orange solution was stirred for 30 min at this temperature. Then a solution of aldehyde **50** (4.73 g, 20.5 mmol, 1.0 equiv) in anhydrous THF (40 mL) was added and the reaction mixture was warmed to ambient temperature and stirred for additional 90 min. The reaction was quenched by the addition of H<sub>2</sub>O (100 mL) and the aqueous layer was extracted with *n*-pentane (3 × 100 mL). The combined organic extracts were dried over anhydrous Na<sub>2</sub>SO<sub>4</sub> and filtered through a plug silica eluting with *n*-pentane. The solvent was removed under reduced pressure to yield alkene **S3** (5.22 g, 20.4 mmol, 99%) as a colourless oil.

<sup>1</sup>H NMR (400 MHz, CDCl<sub>3</sub>): δ = 5.11 (ddq, *J* = 8.5, 5.7, 1.4 Hz, 1H, H-6), 3.60 (t, *J* = 6.6 Hz, 2H, H-1), 2.01 – 1.93 (m, 2H, CH<sub>2</sub>), 1.68 (s, 3H, Me), 1.60 (s, 3H, Me), 1.55 – 1.47 (m, 2H, CH<sub>2</sub>), 1.36 – 1.29 (m, 4H, CH<sub>2</sub>), 0.89 (s, 9H, *t*-Bu), 0.05 (s, 6H, Me) ppm.



To a solution of alkene **S3** (1.77 g, 6.90 mmol, 1.0 equiv) in MeOH (6.9 mL) was added 10 wt% HCl (120 μL, 126 mg, 345 μmol, 5 mol%) and the reaction mixture was stirred at ambient temperature for 1 h. The solvent was removed under reduced pressure (300 mbar, 40 °C) and the residue was dissolved in dichloromethane (10 mL). Brine (10 mL) was added and the mixture was extracted with dichloromethane (3 × 10 mL). The combined organic phases were dried over anhydrous MgSO<sub>4</sub> and concentrated under reduced pressure. Purification of the crude product by column chromatography (SiO<sub>2</sub>, *n*-pentane/Et<sub>2</sub>O, 4:1 to 2:1) afforded alcohol **S4** (837 mg, 5.88 mmol, 85%) as a colourless oil.

<sup>1</sup>H NMR (400 MHz, CDCl<sub>3</sub>): δ = 5.10 (t, *J* = 7.1 Hz, 1H, H-6), 3.62 (t, *J* = 6.6 Hz, 2H, H-1), 2.04 – 1.91 (m, 2H, CH<sub>2</sub>), 1.68 (s, 3H, Me), 1.59 (s, 3H, Me), 1.58 – 1.51 (m, 2H, CH<sub>2</sub>), 1.38 – 1.30 (m, 4H, CH<sub>2</sub>) ppm.

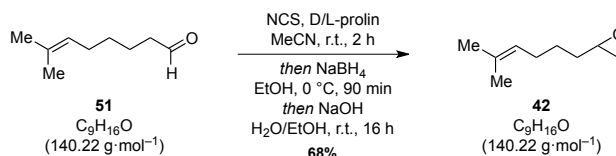


To a solution of alcohol **S4** (2.18 g, 15.3 mmol, 1.0 equiv) in MeCN (30 mL) were added sequentially [Cu(MeCN)<sub>4</sub>]OTf (289 mg, 766 μmol, 5 mol%), 2,2'-bipyridine (120 mg, 766 μmol, 5 mol%), 4-acetamido TEMPO (163 mg, 766 μmol, 5 mol%), and DMAP (187 mg, 1.53 mmol, 10 mol%). The resulting brown reaction mixture was stirred under an oxygen atmosphere at ambient temperature for 3 h. A colour change from brown to green was observed. Then H<sub>2</sub>O (30 mL) was added and the solution was extracted *n*-pentane (3 × 50 mL). The combined organic extracts were washed with brine (50 mL), dried over anhydrous Na<sub>2</sub>SO<sub>4</sub> and filtered through a plug of silica eluting with a 4:1-mixture of *n*-pentane/Et<sub>2</sub>O. The filtrate was concentrated under reduced pressure to yield aldehyde **51** (1.90 g, 13.5 mmol, 88%) as a colourless oil.

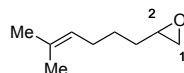


$^1\text{H NMR}$  (400 MHz,  $\text{CDCl}_3$ ):  $\delta = 9.76$  (t,  $J = 1.9$  Hz, 1H, H-1), 5.13 – 5.06 (m, 1H, H-6), 2.42 (td,  $J = 7.4$ , 1.9 Hz, 2H, H-2), 2.00 (q,  $J = 7.4$  Hz, 2H, H-3), 1.69 (s, 3H, Me), 1.67 – 1.61 (m, 2H,  $\text{CH}_2$ ), 1.60 (s, 3H, Me), 1.41 – 1.32 (m, 2H,  $\text{CH}_2$ ) ppm.

### 2-(5-methylhex-4-en-1-yl)oxirane (**42**)

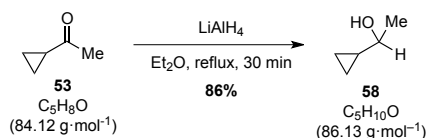


To a solution of aldehyde **51** (587 mg, 4.19 mmol, 1.0 equiv) in MeCN (20 mL) were added racemic prolin (241 mg, 2.09 mmol, 0.5 equiv) and NCS (727 mg, 5.44 mmol, 1.3 equiv) and the reaction mixture was stirred at ambient temperature for 2 h. Then EtOH (5.5 mL) and  $\text{NaBH}_4$  (396 mg, 10.5 mmol, 2.5 equiv) were added at  $0^\circ\text{C}$  and stirring was continued. After 90 min, a solution of NaOH (3.73 g, 93.3 mmol, 22.3 equiv) in a 2:1-mixture of  $\text{H}_2\text{O}/\text{EtOH}$  (28 mL) was added, the cooling bath was removed and the reaction mixture was stirred at ambient temperature for 16 h. The solution was extracted with 8:1-mixture of *n*-pentane/ $\text{Et}_2\text{O}$  ( $3 \times 20$  mL), dried over  $\text{Na}_2\text{SO}_4$ , and concentrated under reduced pressure to yield epoxide **42** (400 mg, 2.85 mmol, 68%) as a colourless oil. The crude was pure enough and used for further experiments without purification.



$^1\text{H NMR}$  (400 MHz,  $\text{CDCl}_3$ ):  $\delta = 5.15 - 5.07$  (m, 1H, H-6), 2.93 – 2.88 (m, 1H, H-2), 2.75 (dd,  $J = 5.0$ , 4.0 Hz, 1H, H-1), 2.46 (dd,  $J = 5.0$ , 2.7 Hz, 1H, H-1), 2.08 – 1.99 (m, 2H,  $\text{CH}_2$ ), 1.68 (s, 3H, H-8), 1.60 (s, 3H, H-9), 1.57 – 1.43 (m, 4H,  $\text{CH}_2$ ) ppm.

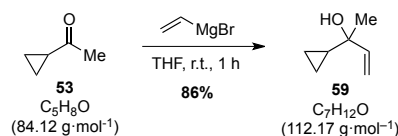
### 1-Cyclopropylethanol (**58**)



A flame-dried two-necked round bottom flask was charged with  $\text{LiAlH}_4$  (720 mg, 19.0 mmol, 0.8 equiv) and anhydrous  $\text{Et}_2\text{O}$  (16 mL) under an argon atmosphere and immersed in an ice bath. Then a solution of cyclopropylmethylketone (**53**) (2.00 g, 23.8 mmol, 1.0 equiv) in anhydrous  $\text{Et}_2\text{O}$  (5 mL) was added dropwise. The reaction mixture was heated to reflux for 30 min and then cooled to  $0^\circ\text{C}$  and quenched with 20 wt% aqueous NaOH (2.4 mL). The resulting suspension was filtered and the phases were separated. The organic layer was dried over anhydrous  $\text{Na}_2\text{SO}_4$  and concentrated under reduced pressure (180 mbar,  $23^\circ\text{C}$ ) to afford cyclopropylcarbinol **58** (1.76 g, 20.4 mmol, 86%) as a colourless liquid.

$^1\text{H NMR}$  (400 MHz,  $\text{CDCl}_3$ ):  $\delta = 3.07$  (dq,  $J = 8.3$ , 6.2 Hz, 1H, H-1), 1.62 – 1.58 (m, 1H, OH), 1.28 (d,  $J = 6.2$  Hz, 3H, Me), 0.95 – 0.85 (m, 1H, H-2), 0.52 – 0.46 (m, 2H,  $\text{CH}_2$ ), 0.30 – 0.24 (m, 1H,  $\text{CH}_2$ ), 0.21 – 0.15 (m, 1H,  $\text{CH}_2$ ) ppm.

### 2-Cyclopropylbut-3-en-2-ol (**59**)

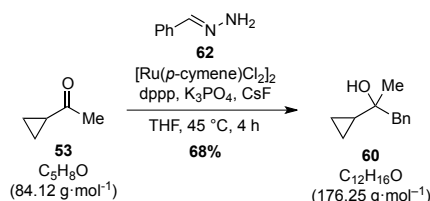


A flame-dried three-necked round bottom flask was charged with vinylmagnesium bromide (1 M in THF, 60 mL, 60.0 mmol, 2.0 equiv) under an argon atmosphere. Then a solution of cyclopropylmethyl ketone (**53**) (2.50 g, 29.8 mmol, 1.0 equiv) in anhydrous THF (20 mL) was added and the resulting reaction mixture was stirred at ambient temperature for 1 h. The reaction was quenched by the addition of saturated aqueous  $\text{NH}_4\text{Cl}$  (4 mL) and  $\text{H}_2\text{O}$  (2 mL). The layers were separated and the aqueous phase was extracted with  $\text{Et}_2\text{O}$  (6  $\times$  15 mL). The combined organic extracts were washed with brine (2  $\times$  15 mL), dried over anhydrous  $\text{MgSO}_4$  and concentrated under reduced pressure. The crude product was purified by column chromatography ( $\text{SiO}_2$ , *n*-pentane/ $\text{Et}_2\text{O}$ , 3:1) to yield cyclopropylcarbinol **59** (3.08 g, 27.4 mmol, 92%) as a colourless liquid.



$^1\text{H NMR}$  (400 MHz,  $\text{CDCl}_3$ ):  $\delta$  = 5.84 (dd,  $J$  = 17.3, 10.7 Hz, 1H, H-2), 5.25 (dd,  $J$  = 17.3, 1.4 Hz, 1H, H-1), 5.05 (dd,  $J$  = 10.7, 1.4 Hz, 1H, H-1), 1.29 (s, 3H, Me), 1.02 (tt,  $J$  = 8.3, 5.5 Hz, 1H, H-4), 0.45 – 0.36 (m, 2H,  $\text{CH}_2$ ), 0.36 – 0.27 (m, 1H,  $\text{CH}_2$ ) ppm.

### 2-Cyclopropyl-1-phenylpropan-2-ol (**60**)



Preparation hydrazone **62**: A flame-dried Schlenk flask was charged with benzaldehyde (7.60 g, 71.3 mmol, 1.2 equiv) and anhydrous THF (30 mL) under an argon atmosphere. Then hydrazine monohydrate (3.76 mL, 3.87 g, 77.3 mmol, 1.3 equiv) was added and the mixture was stirred at ambient temperature for 30 min. The solution was dried by the addition of anhydrous  $\text{Na}_2\text{SO}_4$  prior to use.

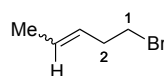
A flame-dried Schlenk flask was charged with  $[\text{Ru}(p\text{-cymene})\text{Cl}_2]_2$  (364 mg, 594  $\mu\text{mol}$ , 1 mol%), dppp (490 mg, 1.19 mmol, 2 mol%),  $\text{CsF}$  (4.51 g, 29.7 mmol, 0.5 equiv), and  $\text{K}_3\text{PO}_4$  (3.15 g, 14.9 mmol, 25 mol%) under an argon atmosphere. The solution of hydrazone **62** and cyclopropylmethyl ketone (**53**) (5.00 g, 59.5 mmol, 1.0 equiv) were added sequentially and the resulting reaction mixture was stirred at 45  $^\circ\text{C}$  for 4 h and then filtered through plug of silica eluting with  $\text{EtOAc}$ . The solvent was removed under reduced pressure and the residue was purified by column chromatography ( $\text{SiO}_2$ , *n*-pentane/ $\text{Et}_2\text{O}$ , 4:1) to yield cyclopropylcarbinol **60** (7.17 g, 40.7 mmol, 68%) as a colourless liquid.

$^1\text{H NMR}$  (400 MHz,  $\text{CDCl}_3$ ):  $\delta$  = 7.33 – 7.23 (m, 5H, Ph), 2.87 (d,  $J$  = 13.1 Hz, 1H,  $\text{CH}_2\text{Ph}$ ), 2.81 (d,  $J$  = 13.1 Hz, 1H,  $\text{CH}_2\text{Ph}$ ), 1.10 (s, 3H, Me), 0.95 – 0.86 (m, 1H, CH), 0.43 – 0.26 (m, 4H,  $\text{CH}_2$ ) ppm.

### 5-Bromopent-2-ene (55)



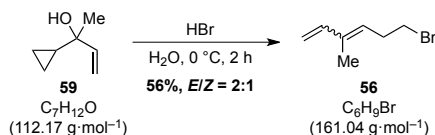
A round bottom flask was charged with cyclopropylcarbinol **58** (1.76 g, 20.4 mmol, 1.0 equiv) and then immersed in an ice bath. Aqueous 48 wt% HBr (24 mL) was added and the reaction mixture was stirred for 2 h. The resulting biphasic mixture was separated and the aqueous layer was extracted with  $\text{Et}_2\text{O}$  ( $3 \times 15 \text{ mL}$ ). The combined organic extracts were washed with saturated aqueous  $\text{NaHCO}_3$  ( $3 \times 15 \text{ mL}$ ) and brine ( $3 \times 15 \text{ mL}$ ) and dried over anhydrous  $\text{MgSO}_4$ . The solvent was removed under reduced pressure and the residue was purified by column chromatography ( $\text{SiO}_2$ ,  $n$ -pentane) to yield bromide **55** (1.67 g, 11.2 mmol, 55%,  $E/Z = 9:1$ ) as a colourless liquid.



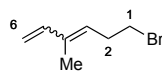
$^1\text{H NMR}$  (400 MHz,  $\text{CDCl}_3$ ):  $\delta = 5.61 - 5.49$  (m, 1H, CH),  $5.47 - 5.36$  (m, 1H, CH),  $3.35$  (t,  $J = 7.1 \text{ Hz}$ , 2H, H-1),  $2.58 - 2.67$  (m, 0.2H, H-2\*),  $2.58 - 2.48$  (m, 1.8H, H-2),  $1.69 - 1.65$  (m, 2.7H),  $1.65 - 1.61$  (m, 0.3H,  $\text{Me}^*$ ) ppm.

The signals of the minor isomer are marked with \*.

### 6-bromo-3-methylhexa-1,3-diene (56)

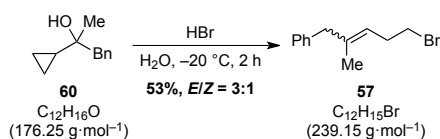


A round bottom flask was charged with cyclopropylcarbinol **59** (2.50 g, 22.3 mmol, 1.0 equiv) and then immersed in an ice bath. Aqueous 48 wt% HBr (26 mL) was added and the reaction mixture was stirred for 2 h. The resulting biphasic mixture was diluted with  $n$ -pentane (20 mL) and the layers were separated. The organic layer was washed with saturated aqueous  $\text{NaHCO}_3$  ( $3 \times 10 \text{ mL}$ ) and brine ( $3 \times 10 \text{ mL}$ ) and dried over anhydrous  $\text{MgSO}_4$ . The solvent was removed under reduced pressure and the residue was purified by column chromatography ( $\text{SiO}_2$ ,  $n$ -pentane) to yield bromide **56** (2.19 g, 12.5 mmol, 56%,  $E/Z = 2:1$ ) as a colourless liquid.

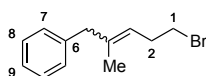


$^1\text{H NMR}$  (400 MHz,  $\text{CDCl}_3$ ):  $\delta = 6.71$  (ddt,  $J = 17.4, 10.9, 0.9 \text{ Hz}$ , 0.33H, H-5\*),  $6.38$  (dd,  $J = 17.4, 10.7 \text{ Hz}$ , 0.67H, H-5),  $5.47$  (t,  $J = 7.3 \text{ Hz}$ , 0.67H, H-3),  $5.37$  (t,  $J = 7.5 \text{ Hz}$ , 0.33H, H-3\*),  $5.27$  (d,  $J = 17.4 \text{ Hz}$ , 1H, H6\*),  $5.21 - 5.13$  (m, 1H, H-6, H-6\*),  $5.01$  (d,  $J = 10.7 \text{ Hz}$ , 1H, H-6),  $3.38$  (q,  $J = 7.3 \text{ Hz}$ , 2H, H-1, H-1\*),  $2.73$  (p,  $J = 7.1 \text{ Hz}$ , 2H, H-2, H-2\*),  $1.84$  (s, 1H,  $\text{Me}^*$ ),  $1.76$  (s, 2H, Me) ppm.

The signals of the minor isomer are marked with \*.

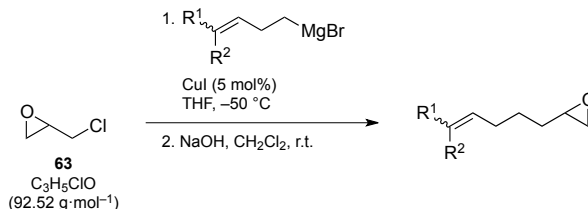
**6-bromo-3-methylhexa-1,3-diene (57)**

A round bottom flask was charged with cyclopropylcarbinol **60** (7.16 g, 40.7 mmol, 1.0 equiv) and then cooled to -20 °C. Aqueous 48 wt% HBr (163 mL) was added and the reaction mixture was stirred for 2 h. The resulting biphasic mixture was diluted with *n*-pentane (200 mL) and the layers were separated. The organic layer was washed with saturated aqueous NaHCO<sub>3</sub> (3 × 100 mL) and dried over anhydrous MgSO<sub>4</sub>. The solvent was removed under reduced pressure and the residue was purified by column chromatography (SiO<sub>2</sub>, *n*-pentane) to yield bromide **57** (5.18 g, 21.7 mmol, 53%, E/Z = 3:1) as a colourless liquid.



<sup>1</sup>H NMR (400 MHz, CDCl<sub>3</sub>): δ = 7.41–7.27 (m, 2H, Ph), 7.22–7.15 (m, 3H, Ph), 5.36–5.30 (m, 0.25H, H-3\*), 5.29–5.24 (m, 0.75H, H-3), 3.42–3.37 (m, 2.5H, H-5\*, H-1), 3.31 (s, 2H, H-5), 2.72 (q, *J* = 7.2 Hz, 0.5H, H-2\*) 2.62 (q, *J* = 7.4 Hz, 1.5H, H-2), 1.66 (s, 0.75H, Me\*), 1.57 (s, 2.25H, Me) ppm.

The signals of the minor isomer are marked with \*.

**General procedure for epoxide formation via epichlorhydrin (GP1):**

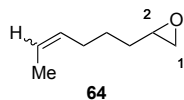
Preparation of the GRIGNARD reagent: To a flame-dried two-necked round bottom flask equipped with a reflux condenser was added freshly ground magnesium (1.5 equiv) and the flask was once more dried by heating with a heat gun under high vacuum while vigorously stirring the magnesium. After cooling to ambient temperature, the vessel was placed under an argon atmosphere and anhydrous THF (1 M) was added and heated to reflux. A small crystal of iodine was added followed by the dropwise addition of the bromide (1.0 equiv). The reaction mixture was stirred at reflux for 90 min and then cooled to ambient temperature.

A flame-dried Schlenk flask was charged with epichlorhydrin (1.0 equiv), CuI (5 mol%) and anhydrous THF (1.5 M) under an argon atmosphere. The suspension was cooled to -50 °C and the Grignard reagent was added dropwise. The resulting reaction mixture was stirred at -50 °C for 2 h and then quenched by the addition of saturated aqueous NH<sub>4</sub>Cl. The layers were separated and the aqueous phase was extracted with Et<sub>2</sub>O (3 ×). The combined organic phases were washed with brine, dried over anhydrous MgSO<sub>4</sub> and concentrated under reduced pressure. The crude product was purified by column chromatography to afford the corresponding chlorohydrin.

The chlorohydrin (1.0 equiv) was dissolved in dichloromethane (0.5 M) and 1 M NaOH (6.0 equiv) was added. The reaction mixture was stirred at ambient temperature for 18 h. The layers were separated and the

aqueous phase was extracted with dichloromethane (3 ×). The combined organic extracts were dried over anhydrous MgSO<sub>4</sub> and the solvent was removed under reduced pressure to afford the corresponding epoxide.

### 2-(Hex-4-en-1-yl)oxirane (64)



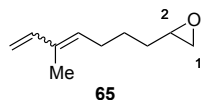
Epoxide **64** was prepared from bromide **55** (580 mg, 3.89 mmol) according to **GP1**. The corresponding chlorohydrin (186 mg, 1.14 mmol, 29%, *E/Z* = 9:1) obtained from the first step afforded epoxide **64** (148 mg, 1.02 mmol, 89%, *E/Z* = 9:1) as a colourless oil.

<sup>1</sup>H NMR (700 MHz, CDCl<sub>3</sub>): δ = 5.48 – 5.36 (m, 2H, H-6, H-7), 2.93 – 2.88 (m, 1H, H-2), 2.74 (t, *J* = 4.5 Hz, 1H, H-1), 2.46 (dd, *J* = 5.2, 2.8 Hz, 1H, H-1), 2.14 – 2.08 (m, 0.2H, H-5\*), 2.06 – 2.01 (m, 1.8H, H-5), 1.64 (d, *J* = 5.5 Hz, 2.7H, Me), 1.60 (d, *J* = 6.8 Hz, 0.3H, Me\*), 1.55 – 1.45 (m, 4H, H-3, H-4) ppm.

<sup>13</sup>C NMR (176 MHz, CDCl<sub>3</sub>): δ = 130.9 (CH), 130.1\*, 125.5 (CH), 124.5\*, 52.4 (C-2), 47.3 (C-1), 32.4 (C-5), 32.2\*, 32.1 (C-3), 29.8\*, 26.7\*, 26.0 (C-4), 18.0 (Me), 12.9\*.

The signals of the minor isomer are marked with \*.

### 2-(5-Methylhepta-4,6-dien-1-yl)oxirane (65)



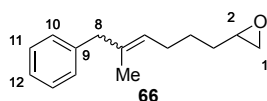
Epoxide **65** was prepared from bromide **56** (589 mg, 3.66 mmol) according to **GP1**. The corresponding chlorohydrin (196 mg, 1.06 mmol, 29%, *E/Z* = 2:1) obtained from the first step afforded epoxide **65** (100 mg, 660 μmol, 62%, *E/Z* = 6:1) as a colourless oil.

<sup>1</sup>H NMR (400 MHz, CDCl<sub>3</sub>): δ = 6.75 (dd, *J* = 17.3, 10.8 Hz, 0.14H, H-8\*), 6.36 (dd, *J* = 17.4, 10.7 Hz, 0.86H, H-8), 5.47 (t, *J* = 7.6 Hz, 0.86H, H-6), 5.37 (t, *J* = 7.6 Hz, 0.14H, H-6\*), 5.20 (d, *J* = 17.3 Hz, 0.14H, H-9\*), 5.14 – 5.03 (m, 1H, H-9, H-9\*), 4.93 (d, *J* = 10.7 Hz, 0.86H, H-9), 2.96 – 2.87 (m, 1H, H-2\*, H-2), 2.75 (dd, *J* = 5.0, 4.1 Hz, 1H, H-1\*, H-1), 2.47 (dd, *J* = 5.0, 2.7 Hz, 1H, H-1\*, H-1), 2.26 – 2.14 (m, 2H, H-5\*, H-5), 1.81 (s, 0.43H, Me\*), 1.73 (s, 2.57H, Me), 1.64 – 1.48 (m, 4H, H-3\*, H-3, H-4\*, H-4) ppm.

<sup>13</sup>C NMR (176 MHz, CDCl<sub>3</sub>): δ = 141.6 (C-8), 134.6 (C-7), 133.7\*, 132.9\*, 132.6 (C-6), 130.6\*, 113.7\*, 110.9 (C-9), 52.3 (C-2), 47.2 (C-1), 32.2 (CH<sub>2</sub>), 32.1\*, 28.0 (C-5), 27.1\*, 26.3\*, 26.0 (CH<sub>2</sub>), 19.9\*, 11.8 (Me) ppm.

The signals of the minor isomer are marked with \*.

### 2-(5-methyl-6-phenylhex-4-en-1-yl)oxirane (66)



Epoxide **66** was prepared from bromide **57** (1.29 g, 5.39 mmol) according to **GP1**. The corresponding chlorohydrin (541 mg, 2.14 mmol, 39%, *E/Z* = 3:1) obtained from the first step afforded epoxide **66** (160 mg, 1.45 mmol, 68%, *E/Z* = 3:1) as a colourless oil.

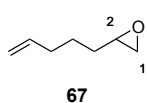
<sup>1</sup>H NMR (700 MHz, CDCl<sub>3</sub>): δ = 7.26 – 7.30 (m, 2H, H-11), 7.18 – 7.21 (m, 1H, H-12), 7.15 – 7.18 (m, 2H, H-10), 5.29 – 5.33 (m, 0.2H, H-6\*), 5.20 – 5.29 (m, 0.8H, H-6), 3.79 – 3.84 (m, 1H, H-2), 3.63 (dd, *J* = 11.1,

3.3 Hz, 1H, H-1), 3.48 (dd,  $J = 11.1, 7.1$  Hz, 1 H, H-1), 3.37 (s, 0.4H, H-8\*), 3.29 (s, 1.6H, H-8), 2.12 – 2.21 (m, 0.4H, H-5\*), 2.05 – 2.12 (m, 1.6H, H-5), 1.63 (s, 0.6H, H-13\*), 1.52 – 1.61 (m, 5.4H, H-13, H-3, H-4), 1.42 – 1.49 (m, 1H, H-4) ppm.

$^{13}\text{C}$  NMR (176 MHz,  $\text{CDCl}_3$ ):  $\delta = 140.5$  (C-9), 140.2\* (C-9), 135.2 (C-7), 134.6\* (C-7), 129.0 (C-10), 128.6\* (C-10), 128.5\* (C-11), 128.3 (C-11), 126.2\* (CH), 126.1 (CH), 126.1 (CH), 126.0\* (CH), 71.54 (C-2), 71.52\* (C-2), 50.7 (C-1), 46.4 (C-8), 38.0\* (C-8), 34.0\* (C-3), 34.0 (C-3), 28.1\* (C-5), 27.9 (C-5), 26.1\* (C-4), 25.8 (C-4), 23.6\* (Me), 16.0 (Me) ppm.

The signals of the minor isomer are marked with \*.

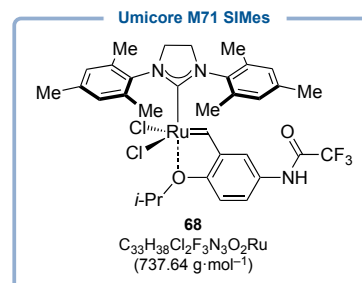
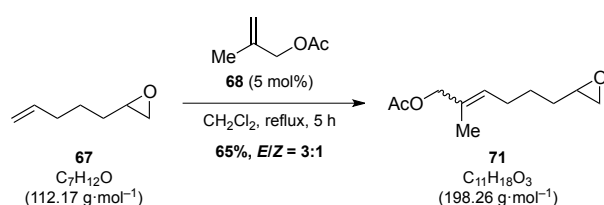
### 2-(5-Methylhepta-4,6-dien-1-yl)oxirane (67)



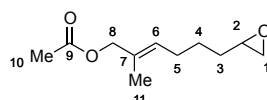
Epoxide **67** was prepared from 4-bromobut-1-ene (1.00 g, 7.41 mmol) according to **GP1**. The corresponding chlorohydrin (1.03 g, 6.97 mmol, 94%) obtained from the first step afforded epoxide **67** (673 mg, 6.00 mol, 86%) as a colourless oil.

$^1\text{H}$  NMR (400 MHz,  $\text{CDCl}_3$ ):  $\delta = 5.85 - 5.75$  (m, 1H, H-6), 5.05 – 4.99 (m, 1H, H-7), 4.99 – 4.95 (m, 1H, H-7), 2.94 – 2.89 (m, 1H, H-2), 2.75 (dd,  $J = 4.9, 4.1$  Hz, 1H, H-1), 2.47 (dd,  $J = 4.9, 2.7$  Hz, 1H, H-1), 2.14 – 2.09 (m, 2H, H-3), 1.62 – 1.51 (m, 4H, H-4, H-5) ppm.

### 2-Methyl-6-(oxiran-2-yl)hex-2-en-1-yl acetate (71)



A Schlenk flask was charged with epoxide **67** (50.0 mg, 450  $\mu\text{mol}$ , 1.0 equiv) and anhydrous and degassed dichloromethane (7.5) under an argon atmosphere. Then 2-methyl acetate (513 mg, 4.50 mmol, 10 equiv) and Umicore M71 SIMes catalyst **68** (16.6 mg, 22.5  $\mu\text{mol}$ , 5 mol%) were added. The reaction mixture was heated to reflux and stirred for 5 h. After cooling to ambient temperature, the solvent was removed under reduced pressure and the residue was purified by column chromatography ( $\text{SiO}_2$ , *n*-pentane/ $\text{Et}_2\text{O}$ , 16:1 to 10:1) to yield epoxide **71** (58.0 mg, 293  $\mu\text{mol}$ , 65%,  $E/Z = 3:1$ ) as a colourless oil.

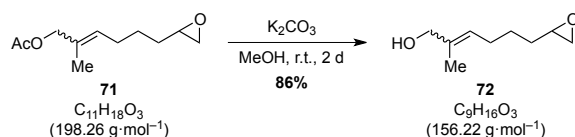


$^1\text{H}$ -NMR (700 MHz,  $\text{CDCl}_3$ ):  $\delta = 5.44 - 5.47$  (m, 0.8H, H-6), 5.37 – 5.41 (m, 0.2H, H-6\*), 4.57 (s, 0.4H, H-8\*), 4.45 (s, 1.6H, H-8), 2.88 – 2.93 (m, 1H, H-2\*, H-2), 2.73 – 2.77 (m, 1H, H-1\*, H-1), 2.44 – 2.49 (m, 1H, H-1\*, H-1), 2.08 – 2.15 (m, 2H, H-5\*, H-5), 2.07 (s, 2.4H, H-10), 2.07 (s, 0.6H, H-10\*), 1.75 (s, 0.6H, H-11\*), 1.65 (s, 2.4 H, H-11), 1.49 – 1.60 (m, 4 H, H-3\*, H-3, H-4\*, H-4) ppm.

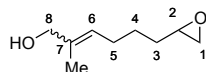
$^{13}\text{C-NMR}$  (176 MHz,  $\text{CDCl}_3$ ):  $\delta$  = 171.2 (C-9\*), 171.0 (C-9), 130.6 (C-7), 130.4\* (C-7), 130.3\* (C-6), 129.2 (C-6), 70.2 (C-8), 63.2 (C-8\*), 52.2 (C-2), 47.1 (C-1), 32.1 (C-3), 32.0 (C-3\*), 27.5\* (C-5), 27.5 (C-5), 26.2 (C-4\*), 25.7 (C-4), 21.5 (C-11\*), 21.1 (C-10), 21.0 (C-10\*), 14.0 (C-11) ppm.

**HRMS** (ESI, pos. mode):  $m/z$  calcd for  $\text{C}_{11}\text{H}_{18}\text{O}_3\text{Na}^+$  [ $\text{M}+\text{Na}$ ] $^+$ : 221.1148, found 221.1158.

### 2-Methyl-6-(oxiran-2-yl)hex-2-en-1-ol (72)



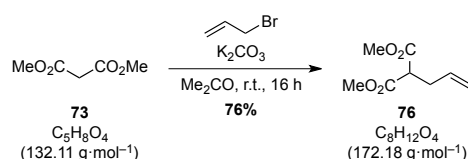
To a solution of epoxide **71** (90.0 mg, 454  $\mu\text{mol}$ , 1.0 equiv) in anhydrous MeOH (5 mL) was added  $\text{K}_2\text{CO}_3$  (120 mg, 900  $\mu\text{mol}$ , 2.0 equiv). The reaction mixture was stirred at ambient temperature for 2 d. Then  $\text{H}_2\text{O}$  (5 mL) was added and the solution was extracted with  $\text{Et}_2\text{O}$  ( $3 \times 15 \text{ mL}$ ). The combined organic phases were dried over anhydrous  $\text{MgSO}_4$  and concentrated under reduced pressure. The crude product was purified by column chromatography ( $\text{SiO}_2$ ,  $n$ -pentane/ $\text{Et}_2\text{O}$ , 4:1) to yield epoxide **72** (60.9 g, 390  $\mu\text{mol}$ , 86%,  $E/Z = 3:1$ ) as a colourless oil.



$^1\text{H NMR}$  (700 MHz,  $\text{CDCl}_3$ ):  $\delta$  = 5.43–5.39 (m, 1H, H-6), 4.01 (s, 2H, H-8), 2.93–2.90 (m, 1H, H-2), 2.77–2.75 (m, 1H, H-1), 2.48–2.47 (m, 1H, H-1), 2.14–2.10 (m, 2H, H-5), 1.67 (s, 3H, Me), 1.59–1.50 (m, 4H, H-4, H-3) ppm.

**HRMS** (ESI, pos. mode):  $m/z$  calcd for  $\text{C}_9\text{H}_{16}\text{O}_2\text{Na}^+$  [ $\text{M}+\text{Na}$ ] $^+$ : 179.1042, found 179.1051.

### Dimethyl 2-allylmalonate (76)

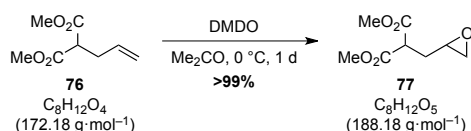


To a suspension of  $\text{K}_2\text{CO}_3$  (52.0 g, 380 mmol, 4.8 equiv) in acetone (250 mL) were added sequentially dimethyl malonate (**73**) (12 mL, 100 mmol, 1.3 equiv) and allyl bromide (6.75 mL, 80.0 mmol, 1.0 equiv) under an argon atmosphere. The reaction mixture was stirred at ambient temperature for 16 h and then quenched by the addition of saturated aqueous  $\text{NH}_4\text{Cl}$  (500 mL). The layers were separated and the aqueous phase was extracted with dichloromethane ( $3 \times 250 \text{ mL}$ ). The combined organic phases were dried over anhydrous  $\text{Na}_2\text{SO}_4$  and the solvent was removed under reduced pressure. The crude product was purified by column chromatography ( $\text{SiO}_2$ ,  $n$ -pentane/ $\text{Et}_2\text{O}$ , 20:1 to 4:1) to afford alkene **76** (10.5 g, 60.8 mmol, 76%) as a colourless oil.

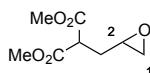
$^1\text{H NMR}$  (400 MHz,  $\text{CDCl}_3$ ):  $\delta$  = 5.76 (ddt,  $J = 17.1, 10.2, 6.8 \text{ Hz}$ , 1H, H-2), 5.12 (d,  $J = 17.1 \text{ Hz}$ , 1H, H-1), 5.06 (d,  $J = 10.2 \text{ Hz}$ , 1H, H-1), 3.74 (s, 6H, OMe), 3.46 (t,  $J = 7.6 \text{ Hz}$ , 1H, H-4), 2.64 (dd,  $J = 7.6, 6.8 \text{ Hz}$ , 2H, H-3) ppm.



### Dimethyl 2-(oxiran-2-ylmethyl)malonate (**77**)

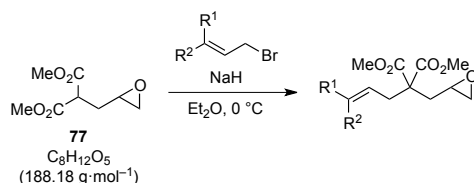


A round bottom flask was charged with alkene **76** (410 mg, 2.38 mmol, 1.0 equiv) and DMDO (0.074 M in acetone, 42 mL, 3.10 mmol, 1.3 equiv) at  $0^\circ C$  and stirred for 25 h while slowly warming to ambient temperature. The solvent was removed under reduced pressure to afford epoxide **77** (447 mg, 2.38 mmol,  $>99\%$ ) as a colourless oil.



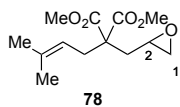
$^1H$  NMR (400 MHz,  $CDCl_3$ ):  $\delta = 3.77$  (s, 3H, OMe), 3.75 (s, 3H, OMe), 3.58 (dd,  $J = 8.6, 6.1$  Hz, 1H, H-4), 3.01 (dtd,  $J = 6.9, 4.2, 2.6$  Hz, 1H, H-2), 2.78 (t,  $J = 4.8, 4.1$  Hz, 1H, H-1), 2.52 (dd,  $J = 4.8, 2.6$  Hz, 1H, H-1), 2.30 (ddd,  $J = 14.4, 8.6, 4.4$  Hz, 1H, H-3), 1.99 (dt,  $J = 14.4, 6.4$  Hz, 1H, H-3) ppm.

### General procedure for epoxide formation via dimethyl malonate (GP2):



A flame-dried Schlenk flask was charged with diester (1.0 equiv) in anhydrous THF (0.1 M) and the solution was cooled to  $0^\circ C$ . Then NaH (60 wt%, 1.2 equiv) was added and the reaction mixture was stirred for 15 min followed by the addition of the alkenyl bromide (1.1 equiv). After 2 h of stirring at  $0^\circ C$ , the mixture was diluted with  $Et_2O$ , washed with  $H_2O$  and dried over anhydrous  $MgSO_4$ . The solvent was removed under reduced pressure and the residue was purified by column chromatography.

### Dimethyl 2-(3-methylbut-2-en-1-yl)-2-(oxiran-2-ylmethyl)malonate (**78**)

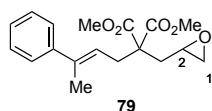


Prepared from epoxide **77** (1.00 g, 5.31 mmol) and prenyl bromide (670  $\mu L$ , 5.84 mmol) according to **GP2**. Purification by column chromatography ( $SiO_2$ ,  $n$ -pentane/ $Et_2O$ , 4:1) afforded **78** (973 mg, 3.80 mmol, 72%) as a colourless oil.

$^1H$  NMR (700 MHz,  $CDCl_3$ ):  $\delta = 4.93 - 4.97$  (m, 1H, H-6), 3.73 (s, 3H, OMe), 3.72 (s, 3H, OMe), 2.93 - 2.99 (m, 1H, H-2), 2.70 - 2.74 (m, 2H, H-4, H-1), 2.41 (dd,  $J = 5.1, 2.6$  Hz, 1H, H-1), 2.15 (dd,  $J = 14.6, 4.8$  Hz, 1H, H-3), 1.97 (dd,  $J = 14.6, 6.9$  Hz, 1H, H-3), 1.69 (s, 3H, Me), 1.61 (s, 3H, Me) ppm.

$^{13}C$  NMR (176 MHz,  $CDCl_3$ ):  $\delta = 171.7$  ( $CO_2Me$ ), 171.7 ( $CO_2Me$ ), 136.3 (C-7), 117.4 (C-6), 56.6 (C-4), 52.7 (OMe), 52.6 (OMe), 48.7 (C-2), 46.9 (C-1), 36.3 (C-3), 32.4 (C-5), 26.1 (Me), 18.0 (Me) ppm.

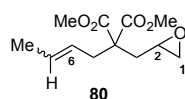
HRMS (ESI, pos. mode):  $m/z$  calcd for  $C_{13}H_{20}ONa^+$  [ $M+Na$ ] $^+$ : 279.1203, found 279.1207.

**(E)-Dimethyl 2-(oxiran-2-ylmethyl)-2-(3-phenylbut-2-en-1-yl)malonate (79)**

Prepared from epoxide **77** (168 mg, 890  $\mu\text{mol}$ ) and bromide **87** (207 mg, 980  $\mu\text{mol}$ ) according to **GP2**. Purification by column chromatography ( $\text{SiO}_2$ , *n*-pentane/EtOAc, 4:1) afforded **79** (197 mg, 620  $\mu\text{mol}$ , 70%) as a colourless oil.

$^1\text{H NMR}$  (400 MHz,  $\text{CD}_2\text{Cl}_2$ ):  $\delta$  = 7.36 – 7.27 (m, 4H, Ph), 7.26 – 7.20 (m, 1H, Ph), 5.58 (tq,  $J$  = 7.5, 1.5 Hz, 1H, H-6), 3.74 (s, 3H, OMe), 3.72 (s, 3H, OMe), 3.00 – 2.87 (m, 3H, H-2, H-5), 2.71 (dd,  $J$  = 5.1, 4.0 Hz, 1H, H-1), 2.42 (dd,  $J$  = 5.1, 2.6 Hz, 1H, H-1), 2.24 (dd,  $J$  = 14.6, 4.6 Hz, 1H, H-3), 2.05 (s, 3H, Me), 2.01 (dd,  $J$  = 14.6, 7.1 Hz, 1H, H-3) ppm.

$^{13}\text{C NMR}$  (176 MHz,  $\text{CD}_2\text{Cl}_2$ ):  $\delta$  = 171.9 (CO<sub>2</sub>Me), 171.8 (CO<sub>2</sub>Me), 144.2 (C-8), 139.4 (C-7), 128.7 (CH), 127.5 (C-11), 126.3 (CH), 121.8 (C-6), 57.2 (C-4), 53.1 (OMe), 53.0 (OMe), 48.9 (C-2), 47.1 (C-1), 37.0 (C-3), 33.3 (C-5), 16.5 (Me) ppm.

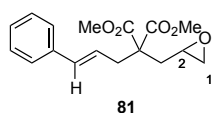
**(E)-Dimethyl 2-(but-2-en-1-yl)-2-(oxiran-2-ylmethyl)malonate (80)**

Prepared from epoxide **77** (150 mg, 790  $\mu\text{mol}$ ) and 1-bromobut-2-ene (110 mg, 870  $\mu\text{mol}$ ) according to **GP2**. Purification by column chromatography ( $\text{SiO}_2$ , *n*-pentane/EtOAc, 6:1) afforded **80** (151 mg, 630  $\mu\text{mol}$ , 79%) as a colourless oil.

$^1\text{H NMR}$  (700 MHz,  $\text{CD}_2\text{Cl}_2$ ):  $\delta$  = 5.62 (dqt,  $J$  = 10.9, 6.9, 1.6 Hz, 0.25H, H-7\*), 5.55 (dqt,  $J$  = 15.5, 6.5, 1.3 Hz, 0.75H, H-7), 5.29 – 5.21 (m, 1H, H-6, H-6\*), 3.71 (s, 0.75H, OMe\*), 3.71 (s, 2.25H, OMe), 3.70 (s, 0.75H, OMe\*), 3.69 (s, 2.25H, OMe), 2.97 – 2.86 (m, 1H, H-2, H-2\*), 2.78 (dddq,  $J$  = 14.8, 7.8, 1.6, 0.9 Hz, 0.25H, H-5\*), 2.73 (dddq,  $J$  = 14.8, 7.5, 1.7, 0.9 Hz, 0.25H, H-5\*), 2.69 (dd,  $J$  = 5.2, 3.9 Hz, 0.25H, H-1\*), 2.69 (dd,  $J$  = 5.1, 4.1 Hz, 1H, H-1), 2.66 (dq,  $J$  = 7.4, 1.1 Hz, 1.5H, H-5), 2.39 (dd,  $J$  = 5.2, 2.6 Hz, 1H, H-1, H-1\*), 2.14 (dd,  $J$  = 14.6, 4.7 Hz, 0.25H, H-3\*), 2.11 (dd,  $J$  = 14.6, 4.6 Hz, 0.75H, H-3), 1.93 (dd,  $J$  = 14.6, 6.9 Hz, 0.25H, H-3\*), 1.92 (dd,  $J$  = 14.6, 7.0 Hz, 0.75H, H-3), 1.64 (ddt,  $J$  = 6.5, 1.7, 1.1 Hz, 2.25H, Me), 1.62 (ddt,  $J$  = 6.9, 1.9, 0.9 Hz, 0.75H, Me\*) ppm.

$^{13}\text{C NMR}$  (176 MHz,  $\text{CD}_2\text{Cl}_2$ ):  $\delta$  = 171.9\*, 171.8\*, 171.8 (CO<sub>2</sub>Me), 171.8 (CO<sub>2</sub>Me), 130.9 (C-7), 128.8\*, 125.0 (C-6), 123.9\*, 57.2 (C-4), 56.9\*, 54.0\*, 53.0 (OMe), 53.0\*, 52.9 (OMe), 48.9\*, 48.8 (C-2), 47.1 (C-1), 47.1\*, 37.3 (C-5), 36.7\*, 36.6 (C-3), 31.4\*, 18.3 (Me), 13.2\* ppm.

The signals of the minor isomer are marked with \*.

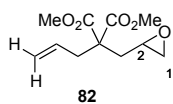
**Dimethyl 2-cinnamyl-2-(oxiran-2-ylmethyl)malonate (81)**

Prepared from epoxide **77** (200 mg, 1.06 mmol) and bromide **86** (150 mg, 1.27 mmol) according to **GP2**. Purification by column chromatography ( $\text{SiO}_2$ , *n*-pentane/EtOAc, 6:1) afforded **81** (250 mg, 821  $\mu\text{mol}$ , 77%) as a colourless oil.

$^1\text{H NMR}$  (500 MHz,  $\text{CDCl}_3$ ):  $\delta$  = 7.36 – 7.24 (m, 4H, H-9, H-10), 7.27 – 7.17 (m, 1H, H-11), 6.47 (dt,  $J$  = 15.7, 1.2 Hz, 1H, H-7), 6.03 (dt,  $J$  = 15.7, 7.6 Hz, 1H, H-6), 3.77 (s, 3H, OMe), 3.76 (s, 3H, OMe), 3.02 (dtd,  $J$  = 7.2, 4.2, 2.6 Hz, 1H, H-2), 2.93 (dt,  $J$  = 7.6, 1.2 Hz, 2H, H-5), 2.76 (t,  $J$  = 5.1, 4.0 Hz, 1H, H-1), 2.45 (dd,  $J$  = 5.1, 2.6 Hz, 1H, H-1), 2.27 (dd,  $J$  = 14.7, 4.4 Hz, 1H, H-3), 2.00 (dd,  $J$  = 14.7, 7.2 Hz, 1H, H-3) ppm.

$^{13}\text{C NMR}$  (126 MHz,  $\text{CDCl}_3$ ):  $\delta$  = 171.3 ( $\text{CO}_2\text{Me}$ ), 171.3 ( $\text{CO}_2\text{Me}$ ), 137.1 (C-8), 134.6 (C-7), 128.7 (C-10), 127.7 (C-11), 126.4 (C-9), 123.6 (C-6), 57.0 (C-4), 52.8 (OMe), 52.8 (OMe), 48.6 (C-2), 46.9 (C-1), 37.5 (C-5), 36.6 (C-3) ppm.

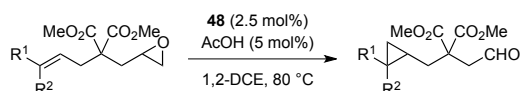
### Dimethyl 2-allyl-2-(oxiran-2-ylmethyl)malonate (**82**)



Prepared from epoxide **77** (20 mg, 100  $\mu\text{mol}$ ) and allyl bromide (95  $\mu\text{L}$ , 13.3 mg, 110  $\mu\text{mol}$ ) according to **GP2**. The crude product was pure enough and **82** (9.3 mg, 40  $\mu\text{mol}$ , 40%) was obtained as a colourless oil.

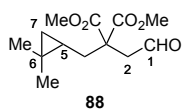
$^1\text{H NMR}$  (400 MHz,  $\text{CDCl}_3$ ):  $\delta$  = 5.66 (ddt,  $J$  = 18.0, 10.1, 7.5 Hz, 1H, H-6), 5.20 – 5.07 (m, 2H, H-7), 3.76 (s, 3H, OMe), 3.74 (s, 3H, OMe), 2.98 (dtd,  $J$  = 7.2, 4.2, 2.6 Hz, 1H, H-2), 2.78 (dt,  $J$  = 7.5, 1.1 Hz, 2H, H-5), 2.74 (dd,  $J$  = 5.1, 3.9 Hz, 1H, H-1), 2.44 (dd,  $J$  = 5.1, 2.6 Hz, 1H, H-1), 2.21 (dd,  $J$  = 14.6, 4.5 Hz, 1H, H-3), 1.97 (dd,  $J$  = 14.6, 7.2 Hz, 1H, H-3) ppm.

### General procedure for epoxide rearrangement (**GP3**):



A GC-vial was charged with epoxide (60.0  $\mu\text{mol}$ , 1.0 equiv) and 1,2-DCE (600  $\mu\text{L}$ ). Then catalyst **48** (800  $\mu\text{g}$ , 1.50  $\mu\text{mol}$ , 2.5 mol%) and acetic acid (0.17  $\mu\text{L}$ , 3.00  $\mu\text{mol}$ , 5 mol%) were added and the reaction mixture was stirred at 80 °C. The reaction progress was monitored by GC-MS.

### Dimethyl 2-((2,2-dimethylcyclopropyl)methyl)-2-(2-oxoethyl)malonate (**88**)



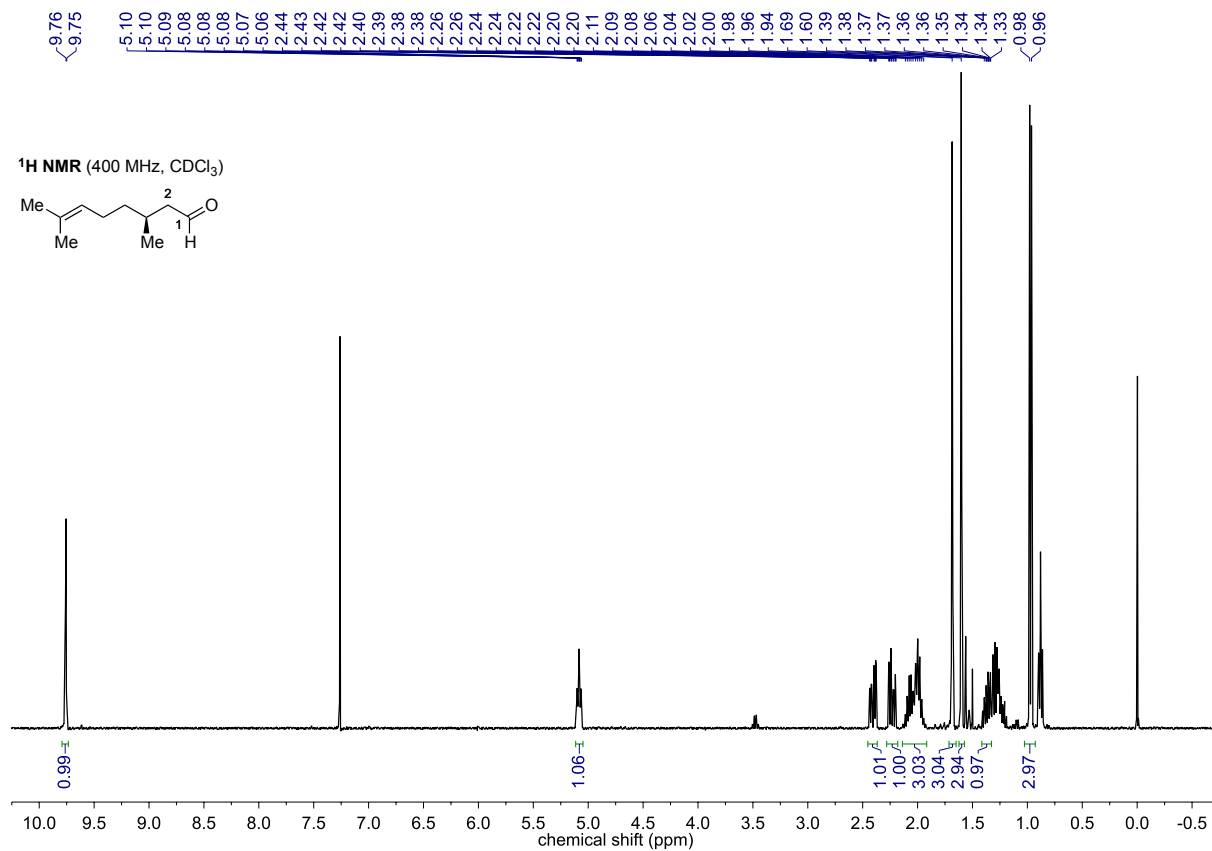
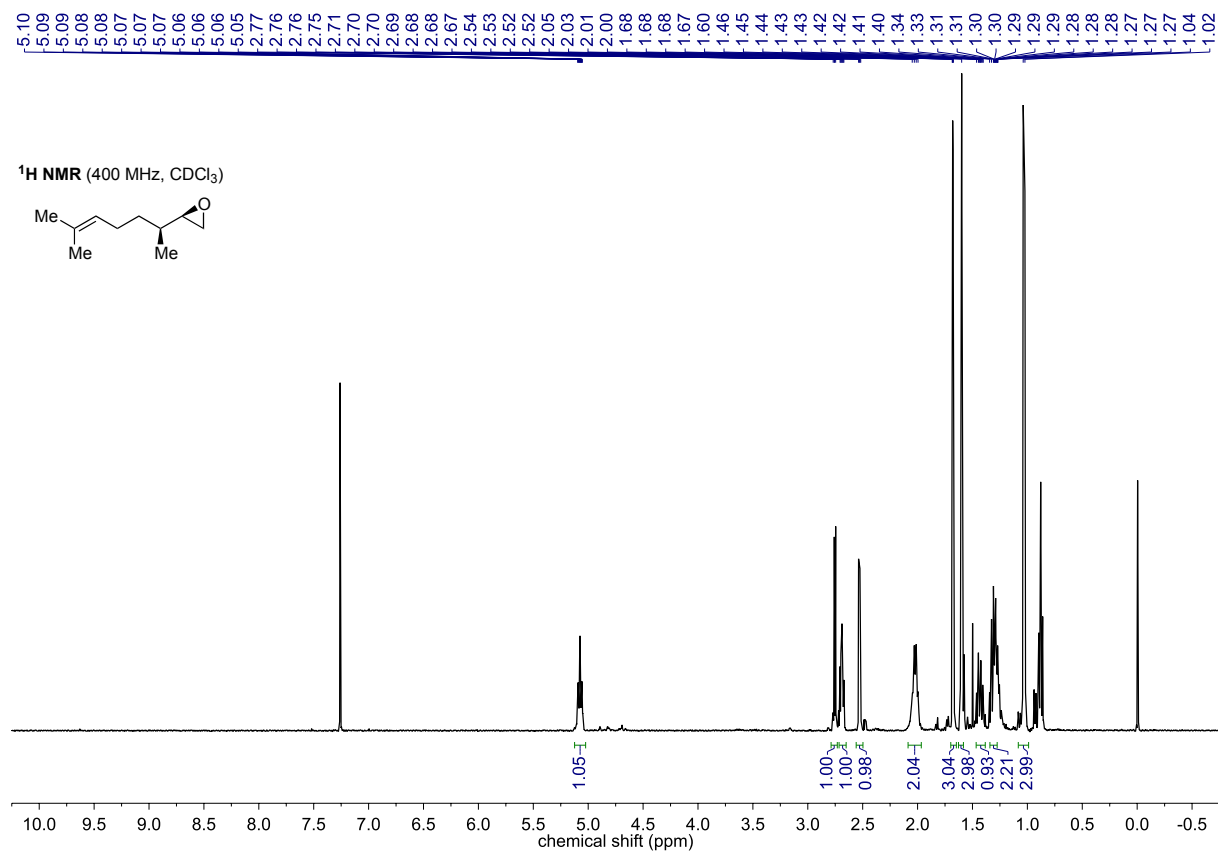
Prepared from epoxide **78** according to **GP3**. Purification by column chromatography ( $\text{SiO}_2$ ,  $n$ -pentane/ $\text{Et}_2\text{O}$ , 4:1) afforded **88** (10.1 mg, 821  $\mu\text{mol}$ , 77%) as a colourless oil.

$^1\text{H NMR}$  (400 MHz,  $\text{CDCl}_3$ ):  $\delta$  = 9.73 (t,  $J$  = 1.4 Hz, 1H, H-1), 3.75 (s, 3H, OMe), 3.75 (s, 3H, OMe), 3.12 (dd,  $J$  = 17.8, 1.4 Hz, 1H, H-2), 3.05 (dd,  $J$  = 17.8, 1.4 Hz, 1H, H-2), 2.26 (dd,  $J$  = 14.5, 5.0 Hz, 1H, H-4), 1.83 (dd,  $J$  = 14.5, 8.7 Hz, 1H, H-4), 1.01 (s, 3H, Me), 1.00 (s, 3H, Me), 0.43 (dd,  $J$  = 8.4, 4.2 Hz, 1H, H-7), 0.34 (tt,  $J$  = 8.6, 5.1 Hz, 1H, H-5), -0.11 (t,  $J$  = 4.8 Hz, 1H, H-7) ppm.

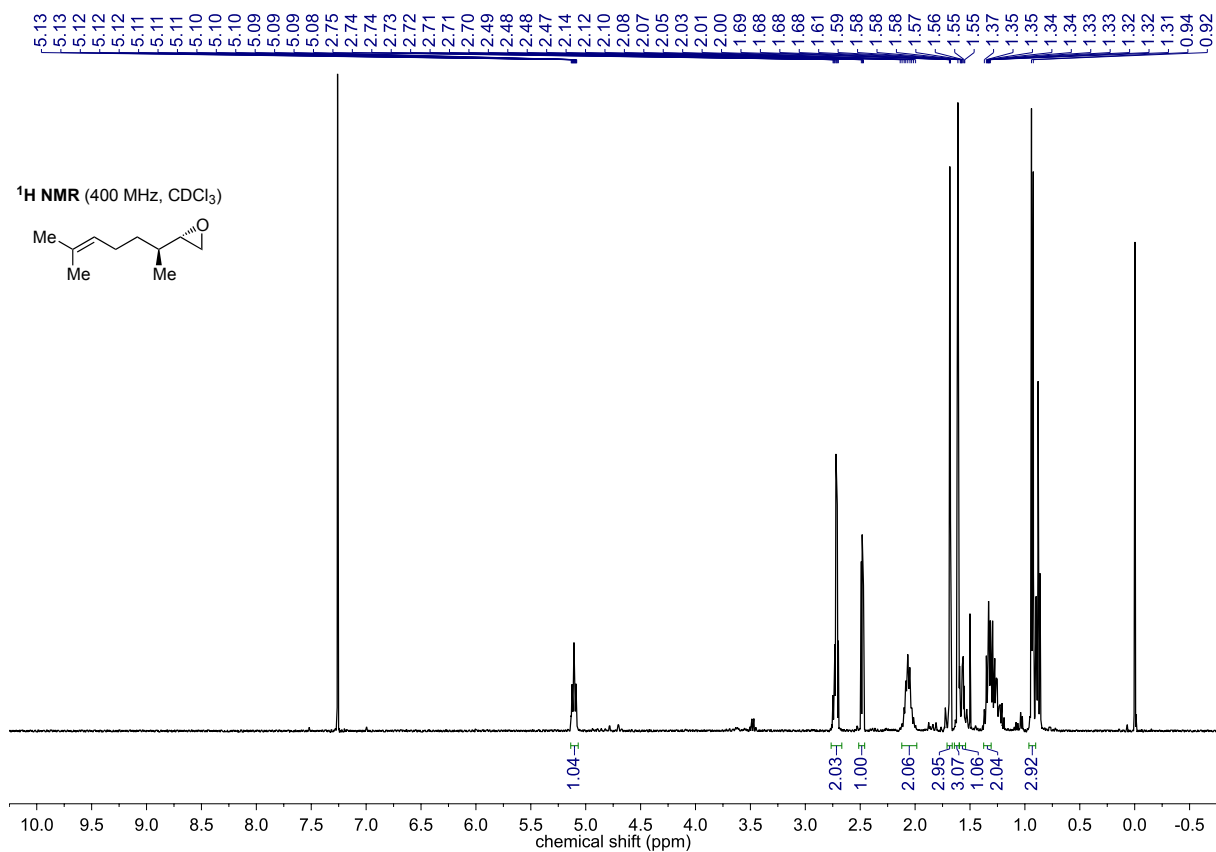
$^{13}\text{C NMR}$  (176 MHz,  $\text{CDCl}_3$ ):  $\delta$  = 199.4 (C-1), 171.2 ( $\text{CO}_2\text{Me}$ ), 171.1 ( $\text{CO}_2\text{Me}$ ), 55.3 (C-3), 53.0 (OMe), 52.9 (OMe), 46.6 (C-2), 34.0 (C-4), 27.3 (Me), 20.2 (Me), 20.1 (C-7), 19.8 (C-5), 15.4 (C-6) ppm.

**HRMS** (ESI, pos. mode):  $m/z$  calcd for  $\text{C}_{13}\text{H}_{20}\text{O}_5\text{Na}^+$  [ $\text{M}+\text{Na}$ ] $^+$ : 279.1230, found 279.1186.

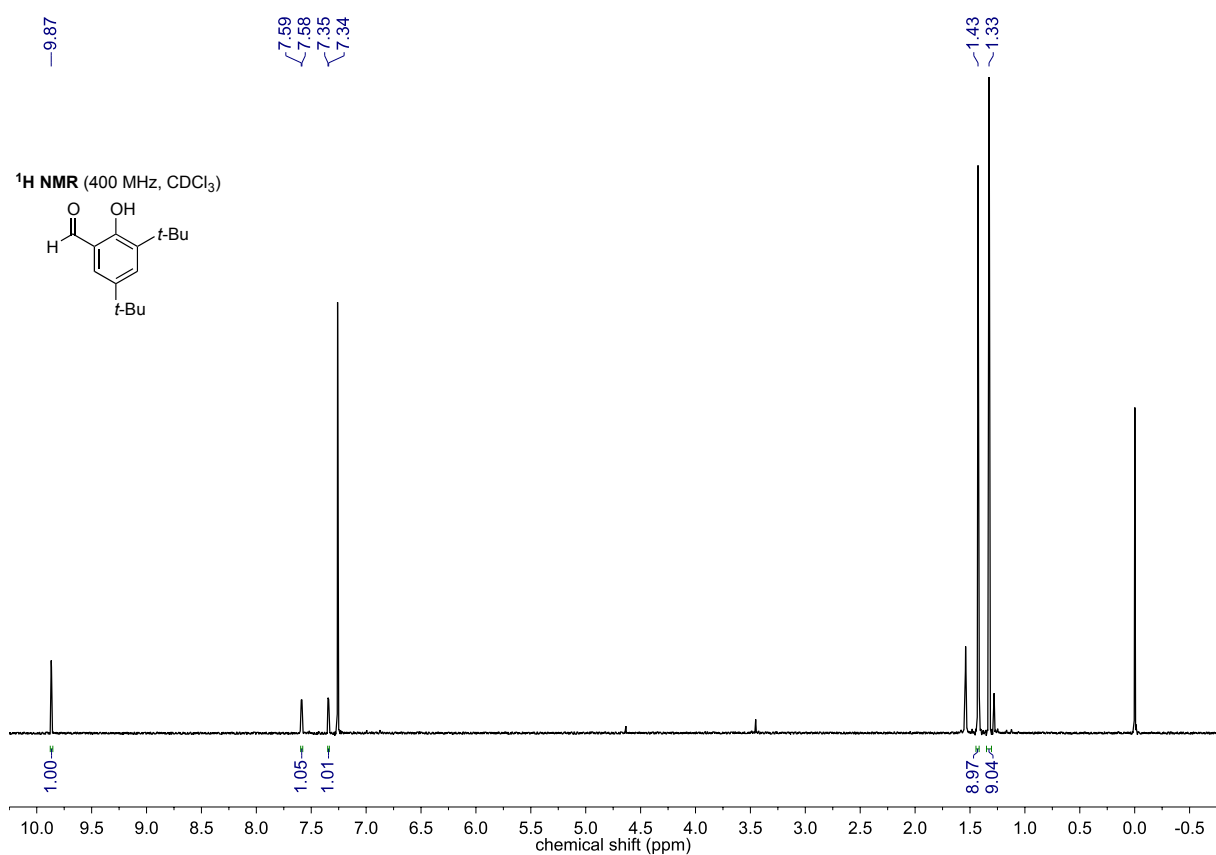
## NMR Spectra

**(S)-Citronellal (43)****Epoxide 40**

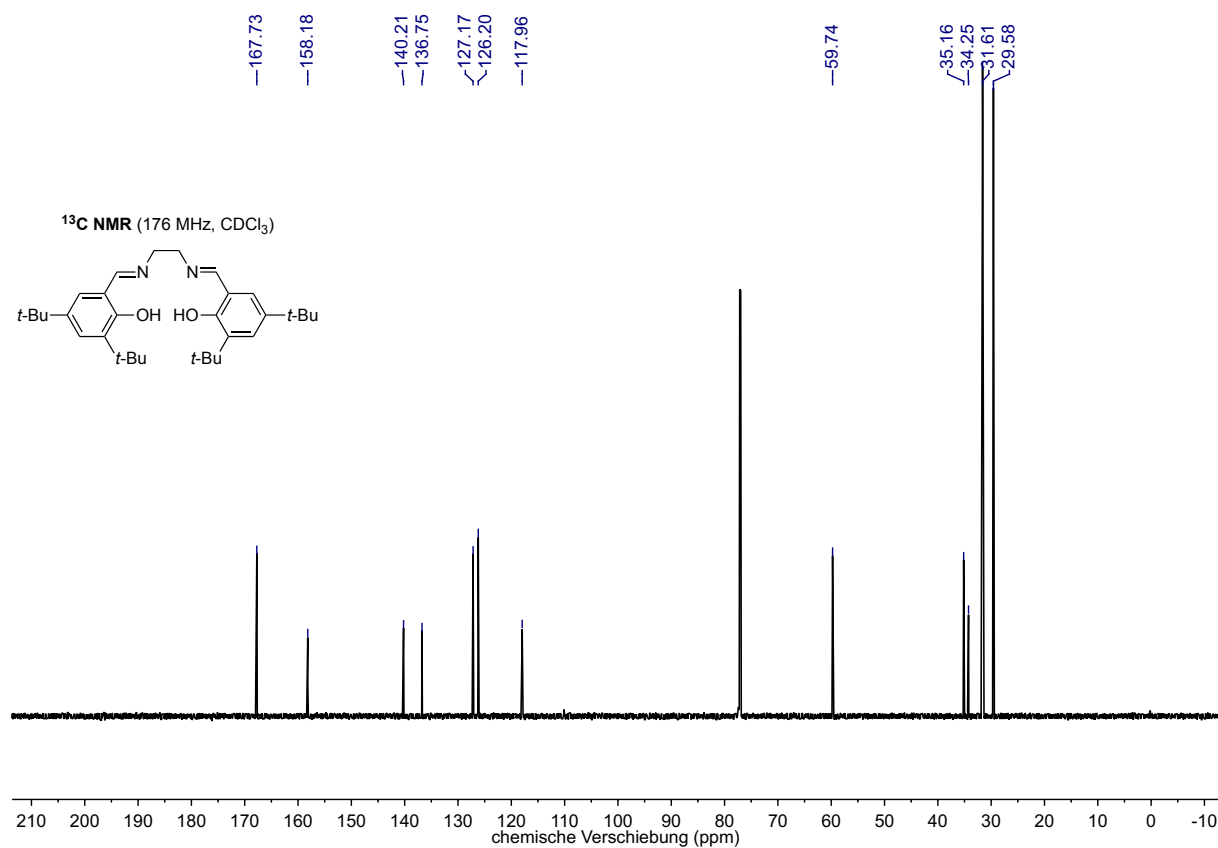
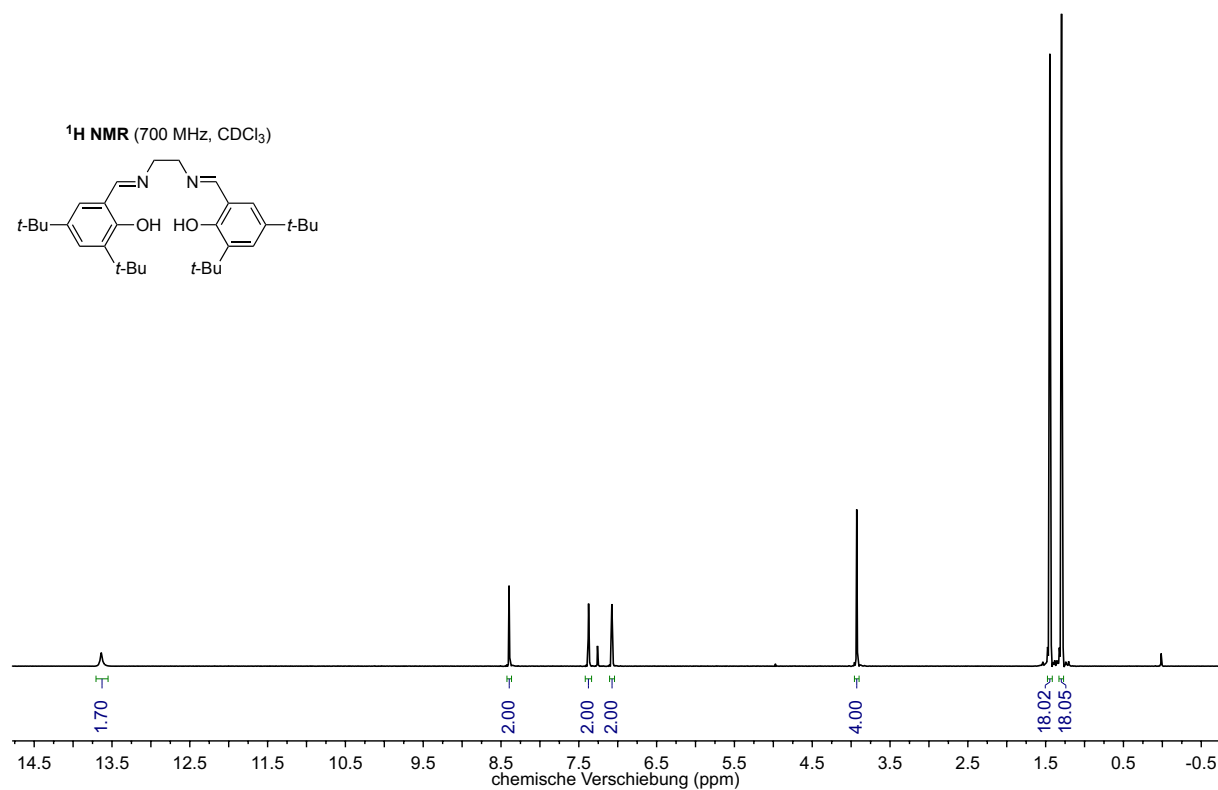
## Epoxide 41



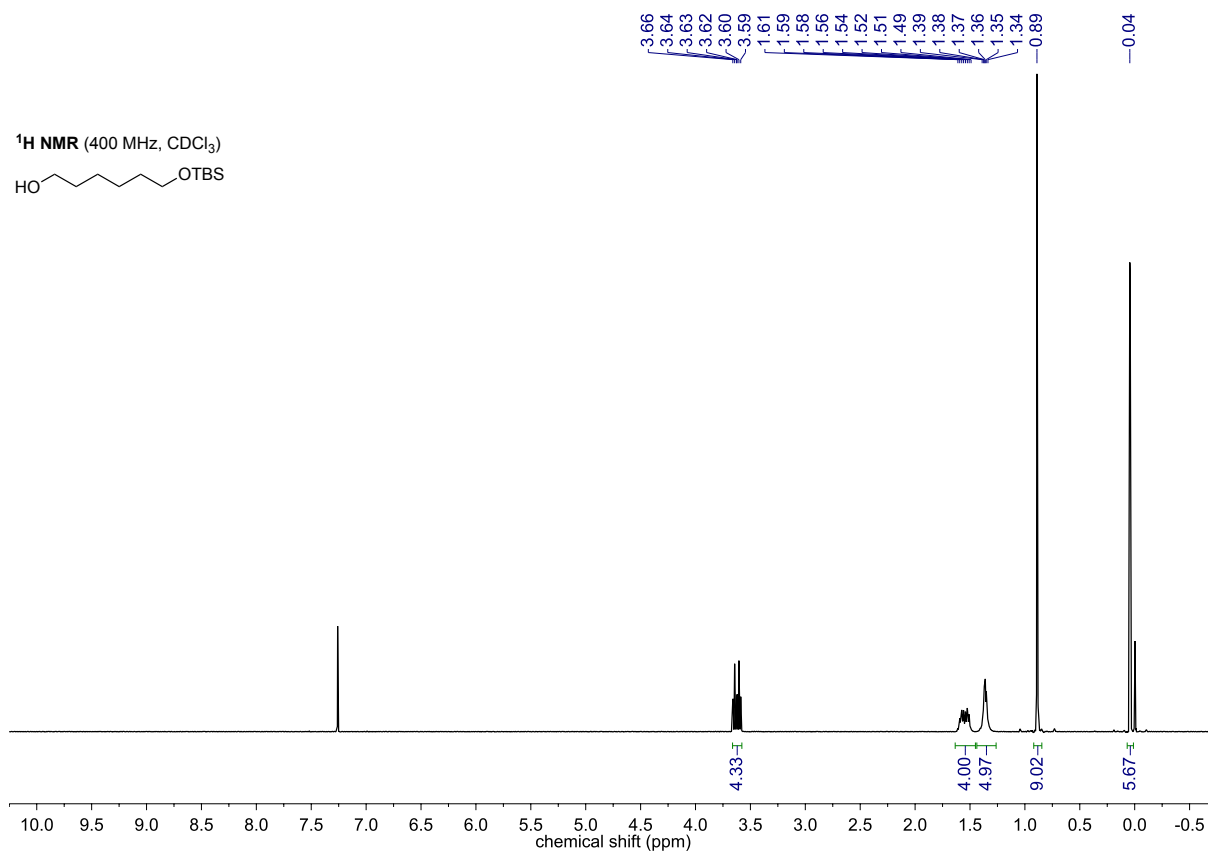
## Aldehyde 47



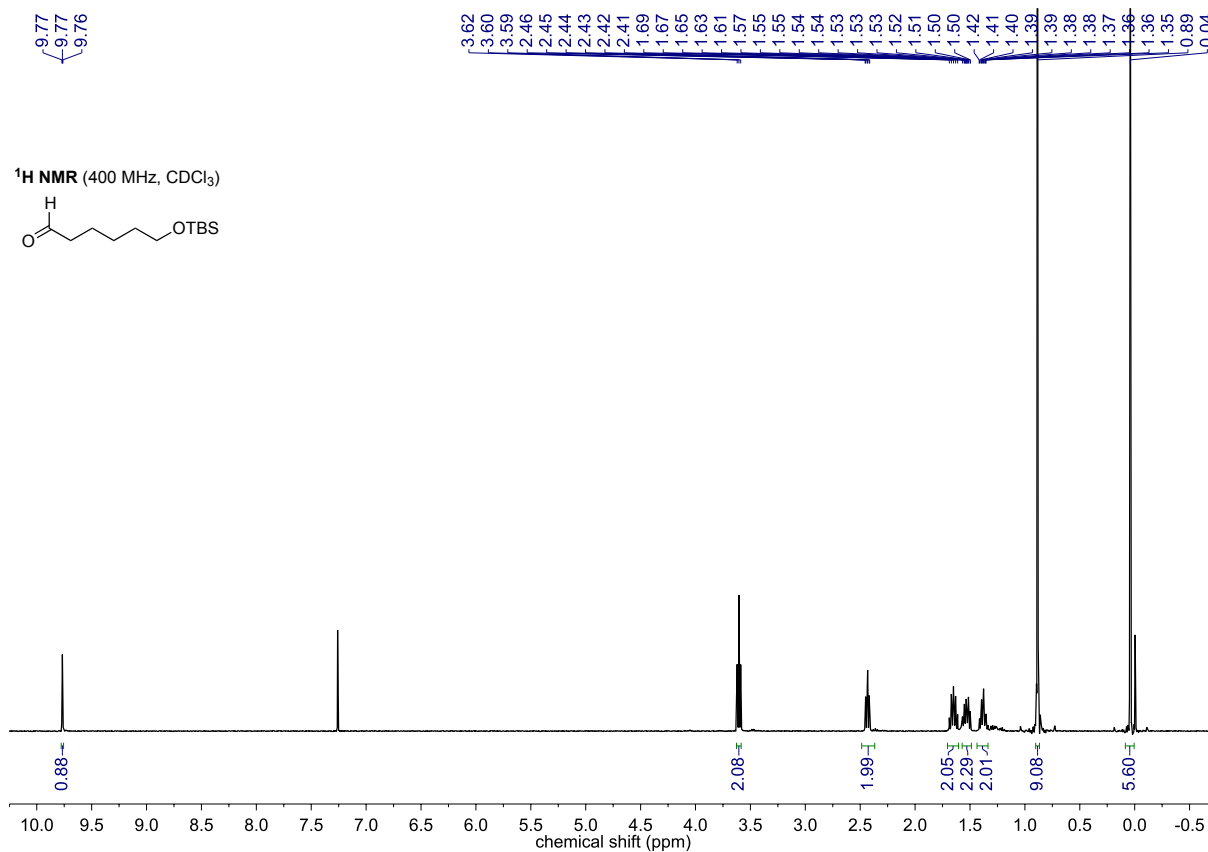
## Ligand S1



## Alcohol S2

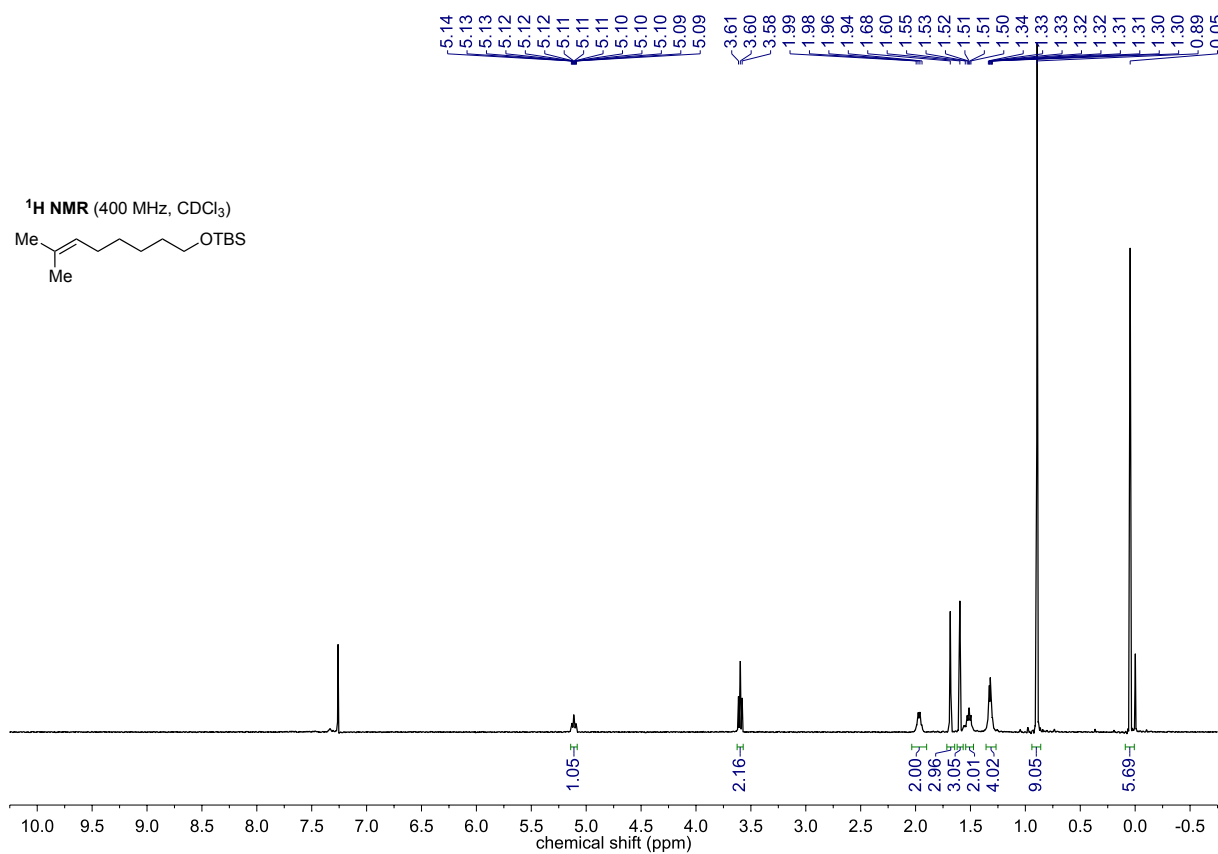


## Aldehyde 50

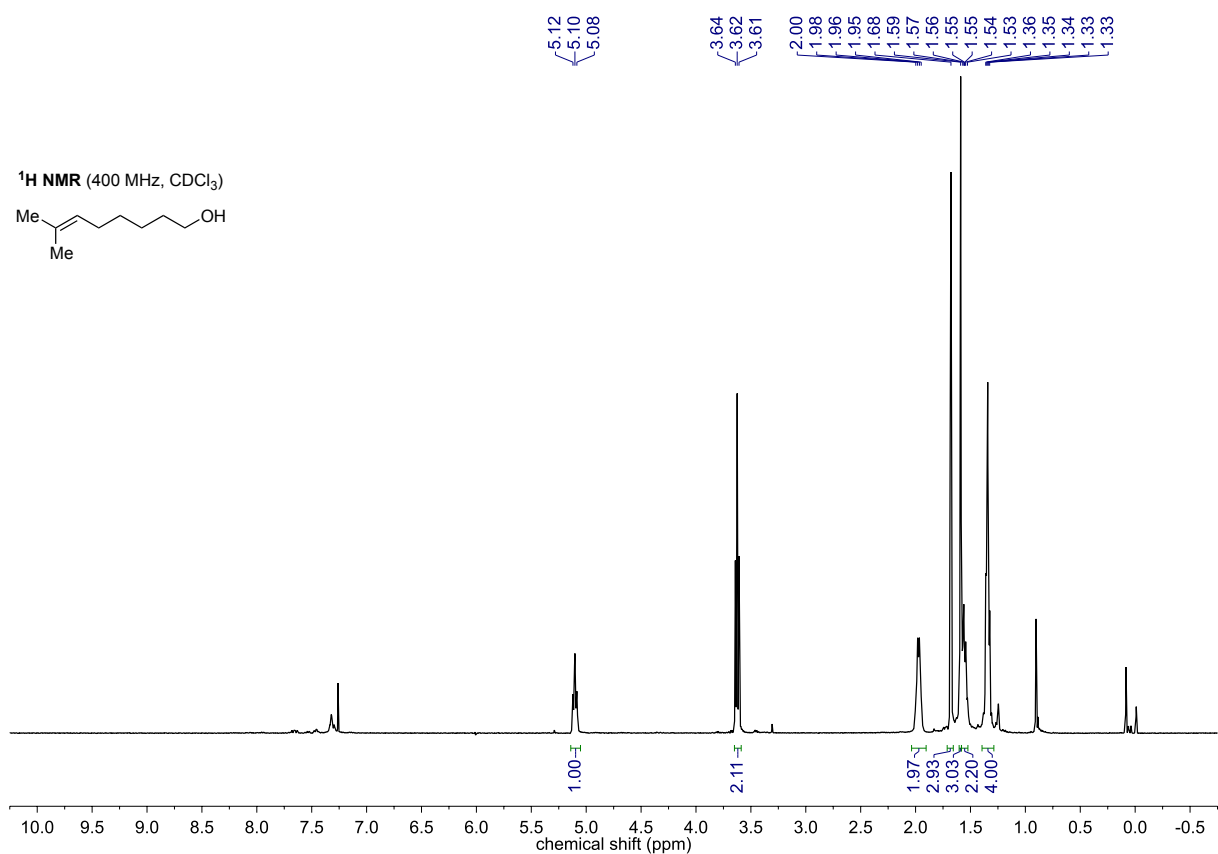




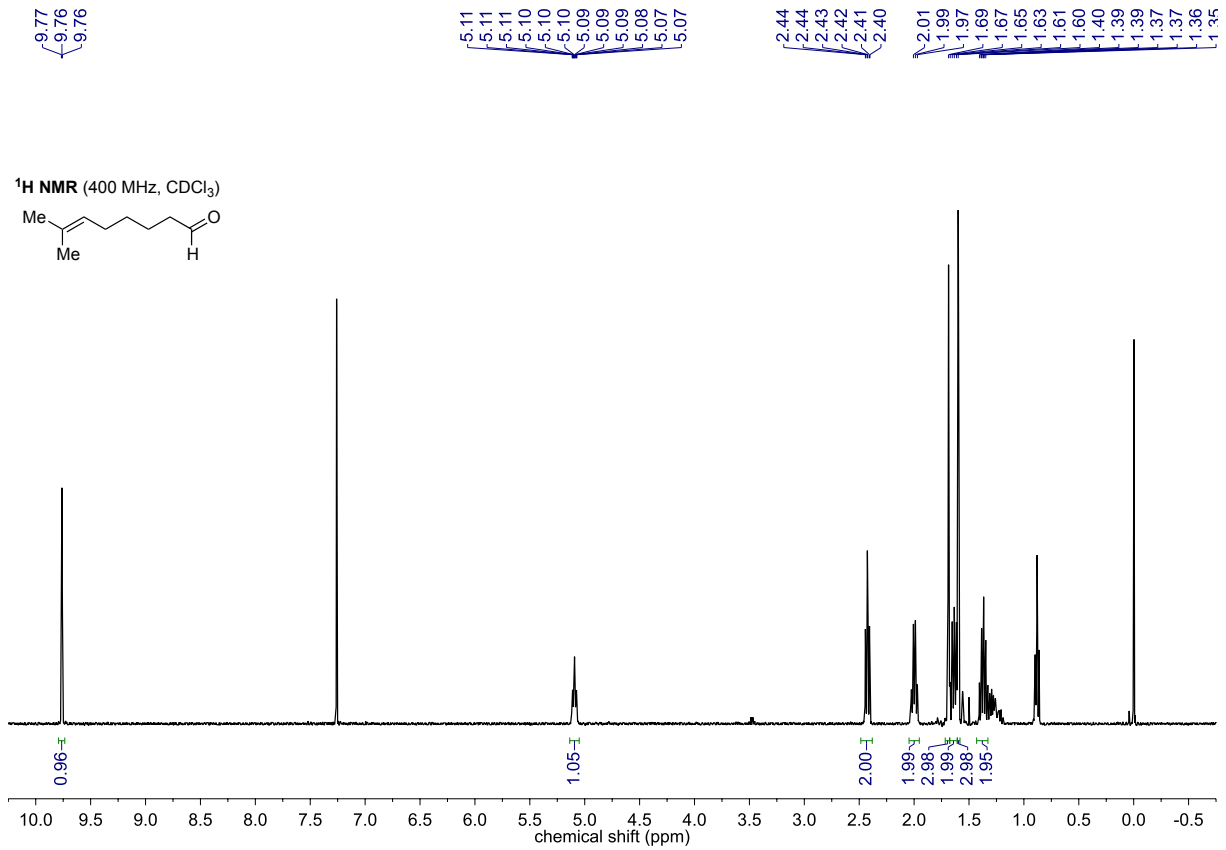
## Alkene S3



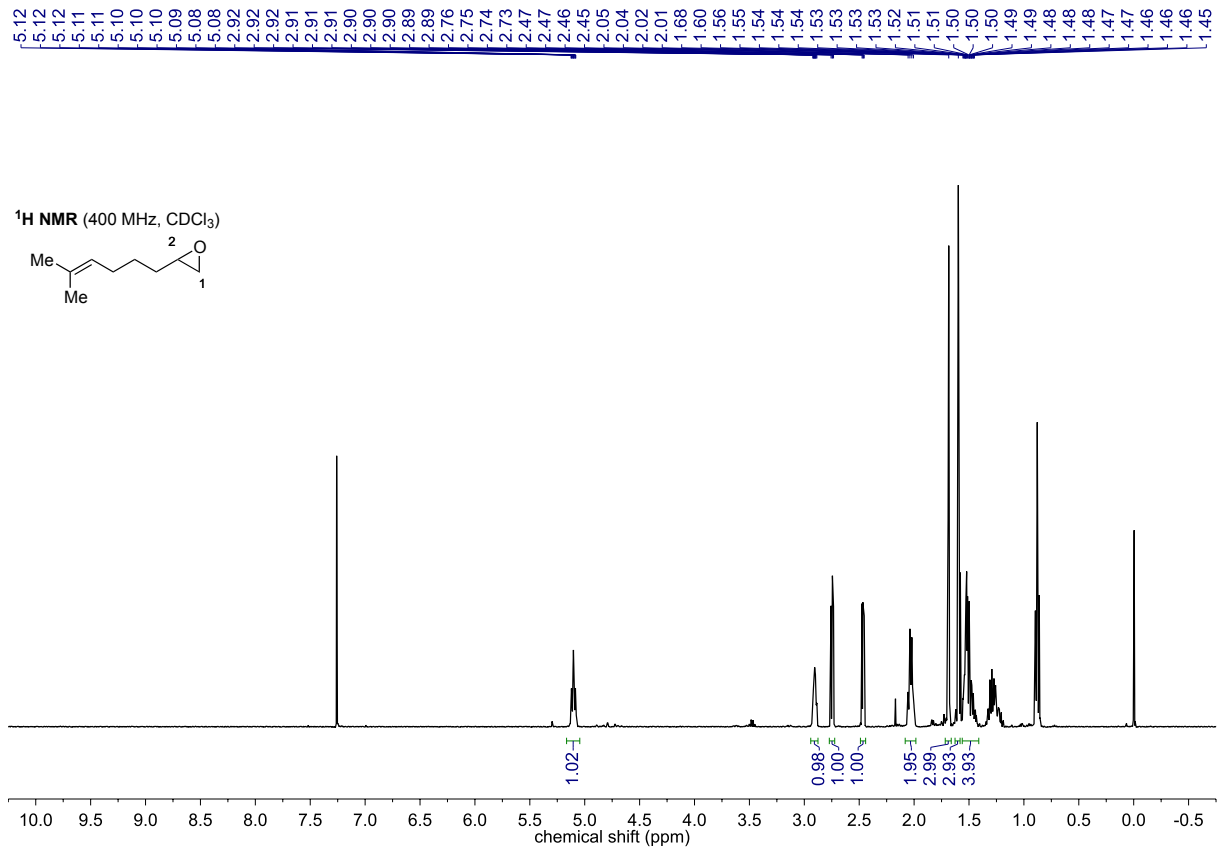
## Alcohol S4



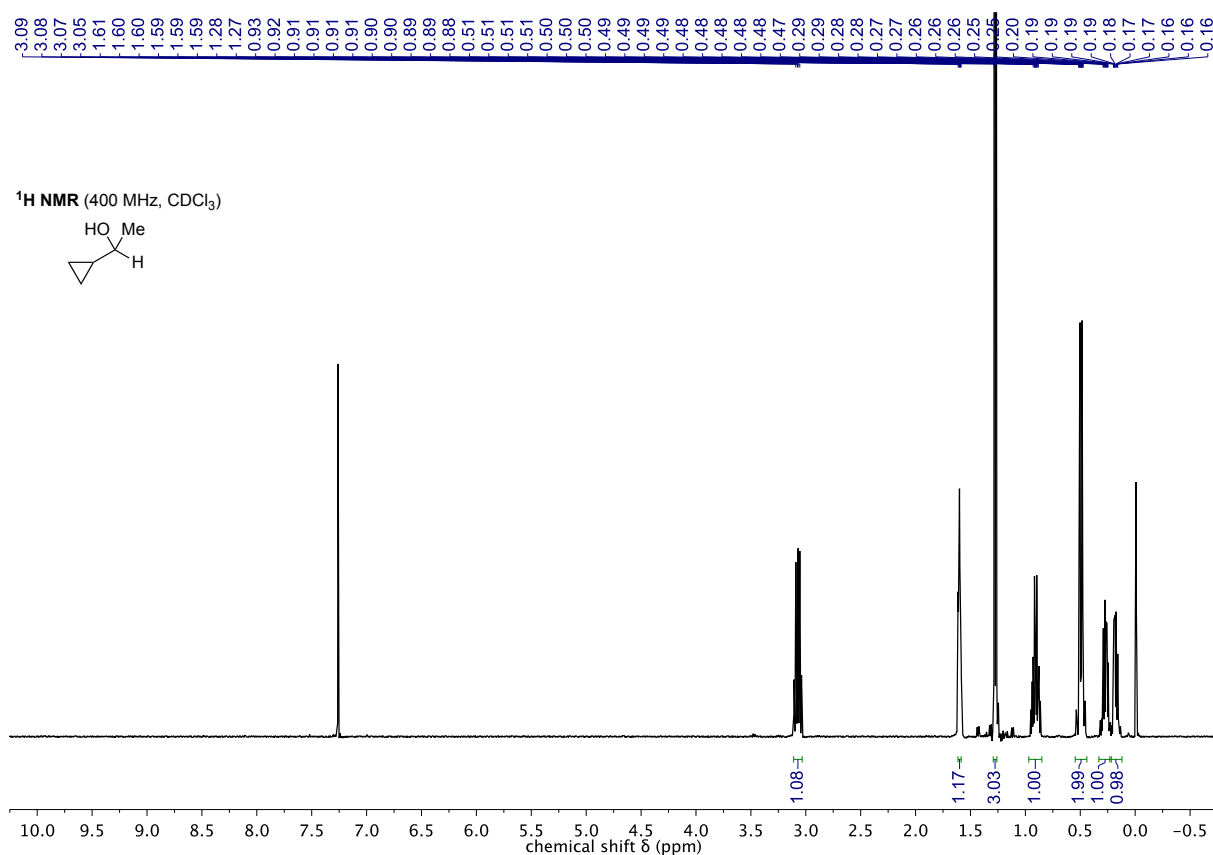
## Aldehyde 51



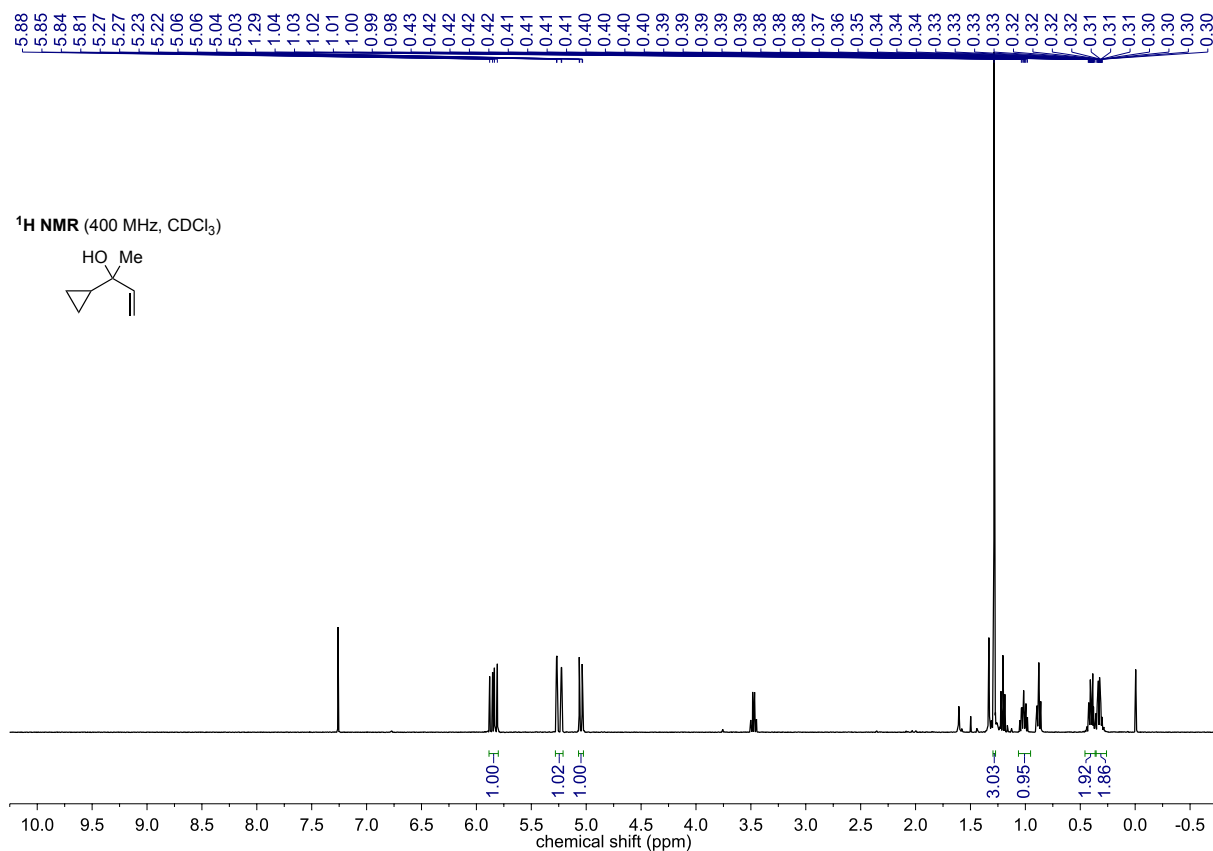
## Epoxide 42



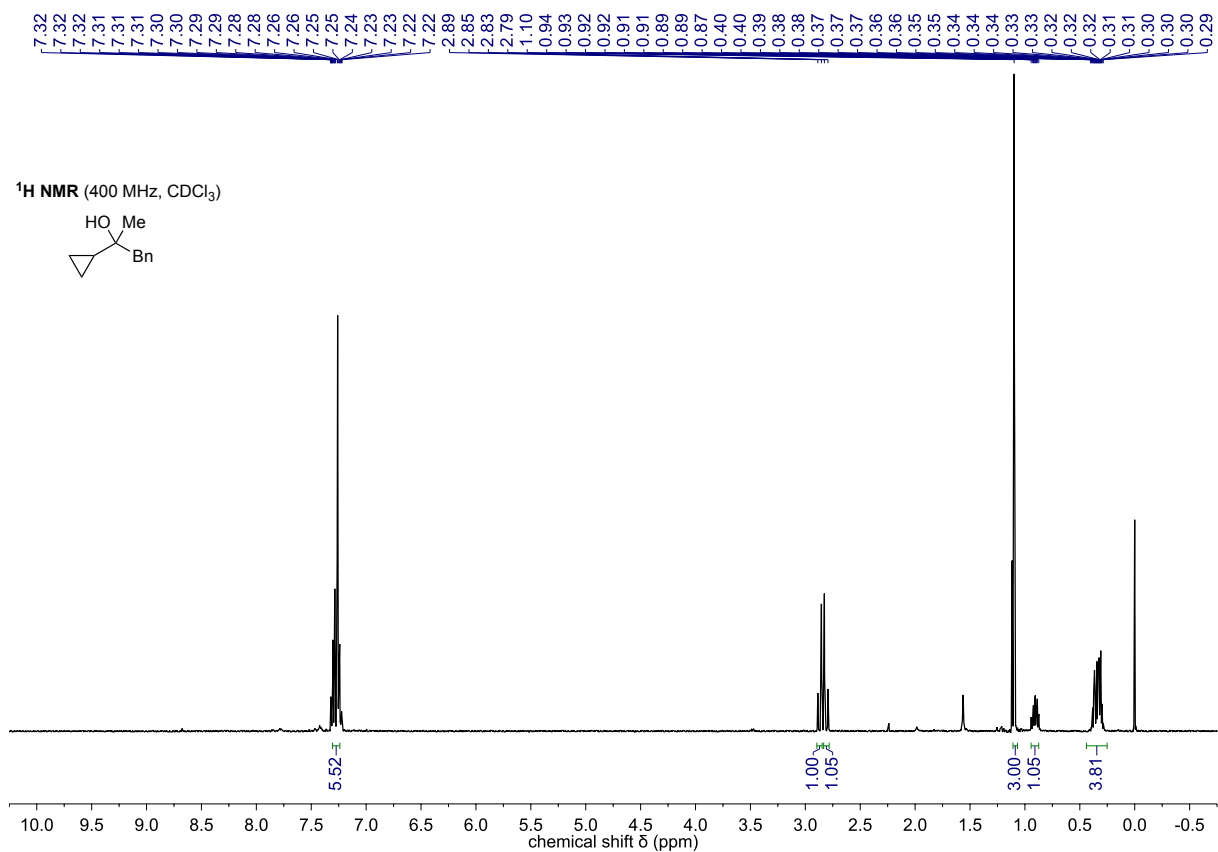
## Cyclopropylcarbinol 58



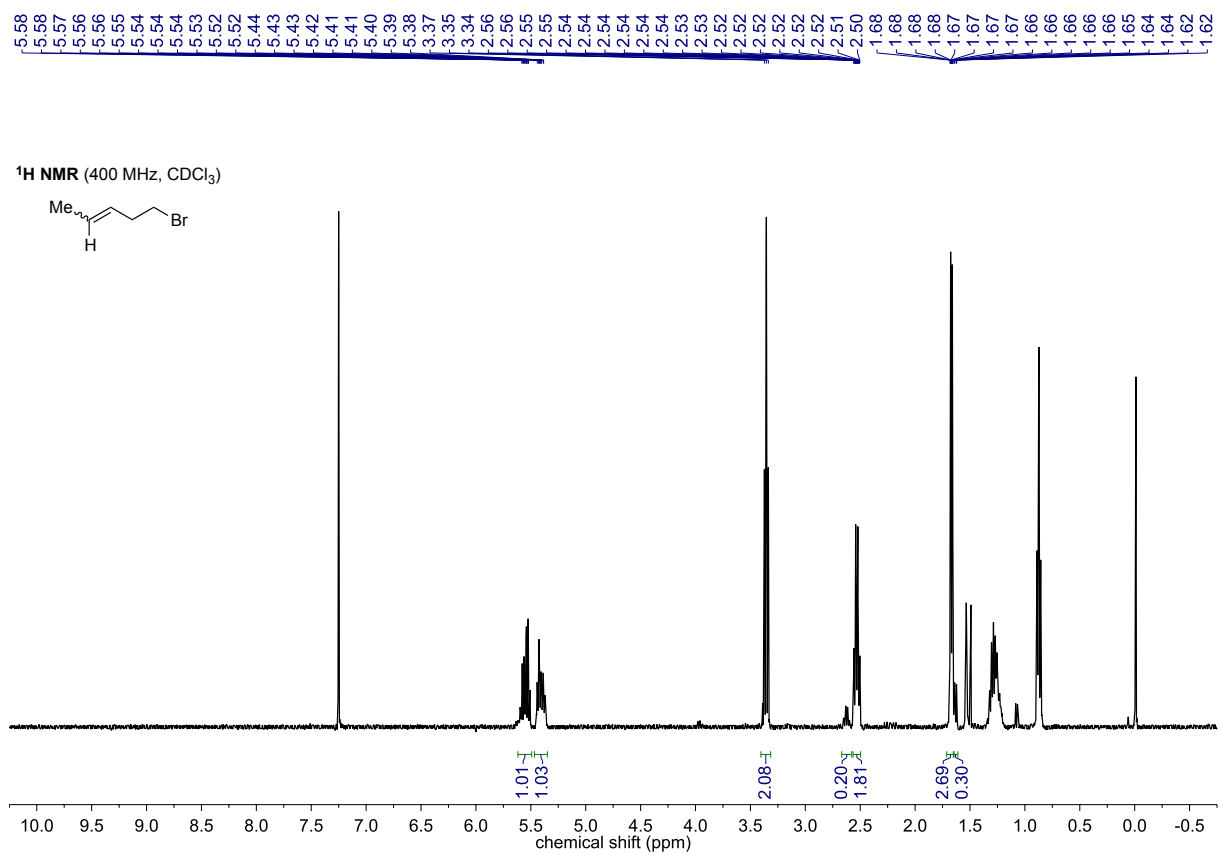
## Cyclopropylcarbinol 59



## Cyclopropylcarbinol 60

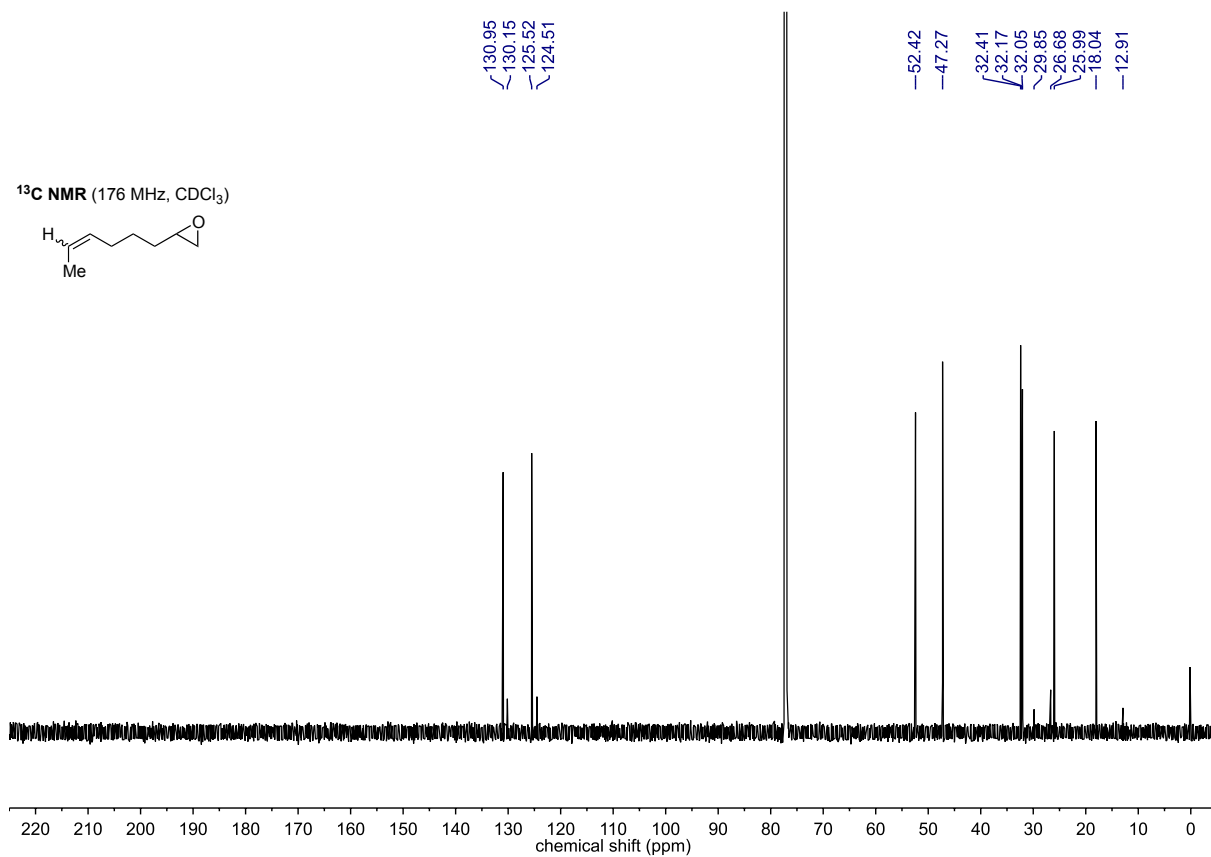
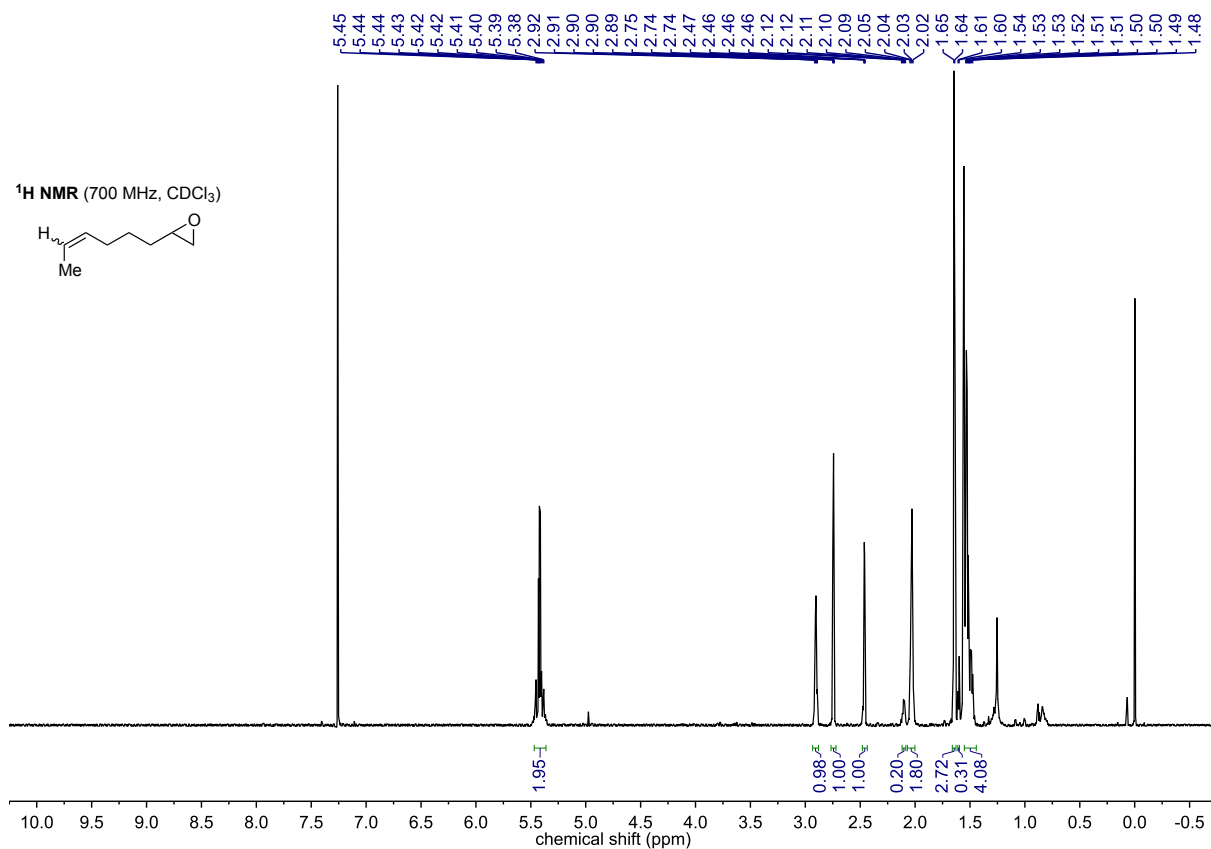


## Bromide 55





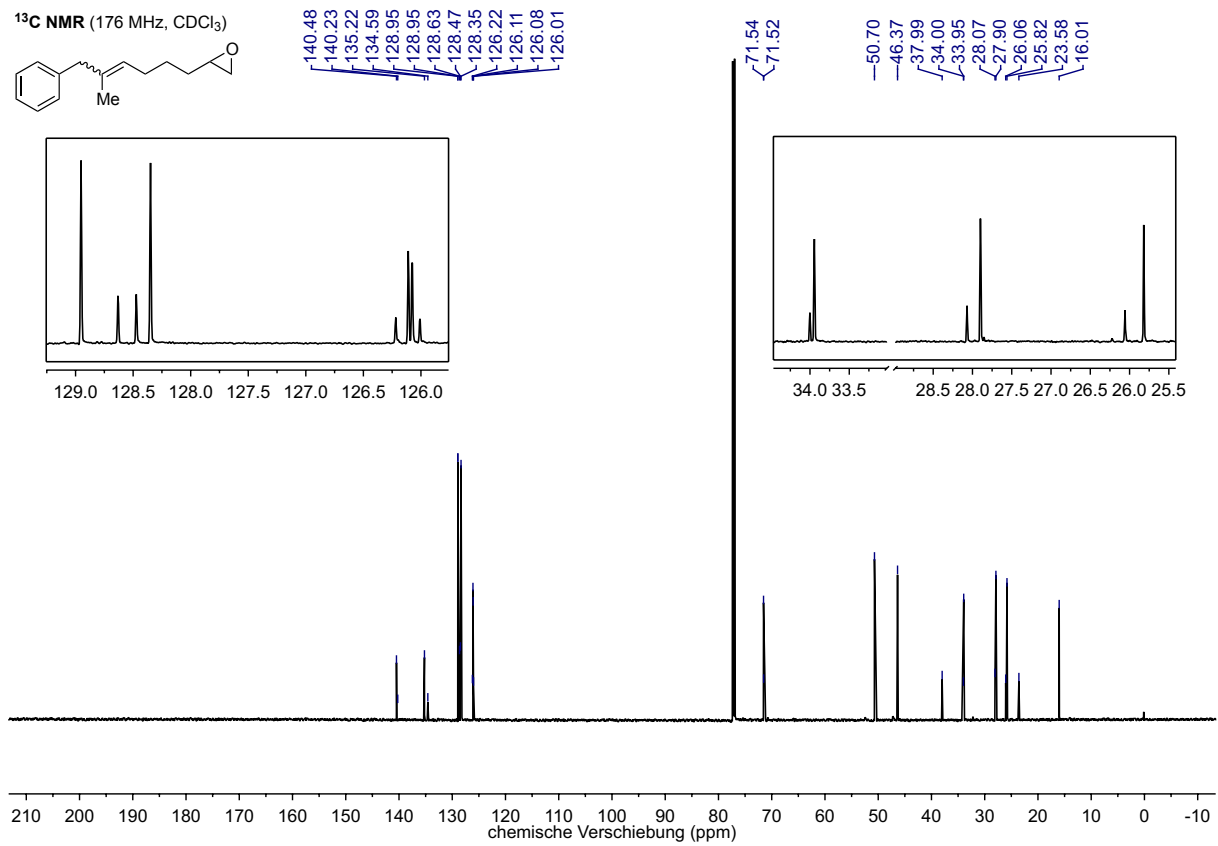
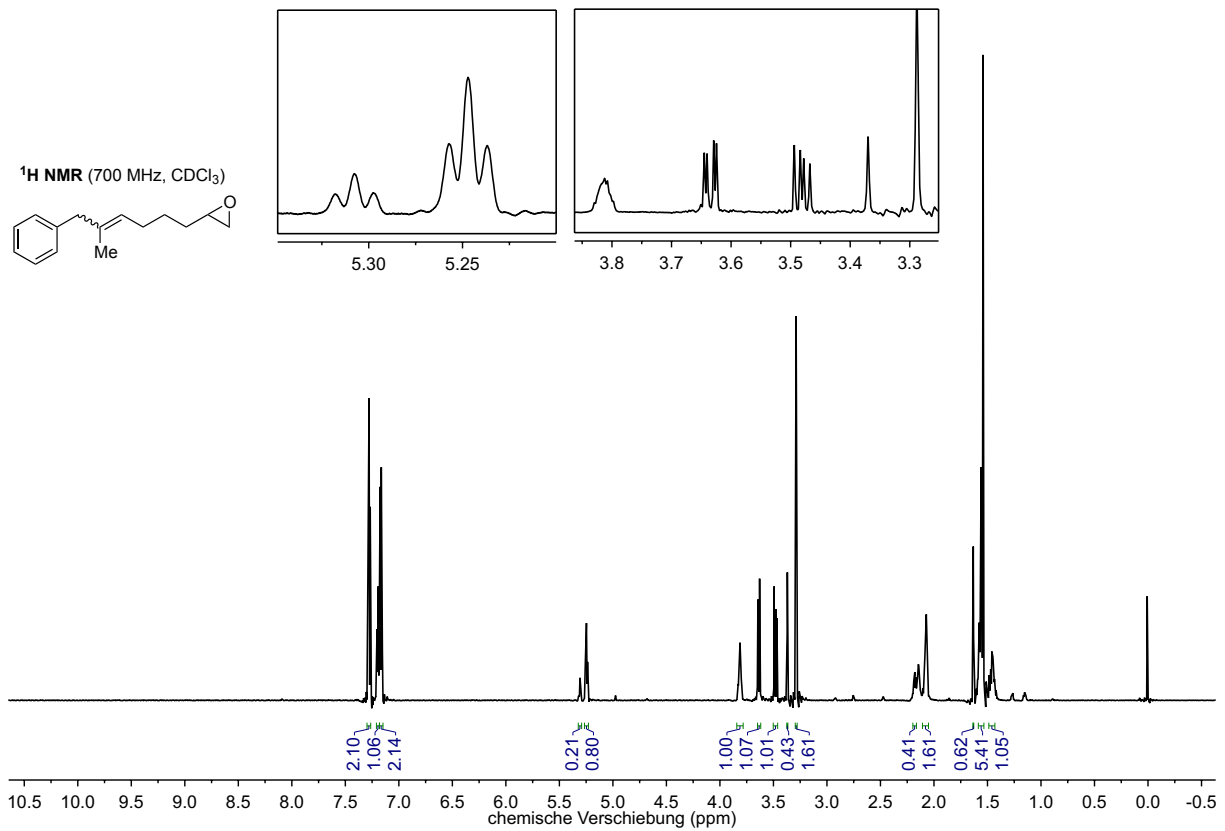
## Epoxide 64



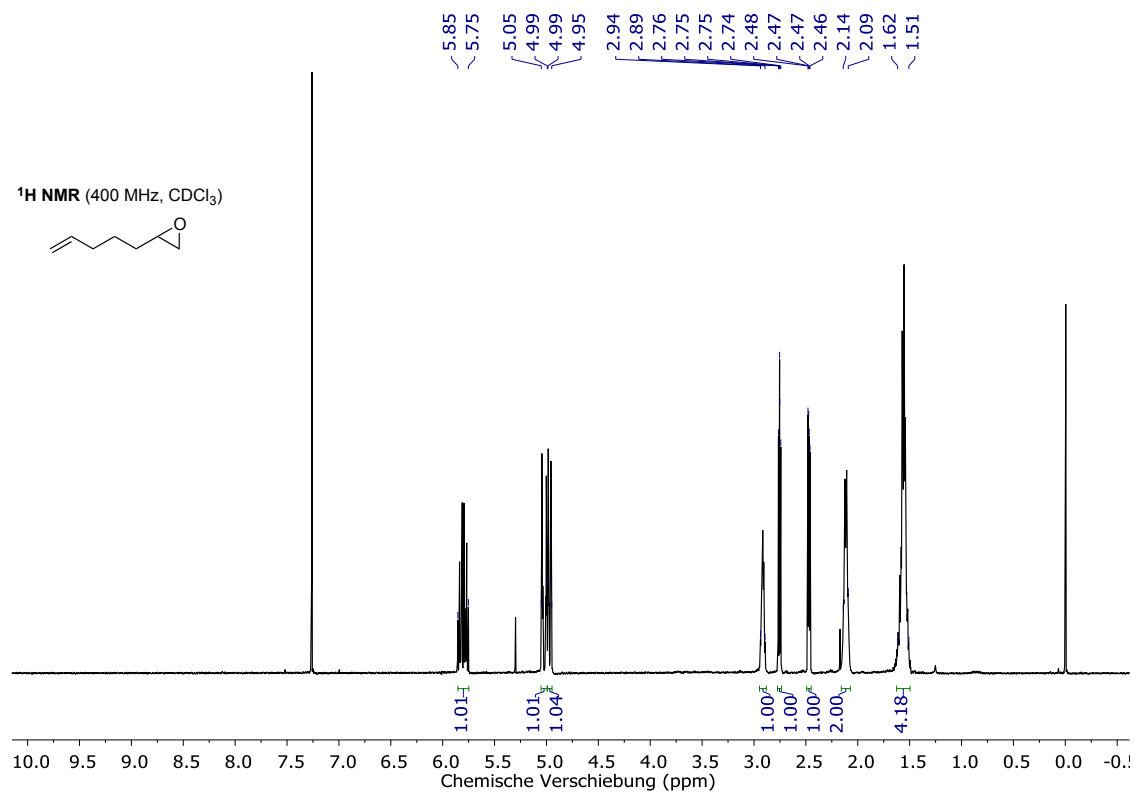




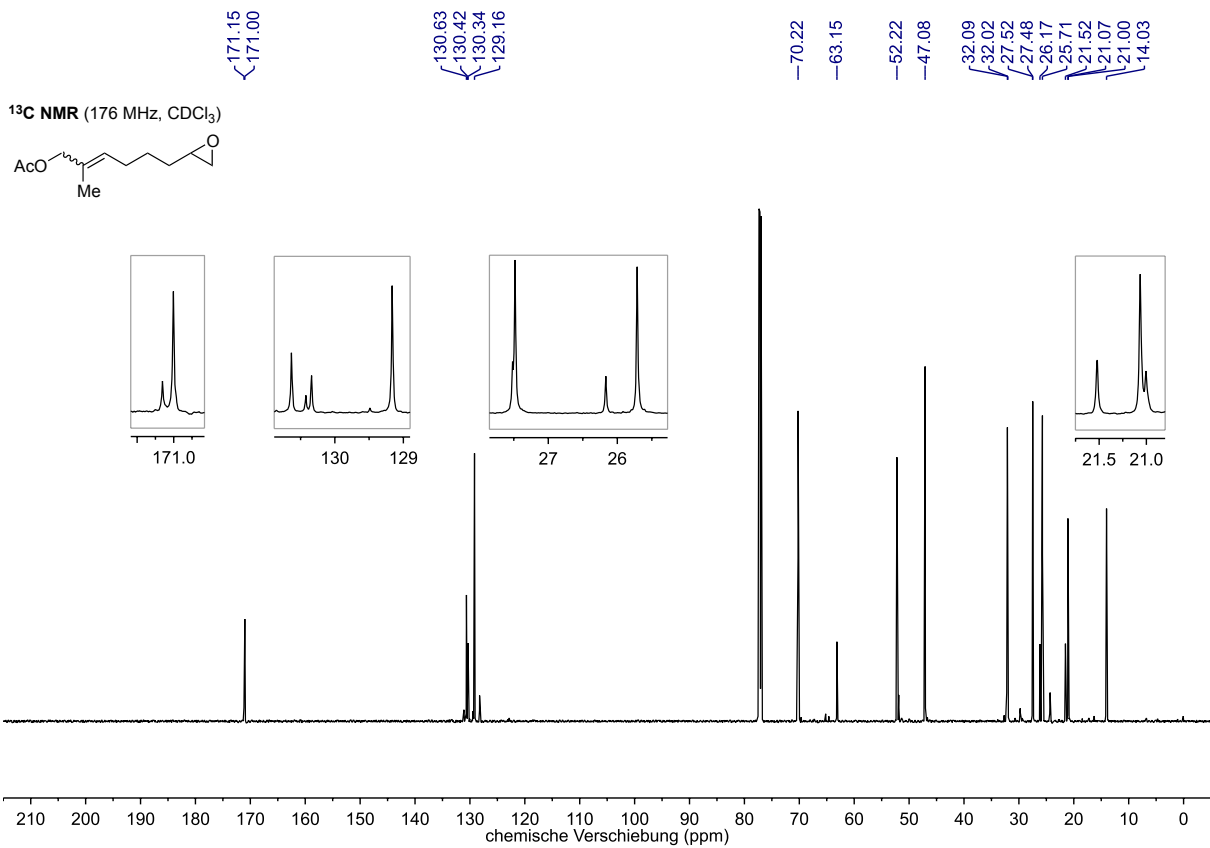
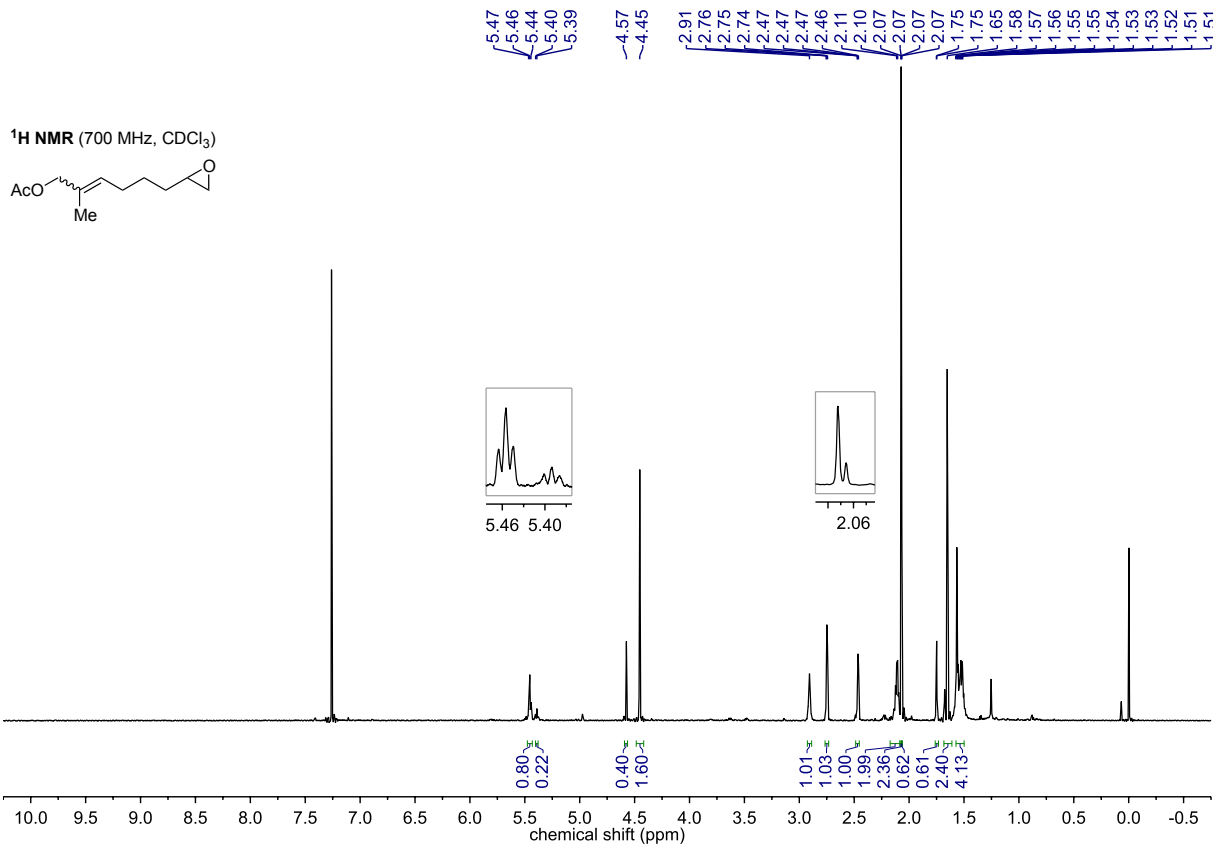
## Epoxide 66



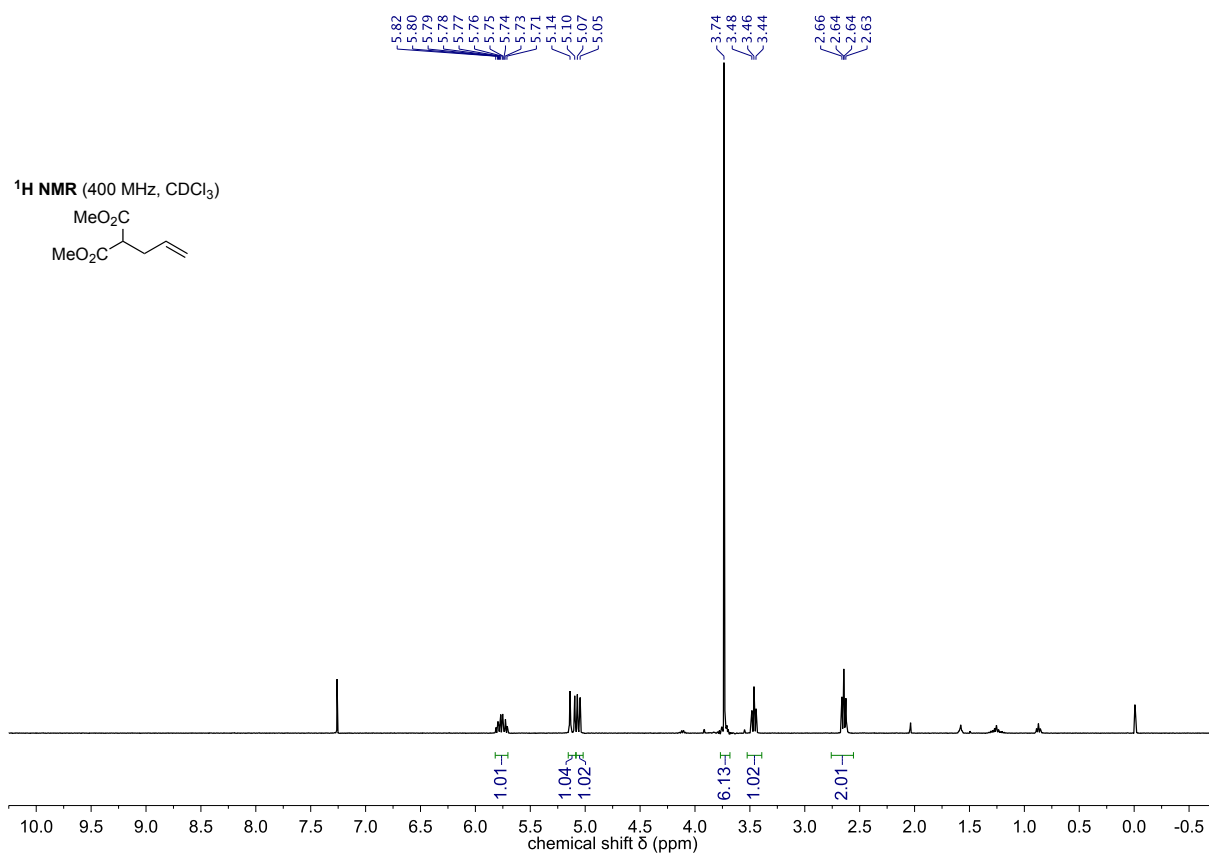
## Epoxide 67



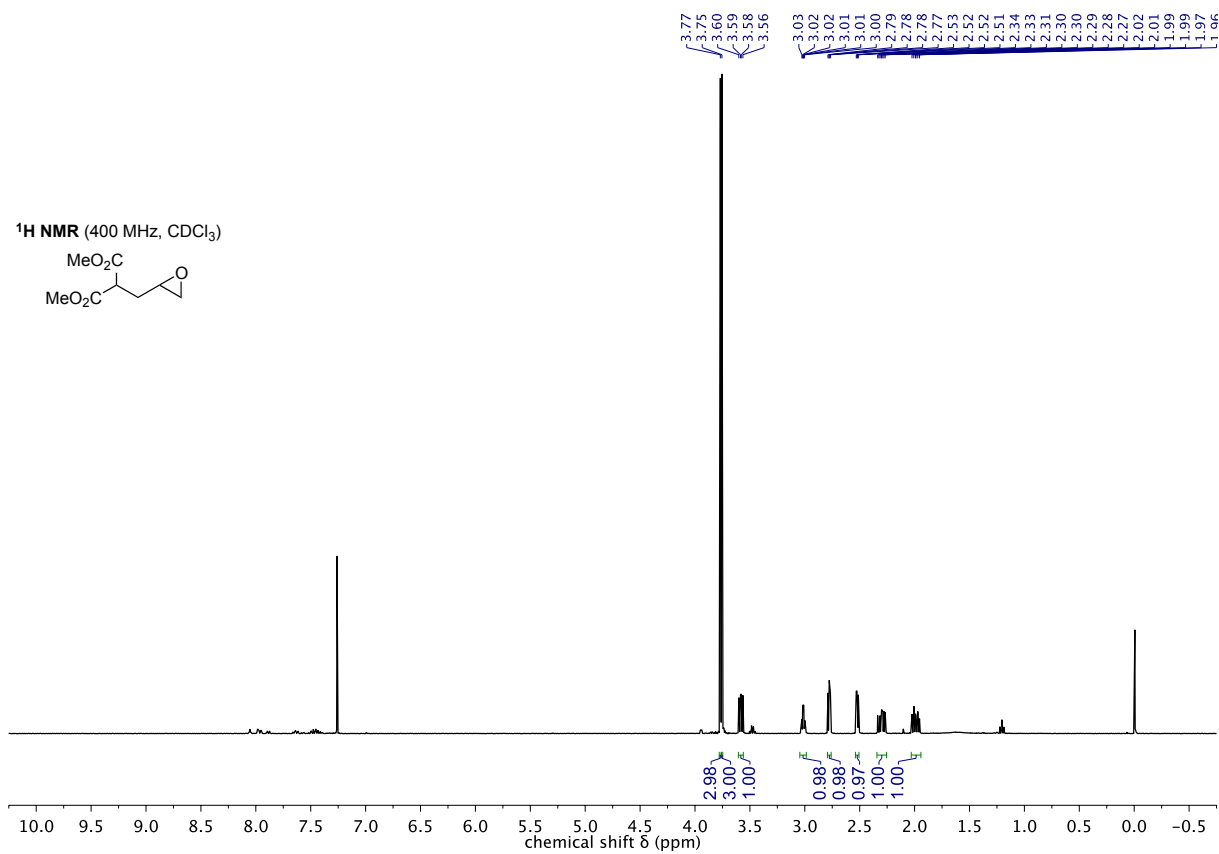
## Acetate 71



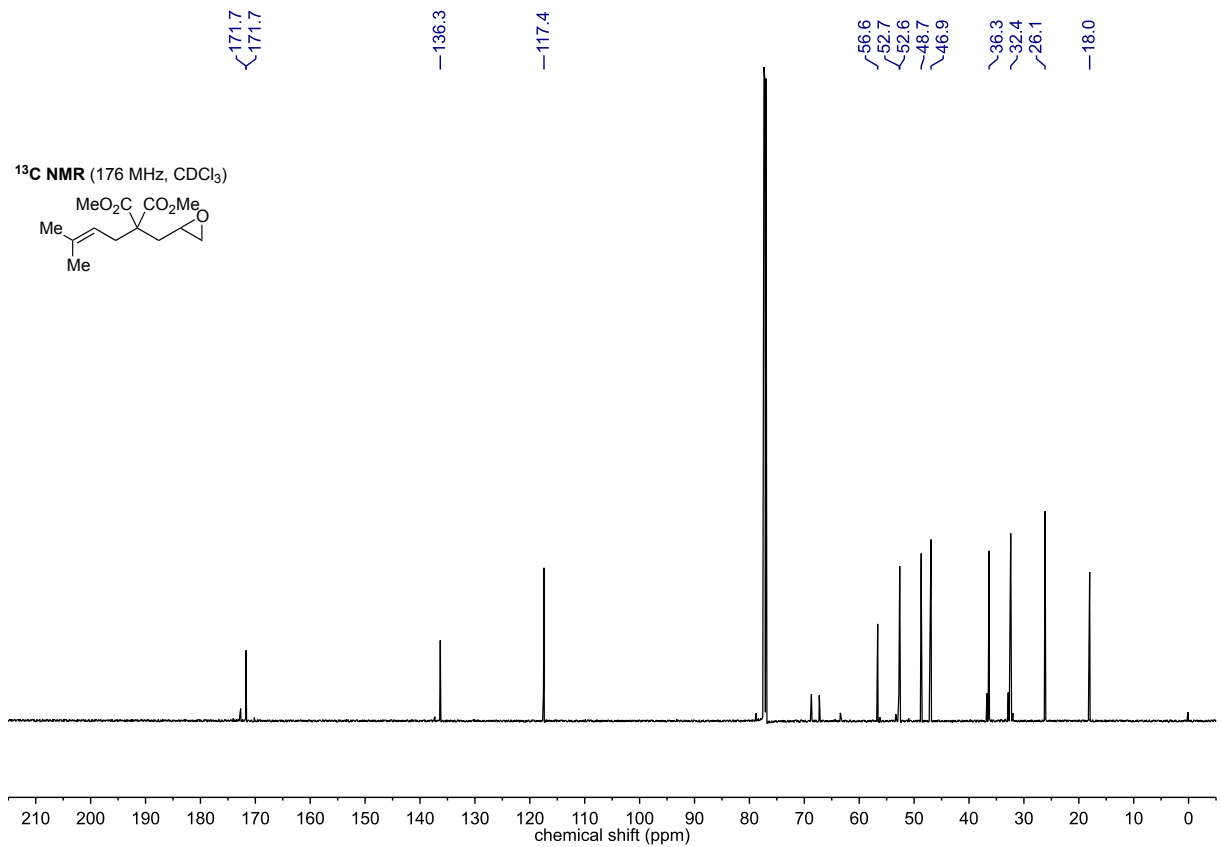
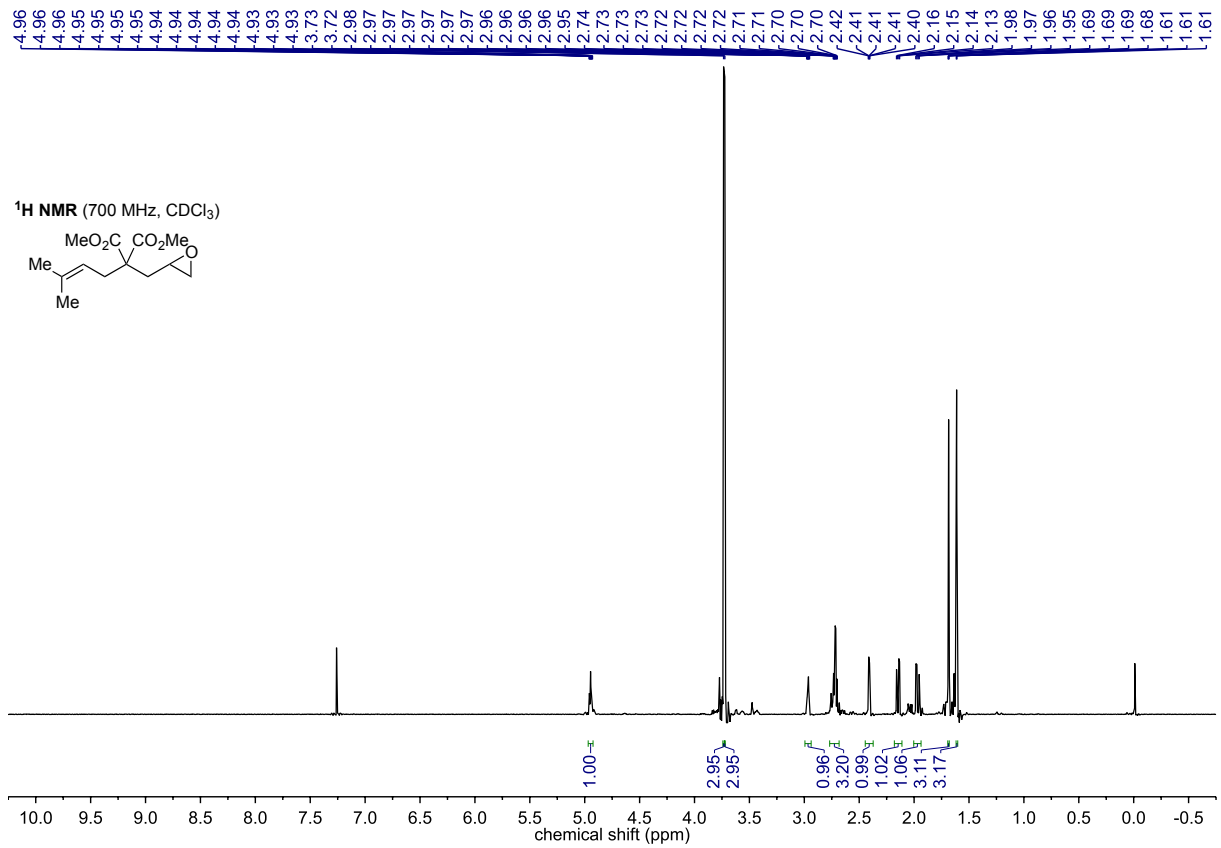
## Alkene 76



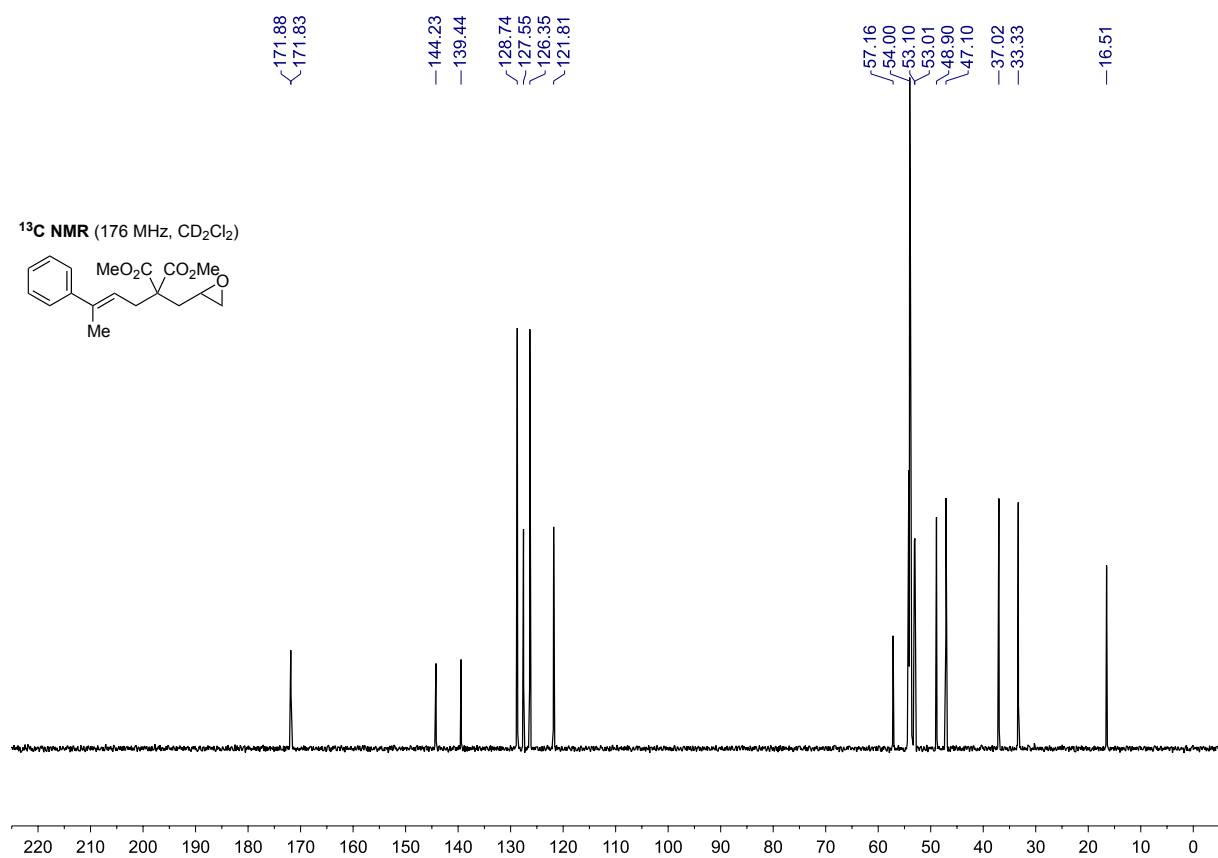
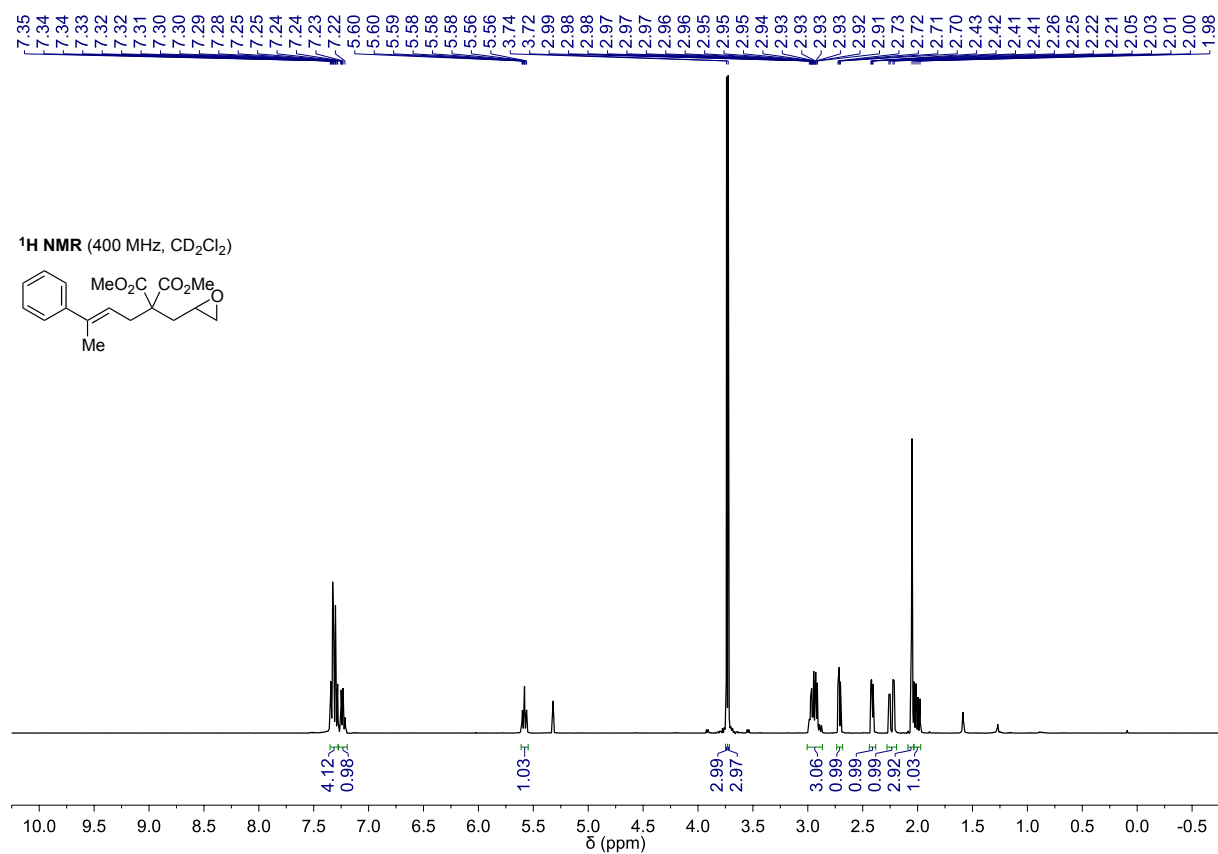
## Epoxide 77



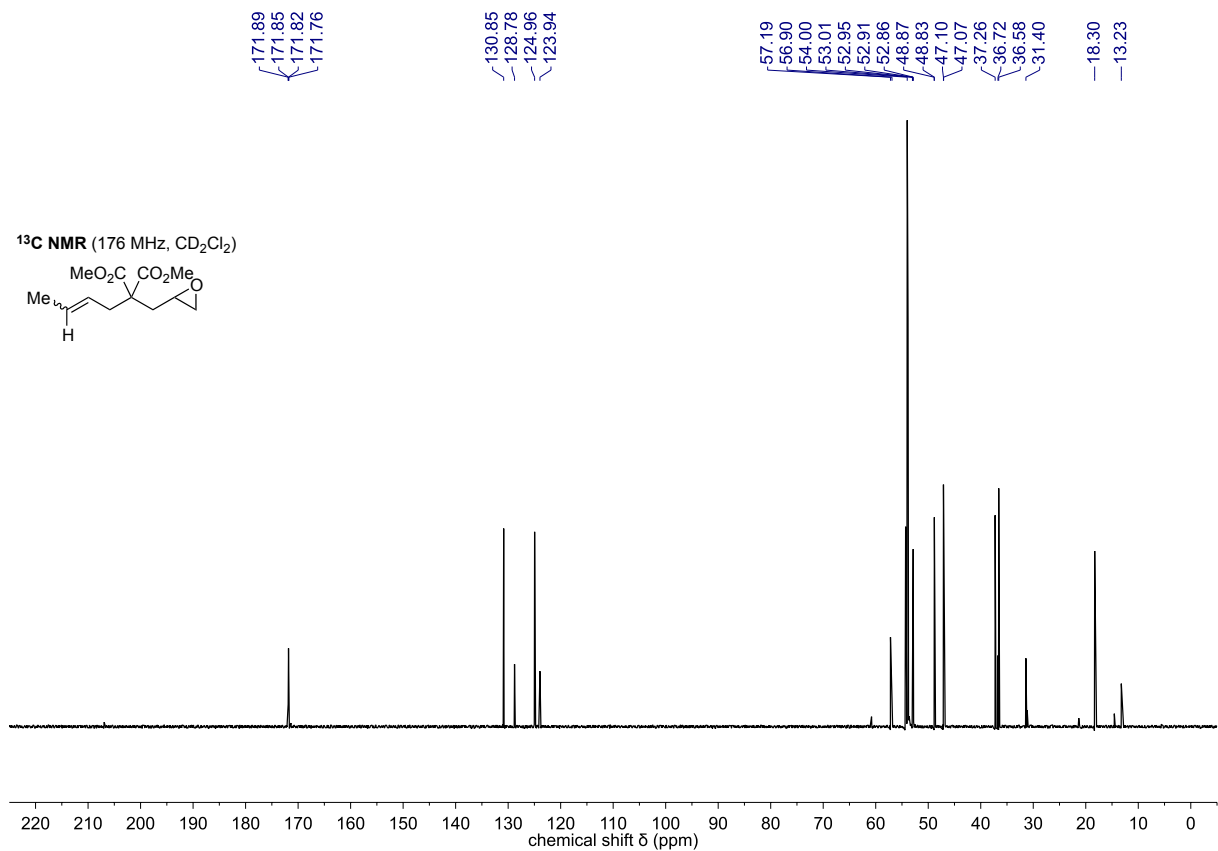
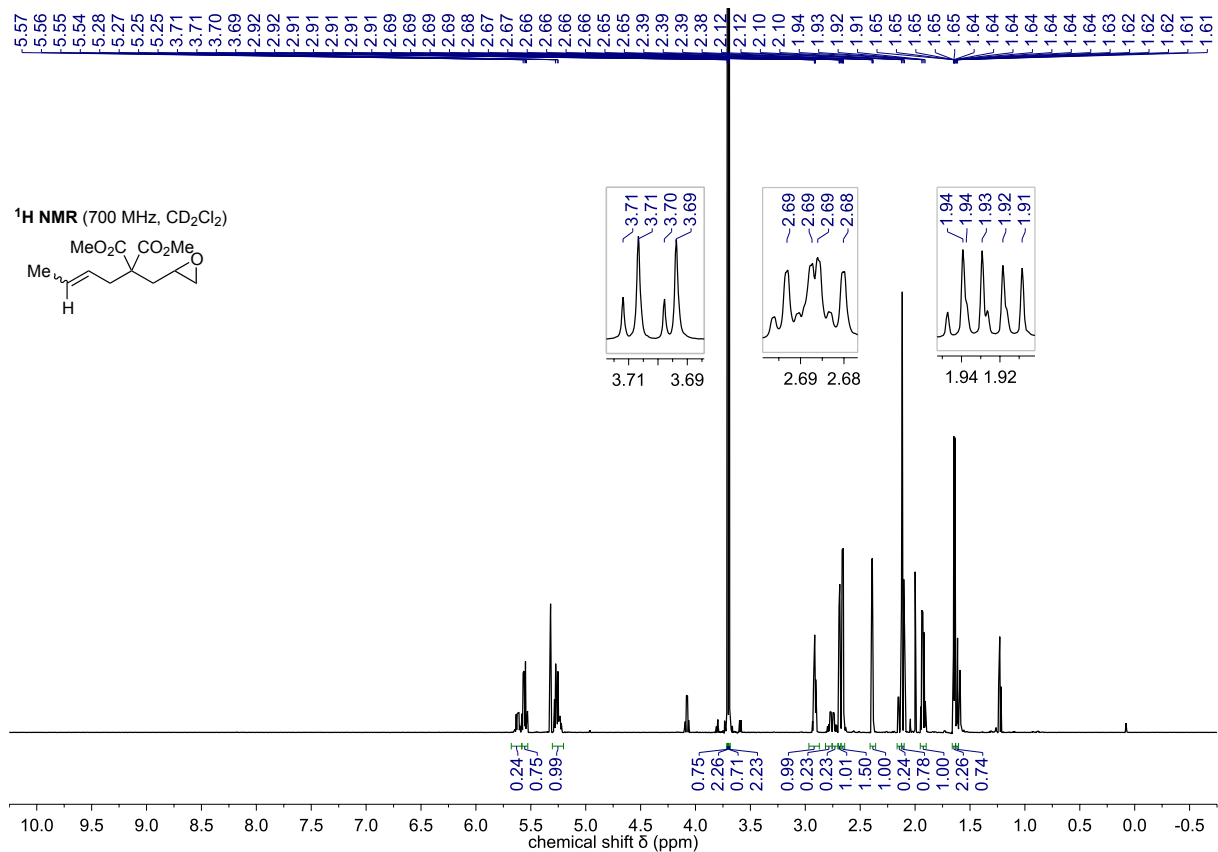
## Epoxide 78



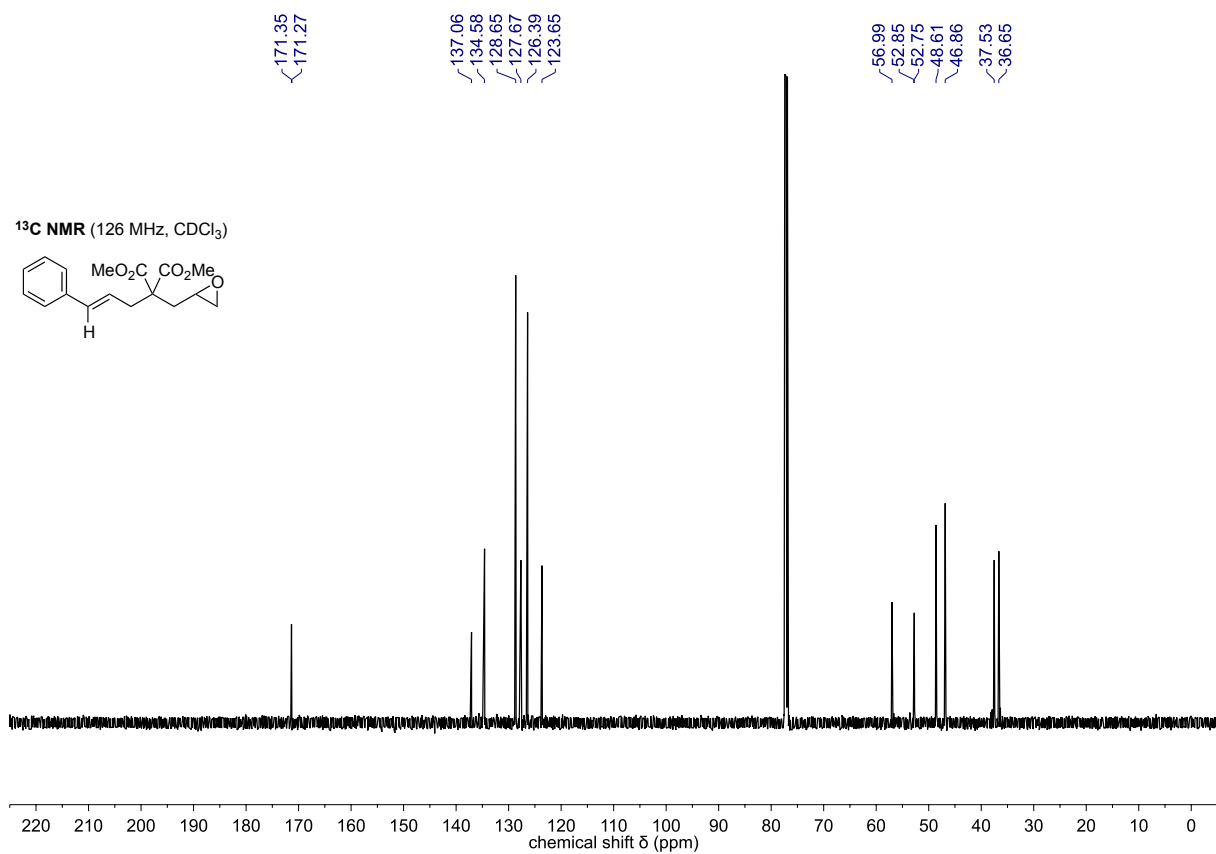
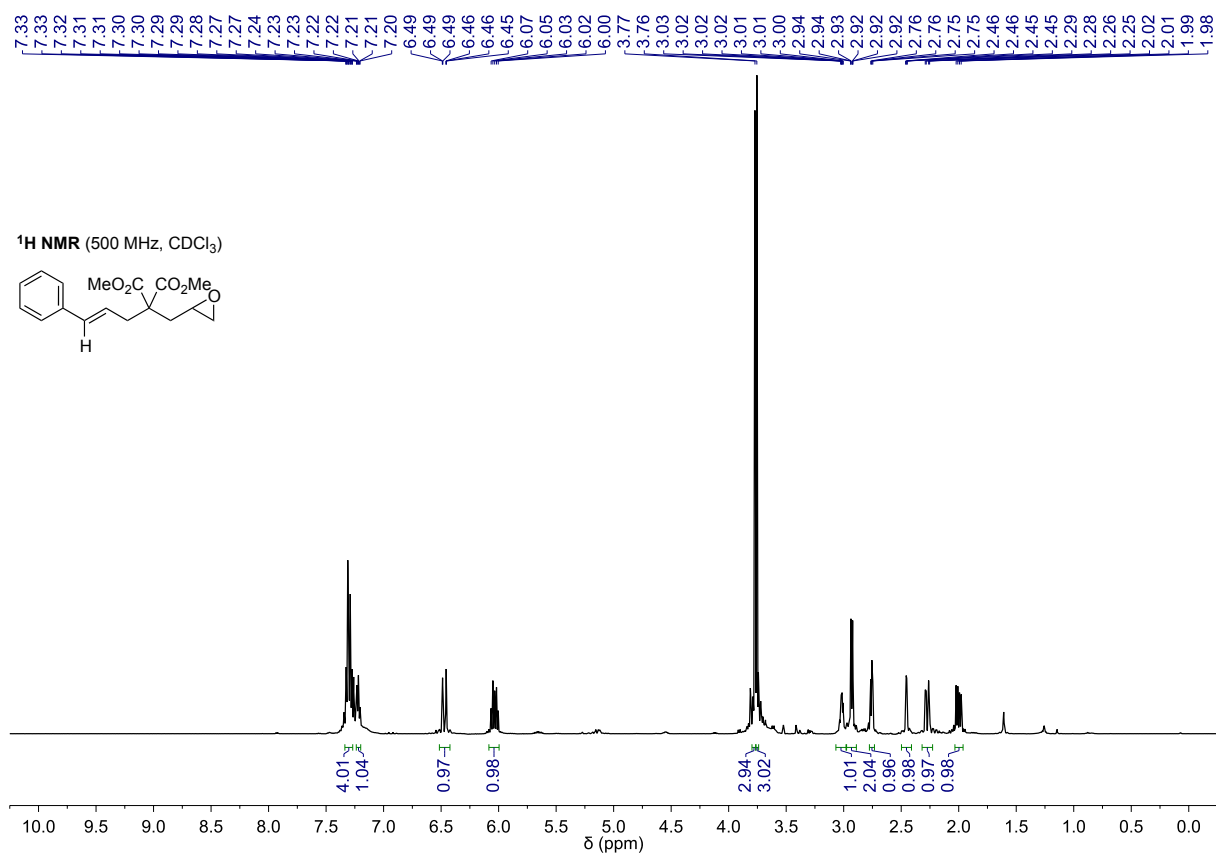
## Epoxide 79



## Epoxide 80

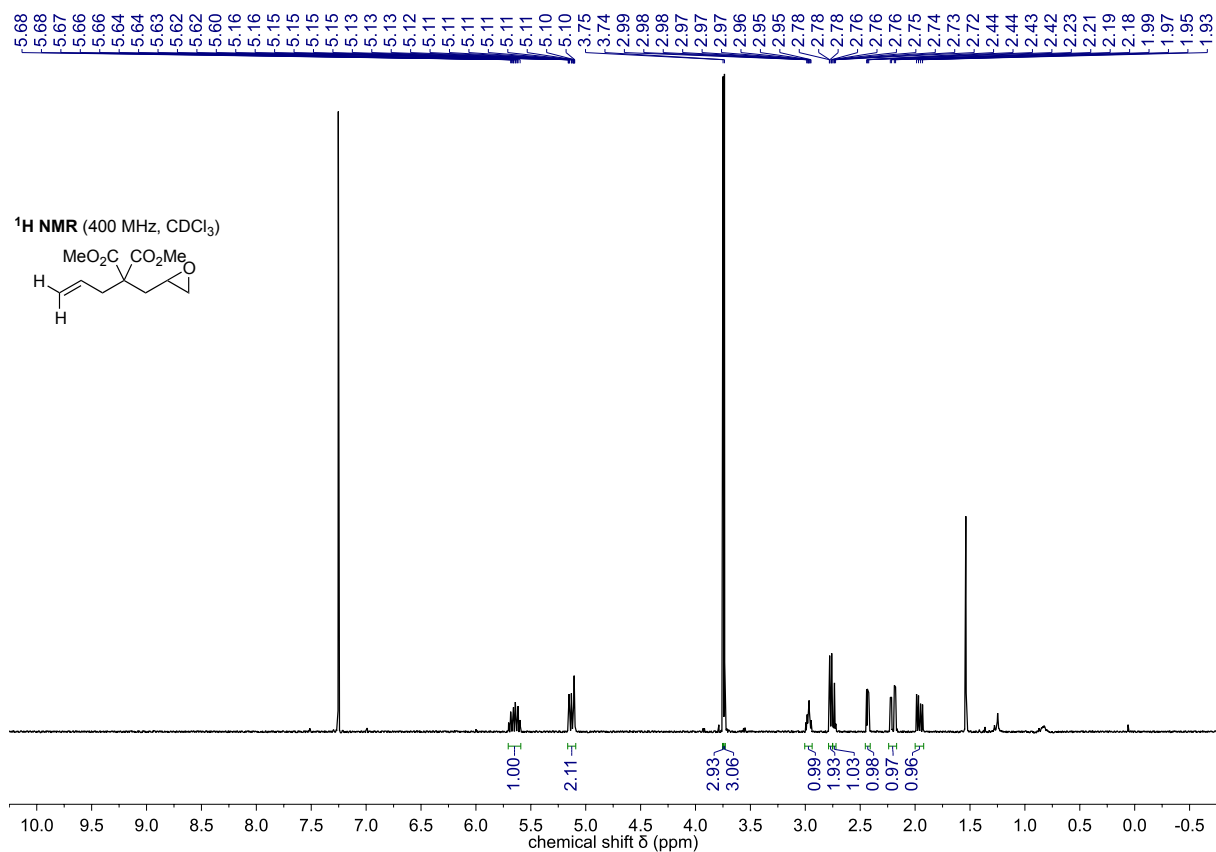


## Epoxide 81

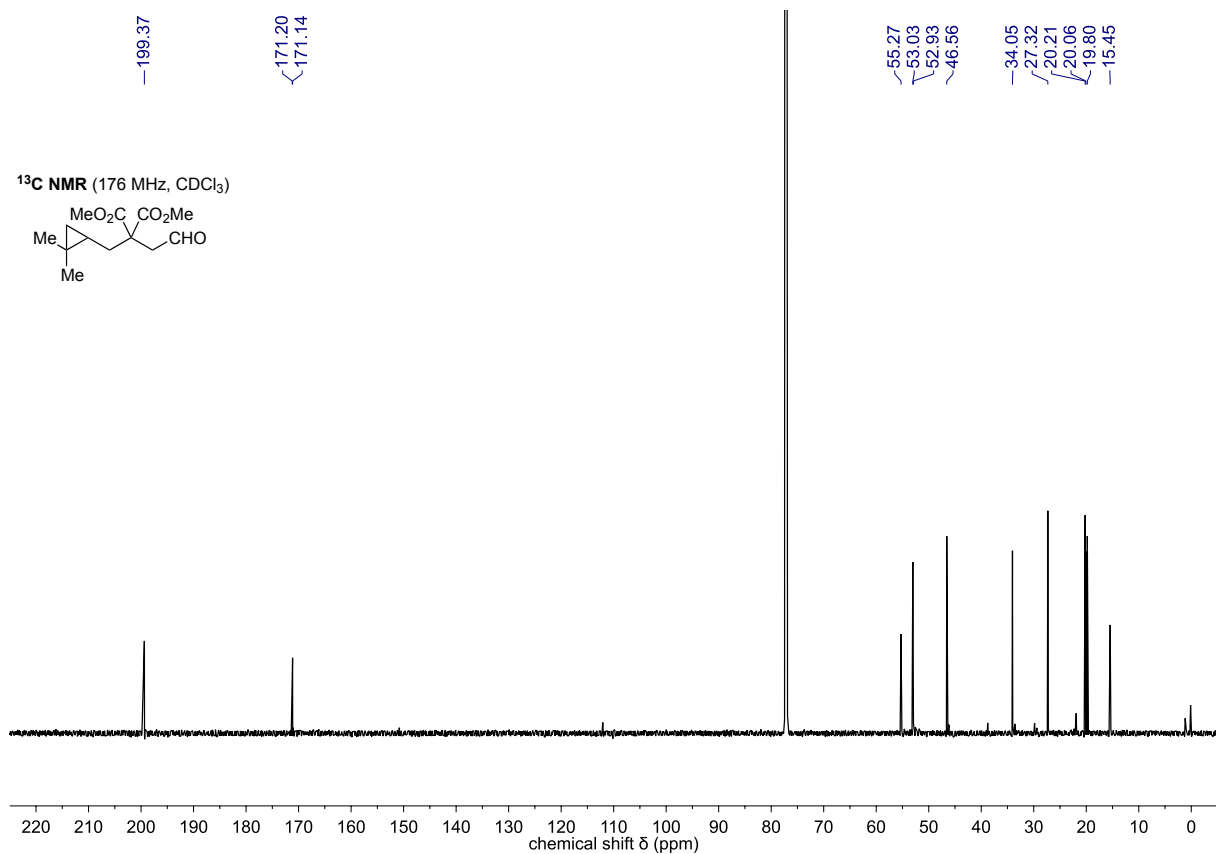
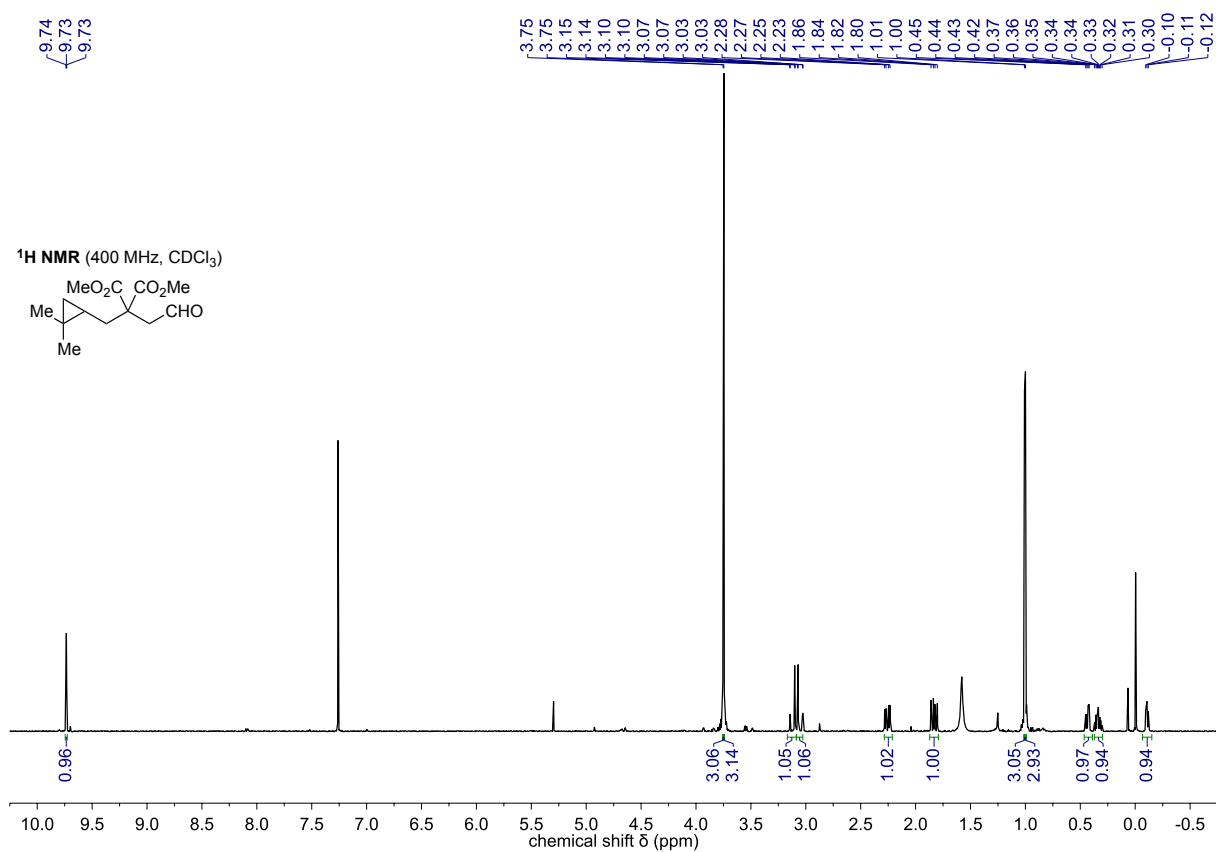




## Epoxide 82



## Cyclopropane 88



## Supporting Information – Synthesis of (+)-Plakortolide E and (–)-Plakortolide I

### Synthesis of Plakortolides E and I Enabled by Base Metal Catalysis

Stefan Leisering, Alexandros Mavroskoufis, Patrick Voßnacker, Reinhold Zimmer, Mathias Christmann\*

Institut für Chemie und Biochemie, Freie Universität Berlin, Takustraße 3, 14195 Berlin, Germany

## Supporting Information

### Table of Content

<b>1. General Information .....</b>	<b>1</b>
1.1 Materials and Methods .....	1
1.2 Analysis.....	1
<b>2. Experimental Procedures and Analytical Data.....</b>	<b>2</b>
2.1 (4 <i>R</i> )-3,4-Dihydroxy-4,8-dimethylnon-7-enenitrile (6).....	2
2.2 (5 <i>R</i> )-4-Hydroxy-5-methyl-5-(4-methylpent-3-ene-1-yl)oxolan-2-one (SI-2) .....	2
2.3 (5 <i>R</i> )-5-Methyl-5-(4-methylpent-3-ene-1-yl)-3-oxolen-2-one (7) .....	3
2.4 (5 <i>R</i> )-5-Methyl-5-(3-oxoprop-1-yl)-3-oxolen-2-one (SI-3) .....	4
2.5 (5 <i>R</i> )-5-Methyl-5-(2-methylene-3-oxoprop-1-yl)-3-oxolen-2-one (SI-4) .....	5
2.6 (5 <i>R</i> )-5-Methyl-5-(3-(acetyloxy)-2-methyleneprop-1-yl)-3-oxolen-2-one (4).....	5
2.7 (5 <i>R</i> )-5-Methyl-5-(12-phenyl-2-methylenedodec-1-yl)-3-oxolen-2-one (3).....	6
2.8 (3 <i>R</i> ,4 <i>aR</i> ,7 <i>aR</i> )-3,4 <i>a</i> -dimethyl-6-oxo-3-(10-phenyldec-1-yl)oxolano[3,2- <i>c</i> ]-1,2-dioxane (1) and (3 <i>S</i> ,4 <i>aR</i> ,7 <i>aR</i> )-3,4 <i>a</i> -dimethyl-6-oxo-3-(10-phenyldec-1-yl)oxolano[3,2- <i>c</i> ]-1,2-dioxane (2) .....	7
<b>3. Comparison of NMR Data.....</b>	<b>9</b>
3.1 (+)-Plakortolide E (1) .....	9
3.2 (–)-Plakortolide I (2).....	10
<b>4. X-ray data .....</b>	<b>11</b>
<b>5. NMR Spectra .....</b>	<b>12</b>
<b>6. References .....</b>	<b>22</b>

## 1. General Information

### 1.1 Materials and Methods

Reactions with air or moisture sensitive substances were carried out under an argon atmosphere using standard Schlenk technique. Ambient or room temperature (RT) refers to 18–23 °C. Heating of reactions was performed with an oil bath unless otherwise noted.

Unless otherwise noted, all starting materials and reagents were purchased from commercial distributors and used without further purification. Anhydrous dichloromethane, tetrahydrofuran and toluene were provided by purification with a MBraun SPS-800 solvent system (BRAUN) using solvents of HPLC grade purchased from FISCHER Scientific and ROTH. Anhydrous *N,N*-dimethylformamide and 1,2-Dichloroethane (99.8+%) were purchased from ACROS Organics. HPLC-grade 2-propanol was purchased from VWR. Triethylamine was distilled from calcium hydride and stored under argon over KOH. Solvents for extraction, crystallization and flash column chromatography were purchased in technical grade and distilled under reduced pressure prior to use.

Column chromatography was performed on silica 60 M (0.040-0.063 mm, 230-400 mesh, MACHEREY-NAGEL).

Medium pressure liquid chromatography (MPLC) was performed with a TELEDYNE ISCO Combi-Flash Rf200 using prepacked silica columns and cartridges from TELDYNE. UV response was monitored at 254 nm and 280 nm. As eluents, cyclohexane (99.5+% quality) and EtOAc (HPLC grade) were used.

The following compounds were prepared according to the literature: **SI-1**,<sup>1</sup> pyridine zinc borohydride,<sup>2</sup> 9-phenylnonanal,<sup>3</sup> (9-bromononyl)benzene.<sup>4</sup>

### 1.2 Analysis

**Reaction monitoring:** Reactions were monitored by thin layer chromatography (TLC). TLC-analysis was performed on silica gel coated aluminum plates ALUGRAM<sup>®</sup> Xtra SIL G/UV<sub>254</sub> purchased from MACHEREY-NAGEL. Products were visualized by UV light at 254 nm and by using staining reagents (based on KMnO<sub>4</sub> and anisaldehyde).

**NMR spectroscopy:** <sup>1</sup>H NMR and <sup>13</sup>C NMR spectral data were recorded on JEOL (ECX 400, ECP 500) and BRUKER (AVANCE III 500, AVANCE III 700) spectrometer in the reported deuterated solvents. The chemical shifts ( $\delta$ ) are listed in parts per million (ppm) and are reported relative to the corresponding residual non-deuterated solvent signal (CDCl<sub>3</sub>:  $\delta_{\text{H}} = 7.26$  ppm,  $\delta_{\text{C}} = 77.16$  ppm). Integrals are in accordance with assignments; coupling constants (*J*) are given in Hz. Multiplicity is indicated as follows: s (singlet), d (doublet), t (triplet), q (quartet), br = broad and combinations thereof. In the case where no multiplicity could be identified, the chemical shift range of the signal is given as m (multiplet). <sup>13</sup>C NMR spectra are <sup>1</sup>H-broadband decoupled. For detailed peak assignments 2D spectra were measured (COSY, HMQC, HMBC).

**High resolution mass spectrometry:** High resolution mass spectra (HRMS) were measured with an AGILENT 6210 ESI-TOF (10  $\mu$ L/min, 1.0 bar, 4 kV) instrument.

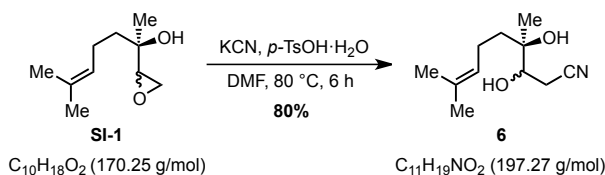
**Optical rotation:** Optical rotation values were measured with a JACSO P-2000 polarimeter at 589 nm using 100 mm cells and the indicated solvent and concentration (g/100 mL) at the given temperatures.

**Melting points:** Melting points were determined by a digital melting point apparatus (Büchi B-545) and are uncorrected.

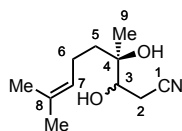
**X-ray:** X-ray diffraction data was collected on a BRUKER D8 Venture CMOS area detector (Photon 100) diffractometer with Cu<sub>K $\alpha$</sub>  radiation. Single crystals were coated with perfluoroether oil and mounted on a 0.2 mm Micromount. The structures were solved with the ShelXT<sup>5</sup> structure solution program using intrinsic phasing and refined with the ShelXL<sup>6</sup> refinement package using least squares on weighted F<sup>2</sup> values for all reflections using OLEX2.<sup>7</sup>

## 2. Experimental Procedures and Analytical Data

### 2.1 (4R)-3,4-Dihydroxy-4,8-dimethylnon-7-enitrile (**6**)



To a flame-dried Schlenk flask containing a suspension of potassium cyanide (5.02 g, 77.0 mmol, 2.5 equiv) and *para*-toluenesulfonic acid monohydrate (7.04 g, 37.0 mmol, 1.2 equiv) in anhydrous *N,N*-dimethylformamide (50 mL) under an argon atmosphere was added a solution of diastereomeric (dr (2*S*, 3*R*):(2*R*, 3*R*)) = 3:2) epoxide **SI-1** (5.25 g, 30.8 mmol, 1.0 equiv) in anhydrous *N,N*-dimethylformamide (10 mL) at 40 °C. The resulting mixture was heated to 80 °C and stirred for 6 h. TLC analysis indicated complete consumption of the starting material. After cooling to 0 °C, the reaction was quenched by the addition of saturated aqueous NaHCO<sub>3</sub> (50 mL) and H<sub>2</sub>O (50 mL). The mixture was extracted with EtOAc (3 × 100 mL). The combined organic extracts were washed with brine (100 mL), dried over anhydrous Na<sub>2</sub>SO<sub>4</sub>, filtered and concentrated under reduced pressure. The crude product was purified by column chromatography (SiO<sub>2</sub>, pentane/EtOAc, 4:1 to 2:1) to afford nitrile **6** (4.88 g, 24.7 mmol, 80%) as a colorless oil.

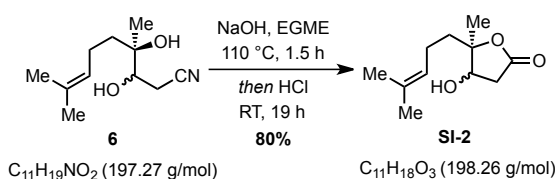


<sup>1</sup>H NMR (700 MHz, CDCl<sub>3</sub>): δ = 5.12 – 5.06 (m, 1H, H-7), 3.83 – 3.73 (m, 1H, H-3), 2.65 – 2.52 (m, 2H, H-2), 2.15 – 1.99 (m, 2H, H-6), 1.62 (s, 3H, Me), 1.68 (s, 3H, Me), 1.59 – 1.51 (m, 1.4H, H-5<sub>S</sub>, H-5<sub>R</sub>), 1.44 – 1.35 (m, 0.6H, H-5<sub>S</sub>), 1.21 (s, 1.8H, H-9<sub>S</sub>), 1.14 (s, 1.2H, H-9<sub>R</sub>) ppm.

<sup>13</sup>C NMR (176 MHz, CDCl<sub>3</sub>): δ = 132.8 (C-8<sub>S</sub>), 132.6 (C-8<sub>R</sub>), 123.81 (C-7<sub>R</sub>), 123.79 (C-7<sub>S</sub>), 119.2 (C-1<sub>S</sub>), 119.0 (C-1<sub>R</sub>), 74.20 (C-4<sub>S</sub>), 74.18 (C-4<sub>R</sub>), 73.3 (C-3<sub>S</sub>), 72.7 (C-3<sub>R</sub>), 38.5 (C-5<sub>R</sub>), 37.4 (C-5<sub>S</sub>), 25.8 (Me), 22.6 (C-9<sub>S</sub>), 22.3 (C-6<sub>R</sub>), 22.1 (C-6<sub>S</sub>), 21.7 (C-9<sub>R</sub>), 21.2 (C-2<sub>R</sub>), 21.1 (C-2<sub>S</sub>), 17.83 (Me<sub>S</sub>), 17.81 (Me<sub>R</sub>) ppm.

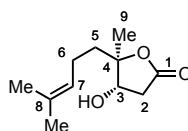
HRMS (ESI, pos.): *m/z* calcd for C<sub>11</sub>H<sub>19</sub>NO<sub>2</sub>Na<sup>+</sup> [M+Na<sup>+</sup>]: 220.1308, found 220.1328.

### 2.2 (5R)-4-Hydroxy-5-methyl-5-(4-methylpent-3-ene-1-yl)oxolan-2-one (**SI-2**)



A solution of nitrile **6** (4.80 g, 24.3 mmol, 1.00 equiv) in ethylene glycol monomethyl ether (25 mL) and aqueous 2 M NaOH (66 mL) was heated to 110 °C and stirred for 1.5 h. After cooling to 0 °C, aqueous 2 M HCl (80 mL) was added until a pH of 2 was reached. The cooling bath was removed and the reaction mixture was stirred for a further 19 h. The solution was extracted with EtOAc (3 × 100 mL) and the combined organic extracts were washed with brine (150 mL), dried over anhydrous Na<sub>2</sub>SO<sub>4</sub>, filtered and concentrated under reduced pressure. The crude product was purified by column chromatography (SiO<sub>2</sub>, pentane/EtOAc, 3:1 to 2:1) to afford lactone **SI-2** (3.84 g, 19.3 mmol, 80%) as a colorless oil.

Both diastereomers could be separated by column chromatography to obtain analytically pure samples which were used for the characterization.

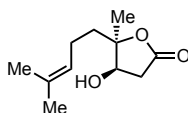
**trans-Lactone SI-2 (major diastereomer)**

$$[\alpha]_{\text{D}}^{22} = +2.6 \quad (c = 1.00, \text{CHCl}_3).$$

$^1\text{H NMR}$  (700 MHz,  $\text{CDCl}_3$ ):  $\delta = 5.08 - 5.02$  (m, 1H, H-7), 4.29 – 4.20 (m, 1H, H-3), 2.89 (dd,  $J = 18.0, 6.9$  Hz, 1H, H-2), 2.84 (d<sub>br</sub>,  $J = 4.8$  Hz, 1H, OH), 2.54 (dd,  $J = 18.0, 4.4$  Hz, 1H, H-2), 2.11 – 2.04 (m, 2H, H-6), 1.67 (s, 3H, Me), 1.66 – 1.57 (m, 2H, H-5), 1.59 (s, 3H, Me), 1.39 (s, 3H, H-9) ppm.

$^{13}\text{C NMR}$  (176 MHz,  $\text{CDCl}_3$ ):  $\delta = 175.2$  (C-1), 132.9 (C-8), 123.1 (C-7), 90.2 (C-4), 72.6 (C-3), 39.4 (C-5), 38.2 (C-2), 25.7 (Me), 22.5 (C-6), 18.6 (C-9), 17.8 (Me) ppm.

**HRMS** (ESI, pos.):  $m/z$  calcd for  $\text{C}_{11}\text{H}_{18}\text{O}_3\text{Na}^+$  [ $\text{M}+\text{Na}^+$ ]: 221.1148, found 221.1146.

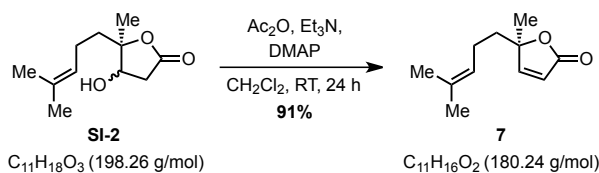
**cis-Lactone SI-2 (minor diastereomer)**

$$[\alpha]_{\text{D}}^{21} = +21.3 \quad (c = 1.00, \text{CHCl}_3).$$

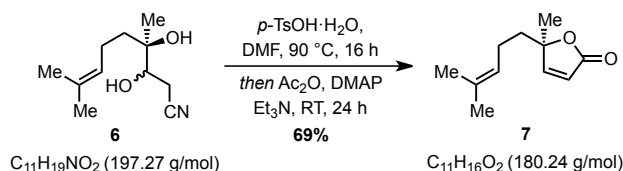
$^1\text{H NMR}$  (700 MHz,  $\text{CDCl}_3$ ):  $\delta = 5.17 - 5.10$  (m, 1H, H-7), 4.20 – 4.15 (m, 1H, H-3), 2.93 (dd,  $J = 18.1, 6.2$  Hz, 1H, H-2), 2.78 (d<sub>br</sub>,  $J = 4.7$  Hz, 1H, OH), 2.50 (dd,  $J = 18.1, 2.4$  Hz, 1H, H-2), 2.16 – 2.05 (m, 2H, H-6), 1.83 (ddd,  $J = 14.0, 9.8, 6.1$  Hz, 1H, H-5), 1.77 (ddd,  $J = 14.0, 10.2, 6.7$  Hz, 1H, H-5), 1.68 (s, 3H, Me), 1.61 (s, 3H, Me), 1.33 (s, 3H, H-9) ppm.

$^{13}\text{C NMR}$  (176 MHz,  $\text{CDCl}_3$ ):  $\delta = 175.5$  (C-1), 133.0 (C-8), 123.5 (C-7), 90.0 (C-4), 74.6 (C-3), 38.6 (C-2), 34.1 (C-5), 25.8 (Me), 23.2 (C-9), 22.5 (C-6), 17.8 (Me) ppm.

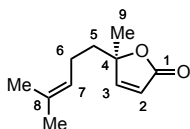
The spectroscopic data are in accordance with the literature.<sup>8</sup>

**2.3 (5R)-5-Methyl-5-(4-methylpent-3-ene-1-yl)-3-oxolen-2-one (7)**

To a flame-dried Schlenk flask containing a solution of lactone **SI-2** (3.65 g, 18.4 mmol, 1.0 equiv) in anhydrous  $\text{CH}_2\text{Cl}_2$  (26 mL) under an argon atmosphere were added  $\text{Ac}_2\text{O}$  (6.97 mL, 74.1 mmol, 4.0 equiv),  $\text{Et}_3\text{N}$  (25.7 mL, 185 mmol, 10 equiv) and 4-(dimethylamino)pyridine (112 mg, 917  $\mu\text{mol}$ , 5 mol%). The reaction mixture was stirred for 24 h at ambient temperature. The reaction was quenched by the addition of saturated aqueous  $\text{NaHCO}_3$  (20 mL), the layers were separated and the aqueous phase was extracted with  $\text{Et}_2\text{O}$  ( $3 \times 20$  mL). The combined organic layers were dried over anhydrous  $\text{Na}_2\text{SO}_4$ , filtered and concentrated under reduced pressure. The crude product was purified by column chromatography ( $\text{SiO}_2$ , pentane/ $\text{EtOAc}$ , 4:1) to afford butenolide **7** (3.01 g, 16.7 mmol, 91%) as a colorless oil.

**One-pot procedure from nitrile 6**

A solution of diastereomeric nitrile **6** (293 mg, 1.49 mmol, 1.0 equiv) and *para*-toluenesulfonic acid monohydrate (2.83 g, 14.9 mmol, 10 equiv) in anhydrous *N,N*-dimethylformamide (6 mL) under an argon atmosphere was heated to 90 °C and stirred for 16 h. After TLC analysis indicated complete consumption of the starting material, Ac<sub>2</sub>O (2.81 mL, 29.7 mmol, 20 equiv), 4-(dimethylamino)pyridine (36.3 mg, 297 μmol, 20 mol%) and Et<sub>3</sub>N (4.12 mL, 29.7 mmol, 20 equiv) were added and stirring was continued for 24 h at ambient temperature. The reaction was quenched by the addition of saturated aqueous NaHCO<sub>3</sub> (10 mL), the layers were separated and the aqueous phase was extracted with Et<sub>2</sub>O (5 × 10 mL). The combined organic extracts were washed with brine (20 mL), dried over anhydrous Na<sub>2</sub>SO<sub>4</sub> and concentrated under reduced pressure. The crude product was purified by column chromatography (SiO<sub>2</sub>, pentane/EtOAc, 4:1) to afford butenolide **7** (186 mg, 1.03 mmol, 69%) as a colorless oil.



$$[\alpha]_{\text{D}}^{20} = -95.6 (c = 1.00, \text{CHCl}_3).$$

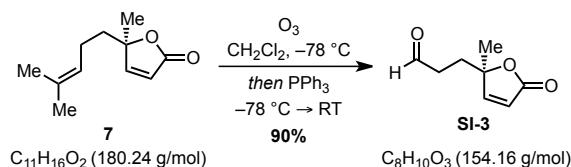
<sup>1</sup>H NMR (700 MHz, CDCl<sub>3</sub>): δ = 7.34 (d, *J* = 5.6 Hz, 1H, H-3), 6.00 (d, *J* = 5.6 Hz, 1H, H-2), 5.04 – 5.00 (m, 1H, H-7), 2.03 – 1.96 (m, 1H, H-6), 1.94 – 1.88 (m, 1H, H-6), 1.85 (ddd, *J* = 14.0 Hz, 10.5, 5.4 Hz, 1H, H-5), 1.72 (ddd, *J* = 14.0, 10.7, 5.2 Hz, 1H, H-5), 1.67 – 1.66 (m, 3H, Me), 1.57 – 1.56 (m, 3H, Me), 1.46 (s, 3H, H-9) ppm.

<sup>13</sup>C NMR (176 MHz, CDCl<sub>3</sub>): δ = 172.7 (C-1), 160.4 (C-3), 132.9 (C-8), 123.0 (C-7), 120.6 (C-2), 89.0 (C-4), 38.4 (C-5), 25.8 (Me), 24.2 (C-9), 22.6 (C-6), 17.8 (Me) ppm.

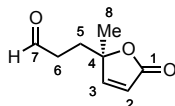
HRMS (ESI, pos.): *m/z* calcd for C<sub>11</sub>H<sub>16</sub>O<sub>2</sub>K<sup>+</sup> [*M*+K<sup>+</sup>]: 219.0782, found 219.0793.

The spectroscopic data are in accordance with the literature.<sup>9</sup>

#### 2.4 (5*R*)-5-Methyl-5-(3-oxoprop-1-yl)-3-oxolen-2-one (SI-3)



A solution of butenolide **7** (1.40 g, 7.77 mmol, 1.0 equiv) in CH<sub>2</sub>Cl<sub>2</sub> (77 mL) was cooled to –78 °C and a stream of ozone was passed through until a blue colour persisted. The excess ozone was then removed by saturating the solution with oxygen until the blue colour faded and triphenylphosphine (2.44 g, 9.30 mmol, 1.2 equiv) was added. The cooling bath was removed and the reaction mixture was warmed to ambient temperature. The crude solution was dry-loaded onto silica and purified by column chromatography (SiO<sub>2</sub>, pentane/EtOAc, 4:1 to 1:1 to 0:1) to afford aldehyde **SI-3** (1.08 g, 7.00 mmol, 90%) as a colorless oil.



$$[\alpha]_{\text{D}}^{22} = -51.1 (c = 1.00, \text{CHCl}_3).$$

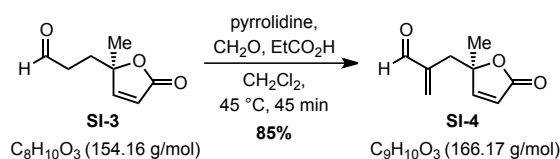
<sup>1</sup>H NMR (700 MHz, CDCl<sub>3</sub>): δ = 9.71 (t, *J* = 0.9 Hz, 1H, H-7), 7.31 (d, *J* = 5.6 Hz, 1H, H-3), 6.01 (d, *J* = 5.6 Hz, 1H, H-2), 2.50 (dddd, *J* = 18.7, 8.2, 6.0, 0.9 Hz, 1H, H-6), 2.39 (dddd, *J* = 18.7, 8.1, 6.5, 0.9 Hz, 1H, H-6), 2.15 (ddd, *J* = 14.6, 8.1, 6.0 Hz, 1H, H-5), 2.08 (ddd, *J* = 14.6, 8.2, 6.5 Hz, 1H, H-5), 1.48 (s, 3H, H-8) ppm.

<sup>13</sup>C NMR (176 MHz, CDCl<sub>3</sub>): δ = 200.5 (C-7), 172.2 (C-1), 160.0 (C-3), 121.0 (C-2), 87.8 (C-4), 38.0 (C-6), 29.7 (C-5), 24.3 (C-8) ppm.

HRMS (ESI, pos.): *m/z* calcd for C<sub>8</sub>H<sub>10</sub>O<sub>3</sub>Na<sup>+</sup> [*M*+Na<sup>+</sup>]: 177.0522, found 177.0515.

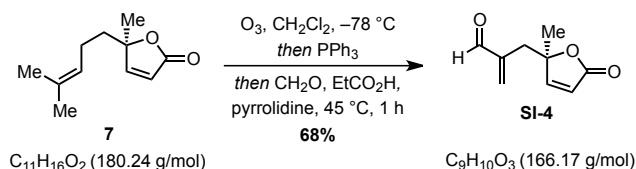
The spectroscopic data are in accordance with the literature.<sup>9</sup>

## 2.5 (5*R*)-5-Methyl-5-(2-methylene-3-oxoprop-1-yl)-3-oxolen-2-one (SI-4)

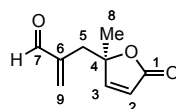


Enal **SI-4** was prepared in analogy to a reported procedure by PIHKO et al. for the  $\alpha$ -methylenation of aldehydes.<sup>10</sup> A solution of aldehyde **SI-3** (500 mg, 3.24 mmol, 1.0 equiv), aqueous formaldehyde (37 wt%, 362  $\mu\text{L}$ , 4.87 mmol, 1.5 equiv), propionic acid (24.0  $\mu\text{L}$ , 324  $\mu\text{mol}$ , 10 mol%) and pyrrolidine (27.0  $\mu\text{L}$ , 324  $\mu\text{mol}$ , 10 mol%) in  $\text{CH}_2\text{Cl}_2$  (13 mL) was heated to 45  $^\circ\text{C}$  and stirred for 1 h. The mixture was cooled to 0  $^\circ\text{C}$ , diluted with EtOAc (10 mL) and carefully quenched with saturated aqueous  $\text{NaHCO}_3$  (10 mL). The layers were separated and the aqueous phase was extracted with EtOAc (3  $\times$  10 mL). The combined organic layers were dried over anhydrous  $\text{Na}_2\text{SO}_4$ , filtered and concentrated under reduced pressure. The residue was purified by column chromatography ( $\text{SiO}_2$ , pentane/ $\text{Et}_2\text{O}$ , 4:1 to 1:2) to afford enal **SI-4** (456 mg, 2.74 mmol, 85%) as a colorless oil.

### One-pot procedure from butenolide 7



A solution of butenolide **7** (190 mg, 1.05 mmol, 1.0 equiv) in  $\text{CH}_2\text{Cl}_2$  (2.5 mL) was cooled to  $-78 ^\circ\text{C}$  and a stream of ozone was passed through until a blue colour persisted. The excess ozone was then removed by saturating the solution with oxygen until the blue colour faded and triphenylphosphine (276 mg, 1.05 mmol, 1.0 equiv) was added. The cooling bath was removed and the reaction mixture was warmed to ambient temperature. Then aqueous formaldehyde solution (37 wt%, 118  $\mu\text{L}$ , 1.58 mmol, 1.5 equiv), propionic acid (8  $\mu\text{L}$ , 105  $\mu\text{mol}$ , 10 mol%) and pyrrolidine (35  $\mu\text{L}$ , 422  $\mu\text{mol}$ , 40 mol%) were added and stirring was continued at 45  $^\circ\text{C}$  for 1 h. The mixture was cooled to 0  $^\circ\text{C}$ , diluted with EtOAc (5 mL) and carefully quenched with saturated aqueous  $\text{NaHCO}_3$  (5 mL). The layers were separated and the aqueous phase was extracted with EtOAc (3  $\times$  5 mL). The combined organic layers were dried over anhydrous  $\text{Na}_2\text{SO}_4$ , filtered and concentrated under reduced pressure. The residue was purified by MPLC (dry-loaded onto Celite<sup>®</sup>,  $\text{SiO}_2$ , cyclohexane/ $\text{EtOAc}$ , 100:0 to 4:1 to 1:1) to afford enal **SI-4** (119 mg, 713  $\mu\text{mol}$ , 68%) as a colorless oil.



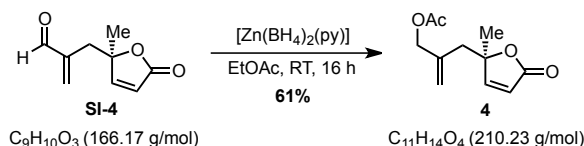
$$[\alpha]_{\text{D}}^{20} = -4.4 \text{ (} c = 1.00, \text{CHCl}_3\text{)}.$$

<sup>1</sup>H NMR (500 MHz,  $\text{CDCl}_3$ ):  $\delta$  = 9.41 (s, 1H, H-7), 7.24 (d,  $J$  = 5.6 Hz, 1H, H-3), 6.49 (s, 1H, H-9), 6.19 (s, 1H, H-9), 5.88 (d,  $J$  = 5.6 Hz, 1H, H-2), 2.88 (d,  $J$  = 13.7 Hz, 1H, H-5), 2.68 (d,  $J$  = 13.7 Hz, 1H, H-5), 1.52 (s, 3H, H-8) ppm.

<sup>13</sup>C NMR (126 MHz,  $\text{CDCl}_3$ ):  $\delta$  = 194.2 (C-7), 172.3 (C-1), 159.5 (C-3), 143.0 (C-6), 140.2 (C-9), 120.9 (C-2), 87.3 (C-4), 35.4 (C-5), 24.5 (C-8) ppm.

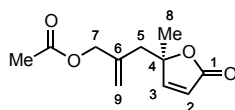
HRMS (ESI, pos.):  $m/z$  calcd for  $\text{C}_9\text{H}_{10}\text{O}_3\text{Na}^+$  [ $\text{M}+\text{Na}^+$ ]: 189.0522, found 189.0526.

## 2.6 (5*R*)-5-Methyl-5-(3-(acetyloxy)-2-methyleneprop-1-yl)-3-oxolen-2-one (4)





Allyl acetate **4** was prepared in analogy to a reported procedure by ZEYNIZADEH and SETAMDIDEH for the reductive acetylation of carbonyl compounds.<sup>11</sup> To a solution of enal **SI-4** (270 mg, 1.63 mmol, 1.0 equiv) in anhydrous EtOAc (4.6 mL) at 0 °C was added zinc borohydride pyridine complex (297 mg, 1.71 mmol, 1.05 equiv). The resulting reaction mixture was warmed to ambient temperature and stirred for 16 h. The reaction was carefully quenched with saturated aqueous NH<sub>4</sub>Cl (5 mL). The layers were separated and the aqueous phase was extracted with EtOAc (3 × 5 mL). The combined organic layers were dried over anhydrous Na<sub>2</sub>SO<sub>4</sub>, filtered and concentrated under reduced pressure. Purification by column chromatography (SiO<sub>2</sub>, pentane/Et<sub>2</sub>O, 2:1 to 1:2) afforded allyl acetate **4** (209 mg, 994 μmol, 61%) as a colorless oil.



$$[\alpha]_{\text{D}}^{20} = -10.2 \quad (c = 1.00, \text{CHCl}_3).$$

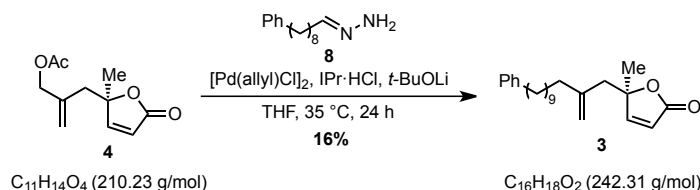
<sup>1</sup>H NMR (500 MHz, CDCl<sub>3</sub>): δ = 7.38 (d, *J* = 5.6 Hz, 1H, H-3), 6.03 (d, *J* = 5.6 Hz, 1H, H-2), 5.25 – 5.24 (m, 1H, H-9), 5.07 – 5.05 (m, 1H, H-9), 4.49 (s, 2H, H-7), 2.59 (d, *J* = 14.3 Hz, 1H, H-5), 2.45 (d, *J* = 14.3 Hz, 1H, H-5), 2.09 (s, 3H, Ac), 1.49 (s, 3H, H-8) ppm.

<sup>13</sup>C NMR (126 MHz, CDCl<sub>3</sub>): δ = 172.2 (C-1), 170.7 (Ac), 159.7 (C-3), 137.6 (C-6), 121.2 (C-2), 118.9 (C-9), 88.0 (C-4), 66.9 (C-7), 41.9 (C-5), 24.1 (C-8), 21.0 (Ac) ppm.

HRMS (ESI, pos.): *m/z* calcd for C<sub>11</sub>H<sub>14</sub>O<sub>4</sub>Na<sup>+</sup> [*M*+Na<sup>+</sup>]: 233.0784, found 233.0787; calcd for C<sub>11</sub>H<sub>14</sub>O<sub>4</sub>K<sup>+</sup> [*M*+K<sup>+</sup>]: 249.0524, found 249.0530.

## 2.7 (5*R*)-5-Methyl-5-(12-phenyl-2-methylenedodec-1-yl)-3-oxolen-2-one (**3**)

### Palladium-catalyzed allylic substitution with hydrazone **8**

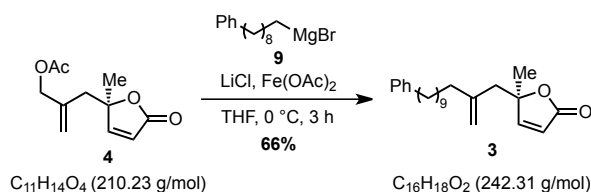


The following procedure was done in analogy to a reported protocol by LI et al. for the palladium-catalyzed alkylation of allyl acetates with hydrazones.<sup>12</sup>

Preparation of the hydrazone **8**: A mixture of 9-phenylnonanal (324 mg, 1.48 mmol, 1.0 equiv), hydrazine monohydrate (86.5 μL, 1.79 mmol, 1.2 equiv) and anhydrous Na<sub>2</sub>SO<sub>4</sub> (120 mg) in THF (1.2 mL) was stirred at ambient temperature for 2 h. Then 5 Å molecular sieves powder (150 mg) was added and the solution was dried over night.

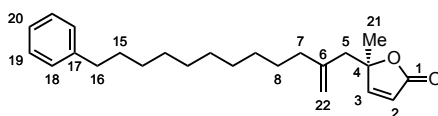
A flame-dried Schlenk tube was charged with 1,3-bis(2,6-diisopropylphenyl)imidazolium chloride (10.0 mg, 24.0 μmol, 10 mol%) and allylpalladium(II) chloride dimer (4.40 mg, 12.0 μmol, 5 mol%) under an argon atmosphere. A solution of *t*-BuOLi (1 M in THF, 48.0 μL, 48.0 μmol, 20 mol%) was added and the mixture was stirred at ambient temperature for 1 h. Then a solution of allyl acetate **4** (50.0 mg, 238 μmol, 1.0 equiv) in THF (0.71 mL) was added and the mixture stirred for another 30 min before a solution of hydrazone **8** (1.25 M in THF, 0.24 mL, 300 μmol, 1.26 equiv) and *t*-BuOLi (1 M in THF, 480 μL, 480 μmol, 2.0 equiv) were added. The reaction mixture was stirred at 35 °C for 24 h and then filtered through a short pad of Celite®, rinsing with CH<sub>2</sub>Cl<sub>2</sub> (3 × 5 mL). The solvent was removed under reduced pressure and the crude product was purified by column chromatography (SiO<sub>2</sub>, pentane/EtOAc, 8:1 to 6:1) to afford alkene **3** (13.8 mg, 389 μmol, 16%) as a colorless oil.

### Iron-catalyzed allylic substitution with Grignard reagent **9**



Preparation of the Grignard reagent (9-phenylnonylmagnesium bromide (**9**)): To a flame-dried Schlenk flask was added freshly ground magnesium (146 mg, 6.00 mmol, 1.5 equiv) and the flask was once more dried by heating with a heat gun under high vacuum while vigorously stirring the magnesium. After cooling to ambient temperature the vessel was placed under an argon atmosphere and a solution of (9-bromononyl)benzene (1.13 g, 4.00 mmol, 1.0 equiv) in anhydrous THF (3 mL) was slowly added over a period of 1 h. Stirring was continued for 16 h and then stopped. After the solids settled down, the clear solution was transferred with a syringe into another flame-dried Schlenk flask and stored under an argon atmosphere. The concentration was determined by titration with menthol in the presence of phenanthroline.<sup>13</sup>

Alkene **3** was prepared in analogy to a procedure by JACOBI VON WANGELIN et al. for the iron-catalyzed alkylation of allyl acetates with alkylmagnesium compounds.<sup>14</sup> A Schlenk tube was charged with anhydrous  $\text{Fe}(\text{OAc})_2$  (4.9 mg, 28  $\mu\text{mol}$ , 10 mol%) and anhydrous LiCl (16.6 mg, 392  $\mu\text{mol}$ , 1.4 equiv) and flame-dried under high vacuum until bubbling ceased. Then a solution of allyl acetate **4** (58.8 mg, 280  $\mu\text{mol}$ , 1.0 equiv) in THF (1.3 mL) was added and the resulting mixture was cooled to 0 °C. The Grignard reagent **9** (0.9 M, 0.44 mL, 1.4 equiv) was added dropwise over a period of 2 h and stirring was continued for further 1 h at 0 °C. The reaction was quenched by the addition of 1 M HCl (2 mL) and the aqueous phase was extracted with EtOAc (3  $\times$  2 mL). The combined organic layers were washed with brine (2 mL), dried over anhydrous  $\text{Na}_2\text{SO}_4$  and concentrated under reduced pressure. The crude product was purified by MPLC (dry-loaded onto Celite®,  $\text{SiO}_2$ , cyclohexane/EtOAc, 100:1 to 10:1 to 6:1) to afford alkene **3** (65.4 mg, 185  $\mu\text{mol}$ , 66%) as a colorless oil.



$$[\alpha]_{\text{D}}^{24} = -12.3 \quad (c = 1.00, \text{CHCl}_3).$$

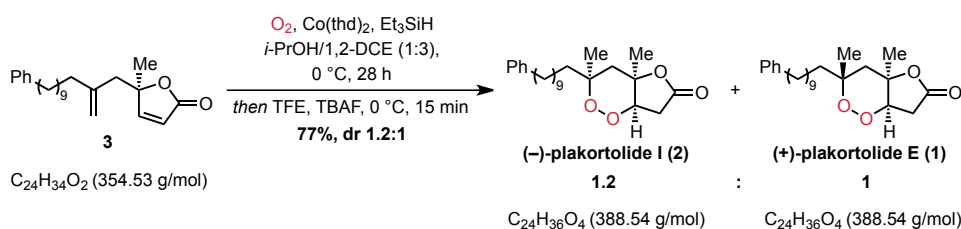
<sup>1</sup>H NMR (700 MHz,  $\text{CDCl}_3$ ):  $\delta$  = 7.35 (d,  $J$  = 5.6 Hz, 1H, H-3), 7.29 – 7.26 (m, 2H, H-19), 7.19 – 7.15 (m, 3H, H-18, H-20), 5.99 (d,  $J$  = 5.6 Hz, 1H, H-2), 4.94 – 4.93 (m, 1H, H-22), 4.81 – 4.79 (m, 1H, H-22), 2.60 (t,  $J$  = 7.7 Hz, 2H, H-16), 2.52 (d,  $J$  = 13.9 Hz, 1H, H-5), 2.40 (d,  $J$  = 13.9 Hz, 1H, H-5), 2.00 (t,  $J$  = 7.7 Hz, 2H, H-7), 1.64 – 1.59 (m, 2H, H-15), 1.46 (s, 3H, H-21), 1.42 – 1.36 (m, 2H, H-9), 1.36 – 1.21 (m, 12H,  $\text{CH}_2$ ) ppm.

<sup>13</sup>C NMR (176 MHz,  $\text{CDCl}_3$ ):  $\delta$  = 172.5 (C-1), 160.4 (C-3), 143.6 (C-6), 143.1 (C-17), 128.5 (2C, C-18), 128.3 (2C, C-19), 125.7 (C-20), 120.6 (C-2), 115.4 (C-22), 88.7 (C-4), 44.9 (C-5), 37.0 (C-7), 36.1 (C-16), 31.6 (C-15), 29.69 ( $\text{CH}_2$ ), 29.66 ( $\text{CH}_2$ ), 29.62 ( $\text{CH}_2$ ), 29.61 ( $\text{CH}_2$ ), 29.44 ( $\text{CH}_2$ ), 29.35 ( $\text{CH}_2$ ), 27.9 (C-8), 24.1 (C-21) ppm.

HRMS (ESI, pos.):  $m/z$  calcd for  $\text{C}_{24}\text{H}_{34}\text{O}_2\text{Na}^+$  [ $\text{M}+\text{Na}^+$ ]: 377.2451, found 377.2465.

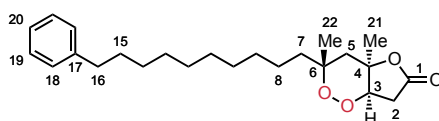
The spectroscopic data are in accordance with the literature.<sup>15</sup>

### 2.8 (3R,4aR,7aR)-3,4a-dimethyl-6-oxo-3-(10-phenyldec-1-yl)oxolano[3,2-c]-1,2-dioxane (**1**) and (3S,4aR,7aR)-3,4a-dimethyl-6-oxo-3-(10-phenyldec-1-yl)oxolano[3,2-c]-1,2-dioxane (**2**)



A flame-dried Schlenk flask was charged with bis(2,2,6,6-tetramethyl-3,5-heptanedionato)cobalt(II) (53.3 mg, 125  $\mu\text{mol}$ , 30 mol%), 1,2-dichloroethane (6 mL) and half the amount of  $\text{Et}_3\text{SiH}$  (80.0  $\mu\text{L}$ , 501  $\mu\text{mol}$ , 1.2 equiv). The solution was saturated with a stream of oxygen for 5 min and stirred for 1 h under an atmosphere of oxygen. Then **3** (148 mg, 417  $\mu\text{mol}$ , 1.0 equiv) and *i*-PrOH (2 mL) were added at 0 °C, followed by the dropwise addition of the remaining half of  $\text{Et}_3\text{SiH}$  (80.0  $\mu\text{L}$ , 501  $\mu\text{mol}$ , 1.2 equiv) in 1,2-dichloroethane (0.05 mL) over 3 h. After stirring for 28 h the reaction mixture was cooled to -5 °C and TFE (300  $\mu\text{L}$ , 4.18 mmol, 10.0 equiv) and TBAF (1 M, 1.00 mL, 2.4 equiv) were added. The mixture was warmed to 0 °C and stirred for 15 min and then diluted with  $\text{H}_2\text{O}$  (5 mL). The layers were separated and the aqueous phase was extracted with  $\text{CH}_2\text{Cl}_2$  ( $3 \times 5$  mL). The combined organic layers were dried over anhydrous  $\text{Na}_2\text{SO}_4$ , filtered and concentrated under reduced pressure. The crude product was purified by column chromatography ( $\text{SiO}_2$ , pentane/ $\text{CH}_2\text{Cl}_2$ , 1:3) to give **1** (57.0 mg, 147  $\mu\text{mol}$ , 35%) as a colorless solid and **2** (68.4 mg, 176  $\mu\text{mol}$ , 42%) as a colorless oil.

### (+)-Plakortolide E (**1**)



$[\alpha]_{\text{D}}^{24} = +10.1$  ( $c = 1.00$ ,  $\text{CHCl}_3$ ); Lit.<sup>16</sup>:  $[\alpha]_{\text{D}} = +8.0$  ( $c = 0.0173$ ,  $\text{CHCl}_3$ ).

**<sup>1</sup>H NMR** (700 MHz,  $\text{CDCl}_3$ ):  $\delta = 7.29 - 7.26$  (m, 2H, H-19), 7.19 - 7.16 (m, 3H, H-18, H-20), 4.45 (d,  $J = 6.2$  Hz, 1H, H-3), 2.91 (dd,  $J = 18.5, 6.2$  Hz, 1H, H-2), 2.65 - 2.58 (m, 1H, H-2), 2.60 (t,  $J = 7.7$  Hz, 2H, H-16), 2.17 (d,  $J = 14.8$  Hz, 1H, H-5), 1.71 (d,  $J = 14.8$  Hz, 1H, H-5), 1.64 - 1.59 (m, 2H, H-15), 1.58 - 1.51 (m, 1H, H-7), 1.51 - 1.46 (m, 1H, H-7), 1.38 (s, 3H, H-21), 1.29 (s, 2H, H-22), 1.38 - 1.24 (m, 14H,  $\text{CH}_2$ ) ppm.

**<sup>13</sup>C NMR** (176 MHz,  $\text{CDCl}_3$ ):  $\delta = 174.4$  (C-1), 143.0 (C-17), 128.5 (2C, C-18), 128.3 (2C, C-19), 125.7 (C-20), 82.9 (C-4), 81.2 (C-3), 80.2 (C-6), 41.1 (C-7), 40.7 (C-5), 36.1 (C-16), 34.4 (C-2), 31.6 (C-15), 30.1 ( $\text{CH}_2$ ), 29.63 (2C,  $\text{CH}_2$ ), 29.59 (2C,  $\text{CH}_2$ ), 29.4 ( $\text{CH}_2$ ), 26.0 (C-21), 23.2 ( $\text{CH}_2$ ), 22.5 (C-22) ppm.

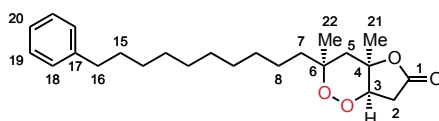
**HRMS** (ESI, pos.):  $m/z$  calcd for  $\text{C}_{24}\text{H}_{36}\text{O}_4\text{Na}^+$  [ $\text{M}+\text{Na}^+$ ]: 411.2506, found 411.2522.

**m. p.:** 54 - 55 °C.

**X-ray:** Crystals were grown by slow evaporation of a solution of **1** in pentane and  $\text{Et}_2\text{O}$  in a 1 mL vial at ambient temperature.

The spectroscopic data are in accordance with the literature.<sup>16</sup>

### (-)-Plakortolide I (**2**)



$[\alpha]_{\text{D}}^{24} = -5.8$  ( $c = 1.00$ ,  $\text{CHCl}_3$ ); Lit.<sup>17</sup>:  $[\alpha]_{\text{D}}^{20} = -8$  ( $c = 0.05$ ,  $\text{CHCl}_3$ ).

**<sup>1</sup>H NMR** (700 MHz,  $\text{CDCl}_3$ ):  $\delta = 7.29 - 7.25$  (m, 2H, H-19), 7.25 - 7.15 (m, 3H, H-18, H-20), 4.47 (d,  $J = 6.0$  Hz, 1H, H-3), 2.90 (dd,  $J = 18.5, 6.0$  Hz, 1H, H-2), 2.60 (t,  $J = 7.8$  Hz, 2H, H-16), 2.56 (d,  $J = 18.5$  Hz, 1H, H-2), 2.27 (d,  $J = 15.0$  Hz, 1H, H-5), 1.77 - 1.70 (m, 1H, H-7), 1.65 (d,  $J = 15.0$  Hz, 1H, H-5), 1.64 - 1.58 (m, 2H, H-15), 1.58 - 1.52 (m, 1H, H-7), 1.37 (s, 3H, H-21), 1.36 - 1.24 (m, 14H,  $\text{CH}_2$ ), 1.20 (s, 3H, H-22) ppm.

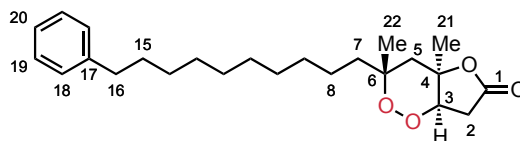
**<sup>13</sup>C NMR** (176 MHz,  $\text{CDCl}_3$ ):  $\delta = 174.2$  (C-1), 143.1 (C-17), 128.5 (2C, C-18), 128.3 (2C, C-19), 125.6 (C-20), 82.6 (C-4), 80.9 (C-3), 80.3 (C-6), 40.3 (C-5), 37.0 (C-7), 36.1 (C-16), 34.2 (C-2), 31.6 (C-15), 30.1 ( $\text{CH}_2$ ), 29.7 ( $\text{CH}_2$ ), 29.64 (2C,  $\text{CH}_2$ ), 29.59 ( $\text{CH}_2$ ), 29.4 ( $\text{CH}_2$ ), 26.0 (C-21), 25.0 (C-22), 23.8 ( $\text{CH}_2$ ) ppm.

**HRMS** (ESI, pos.):  $m/z$  calcd for  $\text{C}_{24}\text{H}_{36}\text{O}_4\text{Na}^+$  [ $\text{M}+\text{Na}^+$ ]: 411.2506, found 411.2524.

The spectroscopic data are in accordance with the literature.<sup>17</sup>

### 3. Comparison of NMR Data

#### 3.1 (+)-Plakortolide E (1)

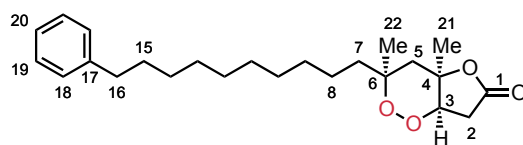


**Table S1. Comparison of  $^1\text{H}$  and  $^{13}\text{C}$  NMR Data for Isolated and Synthetic (+)-plakortolide E.<sup>a</sup>**

No.	Isolation <sup>b</sup>	Synthetic	$\Delta/\text{ppm}$	Isolation <sup>b</sup>	Synthetic	$\Delta/\text{ppm}$
	$^{13}\text{C}$ NMR (125 MHz) $\delta_{\text{C}}/\text{ppm}^{\text{c}}$	$^{13}\text{C}$ NMR (176 MHz) $\delta_{\text{C}}/\text{ppm}^{\text{c}}$		$^1\text{H}$ NMR (500 MHz) $\delta_{\text{H}}/\text{ppm}$ (J in Hz) <sup>d</sup>	$^1\text{H}$ NMR (700 MHz) $\delta_{\text{H}}/\text{ppm}$ (J in Hz) <sup>c</sup>	
1	174.2	174.4	0.2			
2	34.2	34.4	0.2	2.91 dd (12.4, 6.0) 2.70 d (12.4)	2.91 dd (18.5, 6.2) 2.65 – 2.58 m	0
3	80.1	81.2	1.1	4.44 d (6.0)	4.45 d (6.2)	0.01
4	82.0	82.9	0.9			
5	39.5 <sup>e</sup>	40.7	1.2	2.17 d (15.0) 1.71 d (15.0)	2.17 d (14.8) 1.71 d (14.8)	0
6	80.2	80.2	0			
7	41.0 <sup>e</sup>	41.1	0.1	1.50 m	1.58 – 1.51 m 1.51 – 1.46 m	
8	23.0 <sup>e</sup>			1.25 m		
9	29.5			1.25 m		
10	29.5			1.25 m		
11	29.5	30.1, 29.63, 29.63, 29.59, 29.59, 29.4, 23.2		1.25 m	1.38 – 1.24 m	
12	29.5			1.25 m		
13	29.5			1.25 m		
14	29.5			1.25 m		
15	31.4	31.6	0.2	1.58 m	1.64 – 1.59 m	
16	36.0 <sup>e</sup>	36.1	0.1	2.60 t (7.0)	2.60 t (7.7)	0
17	142.2	143.0	0.8			
18	128.3	128.5	0.2		7.19 – 7.16 m	
19	128.2	128.3	0.1	7.20 – 7.25 m	7.29 – 7.26 m	
20	125.5	125.7	0.2		7.19 – 7.16 m	
21	25.8	26.0	0.2	1.37 s	1.38 s	0.01
22	22.4 <sup>e</sup>	22.5	0.1	1.27 s	1.29 s	0.02

a) All data were obtained in  $\text{CDCl}_3$ . b) Data from reference 16; Revised structure (see reference 18), sample originally named as plakortolide I. c) Chemical shifts are reported relative to the corresponding residual non-deuterated solvent signal ( $\text{CDCl}_3$ :  $\delta_{\text{H}} = 7.26$  ppm,  $\delta_{\text{C}} = 77.16$  ppm). d) Chemical shifts are reported relative to TMS ( $\delta_{\text{H}} = 0$  ppm). e) Revised assignments (see reference 18).

## 3.2 (-)-Plakortolide I (2)

Table S2. Comparison of  $^1\text{H}$  and  $^{13}\text{C}$  NMR Data for Isolated and Synthetic (-)-plakortolide I.<sup>a</sup>

No.	Isolation <sup>b</sup>	Synthetic	$\Delta/\text{ppm}$	Isolation <sup>b</sup>	Synthetic	$\Delta/\text{ppm}$
	$^{13}\text{C}$ NMR (100 MHz) $\delta_{\text{C}}/\text{ppm}^{\text{c}}$	$^{13}\text{C}$ NMR (176 MHz) $\delta_{\text{C}}/\text{ppm}^{\text{d}}$		$^1\text{H}$ NMR (300 MHz) $\delta_{\text{H}}/\text{ppm}$ (J in Hz) <sup>c</sup>	$^1\text{H}$ NMR (700 MHz) $\delta_{\text{H}}/\text{ppm}$ (J in Hz) <sup>d</sup>	
1	174.1	174.2	0.1			
2	34.1	34.2	0.1	2.91 dd (18.6, 6.0) 2.59 dd (18.6, 1.5)	2.90 dd (18.5, 6.0) 2.56 d (18.5)	0.01 0.03
3	80.8	80.3	0.5	4.49 d (6.0)	4.47 d (6.0)	0.02
4	82.5	82.6	0.1			
5	40.2	40.3	0.1	2.28 d (15.3) 1.66 d (15.3)	2.27 d (15.0) 1.65 d (15.0)	0.01 0.01
6	80.2	80.3	0.1			
7	36.9	37.0	0.1	1.75 m	1.77 – 1.70 m 1.58 – 1.52 m	
8	23.7			1.27 m		
9	29.5			1.30 m		
10	29.6			1.30 m		
11	29.9	30.1, 29.7, 29.64, 29.64, 29.59, 29.4, 23.8		1.30 m	1.36 – 1.24 m	
12	29.6			1.30 m		
13	29.5			1.30 m		
14	29.3			1.30 m		
15	31.5	31.6	0.1	1.57 m	1.64 – 1.58 m	
16	36.0	36.1	0.1	2.60 t (7.8)	2.60 t (7.8)	0
17	143.0	143.1	0.1			
18	128.4	128.5	0.1	7.19 m	7.25 – 7.15 m	
19	128.2	128.3	0.1	7.27 m	7.29 – 7.25 m	
20	125.5	125.6	0.1	7.19 d (7.2)	7.25 – 7.15 m	
21	25.9	26.0	0.1	1.38 s	1.37 s	0.01
22	24.9	25.0	0.1	1.20 s	1.20 s	0

a) All data were obtained in  $\text{CDCl}_3$ . b) Data from reference 17. c) Reference for chemical shifts not reported. d) Chemical shifts are reported relative to the corresponding residual non-deuterated solvent signal ( $\text{CDCl}_3$ :  $\delta_{\text{H}} = 7.26$  ppm,  $\delta_{\text{C}} = 77.16$  ppm).

#### 4. X-ray data

##### (+)-Plakortolide E (1) (CCDC2074855) (Thermal Ellipsoids at 50% Probability)

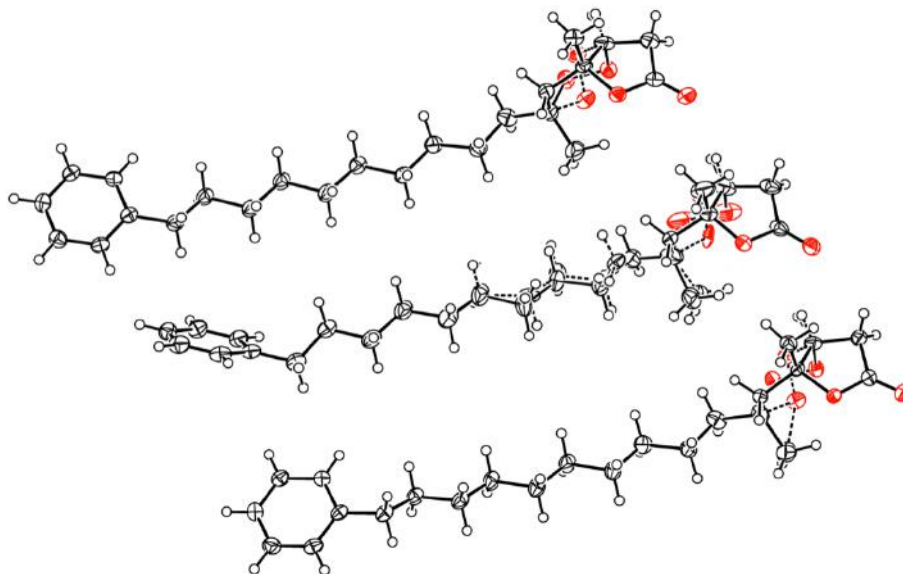
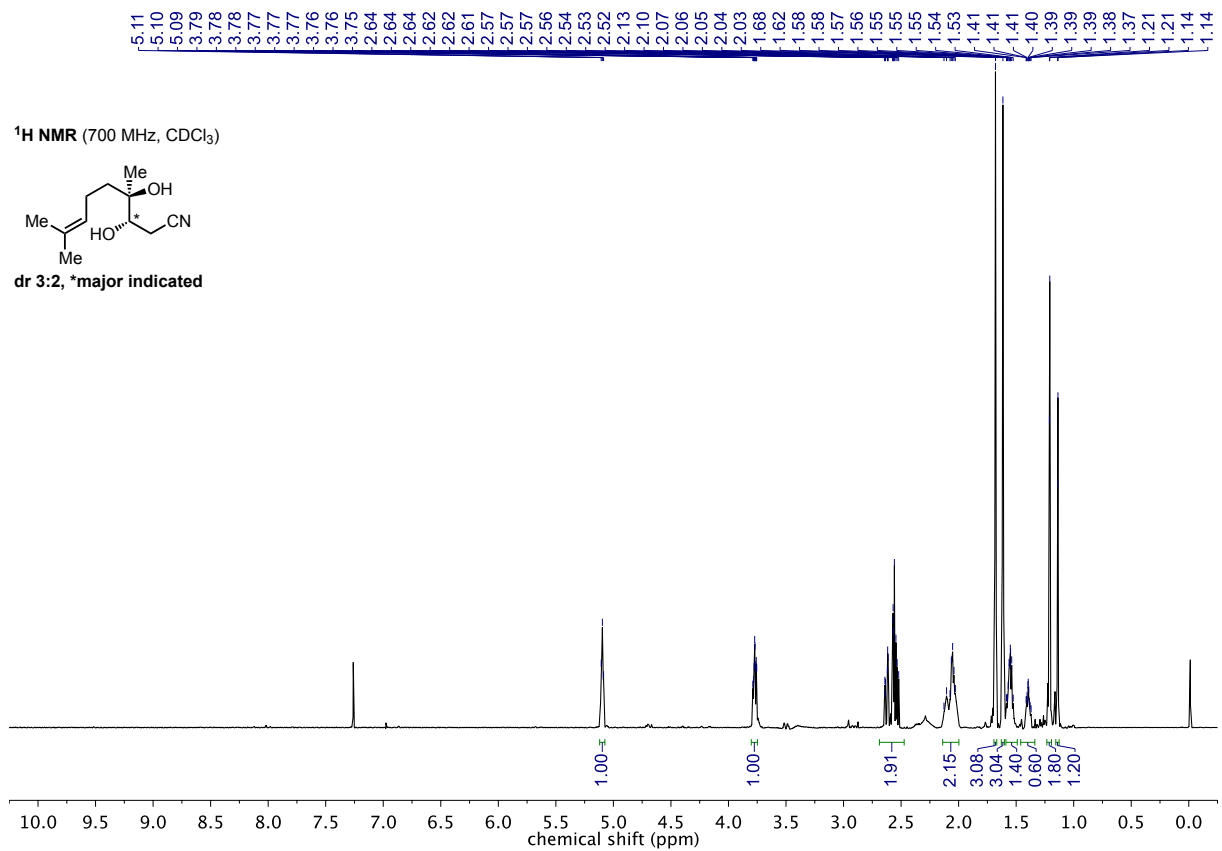


**Table S3. Crystal data of (+)-plakortolide E (1).**

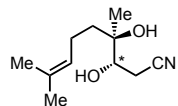
Empirical formula	C <sub>72</sub> H <sub>108</sub> O <sub>12</sub>
Formula weight	1165.58
Temperature/K	100.0
Crystal system	monoclinic
Space group	P2 <sub>1</sub>
a/Å	5.7306(2)
b/Å	17.1506(7)
c/Å	34.0117(14)
α/°	90
β/°	93.473(2)
γ/°	90
Volume/Å <sup>3</sup>	3336.6(2)
Z	2
ρ <sub>calc</sub> /gcm <sup>-3</sup>	1.160
μ/mm <sup>-1</sup>	0.611
F(000)	1272.0
Crystal size/mm <sup>3</sup>	0.754 × 0.126 × 0.052
Radiation	CuKα (λ = 1.54178)
2θ range for data collection/°	5.206 to 136.548
Reflections collected	129589
Independent reflections	12052 [R <sub>int</sub> = 0.0410, R <sub>sigma</sub> = 0.0174]
Data/restraints/parameters	12052/6/860
Goodness-of-fit on F <sup>2</sup>	1.034
Final R indexes [I > 2σ(I)]	R <sub>1</sub> = 0.0380, wR <sub>2</sub> = 0.0906
Final R indexes [all data]	R <sub>1</sub> = 0.0390, wR <sub>2</sub> = 0.0915
Largest diff. peak and hole/e.Å <sup>-3</sup>	0.45 and -0.63
Flack parameter	0.02(2)
CCDC deposition number	2074855

## 5. NMR Spectra

## Nitrile 6

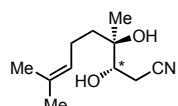


<sup>1</sup>H NMR (700 MHz, CDCl<sub>3</sub>)

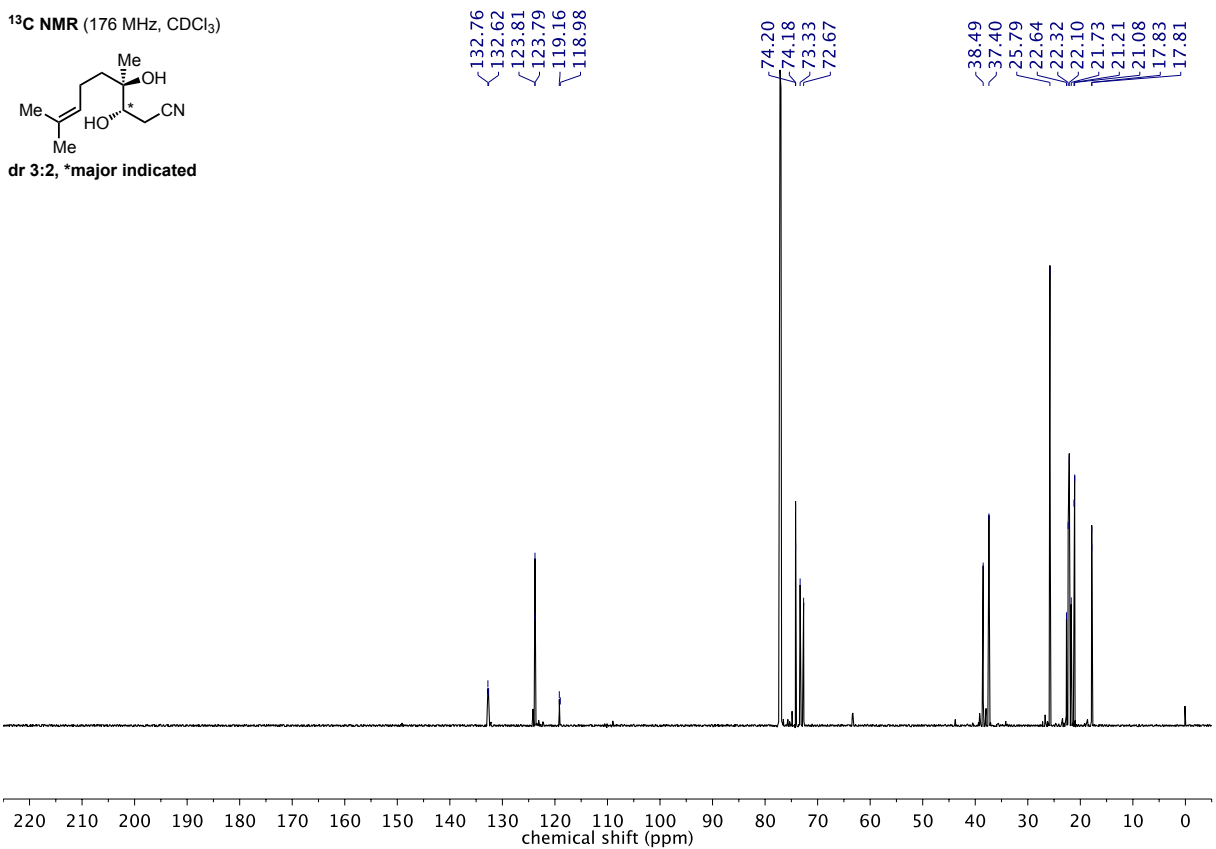


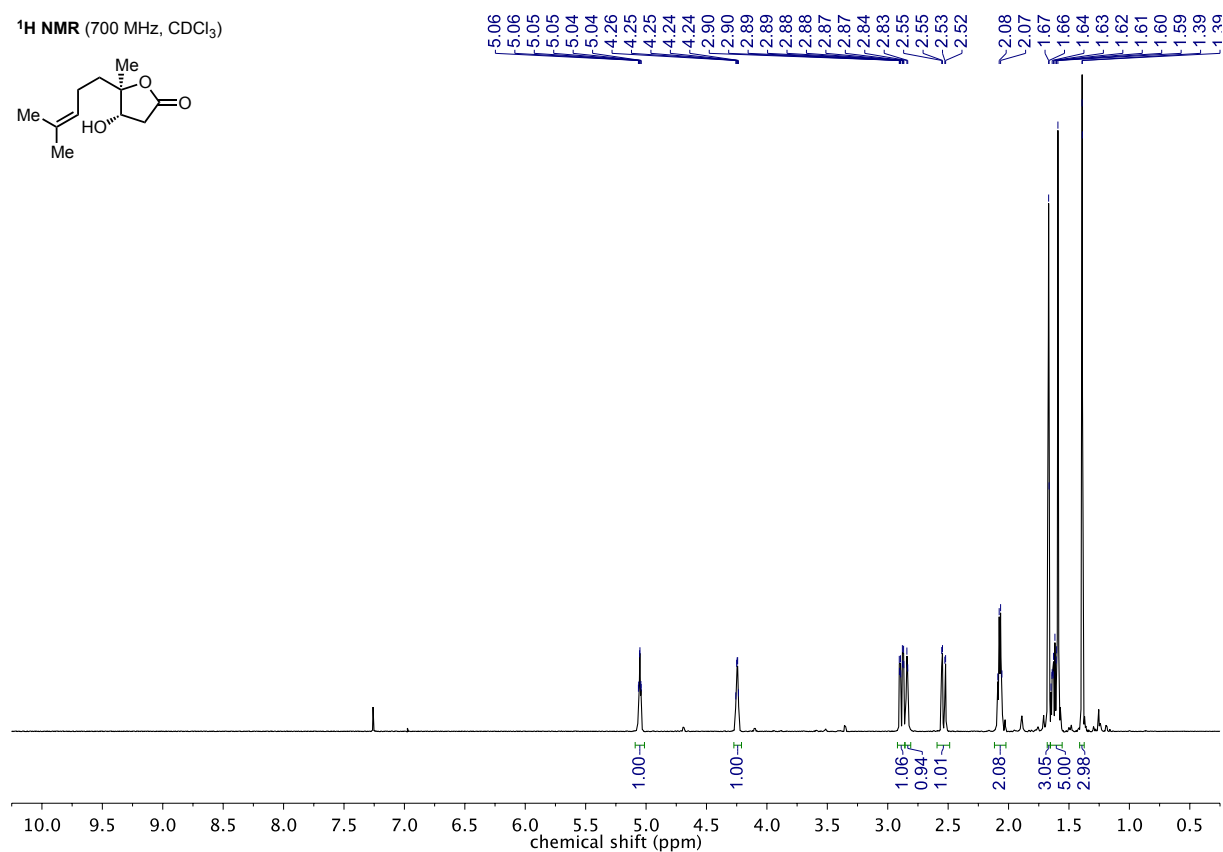
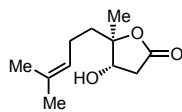
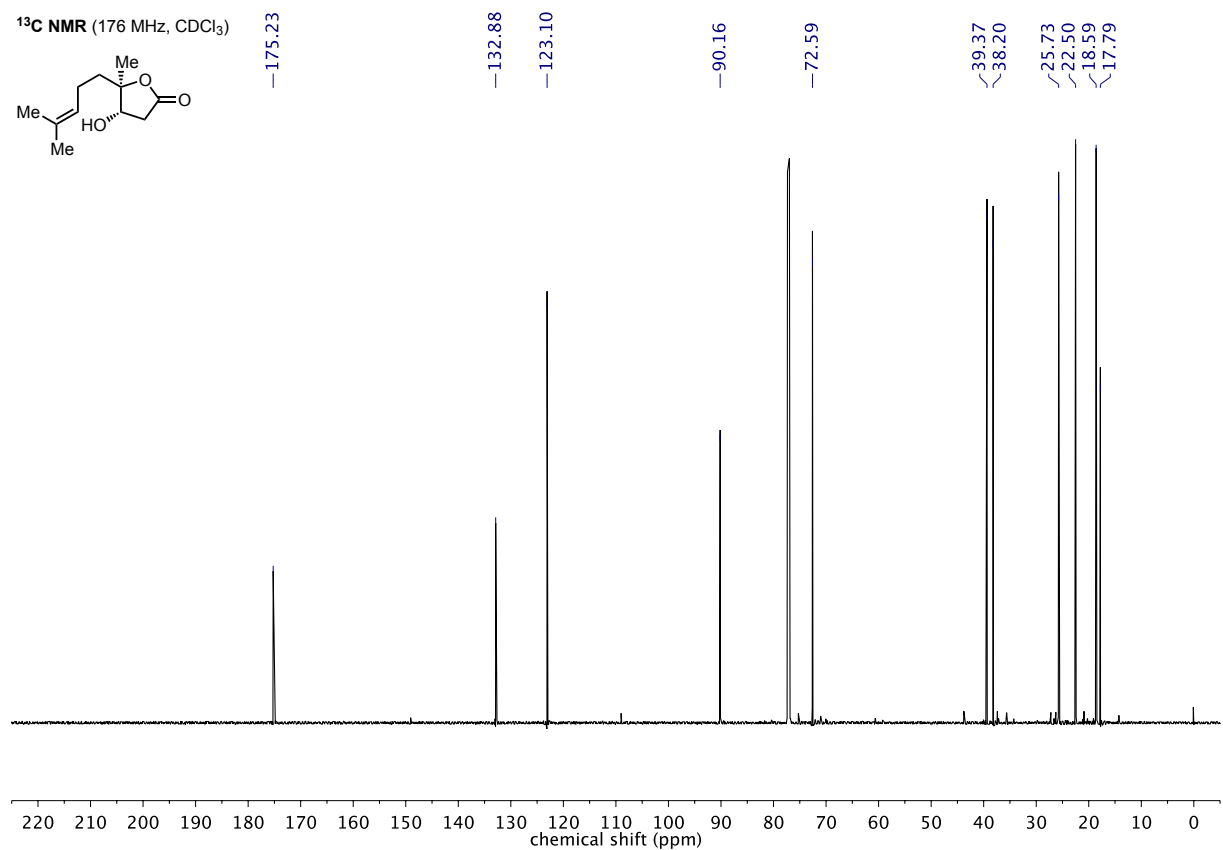
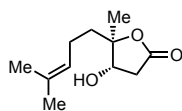
dr 3:2, \*major indicated

<sup>13</sup>C NMR (176 MHz, CDCl<sub>3</sub>)

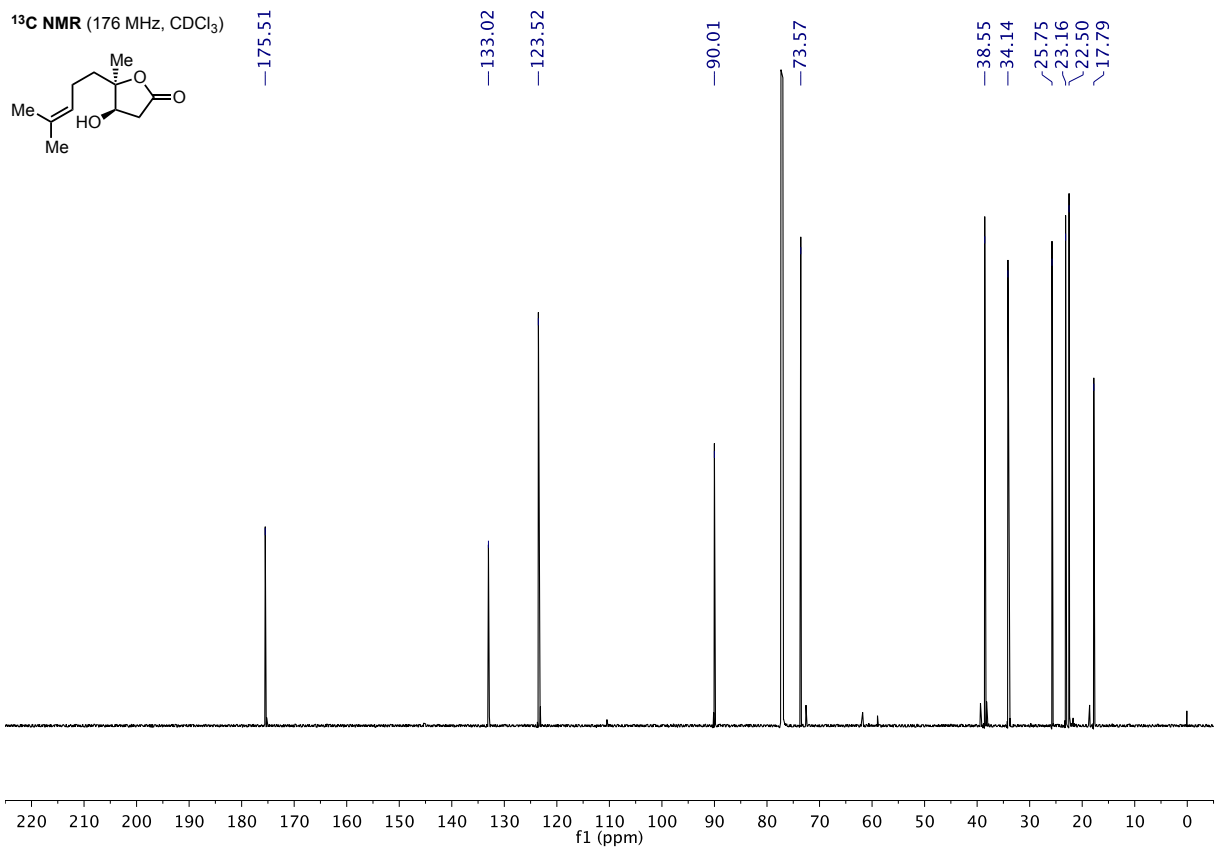
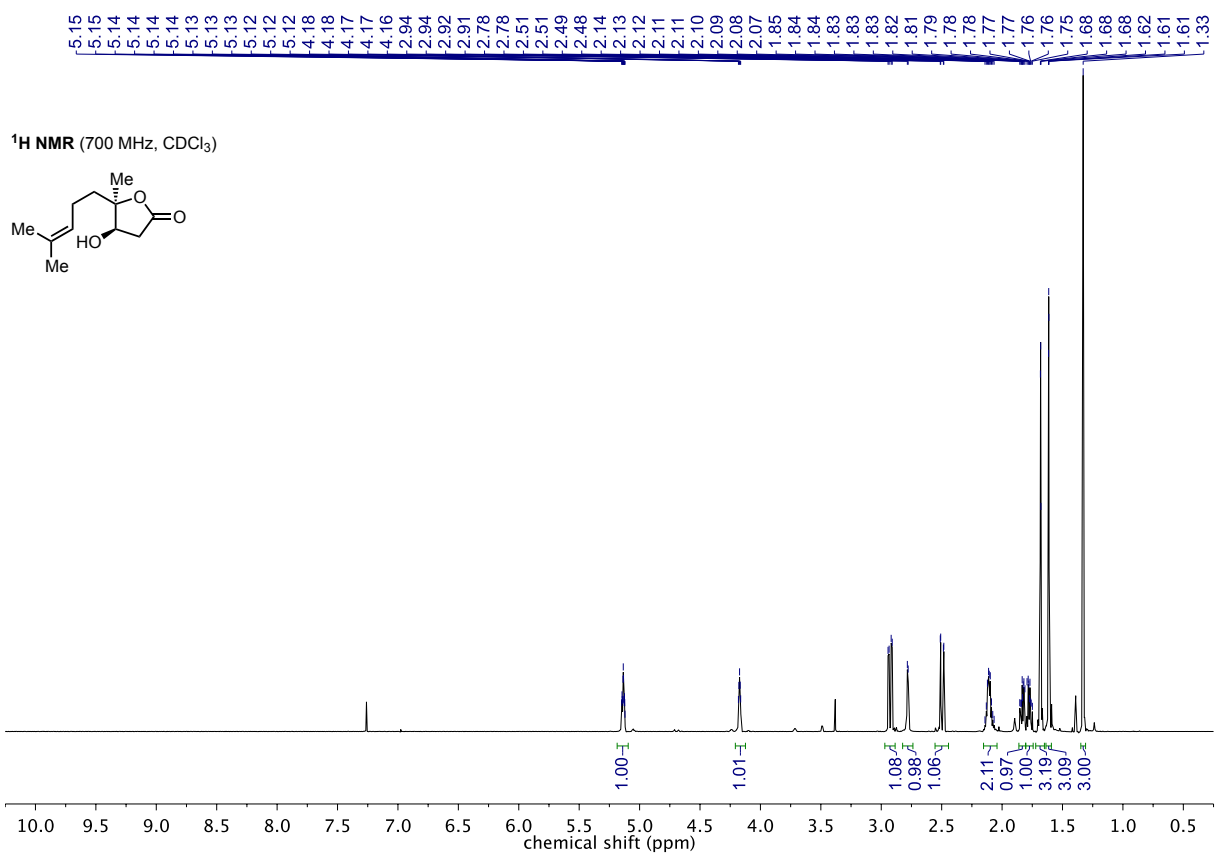


dr 3:2, \*major indicated

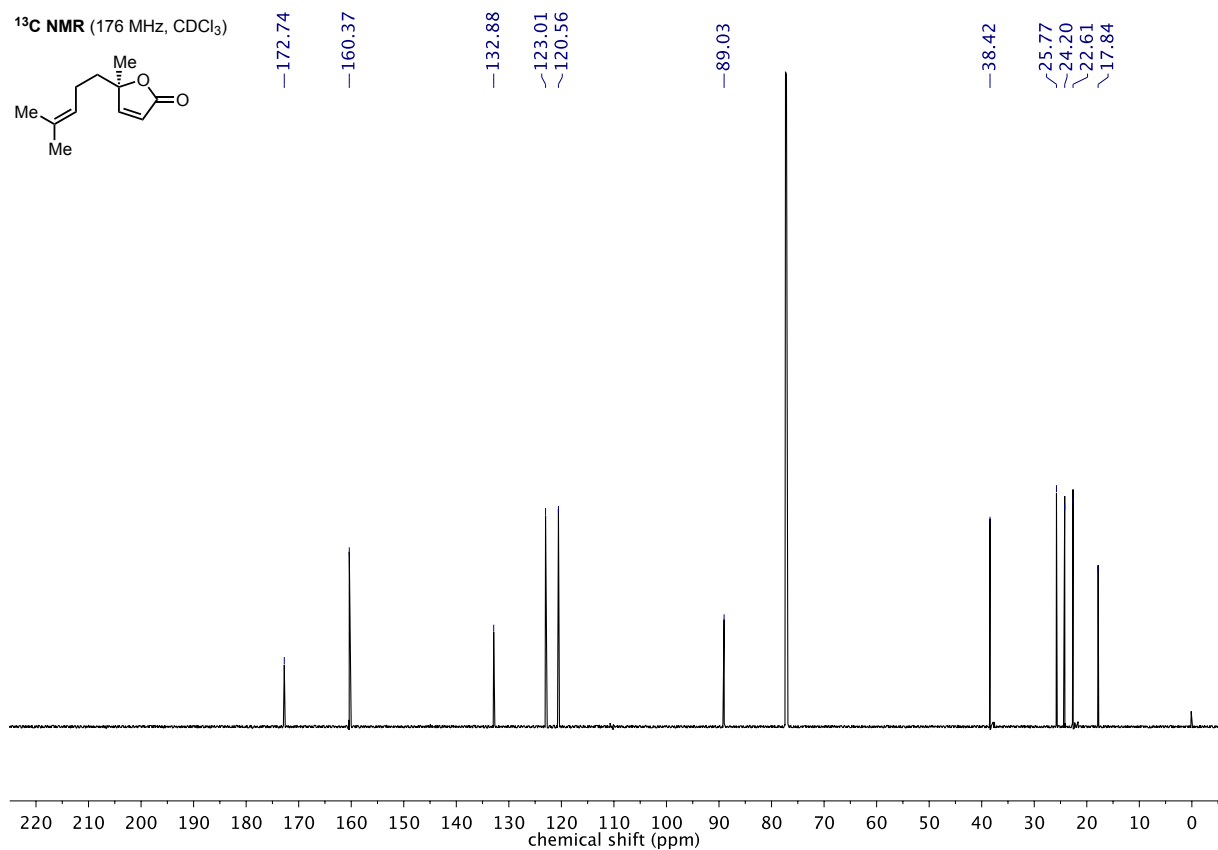
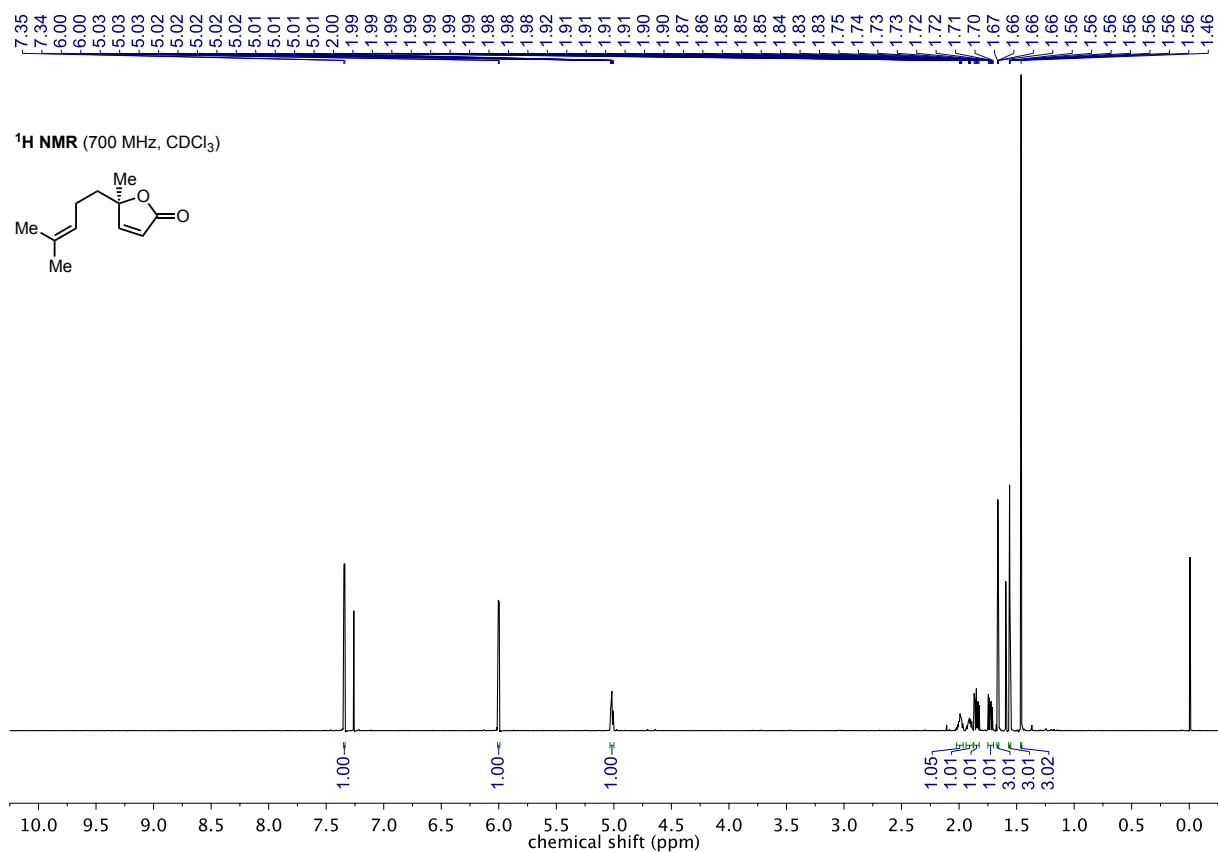


**trans-Lactone SI-2**<sup>1</sup>H NMR (700 MHz, CDCl<sub>3</sub>)<sup>13</sup>C NMR (176 MHz, CDCl<sub>3</sub>)

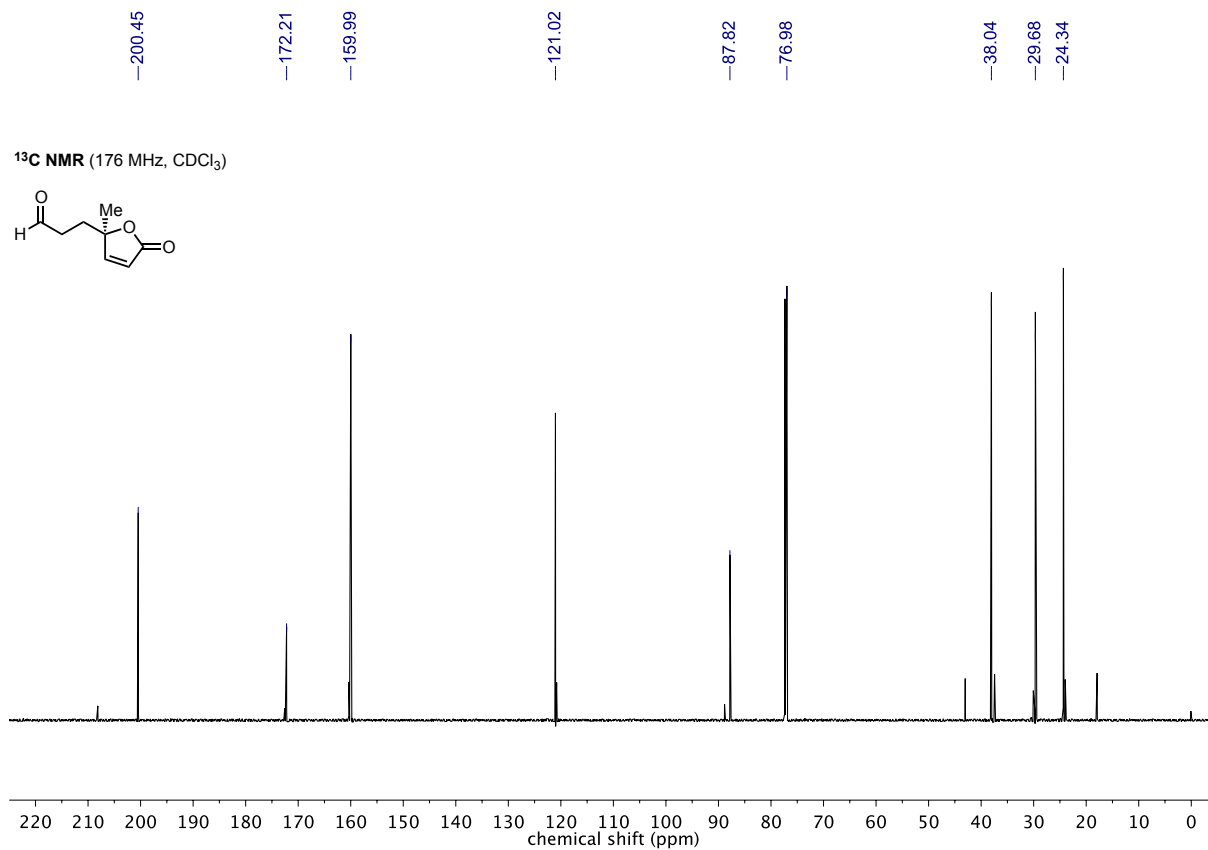
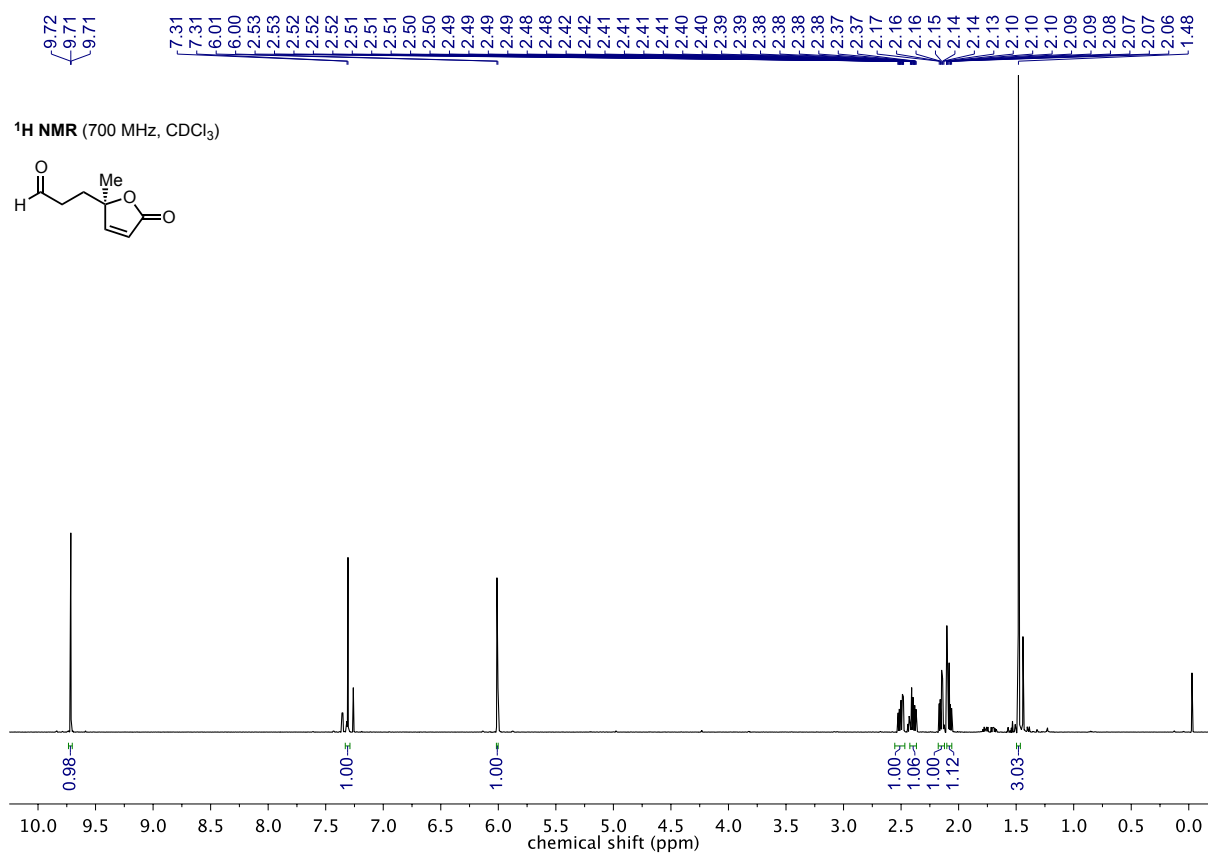


**cis-Lactone SI-2**

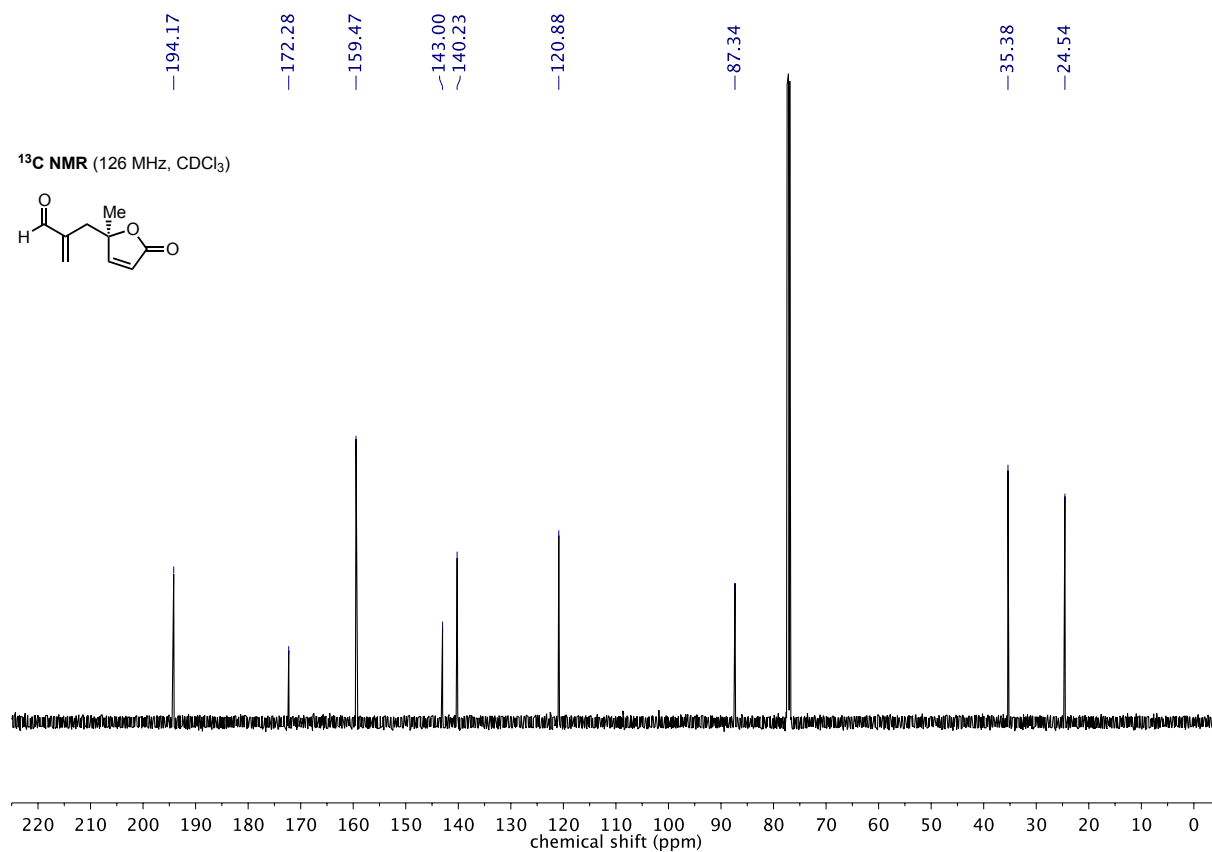
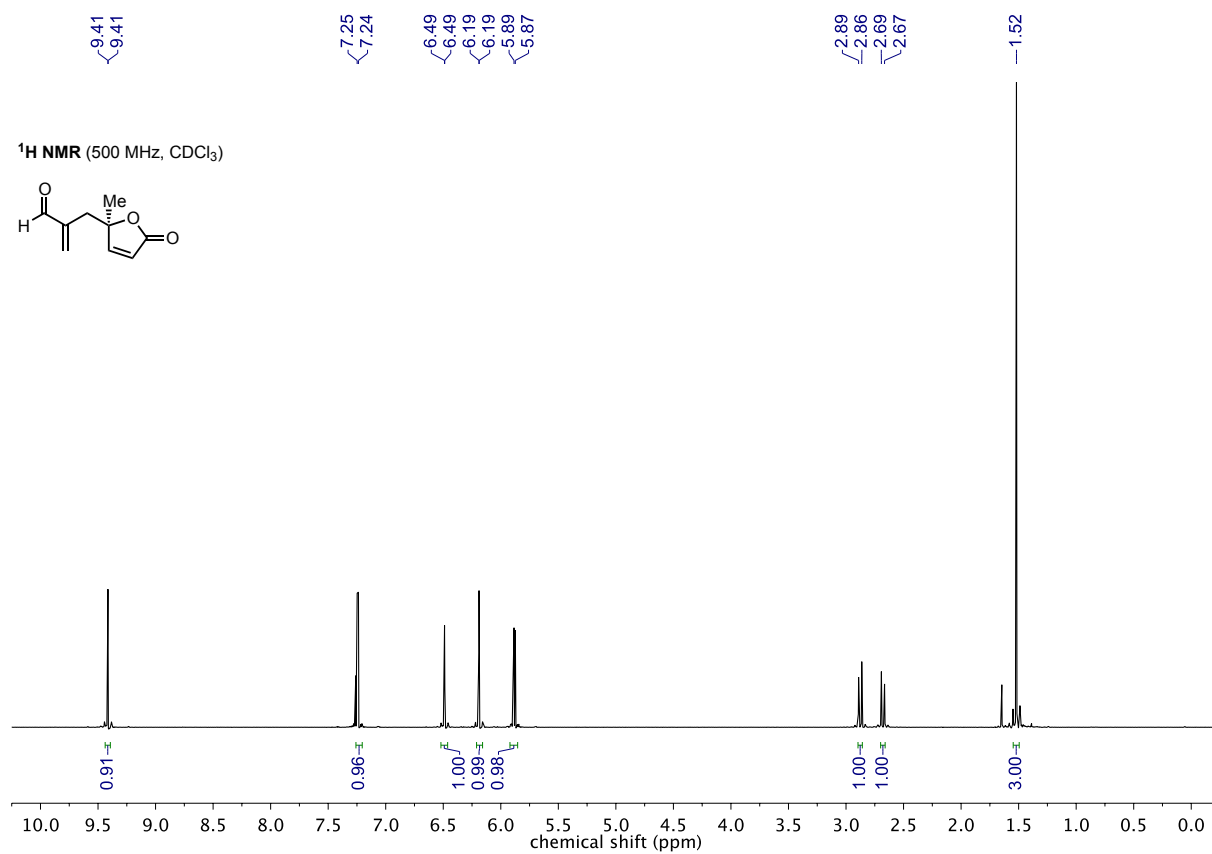
## Butenolide 7



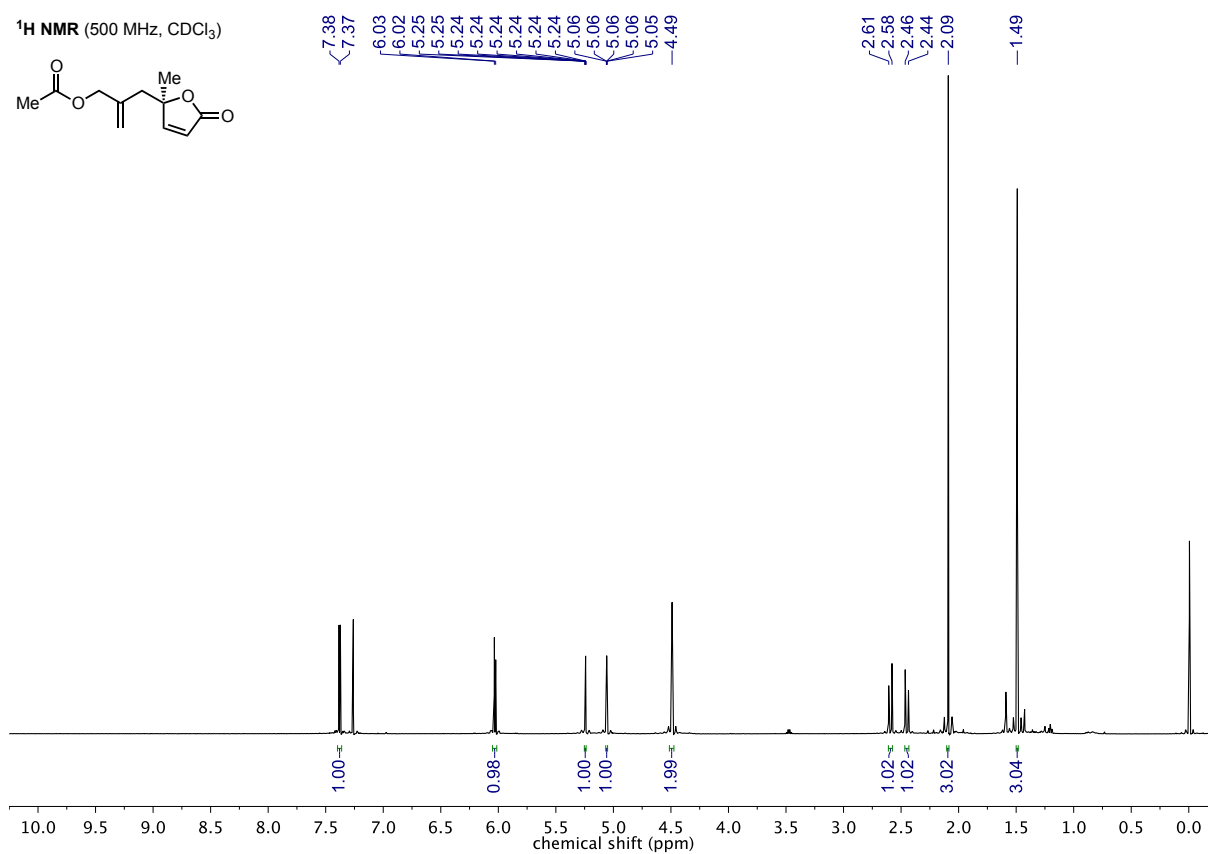
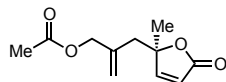
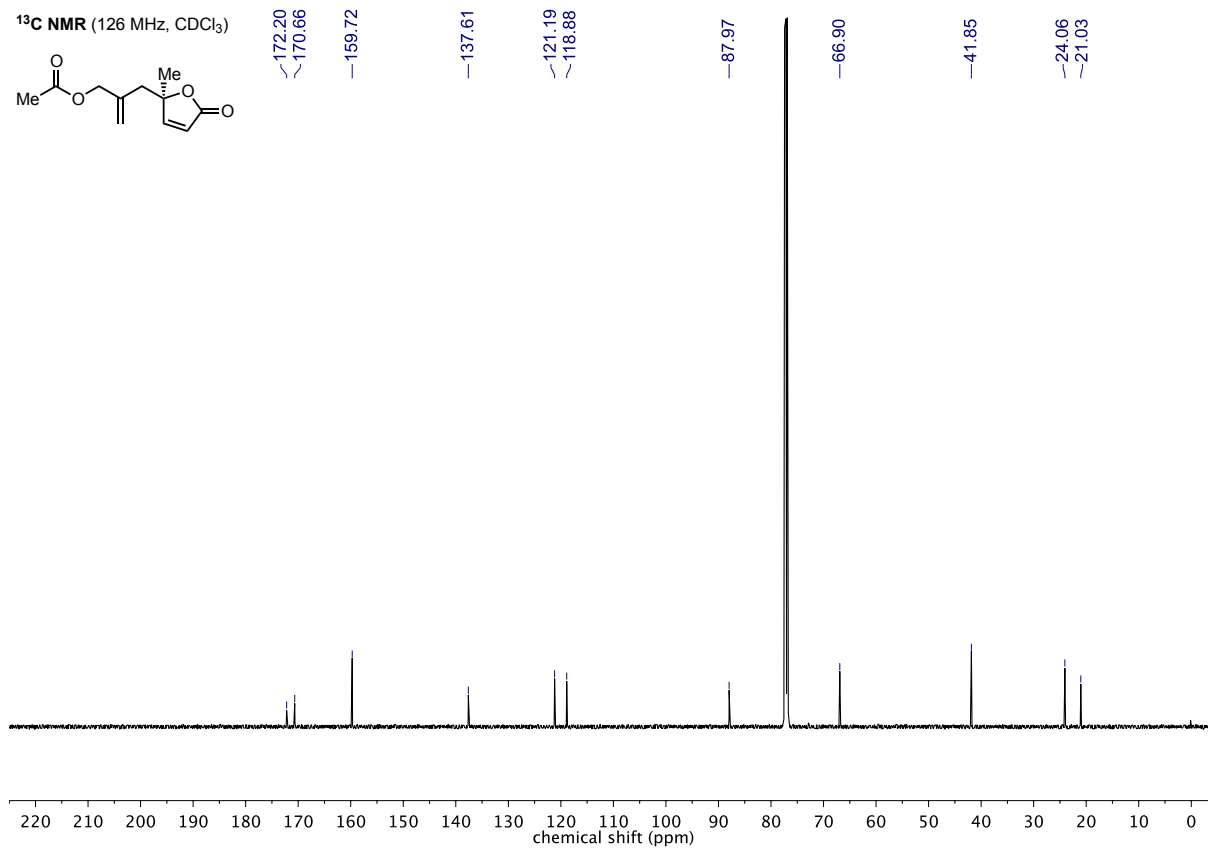
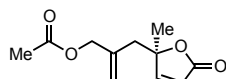
## Aldehyde SI-3



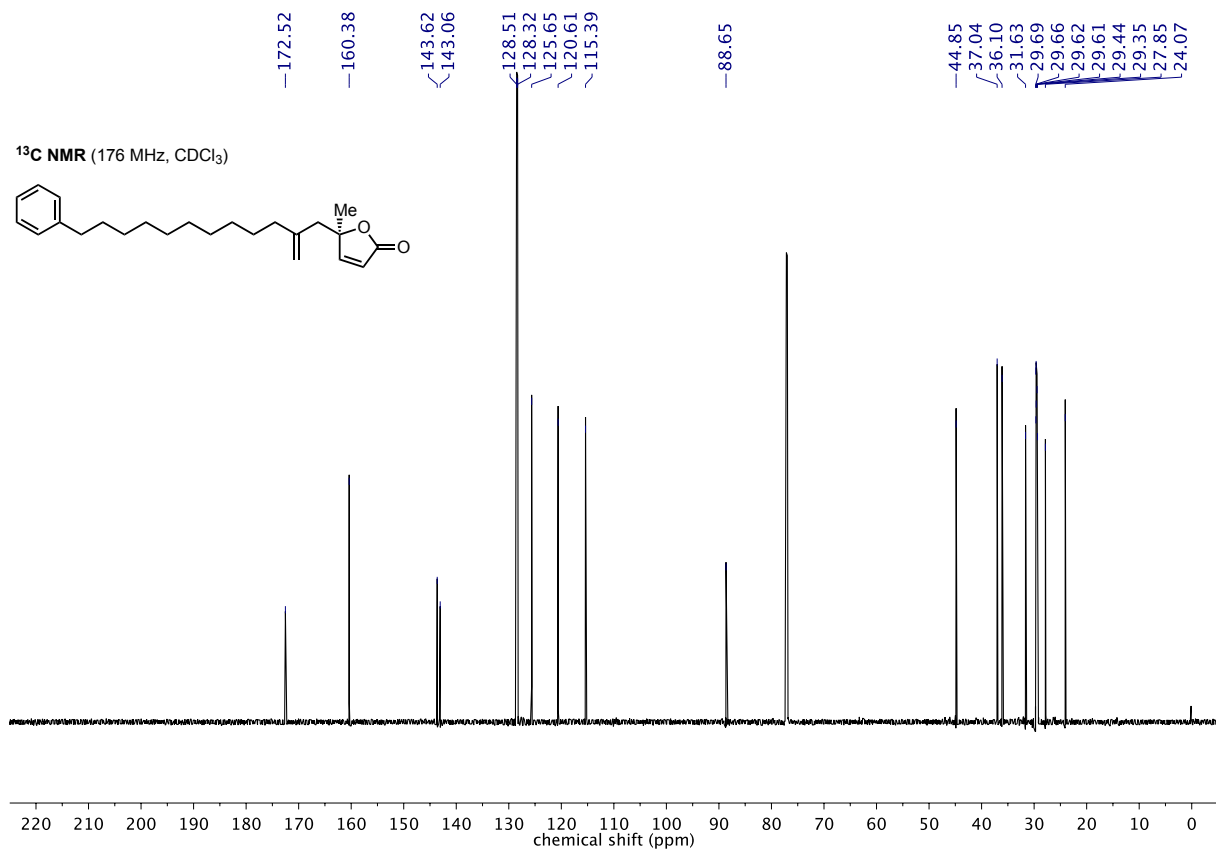
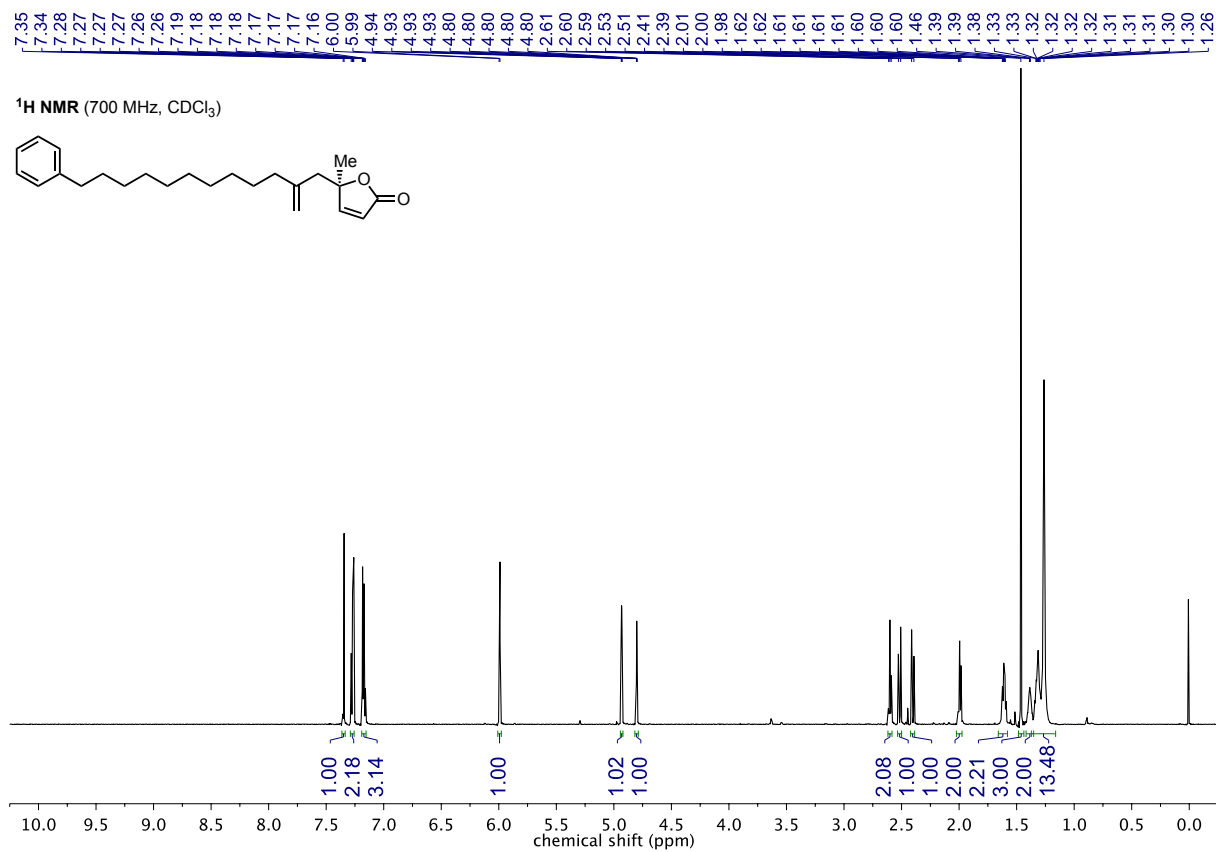
## Enal SI-4

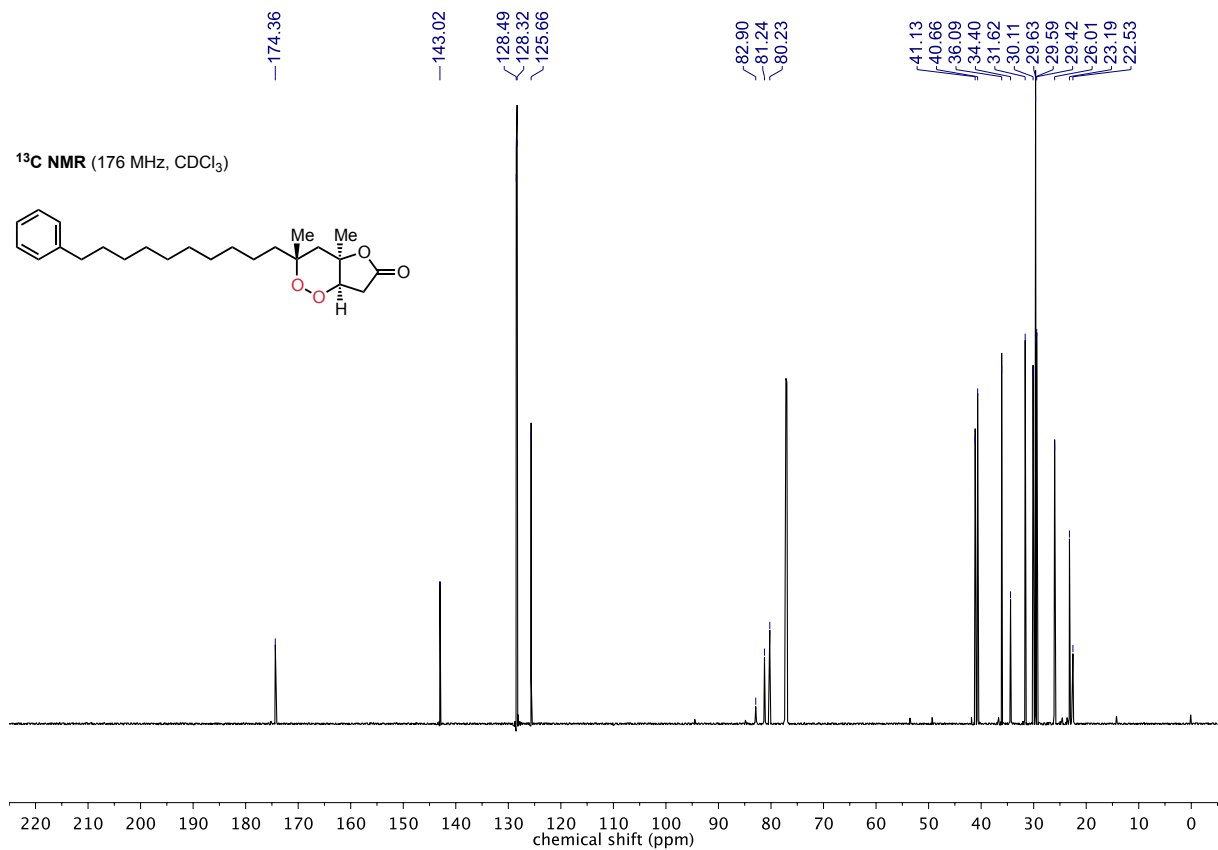
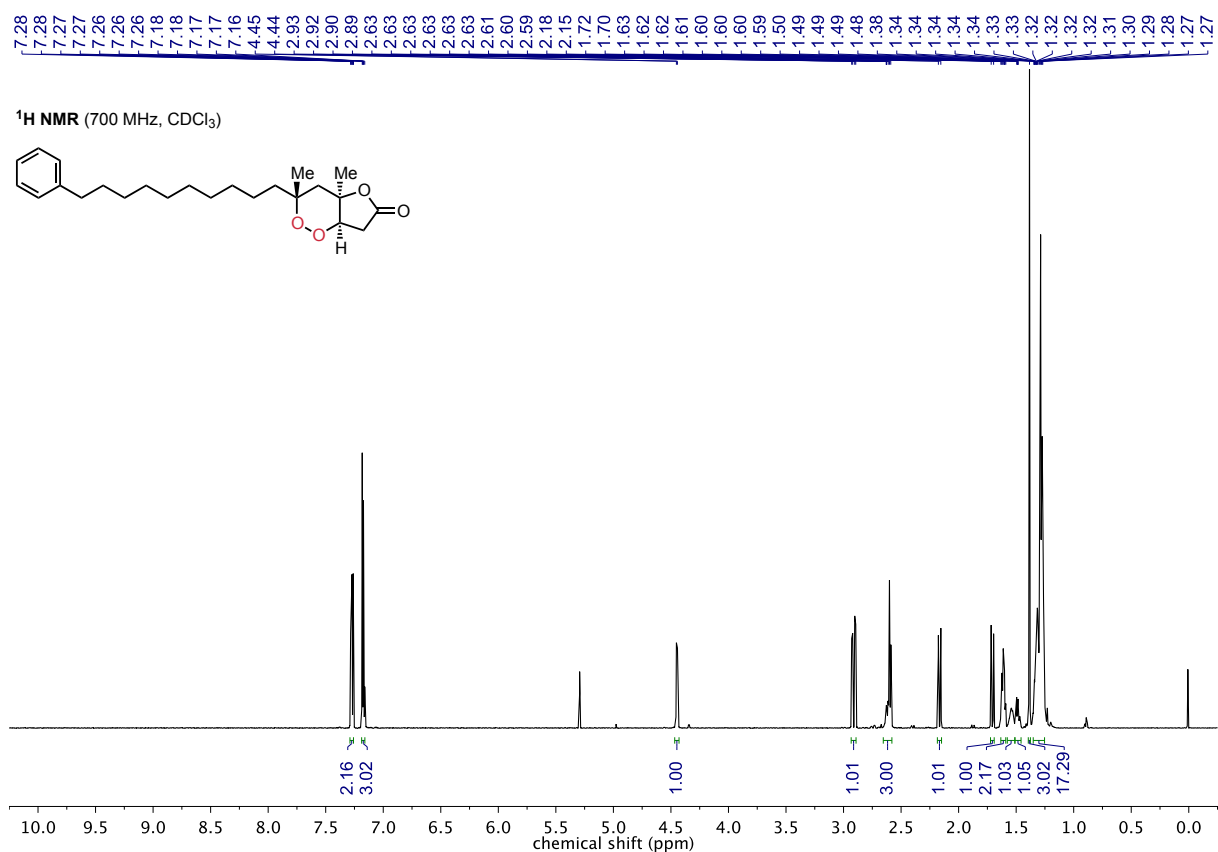


## Allyl acetate 4

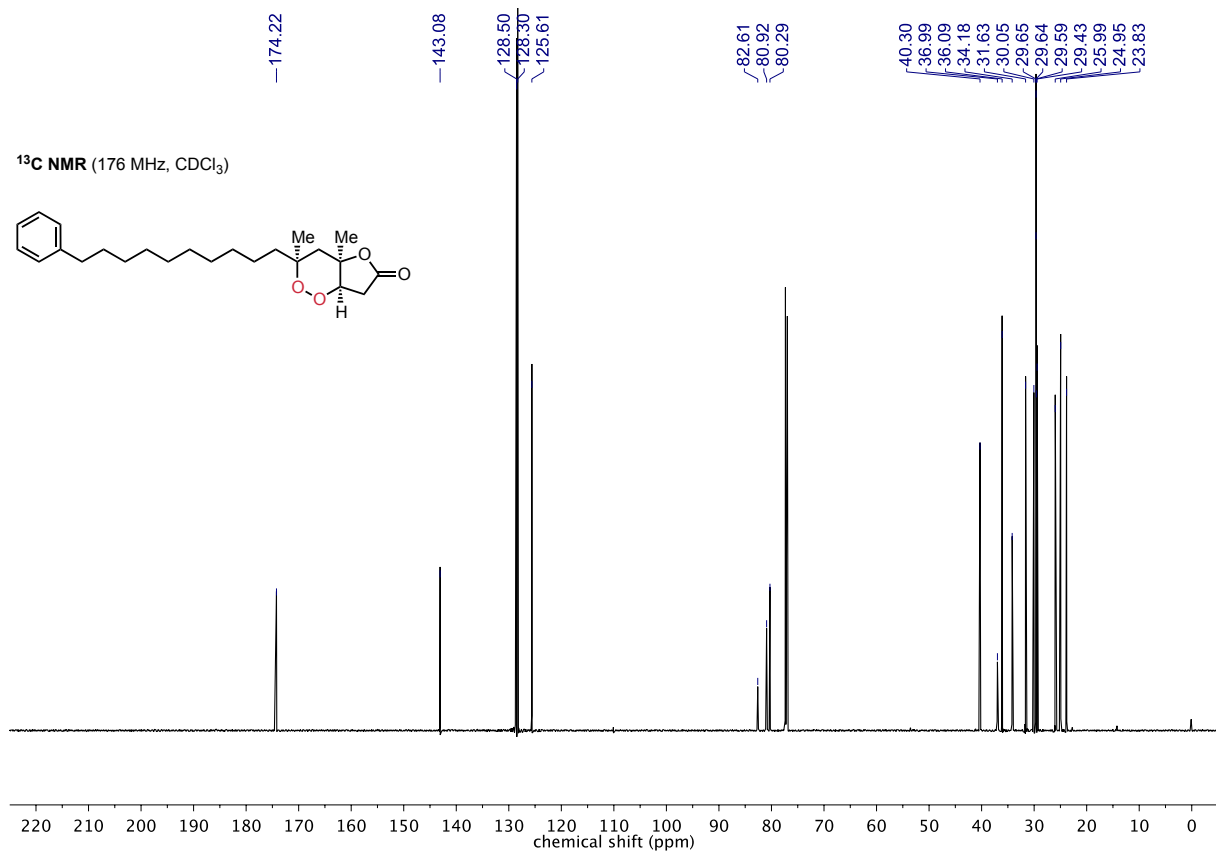
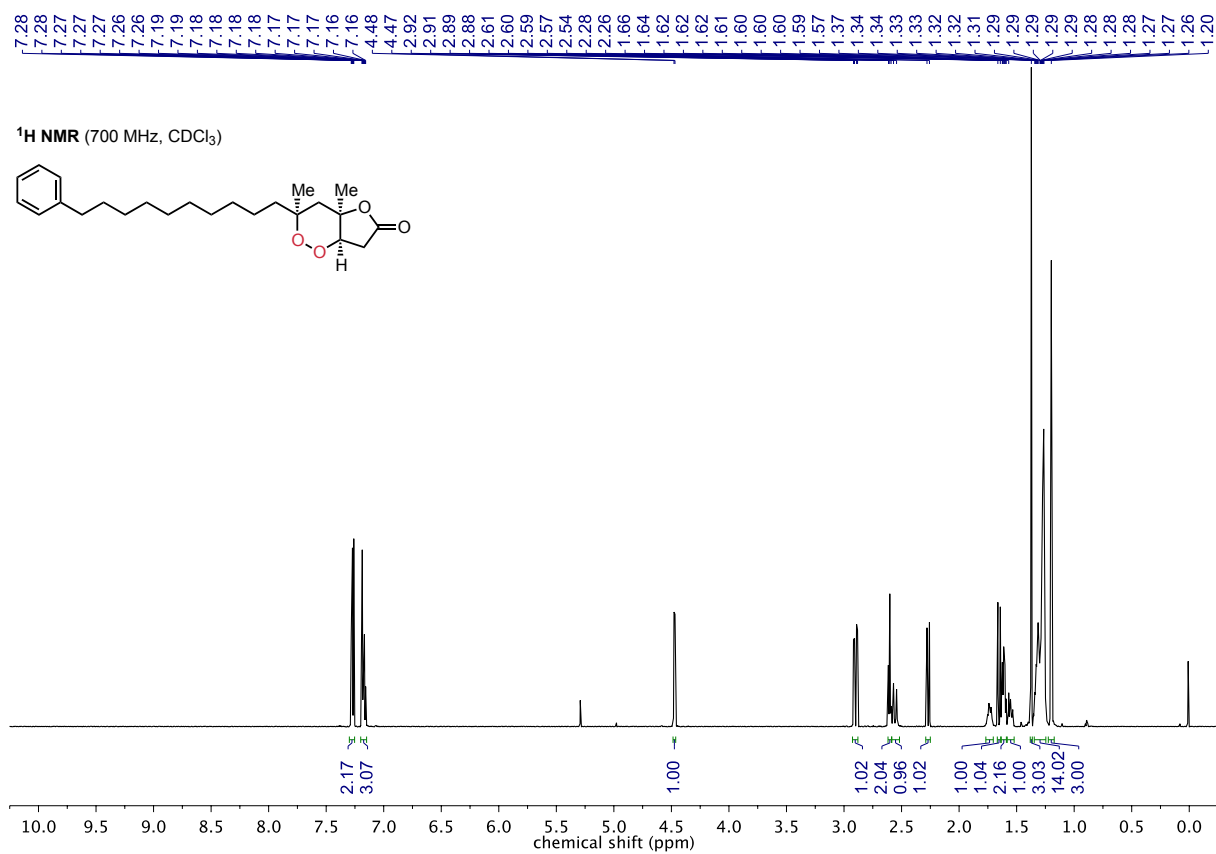
<sup>1</sup>H NMR (500 MHz, CDCl<sub>3</sub>)<sup>13</sup>C NMR (126 MHz, CDCl<sub>3</sub>)

## Alkene 3



**(+)-Plakortolide E (1)**

## (-)-Plakortolide I (2)





## 6. References

- (1) Langhanki, J.; Rudolph, K.; Erkel, G.; Opatz, T. Total synthesis and biological evaluation of the natural product (-)-cyclonerodiol, a new inhibitor of IL-4 signaling. *Org. Biomol. Chem.* **2014**, *12*, 9707–9715.
- (2) Zeynizadeh, B.; Zahmatkesh, K. First and Efficient Method for Reduction of Aliphatic and Aromatic Nitro Compounds with Zinc Borohydride as Pyridine Zinc Tetrahydroborato Complex: A New Stable Ligand-Metal Borohydride. *J. Chin. Chem. Soc.* **2003**, *50*, 267–271.
- (3) Chen, X.; Cheng, Z.; Guo, J.; Lu, Z. Asymmetric remote C-H borylation of internal alkenes via alkene isomerization. *Nat. Commun.* **2018**, *9*, 3939.
- (4) Barnych, B.; Vatèle, J.-M. Total Synthesis of *seco*-Plakortolide E and (-)-*ent*-Plakortolide I: Absolute Configurational Revision of Natural Plakortolide I. *Org. Lett.* **2012**, *14*, 564–567.
- (5) Sheldrick, G. M. A short history of SHELX. *Acta Cryst.* **2008**, *A64*, 112–122.
- (6) Sheldrick, G. M. Crystal structure refinement with SHELX. *Acta Cryst.* **2015**, *C71*, 3–8.
- (7) Dolomanov, O. V.; Bourhis, L. J.; Gildea, R. J.; Howard, J. A. K.; Puschmann, H. OLEX2: a complete structure solution, refinement and analysis program. *J. Appl. Cryst.* **2009**, *42*, 339–341.
- (8) Leisering, S.; Riaño, I.; Depken, C.; Gross, L. J.; Weber, M.; Lentz, D.; Zimmer, R.; Stark, C. B. W.; Breder, A.; Christmann, M. Synthesis of (+)-Greek Tobacco Lactone via a Diastereoselective Epoxidation and a Selenium-Catalyzed Oxidative Cyclization. *Org. Lett.* **2017**, *19*, 1478–1481.
- (9) Siitonen, J. H.; Pihko, P. M. Total Synthesis of (+)-Greek Tobacco Lactone. *Synlett* **2014**, *25*, 1888–1890.
- (10) Benohoud, M.; Erkkilä, A.; Pihko, P. M. ORGANOCATALYTIC  $\alpha$ -METHYLENATION OF ALDEHYDES: PREPARATION OF 3,7-DIMETHYL-2-METHYLENE-6-OCTENAL. *Org. Synth.* **2010**, *87*, 201–208.
- (11) Zeynizadeh, B.; Setamdideh, D.; Faraji, F. Reductive Acetylation of Carbonyl Compounds to Acetates with Pyridine Zinc Borohydride. *Bull. Korean Chem. Soc.* **2008**, *29*, 76–80.
- (12) Zhu, D.; Lv, L.; Li, C.-C.; Ung, S.; Gaom, J.; Li, C.-J. Umpolung of Carbonyl Groups as Alkyl Organometallic Reagent Surrogates for Palladium-Catalyzed Allylic Alkylation. *Angew. Chem. Int. Ed.* **2018**, *57*, 16520–16524.
- (13) Lin, H.-S.; Paquette, L. A. A Convenient Method for Determining the Concentration of Grignard Reagents. *Synth. Commun.* **1994**, *24*, 2503–2506.
- (14) Bernauer, J.; Wu, G.; Jacobi von Wangelin, A. Iron-catalysed allylation-hydrogenation sequence as masked alkyl-alkyl cross-couplings. *RSC Adv.* **2019**, *9*, 31217–31223.
- (15) Barnych, B. Synthetic studies towards plakortolides: asymmetric synthesis of *ent*-plakortolide I and *seco*-plakortolide E. Ph.D. Dissertation, Université Claude Bernard, Lyon I, 2011.
- (16) Rudi, A.; Afanii, R.; Gravalos, L. G.; Akin, M.; Gaydou, E.; Vacelet, J.; Kashman, Y. Three New Cyclic Peroxides from the Marine Sponge *Plakortisaff simplex*. *J. Nat. Prod.* **2003**, *66*, 682–685.
- (17) Qureshi, A.; Salvà, J.; Harper, M.; Faulkner, D. J. New Cyclic Peroxides from the Philippine Sponge *Plakinastrella* sp. *J. Nat. Prod.* **1998**, *61*, 1539–1542.
- (18) Correction of the initially assigned structure to (+)-plakortolide E: Plakortolide Stereochemistry Revisited: Yong, K. W. L.; Barnych, B.; De Voss, J. J.; Vatèle, J.-M.; Garson, M. J. The Checkered History of Plakortolides E and I. *J. Nat. Prod.* **2012**, *75*, 1792–1797.

## Supporting Information – Synthesis of 3-*epi*-Hypatulin B

### Synthesis of 3-*epi*-Hypatulin B Featuring a Late-Stage Photo-Oxidation in Flow

Stefan Leisering, Sebastian Ponath, Kamar Shakeri, Alexandros Mavroskoufis, Merlin Kleoff, Patrick Voßnacker, Simon Steinhauer, Manuela Weber, Mathias Christmann\*

Institut für Chemie und Biochemie, Freie Universität Berlin, Takustraße 3, 14195 Berlin, Germany

## Supporting Information

## Table of Content

<b>1. General Information .....</b>	<b>2</b>
1.1 Materials and Methods .....	2
1.2 Analysis.....	2
1.3 Flow Equipment .....	3
<b>2. Experimental Procedures and Analytical Data.....</b>	<b>4</b>
2.1 Preliminary Studies with Racemic Silyl Enol Ether rac- <b>6</b> .....	5
2.1.1 (2-Methyl-3-(prop-2-en-1-yl)cyclopent-1-en-1-yl)oxy)trimethylsilane (rac- <b>6</b> ) .....	5
2.1.2 Attempted Dieckmann-Type Cyclization.....	5
2.1.3 (1R,3S,4R,5R,6R,8S)-5-methyl-8-((trimethylsilyl)oxy)-2-oxo-3-(oxophenylmethyl)-1,4,6-tris(prop-2-en-1-yl)bicyclo[3.2.1]octan-8-carbonitrile (rac- <b>14</b> ) .....	6
2.2 Synthesis of Enantioenriched 3- <i>epi</i> -Hypatulin B ( <b>17</b> ).....	6
2.2.1 ( <i>S</i> )-2,2'-Bis(methoxymethoxy)-1,1'-binaphthalene ( <b>S-7</b> ).....	6
2.2.2 ( <i>S</i> )-3,3'-Dibromo-2,2'-bis(methoxymethoxy)-1,1'-binaphthalene ( <b>S-8</b> ) .....	7
2.2.3 ( <i>S</i> )-3,3'-Dibromo-[1,1'-binaphthalene]-2,2'-diol ( <b>S-9</b> ) .....	8
2.2.4 ( <i>S</i> )-2-Iodo-1-(prop-2-en-1-yl)cyclopent-2-enol ( <b>S-6</b> ).....	8
2.2.5 ( <i>S</i> )-2-Methyl-1-(prop-2-en-1-yl)cyclopent-2-enol (( <i>S</i> )- <b>S-2</b> ) .....	9
2.2.6 (2 <i>S</i> ,3 <i>S</i> )-2-Methyl-3-(prop-2-en-1-yl)cyclopentan-1-one ( <b>5</b> ).....	10
2.2.7 (( <i>S</i> )-(2-Methyl-3-(prop-2-en-1-yl)cyclopent-1-en-1-yl)oxy)trimethylsilane ( <b>6</b> ) .....	10
2.2.8 (2 <i>R</i> ,3 <i>S</i> )-2-(1-hydroxy-2-(2-phenyl-1,3-dioxolan-2-yl)ethyl)-2-methyl-3-(prop-2-en-1-yl)cyclopentanone ( <b>8</b> ) .....	11
2.2.9 (2 <i>R</i> ,3 <i>S</i> )-2-methyl-2-(( <i>E</i> )-3-oxo-3-phenylprop-1-en-1-yl)-3-(prop-2-en-1-yl)cyclopentan-1-one ( <b>9</b> ).....	12
2.2.10 (2 <i>R</i> ,3 <i>R</i> ,5 <i>R</i> )-2-methyl-2-(( <i>E</i> )-3-oxo-3-phenylprop-1-en-1-yl)-3,5-bis(prop-2-en-1-yl)cyclopentan-1-one ( <b>S-11</b> ).....	13
2.2.11 (1 <i>R</i> ,3 <i>R</i> ,4 <i>R</i> )-methyl 3-methyl-2-oxo-3-(( <i>E</i> )-3-oxo-3-phenylprop-1-en-1-yl)-1,4-bis(prop-2-en-1-yl)cyclopentanecarboxylate ( <b>10</b> ).....	14
2.2.12 (1 <i>R</i> ,3 <i>R</i> ,4 <i>R</i> )-methyl 3-methyl-2-oxo-3-(( <i>R</i> )-1-oxo-1-phenylhex-5-en-3-yl)-1,4-bis(prop-2-en-1-yl)cyclopentanecarboxylate ( <b>11</b> ).....	15
2.2.13 (1 <i>R</i> ,3 <i>R</i> ,4 <i>R</i> )-methyl 3-methyl-2-oxo-3-(( <i>R,E</i> )-1-phenyl-1-((trimethylsilyl)oxy)hexa-1,5-dien-3-yl)-1,4-bis(prop-2-en-1-yl)cyclopentanecarboxylate ( <b>12</b> ) .....	16
2.2.14 (1 <i>R</i> ,3 <i>R</i> ,4 <i>R</i> )-3-methyl-2-oxo-3-(( <i>R,E</i> )-1-phenyl-1-((trimethylsilyl)oxy)hexa-1,5-dien-3-yl)-1,4-bis(prop-2-en-1-yl)cyclopentanecarbaldehyde ( <b>S-14</b> ) .....	17
2.2.15 (1 <i>S</i> ,3 <i>S</i> ,4 <i>R</i> ,5 <i>R</i> ,6 <i>R</i> )-5-methyl-3-(oxophenylmethyl)-1,4,6-tris(prop-2-en-1-yl)bicyclo[3.2.1]octan-2,8-dione ( <b>4</b> ) .....	18
2.2.17 (1 <i>R</i> ,3 <i>S</i> ,4 <i>R</i> ,5 <i>R</i> ,6 <i>R</i> ,8 <i>S</i> )-8-hydroxy-8-(1-methoxypropa-1,2-dien-1-yl)-5-methyl-3-(oxophenylmethyl)-1,4,6-tris(prop-2-en-1-yl)bicyclo[3.2.1]octan-2-one ( <b>15</b> ).....	19
2.2.18 (1 <i>R</i> ,3 <i>S</i> ,4 <i>R</i> ,5 <i>R</i> ,6 <i>R</i> ,8 <i>S</i> )-methyl 8-hydroxy-5-methyl-2-oxo-3-(oxophenylmethyl)-1,4,6-tris(prop-2-en-1-yl)bicyclo[3.2.1]octane-8-carboxylate ( <b>16</b> ) .....	20
2.2.19 (1 <i>R</i> ,3 <i>S</i> ,4 <i>R</i> ,5 <i>R</i> ,6 <i>R</i> ,8 <i>S</i> )-methyl 8-hydroxy-5-methyl-2-oxo-3-(oxophenylmethyl)-1,4,6-tris(3-methylbut-2-en-1-yl)bicyclo[3.2.1]octane-8-carboxylate ( <b>17</b> ) .....	21
<b>4. X-ray data.....</b>	<b>22</b>
<b>5. NMR Spectra .....</b>	<b>26</b>
<b>6. Chiral GC Analysis .....</b>	<b>49</b>
<b>7. References .....</b>	<b>50</b>

## 1. General Information

### 1.1 Materials and Methods

Reactions with air or moisture sensitive substances were carried out under an argon atmosphere using standard Schlenk technique. Ambient or room temperature (r.t.) refers to 18–23 °C. Heating of reactions was performed with an oil bath unless otherwise noted.

Unless otherwise noted, all starting materials and reagents were purchased from commercial distributors and used without further purification. (*S*)-3,3'-Dibromo-[1,1'-binaphthalene]-2,2'-diol (**SI-9**) is commercially available but can easily be prepared in larger quantities. Anhydrous dichloromethane, Tetrahydrofuran (THF) and toluene were provided by purification with a MBraun SPS-800 solvent system (BRAUN) using solvents of HPLC grade purchased from FISCHER Scientific and ROTH. Anhydrous *N,N*-dimethylformamide (DMF) was purchased from ACROS Organics. *t*-BuOH was purchased from GRÜSSING and stored under argon over activated molecular sieves. Triethylamine was distilled from calcium hydride and stored under argon over KOH. Solvents for extraction, crystallization and flash column chromatography were purchased in technical grade and distilled under reduced pressure prior to use.

Column chromatography was performed on silica 60 M (0.040-0.063 mm, 230-400 mesh, MACHEREY-NAGEL).

Medium pressure liquid chromatography (MPLC) was performed with a TELEDYNE ISCO Combi-Flash Rf200 using prepacked silica columns and cartridges from TELDYNE. UV response was monitored at 254 nm and 280 nm. As eluents, cyclohexane (99.5+% quality) and EtOAc (HPLC grade) were used.

Preparative high performance liquid chromatography (HPLC) was performed with a modular system from KNAUER on a chiral column. As eluents, *n*-hexane (HPLC grade) and *i*-PrOH (HPLC grade) were used. The specific conditions are given in each case.

The following compounds were prepared according to the literature: 2-iodocyclopent-2-enone (**SI-4**),<sup>1</sup> *B*-(prop-2-en-1-yl)-1,3,2-dioxaborinane (**SI-5**),<sup>2</sup> 3,3-(ethylenedioxy)-3-phenylpropanal (**7**),<sup>3</sup> silica-supported sodium hydrogen sulfate (NaHSO<sub>4</sub>·SiO<sub>2</sub>).<sup>4</sup>

### 1.2 Analysis

**Reaction monitoring:** Reactions were monitored by thin layer chromatography (TLC). TLC-analysis was performed on silica gel coated aluminum plates ALUGRAM® Xtra SIL G/UV<sub>254</sub> purchased from MACHEREY-NAGEL. Products were visualized by UV light at 254 nm and by using staining reagents (based on KMnO<sub>4</sub> and anisaldehyde).

**NMR spectroscopy:** <sup>1</sup>H NMR and <sup>13</sup>C NMR spectral data were recorded on JEOL (ECX 400, ECP 500) and BRUKER (AVANCE III 500, AVANCE III 700) spectrometer in the reported deuterated solvents. The chemical shifts ( $\delta$ ) are listed in parts per million (ppm) and are reported relative to the corresponding residual non-deuterated solvent signal (CDCl<sub>3</sub>:  $\delta_{\text{H}} = 7.26$  ppm,  $\delta_{\text{C}} = 77.16$  ppm). Integrals are in accordance with assignments; coupling constants (*J*) are given in Hz. Multiplicity is indicated as follows: s (singlet), d (doublet), t (triplet), q (quartet), br = broad and combinations thereof. In the case where no multiplicity could be identified, the chemical shift range of the signal is given as m (multiplet). <sup>13</sup>C NMR spectra are <sup>1</sup>H-broadband decoupled. For detailed peak assignments 2D spectra were measured (COSY, HMQC, HMBC).

**High resolution mass spectrometry:** High resolution mass spectra (HRMS) were measured with an AGILENT 6210 ESI-TOF (10  $\mu$ L/min, 1.0 bar, 4 kV) instrument.

**Optical rotation:** Optical rotation values were measured with a JACSO P-2000 polarimeter at 589 nm using 100 mm cells and the indicated solvent and concentration (g/100 mL) at the given temperatures.

**Melting points:** Melting points were determined by a digital melting point apparatus (Büchi B-545) and are uncorrected.

**Chiral GC:** Enantiomeric excesses was determined by chiral GC using an AGILENT 6850 instrument equipped with a chiral column. The specific conditions are given in each case.

**X-ray:** X-ray diffraction data was collected on a BRUKER D8 Venture CMOS area detector (Photon 100) diffractometer with Cu<sub>K $\alpha$</sub>  and Mo<sub>K $\alpha$</sub>  radiation. Single crystals were coated with perfluoroether oil and mounted on a

0.2 mm Micromount. The structures were solved with the ShelXT<sup>5</sup> structure solution program using intrinsic phasing and refined with the ShelXL<sup>6</sup> refinement package using least squares on weighted F2 values for all reflections using OLEX2.<sup>7</sup>

### 1.3 Flow Equipment

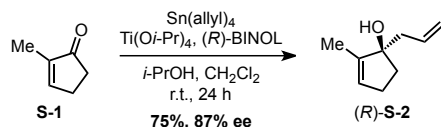
All flow experiments were carried out using a self-assembled flow platform as previously reported.<sup>8</sup>

**Tubings, connectors and valves:** FEP tubing (outer diameter 1/16", inner diameter 1/32") were obtained from the company BOLA. T-mixers made from stainless steel 316L were provided by the company VICI. Tubings and mixers were connected using either coned 10-32 UNF fittings made from stainless steel 316L obtained from UPCHURCH SCIENTIFIC or flat bottom 1/4-28 UNF gripper fittings made from PP or ETFE obtained from DIBAFIT. Adapters for 1/4-28 UNF systems were made from PP or PTFE and were provided from UPCHURCH SCIENTIFIC.

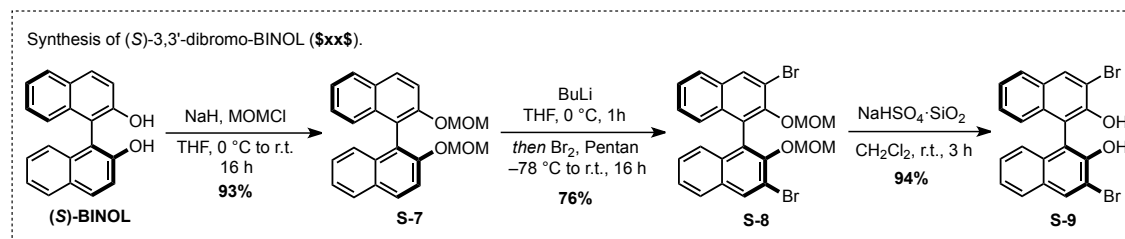
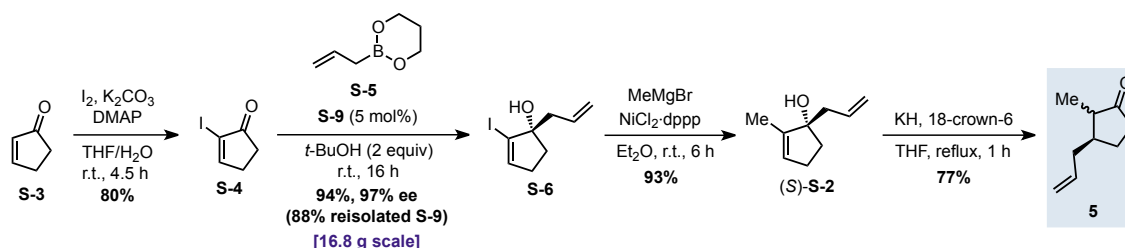
## 2. Experimental Procedures and Analytical Data

Ketone **5** was prepared starting from cyclopent-2-enone (**S-3**) in analogy to reported procedures. Although allylic alcohol **S-2** can be prepared by the direct asymmetric allylation of 2-methylcyclopent-2-enone (**S-1**) according to a procedure by WALSH and co-workers,<sup>9</sup> we found that the strategy by TABER and co-workers via 2-iodocyclopent-2-enone (**S-4**) gives higher enantiomeric excess.<sup>10</sup>

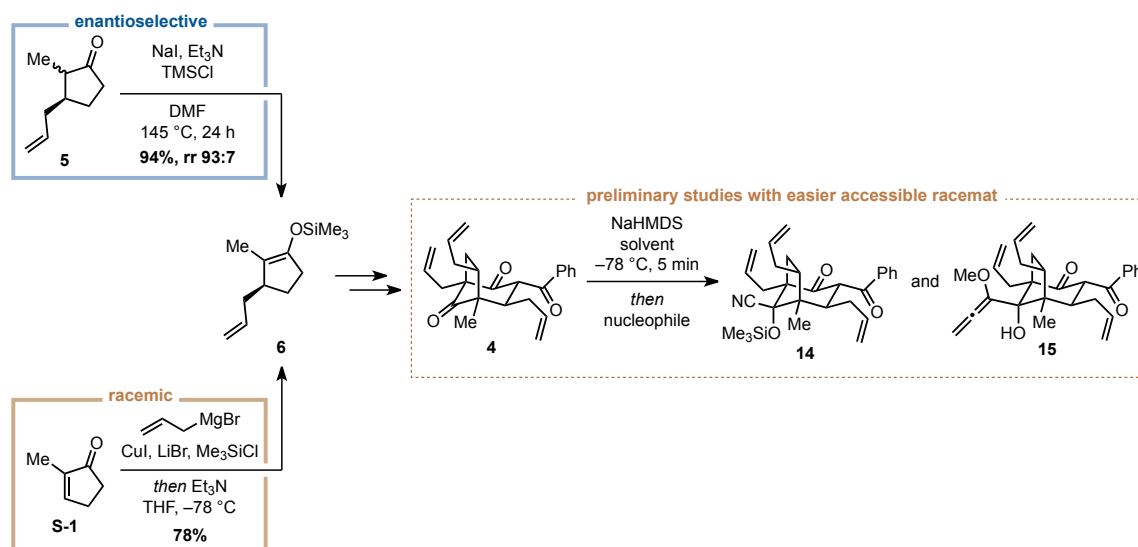
A – Asymmetric allylation strategy by WALSH and co-workers.



B – Asymmetric allylation strategy by TABER and co-workers.



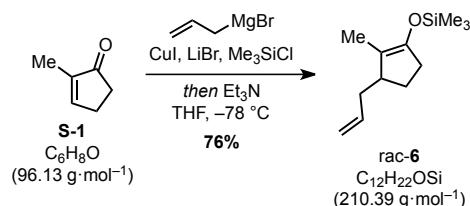
Preliminary studies were conducted with the easier accessible racemat of silyl enol ether **6**, which can be prepared by copper-mediated conjugate addition of allylmagnesium bromide to 2-methylcyclopent-2-enone **S-1**. Thus, crystals structures for the compounds **4**, **14** and **15** were obtained as racemates. Cyanhydrin **14** was only prepared in racemic form.



## 2.1 Preliminary Studies with Racemic Silyl Enol Ether rac-6

All reaction conditions with racemic compounds are identical to those starting from enantioenriched silyl enol ether **6**. Procedures for compounds, that were only obtained as racemates, are reported in this section.

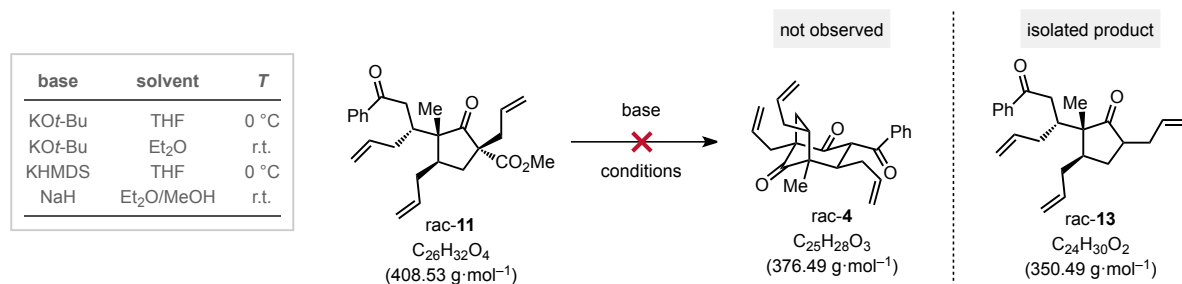
### 2.1.1 (2-Methyl-3-(prop-2-en-1-yl)cyclopent-1-en-1-yl)oxy)trimethylsilane (rac-6)



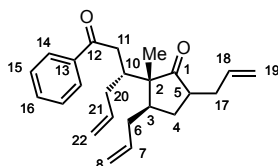
Racemic silyl enol ether **rac-6** was prepared according to a reported procedure by WICHA et al.<sup>11</sup> A flame-dried three-neck round-bottom flask equipped with a dropping funnel was charged with LiBr (54.2 g, 624 mmol, 3.0 equiv) and CuI (119 g, 624 mmol, 3.0 equiv) and the salts were flame-dried under high vacuum until bubbling ceased. Anhydrous THF (1 L) was added and the suspension was cooled to  $-78^\circ\text{C}$ . The allylmagnesium bromide (1 M in Et<sub>2</sub>O, 541 mL, 541 mmol, 2.6 equiv) was added dropwise and the resulting suspension was stirred for 30 min. Then 2-methylcyclopent-2-enone **S-1** (20.0 g, 208 mmol, 1.0 equiv) and trimethylsilyl chloride (81.5 mL, 645 mmol, 3.1 equiv) were added and the reaction mixture was stirred for 60 min at  $-78^\circ\text{C}$ . Then Et<sub>3</sub>N (130 mL) was added and the mixture was warmed to ambient temperature. A second portion of Et<sub>3</sub>N (130 mL) was added and the mixture was diluted with *n*-pentane (1 L) and was left to rest for 15 min. The precipitate was removed by filtration and the residue was rinsed with *n*-pentane (3 ×). The filtrate was washed with saturated aqueous NaHCO<sub>3</sub> (1 L) and the aqueous layer was extracted with *n*-pentane (3 × 500 mL). The combined organic layers were washed with brine (500 mL), dried over anhydrous Na<sub>2</sub>SO<sub>4</sub> and concentrated under reduced pressure. The crude product was purified by distillation (90 °C, 5 mbar) to yield silyl enol ether **rac-6** (33.2 g, 158 mmol, 76%) as a colorless liquid.

The analytical data are identical with those for enantioenriched silyl enol ether **6**.

### 2.1.2 Attempted Dieckmann-Type Cyclization



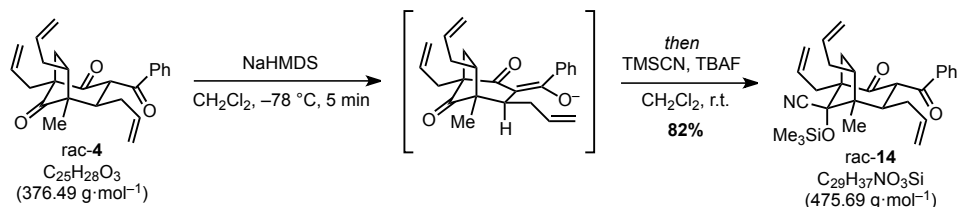
All reactions were performed on a 1–5 mg scale. Formation of the decarboxylation product **rac-13** was observed within several minutes in all cases. Purification was done either by column chromatography or preparative TLC (SiO<sub>2</sub>, *n*-pentane/EtOAc, 50:1).



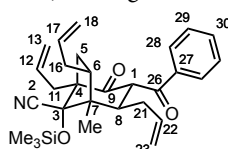
<sup>1</sup>H NMR (700 MHz, CD<sub>2</sub>Cl<sub>2</sub>): δ = 7.96 – 7.94 (m, 2H, H-14), 7.57 – 7.54 (m, 1H, H-16), 7.48 – 7.45 (m, 2H, H-15), 5.89 (dddd, *J* = 17.1, 10.1, 7.7, 6.2 Hz, 1H, H-7), 5.74 (ddt, *J* = 17.1, 10.1, 7.0 Hz, 1H, H-18), 5.68 (dddd, *J* = 17.1, 10.1, 8.7, 5.3 Hz, 1H, H-21), 5.13 – 5.09 (m, 1H, H-8), 5.07 – 5.03 (m, 2H, H-8, H-19), 5.01 – 4.95 (m, 2H, H-19, H-22), 4.91 – 4.88 (m, 1H, H-22), 3.31 (dd, *J* = 17.6, 5.6 Hz, 1H, H-11), 2.99 (dd, *J* = 17.6, 6.0 Hz, 1H, H-11), 2.61 (dddd, *J* = 9.8, 6.0, 5.6, 3.5 Hz, 1H, H-10), 2.49 (dddt, *J* = 14.2, 6.9, 4.2, 1.3 Hz, 2H, H-17), 2.44 – 2.35 (m, 2H, H-6, H-20), 2.29 – 2.21 (m, 2H, H-3, H-4), 2.20 – 2.14 (m, 1H, H-5), 2.04 (dddt, *J* = 14.2, 8.5, 7.2, 1.2 Hz, 1H, H-17), 1.96 – 1.88 (m, 2H, H-6, H-20), 1.19 – 1.12 (m, 1H, H-4), 0.83 (s, 3H, Me) ppm.

$^{13}\text{C}$  NMR (176 MHz,  $\text{CD}_2\text{Cl}_2$ ):  $\delta$  = 223.4 (C-1), 200.4 (C-12), 138.0 (C-21), 137.9 (C-13), 136.6 (C-18), 133.3 (C-16), 129.1 (C-15), 128.6 (C-14), 117.0 (C-22), 116.6 (C-19), 116.3 (C-8), 54.0 (C-2), 50.1 (C-5), 40.9 (C-3), 39.7 (C-11), 38.5 (C-10), 36.3 (C-20), 35.6 (C-6), 34.6 (C-17), 31.9 (C-4), 16.7 (Me) ppm.

### 2.1.3 (1R,3S,4R,5R,6R,8S)-5-methyl-8-((trimethylsilyl)oxy)-2-oxo-3-(oxophenylmethyl)-1,4,6-tris(prop-2-en-1-yl)bicyclo[3.2.1]octan-8-carbonitrile (rac-14)



A flame-dried Schlenk tube was charged with racemic triketone rac-4 (20.0 mg, 53.0  $\mu\text{mol}$ , 1.0 equiv) and anhydrous  $\text{CH}_2\text{Cl}_2$  (200  $\mu\text{L}$ ) under an argon atmosphere. Sodium hexamethyldisilazide (1.9 M in THF, 28  $\mu\text{L}$ , 53.0  $\mu\text{mol}$ , 1.0 equiv) was added at  $-78^\circ\text{C}$  and the solution was stirred for 5 min. Then trimethylsilyl cyanide (33.2  $\mu\text{L}$ , 266  $\mu\text{mol}$ , 5.0 equiv) was added and the mixture was warmed to  $0^\circ\text{C}$ , followed by the addition of tetrabutylammonium fluoride (1 M in THF, 53.1  $\mu\text{L}$ , 53.0  $\mu\text{mol}$ , 1.0 equiv) and removal of the cooling bath. After stirring for 3 h at ambient temperature the reaction was quenched by the addition of saturated aqueous  $\text{NaHCO}_3$  (2 mL). The layers were separated, the aqueous phase was extracted with  $\text{Et}_2\text{O}$  ( $3 \times 2 \text{ mL}$ ), dried over  $\text{Na}_2\text{SO}_4$ , and concentrated under reduced pressure. The crude product was purified by preparative TLC ( $\text{SiO}_2$ , *n*-pentane/ $\text{EtOAc}$ , 6:1) to yield cyanohydrin rac-14 (20.7 mg, 435  $\mu\text{mol}$ , 82%) as a colorless solid.



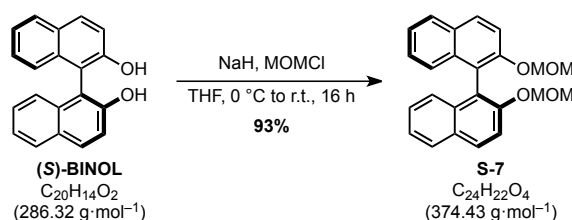
$^1\text{H}$  NMR (400 MHz,  $\text{CDCl}_3$ ):  $\delta$  = 7.80 – 7.75 (m, 2H, H-28), 7.56 – 7.50 (m, 1H, H-30), 7.48 – 7.39 (m, 2H, H-29), 5.83 – 5.68 (m, 2H, H-12, H-17), 5.63 – 5.50 (m, 1H, H-22), 5.19 – 5.06 (m, 3H, H-13, H-18), 5.01 (d,  $J$  = 10.2 Hz, 1H, H-13), 4.84 – 4.78 (m, 1H, H-23), 4.74 – 4.69 (m, 1H, H-23), 4.11 (d,  $J$  = 11.0 Hz, 1H, H-1), 3.07 – 3.00 (m, 1H, H-8), 2.87 (dd,  $J$  = 13.3, 5.2 Hz, 1H, H-11), 2.46 – 2.23 (m, 4H, H-6, H-16, H-21), 2.17 (dd,  $J$  = 13.3, 9.0 Hz, 1H, H-11), 2.06 (dd,  $J$  = 15.4, 8.9 Hz, 1H, H-5), 1.93 (dt,  $J$  = 15.0, 7.8 Hz, 1H, H-21), 1.64 (dd,  $J$  = 15.4, 5.7 Hz, 1H, H-5), 1.36 (s, 3H, Me), 0.30 (s, 9H,  $\text{SiMe}_3$ ) ppm.

$^{13}\text{C}$  NMR (176 MHz,  $\text{CD}_2\text{Cl}_2$ ):  $\delta$  = 207.2 (C-9), 197.5 (C-26), 145.7 (C-2), 139.2 (C-27), 137.2 (C-22), 136.9 (C-17), 135.1 (C-12), 133.4 (C-30), 129.1 (C-29), 128.8 (C-28), 118.3 (C-13), 117.5 (C-23), 117.2 (C-18), 87.6 (C-3), 62.7 (C-4), 58.3 (C-1), 52.8 (C-7), 42.9 (C-8), 38.5 (C-16), 36.9 (C-11), 36.7 (C-6), 36.4 (C-5), 35.7 (C-21), 18.3 (Me), 1.7 ( $\text{SiMe}_3$ ) ppm.

**X-ray:** Crystals were grown by addition of *n*-pentane to a concentrated solution of **15** in  $\text{Et}_2\text{O}$  in a 1 mL vial until a nearly saturated solution was reached. The solution was then left to rest at ambient temperature.

## 2.2 Synthesis of Enantioenriched 3-*epi*-Hypatulin B (17).

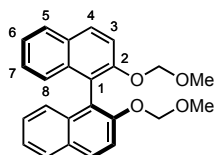
### 2.2.1 (*S*)-2,2'-Bis(methoxymethoxy)-1,1'-binaphthalene (S-7)



BINOL **S-7** was prepared according to a procedure by and et al.<sup>12</sup> NaH (60 wt%, 1.12 g, 27.9 mmol, 4.0 equiv) was added to a flame-dried round-bottom flask under an argon atmosphere, washed with hexane and then suspended



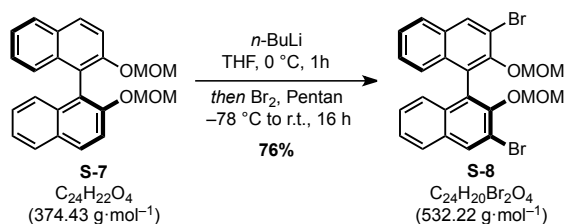
in anhydrous THF (20 mL). The flask was immersed in an ice bath and a solution of (*S*)-BINOL (2.00 g, 6.99 mmol, 1.0 equiv) in anhydrous THF (12 mL) was added dropwise. The mixture was stirred at 0 °C until the evolution of gas ceased and then stirred for additional 30 min. Then chloro(methoxy)methane (1.11 mL, 14.7 mmol, 2.1 equiv) was added dropwise and stirring was continued for 16 h, while warming to ambient temperature. The mixture was diluted with Et<sub>2</sub>O (80 mL), washed with water (3 × 25 mL), dried over anhydrous MgSO<sub>4</sub>, and filtered through a plug of silica. The solvent was removed under reduced pressure and the crude product was purified by column chromatography (SiO<sub>2</sub>, *n*-pentane/Et<sub>2</sub>O, 4:1) to give ether **S-7** (2.42 g, 6.46 mmol, 93%) as a colorless solid.



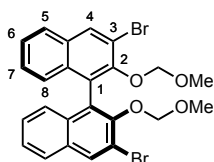
<sup>1</sup>H NMR (400 MHz, CDCl<sub>3</sub>): δ = 7.95 (d, *J* = 9.0 Hz, 2H, H-4), 7.88 (d, *J* = 8.2 Hz, 2H, H-5), 7.58 (d, *J* = 9.0 Hz, 2H, H-3), 7.35 (ddd, *J* = 8.2, 6.7, 1.3 Hz, 2H, H-6), 7.23 (ddd, *J* = 8.5, 6.7, 1.3 Hz, 2H, H-7), 7.16 (d, *J* = 8.5 Hz, 2H, H-8), 5.09 (d, *J* = 6.8 Hz, 2H, CH<sub>2</sub>), 4.98 (d, *J* = 6.8 Hz, 2H, CH<sub>2</sub>), 3.15 (s, 6H, OMe) ppm.

The spectroscopic data are in accordance with the literature.<sup>12</sup>

### 2.2.2 (*S*)-3,3'-Dibromo-2,2'-bis(methoxymethoxy)-1,1'-binaphthalene (**S-8**)



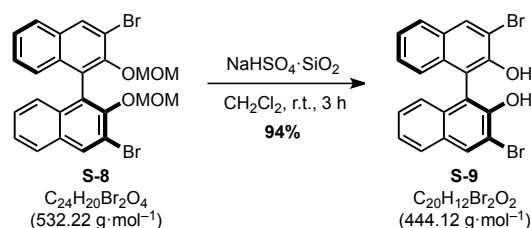
BINOL **S-8** was prepared according to a procedure by WILLS and et al.<sup>12</sup> To a flame-dried Schlenk flask containing a solution of ether **S-7** (3.18 g, 8.49 mmol, 1.0 equiv) in anhydrous THF (37 mL) under an argon atmosphere was added *n*-BuLi (2.5 M in hexanes, 8.15 mL, 20.4 mmol, 2.4 equiv) at -78 °C. The mixture was then warmed to 0 °C, stirred for 1 h and then cooled to -78 °C again. A solution of bromine (1.30 mL, 25.5 mmol, 3.0 equiv) in *n*-pentane (6.8 mL) was added over a period of 20 min. After complete addition the reaction mixture was warmed to ambient temperature and stirred for 16 h. The reaction was quenched by the addition of saturated aqueous Na<sub>2</sub>SO<sub>3</sub> (20 mL), and the aqueous phase was extracted with EtOAc (3 × 20 mL). The combined organic layers were dried over anhydrous Na<sub>2</sub>SO<sub>4</sub> and concentrated under reduced pressure. The crude product was purified by column chromatography (SiO<sub>2</sub>, *n*-pentane/Et<sub>2</sub>O, 10:1 to 4:1) to give ether **S-8** (3.45 g, 6.48 mmol, 76%) as a colorless solid.



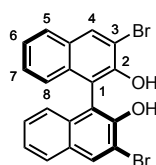
<sup>1</sup>H NMR (400 MHz, CDCl<sub>3</sub>): δ = 8.27 (s, 2H, H-4), 7.80 (d<sub>br</sub>, *J* = 8.2 Hz, 2H, H-5), 7.44 (ddd, *J* = 8.2, 6.8, 1.1 Hz, 2H, H-6), 7.30 (ddd, *J* = 8.5, 6.8, 1.3 Hz, 2H, H-7), 7.18 (dd, *J* = 8.5, 1.1 Hz, 2H, H-8), 4.83 (d, *J* = 5.8 Hz, 2H, CH<sub>2</sub>), 4.81 (d, *J* = 5.8 Hz, 2H, CH<sub>2</sub>), 2.57 (s, 6H, OMe) ppm.

The spectroscopic data are in accordance with the literature.<sup>12</sup>

### 2.2.3 (S)-3,3'-Dibromo-[1,1'-binaphthalene]-2,2'-diol (S-9)



BINOL **S-9** was prepared in analogy to a reported procedure by DAS et al. for the deprotection of phenolic methoxymethyl ethers.<sup>13</sup> Activated (vacuum-dried and hot)  $\text{NaHSO}_4 \cdot \text{SiO}_2$  (5.1 g) was added to a solution of ether **S-8** (2.30 g, 4.32 mmol) in anhydrous  $\text{CH}_2\text{Cl}_2$  (60 mL) and the reaction mixture was stirred at ambient temperature. After 2 h TLC analysis indicated incomplete conversion of the starting material and additional  $\text{NaHSO}_4 \cdot \text{SiO}_2$  (2.0 g) was added and stirring was continued for 1 h. The mixture was dry-loaded onto silica and purified by column chromatography ( $\text{SiO}_2$ , *n*-pentane/ $\text{Et}_2\text{O}$ , 5:1) to give BINOL **S-9** (1.80 g, 4.05 mmol, 94%) as a colorless solid.

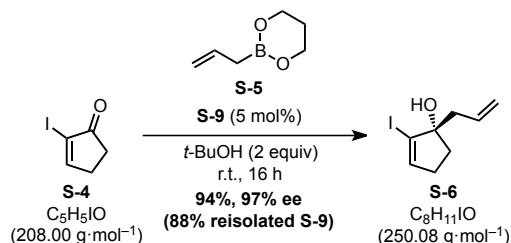


$^1\text{H NMR}$  (400 MHz,  $\text{CDCl}_3$ ):  $\delta$  = 8.26 (s, 2H, H-4), 7.82 (d,  $J$  = 8.2 Hz, 2H, H-5), 7.39 (ddd,  $J$  = 8.2, 6.8, 1.3 Hz, 2H, H-6), 7.31 (ddd,  $J$  = 8.5, 6.8, 1.2 Hz, 2H, H-7), 7.10 (d,  $J$  = 8.5 Hz, 2H, H-8), 5.54 (s, 2H, OH) ppm.

**m.p.**: 255 – 257 °C

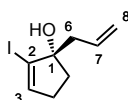
The spectroscopic data are in accordance with the literature.<sup>12</sup>

### 2.2.4 (S)-2-Iodo-1-(prop-2-en-1-yl)cyclopent-2-enol (S-6)



Alcohol **S-6** was prepared according to a reported procedure by TABER and et al.<sup>10</sup> A flame-dried Schlenk flask was charged with BINOL **S-9** (1.79 g, 4.03 mmol, 5 mol%), allyl boronate **S-5** (15.2 g, 121 mmol, 1.5 equiv), and anhydrous *t*-BuOH (15.1 mL, 161 mmol, 2.0 equiv) under an argon atmosphere. The suspension was stirred for about 10 min at ambient temperature until the catalyst was completely dissolved. Then enon **S-4** (16.8 g, 80.6 mmol, 1.0 equiv) was added and the reaction mixture was stirred at ambient temperature for 16 h. The solution was diluted with  $\text{Et}_2\text{O}$  (10 mL) and washed with 1 M aqueous NaOH ( $3 \times 10$  mL). The aqueous phase was extracted with  $\text{Et}_2\text{O}$  ( $3 \times 10$  mL) and the combined organic extracts were dried over anhydrous  $\text{Na}_2\text{SO}_4$  and concentrated under reduced pressure. The crude product was purified by column chromatography ( $\text{SiO}_2$ , *n*-pentane/ $\text{Et}_2\text{O}$ , 8:1 to 6:1) to give alcohol **S-6** (18.9 g, 75.7 mmol, 94%, 97% ee) as a yellow wax.

The combined aqueous layers were acidified with 1 M HCl until a pH value of 1 was reached and then extracted with  $\text{Et}_2\text{O}$  ( $3 \times 10$  mL). The combined organic extracts were dried over anhydrous  $\text{Na}_2\text{SO}_4$  and concentrated under reduced pressure. BINOL **S-9** (1.58 g, 3.56 mmol, 88%) was reisolated as a colorless solid, that was pure enough for further use.



$[\alpha]_{\text{D}}^{23} = +9.0$  ( $c = 1.00$ ,  $\text{CHCl}_3$ ).

**$^1\text{H NMR}$**  (600 MHz,  $\text{CDCl}_3$ ):  $\delta = 6.25$  (t,  $J = 2.5$  Hz, 1H, H-3), 5.78 – 5.70 (m, 1H, H-7), 5.21 – 5.16 (m, 1H, H-8), 5.15 – 5.12 (m, 1H, H-8), 2.49 – 2.42 (m, 1H, H-4), 2.39 (dd,  $J = 13.7, 7.9$  Hz, 1H, H-6), 2.30 (dd,  $J = 13.7, 6.7$  Hz, 1H, H-6), 2.29 – 2.19 (m, 2H, H-4, H-5), 1.96 – 1.90 (m, 1H, H-5), 1.88 (s, 1H, OH) ppm.

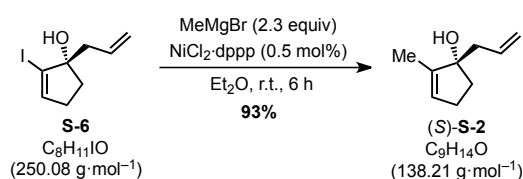
**$^{13}\text{C NMR}$**  (151 MHz,  $\text{CDCl}_3$ ):  $\delta = 141.9$  (C-3), 132.7 (C-7), 119.2 (C-8), 106.7 (C-2), 86.2 (C-1), 44.8 (C-6), 33.3 (C-5), 33.0 (C-4) ppm.

**HRMS** (ESI, pos.):  $m/z$  calcd for  $\text{C}_8\text{H}_{11}\text{IONa}^+$  [ $\text{M}+\text{Na}^+$ ]: 272.9747, found 272.9748.

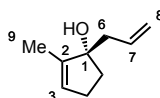
**GC** (Hydrodex- $\beta$ -TBDAC; temperature gradient 50–190 °C; 1.1 mL/min; split 50:1; FID 300 °C):  $t_{\text{R}}$ (minor) = 11.27 min,  $t_{\text{R}}$ (major) = 11.49 min.

The spectroscopic data are in accordance with the literature.<sup>10</sup>

### 2.2.5 (*S*)-2-Methyl-1-(prop-2-en-1-yl)cyclopent-2-enol ((*S*)-**S-2**)



Alcohol (*S*)-**S-2** was prepared in analogy to a reported procedure by TABER and BERRY.<sup>2</sup> A flame-dried Schlenk flask was charged with dichloro(1,3-bis(diphenylphosphino)propane)nickel (51.0 mg, 94.0  $\mu\text{mol}$ , 5 mol%) and anhydrous  $\text{Et}_2\text{O}$  (85 mL) under an argon atmosphere. A solution of methylmagnesium bromide (3 M, 14.4 mL, 43.2 mmol, 2.3 equiv) was added and the mixture was stirred for 10 min. A change of color from orange to yellow occurred during the addition. The flask was immersed in a water bath (16 °C) and a solution of vinyl iodide **S-6** (4.70 g, 18.8 mmol, 1.0 equiv) in anhydrous  $\text{Et}_2\text{O}$  (23 mL) was added dropwise. The reaction mixture was stirred at room temperature for 5 h. After analysis indicated complete consumption of the starting material  $\text{Na}_2\text{SO}_3$  (10.5 g) was added and the mixture was stirred vigorously for 15 min. The solution was degassed with argon while ice-cold saturated aqueous  $\text{Na}_2\text{S}_2\text{O}_3$  (105 mL) was added. The mixture was rapidly transferred to a separatory funnel and the layers were separated. The aqueous phase was extracted with  $\text{Et}_2\text{O}$  ( $3 \times 85$  mL). The organic layers were collected in an Erlenmeyer flask charged with  $\text{Na}_2\text{SO}_3$ ,  $\text{Na}_2\text{SO}_4$  and a magnetic stir bar and vigorously stirred to ensure complete removal of water. The combined organic extracts were filtered through a pad of silica and concentrated under reduced pressure (40 °C, 400 mbar and then 25 °C, 150 mbar). The crude product was immediately purified by column chromatography ( $\text{SiO}_2$ , *n*-pentane/ $\text{Et}_2\text{O}$ , 2:1) to give alcohol (*S*)-**S-2** (2.42 g, 17.5 mmol, 93%) as a light yellow oil.



$[\alpha]_{\text{D}}^{25} = +2.7$  ( $c = 1.00$ ,  $\text{CH}_2\text{Cl}_2$ ).

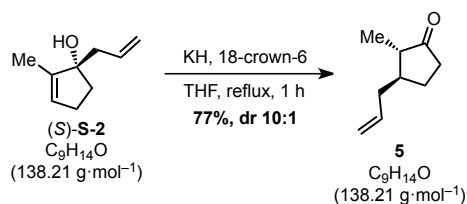
**$^1\text{H NMR}$**  (700 MHz,  $\text{CD}_2\text{Cl}_2$ ):  $\delta = 5.77$  (dddd,  $J = 17.1, 10.2, 7.8, 6.8$  Hz, 1H, H-7), 5.48 (tq,  $J = 2.3, 1.5$  Hz, 1H, H-3), 5.12 (ddt,  $J = 17.1, 2.2, 1.5$  Hz, 1H, H-8), 5.07 (ddt,  $J = 10.2, 2.2, 1.1$  Hz, 1H, H-8), 2.39 (ddt,  $J = 13.6, 7.8, 1.3$  Hz, 1H, H-6), 2.31 – 2.25 (m, 2H, H-4, H-6), 2.17 – 2.07 (m, 2H, H-4, H-5), 1.78 – 1.74 (m, 1H, H-5), 1.69 – 1.68 (m, 4H, Me, OH) ppm.

**$^{13}\text{C NMR}$**  (176 MHz,  $\text{CD}_2\text{Cl}_2$ ):  $\delta = 143.9$  (C-2), 134.9 (C-7), 128.0 (C-3), 118.2 (C-8), 85.6 (C-1), 43.6 (C-6), 38.1 (C-5), 29.3 (C-4), 11.8 (Me) ppm.

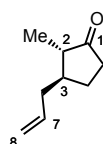
**HRMS** (ESI, pos.):  $m/z$  calcd for  $\text{C}_9\text{H}_{14}\text{ONa}^+$  [ $\text{M}+\text{Na}^+$ ]: 161.0937, found 161.0943.

The spectroscopic data are in accordance with the literature.<sup>9</sup>

### 2.2.6 ((2*S*,3*S*))-2-Methyl-3-(prop-2-en-1-yl)cyclopentan-1-one (**5**)



Ketone **5** was prepared in analogy to a reported procedure by TABER and et al. for the oxy-Cope rearrangement of 1,2-allylated cyclic enones.<sup>10</sup> A flame-dried two-neck round-bottom flask equipped with a reflux condenser was charged with KH (30 wt%, 5.80 g, 43.4 mmol, 1.5 equiv) under an argon atmosphere. The KH was washed with three portions of *n*-pentane and dried under reduced pressure. The flask was flushed with argon again and anhydrous THF (340 mL) was added, followed by the addition of a solution of alcohol (*S*)-**S-2** (4.00 g, 28.9 mmol, 1.0 equiv) and 18-crown-6 (8.14 g, 30.8 mmol, 1.07 equiv) in anhydrous THF (50 mL). The reaction mixture was heated to reflux for 1 h, then cooled to 0 °C and quenched with aqueous 2M HCl (200 mL). The solution was diluted with Et<sub>2</sub>O (200 mL) and the layers were separated. The aqueous layer was extracted with Et<sub>2</sub>O (2 × 100 mL) and the combined organic extracts were washed with brine (200 mL), dried over anhydrous Na<sub>2</sub>SO<sub>4</sub> and concentrated under reduced pressure (25 °C, 180 mbar and then 0 °C, 80 mbar). The crude product was purified by column chromatography (SiO<sub>2</sub>, *n*-pentane/Et<sub>2</sub>O, 1:0, then 10:1 to 6:1) to give ketone **5** (3.07 g, 22.2 mmol, 77%, dr 10:1) as a yellow oil.



$$[\alpha]_{\text{D}}^{25} = +60.2 \quad (c = 1.00, \text{CHCl}_3).$$

**<sup>1</sup>H NMR** (700 MHz, CDCl<sub>3</sub>): δ = 5.82 (ddt, *J* = 17.2, 10.2, 7.1 Hz, 1H, H-7), 5.08 (d, *J* = 17.2 Hz, 1H, H-8), 5.05 (d, *J* = 10.2 Hz, 1H, H-8), 2.46 – 2.41 (m, 1H, H-6), 2.34 (dd, *J* = 17.3, 8.6 Hz, 1H, H-5), 2.16 – 2.02 (m, 3H, H-4, H-5, H-6), 1.79 – 1.68 (m, 3H, H-2, H-3), 1.49 – 1.39 (m, 1H, H-4), 1.07 (d, *J* = 6.4 Hz, 3H, Me) ppm.

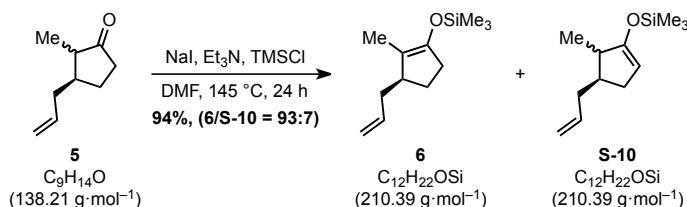
**<sup>13</sup>C NMR** (176 MHz, CDCl<sub>3</sub>): δ = 221.7\*, 221.1 (C-1), 136.8\*, 135.9 (C-7), 116.7 (C-8), 116.3\*, 49.8 (C-2), 47.1\*, 44.5 (C-3), 39.6\*, 38.4 (C-6), 37.4 (C-5), 35.9\*, 33.8\*, 26.9 (C-4), 25.1\*, 12.7 (Me), 9.8\* ppm.

Signals of the minor isomer indicated by \*.

**HRMS** (ESI, pos.): *m/z* calcd for C<sub>9</sub>H<sub>14</sub>ONa<sup>+</sup> [*M*+Na<sup>+</sup>]: 161.0937, found 161.0939.

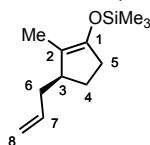
The spectroscopic data are in accordance with the literature.<sup>14</sup>

### 2.2.7 ((*S*))-2-Methyl-3-(prop-2-en-1-yl)cyclopent-1-en-1-yl)oxy)trimethylsilane (**6**)



A pressure tube was flushed with argon and charged with ketone **5** (3.70 g, 26.8 mmol, 1.0 equiv), anhydrous *N,N*-dimethylformamide (8.1 mL), NaI (201 mg, 1.34 mmol, 5 mol%), Et<sub>3</sub>N (12.3 mL, 88.3 mmol, 3.3 equiv) and trimethylsilyl chloride (10.1 mL, 80.3 mmol, 3.0 equiv). The reaction mixture was heated to 145 °C and stirred for 24 h. The conversion and ratio of regioisomers was monitored by <sup>1</sup>H NMR spectroscopy. The mixture was cooled to 0 °C, diluted with *n*-pentane (100 mL) and quenched with ice-cold saturated aqueous NaHCO<sub>3</sub> (100 mL). The layers were separated and the aqueous phase was extracted with *n*-pentane (3 × 100 mL). The combined organic layers were dried over anhydrous MgSO<sub>4</sub>, filtered through a pad of silica with *n*-pentane and concentrated under

reduced pressure to give a mixture of both silyl enol ethers **6** and **S-10** (5.30 g, 25.2 mmol, 94%, **6/S-10** = 93:7) as a yellow oil. The obtained product was pure enough and directly used in the next step without further purification.



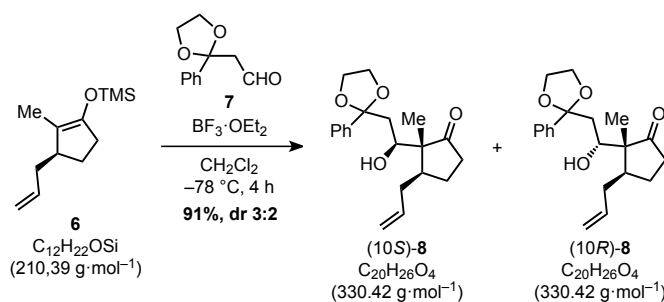
$$[\alpha]_{\text{D}}^{25} = -3.9 \quad (c = 1.00, \text{CH}_2\text{Cl}_2).$$

**<sup>1</sup>H NMR** (600 MHz,  $\text{C}_6\text{D}_6$ ):  $\delta = 5.77$  (ddt,  $J = 17.2, 10.1, 7.0$  Hz, 1H, H-7), 5.07 – 5.01 (m, 2H, H-8), 2.49 ( $s_{\text{br}}$ , 1H, H-3), 2.30 – 2.16 (m, 3H, H-5, H-6), 1.97 – 1.91 (m, 1H, H-6), 1.91 – 1.84 (m, 1H, H-4), 1.59 (s, 3H, Me), 1.55 – 1.43 (m, 1H, H-4), 0.14 (s, 9H,  $\text{SiMe}_3$ ) ppm.

**<sup>13</sup>C NMR** (151 MHz,  $\text{C}_6\text{D}_6$ ):  $\delta = 147.6$  (C-1), 137.4 (C-7), 115.9 (C-8), 115.4 (C-2), 44.7 (C-3), 39.0 (C-6), 33.1 (C-5), 26.2 (C-4), 10.6 (Me), 0.7 ( $\text{SiMe}_3$ ) ppm.

The spectroscopic data are in accordance with the literature.<sup>11</sup>

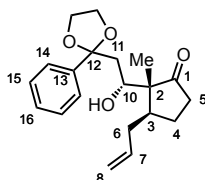
### 2.2.8 (2*R*,3*S*)-2-(1-hydroxy-2-(2-phenyl-1,3-dioxolan-2-yl)ethyl)-2-methyl-3-(prop-2-en-1-yl)cyclopentanone (**8**)



Ketone **8** was prepared in analogy to a reported procedure by LEI et al.<sup>15</sup> A flame-dried Schlenk flask was charged with silyl enol ether **6** (13.0 g, 61.8 mmol, 1.0 equiv) and anhydrous  $\text{CH}_2\text{Cl}_2$  (600 mL). The solution was cooled to  $-78$  °C and aldehyde **7** (61.8 g, 61.8 mmol, 1.0 equiv) was added, followed by the dropwise addition of boron trifluoride etherate (8.61 mL, 67.9 mmol, 1.1 equiv). The reaction mixture was stirred for 3 h, then allowed to warm to  $-20$  °C and quenched with saturated aqueous  $\text{NaHCO}_3$  (300 mL). The layers were separated and the aqueous phase was extracted with  $\text{CH}_2\text{Cl}_2$  ( $3 \times 200$  mL). The combined organic layers were washed with brine (200 mL), dried over anhydrous  $\text{Na}_2\text{SO}_4$  and concentrated under reduced pressure. The crude product was purified by column chromatography ( $\text{SiO}_2$ , *n*-pentane/ $\text{EtOAc}$ , 10:1, then 5:1) to yield a mixture of epimeric ketones (10*S*)-**8** and (10*R*)-**8** (18.6 g, 56.3 mmol, 91%, dr 3:2) as a colorless oil.

A sample of both diastereoisomers could be separated by column chromatography and characterized.

### (2*R*,3*S*)-2-((*R*)-1-hydroxy-2-(2-phenyl-1,3-dioxolan-2-yl)ethyl)-2-methyl-3-(prop-2-en-1-yl)cyclopentanone ((10*R*)-**8**)



$$[\alpha]_{\text{D}}^{24} = +25.8 \quad (c = 1.00, \text{CH}_2\text{Cl}_2).$$

**<sup>1</sup>H NMR** (700 MHz,  $\text{CDCl}_3$ ):  $\delta = 7.46$  – 7.43 (m, 2H, H-14), 7.37 – 7.33 (m, 2H, H-15), 7.33 – 7.29 (m, 1H, H-16), 5.85 – 5.77 (m, 1H, H-7), 5.05 (d,  $J = 17.2$  Hz, 1H, H-8), 4.99 (d,  $J = 10.6$  Hz, 1H, H-8), 4.14 – 4.07 (m, 1H,  $\text{OCH}_2$ ), 4.07 – 4.02 (m, 1H,  $\text{OCH}_2$ ), 3.94 (d,  $J = 10.8$  Hz, 1H, H-10), 3.87 – 3.81 (m, 1H,  $\text{OCH}_2$ ), 3.75 – 3.69 (m, 2H,  $\text{OCH}_2$ , OH), 2.55 – 2.48 (m, 1H, H-3), 2.43 – 2.37 (m, 2H, H-6, H-11), 2.26 (dd,  $J = 18.1, 8.0$  Hz, 1H, H-5), 2.17 – 2.01 (m, 3H, H-4, H-5, H-11), 1.94 – 1.87 (m, 1H, H-6), 1.38 – 1.30 (m, 1H, H-4), 0.86 (s, 3H, Me) ppm.

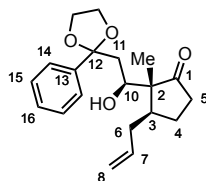
$^{13}\text{C}$  NMR (176 MHz,  $\text{CDCl}_3$ ):  $\delta$  = 222.6 (C-1), 142.0 (C-13), 137.3 (C-7), 128.5 (C-15), 128.4 (C-16), 125.7 (C-14), 115.9 (C-8), 111.0 (C-12), 71.0 (C-10), 64.8 ( $\text{OCH}_2$ ), 64.0 ( $\text{OCH}_2$ ), 54.2 (C-2), 41.3 (C-11), 40.9 (C-3), 38.9 (C-5), 35.1 (C-6), 25.2 (C-4), 14.6 (Me) ppm.

HRMS (ESI, pos.):  $m/z$  calcd for  $\text{C}_{20}\text{H}_{26}\text{O}_4\text{Na}^+$  [ $\text{M}+\text{Na}^+$ ]: 353.1723, found 353.1727.

m.p.: 52 – 58 °C.

X-ray: Crystals were grown by slow evaporation of a solution of (10R)-8 in *n*-pentane and  $\text{Et}_2\text{O}$  in a 1 mL vial at ambient temperature.

(2R,3S)-2-((S)-1-hydroxy-2-(2-phenyl-1,3-dioxolan-2-yl)ethyl)-2-methyl-3-(prop-2-en-1-yl)cyclopentanone ((10S)-8)



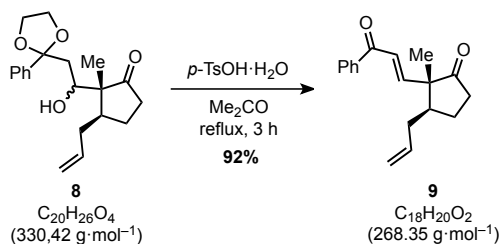
$[\alpha]_{\text{D}}^{24} = +25.9$  ( $c = 1.00$ ,  $\text{CH}_2\text{Cl}_2$ ).

$^1\text{H}$  NMR (700 MHz,  $\text{CDCl}_3$ ):  $\delta$  = 7.46 – 7.43 (m, 2H, H-14), 7.38 – 7.34 (m, 2H, H-15), 7.33 – 7.30 (m, 1H, H-16), 5.78 (dddd,  $J = 17.1, 10.1, 8.2, 5.8$  Hz, 1H, H-7), 5.04 – 5.00 (m, 1H, H-8), 4.99 – 4.96 (m, 1H, H-8), 4.13 – 4.07 (m, 2H, H-10,  $\text{OCH}_2$ ), 4.04 (td,  $J = 7.5, 5.5$  Hz, 1H,  $\text{OCH}_2$ ), 3.83 (td,  $J = 7.6, 5.5$  Hz, 1H,  $\text{OCH}_2$ ), 3.71 (td,  $J = 7.6, 6.4$  Hz, 1H,  $\text{OCH}_2$ ), 3.53 (d,  $J = 1.3$  Hz, 1H, OH), 2.56 (tdd,  $J = 11.4, 6.1, 3.4$  Hz, 1H, H-3), 2.32 – 2.24 (m, 2H, H-5, H-6), 2.20 – 2.11 (m, 3H, H-4, H-5, H-11), 1.95 (dd,  $J = 14.7, 10.4$  Hz, 1H, H-11), 1.85 (dddd,  $J = 13.6, 11.4, 8.2, 1.1$  Hz, 1H, H-6), 1.31 – 1.24 (m, 1H, H-4), 0.78 (s, 3H, Me) ppm.

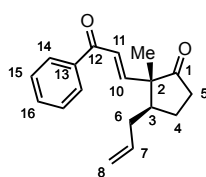
$^{13}\text{C}$  NMR (176 MHz,  $\text{CDCl}_3$ ):  $\delta$  = 222.9 (C-1), 141.9 (C-13), 137.0 (C-7), 128.6 (C-15), 128.4 (C-16), 125.6 (C-14), 116.0 (C-8), 110.8 (C-12), 72.0 (C-10), 64.8 ( $\text{OCH}_2$ ), 64.2 ( $\text{OCH}_2$ ), 54.1 (C-2), 41.6 (C-11), 38.9 (C-3), 38.7 (C-5), 36.7 (C-6), 25.8 (C-4), 14.2 (Me) ppm.

HRMS (ESI, pos.):  $m/z$  calcd for  $\text{C}_{20}\text{H}_{26}\text{O}_4\text{Na}^+$  [ $\text{M}+\text{Na}^+$ ]: 353.1723, found 353.1719.

2.2.9 (2R,3S)-2-methyl-2-((E)-3-oxo-3-phenylprop-1-en-1-yl)-3-(prop-2-en-1-yl)cyclopentan-1-one (9)



A solution of **8** (13.1 g, 39.5 mmol, 1.0 equiv) and *para*-toluenesulfonic acid monohydrate (15.0 g, 79.1 mmol, 2.0 equiv) in acetone (400 mL) was heated to reflux for 3 h and then cooled to room temperature. The mixture was concentrated to about half its volume under reduced pressure and saturated aqueous  $\text{NaHCO}_3$  (150 mL) was added. The layers were separated and the aqueous phase was extracted with  $\text{EtOAc}$  ( $3 \times 100$  mL). The combined organic layers were dried over anhydrous  $\text{Na}_2\text{SO}_4$  and concentrated under reduced pressure. The crude product was purified by column chromatography ( $\text{SiO}_2$ , *n*-pentane/ $\text{EtOAc}$ , 5:1) to give enone **9** (9.75 g, 36.3 mmol, 92%) as a yellow oil.



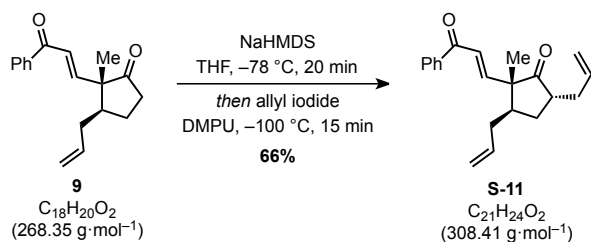
$[\alpha]_{\text{D}}^{24} = -36.0$  ( $c = 1.00$ ,  $\text{CHCl}_3$ ).

**<sup>1</sup>H NMR** (700 MHz, CDCl<sub>3</sub>): δ = 7.92 (d, *J* = 7.2 Hz, 2H, H-14), 7.56 (t, *J* = 7.4 Hz, 1H, H-16), 7.47 (t, *J* = 7.7 Hz, 2H, H-15), 6.95 (d, *J* = 15.7 Hz, 1H, H-11), 6.91 (d, *J* = 15.7 Hz, 1H, H-10), 5.84 – 5.74 (m, 1H, H-7), 5.10 (d<sub>br</sub>, *J* = 17.0 Hz, 1H, H-8), 5.05 (d<sub>br</sub>, *J* = 10.1 Hz, 1H, H-8), 2.48 (ddd, *J* = 19.2, 8.5, 1.8 Hz, 1H, H-5), 2.34 – 2.26 (m, 3H, H-3, H-4, H-6), 2.23 – 2.15 (m, 1H, H-5), 2.07 – 1.99 (m, 1H, H-6), 1.66 – 1.57 (m, 1H, H-4), 1.16 (s, 3H, Me) ppm.

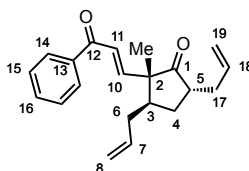
**<sup>13</sup>C NMR** (176 MHz, CDCl<sub>3</sub>): δ = 218.5 (C-1), 190.6 (C-12), 150.3 (C-10), 137.9 (C-13), 136.1 (C-7), 133.0 (C-16), 128.8 (C-14), 128.7 (C-15), 125.9 (C-11), 116.8 (C-8), 55.0 (C-2), 46.3 (C-3), 37.1 (C-5), 34.5 (C-6), 25.1 (C-4), 15.7 (Me) ppm.

**HRMS** (ESI, pos.): *m/z* calcd for C<sub>18</sub>H<sub>21</sub>O<sub>2</sub><sup>+</sup> [M+H<sup>+</sup>]: 269.1536, found 269.1539.

### 2.2.10 (2*R*,3*R*,5*R*)-2-methyl-2-((*E*)-3-oxo-3-phenylprop-1-en-1-yl)-3,5-bis(prop-2-en-1-yl)cyclopentan-1-one (S-11)



A flame-dried Schlenk flask was charged with enone **9** (11.1 g, 41.4 mmol, 1.0 equiv) and anhydrous THF (480 mL) under an argon atmosphere. Sodium hexamethyldisilazide (1.9 M in THF, 21.8 mL, 41.4 mmol, 1.0 equiv) was added at  $-78\text{ }^\circ\text{C}$  and the reaction mixture was stirred for 20 min. The resulting orange solution was cooled to  $-100\text{ }^\circ\text{C}$  and allyl iodide (3.8 mL, 41.4 mmol, 1.0 equiv) in 1,3-dimethyl-1,3-diazinan-2-one (DMPU, 80 mL) was added over 15 min. After the addition, TLC indicated complete consumption of the starting material and the reaction was quenched with saturated aqueous NaHCO<sub>3</sub> (200 mL) and diluted with EtOAc (200 mL). The layers were separated and the aqueous phase was extracted with EtOAc (3 × 200 mL) and the combined organic layers were washed with brine (200 mL), dried over Na<sub>2</sub>SO<sub>4</sub>, and concentrated under reduced pressure. The crude product was purified by MPLC (dry-loaded onto Celite®, SiO<sub>2</sub>, cyclohexane/EtOAc, 20:1) to afford enon **S-11** (8.36 g, 27.1 mmol, 66%) as a colorless oil.



$[\alpha]_{\text{D}}^{24} = +2.3$  (*c* = 1.00, CHCl<sub>3</sub>).

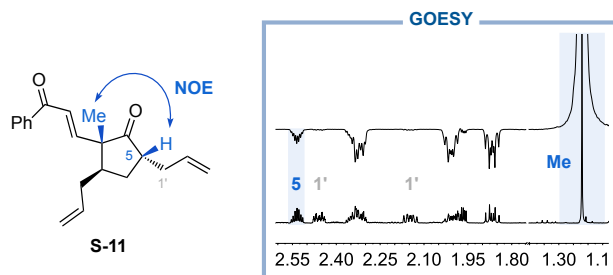
**<sup>1</sup>H NMR** (600 MHz, CDCl<sub>3</sub>): δ = 7.96 – 7.88 (m, 2H, H-14), 7.58 – 7.54 (tt, *J* = 6.8, 1.2 Hz, 1H, H-16), 7.46 (d, *J* = 8.0 Hz, 2H, H-15), 6.92 (d, *J* = 15.7, 1H, H-11), 6.89 (d, *J* = 15.7 Hz, 1H, H-10), 5.83 – 5.66 (m, 2H, H-7, H-18), 5.13 – 5.00 (m, 4H, H-8, H-19), 2.51 (tt, *J* = 9.2, 4.3, 1H, H-5), 2.46 – 2.40 (m, 1H, H-17), 2.35 – 2.26 (m, 2H, H-3, H-6), 2.16 – 2.08 (m, 1H, H-17), 2.02 – 1.91 (m, 2H, H-4, H-6), 1.83 (dt, *J* = 13.5, 9.2, 1H, H-4), 1.19 (s, 3H, Me) ppm.

**<sup>13</sup>C NMR** (151 MHz, CDCl<sub>3</sub>): δ = 219.8 (C-1), 190.4 (C-12), 150.3 (C-10), 137.8 (C-13), 136.1 (C-7), 135.4 (C-18), 133.0 (C-16), 128.8 (C-14), 128.7 (C-15), 125.9 (C-11), 117.3 (C-19), 116.8 (C-8), 55.7 (C-2), 45.6 (C-5), 43.6 (C-3), 35.6 (C-17), 34.5 (C-6), 30.0 (C-4), 16.3 (Me) ppm.

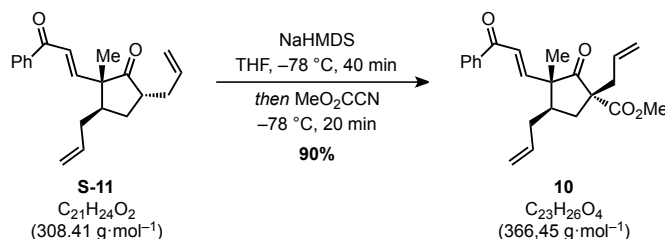
**HRMS** (ESI, pos.): *m/z* calcd for C<sub>21</sub>H<sub>24</sub>O<sub>2</sub>Na<sup>+</sup> [M+Na<sup>+</sup>]: 331.1669, found 331.1681.

The relative configuration was deduced by NOE correlations.

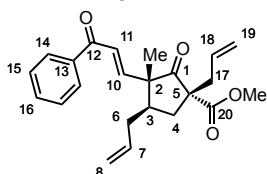




### 2.2.11 (1*R*,3*R*,4*R*)-methyl 3-methyl-2-oxo-3-((*E*)-3-oxo-3-phenylprop-1-en-1-yl)-1,4-bis(prop-2-en-1-yl)cyclopentanecarboxylate (**10**)



A flame-dried Schlenk flask was charged with enone **S-11** (4.04 g, 13.1 mmol, 1.0 equiv) and anhydrous THF (160 mL) under an argon atmosphere. Sodium hexamethyldisilazide (1.9 M in THF, 14.4 mL, 28.8 mmol, 2.2 equiv) was added at  $-78\text{ }^{\circ}\text{C}$  and the reaction mixture was stirred for 40 min. To the dark red solution was added methyl cyanofornate (2.50 mL, 31.4 mmol, 2.4 equiv) and stirring at  $-78\text{ }^{\circ}\text{C}$  was continued for 20 min. The reaction was quenched by addition of saturated aqueous  $\text{NaHCO}_3$  (50 mL),  $\text{H}_2\text{O}$  (50 mL), and brine (50 mL) and diluted with EtOAc (50 mL). The layers were separated and the aqueous phase was extracted with EtOAc ( $3 \times 50\text{ mL}$ ) and the combined organic layers were dried over  $\text{Na}_2\text{SO}_4$  and concentrated under reduced pressure. The crude product was purified by MPLC (dry-loaded onto Celite<sup>®</sup>,  $\text{SiO}_2$ , cyclohexane/EtOAc, 20:1 to 6:1) to give ester **10** (4.34 g, 11.9 mmol, 90%) as a colorless oil.



$$[\alpha]_{\text{D}}^{24} = -45.0 \quad (c = 1.00, \text{CHCl}_3).$$

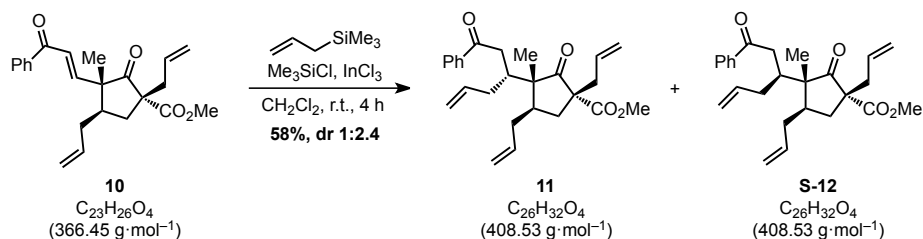
**<sup>1</sup>H NMR** (600 MHz,  $\text{CDCl}_3$ ):  $\delta$  = 7.94 – 7.91 (m, 2H, H-14), 7.58 – 7.54 (m, 1H, H-16), 7.49 – 7.45 (m, 2H, H-15), 6.96 (d,  $J$  = 15.7 Hz, 1H, H-11), 6.90 (d,  $J$  = 15.7 Hz, 1H, H-10), 5.78 (ddt,  $J$  = 17.0, 10.1, 6.8 Hz, 1H, H-7), 5.69 – 5.60 (m, 1H, H-18), 5.15 – 5.14 (m, 1H, H-19), 5.13 – 5.08 (m, 2H, H-8, H-19), 5.07 – 5.04 (m, 1H, H-8), 3.70 (s, 3H, OMe), 2.71 (dd,  $J$  = 13.9, 7.8 Hz, 1H, H-17), 2.55 – 2.47 (m, 3H, H-3, H-4, H-17), 2.32 – 2.25 (m, 1H, H-6), 2.06 – 1.99 (m, 1H, H-6), 1.65 – 1.59 (m, 1H, H-4), 1.14 (s, 3H, Me) ppm.

**<sup>13</sup>C NMR** (151 MHz,  $\text{CDCl}_3$ ):  $\delta$  = 213.9 (C-1), 190.5 (C-12), 171.0 (C-20), 150.1 (C-10), 137.9 (C-13), 135.9 (C-7), 133.0 (C-16), 132.8 (C-18), 128.8 (C-14), 128.7 (C-15), 125.6 (C-11), 119.8 (C-19), 116.9 (C-8), 61.4 (C-5), 55.1 (C-2), 53.0 (OMe), 43.3 (C-3), 39.0 (C-17), 35.1 (C-4), 34.5 (C-6), 16.6 (Me) ppm.

**HRMS** (ESI, pos.):  $m/z$  calcd for  $\text{C}_{23}\text{H}_{26}\text{O}_4\text{Na}^+$  [ $\text{M}+\text{Na}^+$ ]: 389.1723, found 389.1741.



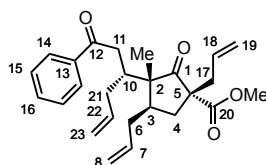
**2.2.12 (1R,3R,4R)-methyl 3-methyl-2-oxo-3-((R)-1-oxo-1-phenylhex-5-en-3-yl)-1,4-bis(prop-2-en-1-yl)cyclopentanecarboxylate (11)**



Ketone **12** was prepared in analogy to a procedure by LEE et al.<sup>16</sup> Anhydrous  $\text{InCl}_3$  (42.6 mg, 192  $\mu\text{mol}$ , 15 mol%), trimethylsilyl chloride (814  $\mu\text{L}$ , 6.14 mmol, 5.0 equiv), and allyltrimethylsilane (306  $\mu\text{L}$ , 1.92 mmol, 1.5 equiv) were added sequentially to a solution of enone **10** (470 mg, 1.28 mmol, 1.0 equiv) in anhydrous  $\text{CH}_2\text{Cl}_2$  (3.9 mL). The reaction mixture was stirred for 4 h at ambient temperature and then washed with saturated aqueous  $\text{NaHCO}_3$  (4 mL). The aqueous phase was extracted with  $\text{CH}_2\text{Cl}_2$  ( $3 \times 5$  mL) and the combined organic layers were dried over  $\text{Na}_2\text{SO}_4$  and concentrated under reduced pressure. After purification by column chromatography ( $\text{SiO}_2$ , *n*-pentane/ $\text{EtOAc}$ , 30:1) to give a mixture of epimeric ketones **11** and **S-12** (302 mg, 739  $\mu\text{mol}$ , 58%, dr 1:2.4) was obtained as a colorless oil.

Both epimers **11** and **S-12** can be separated by HPLC (1% *i*-PrOH/*n*-hexane, Chiralpak IA, 32 mm  $\times$  250 mm, UV detection at 254 nm, 18 mL/min,  $t_{\text{R}}$ (minor) = 11.19 min,  $t_{\text{R}}$ (major) = 12.53 min.). Alternatively, the mixture can be used for the next steps and both corresponding diastereomers can be separated at the stage of the triketone **4**.

**(1R,3R,4R)-methyl 3-methyl-2-oxo-3-((R)-1-oxo-1-phenylhex-5-en-3-yl)-1,4-bis(prop-2-en-1-yl)cyclopentanecarboxylate (11)**



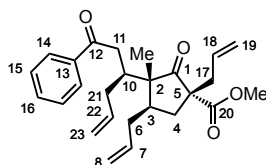
$[\alpha]_{\text{D}}^{27} = +12.1$  ( $c = 1.00$ ,  $\text{CH}_2\text{Cl}_2$ ).

**$^1\text{H NMR}$**  (700 MHz,  $\text{CDCl}_3$ )  $\delta = 8.01 - 7.93$  (m, 2H, H-14), 7.59 – 7.50 (m, 1H, H-16), 7.50 – 7.40 (m, 2H, H-15), 5.88 (dddd,  $J = 17.1, 10.2, 7.6, 6.1$  Hz, 1H, H-7), 5.69 – 5.54 (m, 2H, H-18, H-22), 5.18 – 5.09 (m, 1H, H-8), 5.13 – 5.03 (m, 3H, H-8, H-19), 4.94 (dtd,  $J = 17.1, 1.9, 1.1$  Hz, 1H, H-23), 4.89 (dtd,  $J = 10.1, 1.7, 0.7$  Hz, 1H, H-23), 3.67 (s, 3H, OMe), 3.47 (dd,  $J = 18.1, 5.8$  Hz, 1H, H-11), 2.95 (dd,  $J = 18.1, 5.4$  Hz, 1H, H-11), 2.77 (ddt,  $J = 13.9, 7.5, 1.1$  Hz, 1H, H-17), 2.67 – 2.62 (m, 2H, H-4, H-10), 2.49 (dddd,  $J = 12.0, 10.4, 6.6, 3.9$  Hz, 1H, H-3), 2.45 – 2.40 (m, 1H, H-6), 2.31 – 2.25 (m, 2H, H-17, H-21), 1.93 (dddt,  $J = 13.9, 10.4, 7.6, 1.2$  Hz, 1H, H-6), 1.76 (dddt,  $J = 14.1, 10.3, 8.5, 0.9$  Hz, 1H, H-21), 1.41 (t,  $J = 13.4, 12.0$  Hz, 1H, H-4), 0.90 (s, 3H, Me) ppm.

**$^{13}\text{C NMR}$**  (176 MHz,  $\text{CDCl}_3$ )  $\delta = 217.9$  (C-1), 200.1 (C-12), 170.0 (C-20), 137.4 (C-22), 137.3 (C-13), 136.5 (C-7), 133.1 (C-18), 133.0 (C-16), 128.7 (C-15), 128.2 (C-14), 119.1 (C-19), 117.0 (C-23), 116.5 (C-8), 61.9 (C-5), 54.8 (C-2), 52.8 (OMe), 40.8 (C-17), 39.7 (C-3), 38.9 (C-11), 37.2 (C-10), 35.6 (C-21), 34.9 (C-6), 34.7 (C-4), 17.6 (Me).

**HRMS** (ESI, pos.):  $m/z$  calcd for  $\text{C}_{26}\text{H}_{32}\text{O}_4\text{Na}^+$  [ $\text{M}+\text{Na}^+$ ]: 431.2193, found 431.2208.

**(1R,3R,4R)-methyl 3-methyl-2-oxo-3-((S)-1-oxo-1-phenylhex-5-en-3-yl)-1,4-bis(prop-2-en-1-yl)cyclopentanecarboxylate (S-12)**



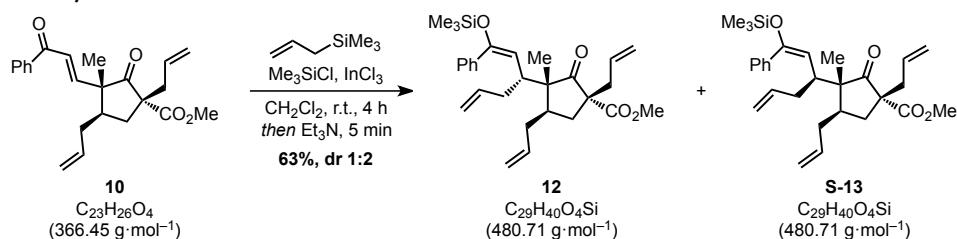
**$^1\text{H NMR}$**  (600 MHz,  $\text{CDCl}_3$ ):  $\delta = 7.89 - 7.86$  (m, 2H, H-14), 7.55 – 7.51 (m, 1H, H-16), 7.45 – 7.41 (m, 2H, H-15), 5.82 (dddd,  $J = 16.9, 10.1, 7.8, 6.0$  Hz, 1H, H-7), 5.67 – 5.58 (m, 2H, H-18, H-22), 5.13 – 5.04 (m, 4H, H-8, H-19), 4.94 (dtd,  $J = 16.9, 1.9, 1.0$  Hz, 1H, H-23), 4.83 (dt,  $J = 10.1, 1.7$  Hz, 1H, H-23), 3.65 (s, 3H, OMe), 2.98 (dd,  $J$

= 17.9, 4.1 Hz, 1H, H-11), 2.91 (dd,  $J = 17.9, 6.5$  Hz, 1H, H-11), 2.76 (dd,  $J = 13.9, 7.5$  Hz, 1H, H-17), 2.66 (ddt,  $J = 10.5, 6.5, 4.1$  Hz, 1H, H-10), 2.58 (dd,  $J = 13.5, 6.6$  Hz, 1H, H-4), 2.51 – 2.40 (m, 1H, H-6), 2.36 – 2.22 (m, 3H, H-3, H-17, H-21), 2.17 (dt,  $J = 13.9, 9.7$  Hz, 1H, H-21), 1.90 (ddd,  $J = 13.7, 10.8, 7.8$  Hz, 1H, H-6), 1.39 (dd,  $J = 13.5, 11.9$  Hz, 1H, H-4), 0.98 (s, 3H, Me) ppm.

$^{13}\text{C}$  NMR (151 MHz,  $\text{CDCl}_3$ ):  $\delta = 217.5$  (C-1), 199.1 (C-12), 170.3 (C-20), 137.7 (C-22), 137.4 (C-13), 136.5 (C-7), 133.1 (C-18), 132.9 (C-16), 128.6 (C-15), 128.0 (C-14), 119.1 (C-19), 116.8 (C-23), 116.5 (C-8), 61.4 (C-5), 54.7 (C-2), 52.8 (OMe), 40.5 (C-3), 40.5 (C-17), 39.4 (C-11), 38.0 (C-10), 35.8 (C-21), 35.5 (C-6), 35.0 (C-4), 16.6 (Me) ppm.

### 2.2.13 (1R,3R,4R)-methyl 3-methyl-2-oxo-3-((R,E)-1-phenyl-1-((trimethylsilyl)oxy)hexa-1,5-dien-3-yl)-1,4-bis(prop-2-en-1-yl)cyclopentanecarboxylate (**12**)

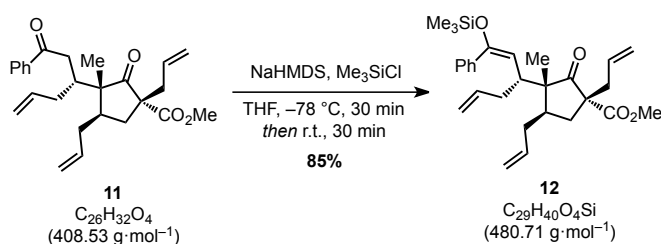
#### Preparation of silyl enol ether **12** from enone **10**



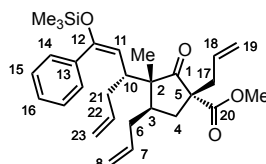
Anhydrous  $\text{InCl}_3$  (60.4 mg, 273  $\mu\text{mol}$ , 20 mol%), trimethylsilyl chloride (1.73 mL, 13.6 mmol, 10 equiv), and allyltrimethylsilane (1.08 mL, 6.82 mmol, 5.0 equiv) were added sequentially to a solution of enone **10** (500 mg, 1.36 mmol, 1.0 equiv) in anhydrous  $\text{CH}_2\text{Cl}_2$  (4.0 mL). The reaction mixture was stirred at ambient temperature, while the reaction progress was monitored by TLC. After 60 min TLC analysis indicated complete consumption of the starting material, anhydrous  $\text{Et}_3\text{N}$  (1.90 mL, 13.6 mmol, 1.0 equiv) was added and stirring was continued for 5 min. Then *n*-pentane (4 mL) was added and the resulting suspension was filtered through a plug of Celite®. The filtrate was washed with saturated aqueous  $\text{NaHCO}_3$  (8 mL) and the aqueous phase was extracted with  $\text{CH}_2\text{Cl}_2$  (3  $\times$  8 mL). The combined organic layers were dried over  $\text{Na}_2\text{SO}_4$  and the solvent was removed under reduced pressure. The crude product was purified by column chromatography ( $\text{SiO}_2$ , *n*-pentane/ $\text{EtOAc}$ , 100:1 to 50:1) to give a mixture of epimeric silyl enol ethers **12** and **S-13** (410 mg, 853  $\mu\text{mol}$ , 58%, dr 1:2) as a colorless oil.

The mixture can be used for the next steps and both **12** and **S-13** can be separated at the stage of the triketone **4**.

#### Preparation of silyl enol ether **12** from ketone **11**



A flame-dried Schlenk tube was charged with ketone **11** (146 mg, 358  $\mu\text{mol}$ , 1.0 equiv) and anhydrous THF (4.7 mL) under an argon atmosphere. Sodium hexamethyldisilazide (1.9 M in THF, 0.28 mL, 537  $\mu\text{mol}$ , 1.5 equiv) was added at  $-78$   $^\circ\text{C}$  and the solution was stirred for 30 min. Then trimethylsilyl chloride (226  $\mu\text{L}$ , 1.79 4.67 mmol, 5.0 equiv) was added and the reaction mixture was warmed to ambient temperature and stirred for 2 h. The reaction was quenched by the addition of saturated aqueous  $\text{NaHCO}_3$  (4 mL) and the aqueous phase was extracted with  $\text{CH}_2\text{Cl}_2$  (3  $\times$  8 mL). The combined organic layers were dried over  $\text{Na}_2\text{SO}_4$  and the solvent was removed under reduced pressure. The crude product was purified by column chromatography ( $\text{SiO}_2$ , *n*-pentane/ $\text{EtOAc}$ , 100:1 to 50:1) to give silyl enol ether **12** (146 mg, 304  $\mu\text{mol}$ , 85%) as a colorless oil.

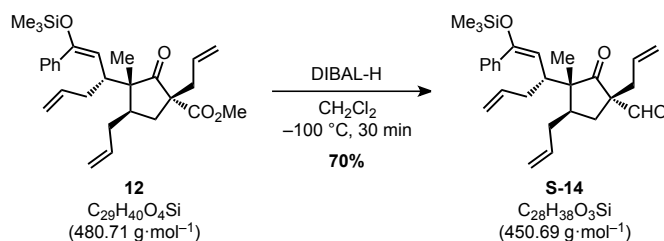


$^1\text{H NMR}$  (700 MHz,  $\text{CD}_2\text{Cl}_2$ ):  $\delta$  = 7.46 – 7.38 (m, 2H, H-14), 7.34 – 7.28 (m, 2H, H-15), 7.27 – 7.23 (m, 1H, H-16), 5.89 (dddd,  $J$  = 17.1, 10.1, 7.9, 6.0 Hz, 1H, H-7), 5.83 – 5.70 (m, 1H, H-22), 5.61 (ddt,  $J$  = 17.3, 10.1, 7.3 Hz, 1H, H-18), 5.12 – 5.08 (m, 1H, H-8), 5.12 (d,  $J$  = 10.4 Hz, 1H, H-11), 5.08 – 5.00 (m, 4H, H-8, H-19, H-23), 4.94 (ddt,  $J$  = 10.0, 2.1, 1.0 Hz, 1H, H-23), 3.55 (s, 3H, OMe), 2.78 (td,  $J$  = 11.1, 10.4, 3.1 Hz, 1H, H-21), 2.74 (ddt,  $J$  = 13.9, 7.5, 1.1 Hz, 1H, H-17), 2.64 (dd,  $J$  = 13.4, 6.6 Hz, 1H, H-4), 2.48 (tdd,  $J$  = 10.6, 6.7, 3.6 Hz, 1H, H-3), 2.42 – 2.35 (m, 2H, H-6, H-21), 2.24 – 2.20 (m, 1H, H-17), 1.93 – 1.84 (m, 2H, H-6, H-21), 1.42 – 1.32 (m, 1H, H-4), 0.94 (s, 3H, Me), 0.10 (s, 9H,  $\text{SiMe}_3$ ) ppm.

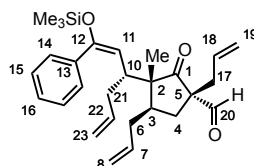
$^{13}\text{C NMR}$  (176 MHz,  $\text{CD}_2\text{Cl}_2$ ):  $\delta$  = 217.0 (C-1), 170.5 (C-20), 151.6 (C-12), 140.2 (C-13), 138.5 (C-22), 137.6 (C-7), 134.0 (C-18), 128.6 (C-15), 128.3 (C-16), 126.6 (C-14), 118.9 (C-19), 116.3 (C-8), 115.9 (C-23), 111.9 (C-11), 61.9 (C-5), 55.8 (C-2), 52.9 (OMe), 42.1 (C-10), 41.1 (C-17), 40.4 (C-3), 36.1 (C-6), 35.6 (C-21), 35.2 (C-4), 16.7 (Me), 1.3 ( $\text{SiMe}_3$ ) ppm.

**HRMS** (ESI, pos.):  $m/z$  calcd for  $\text{C}_{29}\text{H}_{40}\text{O}_4\text{SiNa}^+$  [ $\text{M}+\text{Na}^+$ ]: 503.2588, found 503.2610.

#### 2.2.14 (1R,3R,4R)-3-methyl-2-oxo-3-((R,E)-1-phenyl-1-((trimethylsilyl)oxy)hexa-1,5-dien-3-yl)-1,4-bis(prop-2-en-1-yl)cyclopentanecarbaldehyde (S-14)



A flame-dried Schlenk flask was charged with ester **12** (840 mg, 1.75 mmol, 1.0 equiv) and anhydrous  $\text{CH}_2\text{Cl}_2$  (13 mL) under an argon atmosphere. The solution was cooled to  $-100\text{ }^\circ\text{C}$  and diisobutylaluminum hydride (1 M in hexane, 4.37 mL, 4.37 mmol, 2.5 equiv) was added over a period of 30 min. Then the reaction was quenched by the addition of EtOAc (1.71 mL, 17.5 mmol, 10 equiv) followed by saturated aqueous  $\text{NaHCO}_3$  (15 mL). The layers were crudely separated and the organic layer was washed with saturated aqueous  $\text{NaHCO}_3$  again. This process was repeated until a clear separation was observed. The collected aqueous phases were extracted with EtOAc (3  $\times$  15 mL) and the combined organic extracts were washed with brine (15 mL), dried over anhydrous over  $\text{Na}_2\text{SO}_4$  and concentrated under reduced pressure. The crude product was purified by MPLC (dry-loaded onto Celite<sup>®</sup>,  $\text{SiO}_2$ , cyclohexane/EtOAc, 80:1 to 50:1 to 20:1) to give aldehyde **S-14** (550 mg, 1.22 mmol, 70%) as a colorless oil.



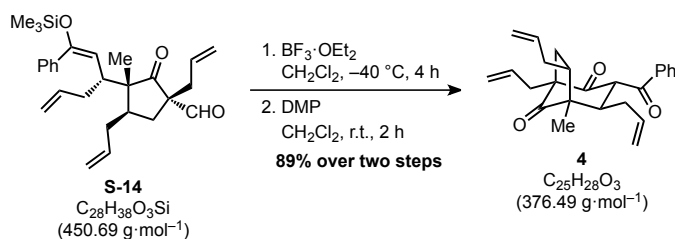
$[\alpha]_{\text{D}}^{26} = -13.1$  ( $c$  = 1.00,  $\text{CH}_2\text{Cl}_2$ ).

$^1\text{H NMR}$  (400 MHz,  $\text{CD}_2\text{Cl}_2$ )  $\delta$  = 9.24 (d,  $J$  = 1.4 Hz, 1H, H-20), 7.44 – 7.37 (m, 2H, H-14), 7.34 – 7.22 (m, 3H, H-15, H-16), 5.96 – 5.83 (m, 1H, H-7), 5.73 (ddt,  $J$  = 17.1, 10.1, 7.1 Hz, 1H, H-22), 5.52 (dddd,  $J$  = 17.0, 10.2, 7.8, 6.9 Hz, 1H, H-18), 5.15 – 4.91 (m, 7H, H-8, H-11, H-19, H-23), 2.77 (td,  $J$  = 10.8, 3.2 Hz, 1H, H-10), 2.68 – 2.56 (m, 2H, H-4, H-17), 2.45 – 2.25 (m, 3H, H-3, H-6, H-17), 1.97 – 1.82 (m, 2H, H-21), 1.39 (dt,  $J$  = 11.0, 2.4 Hz, 1H, H-4), 0.94 (s, 3H, Me), 0.09 (s, 9H,  $\text{SiMe}_3$ ) ppm.

$^{13}\text{C NMR}$  (176 MHz,  $\text{CD}_2\text{Cl}_2$ ):  $\delta$  = 217.4 (C-1), 197.8 (C-20), 151.8 (C-12), 140.1 (C-13), 138.2 (C-22), 137.4 (C-7), 132.7 (C-18), 128.6 (C-15), 128.3 (C-16), 126.6 (C-14), 119.7 (C-19), 116.5 (C-8), 116.1 (C-23), 111.9 (C-11), 68.9 (C-5), 55.9 (C-2), 41.6 (C-10), 39.6 (C-3), 38.5 (C-17), 36.1 (C-6), 35.8 (21), 31.0 (C-4), 16.6 (Me), 1.3 ( $\text{SiMe}_3$ ) ppm.

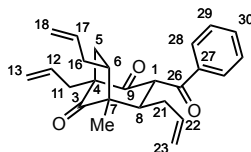
**HRMS** (ESI, pos.):  $m/z$  calcd for  $C_{28}H_{38}O_3SiNa^+$  [ $M+Na^+$ ]: 473.2482, found 473.2478.

**2.2.15 (1*S*,3*S*,4*R*,5*R*,6*R*)-5-methyl-3-(oxophenylmethyl)-1,4,6-tris(prop-2-en-1-yl)bicyclo[3.2.1]octan-2,8-dione (4)**



A flame-dried Schlenk flask was charged with aldehyde **S-14** (550 mg, 1.22 mmol, 1.0 equiv) and anhydrous  $CH_2Cl_2$  (16 mL) under an argon atmosphere. To the solution was added boron trifluoride etherate (619  $\mu L$ , 4.88 mmol, 4.0 equiv) at  $-78^\circ C$ . The reaction mixture was then warmed to  $-40^\circ C$  and stirred for 4 h. The reaction was quenched with saturated aqueous  $NaHCO_3$  (15 mL) and extracted with  $CH_2Cl_2$  ( $3 \times 15$  mL). The combined organic phases were washed with brine (15 mL) and dried over anhydrous  $Na_2SO_4$ . The solvent was removed under reduced pressure to give a crude mixture of diastereomeric  $\beta$ -hydroxy ketones.

The crude product was dissolved in anhydrous  $CH_2Cl_2$  (12 mL) and Dess-Martin periodinane (555 mg, 1.31 mmol, 1.1 equiv) was added. The reaction mixture was stirred at ambient temperature for 2 h. Then *n*-pentane (30 mL) was added and the suspension was filtered through a plug of Celite®. The filtrate was dry-loaded onto Celite® and purified by column chromatography ( $SiO_2$ , *n*-pentane/ $EtOAc$ , 20:1 to 8:1) to afford triketone **4** (405 mg, 1.08 mmol, 89% over two steps) as a colorless solid.



$[\alpha]_D^{26} = +8.2$  ( $c = 1.00$ ,  $CH_2Cl_2$ ).

**$^1H$  NMR** (700 MHz,  $CDCl_3$ ):  $\delta = 7.81$  (d,  $J = 7.8$  Hz, 2H, H-28), 7.56 (t,  $J = 7.8$  Hz, 1H, H-30), 7.45 (t,  $J = 7.8$  Hz, 1H, H-29), 5.75 – 5.66 (m, 2H, H-12, H-17), 5.61 – 5.53 (m, 1H, H-22), 5.14 – 5.05 (m, 4H, H-13, H-18), 4.84 (d,  $J = 16.6$  Hz, 1H, H-23), 4.74 (d,  $J = 10.5$  Hz, 1H, H-23), 4.61 (d,  $J = 11.3$  Hz, 1H, H-1), 2.53 – 2.46 (m, 3H, H-6, H-8, H-11), 2.46 – 2.39 (m, 2H, H-11, H-21), 2.32 – 2.28 (m, 1H, H-16), 2.20 (dd,  $J = 14.8, 9.7$  Hz, 1H, H-5), 2.13 – 2.07 (m, 1H, H-21), 1.82 (dd,  $J = 14.8, 4.3$  Hz, 1H, H-5), 1.73 – 1.67 (m, 1H, H-16), 1.23 (s, 3H, Me) ppm.

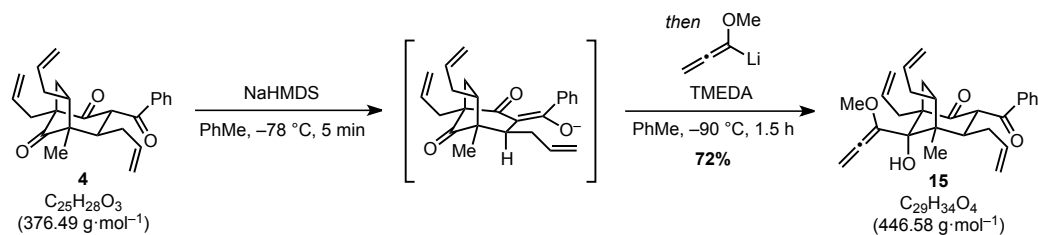
**$^{13}C$  NMR** (176 MHz,  $CDCl_3$ ):  $\delta = 209.6$  (C-3), 203.9 (C-9), 196.8 (C-26), 138.2 (C-27), 135.7 (C-22), 135.2 (C-17), 133.8 (C-12), 133.3 (C-30), 128.8 (C-29), 128.5 (C-28), 118.9 (C-13), 118.3 (C-23), 118.2 (s), 67.5 (C-4), 57.8 (C-1), 54.5 (C-7), 43.4 (C-8), 37.8 (C-16), 35.1 (C-21), 34.0 (C-6), 33.6 (C-5), 31.7 (C-11), 15.4 (Me) ppm.

**HRMS** (ESI, pos.):  $m/z$  calcd for  $C_{25}H_{28}O_3Na^+$  [ $M+Na^+$ ]: 399.1931, found 399.1938.

**m.p.:** 106 – 108  $^\circ C$ .

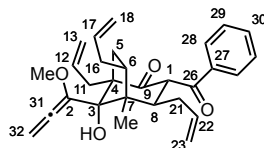
**X-ray:** Crystals were grown by addition of *n*-pentane to a concentrated solution of **4** in  $Et_2O$  in a 1 mL vial until a nearly saturated solution was reached. The solution was then left to rest at ambient temperature.

**2.2.17 (1R,3S,4R,5R,6R,8S)-8-hydroxy-8-(1-methoxypropa-1,2-dien-1-yl)-5-methyl-3-(oxophenylmethyl)-1,4,6-tris(prop-2-en-1-yl)bicyclo[3.2.1]octan-2-one (15)**



Preparation of methoxyallenyllithium: To a flame-dried Schlenk tube was added anhydrous toluene (660  $\mu\text{L}$ ) and methoxyallene (104  $\mu\text{L}$ , 1.07 mmol, 6.1 equiv) under an argon atmosphere. The reaction was cooled to  $-50\text{ }^\circ\text{C}$  and *n*-BuLi (2.5 M in hexanes, 420  $\mu\text{L}$ , 1.05 mmol, 6.0 equiv) was added. The reaction mixture was stirred at  $-50\text{ }^\circ\text{C}$  to  $-40\text{ }^\circ\text{C}$  over 5 min. Then anhydrous *N,N,N,N*-tetramethylethylenediamine (158  $\mu\text{L}$ , 1.05 mmol, 6.0 equiv) was added and the mixture was cooled to  $-78\text{ }^\circ\text{C}$ .

A flame-dried Schlenk tube was charged with triketone **4** (66.0 mg, 175  $\mu\text{mol}$ , 1.0 equiv) and anhydrous toluene (660  $\mu\text{L}$ ) under an argon atmosphere. Sodium hexamethyldisilazide (1.9 M in THF, 102  $\mu\text{L}$ , 193  $\mu\text{mol}$ , 1.1 equiv) was added at  $-78\text{ }^\circ\text{C}$  and the solution was stirred for 5 min. Then the mixture cooled to  $-90\text{ }^\circ\text{C}$  and the prepared solution of methoxyallenyllithium was added. Stirring was continued at  $-90\text{ }^\circ\text{C}$  for 1.5 h. The reaction was quenched by the addition of saturated aqueous  $\text{NaHCO}_3$  (5 mL). The layers were separated, the aqueous phase was extracted with  $\text{Et}_2\text{O}$  (3  $\times$  5 mL), and the combined organic layers were washed with brine (20 mL), dried over  $\text{Na}_2\text{SO}_4$ , and concentrated under reduced pressure. The crude product was purified by MPLC (dry-loaded onto Celite<sup>®</sup>,  $\text{SiO}_2$ , cyclohexane/ $\text{EtOAc}$ , 25:1 to 10:1) to yield methoxyallene **15** (56.4 mg, 126  $\mu\text{mol}$ , 72%) as a colorless solid.



$$[\alpha]_{\text{D}}^{24} = -3.44 \quad (c = 1.00, \text{CH}_2\text{Cl}_2).$$

**<sup>1</sup>H NMR** (700 MHz,  $\text{CD}_2\text{Cl}_2$ ):  $\delta = 7.84 - 7.82$  (m, 2H, H-28),  $7.56 - 7.52$  (m, 1H, 30),  $7.46 - 7.42$  (m, 2H, H-29),  $5.91 - 5.79$  (m, 2H, 9, H-12, H-17),  $5.76$  (d,  $J = 7.9$  Hz, 1H, H-32),  $5.71$  (d,  $J = 7.9$  Hz, 1H, H-32),  $5.55$  (dddd,  $J = 16.9, 9.9, 8.4, 6.1$  Hz, 1H, H-22),  $5.08$  (d,  $J = 17.2$ , 1H, H-18),  $5.04 - 4.98$  (m, 2H, H-13, H-18),  $4.94$  (d,  $J = 10.1$  Hz, 1H, H-13),  $4.78$  (dq,  $J = 17.0, 1.8$  Hz, 1H, H-23),  $4.63$  (d,  $J = 10.0$  Hz, 1H, H-23),  $4.13$  (d,  $J = 10.4$  Hz, 1H, H-1),  $3.48$  (s, 3H, OMe),  $3.14$  (ddd,  $J = 10.4, 7.6, 4.9$  Hz, 1H, H-8),  $2.44$  (dd,  $J = 13.5, 6.9$  Hz, 1H, H-11),  $2.39 - 2.31$  (m, 3H, H-6, H-16, H-21),  $2.28 - 2.23$  (m, 1H, H-16),  $2.23 - 2.17$  (m, 1H, H-11),  $1.93 - 1.81$  (m, 3H, H-5, H-21),  $1.03$  (s, 3H, Me) ppm.

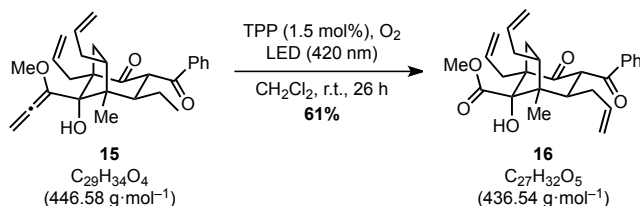
**<sup>13</sup>C NMR** (176 MHz,  $\text{CD}_2\text{Cl}_2$ ):  $\delta = 209.8$  (C-9),  $199.1$  (C-26),  $199.0$  (C-31),  $139.6$  (C-27),  $138.7$  (C-17),  $137.3$  (C-22),  $136.9$  (C-12),  $133.0$  (C-30),  $129.0$  (C-28),  $128.9$  (C-29),  $116.9$  (C-13),  $116.7$  (C-23),  $116.0$  (C-18),  $96.4$  (C-32),  $86.3$  (C-3),  $63.3$  (C-4),  $59.6$  (C-1),  $56.5$  (OMe),  $52.5$  (C-7),  $44.0$  (C-8),  $38.5$  (C-6),  $38.0$  (C-5),  $37.2$  (C-16),  $36.1$  (C-21),  $35.4$  (C-11),  $16.4$  (Me) ppm.

**HRMS** (ESI, pos.):  $m/z$  calcd for  $\text{C}_{29}\text{H}_{34}\text{O}_4\text{Na}^+$  [ $\text{M}+\text{Na}^+$ ]: 469.2349, found 469.2360.

**X-ray**: Crystals were grown by addition of *n*-pentane to a concentrated solution of **15** in  $\text{Et}_2\text{O}$  in a 1 mL vial until a nearly saturated solution was reached. The solution was then left to rest at ambient temperature.

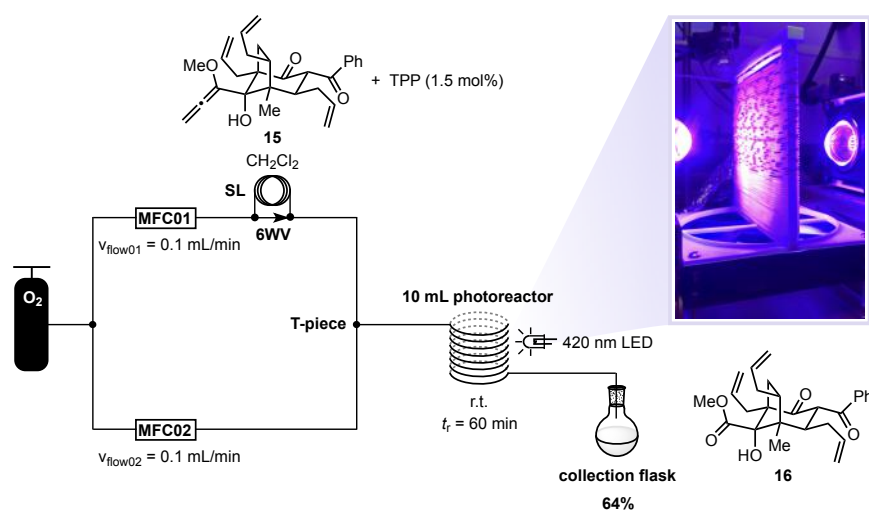
## 2.18 (1*R*,3*S*,4*R*,5*R*,6*R*,8*S*)-methyl 8-hydroxy-5-methyl-2-oxo-3-(oxophenylmethyl)-1,4,6-tris(prop-2-en-1-yl)bicyclo[3.2.1]octane-8-carboxylate (**16**)

### Preparation of ester **16** in batch

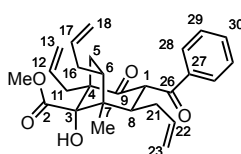


A solution of methoxyallene **15** (46.0 mg, 103  $\mu\text{mol}$ , 1.0 equiv) and tetraphenylporphyrine (1.0 mg, 1.5  $\mu\text{mol}$ , 1.5 mol%) in  $\text{CH}_2\text{Cl}_2$  (4.0 mL) was stirred at ambient temperature. The reaction mixture was irradiated using a LED chip (420 nm, max 30 W) at ambient temperature and a stream of oxygen was passed through until TLC analysis indicated complete consumption of the starting material. After 26 h the solvent was removed under reduced pressure and the crude product was purified by column chromatography ( $\text{SiO}_2$ , *n*-pentane/EtOAc, 8:1) to yield ester **16** (27.5 mg, 63.0  $\mu\text{mol}$ , 61%) as a reddish oil.

### Preparation of ester **16** in flow



In a small vial, a solution of allene **15** (56.4 mg, 126  $\mu\text{mol}$ , 1.0 equiv) and tetraphenylporphyrine (1.2 mg, 1.9  $\mu\text{mol}$ , 1.5 mol%) in  $\text{CH}_2\text{Cl}_2$  (4.8 mL) was prepared and loaded on the sample loop **SL** ( $V = 2.2$  mL). This solution was driven by an oxygen flow using mass flow controller **MFC01** ( $v_{\text{flow01}} = 0.1$  mL/min) and mixed with an oxygen flow controlled by mass flow controller **MFC02** ( $v_{\text{flow02}} = 0.1$  mL/min) resulting in a segmented gas-liquid flow with an initial flow rate of  $v_{\text{flow\_tot}} = v_{\text{flow01}} + v_{\text{flow02}} = 0.2$  mL/min. Due to the oxygen consumption during the reaction, the real flow rate was decreasing over time. This segmented gas-liquid-flow was passed through a tailor made, 3D-printed photoreactor ( $V = 10$  mL) and irradiated using a LED chip (420 nm, max 30 W) at ambient temperature with a residence time of  $t_r = 60$  min. At the end of the reactor, the reaction mixture was collected in a **collection flask**. The solvent was removed under reduced pressure and the crude product was purified by MPLC (dry-loaded onto Celite®,  $\text{SiO}_2$ , cyclohexane/EtOAc, 20:1 to 6:1) to yield ester **16** (35.4 mg, 81.1  $\mu\text{mol}$ , 64%) as a reddish oil.



$$[\alpha]_{\text{D}}^{24} = -19.21 \quad (c = 1.00, \text{CH}_2\text{Cl}_2).$$

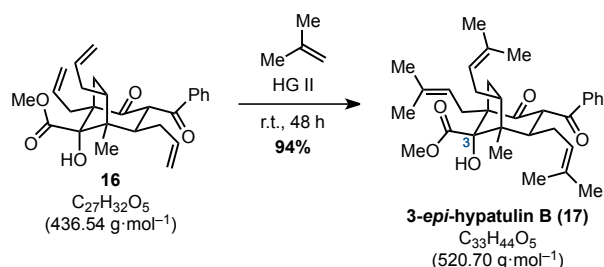


**<sup>1</sup>H NMR** (700 MHz, CDCl<sub>3</sub>): δ = 7.92 – 7.88 (m, 2H, H-28), 7.56 – 7.52 (m, 1H, H-30), 7.47 – 7.43 (m, 2H, H-29), 5.93 – 5.77 (m, 2H, H-12, H-17), 5.61 – 5.50 (m, 1H, H-22), 5.14 (dq, *J* = 17.0, 1.6 Hz, 1H, H-18), 5.10 – 5.07 (m, 1H, H-18), 4.95 – 4.91 (m, 2H, H-13), 4.83 (dq, *J* = 17.0, 1.6 Hz, 1H, H-23), 4.69 (d, *J* = 10.1 Hz, 1H, H-23), 4.13 (d, *J* = 10.4 Hz, 1H, H-1), 3.89 (s, 3H, OMe), 3.28 (ddd, *J* = 10.4, 7.5, 4.9 Hz, 1H, H-8), 2.46 – 2.38 (m, 2H, H-6, H-11), 2.38 – 2.25 (m, 3H, H-16, H-21), 2.22 – 2.11 (m, 1H, H-11), 2.01 – 1.98 (m, 2H, H-5), 1.95 – 1.90 (m, 1H, H-21), 1.00 (s, 3H, Me) ppm.

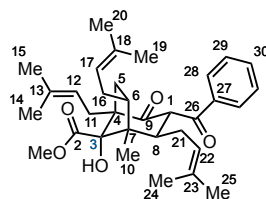
**<sup>13</sup>C NMR** (176 MHz, CDCl<sub>3</sub>): δ = 207.8 (C-9), 198.1 (C-26), 173.1 (C-2), 138.7 (C-27), 137.3 (C-17), 136.8 (C-22), 135.4 (C-12), 132.8 (C-30), 128.8 (C-28), 128.5 (C-29), 117.1 (C-23), 117.0 (C-13), 116.5 (C-18), 89.6 (C-3), 62.1 (C-4), 59.0 (C-1), 52.7 (OMe), 51.8 (C-7), 43.2 (C-8), 38.0 (C-6), 37.8 (C-5), 36.7 (C-16), 35.4 (C-11), 35.2 (C-21), 15.9 (Me) ppm.

**HRMS** (ESI, pos.): *m/z* calcd for C<sub>27</sub>H<sub>32</sub>O<sub>5</sub>Na<sup>+</sup> [*M*+Na<sup>+</sup>]: 459.2142, found 459.2141.

### 2.19 (1*R*,3*S*,4*R*,5*R*,6*R*,8*S*)-methyl 8-hydroxy-5-methyl-2-oxo-3-(oxophenylmethyl)-1,4,6-tris(3-methylbut-2-en-1-yl)bicyclo[3.2.1]octane-8-carboxylate (**17**)



The alkene metathesis was performed in analogy to a reported procedure by NAKADA and UWAMORI.<sup>17</sup> A pressure tube was placed under an argon atmosphere, charged with ester **16** (8.0 mg, 18 μmol, 1.0 equiv) and then submerged into a cooling bath with a temperature of –78 °C. Liquid 2-methylbut-2-ene (1.8 mL) and Hoveyda-Grubbs II catalyst (3.0 mg, 5 μmol, 26 mol%) were added. The tube was sealed and the cooling bath was removed. The reaction mixture was warmed to ambient temperature and stirred for 48 h. The solution was cooled to –78 °C before opening the pressure tube and then diluted with CH<sub>2</sub>Cl<sub>2</sub> (2 mL). The cooling bath was removed and the tube was warmed to ambient temperature to vent off all volatile compounds. The residue was purified by preparative TLC (SiO<sub>2</sub>, *n*-pentane/EtOAc, 8:1) to afford 3-*epi*-hypatulin B (**17**) (9.0 mg, 17.3 μmol, 94%) as a colorless oil.



$[\alpha]_{\text{D}}^{27} = +3.78$  (*c* = 1.00, CH<sub>2</sub>Cl<sub>2</sub>).

**<sup>1</sup>H NMR** (700 MHz, CD<sub>3</sub>OD): δ = 7.91 – 7.89 (m, 2H, H-28), 7.56 – 7.53 (m, 1H, H-30), 7.49 – 7.45 (m, 2H, H-29), 5.22 – 5.18 (m, 1H, H-12), 5.14 – 5.10 (m, 1H, H-17), 4.74 – 4.70 (m, 1H, H-22), 4.14 (d, *J* = 10.2 Hz, 1H, H-1), 3.83 (s, 1H, OMe), 3.16 (ddd, *J* = 10.2, 9.5, 4.9 Hz, 1H, H-8), 2.53 – 2.46 (m, 1H, H-6), 2.46 – 2.36 (m, 2H, H-11, H-16), 2.15 – 2.08 (m, 2H, H-5, H-11), 2.07 – 1.93 (m, 4H, H-5, H-16, H-21), 1.74 (s, 3H, H-15), 1.71 (s, 3H, H-14), 1.63 (s, 3H, H-20), 1.57 (s, 3H, H-19), 1.33 (s, 3H, H-24), 1.13 (s, 3H, H-25), 1.00 (s, 3H, H-10) ppm.

**<sup>13</sup>C NMR** (176 MHz, CD<sub>3</sub>OD): δ = 210.8 (C-9), 200.4 (C-26), 174.6 (C-2), 139.7 (C-27), 134.2 (C-23), 133.6 (C-30), 133.3 (C-18), 133.2 (C-13), 129.8 (C-28), 129.4 (C-29), 125.3 (C-22), 125.0 (C-12), 122.3 (C-17), 91.4 (C-3), 64.2 (C-4), 59.8 (C-1), 53.1 (C-7), 52.5 (OMe), 46.4 (C-8), 40.2 (C-6), 38.0 (C-21), 31.7 (C-11), 29.7 (C-5), 29.4 (C-16), 26.1 (C-20), 26.0 (C-15), 25.8 (C-25), 18.3 (C-14), 18.0 (C-19), 17.6 (C-24), 16.2 (C-10) ppm.

**HRMS** (ESI, pos.): *m/z* calcd for C<sub>33</sub>H<sub>44</sub>O<sub>5</sub>Na<sup>+</sup> [*M*+Na<sup>+</sup>]: 542.3081, found 543.3106.

#### 4. X-ray data

##### Ketone ((10R)-8) (CCDC2154248) (Thermal Ellipsoids at 50% Probability)

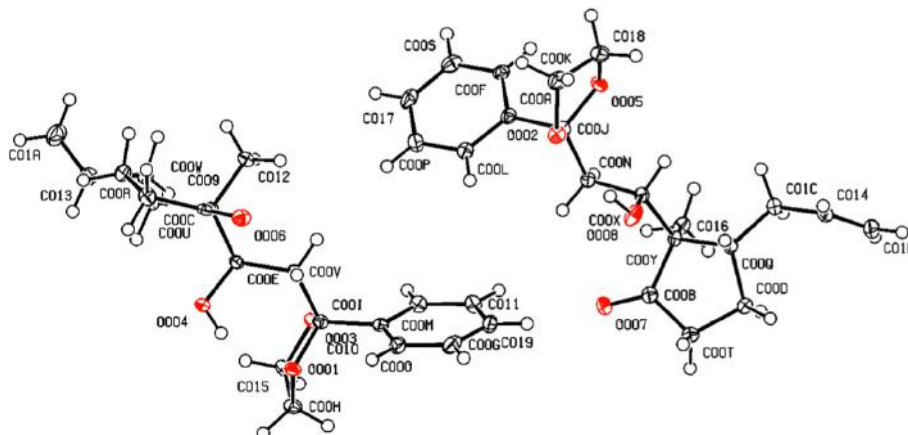


**Table S1.** Crystal data of ketone ((10R)-8).

Empirical formula	C <sub>20</sub> H <sub>26</sub> O <sub>4</sub>
Formula weight	330.41
Temperature/K	100.01
Crystal system	triclinic
Space group	<i>P</i> 1
<i>a</i> /Å	8.961(4)
<i>b</i> /Å	9.353(4)
<i>c</i> /Å	11.693(6)
$\alpha$ /°	92.43(3)
$\beta$ /°	110.673(18)
$\gamma$ /°	102.285(16)
Volume/Å <sup>3</sup>	888.5(7)
<i>Z</i>	2
$\rho_{\text{calc}}$ /gcm <sup>-3</sup>	1.235
$\mu$ /mm <sup>-1</sup>	0.682
<i>F</i> (000)	356.0
Crystal size/mm <sup>3</sup>	0.5 × 0.34 × 0.21
Radiation	CuK $\alpha$ ( $\lambda$ = 1.54178)
2 $\theta$ range for data collection/°	8.15 to 143.936
Reflections collected	27548
Independent reflections	6594 [ <i>R</i> <sub>int</sub> = 0.0311, <i>R</i> <sub>sigma</sub> = 0.0283]
Data/restraints/parameters	6594/3/437
Goodness-of-fit on <i>F</i> <sup>2</sup>	1.082
Final <i>R</i> indexes [ <i>I</i> > 2 $\sigma$ ( <i>I</i> )]	<i>R</i> <sub>1</sub> = 0.0292, <i>wR</i> <sub>2</sub> = 0.0760
Final <i>R</i> indexes [all data]	<i>R</i> <sub>1</sub> = 0.0295, <i>wR</i> <sub>2</sub> = 0.0761
Largest diff. peak and hole/e.Å <sup>-3</sup>	0.20 and -0.20
Flack parameter	0.06(3)
CCDC deposition number	2154248



(±)-Triketone (rac-4) (CCDC2151468) (Thermal Ellipsoids at 50% Probability)

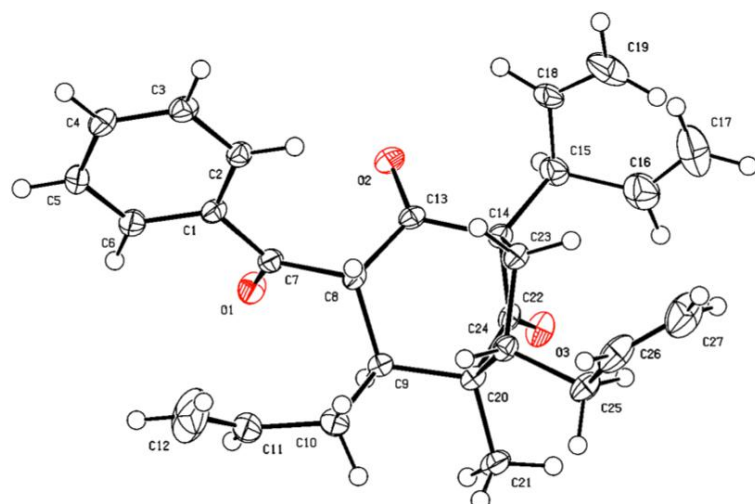
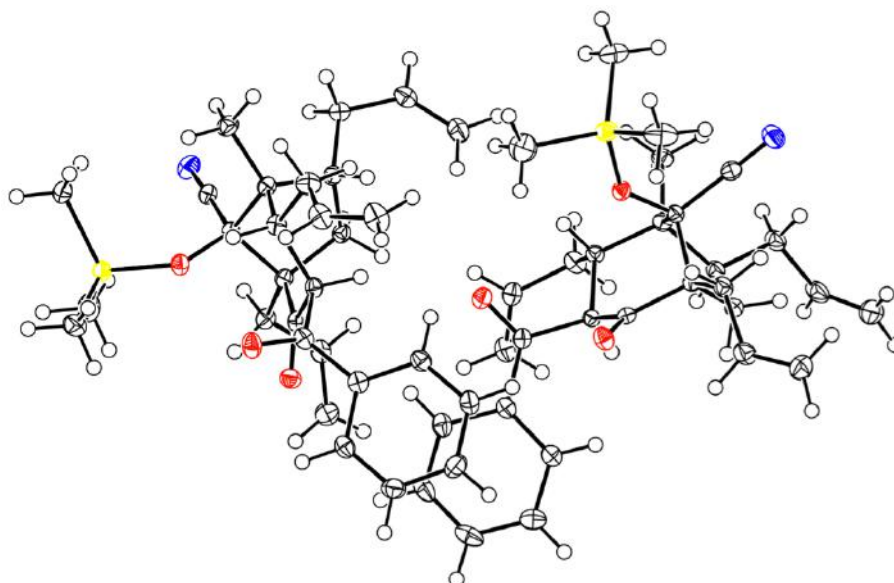


Table S2. Crystal data of (±)-triketone (rac-4).

Empirical formula	C <sub>25</sub> H <sub>28</sub> O <sub>3</sub>
Formula weight	375.46
Temperature/K	100.00
Crystal system	monoclinic
Space group	<i>P</i> 2 <sub>1</sub> / <i>n</i>
<i>a</i> /Å	8.43994(5)
<i>b</i> /Å	12.19920(8)
<i>c</i> /Å	21.41911(3)
$\alpha$ /°	90
$\beta$ /°	96.3817(2)
$\gamma$ /°	90
Volume/Å <sup>3</sup>	2191.66(2)
<i>Z</i>	4
$\rho_{\text{calc}}/\text{gcm}^{-3}$	1.138
$\mu/\text{mm}^{-1}$	0.580
<i>F</i> (000)	804.0
Crystal size/mm <sup>3</sup>	0.58 × 0.24 × 0.06
Radiation	CuK $\alpha$ ( $\lambda$ = 1.54178)
2 $\theta$ range for data collection/°	8.308 to 140.628
Reflections collected	97662
Independent reflections	4161 [ <i>R</i> <sub>int</sub> = 0.0346, <i>R</i> <sub>sigma</sub> = 0.0146]
Data/restraints/parameters	4161/0/272
Goodness-of-fit on <i>F</i> <sup>2</sup>	0.977
Final <i>R</i> indexes [ <i>I</i> ≥ 2 $\sigma$ ( <i>I</i> )]	<i>R</i> <sub>1</sub> = 0.0408, <i>wR</i> <sub>2</sub> = 0.1022
Final <i>R</i> indexes [all data]	<i>R</i> <sub>1</sub> = 0.0411, <i>wR</i> <sub>2</sub> = 0.1024
Largest diff. peak and hole/e.Å <sup>-3</sup>	0.35 and -0.47
CCDC deposition number	2151468

(±)-Cyanhydrin (rac-14) (CCDC2151470) (Thermal Ellipsoids at 50% Probability)



**Table S3. Crystal data of (±)-cyanhydrin (rac-14).**

Empirical formula	C <sub>29</sub> H <sub>37</sub> NO <sub>3</sub> Si
Formula weight	475.68
Temperature/K	100(2)
Crystal system	triclinic
Space group	$P\bar{1}$
a/Å	12.028(4)
b/Å	14.201(5)
c/Å	16.489(5)
$\alpha$ /°	105.487(7)
$\beta$ /°	97.062(13)
$\gamma$ /°	93.370(7)
Volume/Å <sup>3</sup>	2681.2(15)
Z	4
$\rho_{\text{calc}}/\text{gcm}^{-3}$	1.178
$\mu/\text{mm}^{-1}$	0.117
F(000)	1024.0
Crystal size/mm <sup>3</sup>	0.51 × 0.32 × 0.19
Radiation	MoK $\alpha$ ( $\lambda$ = 0.71073)
2 $\theta$ range for data collection/°	3.988 to 51.474
Reflections collected	61969
Independent reflections	10234 [ $R_{\text{int}}$ = 0.0333, $R_{\text{sigma}}$ = 0.0200]
Data/restraints/parameters	10234/0/621
Goodness-of-fit on F <sup>2</sup>	1.033
Final R indexes [ $I > 2\sigma(I)$ ]	$R_1$ = 0.0347, $wR_2$ = 0.0825
Final R indexes [all data]	$R_1$ = 0.0391, $wR_2$ = 0.0853
Largest diff. peak and hole/e.Å <sup>-3</sup>	0.34 and -0.27
CCDC deposition number	2151470

(±)-Methoxyallene (rac-15) (CCDC2151469) (Thermal Ellipsoids at 50% Probability)

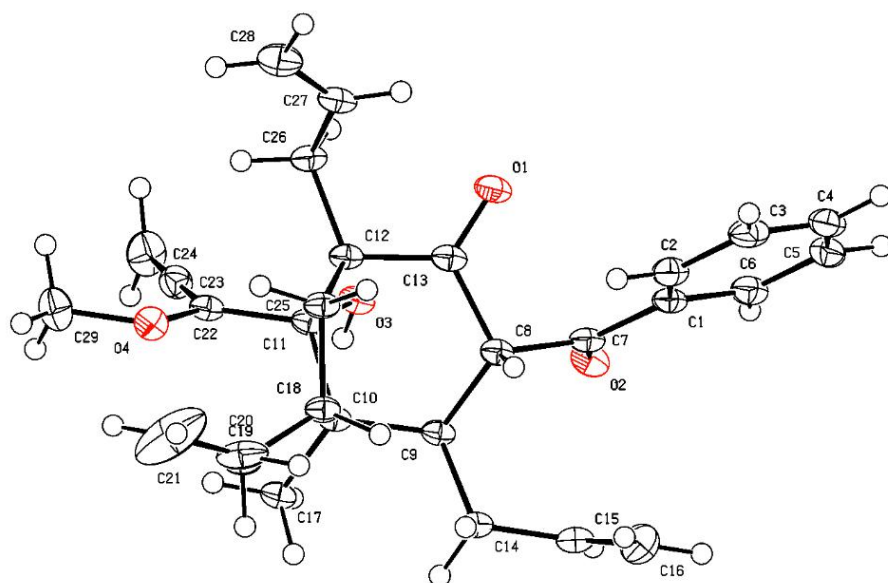
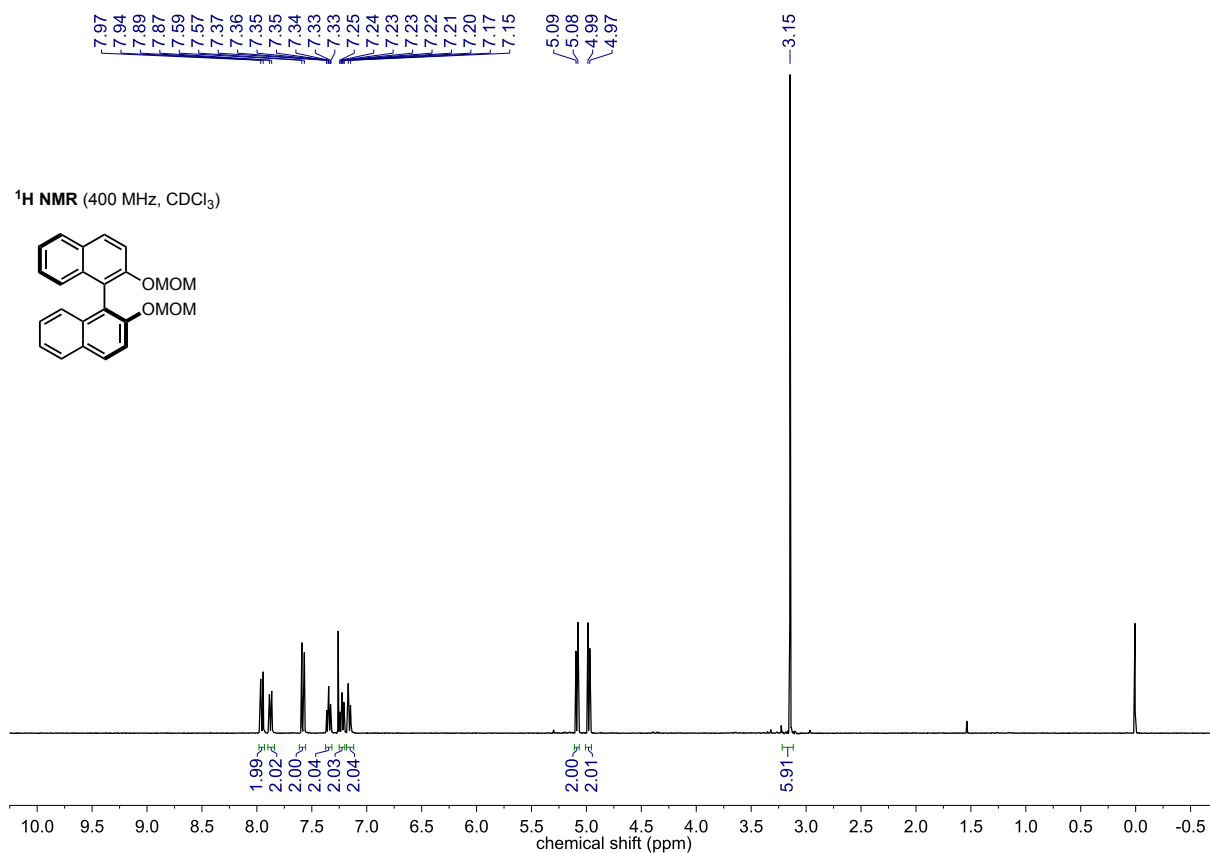


Table S4. Crystal data of (±)-methoxyallene (rac-15).

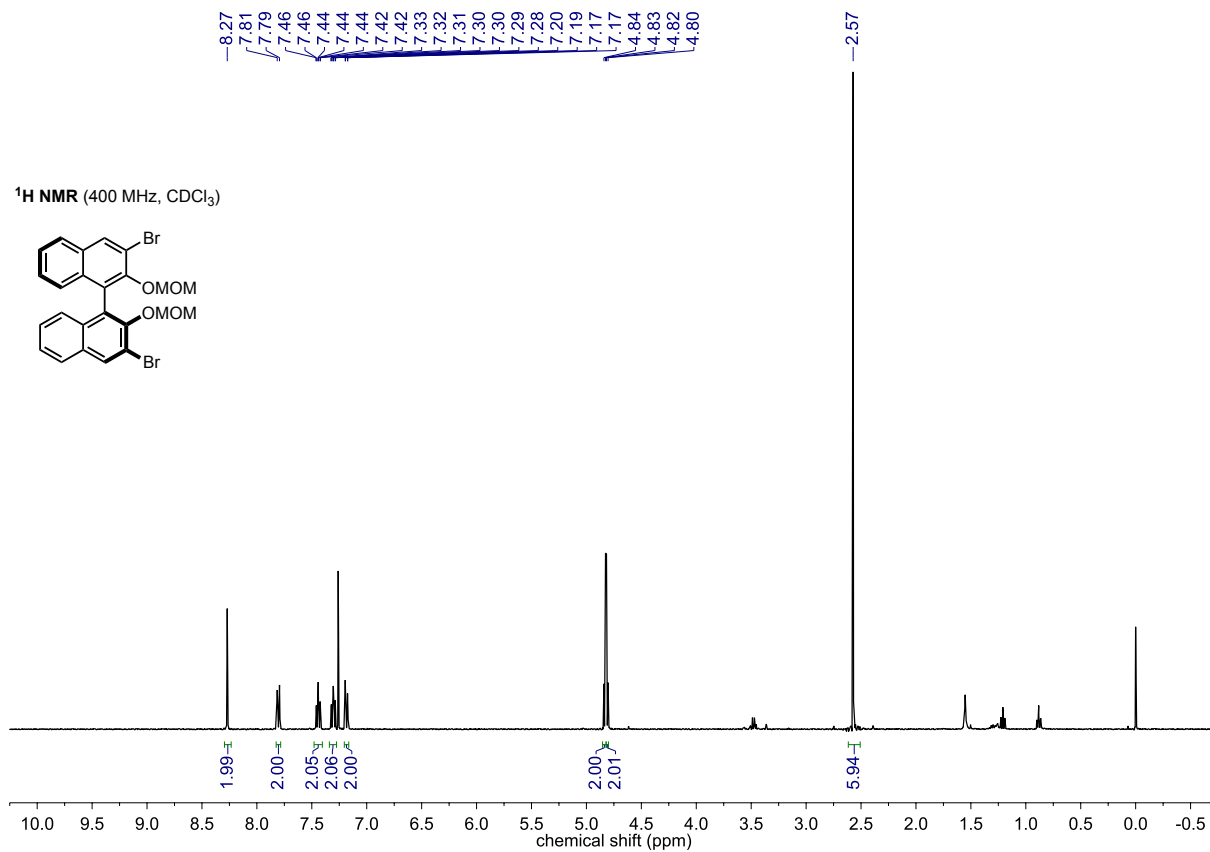
Empirical formula	C <sub>29</sub> H <sub>34</sub> O <sub>4</sub>
Formula weight	446.56
Temperature/K	100(2)
Crystal system	monoclinic
Space group	<i>P</i> 2 <sub>1</sub> / <i>n</i>
<i>a</i> /Å	14.8004(14)
<i>b</i> /Å	11.7432(11)
<i>c</i> /Å	15.7166(15)
$\alpha$ /°	90
$\beta$ /°	113.198(3)
$\gamma$ /°	90
Volume/Å <sup>3</sup>	2510.8(4)
<i>Z</i>	4
$\rho_{\text{calc}}/\text{g cm}^{-3}$	1.181
$\mu/\text{mm}^{-1}$	0.613
<i>F</i> (000)	960.0
Crystal size/mm <sup>3</sup>	0.24 × 0.17 × 0.03
Radiation	CuK $\alpha$ ( $\lambda$ = 1.54178)
2 $\theta$ range for data collection/°	6.952 to 140.28
Reflections collected	124225
Independent reflections	4757 [ <i>R</i> <sub>int</sub> = 0.0362, <i>R</i> <sub>sigma</sub> = 0.0112]
Data/restraints/parameters	4757/0/308
Goodness-of-fit on <i>F</i> <sup>2</sup>	1.021
Final <i>R</i> indexes [ <i>I</i> > 2 $\sigma$ ( <i>I</i> )]	<i>R</i> <sub>1</sub> = 0.0351, <i>wR</i> <sub>2</sub> = 0.0837
Final <i>R</i> indexes [all data]	<i>R</i> <sub>1</sub> = 0.0362, <i>wR</i> <sub>2</sub> = 0.0845
Largest diff. peak and hole/e.Å <sup>-3</sup>	0.26 and -0.29
CCDC deposition number	2151469

## 5. NMR Spectra

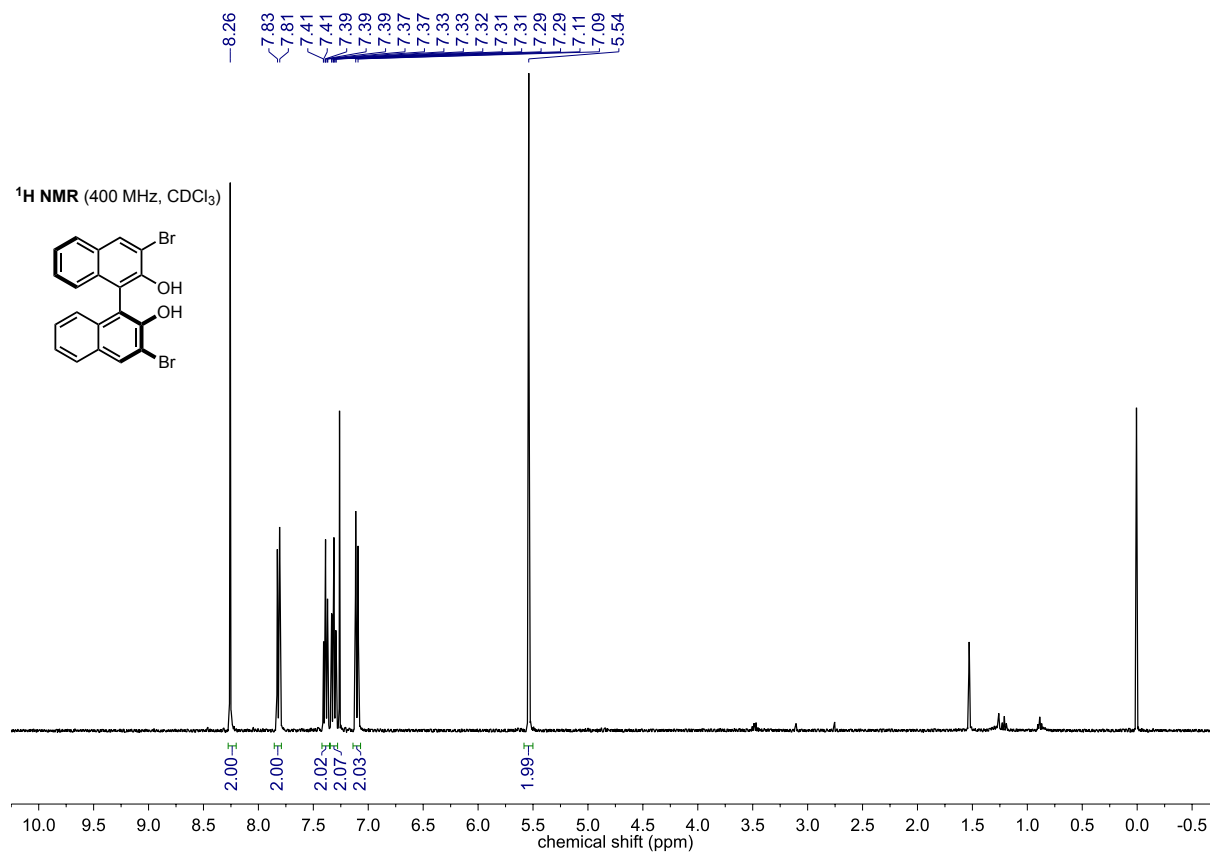
## BINOL S-7



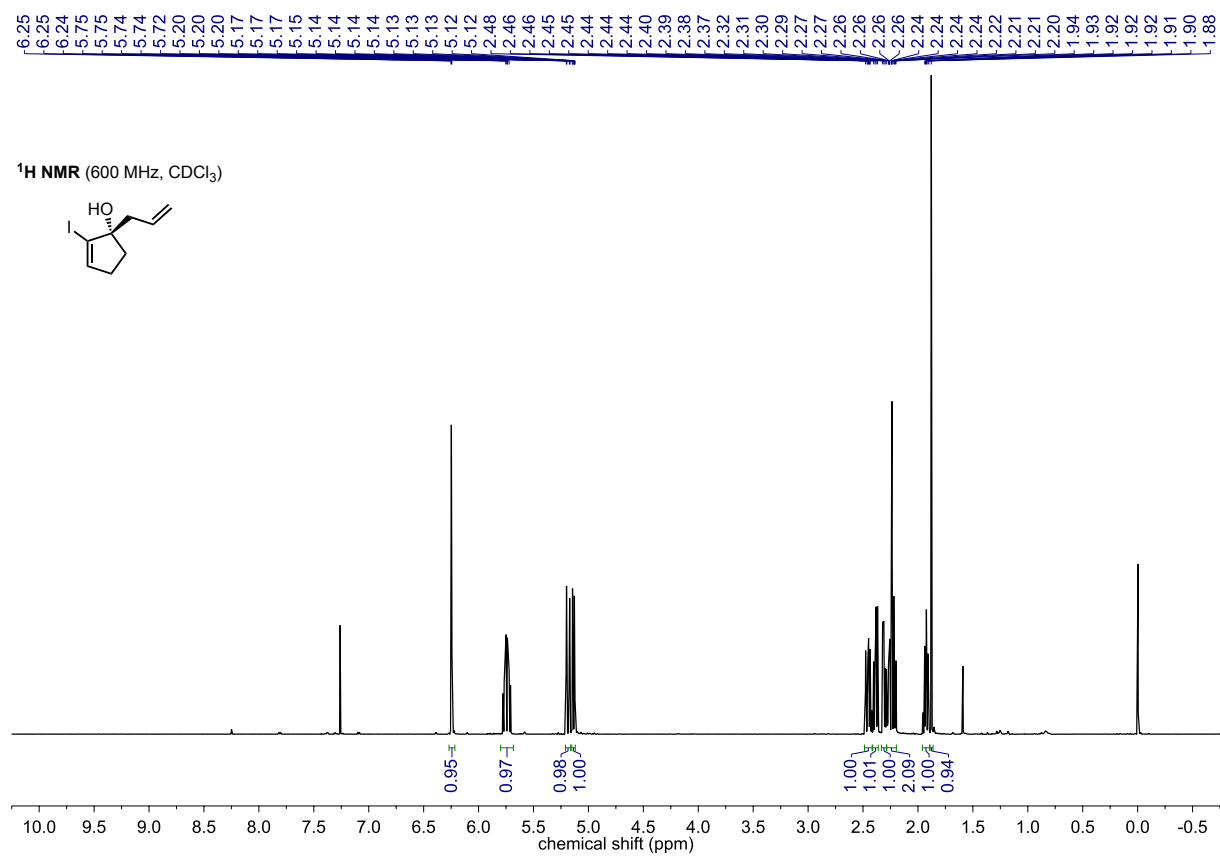
## BINOL S-8



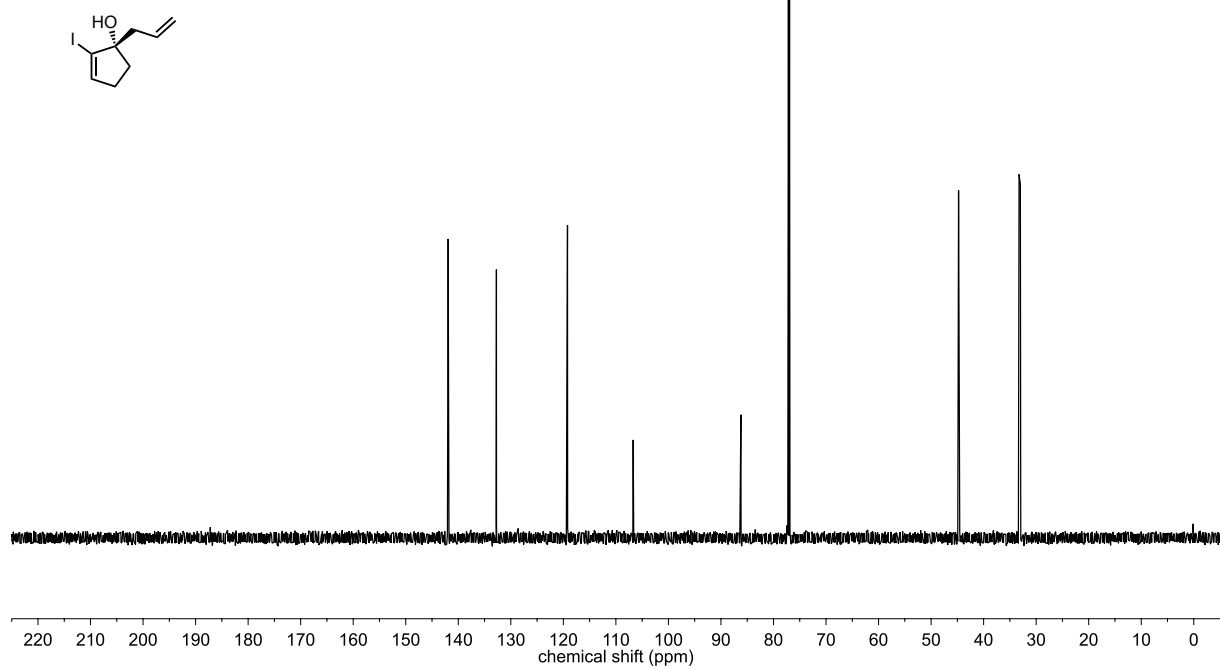
## BINOL S-9



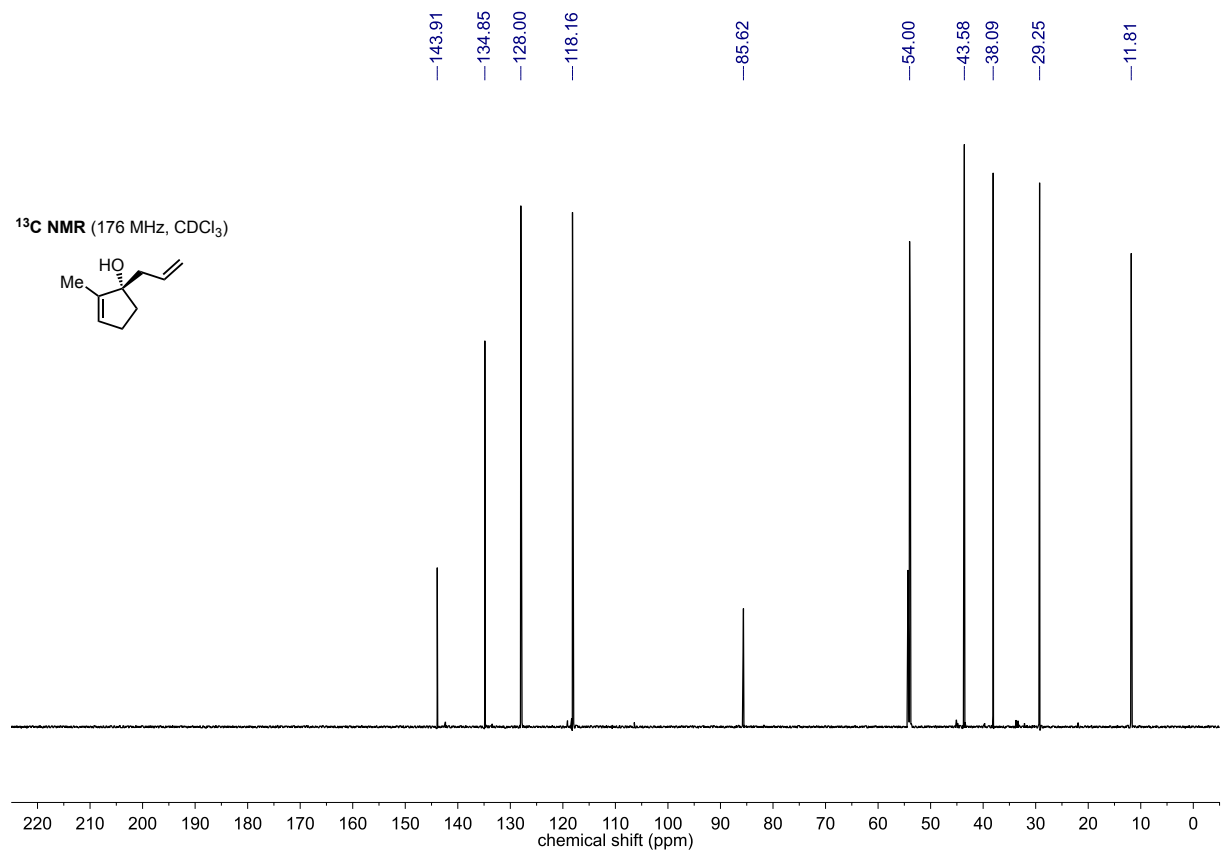
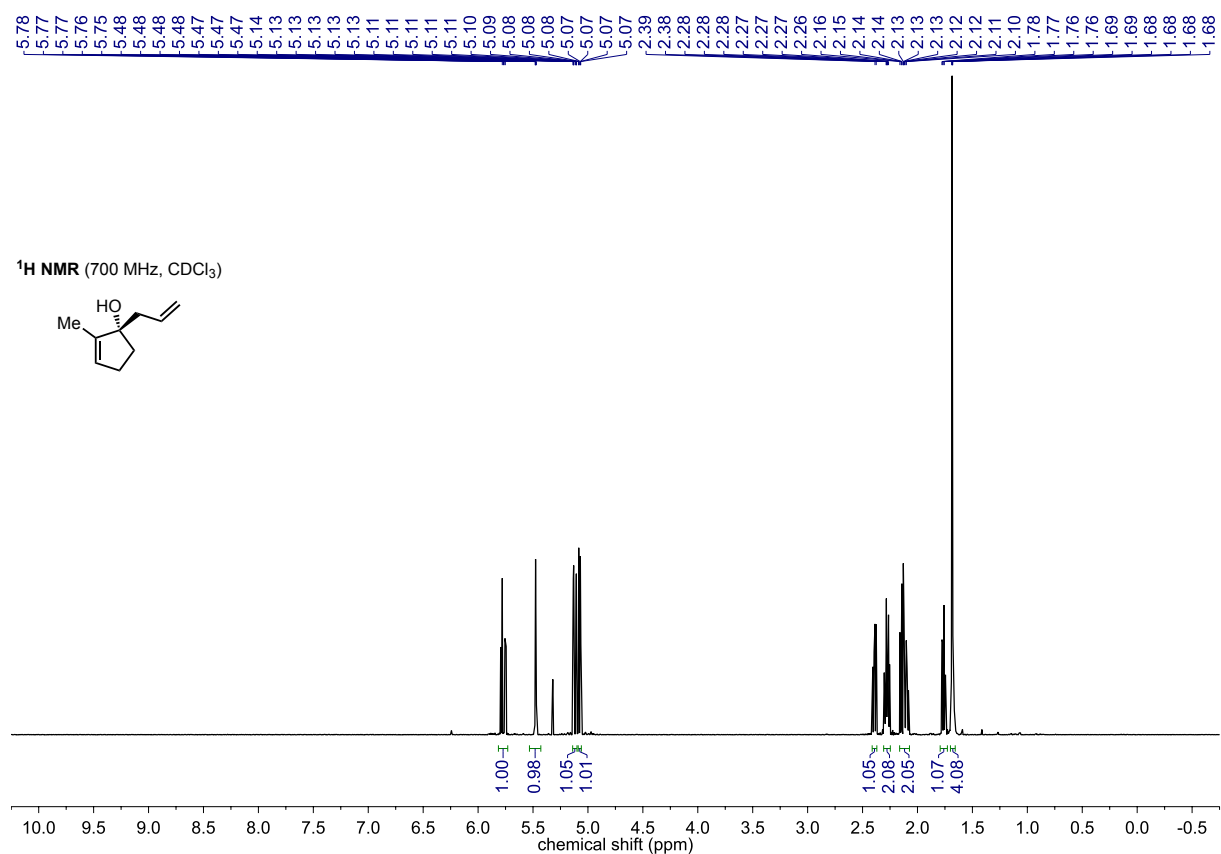
## Alcohol S-6



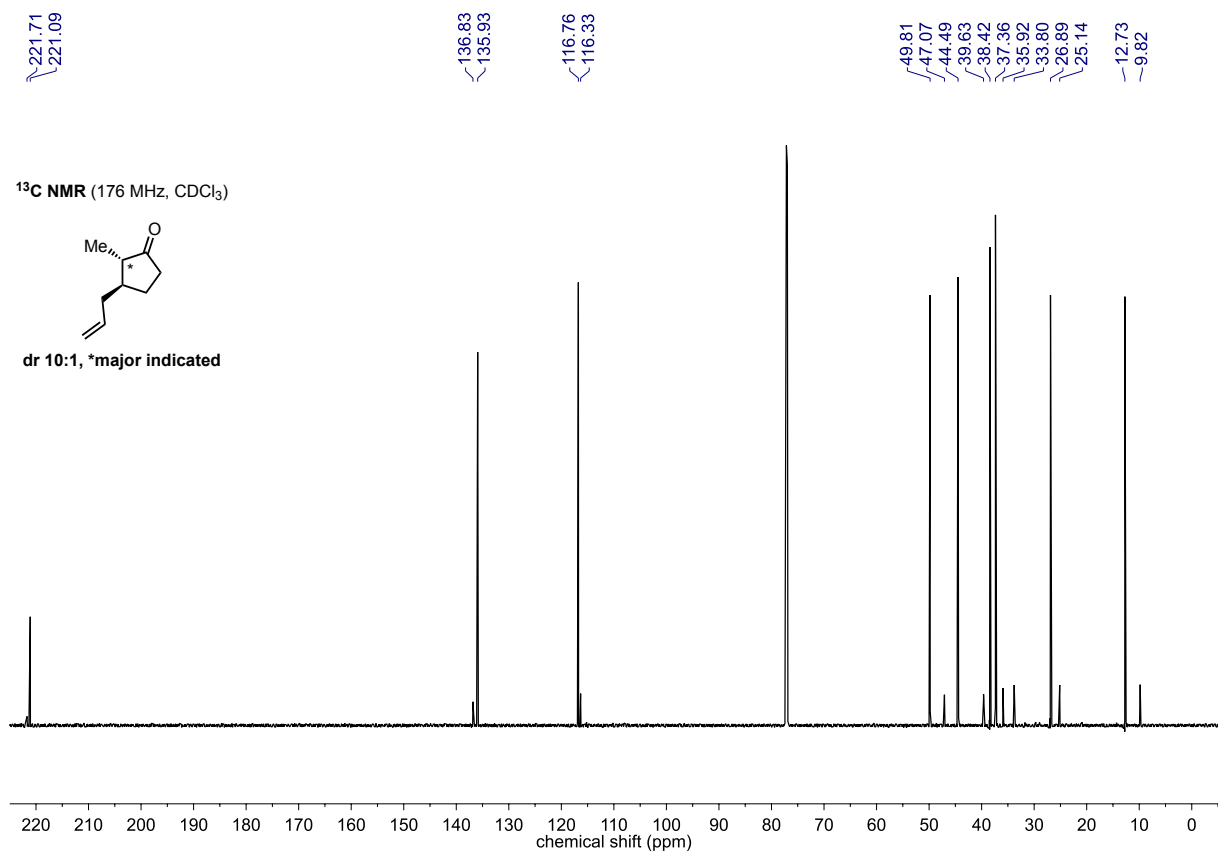
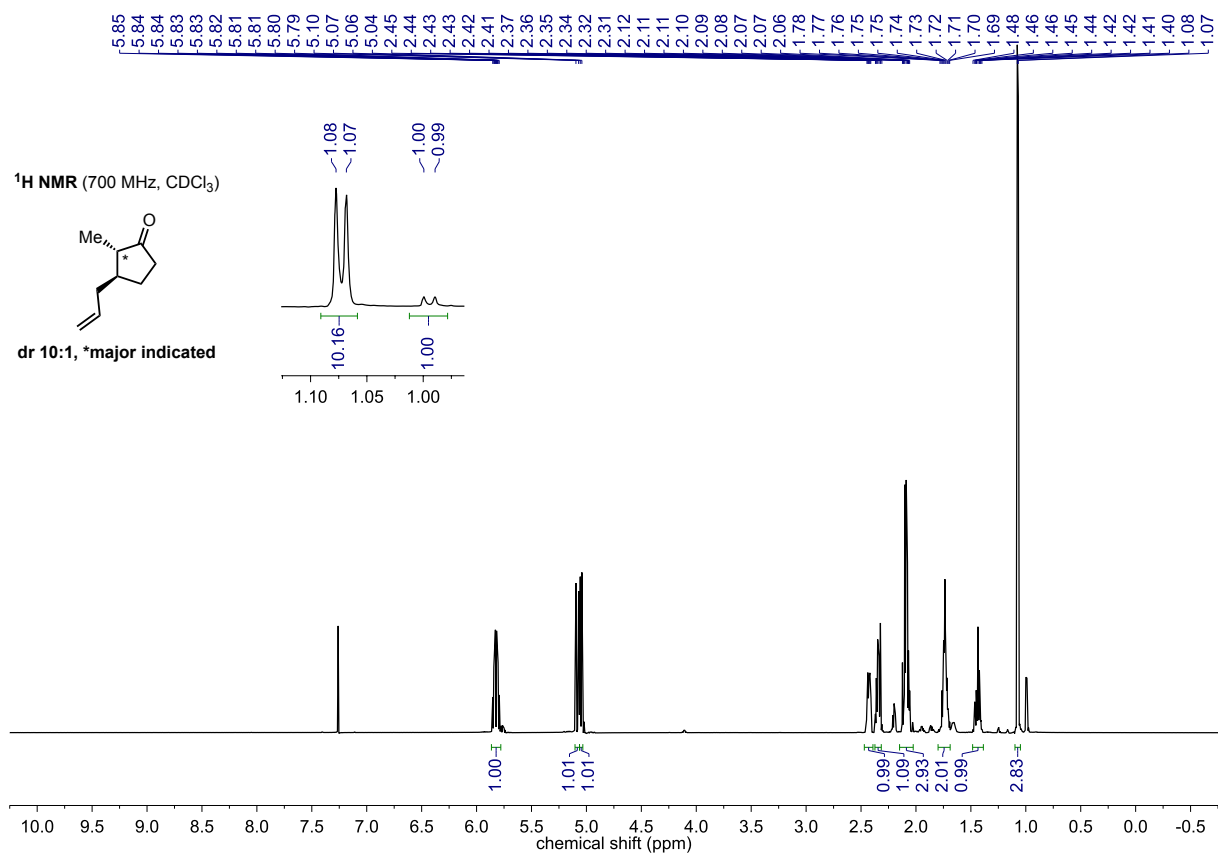
<sup>13</sup>C NMR (151 MHz, CDCl<sub>3</sub>)



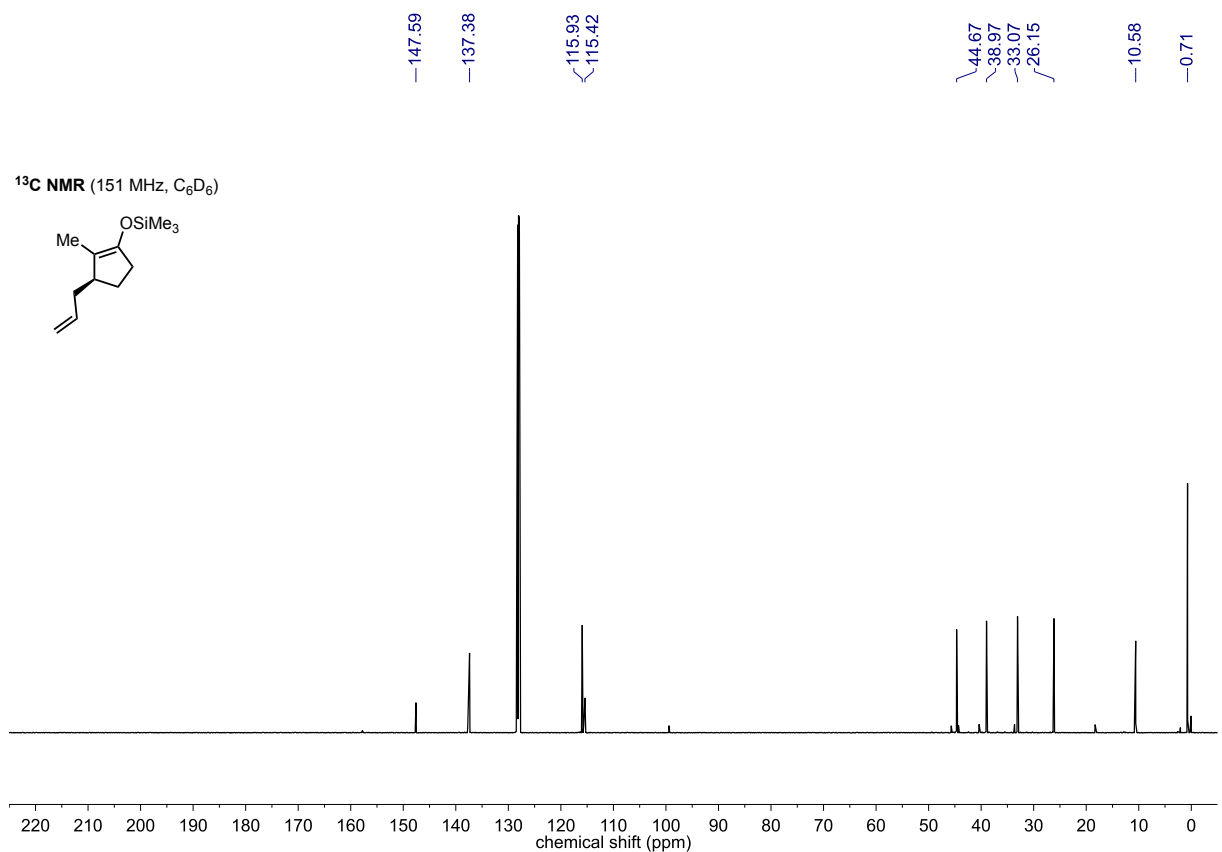
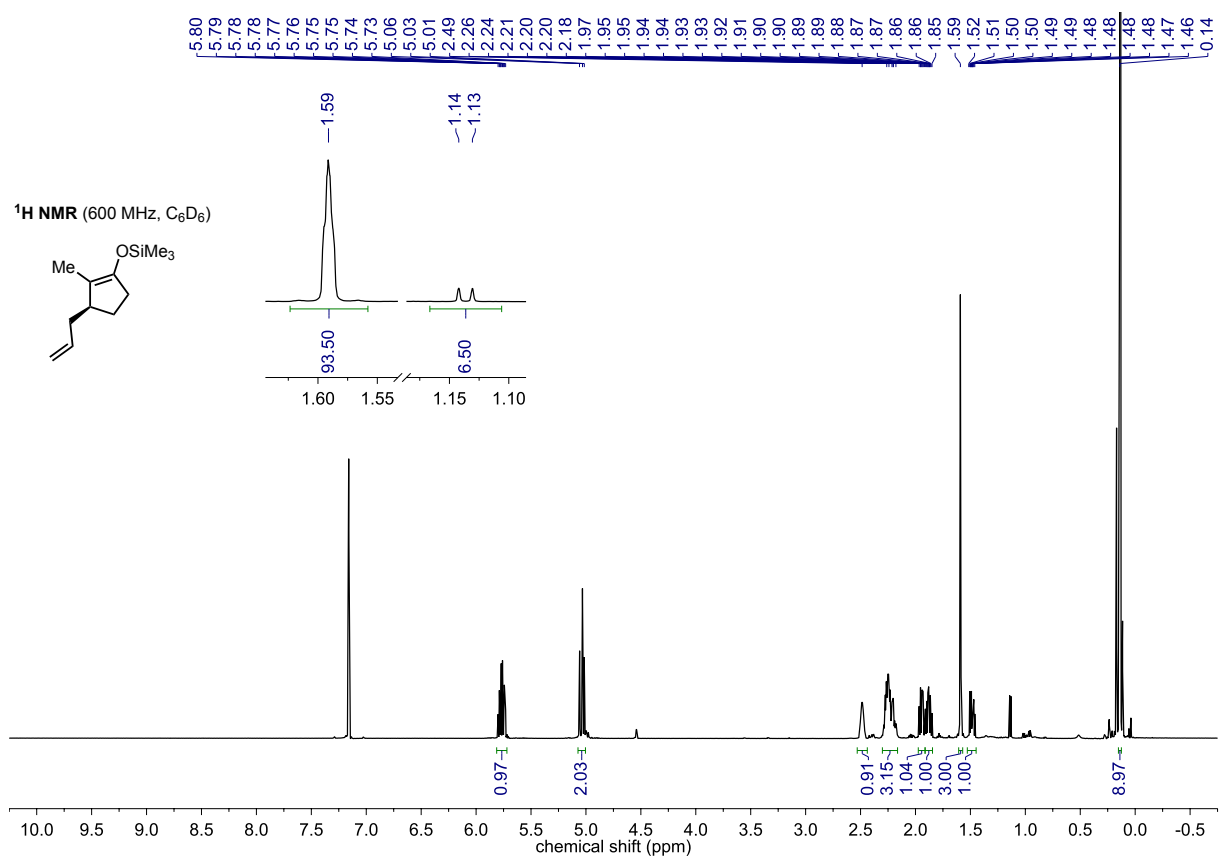
## Alcohol (S)-S-2



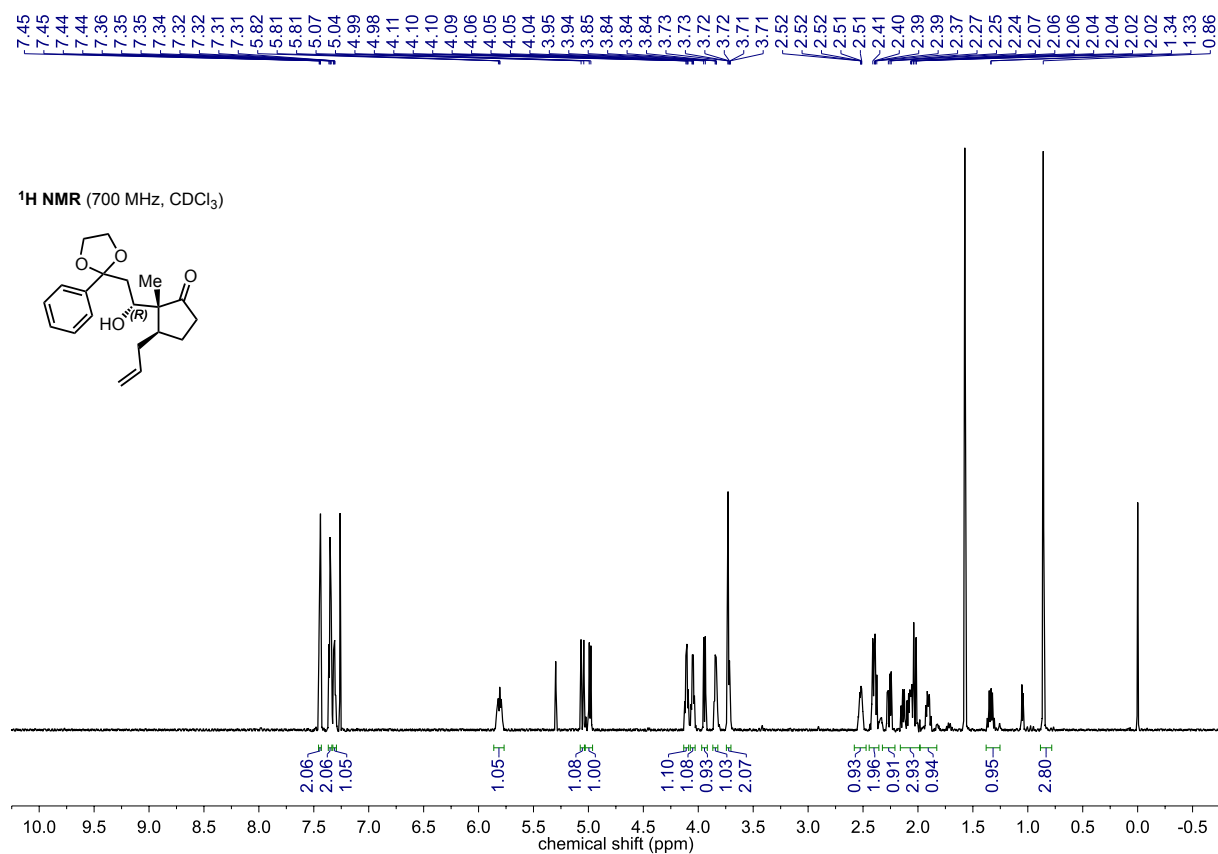
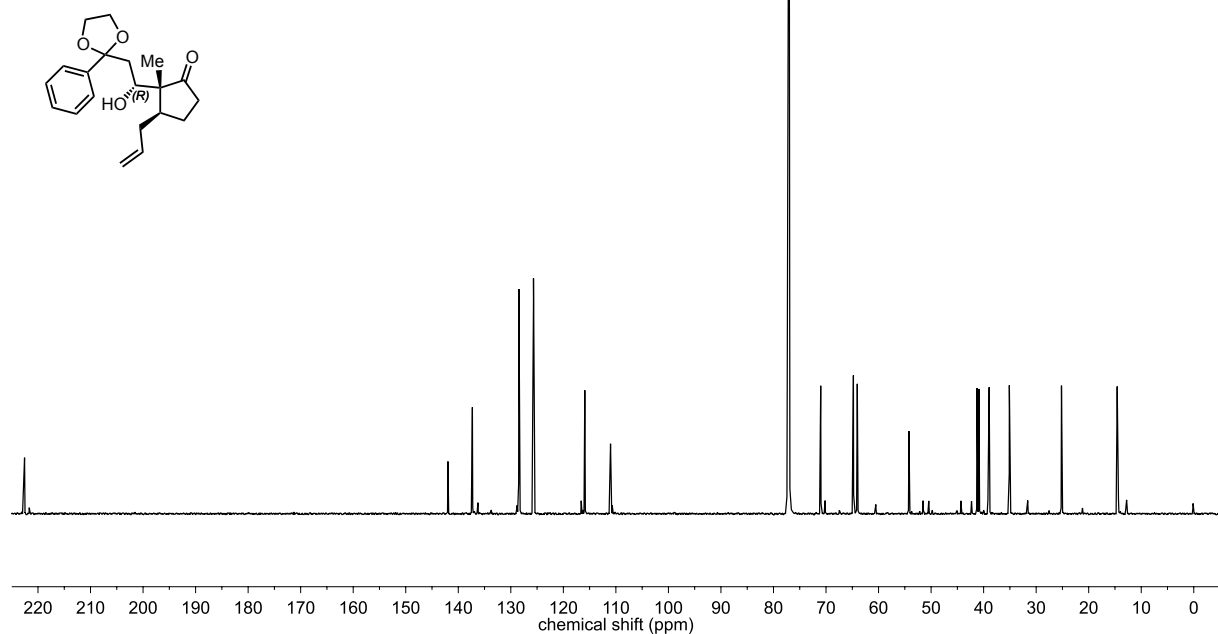
## Ketone 5





Silyl enol ether **6**

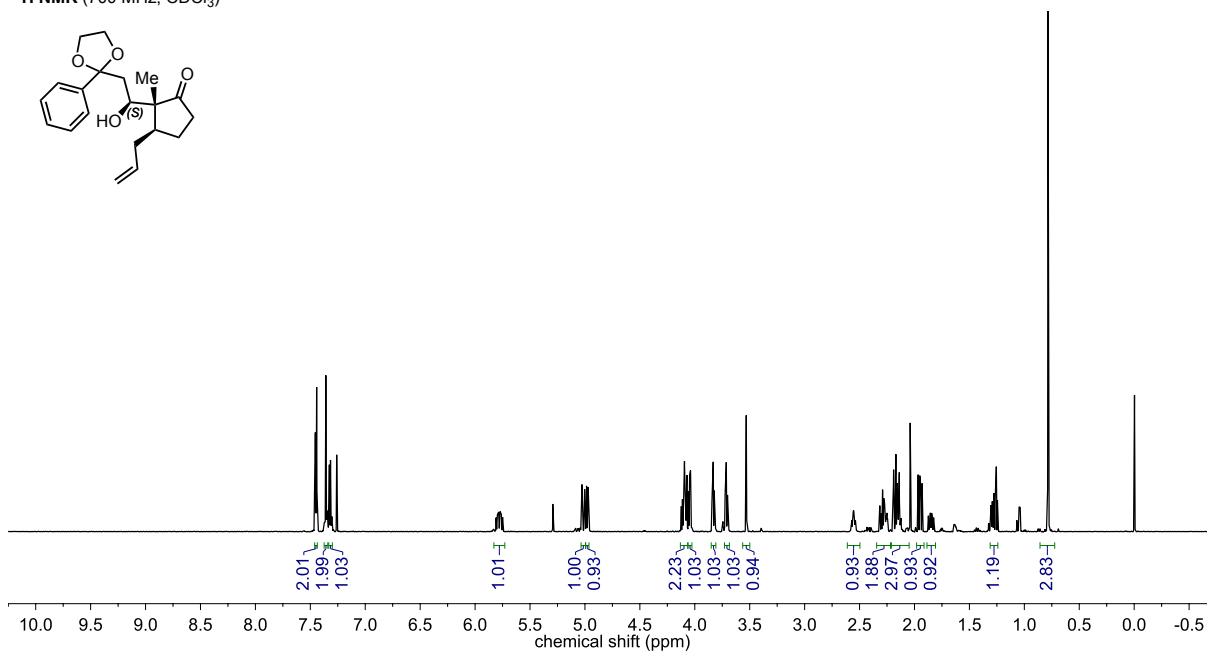
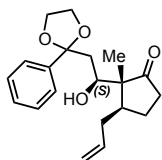
## Acetal (10R)-8

<sup>13</sup>C NMR (176 MHz, CDCl<sub>3</sub>)

## Acetal (10S)-8

7.46  
7.45  
7.44  
7.44  
7.44  
7.37  
7.37  
7.36  
7.36  
7.35  
7.35  
7.33  
7.32  
7.32  
5.03  
5.03  
5.00  
5.00  
4.99  
4.98  
4.97  
4.10  
4.10  
4.09  
4.09  
4.09  
4.09  
4.08  
4.08  
4.07  
4.07  
4.05  
4.05  
4.04  
4.04  
3.83  
3.82  
3.82  
3.72  
3.71  
3.70  
3.53  
3.53  
2.29  
2.19  
2.19  
2.19  
2.17  
2.17  
2.17  
2.16  
2.16  
2.14  
2.14  
1.95  
1.95  
1.93  
1.93  
1.25  
1.25  
0.78

<sup>1</sup>H NMR (700 MHz, CDCl<sub>3</sub>)

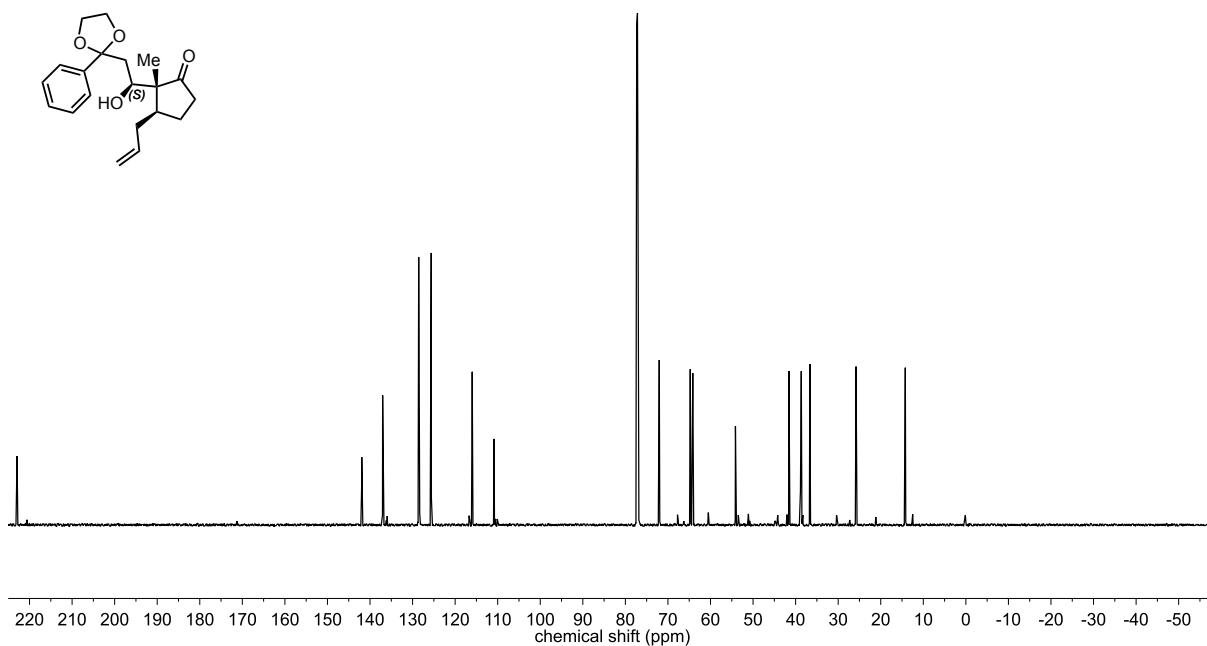
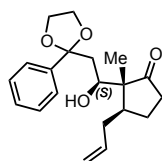


-222.93

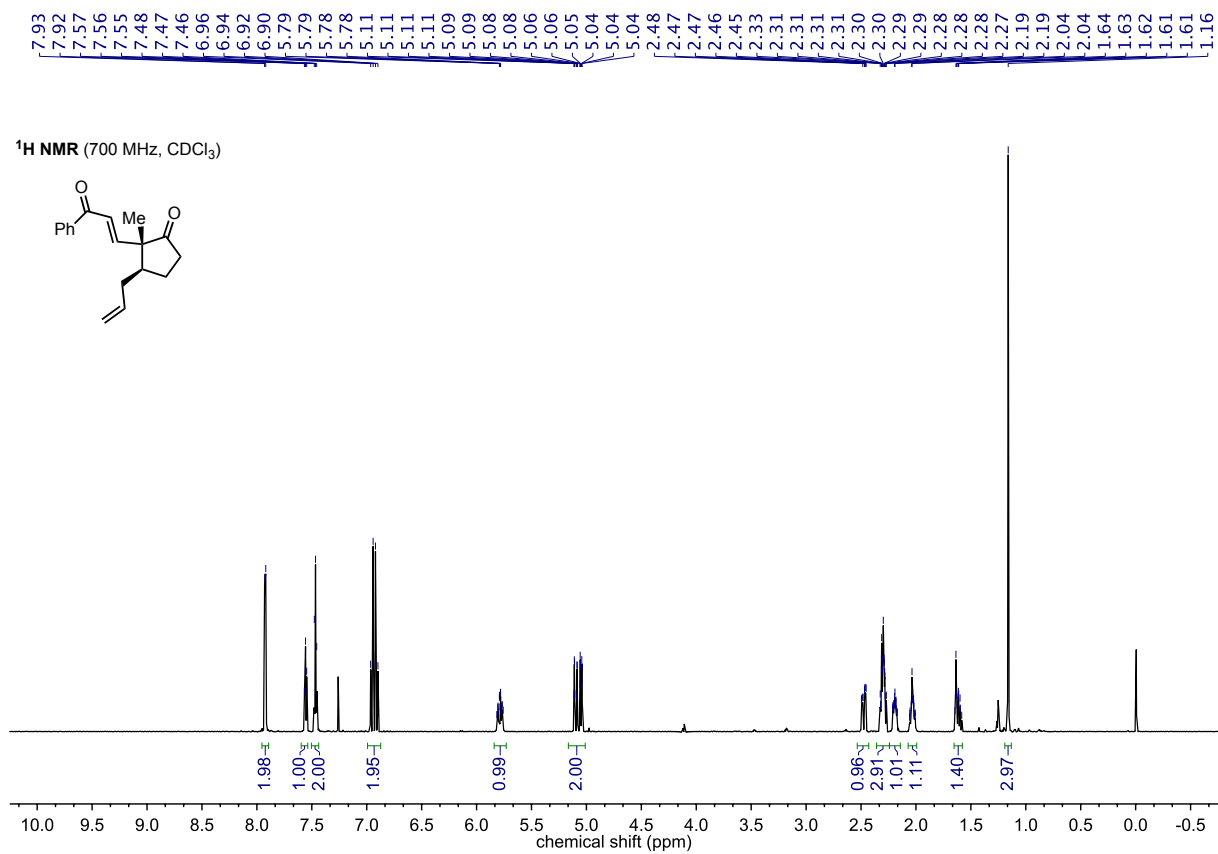
141.94  
137.04  
128.56  
128.44  
125.61  
115.98  
110.84

72.04  
64.75  
64.16  
54.14  
41.58  
38.85  
38.67  
36.65  
25.80  
14.23

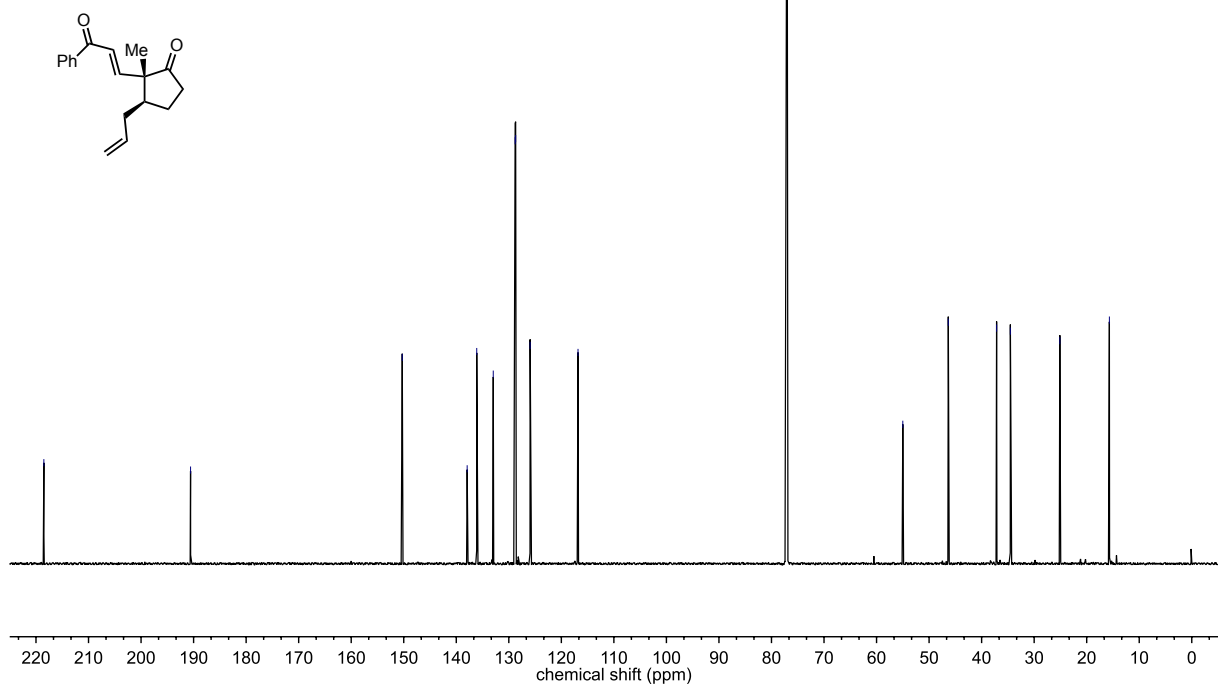
<sup>13</sup>C NMR (176 MHz, CDCl<sub>3</sub>)



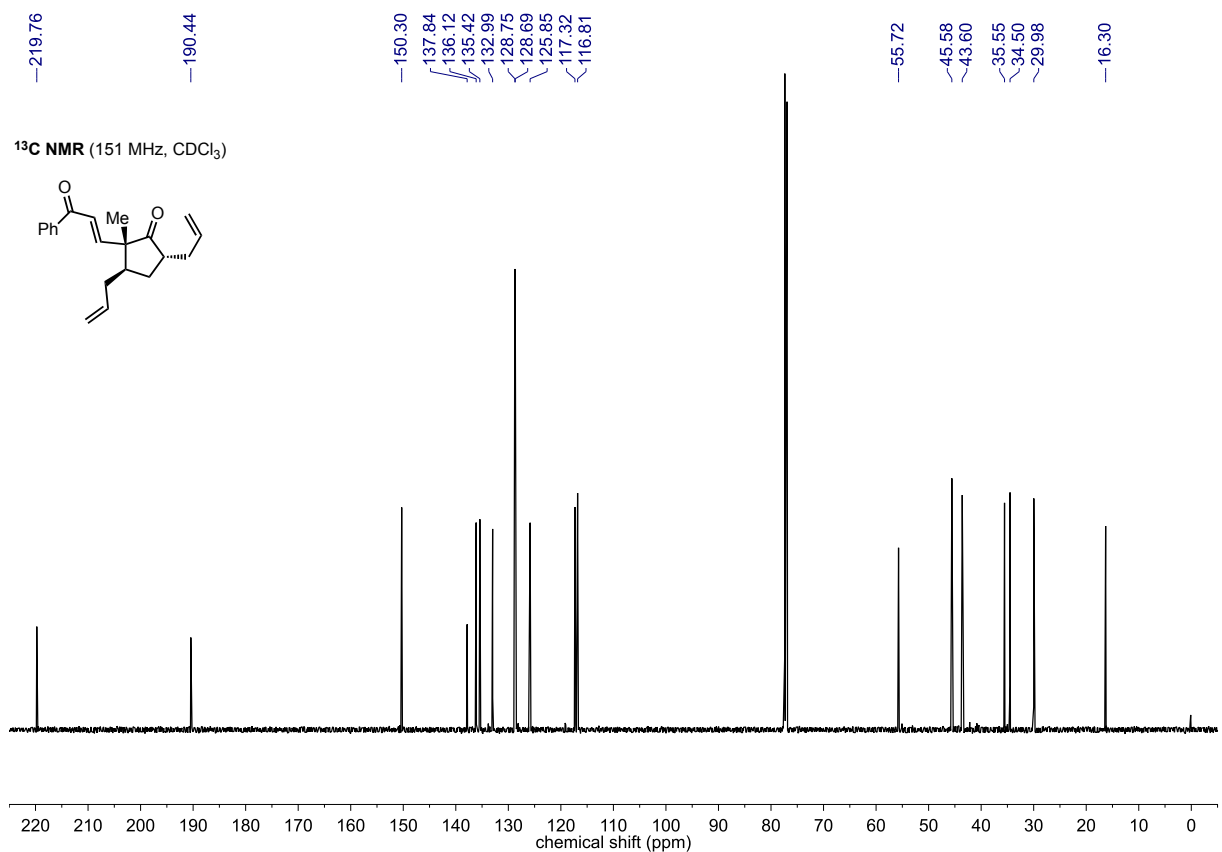
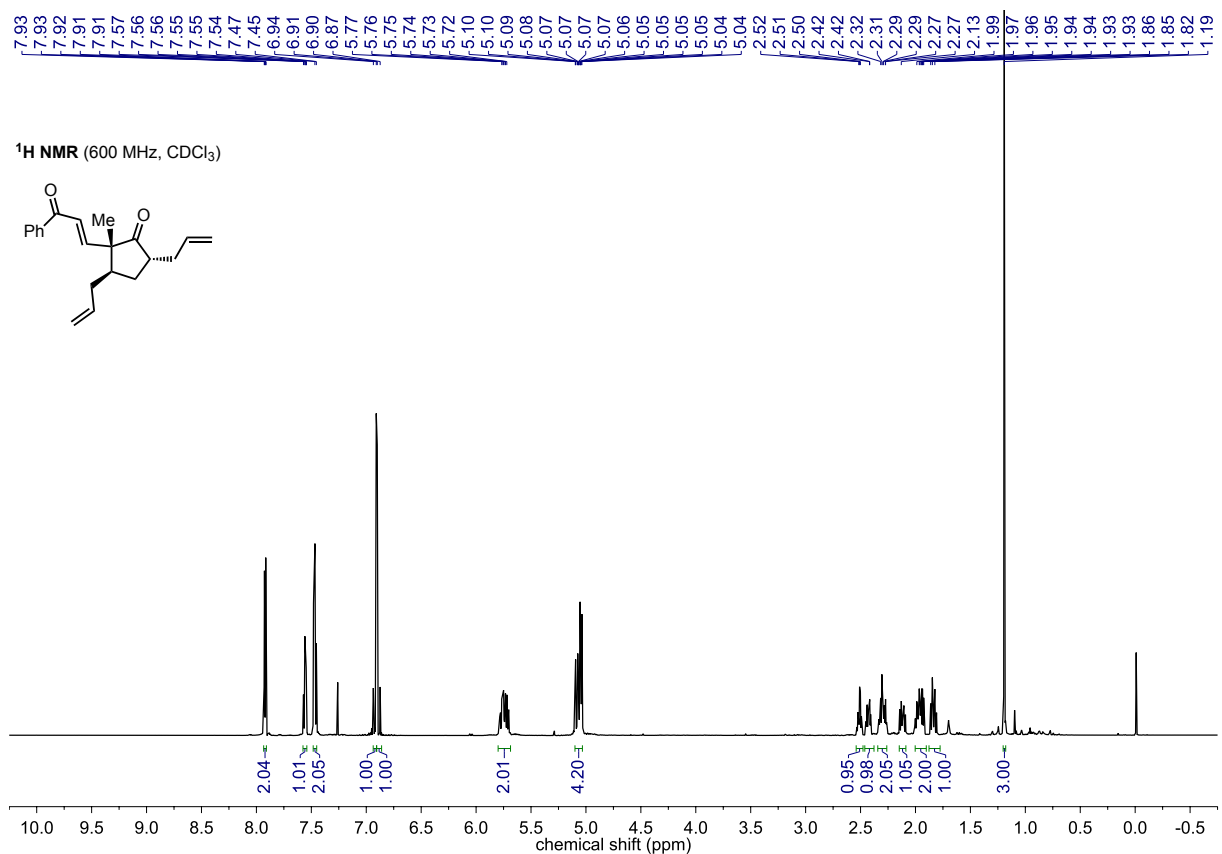
## Enone 9



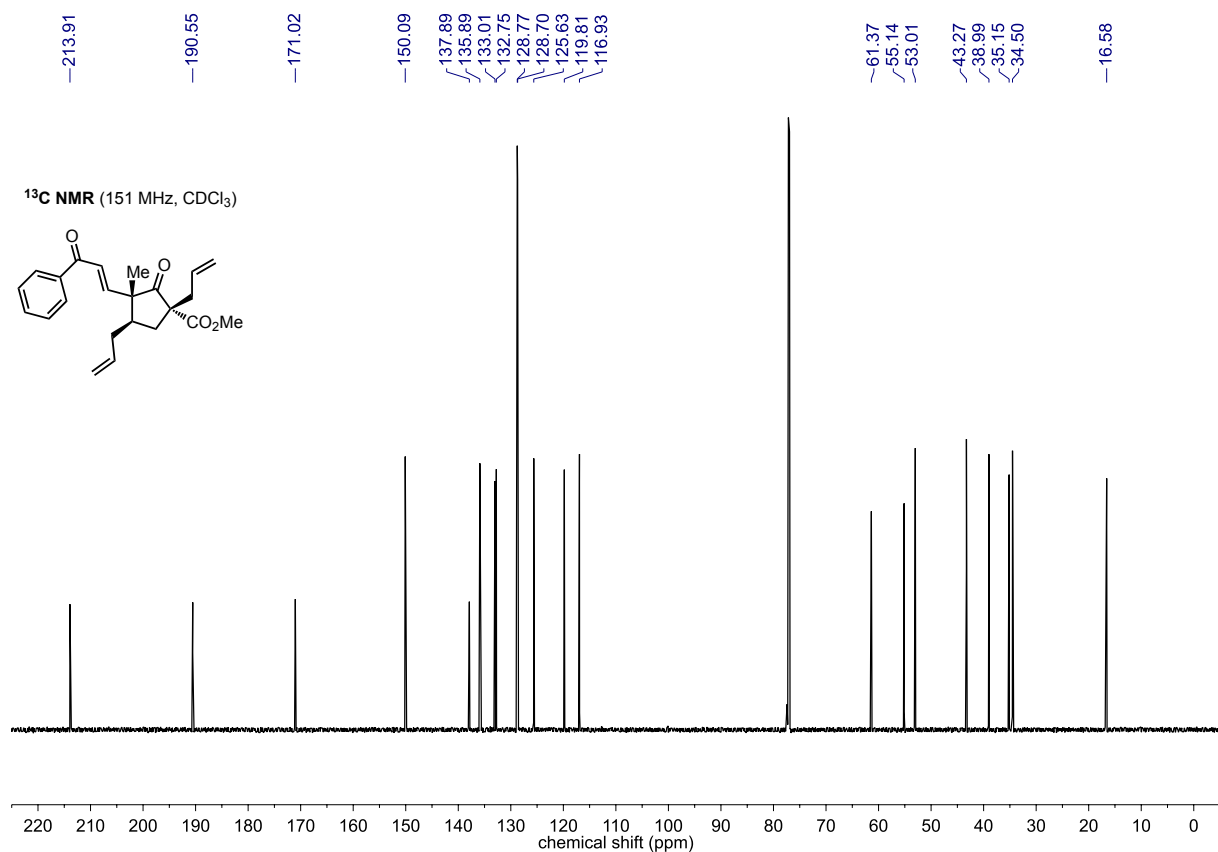
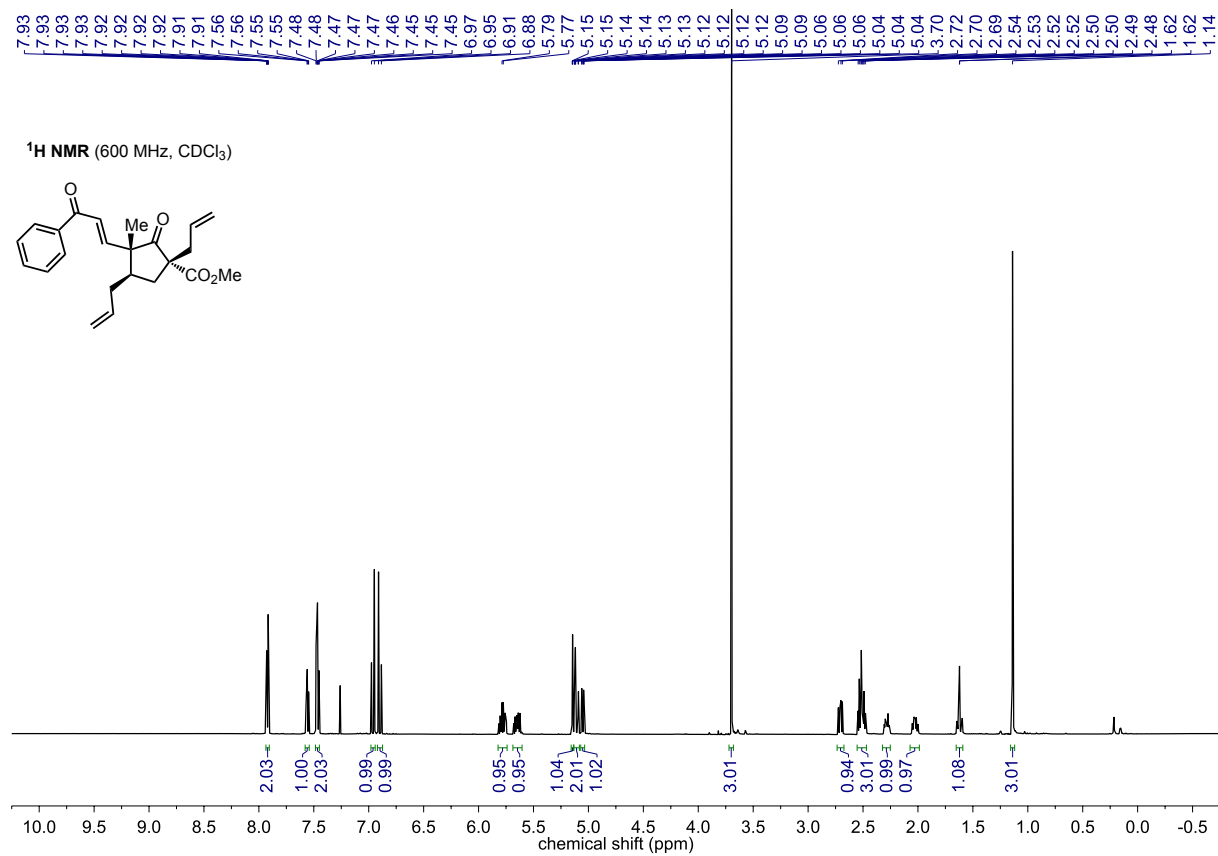
<sup>13</sup>C NMR (176 MHz, CDCl<sub>3</sub>)



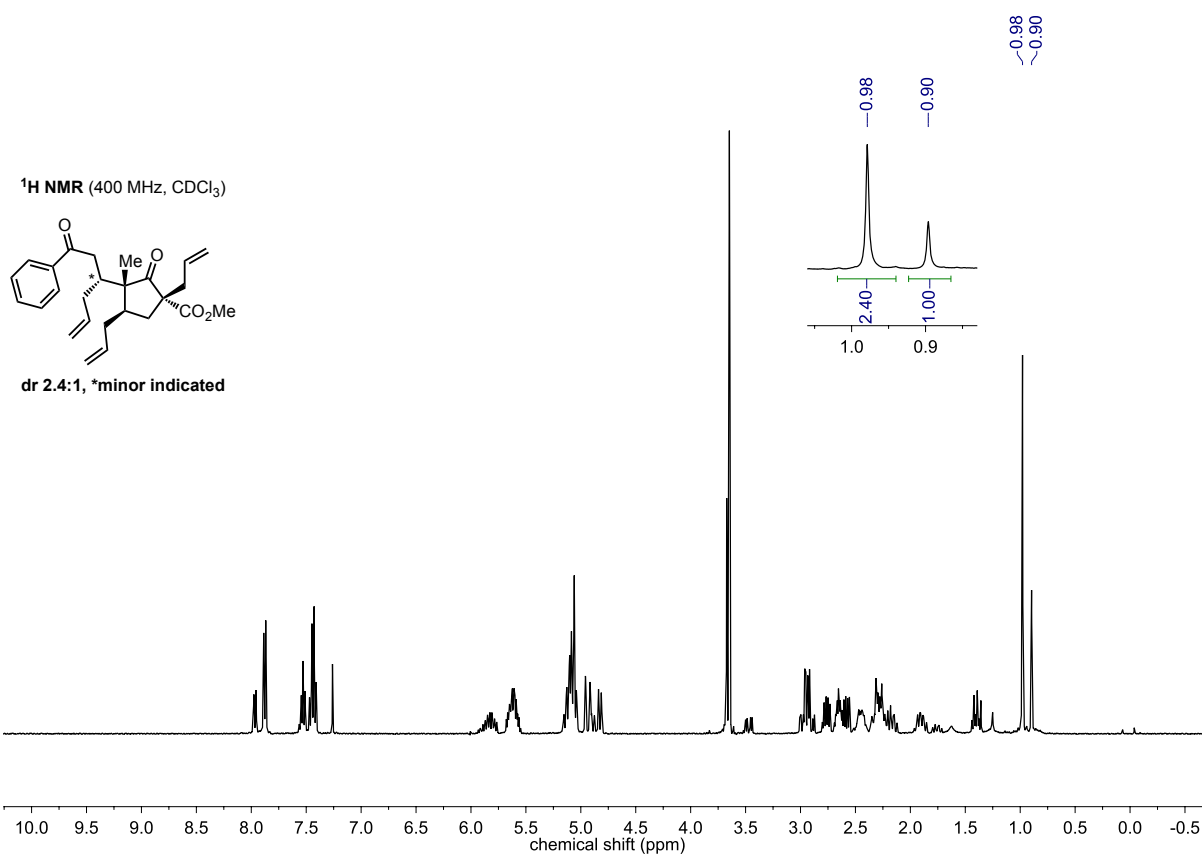
## Enone S-11



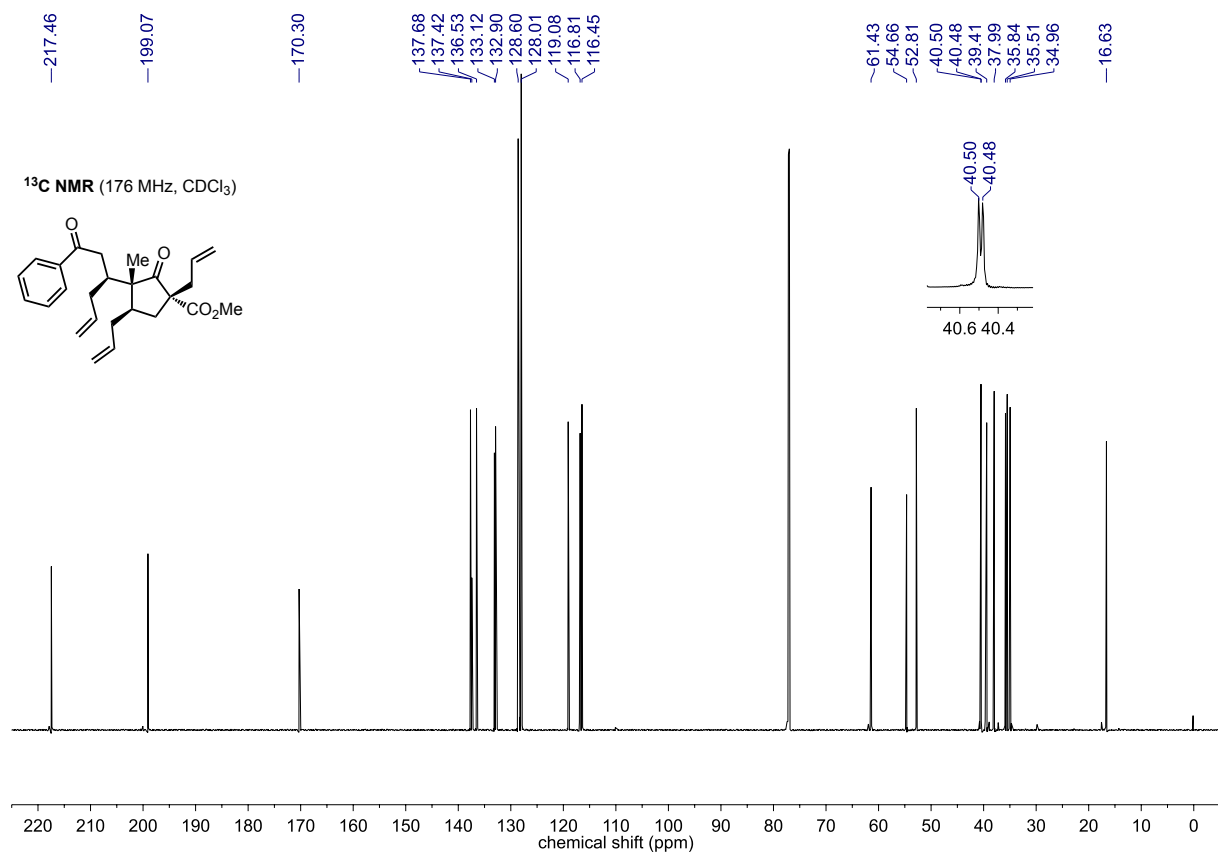
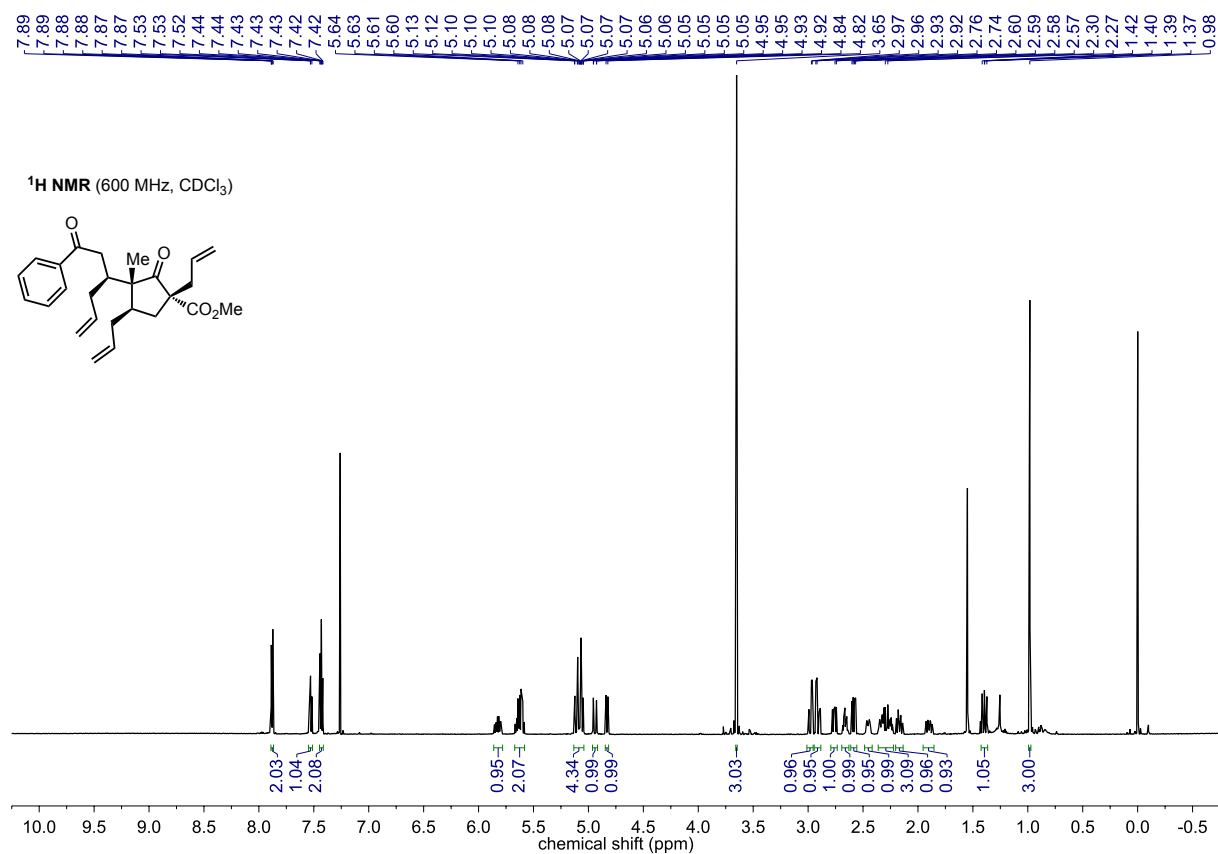
## Ester 10



## Ketones 11 and S-12

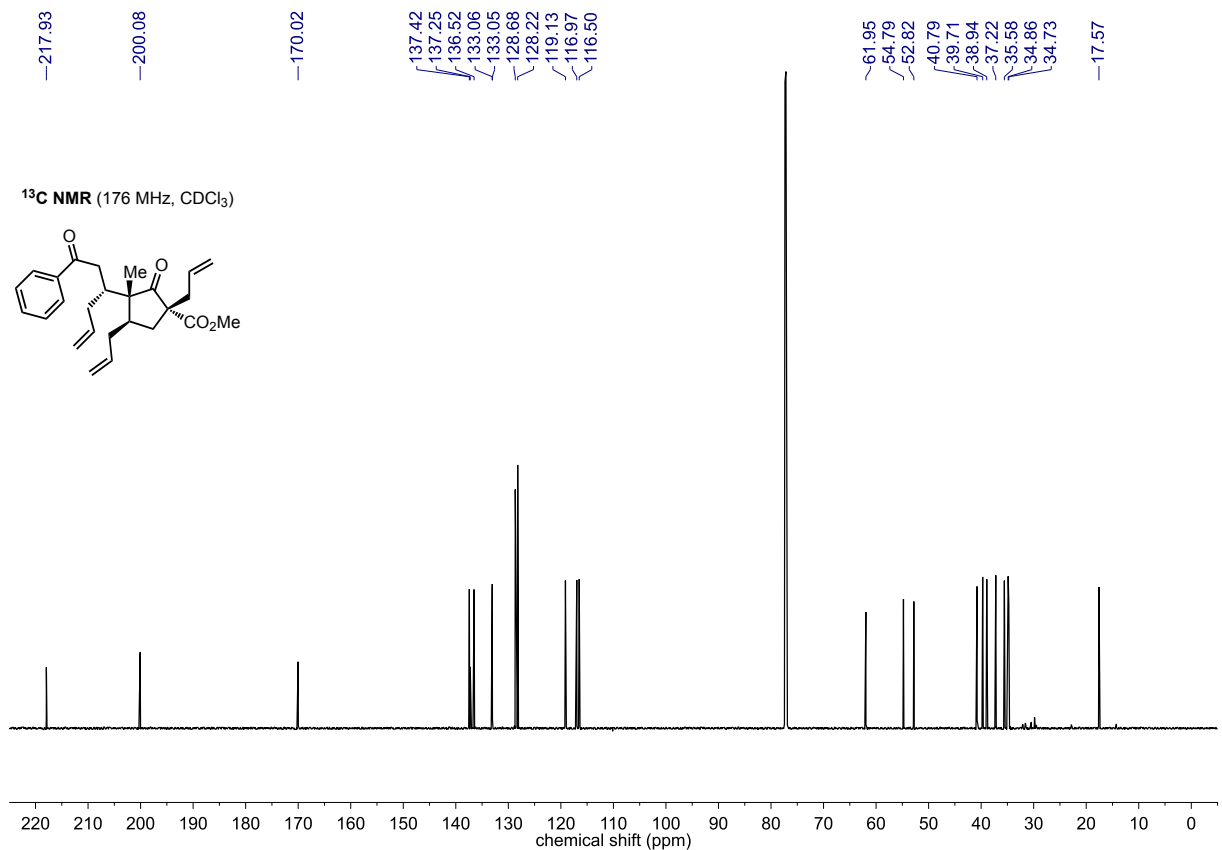
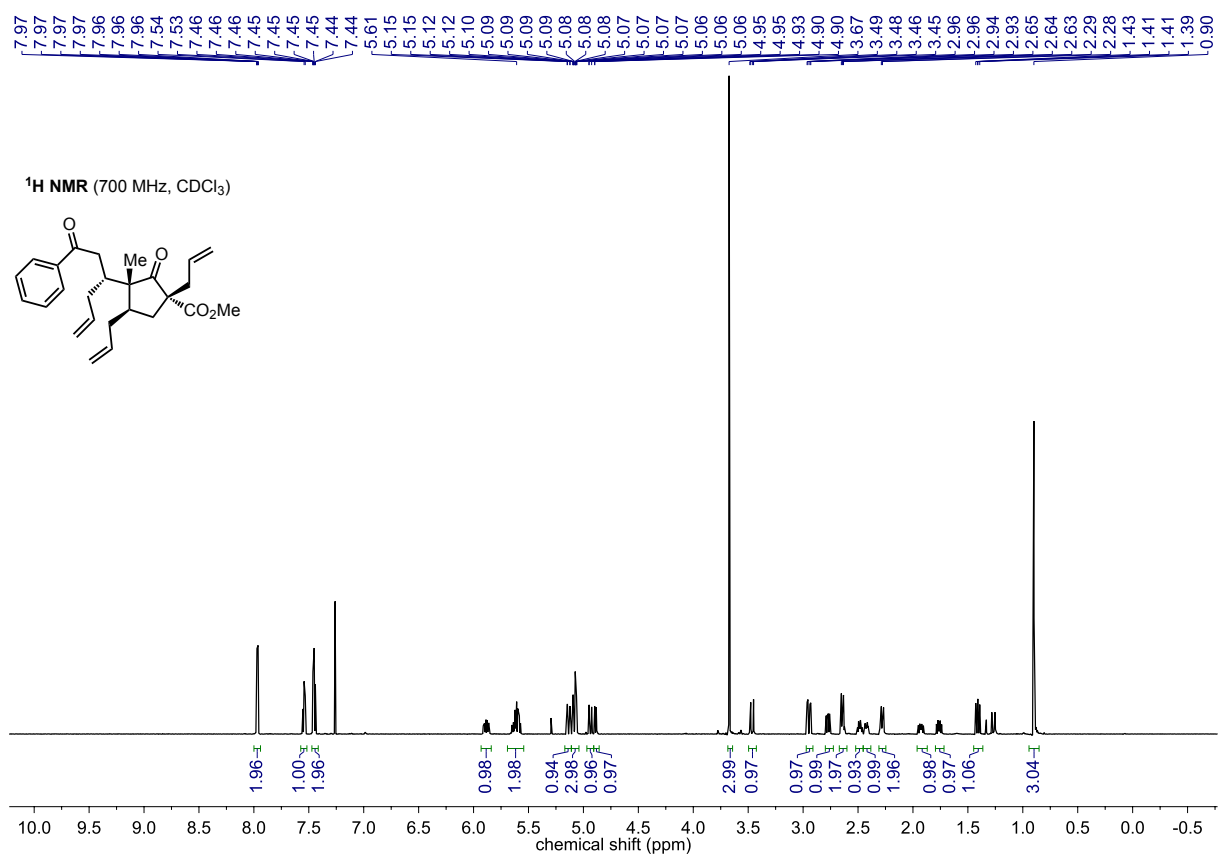


## Ketone S-12



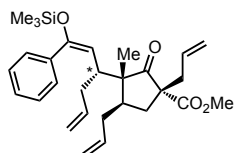


## Ketone 11

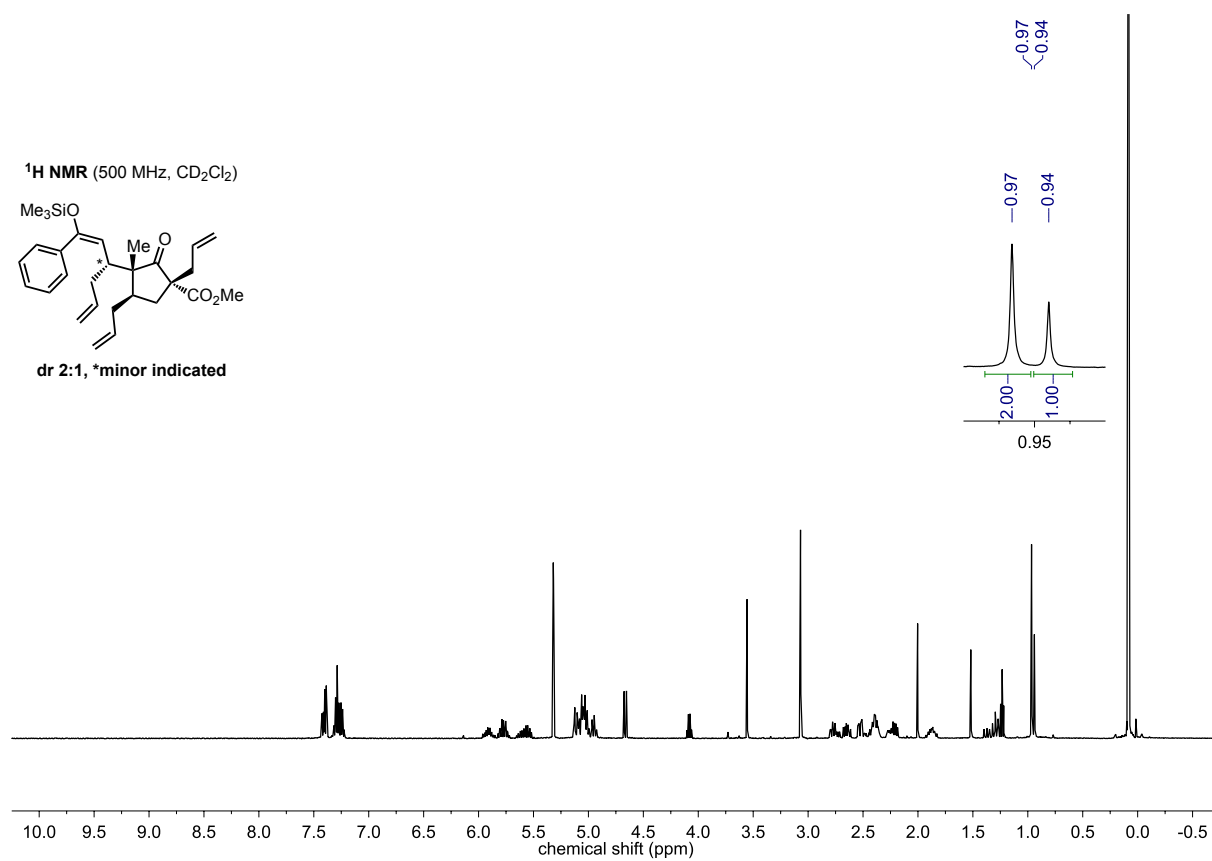


## Silyl enol ethers 12 und S-13

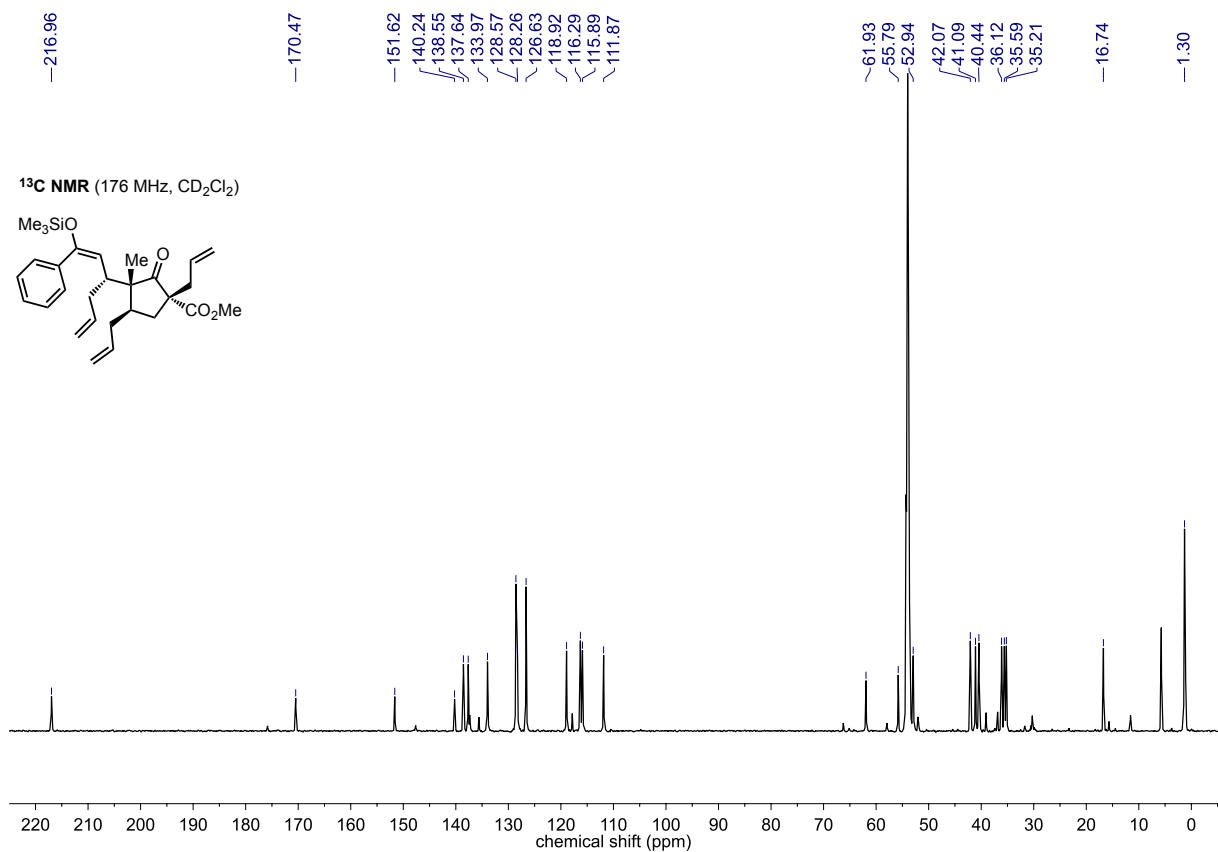
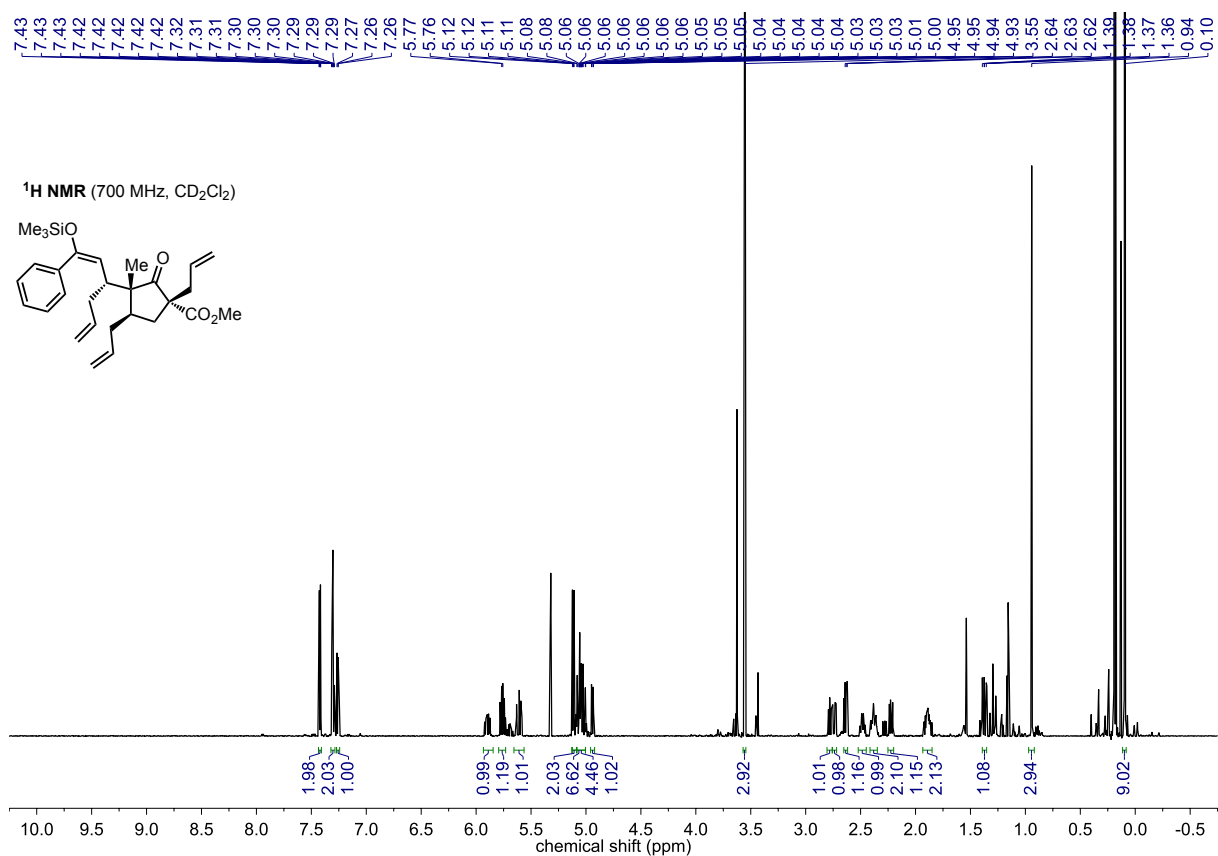
<sup>1</sup>H NMR (500 MHz, CD<sub>2</sub>Cl<sub>2</sub>)



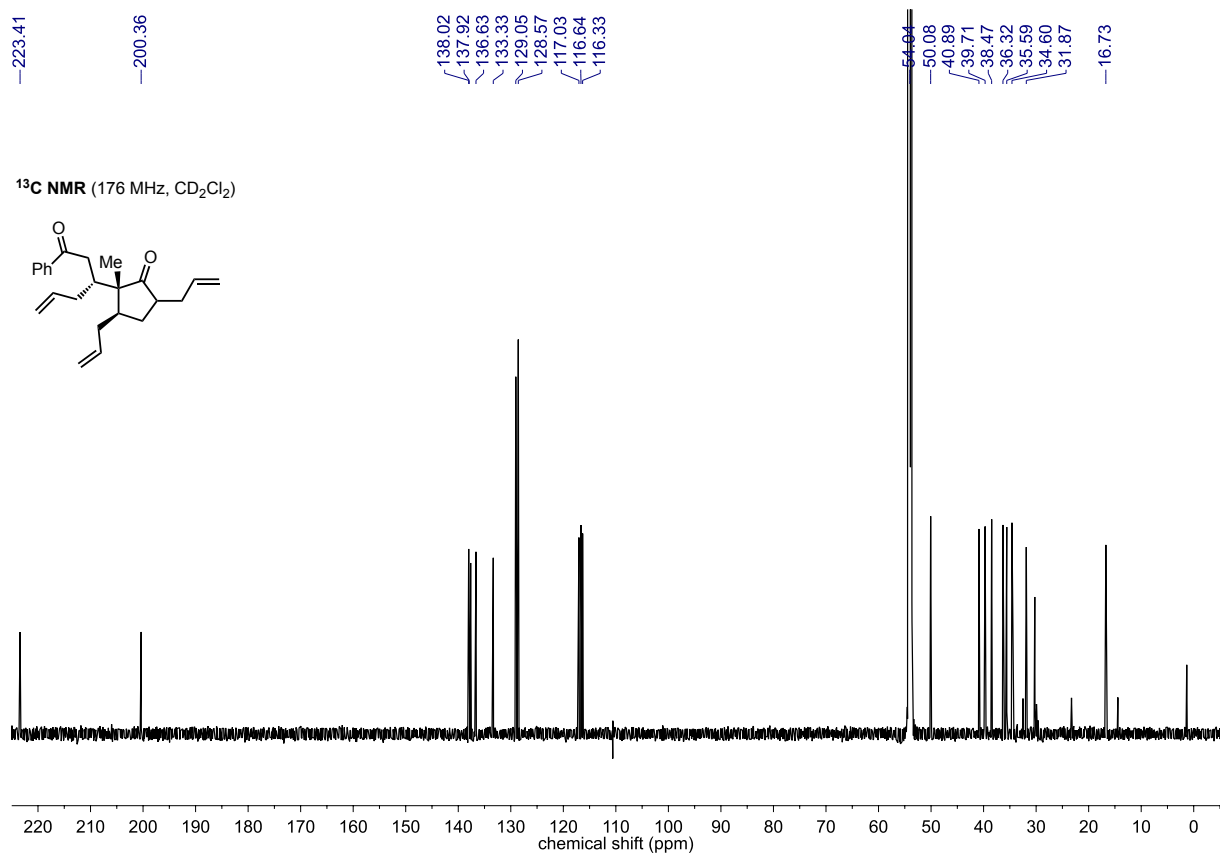
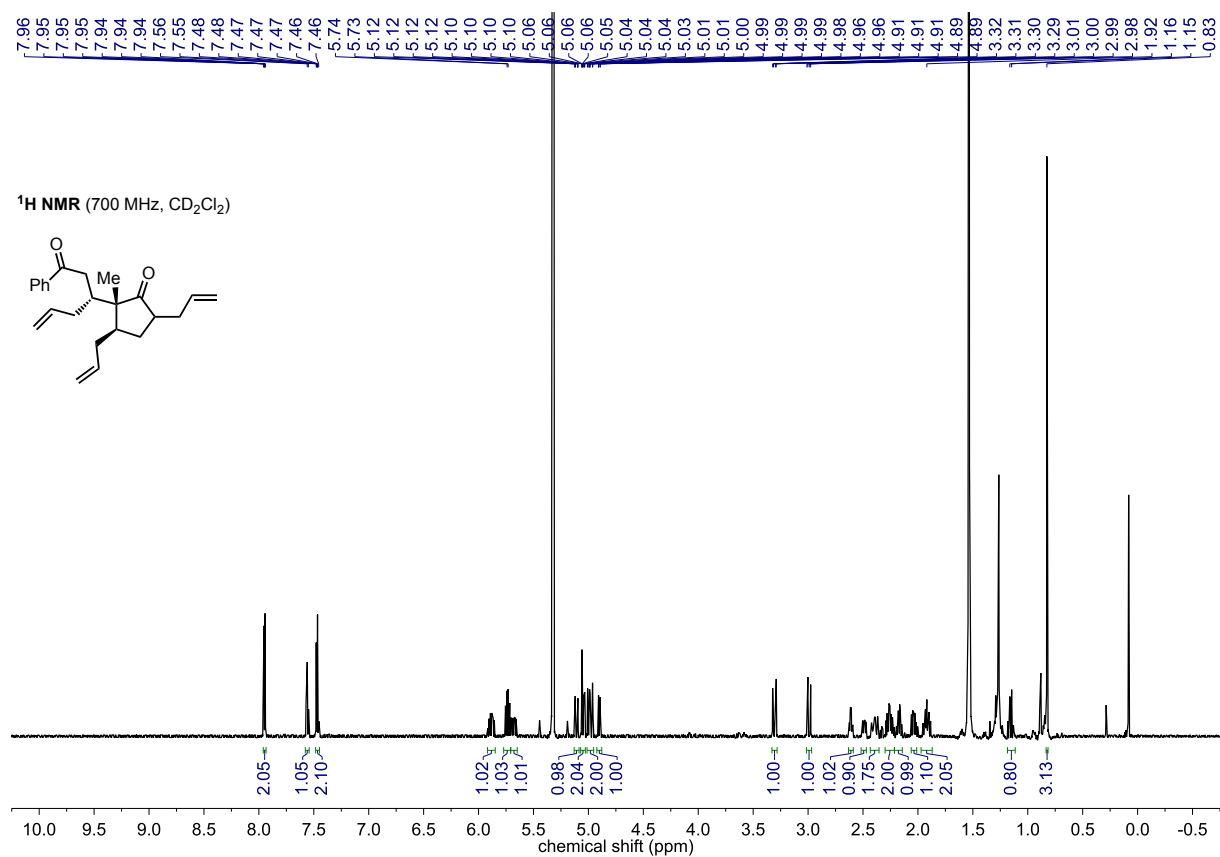
dr 2:1, \*minor indicated



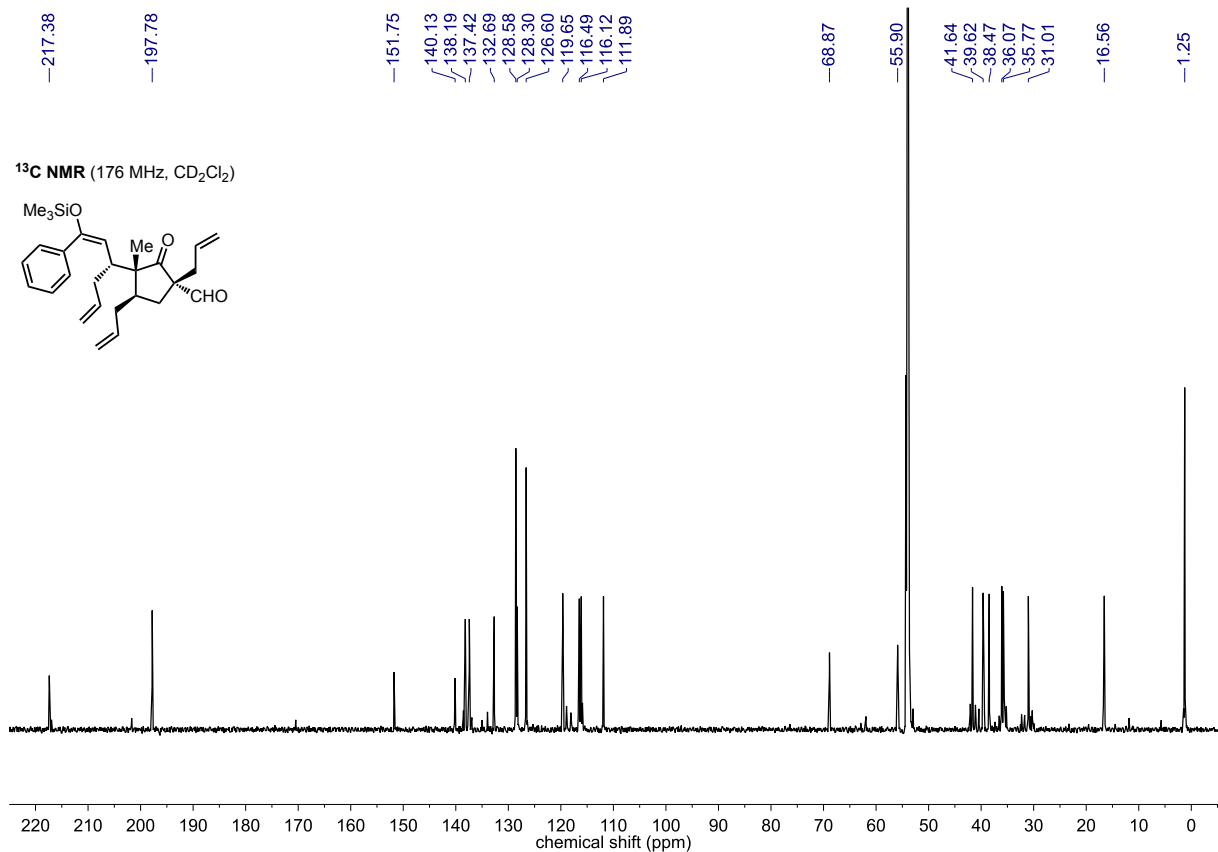
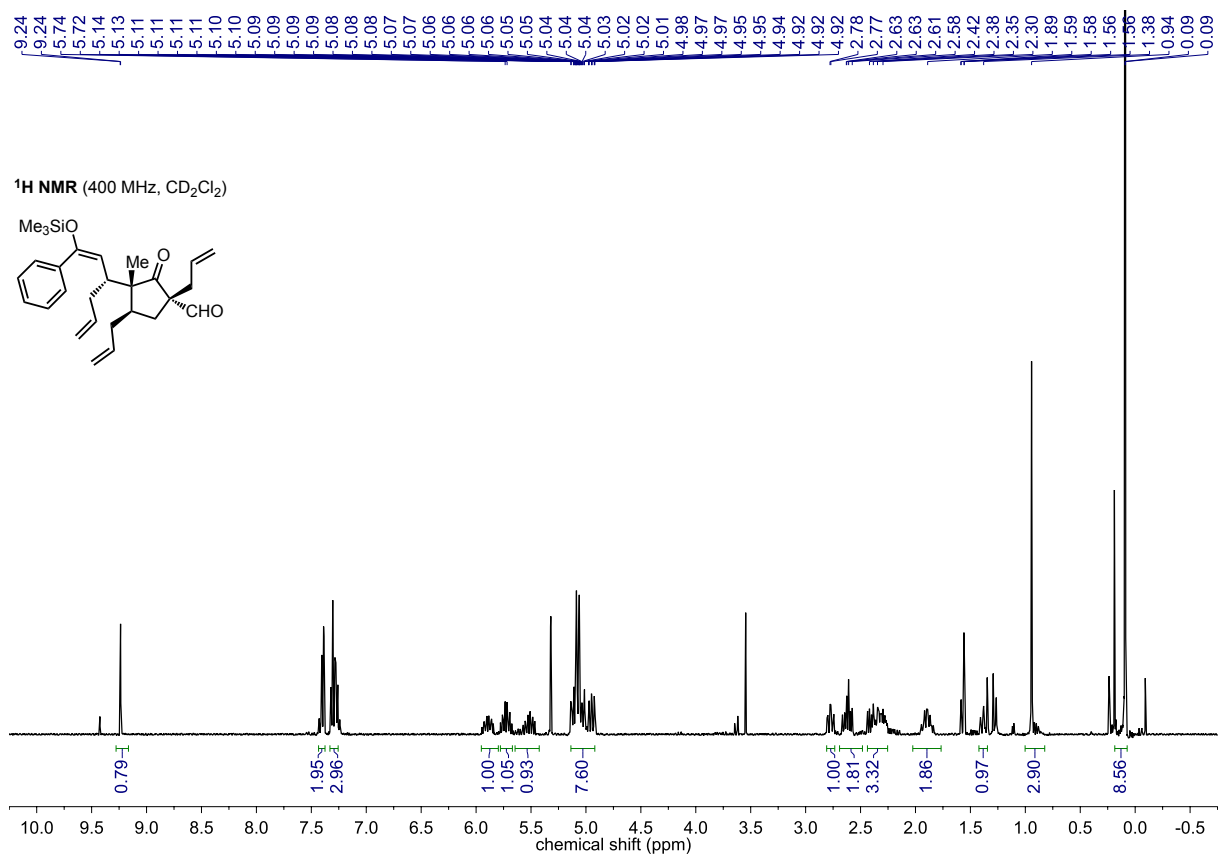
## Silyl enol ether 12



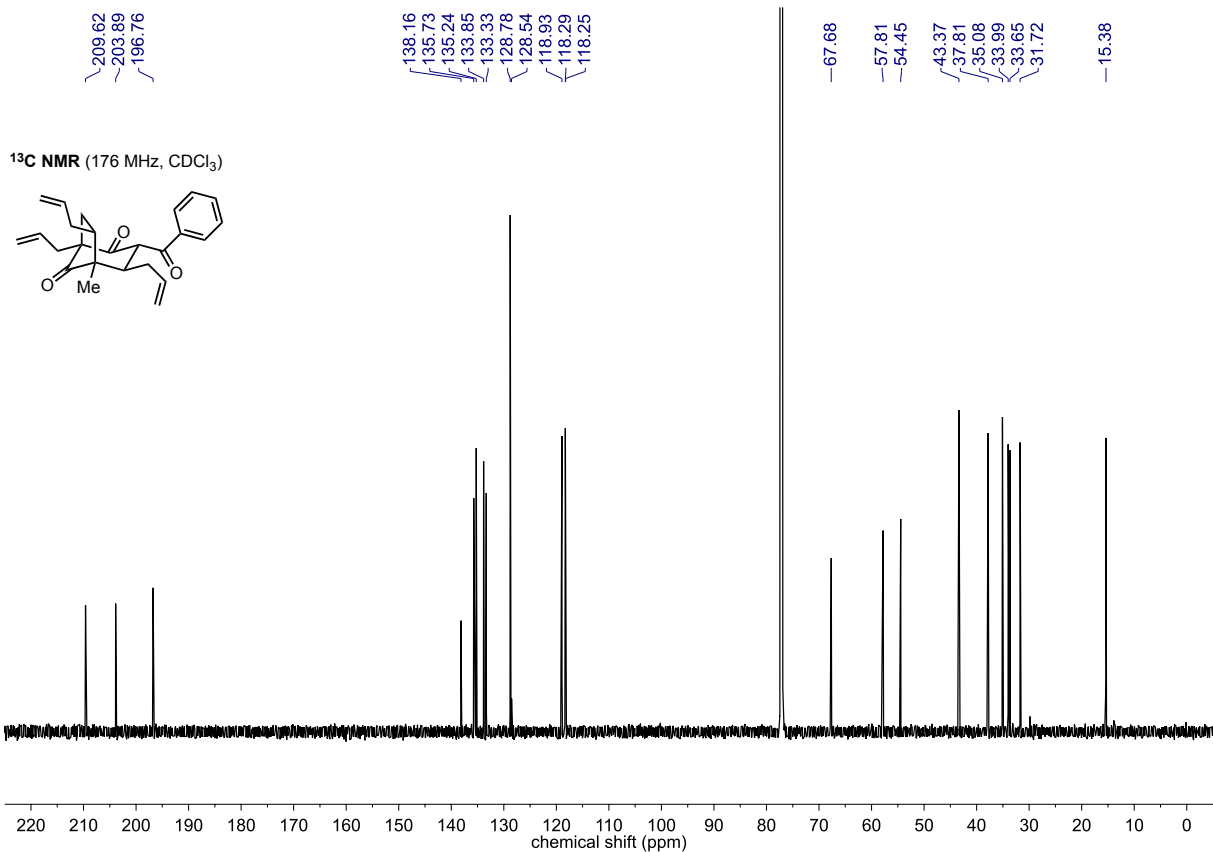
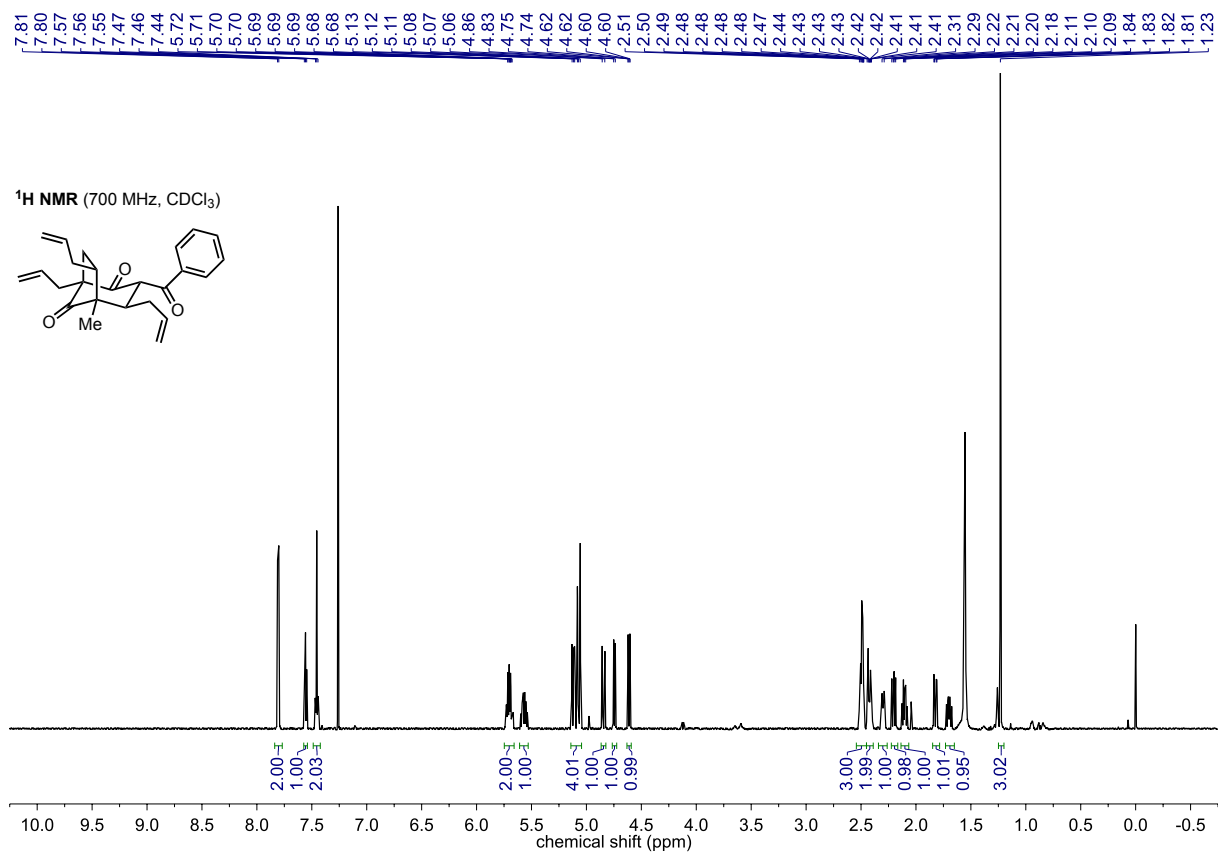
## Decarboxylation Product rac-13



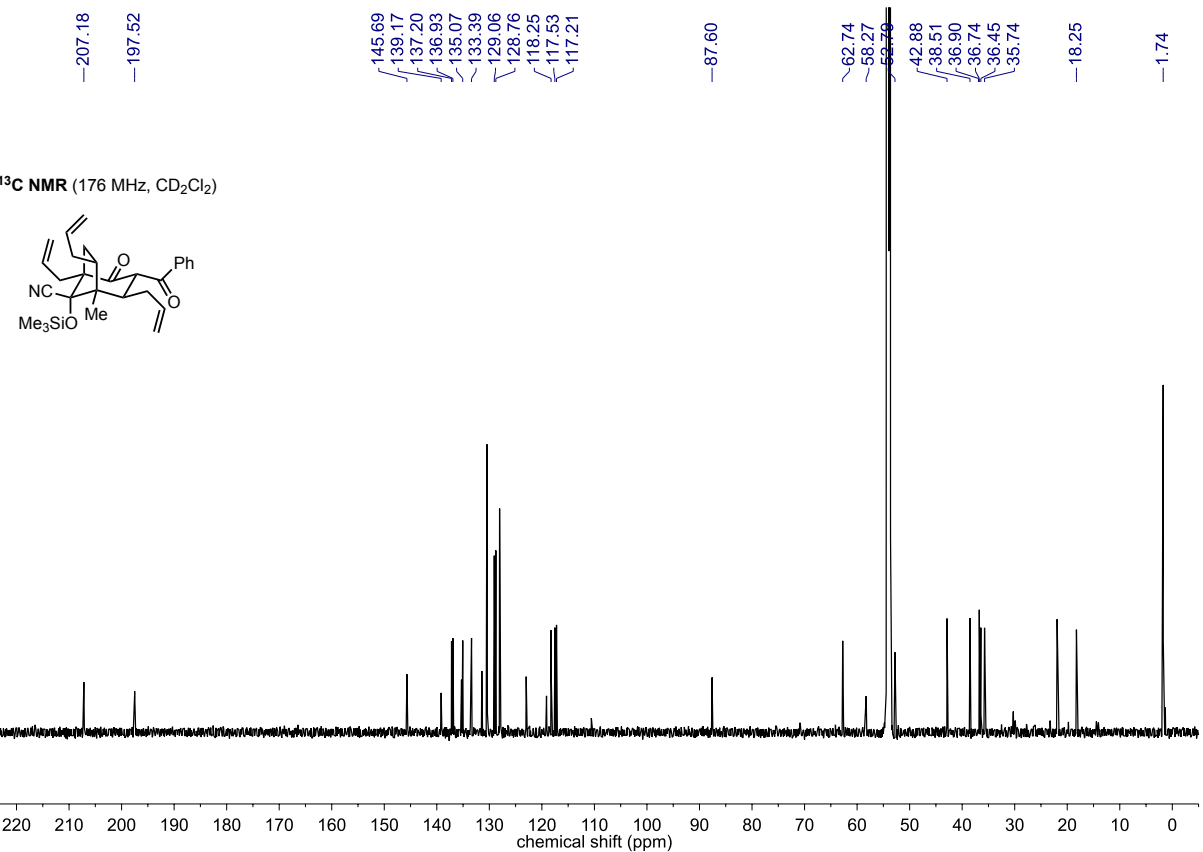
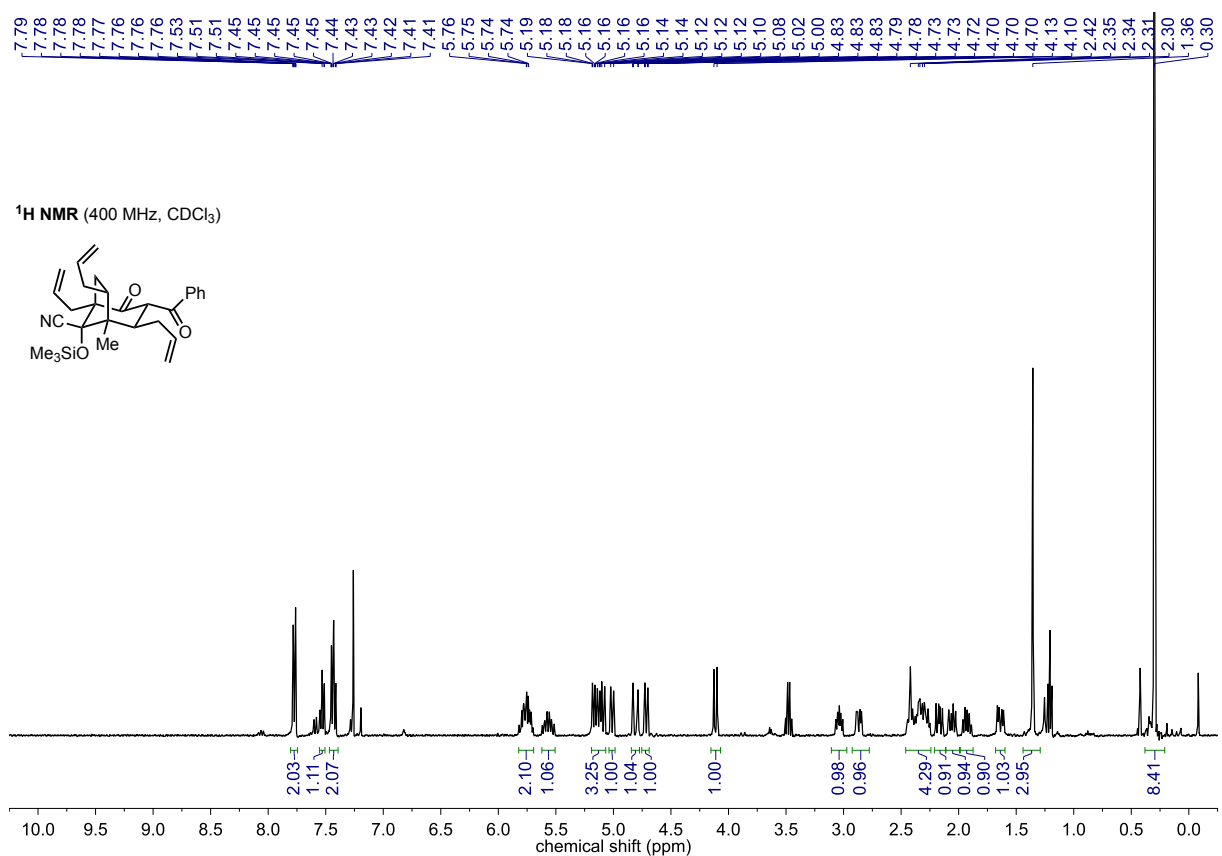
## Aldehyde S-14



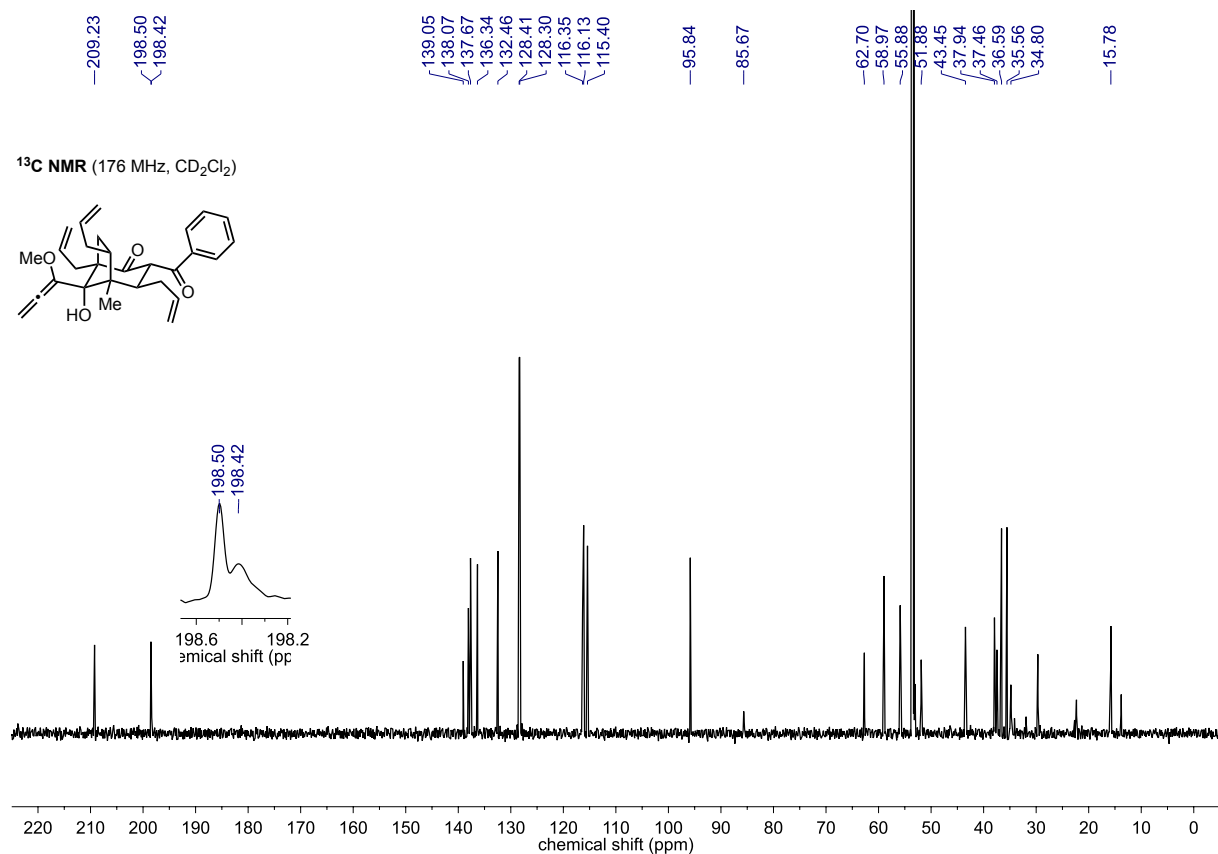
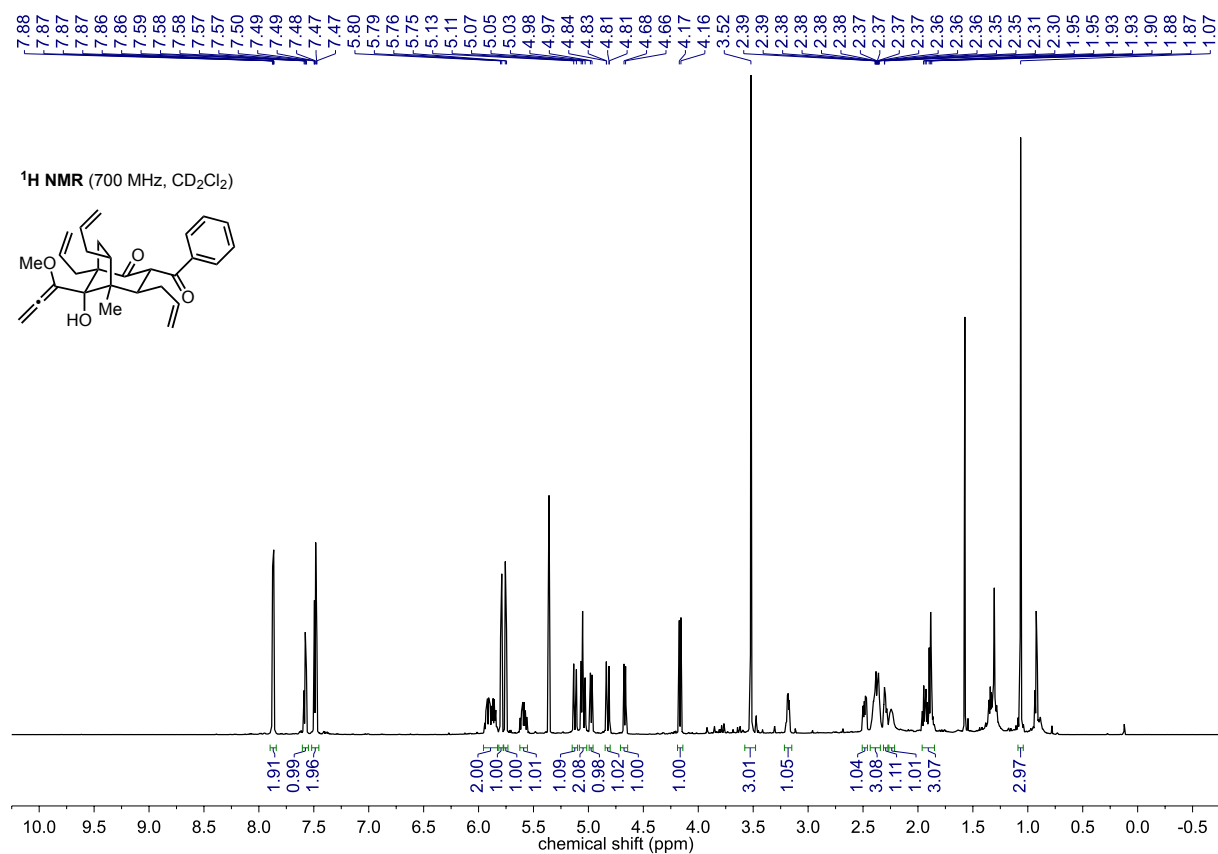
## Triketone 4



## Cyanhydrin rac-14



## Methoxyallene 15

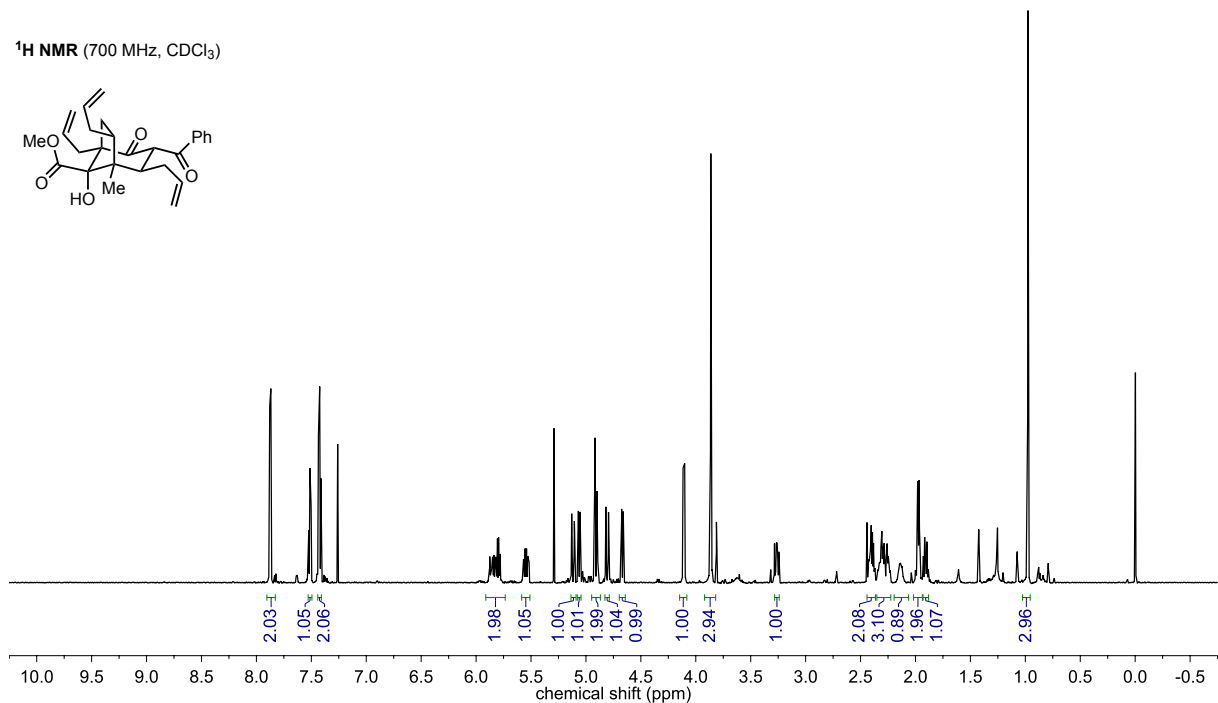
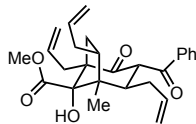




## Ester 16

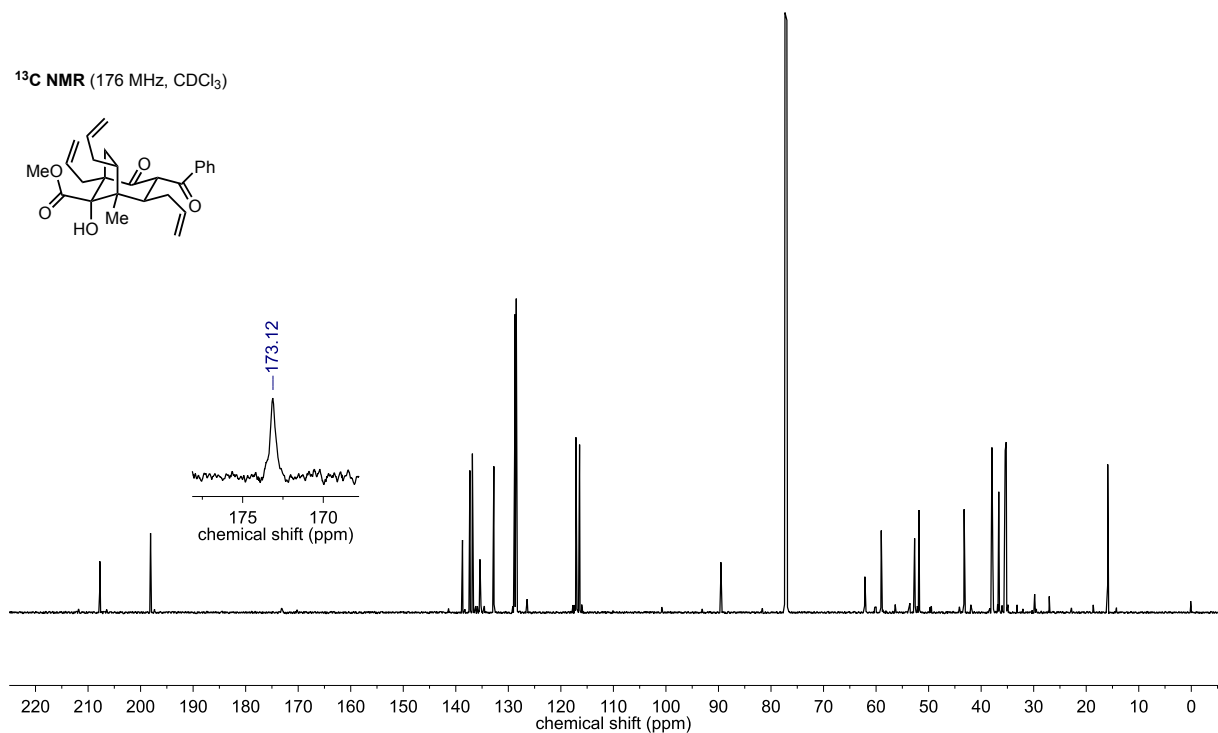
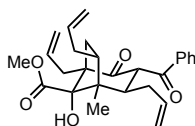
7.88  
7.88  
7.87  
7.87  
7.52  
7.51  
7.50  
7.44  
7.43  
7.42  
7.42  
7.42  
7.41  
5.81  
5.80  
5.13  
5.13  
5.11  
5.10  
5.07  
5.07  
5.07  
5.05  
5.05  
5.05  
4.92  
4.92  
4.92  
4.92  
4.90  
4.90  
4.90  
4.89  
4.89  
4.89  
4.82  
4.82  
4.79  
4.79  
4.67  
4.66  
4.12  
4.10  
3.86  
2.39  
2.31  
2.30  
2.30  
1.98  
1.98  
1.97  
1.96  
1.92  
0.98

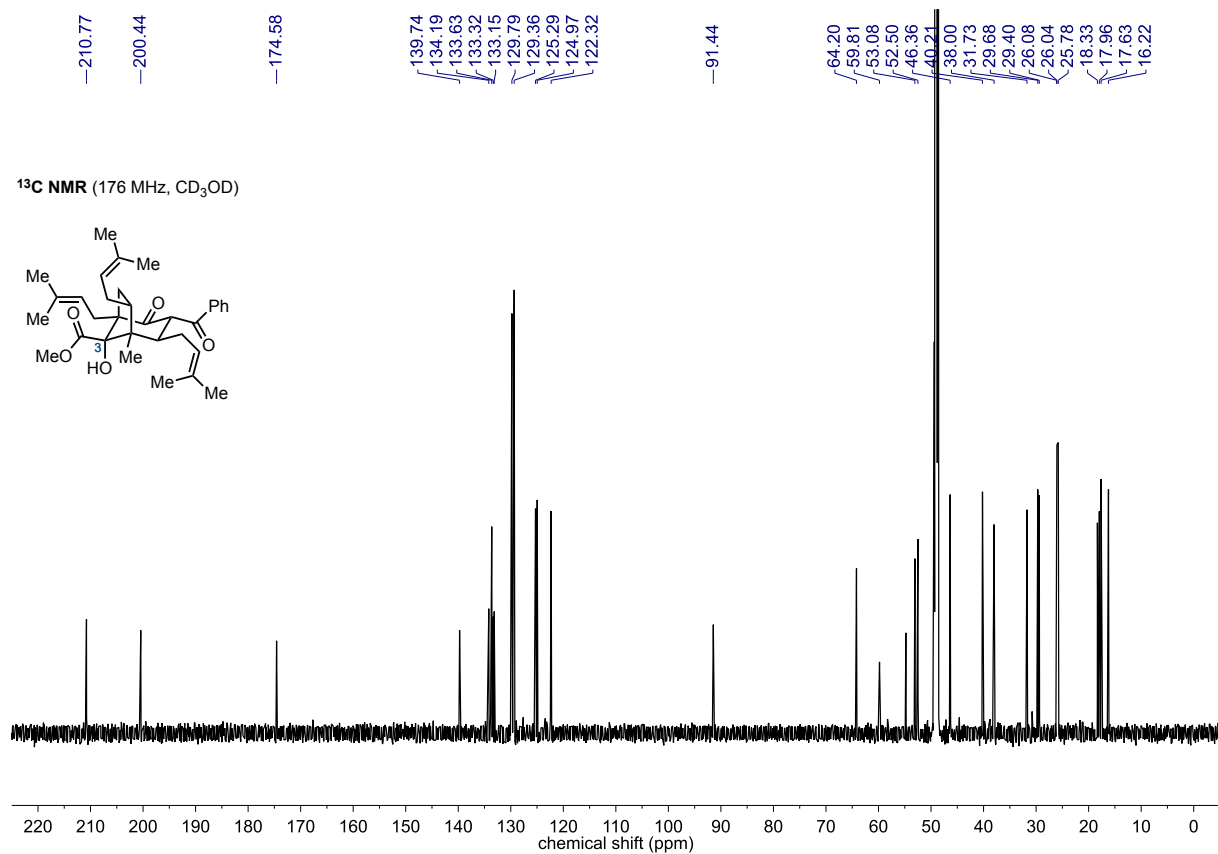
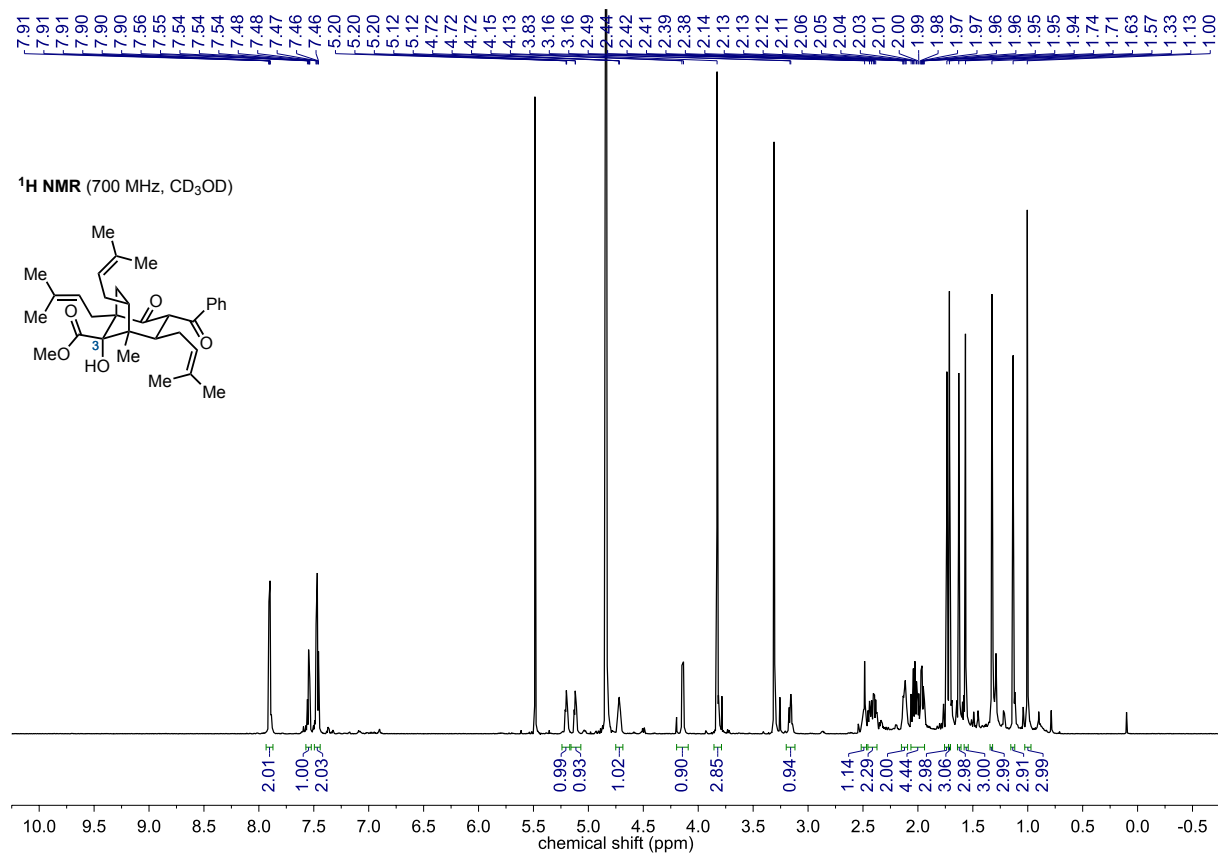
<sup>1</sup>H NMR (700 MHz, CDCl<sub>3</sub>)



-207.75  
-198.10  
-173.12  
138.72  
137.32  
136.84  
135.40  
132.76  
128.77  
128.49  
117.13  
117.01  
116.44  
-89.55  
-62.13  
-59.01  
-52.66  
-51.83  
-43.24  
-37.95  
-37.76  
-36.65  
-35.43  
-35.23  
-15.90

<sup>13</sup>C NMR (176 MHz, CDCl<sub>3</sub>)



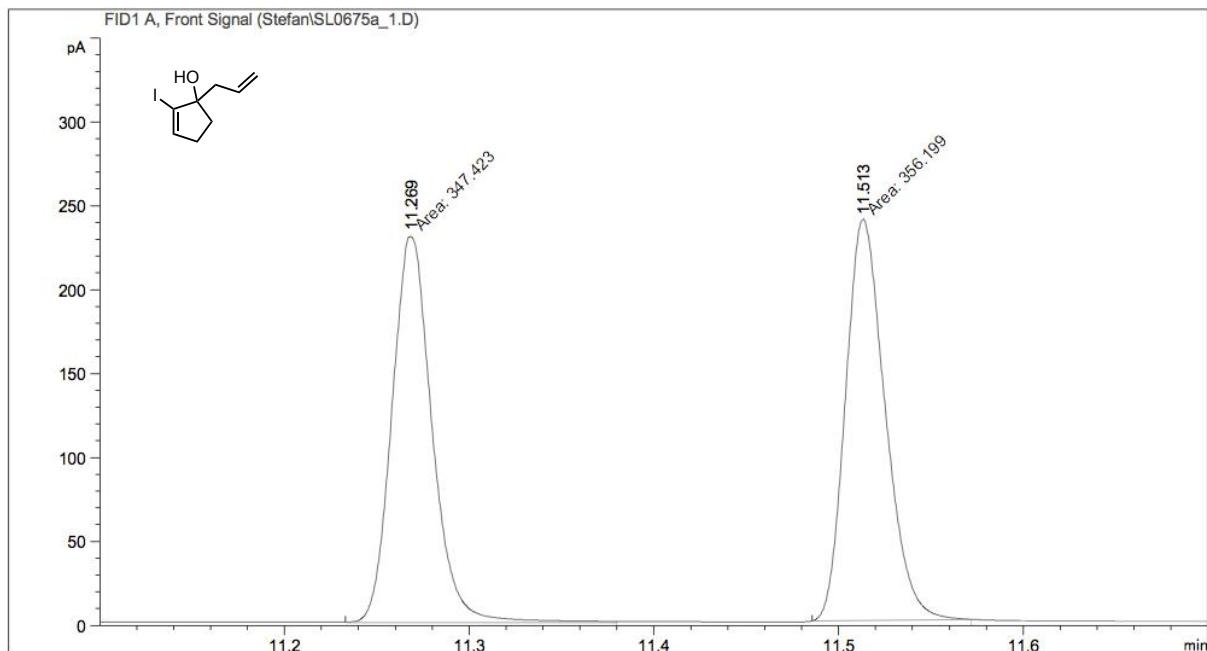
3-*epi*-Hypatulin B (17)

## 6. Chiral GC Analysis

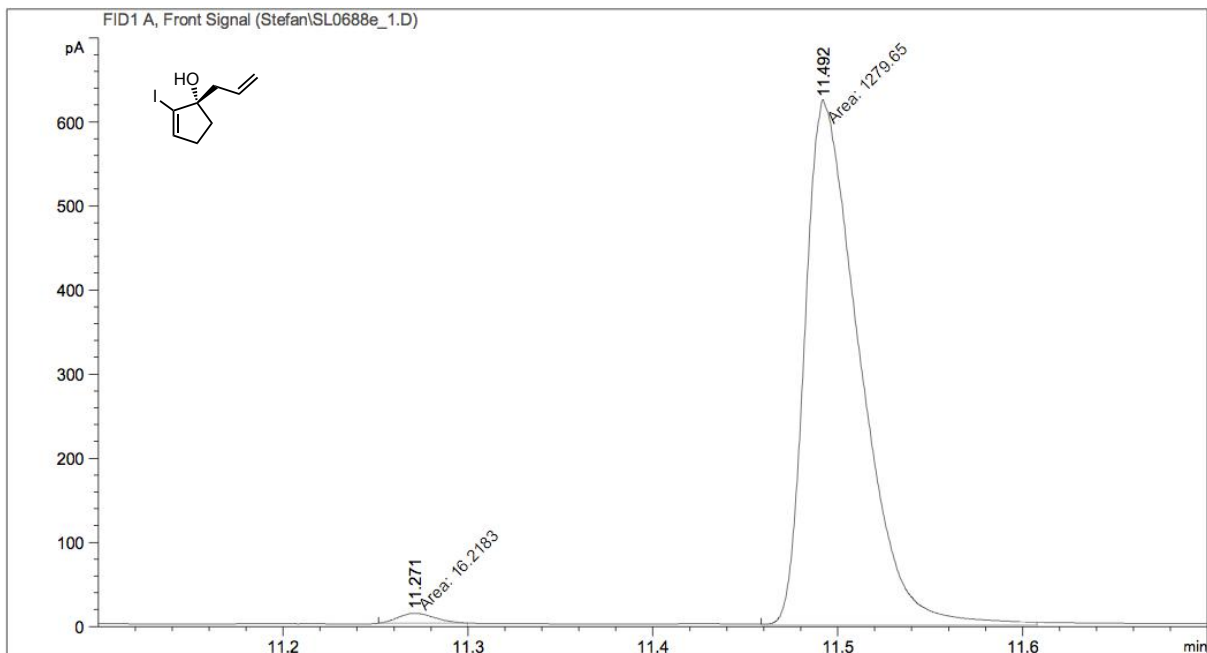
### (S)-2-Methyl-1-(prop-2-en-1-yl)cyclopent-2-enol (SI-6)

Hydrodex-TBDAC; temperature gradient 50–190 °C; 1.1 mL/min; split 50:1; FID 300 °C

#### Racemic mixture



#### Enantioenriched



Signal 1: FID1 A, Front Signal

Peak #	RetTime [min]	Type	Width [min]	Area [pA*s]	Height [pA]	Area %
1	11.271	MM T	0.0227	16.21828	11.90638	1.25154
2	11.492	MM T	0.0342	1279.64709	623.27820	98.74846

Totals :                                    1295.86538    635.18458

## 7. References

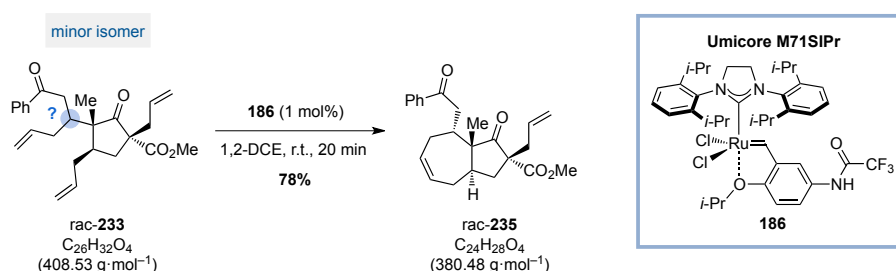
- (1) Lin, H.; Xiao, L.-J.; Zhou, M.-J.; Yu, H.-M.; Xie, J.-H.; Zhou, Q.-L. Enantioselective Approach to (-)-Hamigeran B and (-)-4-Bromohamigeran B via Catalytic Asymmetric Hydrogenation of Racemic Ketone To Assemble the Chiral Core Framework. *Org. Lett.* **2016**, *18*, 1434–1437.
- (2) Barnett, D. S.; Moquist, P. N.; Schaus, S. E. The Mechanism and an Improved Asymmetric Allylboration of Ketones Catalyzed by Chiral Biphenols. *Angew. Chem. Int Ed.* **2009**, *48*, 8679–8682.
- (3) (a) Lui, K.-H.; Sammes, M. P. Synthesis and chemistry of azolenines. Part 16. Preparation of both 3*H*- and 2*H*-pyrroles from 2,2-disubstituted 1,4-diketones via the Paal-Knorr reaction, and isolation of intermediate 2-hydroxy-3,4-dihydro-2*H*-pyrroles. *J. Chem Soc. Perkin Trans. 1* **1990**, *3*, 457–468; (b)
- (4) Breton, G. W. Selective Monoacetylation of Unsymmetrical Diols Catalyzed by Silica Gel-Supported Sodium Hydrogen Sulfate. *J. Org. Chem.* **1997**, *62*, 8952–8954.
- (5) Sheldrick, G. M. A short history of SHELX. *Acta Cryst.* **2008**, *A64*, 112–122.
- (6) Sheldrick, G. M. Crystal structure refinement with SHELX. *Acta Cryst.* **2015**, *C71*, 3–8.
- (7) Dolomanov, O. V.; Bourhis, L. J.; Gildea, R. J.; Howard, J. A. K.; Puschmann, H. OLEX2: a complete structure solution, refinement and analysis program. *J. Appl. Cryst.* **2009**, *42*, 339–341.
- (8) Kleoff, M.; Schwan, J.; Christmann, M.; Heretsch, P. A Modular, Argon-Driven Flow Platform for Natural Product Synthesis and Late-Stage Transformations. *Org. Lett.* **2021**, *23*, 2370–2374.
- (9) Kim, J. G.; Waltz, K. M.; Garcia, I. F.; Kwiatkowski, D.; Walsh, P. J. Catalytic Asymmetric Allylation of Ketones and a Tandem Asymmetric Allylation/Diastereoselective Epoxidation of Cyclic Enones. *J. Am. Chem. Soc.* **2004**, *126*, 12580–12585.
- (10) Taber, D. F.; Gerstenhaber, D. A.; Berry, J. F. Enantioselective Conjugate Allylation of Cyclic Enones. *J. Org. Chem.* **2011**, *76*, 7614–7617.
- (11) Michalak, K.; Michalak, M.; Wicha, J. Construction of the Tricyclic 5–7–6 Scaffold of Fungi-Derived Diterpenoids. Total Synthesis of (±)-Heptemerone G and an Approach to Danishefsky's Intermediate for Guanacastepene A Synthesis. *J. Org. Chem.* **2010**, *75*, 8337–8350.
- (12) Xu, Y.; Clarkson, G. C.; Docherty, G.; North, C. L.; Woodward, G.; Wills, M. Ruthenium(II) Complexes of Monodonor Ligands: Efficient Reagents for Asymmetric Ketone Hydrogenation. *J. Org. Chem.* **2005**, *70*, 8079–8087.
- (13) Ramesh, C.; Ravindranath, N.; Das, B. Simple, Efficient and Selective Deprotection of Phenolic Methoxymethyl Ethers Using Silica-Supported Sodium Hydrogen Sulfate as a Heterogeneous Catalyst. *J. Org. Chem.* **2003**, *68*, 7101–7103.
- (14) Li, K.; Wang, C.; Yin, G.; Gao, S. Construction of the basic skeleton of ophiobolin A and variecolin. *Org. Biomol. Chem.* **2013**, *11*, 7550–7558.
- (15) Li, C.; Tu, S.; Wen, S.; Li, S.; Chang, J.; Shao, F.; Lei, X. Total Synthesis of the G2/M DNA Damage Checkpoint Inhibitor Psilostachyin C. *J. Org. Chem.* **2011**, *76*, 3566–3570.
- (16) Lee, P. H.; Lee, K.; Sung, S.-y.; Chang, S. The Catalytic Sakurai Reaction. *J. Org. Chem.* **2001**, *66*, 8646–8649.
- (17) Uwamori, M.; Nakada, M. Stereoselective total synthesis of (±)-hyperforin via intramolecular cyclopropanation. *Tetrahedron Lett.* **2013**, *54*, 2022–2025.

## Unpublished Results – Additional Experiments Towards 3-*epi*-Hypatulin B

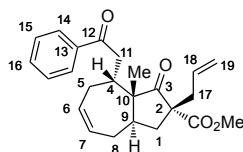
The same general working methods have been used.

### Experimental Procedures and Analytical Data

(2*R*,3*aR*,4*R*,8*aR*)-methyl-3*a*-methyl-3-oxo-4-(2-oxo-2-phenylethyl)-2-(prop-2-en-1-yl)-1,2,3,3*a*,4,5,8,8*a*-octahydroazulene-2-carboxylate (**rac-235**)



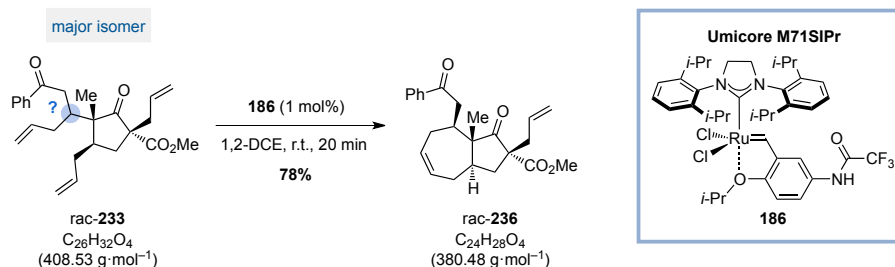
A closed vial was charged with the minor isomer of keton **rac-233** (22.8 mg, 55.8 μmol, 1.0 equiv), Umicore catalyst **186** (460 μg, 0.588 μmol, 1 mol%) and 1,2-DCE (1,24 mL) under an argon atmosphere. The reaction mixture was stirred at ambient temperature for 20 min and then concentrated under reduced pressure. The crude product was purified by preparative TLC (SiO<sub>2</sub>, *n*-pentane/EtOAc, 14:1) to afford **rac-235** (16.6 mg, 43.6 μmol, 78%) as a colourless oil.



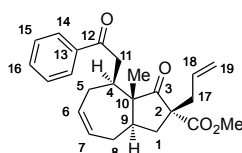
<sup>1</sup>H NMR (700 MHz, CDCl<sub>3</sub>): δ = 7.95 – 7.92 (m, 2H, H-14), 7.56 – 7.52 (m, 1H, H-16), 7.47 – 7.43 (m, 2H, C-15), 5.76 – 5.67 (m, 2H, H-7, H-18), 5.53 – 5.47 (m, 1H, H-6), 5.15 – 5.09 (m, 2H, H-19), 3.69 (s, 3H, OMe), 2.96 (dd, *J* = 15.3, 11.3 Hz, 1H, H-11), 2.85 (ddt, *J* = 14.0, 7.2, 1.2 Hz, 1H, H-17), 2.76 – 2.72 (m, 1H, H-4), 2.58 (dt, *J* = 15.3, 1.9 Hz, 1H, H-11), 2.54 (ddd, *J* = 12.4, 6.1, 3.2 Hz, 1H, H-9), 2.42 – 2.34 (m, 3H, H-1, H-5, H-17), 2.27 (ddd, *J* = 16.5, 8.0, 3.2 Hz, 1H, H-8), 2.21 (ddd, *J* = 17.4, 8.0, 3.1 Hz, 1H, H-5), 2.12 – 2.03 (m, 1H, H-8), 1.64 (t, *J* = 12.9 Hz, 1H, H-1), 1.04 (s, 3H, Me) ppm.

<sup>13</sup>C NMR (176 MHz, CDCl<sub>3</sub>): δ = 217.2 (C-3), 199.6 (C-12), 170.9 (CO<sub>2</sub>Me), 137.0 (C-13), 133.3 (C-18), 133.1 (C-16), 129.6 (C-7), 128.7 (C-15), 128.4 (C-14), 128.1 (C-6), 119.2 (C-19), 61.5 (C-2), 56.3 (C-10), 52.9 (OMe), 40.7 (C-17), 39.2 (C-11), 37.0 (C-9), 36.8 (C-4), 35.5 (C-1), 29.7 (C-8), 27.4 (C-5), 16.3 (Me) ppm.

**(2*R*,3*aR*,4*S*,8*aR*)-methyl-3*a*-methyl-3-oxo-4-(2-oxo-2-phenylethyl)-2-(prop-2-en-1-yl)-1,2,3,3*a*,4,5,8,8*a*-octahydroazulene-2-carboxylate (rac-236)**



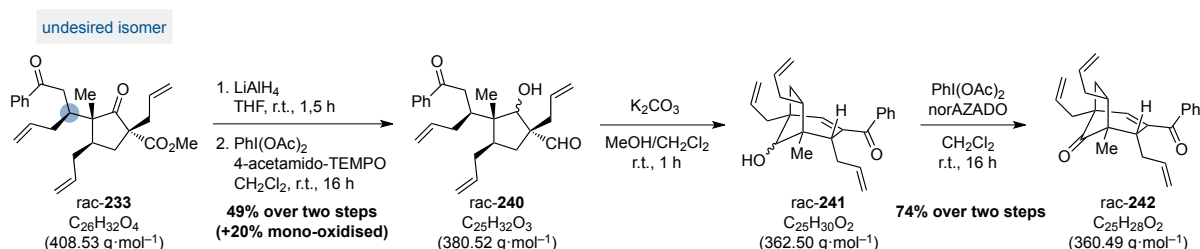
A closed vial was charged with the minor isomer of keton rac-233 (4.4 mg, 11  $\mu\text{mol}$ , 1.0 equiv), Umicore catalyst **186** (89  $\mu\text{g}$ , 0.11  $\mu\text{mol}$ , 1 mol%) and 1,2-DCE (0,24 mL) under an argon atmosphere. The reaction mixture was stirred at ambient temperature for 20 min and then diluted with pentane and filtered through a plug of Celite®, rinsing with a 5:1-mixture of *n*-pentane/Et<sub>2</sub>O. The product rac-236 (3.0 mg, 7.9  $\mu\text{mol}$ , 73%) was obtained as a colourless oil.



<sup>1</sup>H NMR (700 MHz, CDCl<sub>3</sub>):  $\delta$  = 7.97 – 7.93 (m, 2H, H-14), 7.57 – 7.52 (m, 1H, H-30), 7.47 – 7.43 (m, 2H, H-29), 5.67 – 5.59 (m, 2H, H-7, H-18), 5.55 – 5.50 (m, 1H, H-6), 5.11 – 5.05 (m, 2H, H-19), 4.16 – 4.10 (m, 1H, H-11), 3.76 (s, 3H, OMe), 2.67 (ddt, *J* = 14.0, 7.9, 1.0 Hz, 1H, H-17), 2.62 – 2.55 (m, 2H, H-4, H-11), 2.44 – 2.34 (m, 3H, H-1, H-9, H-17), 2.31 – 2.22 (m, 2H, H-5, H-8), 2.10 – 1.93 (m, 2H, H-5, H-8), 1.56 – 1.50 (m, 1H, H-1), 0.92 (s, 3H, Me) ppm.

<sup>13</sup>C NMR (176 MHz, CDCl<sub>3</sub>):  $\delta$  = 218.0 (C-3), 199.8 (C-12), 171.2 (CO<sub>2</sub>Me), 137.6 (C-13), 133.2 (C-18), 132.9 (C-16), 128.9 (C-7), 128.6 (C-15), 128.4 (C-6), 128.2 (C-14), 119.2 (C-19), 62.2 (C-2), 52.9 (OMe), 52.3 (C-10), 45.2 (C-9), 40.9 (C-4), 40.4 (C-11), 39.3 (C-17), 35.6 (C-1), 30.8 (C-8), 11.5 (Me) ppm.

**Sequence for the aldol cyclisation via global reduction**

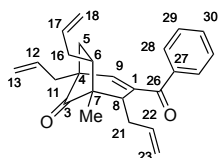


A flame-dried Schlenk flask was charged with the undesired isomer of rac-233 (250 mg, 612  $\mu\text{mol}$ , 1.0 equiv) and anhydrous THF (2.6 mL). Then lithium aluminium hydride (139 mg, 3.67 mmol, 6.0 equiv) was carefully added in small portions at 0 °C. After complete addition, the reaction mixture warmed to ambient temperature and stirred for 1.5 h. The reaction was diluted with Et<sub>2</sub>O (2 mL), cooled to 0 °C and quenched by the addition of H<sub>2</sub>O (0.2 mL) and 4 M NaOH (0.4 mL). Filtration through a plug of Celite®, rinsing with Et<sub>2</sub>O and concentration under reduced pressure afforded a crude mixture of four diastereomeric products.

The crude mixture was dissolved in dichloromethane (10 mL) and 4-acetamido-TEMPO (26.1 mg, 122  $\mu\text{mol}$ , 20 mol%) and  $\text{PhI}(\text{OAc})_2$  (433 mg, 1.34 mmol, 2.2 equiv) were added. The reaction mixture was stirred at ambient temperature for 16 h and then dry-loaded onto silica and purified by column chromatography ( $\text{SiO}_2$ , *n*-pentane/ $\text{Et}_2\text{O}$ , 5:1 to 3:1) to afford a mixture of diastereomeric alcohols **rac-240** (115 mg, 302  $\mu\text{mol}$ , 49% over two steps) as a colourless oil and a mono-oxidised product containing an aldehyde (46.0 mg, 120  $\mu\text{mol}$ , 20%).

The mixture of **rac-240** (115 mg, 302  $\mu\text{mol}$ ) was dissolved in a 9:1-mixture of dichloromethane and MeOH (28 mL) and  $\text{K}_2\text{CO}_3$  (418 mg, 3.02 mmol, 10 equiv) was added. The reaction mixture was stirred at ambient temperature for 1 h. Then  $\text{H}_2\text{O}$  (10 mL) was added and the aqueous layer was extracted with dichloromethane ( $3 \times 10 \text{ mL}$ ), dried over anhydrous  $\text{Na}_2\text{SO}_4$  and concentrated under reduced pressure.

The crude mixture was dissolved in dichloromethane (6 mL) and norAZADO (2.1 mg, 15  $\mu\text{mol}$ , 5 mol%) and  $\text{PhI}(\text{OAc})_2$  (236 mg, 732  $\mu\text{mol}$ , 2.4 equiv) were added. The reaction mixture was stirred at ambient temperature for 16 h and then dry-loaded onto silica and purified by column chromatography ( $\text{SiO}_2$ , *n*-pentane/ $\text{Et}_2\text{O}$ , 10:1) to afford **rac-242** (80.6 mg, 224  $\mu\text{mol}$ , 74% over two steps) as a colourless oil.

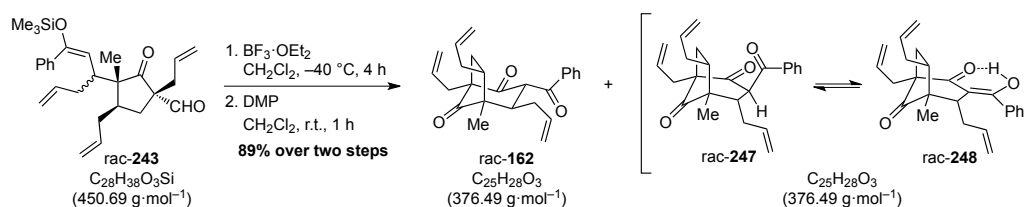


$^1\text{H NMR}$  (600 MHz,  $\text{CDCl}_3$ ):  $\delta = 7.72 - 7.67$  (m, 2H, H-28),  $7.57 - 7.50$  (m, 1H, H-30),  $7.44 - 7.38$  (m, 2H, H-29),  $6.27$  (s, 1H, H-9),  $5.92 - 5.84$  (m, 1H, H-12),  $5.72 - 5.57$  (m, 2H, H-17, H-22),  $5.10 - 5.07$  (m, 1H, H-13),  $5.06 - 4.99$  (m, 3H, H-13, H-18),  $4.89 - 4.84$  (m, 1H, H-23),  $4.80 - 4.75$  (m, 1H, H-23),  $3.56$  (dd,  $J = 8.2, 5.1 \text{ Hz}$ , 1H, H-8),  $2.46 - 2.32$  (m, 3H, H-11, H-16, H-21),  $2.27 - 2.11$  (m, 3H, H-5, H-6, H-11),  $2.03$  (dtd,  $J = 14.2, 8.1, 1.0 \text{ Hz}$ , 1H, H-21),  $1.84 - 1.75$  (m, 1H, H-16),  $1.18$  (dd,  $J = 12.7, 8.9 \text{ Hz}$ , 1H, H-5),  $1.12$  (s, 3H, Me) ppm.

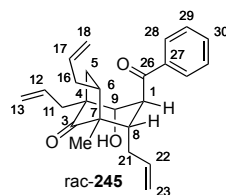
$^{13}\text{C NMR}$  (151 MHz,  $\text{CDCl}_3$ ):  $\delta = 215.7$  (C-3),  $196.3$  (C-26),  $146.6$  (C-9),  $140.3$  (C-1),  $137.2$  (C-27),  $135.9$  (C-17),  $132.6$  (C-30),  $130.0$  (C-28),  $128.2$  (C-29),  $56.5$  (C-8),  $51.2$  (C-4),  $50.7$  (C-7),  $42.3$  (C-5),  $41.5$  (C-6),  $37.6$  (C-16),  $35.5$  (C-21),  $35.4$  (C-11),  $13.0$  (Me) ppm.

### Characterisation of compounds **rac-245**, **rac-246**, **rac-162** and **rac-247/248**

The reactions were performed as described in the supporting information.



After the first step, samples of the two major aldol products were isolated and characterised.

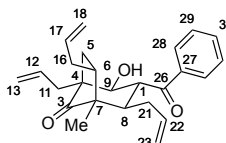


**<sup>1</sup>H NMR** (700 MHz, CD<sub>2</sub>Cl<sub>2</sub>): δ = 7.81 – 7.78 (m, 2H, H-28), 7.58 – 7.54 (m, 1H, H-30), 7.50 – 7.46 (m, 2H, H-29), 5.76 (dtd, *J* = 16.8, 9.9, 9.3, 5.3 Hz, 1H, H-22), 5.70 (dddd, *J* = 17.1, 10.1, 9.1, 5.8 Hz, 1H, H-12), 5.63 (dddd, *J* = 17.1, 10.3, 7.6, 5.7 Hz, 1H, H-17), 5.17 – 5.11 (m, 2H, H-23), 5.09 (dtd, *J* = 17.1, 1.9, 1.1 Hz, 1H, H-13), 5.04 (dddd, *J* = 10.1, 2.1, 1.4, 0.7 Hz, 1H, H-13), 5.01 (dddd, *J* = 10.3, 2.2, 1.5, 0.9 Hz, 1H, H-18), 4.97 (dtd, *J* = 17.1, 1.9, 1.3 Hz, 1H, H-18), 4.74 (ddd, *J* = 4.8, 2.1, 1.2 Hz, 1H, H-9), 3.68 (t, *J* = 1.2 Hz, 1H, H-1), 2.87 (ddt, *J* = 11.7, 3.7, 2.1, 1.5 Hz, 1H, H-8), 2.46 (dddt, *J* = 13.9, 5.3, 3.7, 1.5 Hz, 1H, H-21), 2.37 (ddt, *J* = 14.3, 9.1, 0.9 Hz, 1H, H-11), 2.30 – 2.24 (m, 1H, H-6), 2.23 – 2.15 (m, 2H, H-11, H-16), 2.11 (ddd, *J* = 13.9, 11.7, 9.3 Hz, 1H, H-21), 1.88 (dd, *J* = 14.4, 9.7 Hz, 1H, H-5), 1.59 – 1.54 (m, 1H, H-16), 1.24 (dd, *J* = 14.4, 5.0 Hz, 1H, H-5), 1.00 (s, 3H, Me) ppm.

**<sup>13</sup>C NMR** (176 MHz, CD<sub>2</sub>Cl<sub>2</sub>): δ = 218.4 (C-3), 202.7 (C-26), 138.2 (C-22), 137.7 (C-27), 136.8 (C-17), 134.7 (C-12), 133.0 (C-30), 129.2 (C-29), 128.9 (C-28), 118.9 (C-23), 118.6 (C-13), 117.2 (C-18), 82.5 (C-9), 54.4 (C-4), 52.9 (C-7), 52.3 (C-1), 52.0 (C-8), 39.0 (C-16), 37.8 (C-6), 36.1 (C-21), 35.6 (C-11), 32.5 (C-5), 14.2 (Me) ppm.

**HRMS** (ESI, pos. mode): *m/z* calcd for C<sub>25</sub>H<sub>30</sub>O<sub>3</sub>Na<sup>+</sup> [M+H]<sup>+</sup>: 401.2087, found 401.2098.

**X-ray:** Crystals were grown by addition of *n*-pentane to a concentrated solution of rac-245 in Et<sub>2</sub>O in a 1 mL vial until a nearly saturated solution was reached. The solution was then left to rest at ambient temperature.



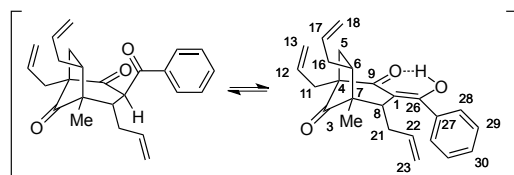
**<sup>1</sup>H NMR** (700 MHz, CD<sub>2</sub>Cl<sub>2</sub>): δ = 8.04 – 8.01 (m, 2H, H-28), 7.60 – 7.56 (m, 1H, H-30), 7.50 – 7.46 (m, 2H, H-29), 5.98 (ddt, *J* = 17.2, 10.1, 7.3 Hz, 1H, H-12), 5.76 (dddd, *J* = 16.5, 10.6, 7.7, 5.9 Hz, 1H, H-17), 5.52 (dddd, *J* = 16.7, 10.2, 7.6, 6.4 Hz, 1H, H-22), 5.10 – 5.03 (m, 4H, H-13, H-18), 4.69 – 4.64 (m, 2H, H-23), 3.83 – 3.78 (m, 2H, H-1, H-9), 2.44 (dd, *J* = 14.2, 10.0 Hz, 1H, H-5), 2.34 – 2.27 (m, 3H, H-11, H-21), 2.23 – 2.14 (m, 2H, H-16, H-21), 1.99 – 1.93 (m, 3H, H-6, H-8, OH), 1.62 (dddt, *J* = 13.4, 11.1, 7.7, 0.9 Hz, 1H, H-11), 1.31 (ddd, *J* = 14.2, 4.4, 0.8 Hz, 1H, H-5), 1.00 (s, 3H, Me) ppm.

**<sup>13</sup>C NMR** (176 MHz, CD<sub>2</sub>Cl<sub>2</sub>): δ = 217.9 (C-3), 203.6 (C-26), 139.9 (C-27), 136.9 (C-22), 136.8 (C-17), 136.2 (C-12), 133.6 (C-30), 129.2 (C-28), 129.0 (C-29), 118.2 (C-13), 117.4 (C-18), 117.3 (C-23), 80.3 (C-9), 55.9 (C-4), 53.4 (C-7), 51.7 (C-1), 48.1 (C-8), 38.6 (C-16), 36.1 (C-11), 35.0 (C-21), 34.5 (C-6), 30.0 (C-5), 15.1 (Me) ppm.

**X-ray:** Crystals were grown by addition of *n*-pentane to a concentrated solution of rac-246 in Et<sub>2</sub>O in a 1 mL vial until a nearly saturated solution was reached. The solution was then left to rest at ambient temperature.



After the second step, both triketones **rac-162** and **rac-247** could be separated and characterised. The analytical data for compound **rac-162** are identical with those reported in the supporting information



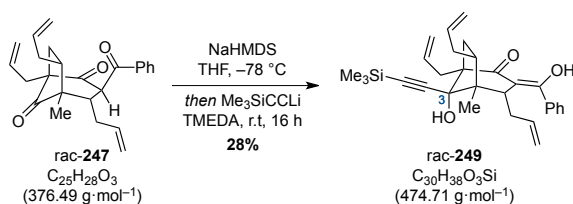
$^1\text{H NMR}$  (700 MHz,  $\text{CD}_3\text{CN}$ ):  $\delta$  = 15.75 (s, **1H**, OH), 7.87 – 7.84 (m, **1H**<sup>\*</sup>), 7.63 – 7.59 (m, 0.5H<sup>\*</sup>), 7.58 – 7.54 (m, **2H**, H-28), 7.51 – 7.47 (m, **3H**+**1H**<sup>\*</sup>, H-29, H-30), 5.91 (ddt,  $J$  = 17.3, 10.2, 7.1 Hz, **1H**, H-17), 5.86 – 5.80 (m, 0.5H<sup>\*</sup>), 5.81 – 5.67 (m, **1H**+0.5H<sup>\*</sup>, H-12), 5.49 (dddd,  $J$  = 17.1, 10.1, 9.0, 5.5 Hz, 0.5H<sup>\*</sup>), 5.15 – 4.99 (m, **5H**+**2H**<sup>\*</sup>, H-13, H-18, H-22), 4.98 – 4.94 (m, 0.5H<sup>\*</sup>), 4.80 – 4.76 (m, 0.5H<sup>\*</sup>), 4.68 (ddt,  $J$  = 10.1, 2.0, 1.1 Hz, **1H**, H-23), 4.62 – 4.58 (m, **1H**, H-23), 4.30 (d,  $J$  = 5.1 Hz, **1H**<sup>\*</sup>), 3.13 (t,  $J$  = 5.9 Hz, **1H**, H-8), 2.74 (dt,  $J$  = 10.8, 5.1, 3.8 Hz, **1H**<sup>\*</sup>), 2.55 – 2.48 (m, **3H**, H-6, H-16), 2.44 – 2.37 (m, **1H**+**2H**<sup>\*</sup>, H-11), 2.24 – 2.19 (m, **1H**+0.5H<sup>\*</sup>+H<sub>2</sub>O, H-5), 2.03 – 1.96 (m, **1H**+0.5H<sup>\*</sup>, H-21), 1.85 – 1.71 (m, **1H**+**1H**<sup>\*</sup>, H-11), 1.68 (dddd,  $J$  = 14.6, 7.3, 5.9, 1.3 Hz, **1H**, H-21), 1.48 (dd,  $J$  = 13.4, 8.2 Hz, **1H**, H-5), 1.39 (dd,  $J$  = 13.4, 8.8 Hz, 0.5H<sup>\*</sup>), 1.15 (s, 1.5H<sup>\*</sup>), 1.05 (s, **3H**, Me) ppm.

$^{13}\text{C NMR}$  (176 MHz,  $\text{CD}_3\text{CN}$ ):  $\delta$  = 212.3<sup>\*</sup>, 211.9 (C-3), 207.4<sup>\*</sup>, 202.8 (C-9), 198.3<sup>\*</sup>, 181.4 (C-26), 138.0<sup>\*</sup>, 137.2 (C-12), 137.1<sup>\*</sup>, 136.9 (C-22), 136.7<sup>\*</sup>, 136.6 (C-27), 135.8 (C-17), 134.8<sup>\*</sup>, 134.3<sup>\*</sup>, 131.3 (C-30), 129.8<sup>\*</sup>, 129.5 (C-29), 129.3 (C-28), 119.3<sup>\*</sup>, 118.8<sup>\*</sup>, 118.2 (C-18), 117.4<sup>\*</sup>, 117.4 (C-23), 117.3 (C-13), 109.9 (C-1), 67.5<sup>\*</sup>, 63.2 (C-4), 63.2<sup>\*</sup>, 53.0 (C-7), 49.0 (C-8), 45.8<sup>\*</sup>, 41.4<sup>\*</sup>, 40.4 (C-6), 40.0 (C-5), 38.6<sup>\*</sup>, 38.0 (C-21), 37.9<sup>\*</sup>, 36.6<sup>\*</sup>, 36.5<sup>\*</sup>, 32.7<sup>\*</sup>, 32.0 (C-16), 13.8 (Me), 13.1<sup>\*</sup> ppm.

Signals for the 1,3-diketone form **rac-247** are marked with \* and were not assigned.

**HRMS** (ESI, pos. mode):  $m/z$  calcd for  $\text{C}_{25}\text{H}_{30}\text{O}_3\text{Na}^+$  [ $\text{M}+\text{H}$ ]<sup>+</sup>: 399.1931, found 399.1944.

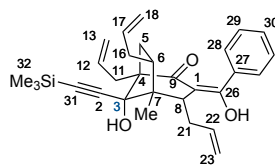
**(1R,4R,5R,6R,8S)-8-hydroxy-3-(hydroxy(phenyl)methylene)-5-methyl-8-((trimethylsilyl)ethynyl)-1,4,6-tris(prop-2-en-1-yl)bicyclo[3.2.1]octan-2-one (rac-249)**



Preparation of the organolithium reagent: To a flame-dried Schlenk tube was added anhydrous THF (0.2 mL), TMEDA (24.0  $\mu\text{L}$ , 150  $\mu\text{mol}$ , 3.0 equiv) and trimethylsilylacetylene (22.4  $\mu\text{L}$ , 15.7 mg, 159  $\mu\text{mol}$ , 3.0 equiv) under an argon atmosphere. The reaction was cooled to  $-78\text{ }^\circ\text{C}$  and *n*-BuLi (2.5 M in hexanes, 63.7  $\mu\text{L}$ , 159  $\mu\text{mol}$ , 3.0 equiv) was added.

A flame-dried Schlenk tube was charged with ketone **rac-247** (20.0 mg, 53.0  $\mu\text{mol}$ , 1.0 equiv) and anhydrous THF (0.25 mL) under an argon atmosphere. The solution was cooled to  $-78\text{ }^\circ\text{C}$  and NaHMDS (1.9 M in THF, 28.0  $\mu\text{L}$ , 1.0 equiv) was added. After stirring for 5 min, the prepared solution of lithium (trimethylsilyl)acetylide was added. The reaction mixture was stirred for 16 h while slowly warming to ambient temperature. The reaction was quenched by the addition of saturated aqueous  $\text{NH}_4\text{Cl}$  (1 mL) and

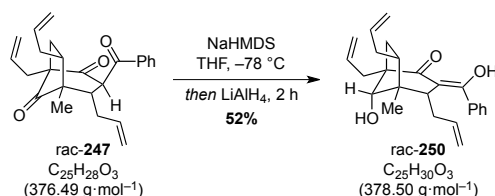
extracted with EtOAc ( $3 \times 1$  mL). The combined organic layers were dried over anhydrous  $\text{Na}_2\text{SO}_4$  and concentrated under reduced pressure. The crude product was purified by preparative TLC ( $\text{SiO}_2$ ,  $n$ -pentane/EtOAc, 30:1) to afford alkyne **rac-249** (6.3 mg, 151  $\mu\text{mol}$ , 28%) as a colourless oil.



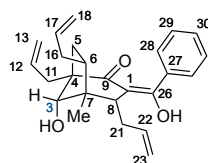
$^1\text{H NMR}$  (600 MHz,  $\text{CDCl}_3$ ):  $\delta$  = 7.46 – 7.42 (m, 5H, Ph), 6.24 (dtd,  $J$  = 17.3, 10.1, 4.5 Hz, 1H, H-12), 5.69 (dddd,  $J$  = 17.0, 10.1, 8.2, 5.7 Hz, 1H, H-17), 5.33 (dt,  $J$  = 17.3, 1.9 Hz, 1H, H-13), 5.17 (ddd,  $J$  = 10.0, 2.5, 1.2 Hz, 1H, H-13), 5.04 (dq,  $J$  = 17.0, 1.7 Hz, 1H, H-18), 5.01 (ddt,  $J$  = 10.1, 2.0, 1.0 Hz, 1H, H-18), 4.84 (dddd,  $J$  = 17.0, 10.1, 8.1, 6.0 Hz, 1H, H-22), 4.44 (dtd,  $J$  = 10.1, 1.8, 0.8 Hz, 1H, H-23), 4.34 (dtd,  $J$  = 17.0, 1.9, 1.3 Hz, 1H, H-23), 3.04 (ddt,  $J$  = 13.4, 4.5, 1.4 Hz, 1H, H-11), 2.95 (dt,  $J$  = 15.9, 7.7 Hz, 1H, H-21), 2.71 (dd,  $J$  = 7.4, 2.2 Hz, 1H, H-8), 2.63 (s, 1H, OH), 2.55 (dd,  $J$  = 13.4, 10.2 Hz, 1H, H-11), 2.42 – 2.38 (m, 1H, H-16), 2.13 (td,  $J$  = 12.6, 8.2 Hz, 1H, H-16), 2.06 (dd,  $J$  = 13.5, 9.1 Hz, 1H, H-5), 1.94 – 1.81 (m, 1H, H-6), 1.74 (ddq,  $J$  = 16.1, 6.1, 2.0 Hz, 1H, H-21), 1.51 (dd,  $J$  = 13.5, 7.8 Hz, 1H, H-5), 1.20 (s, 3H, Me), 0.24 (s, 9H,  $\text{SiMe}_3$ ) ppm.

$^{13}\text{C NMR}$  (151 MHz,  $\text{CDCl}_3$ )  $\delta$  = 198.3 (C-9), 185.8 (C-26), 140.4 (C-21), 137.6 (C-12), 137.3 (C-17), 137.0 (C-27), 130.1 (C-30), 128.7 (CH), 127.9 (CH), 118.9 (C-13), 116.1 (C-18), 114.0 (C-23), 111.4 (C-1), 105.5 (C-2), 94.2 (C-31), 82.3 (C-3), 58.8 (C-4), 50.4 (C-8), 49.4 (C-7), 44.9 (C-6), 44.0 (C-5), 40.4 (C-21), 38.5 (C-16), 36.4 (C-11), 17.9 (Me), -0.1 ( $\text{SiMe}_3$ ) ppm.

**(1R,4R,5R,6R,8S)-8-hydroxy-3-(hydroxy(phenyl)methylene)-5-methyl-1,4,6-tris(prop-2-en-1-yl)bicyclo[3.2.1]octan-2-one (rac-250)**



A flame-dried Schlenk tube was charged with ketone **rac-247** (100 mg, 266  $\mu\text{mol}$ , 1.0 equiv) and anhydrous THF (2.6 mL) under and argon atmosphere. The solution was cooled to  $-78^\circ\text{C}$  and NaHMDS (1.9 M in THF, 140  $\mu\text{L}$ , 1.0 equiv) was added. After stirring for 5 min, lithium aluminium hydride (15.1 mg, 398  $\mu\text{mol}$ , 1.5 equiv) were added and the reaction mixture was stirred for 2 h. The reaction was quenched by the addition of 1 M HCl (1 mL) and extracted with EtOAc ( $3 \times 2$  mL). The combined organic layers were dried over anhydrous  $\text{Na}_2\text{SO}_4$  and concentrated under reduced pressure. The crude product was purified by column chromatography ( $\text{SiO}_2$ ,  $n$ -pentane/EtOAc, 10:1) to afford alcohol **rac-250** (52 mg, 137  $\mu\text{mol}$ , 52%) as a colourless oil.

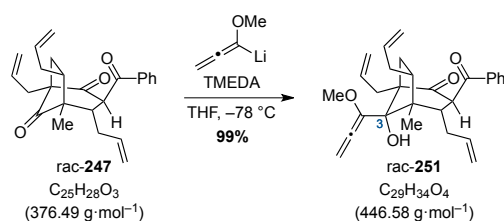


**<sup>1</sup>H NMR** (700 MHz, CDCl<sub>3</sub>): δ = 7.48 – 7.46 (m, 2H, H-28), 7.45 – 7.42 (m, 3H, H-29, H-30), 6.10 (dddd, *J* = 17.1, 10.0, 8.5, 6.3 Hz, 1H, H-12), 5.70 (dddd, *J* = 17.1, 10.2, 7.6, 6.0 Hz, 1H, H-17), 5.21 (ddt, *J* = 17.1, 2.1, 1.3 Hz, 1H, H-13), 5.14 (ddd, *J* = 10.0, 2.1, 1.0 Hz, 1H, H-13), 5.06 (dq, *J* = 17.1, 1.7 Hz, 1H, H-18), 5.04 – 4.97 (m, 2H, H-18, H-22), 4.52 – 4.48 (m, 1H, H-23), 4.36 (dtd, *J* = 17.1, 1.9, 1.3 Hz, 1H, H-23), 3.67 (s, 1H, H-3), 2.85 (dtt, *J* = 15.5, 7.7, 1.1 Hz, 1H, H-21), 2.78 (dtt, *J* = 14.1, 6.3, 1.4 Hz, 1H, H-11), 2.71 (dd, *J* = 7.7, 2.7 Hz, 1H, H-8), 2.40 (dddt, *J* = 13.3, 5.8, 4.1, 1.6 Hz, 1H, H-16), 2.34 (dd, *J* = 14.1, 8.5 Hz, 1H, H-11), 2.05 (s, 1H, OH), 2.02 (dd, *J* = 13.6, 9.1 Hz, 1H, H-5), 1.87 (dddd, *J* = 11.4, 9.1, 7.3, 4.1 Hz, 1H, H-6), 1.84 – 1.75 (m, 1H, H-16, H-21), 1.29 (dd, *J* = 13.6, 7.3 Hz, 1H, H-5), 1.09 (s, 3H, Me) ppm.

**<sup>13</sup>C NMR** (176 MHz, CDCl<sub>3</sub>): δ = 199.4 (C-9), 185.9 (C-26), 139.9 (C-22), 137.2 (C-27), 136.9 (C-17), 136.3 (C-12), 130.1 (C-30), 128.6 (C-29), 127.9 (C-28), 118.1 (C-13), 116.4 (C-18), 114.4 (C-23), 110.7 (C-1), 81.9 (C-3), 54.7 (C-4), 49.0 (C-8), 45.1 (C-7), 44.4 (C-6), 41.3 (C-5), 40.0 (C-21), 38.7 (C-16), 36.4 (C-11), 19.4 (Me).

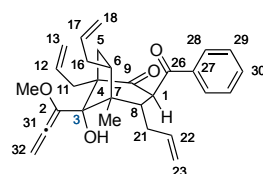
**HRMS** (ESI, pos. mode): *m/z* calcd for C<sub>25</sub>H<sub>30</sub>O<sub>3</sub>Na<sup>+</sup> [M+H]<sup>+</sup>: 401.2087, found 401.2096.

**(1R,3R,4S,5R,6R,8S)-8-hydroxy-8-(1-methoxypropa-1,2-dien-1-yl)-5-methyl-3-(oxophenylmethyl)-1,4,6-tris(prop-2-en-1-yl)bicyclo[3.2.1]octan-2-one (rac-251)**



Preparation of methoxyallenyllithium: To a flame-dried Schlenk tube was added THF (190 μL) and methoxyallene (19.2 μL, 198 μmol, 3.1 equiv) under an argon atmosphere. The reaction was cooled to –50 °C and *n*-BuLi (2.5 M in hexanes, 76.5 μL, 191 μmol, 3.0 equiv) was added. The reaction mixture was stirred at –50 °C to –40 °C over 5 min. Then anhydrous *N,N,N',N'*-tetramethylethylenediamine (28.7 μL, 191 μmol, 3.0 equiv) was added and the mixture was cooled to –78 °C.

A flame-dried Schlenk tube was charged with triketone rac-**247** (24.0 mg, 64.0 μmol, 1.0 equiv) and anhydrous toluene (240 μL) under an argon atmosphere. Then the mixture cooled to –78 °C and the prepared solution of methoxyallenyllithium was added. After stirring for 10 min, the reaction was quenched diluted with Et<sub>2</sub>O (5 mL) by the addition of saturated aqueous NaHCO<sub>3</sub> (5 mL). The layers were separated, the aqueous phase was extracted with Et<sub>2</sub>O (3 × 5 mL), and the combined organic layers were dried over Na<sub>2</sub>SO<sub>4</sub>, and concentrated under reduced pressure. The crude product was purified by column chromatography (SiO<sub>2</sub>, cyclohexane/EtOAc, 40:1) to yield methoxyallene rac-**251** (28.6 mg, 64.0 μmol, >99%) as a colorless solid.



**<sup>1</sup>H NMR** (700 MHz, CD<sub>2</sub>Cl<sub>2</sub>): δ = 7.93 – 7.90 (m, 2H, H-28), 7.57 – 7.53 (m, 1H, H-30), 7.48 – 7.44 (m, 2H, H-29), 5.86 (dddd, *J* = 17.2, 10.1, 8.9, 5.7 Hz, 1H, H-12), 5.79 – 5.66 (m, 3H, H-17, H-32), 5.31 – 5.28 (m,

1H, H-22), 5.06 – 5.00 (m, 2H, H-13, H-18), 4.99 – 4.95 (m, 2H, , H-13, H-18), 4.89 – 4.85 (m, 1H, H-23), 4.63 (d,  $J = 5.0$  Hz, 1H, H-8), 4.55 – 4.53 (m, 1H, H-23), 3.47 (s, 3H, OMe), 2.68 (ddt,  $J = 14.0, 5.7, 1.6$  Hz, 1H, H-11), 2.56 – 2.48 (m, 2H, H-1, H-21), 2.44 – 2.33 (m, 3H, H-6, H-16, H-21), 2.23 – 2.12 (m, 2H, H-11, H-16), 1.78 (dd,  $J = 13.5, 9.1$  Hz, 1H, H-5), 1.56 (dd,  $J = 13.5, 9.6$  Hz, 1H, H-5), 1.07 (s, 3H, Me) ppm.

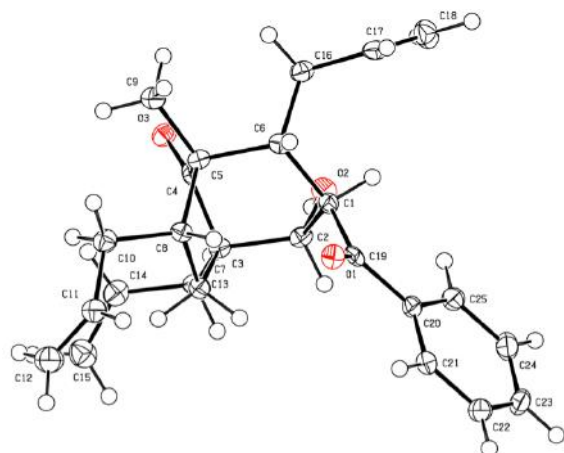
$^{13}\text{C}$  NMR (176 MHz,  $\text{CD}_2\text{Cl}_2$ ):  $\delta = 211.3$  (C-9), 200.6 (C-26), 199.6 (C-31), 138.8 (C-27), 138.8 (C-17), 138.8 (C-22), 138.4 (C-2), 136.8 (C-12), 133.1 (C-30), 129.9 (C-28), 128.7 (C-29), 117.5 (C-23), 117.0 (C-13), 115.6 (C-18), 95.9 (C-32), 86.4 (C-3), 65.0 (C-4), 61.5 (C-1), 56.5 (OMe), 51.1 (C-8), 49.9 (C-7), 45.5 (C-6), 40.5 (C-5), 39.3 (C-21), 37.0 (C-16), 36.1 (C-11), 16.4 (Me).

**HRMS** (ESI, pos. mode):  $m/z$  calcd for  $\text{C}_{29}\text{H}_{34}\text{O}_3\text{Na}^+ [\text{M}+\text{H}]^+$ : 469.2349, found 469.2360.

**X-ray**: Crystals were grown by addition of *n*-pentane to a concentrated solution of rac-**251** in Et<sub>2</sub>O in a 1 mL vial until a nearly saturated solution was reached. The solution was then left to rest at ambient temperature.

## X-ray Data

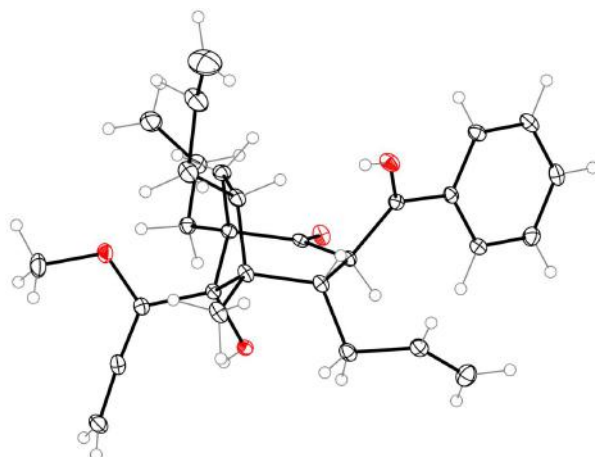
### Compound (rac-245) (Thermal Ellipsoids at 50% Probability)



**Table S1. Crystal data of compound (rac-245).**

Empirical formula	C <sub>25</sub> H <sub>30</sub> O <sub>3</sub>
Formula weight	378.49
Temperature/K	100.0
Crystal system	triclinic
Space group	$P\bar{1}$
a/Å	8.1210(2)
b/Å	12.2495(4)
c/Å	13.3618(4)
$\alpha$ /°	71.511(2)
$\beta$ /°	84.704(2)
$\gamma$ /°	81.242(2)
Volume/Å <sup>3</sup>	1244.53(7)
Z	2
$\rho_{\text{calc}}/\text{gcm}^{-3}$	1.010
$\mu/\text{mm}^{-1}$	0.511
F(000)	408.0
Crystal size/mm <sup>3</sup>	0.472 × 0.241 × 0.121
Radiation	CuK $\alpha$ ( $\lambda$ = 1.54178)
2 $\theta$ range for data collection/°	6.984 to 94.478
Reflections collected	22683
Independent reflections	2246 [ $R_{\text{int}}$ = 0.0536, $R_{\text{sigma}}$ = 0.0234]
Data/restraints/parameters	2246/0/255
Goodness-of-fit on F <sup>2</sup>	1.122
Final R indexes [ $I \geq 2\sigma(I)$ ]	$R_1$ = 0.0341, $wR_2$ = 0.0858
Final R indexes [all data]	$R_1$ = 0.0370, $wR_2$ = 0.0876
Largest diff. peak and hole/e.Å <sup>-3</sup>	0.11 and -0.24

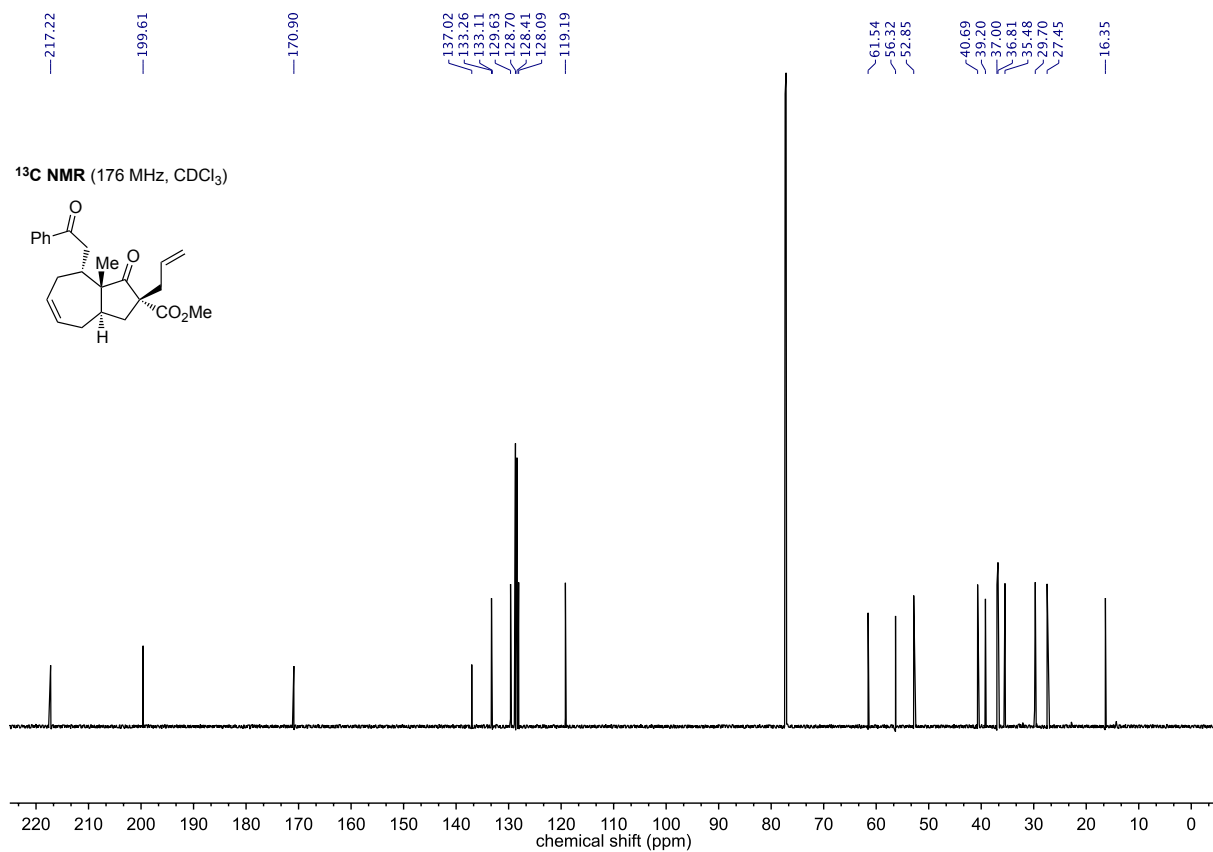
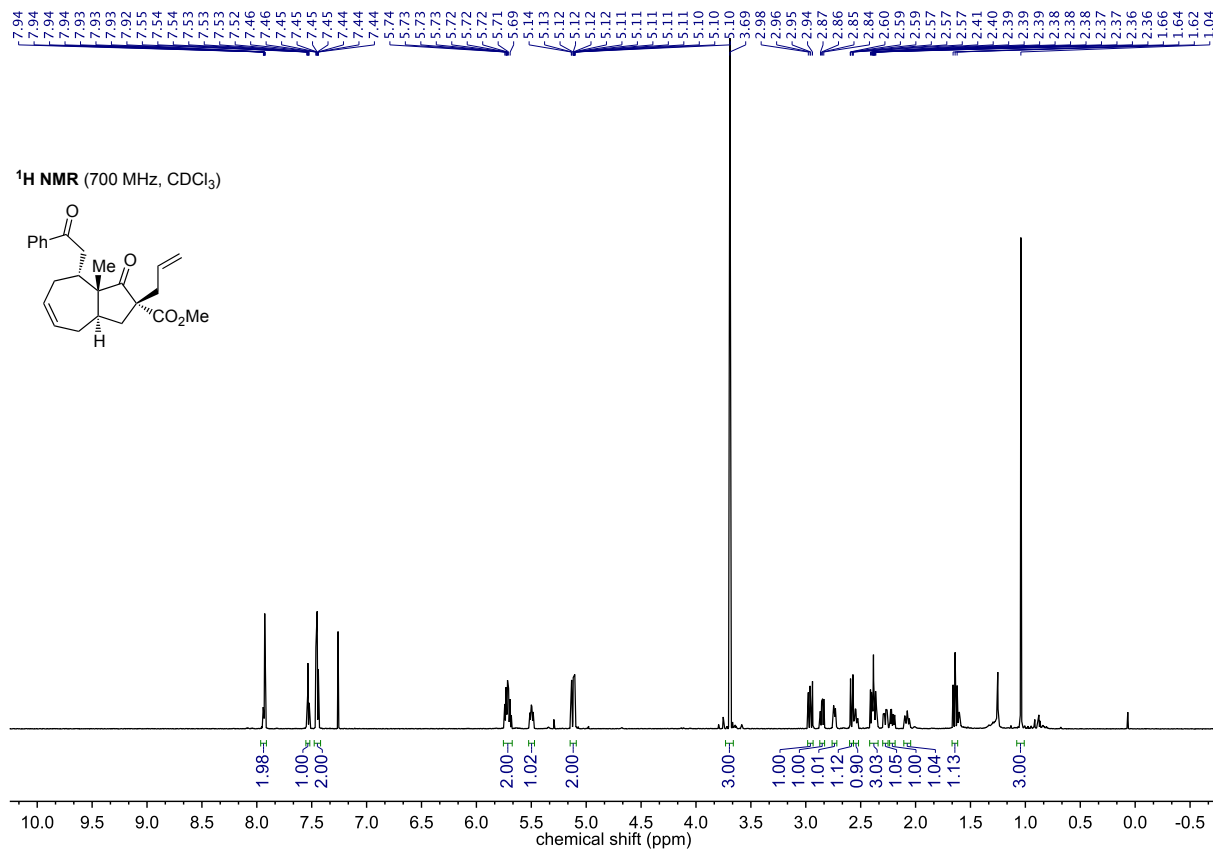


**Compound (rac-251) (Thermal Ellipsoids at 50% Probability)**

**Table S1. Crystal data of compound (rac-251).**

Empirical formula	C <sub>29</sub> H <sub>34</sub> O <sub>4</sub>
Formula weight	446.591
Temperature/K	100.0
Crystal system	monoclinic
Space group	<i>P</i> 2 <sub>1</sub> / <i>n</i>
<i>a</i> /Å	9.7347(4)
<i>b</i> /Å	24.2605(9)
<i>c</i> /Å	21.1414(8)
$\alpha$ /°	90
$\beta$ /°	93.452(2)
$\gamma$ /°	90
Volume/Å <sup>3</sup>	4983.9(3)
<i>Z</i>	8
$\rho_{\text{calc}}/\text{gcm}^{-3}$	1.190
$\mu/\text{mm}^{-1}$	0.617
<i>F</i> (000)	1926.1
Radiation	CuK $\alpha$ ( $\lambda$ = 1.54178)
2 $\Theta$ range for data collection/°	5.56 to 176.18
Reflections collected	60569
Independent reflections	5770 [ <i>R</i> <sub>int</sub> = 0.5485, <i>R</i> <sub>sigma</sub> = 0.1552]
Data/restraints/parameters	5770/48/659
Goodness-of-fit on <i>F</i> <sup>2</sup>	15.245
Final <i>R</i> indexes [ <i>I</i> > 2 $\sigma$ ( <i>I</i> )]	<i>R</i> <sub>1</sub> = 0.6842, <i>wR</i> <sub>2</sub> = 0.8920
Final <i>R</i> indexes [all data]	<i>R</i> <sub>1</sub> = 0.6914, <i>wR</i> <sub>2</sub> = 0.9026
Largest diff. peak and hole/e.Å <sup>-3</sup>	13.42 and -8.58

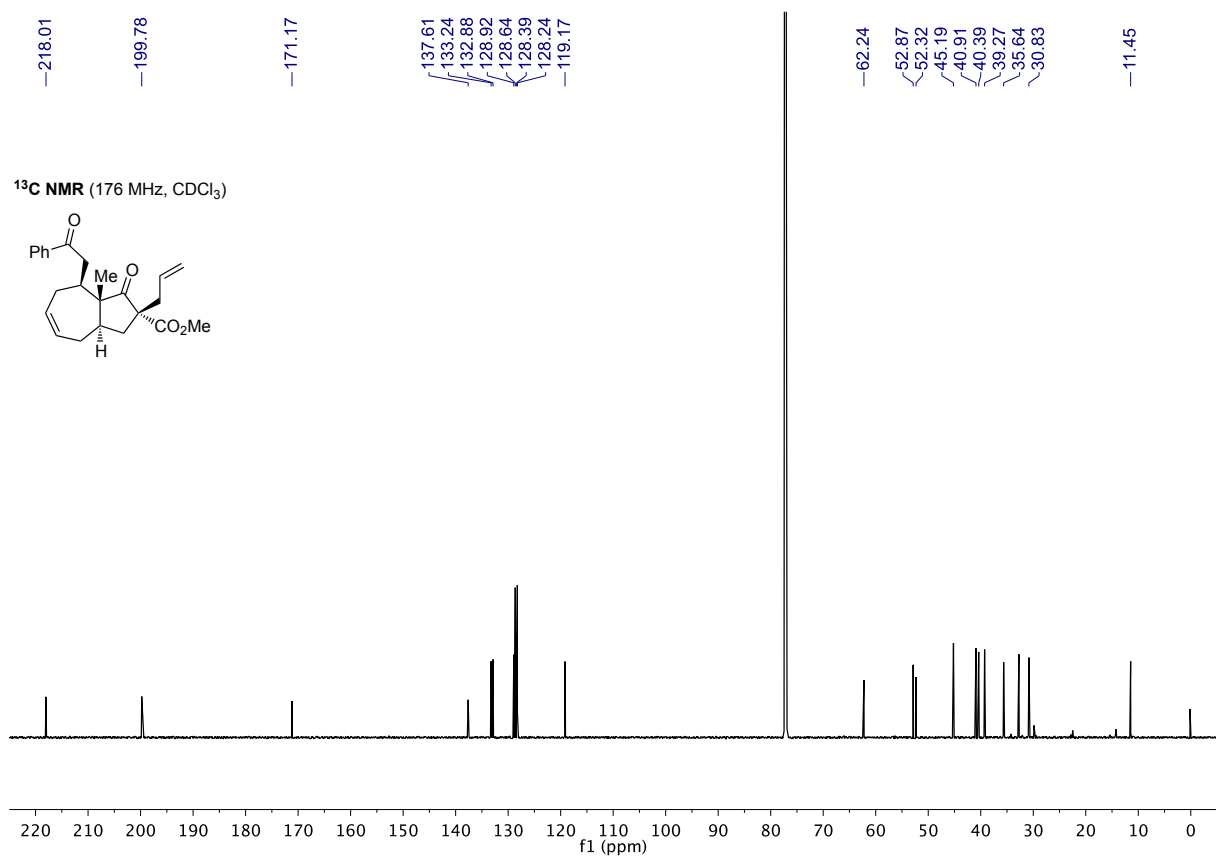
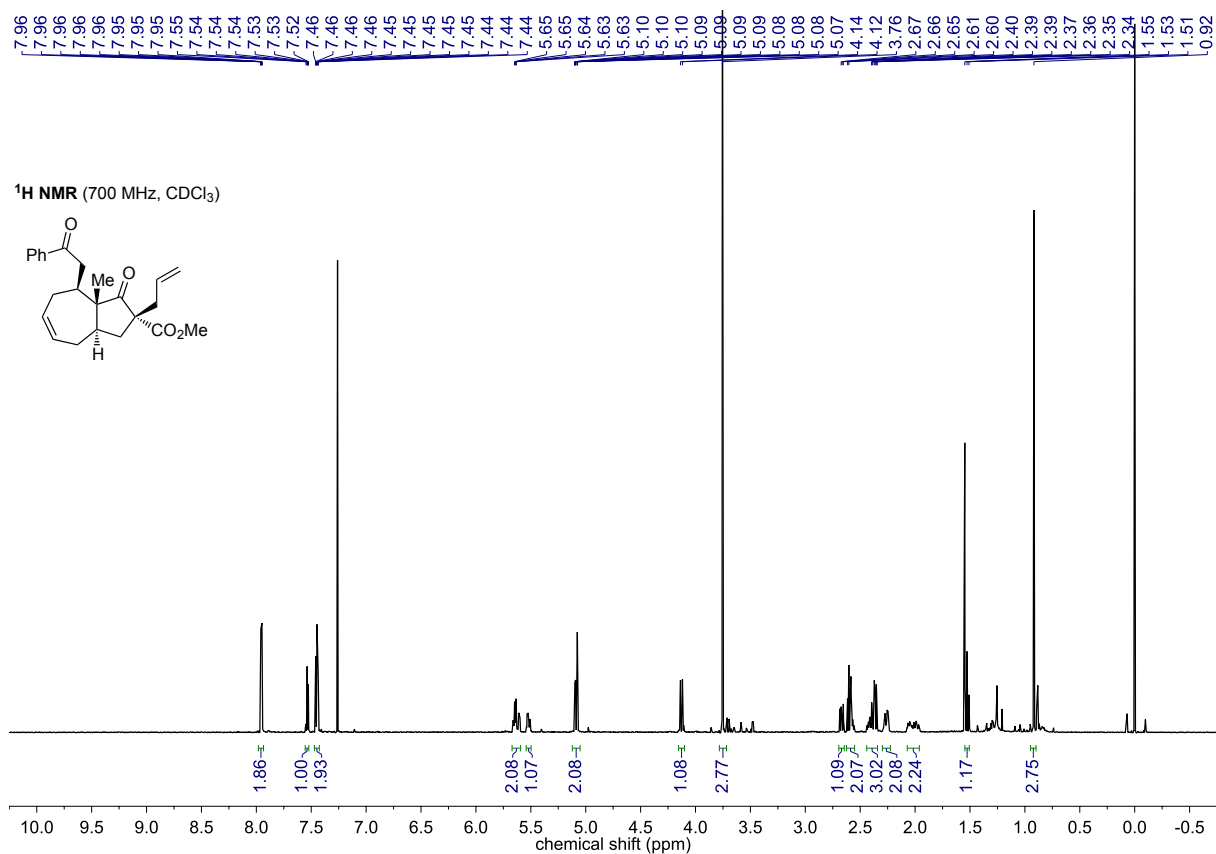
## NMR Spectra

## Compound rac-235

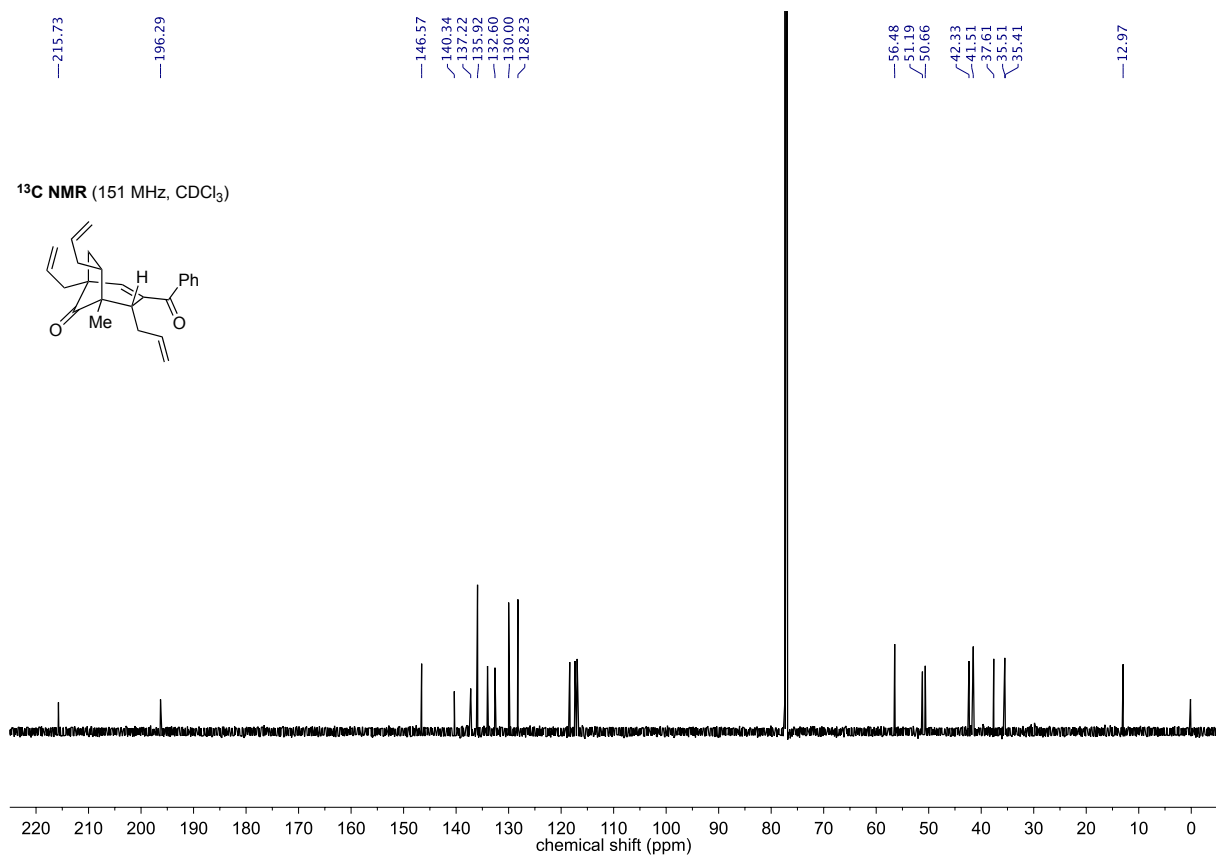
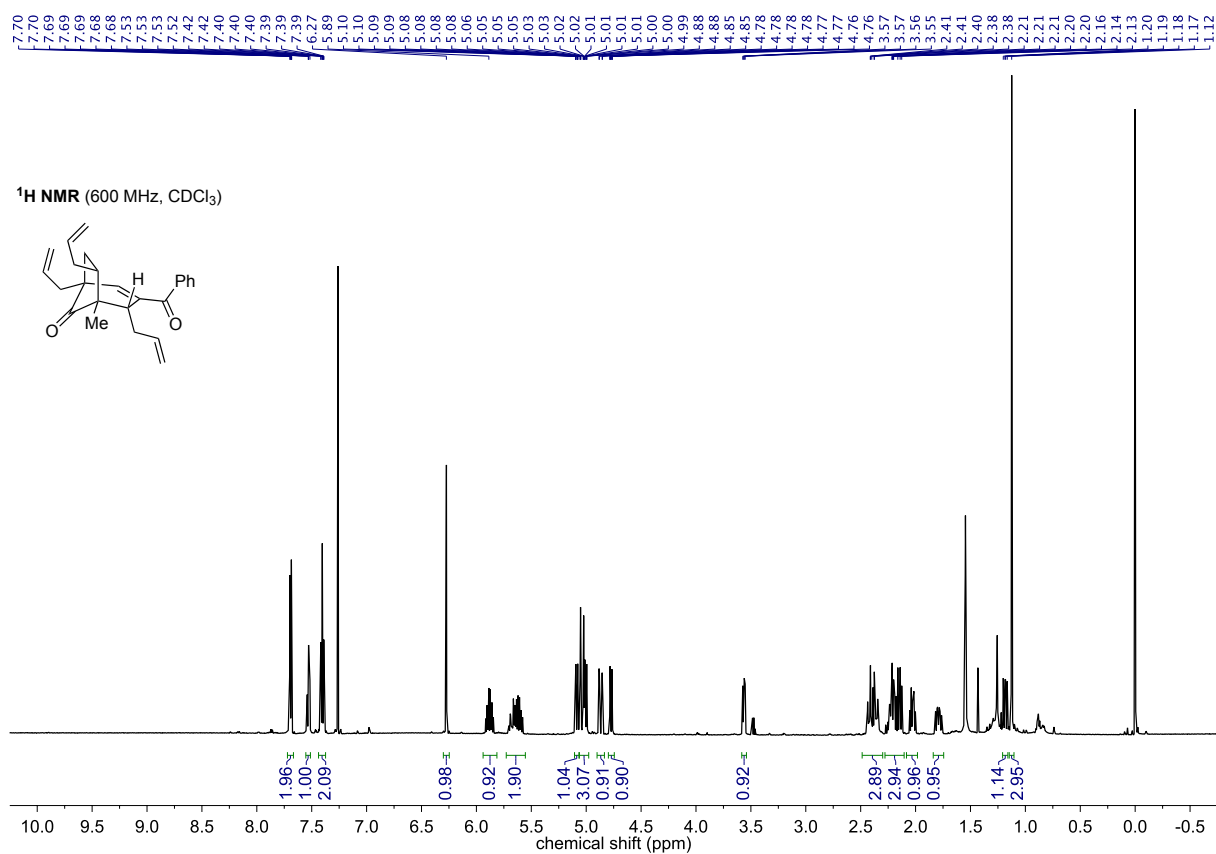




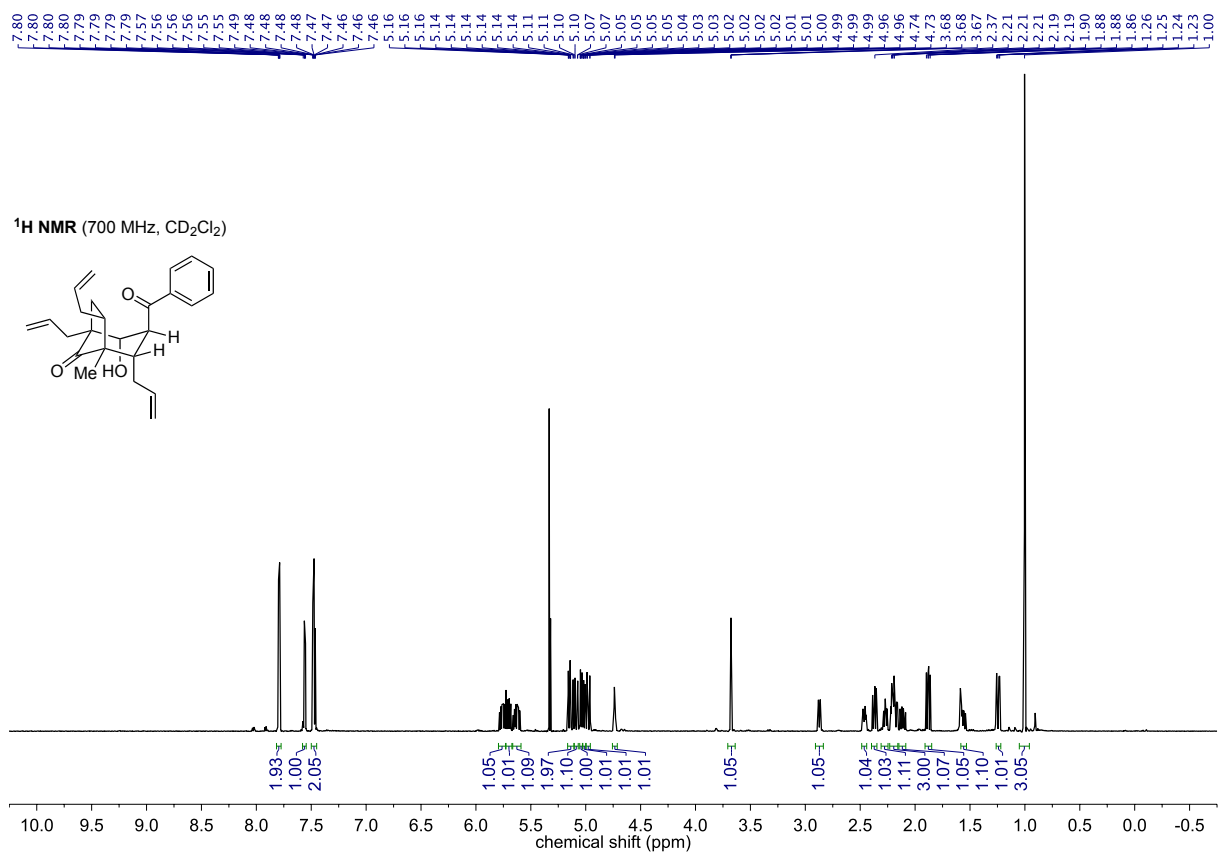
## Compound rac-236



## Compound rac-242



## Compound rac-245



-218.44

-202.74

138.17

137.75

136.79

134.68

133.01

129.23

128.86

118.86

118.63

117.22

-82.46

54.43

52.91

52.28

51.98

39.03

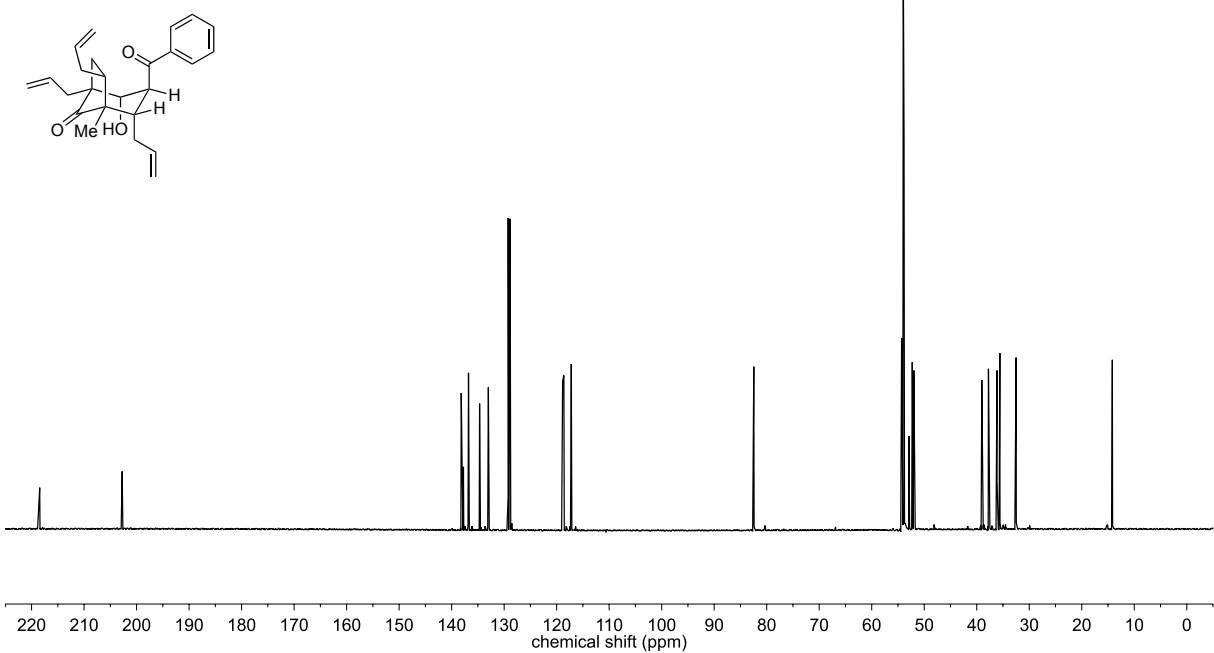
37.77

36.14

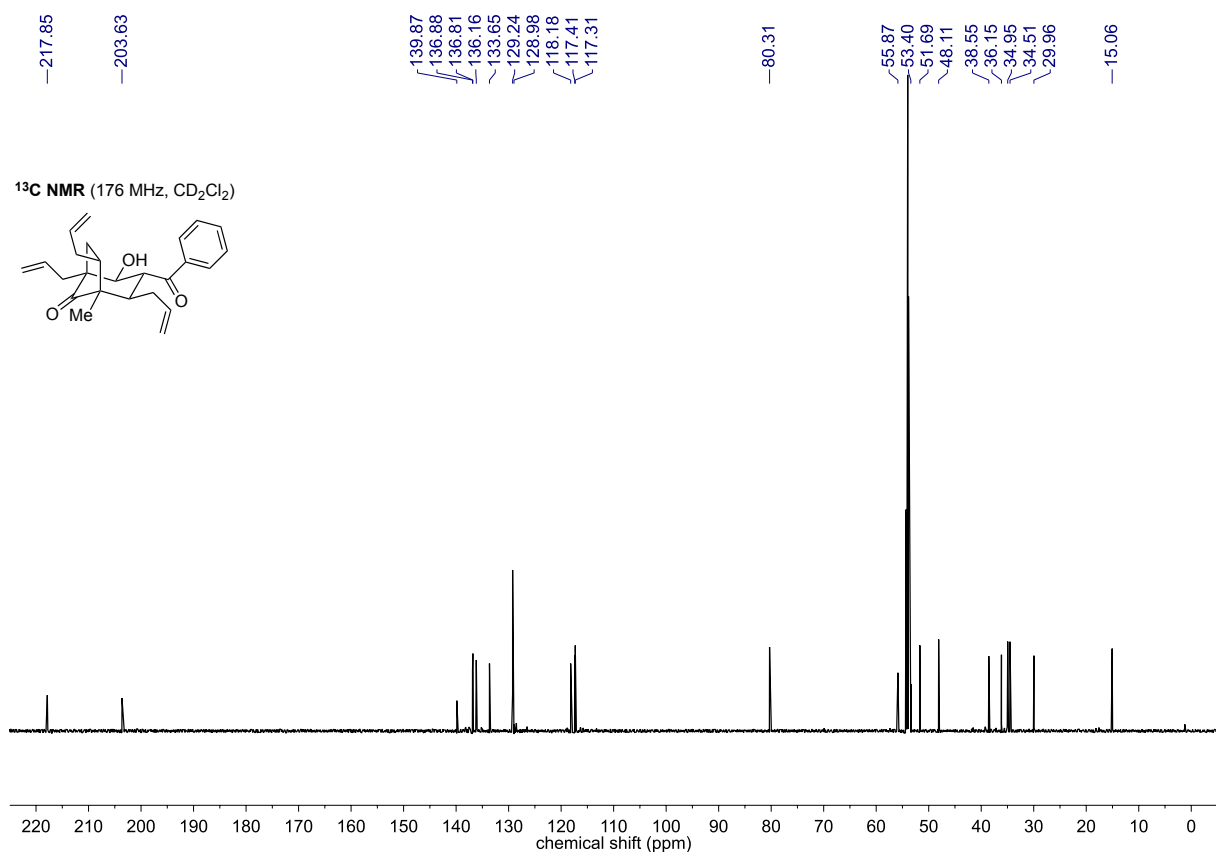
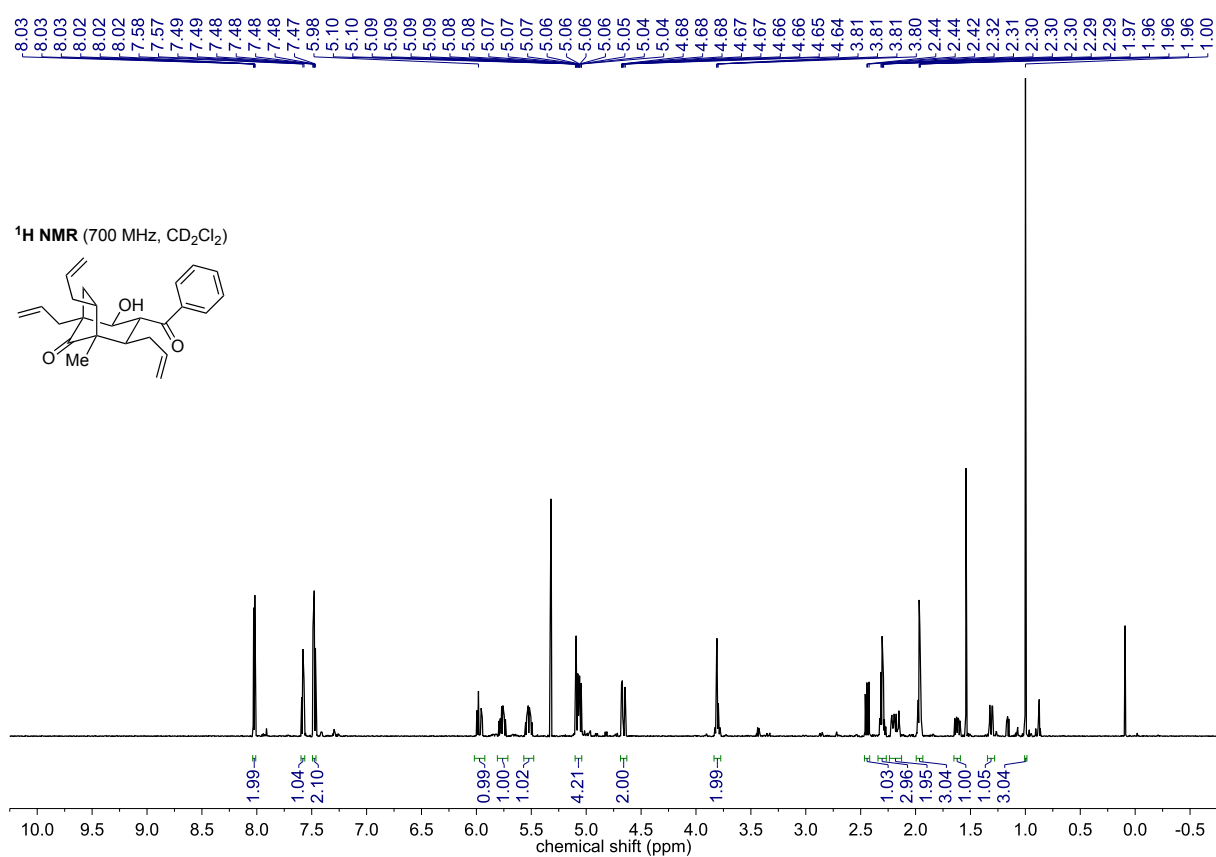
35.60

32.30

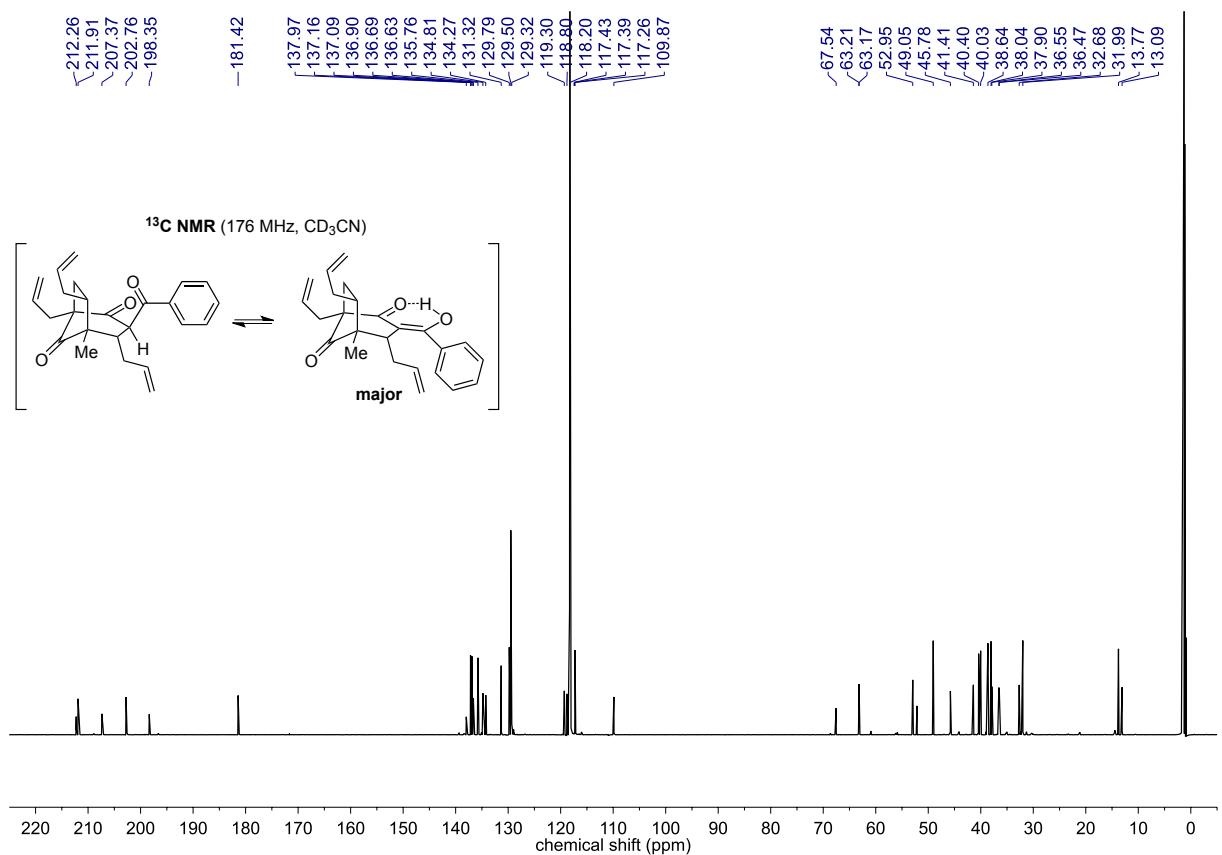
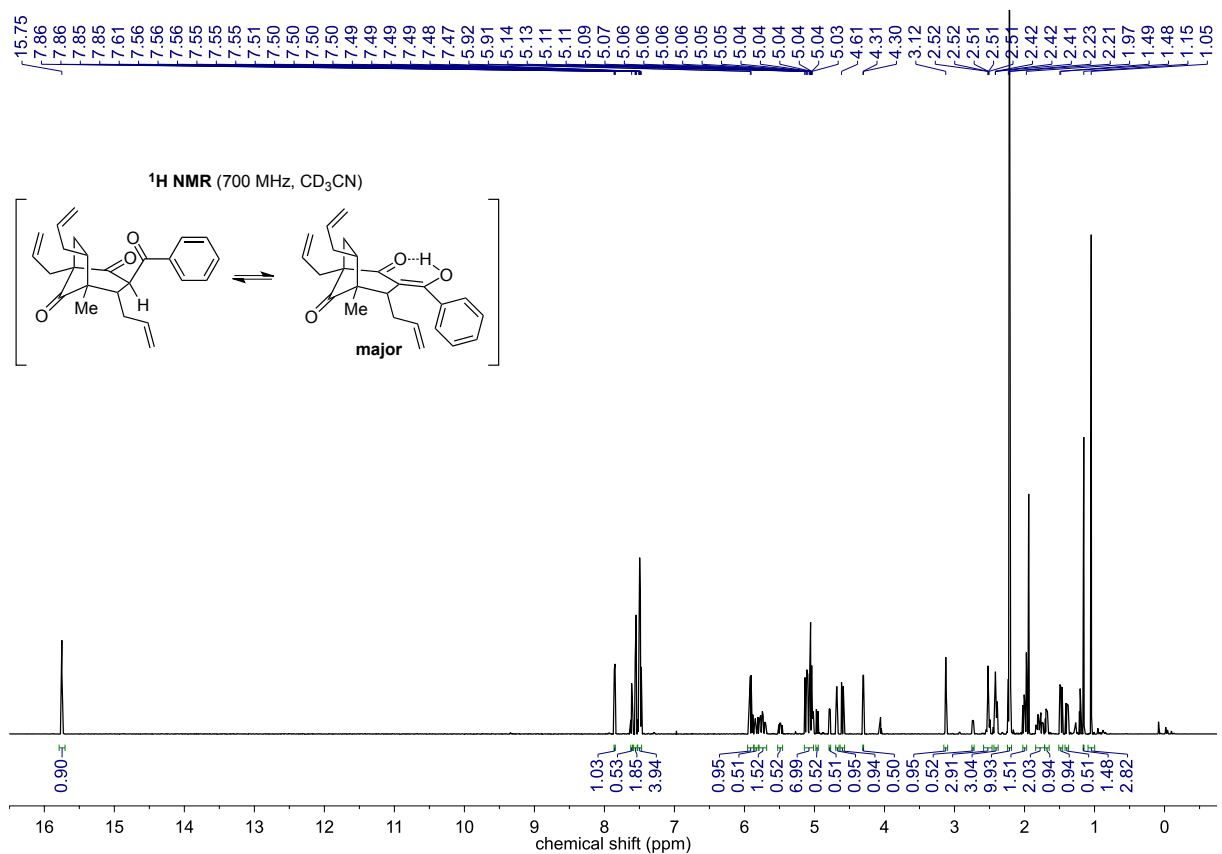
-14.18

<sup>13</sup>C NMR (176 MHz, CD<sub>2</sub>Cl<sub>2</sub>)

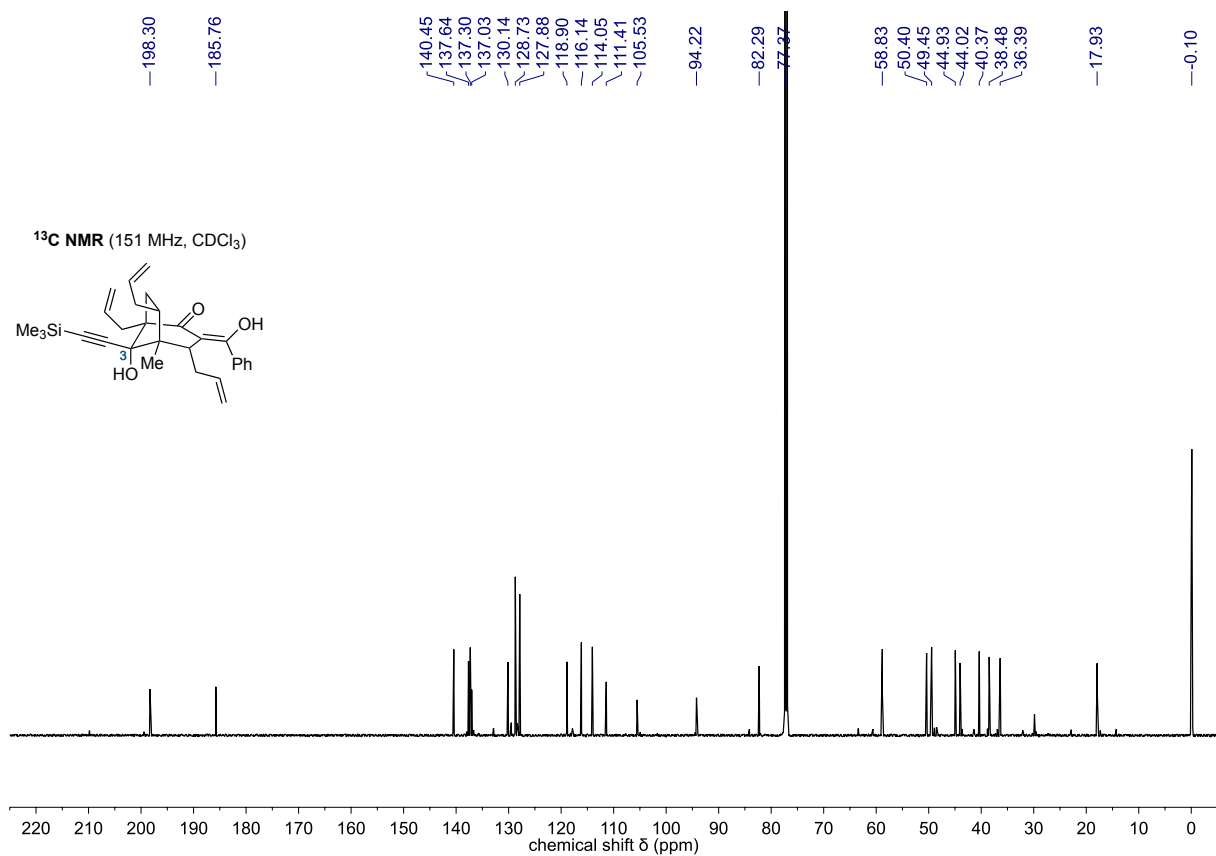
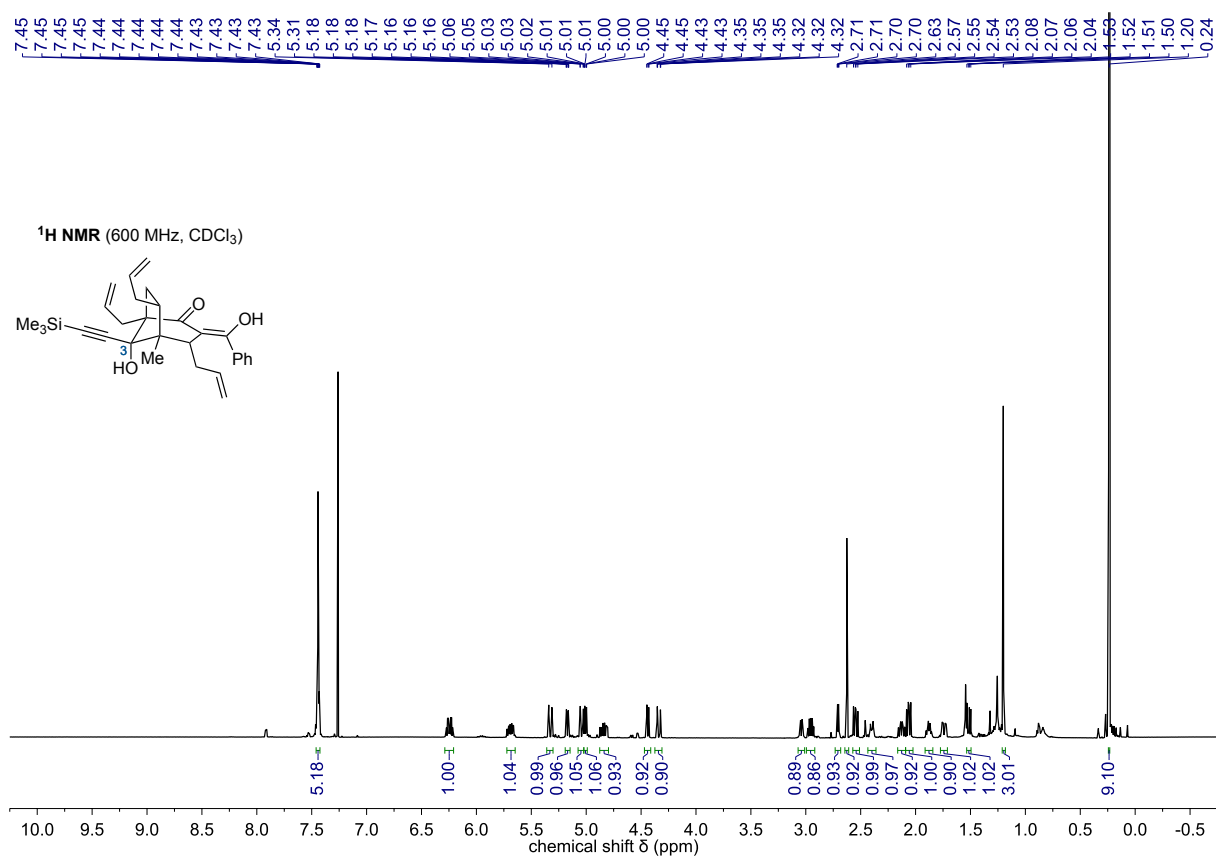
## Compound rac-246



## Compound rac-247/248



## Compound rac-249



## Compound rac-250

